

PV-AAT-ES5
41690

LIMA DISASTER PREPAREDNESS REPORT

VOLUME XIII-D

SELECTED AVAILABLE DOCUMENTATION:

THE BRADY EARTHQUAKE PREDICTIONS

BOOK D: Published and Unpublished Technical Papers

Office of U. S. Foreign Disaster Assistance
Agency for International Development

October 1982

FOREWORD

This is one of four books which together form a compilation of documentation available to the author concerning the earthquake predictions for Peru in 1981 of Dr. Brian T. Brady. The set of four books together comprise Volume XIII of a fifteen volume report concerning disaster preparedness in Lima, Peru. It was researched in Lima by a team of disaster specialists during the period July - November, 1981, for the Agency for International Development's Office of Foreign Disaster Assistance and USAID Mission in Peru. Further research was conducted in the Office of Foreign Disaster Assistance, Washington, D. C., in Fall, 1982.

October 1982

This work was done under Contract #PDC-0018-0-OC-2075-00
by Robert Gersony.

The Lima Disaster Preparedness Report has 15 sections:

Volume I	Methodology Employed
Volume II	Port of Callao Infrastructure Security and Emergency Evacuation Needs
Volume III	Electricity
Volume IV	Water and Sewerage
Volume V	Heavy Equipment Rehabilitation and Maintenance
Volume VI	Airport and Aircraft Resources
Volume VII	Education
Volume VIII	Food Supply and Consumption
Volume IX	Low-Income Housing
Volume X	Emergency Medical Care
Volume XI	International Donor Coordination
Volume XII	Critical Abstracts from the Literature: A Field Perspective on Major Earthquakes Peru, 5-31-70 Nicaragua, 12-23-72 Guatemala, 2-4-76
Volume XIII	Selected Available Documentation: The Brady Earthquake Predictions
Volume XIV	Sewerage and Water: Supplementary Information
Volume XV	Summary

COMMONLY USED ABBREVIATIONS

USGS	U. S. Geological Survey [U. S. Department of the Interior]
USBM	U. S. Bureau of Mines [U. S. Department of the Interior]
DOI/OES	U. S. Department of the Interior/ Office of Earthquake Studies
AID	Agency for International Development
OFDA	Office of U. S. Foreign Disaster Assistance [Agency for International Development]
IGP	<u>Instituto Geofísico Peruano</u>
CERESIS	<u>Centro Regional de Sismología para</u> <u>América del Sur</u>

TABLE OF CONTENTS

<u>Approximate Date of Document*</u>	<u>Reference/Description*</u>	<u>Page No.</u>
1915	Billings, L. G., 1915, Some Personal Experiences With Earthquakes, National Geographic Magazine, pp. 57 - 70	647
June, 1971	Cloud, W. K., and Perez, V., June, 1971, Unusual Accelerograms Recorded at Lima, Peru, Bulletin of Seismological Society of America, Vol. 61, No. 3, pp. 633 - 640	653
August, 1973	Stauder, W., August 10, 1973, Mechanism and Spatial Distribution of Chilean Earthquakes With Relation to Subduction of the Oceanic Plate, Journal of Geophysical Research, Vol. 78, No. 23, p. 5033 [Abstract Only]	656(a)
March, 1974	Kisslinger, C., March, 1974, Earthquake Prediction, Physics Today	657
March, 1975	Stauder, W., March 10, 1975, Subduction of the Nazca Plate Under Peru as Evidenced by Focal Mechanisms and by Seismicity, Journal of Geophysical Research, Vol. 80, No. 8, pp. 1053 - 1064	664
1974	Brady, B. T., 1974, Theory of earthquakes - I. A scale independent theory of rock failure, Pure appl. Geophys, 112, 701 - 725	676
1975	Brady, B. T., Theory of earthquakes - II. Inclusion theory of crustal earthquakes, Pure appl. Geophys, 113, 149 - 168	701
1976	Brady, B. T., 1976, Theory of earthquakes - Part III: Inclusion collapse theory of deep earthquakes, Pure appl. Geophys, 114, 119 - 139	721
1976	Brady, B. T., 1976, Theory of earthquakes - IV. General implications for earthquake prediction, Pure appl. Geophys, 114, 1031 - 1082	742

* Based on best available information from sources of documents, with some estimations of date for undated manuscripts.

<u>Approximate Date of Document</u>	<u>Reference/Description</u>	<u>Page No.</u>
November, 1976	Barzangi, M., and Isacks, B. L., November, 1976, Spatial distribution of earthquakes and subduction of the Nazca plate beneath South America, Geology, Vol. 4, pp. 686 - 692	768
July, 1977	Kanamori, H., July 10, 1977, The Energy Release in Great Earthquakes, Journal of Geophysical Research, Vol. 82, No. 20, pp. 2981 - 2987	775
1977 [?]	Brady, B. T., [undated manuscript], The 3 October and 9 November 1974 Peru Earthquakes: Seismological Implications	782
October, 1977	Espinosa, A. F., Husid, R., Algermissen, S. T., de las Casas, J., October, 1977, The Lima Earthquake of October 3, 1974: Intensity Distribution, Bulletin of the Seismological Society of America, Vol. 67, No. 5, pp. 1429 - 1439	823
1979 [?]	Kolub, R.F., & Brady, B.T., [undated manuscript] The Effect of Stress on Radon Emanation From Rock	834
January, 1978	Conference Report: Toward Earthquake Prediction on a Global Scale, January, 1978, EOS, Vol. 59, No. 1, pp. 36 - 42	853
1979	Dewey, J. W., and Spence, W., 1979, Seismic Gaps and Source Zones of Recent Large Earthquakes in Coastal Peru, Pure and Applied Geophysics, Vol. 117, No. 6, pp. 1148 - 1171	861
1979 [?]	Brady, B. T., Rowell, G. A., Yoder, L. P., [undated manuscript], Physical Precursors of Rock Failure: A Laboratory Investigation	886
April, 1980	Ocola, L., April, 1980, <u>Prediccion Sismica en el Peru: Parametros Importantes, Programa General, y Equipamiento</u> , report by <u>Direccion de Investigacion Cientifica de Geofisica Aplicada, Instituto Geofisico Peruano</u> , Lima, Peru	907
December, 1980	Roberts, J., December, 1980, Reflections on a forecast which may lead to the prediction of a strong earthquake near Lima, Peru [manuscript]	947
January, 1981	Aki, K., January 20, 1981, A Probabilistic Synthesis of Precursory Phenomena [manuscript]	976

<u>Approximate Date of Document</u>	<u>Reference/Description</u>	<u>Page No.</u>
October, 1982	Roberts, J.L., October, 1982 [?], Notes on procedure for conveying earthquake forecasts by foreign scientists suggested by experience of forecasts issued for central coastal area of Peru in October, 1980, [manuscript] comprising part of UNESCO Seminar on Earthquake Prediction Case Histories	1005
October, 1982	Giesecke, A.A., 12 October 1982, Case History of the Peru Prediction for 1980 - 81, [manuscript] comprising part of UNDRO/UNESCO Seminar on Earthquake Prediction Case Histories	1014

SOME PERSONAL EXPERIENCES WITH EARTHQUAKES

By REAR ADMIRAL L. G. BILLINGS, U. S. NAVY, RETIRED

THERE is no natural phenomenon more deeply interesting and yet so little understood as the seismic disturbances which have from earliest history devastated the earth and carried terror and dismay into the hearts of all survivors.

Up to 1903, it is computed by an eminent scientist, Compté de Balloré, there had been 159,782 recorded earthquakes. Of later years, when more accurate records have been kept, they have averaged about 60 per annum. There is comfort to the dwellers in most of the world to know that 94 per cent of recorded shocks have occurred in two narrow, well-defined belts—one called the Mediterranean, with 53 per cent to its credit, and, the other, the Circum-Pacific, with 41 per cent—while the remainder of the world has only 6 per cent, widely distributed.

The United States has been singularly free from recorded seismic disturbance, perhaps the most disastrous being in 1811, when a very severe shock occurred in the Mississippi Valley south of the Ohio, which was felt in New York in one direction and in the West Indies in another. This earthquake changed the face of the earth. A vast extent of land was sunk, lakes were formed, and even the course of the Mississippi River was obstructed for a time (see page 67).

Most of the earthquakes occurring of late years can hardly be classed with the great ones of history, nearly all of the destruction being caused by uncontrollable fires. In the more stable zones long periods may elapse between shocks, as, for instance, in Kingston, Jamaica, 215 years intervened.

While the Panama Canal is not situated in the earthquake zone proper, it has experienced numerous shocks, though none in historic times have been fatal.

THE CAUSE OF EARTHQUAKES

The cause of earthquakes and volcanoes is an elusive problem, not yet set-

tled to the satisfaction of the scientist. Tremors of the earth may be caused by many things. The explosion of mines, falling in of caves, slipping of rock strata, and many other movements of the earth may cause them; but for the great shocks which have recurred almost since the history of the world began we must look further.

For ages theories have been evolved, and, though most of them have received the earnest consideration of our modern scientists, they seem to be advanced only to be combated and denied; so that, after all, we must confess to the humiliating fact that we know very little about the cause of earthquakes.

Though many times there seem to be an intimate connection between earthquakes and volcanoes, the law regarding them has not been established. Some remarkable coincidences have been observed in late years. The terrible cataclysm of Mount Pelee, which, on May 8, 1902, almost instantly killed 30,000 inhabitants, was preceded by the earthquake which in January and April of the same year wrecked a number of cities in Mexico and Guatemala. The distance between these points is at least 2,000 miles, showing how deep-seated must have been the disturbance, if, as has been suggested, there was communication between them. The great San Francisco earthquake was preceded only two days by one of the most violent eruptions of Vesuvius recorded in many years.

THE BEHAVIOR OF BOGOSLOF

It is also a significant fact that the fuming island off the coast of Alaska, called Bogoslof No. 3, appeared at almost the same time. A revenue cutter, visiting this island, was astonished to see that the mountain, or hill, some 400 feet high, on the island, had disappeared, and in its place a bay had been formed. Soundings showed a depth of from 8 to 25 fathoms of water.

Nor is that the only time Bogoslof has changed. When the revenue cutter "Tahoma" called there on September 10, 1910, it was found that what was once a group of islands had now become a single mass of land, with several peaks. The cutter's officers found on the new-born land the skeletons of myriads of sea-birds that had been roasted alive before they could fly away from the terrible upheaval caused by the submarine explosion. They had been burned in such a fervent heat that the skeletons crumbled to dust upon being touched. Nine days later the "Tahoma" visited Bogoslof again, and when 25 miles off, witnessed another eruption, which resulted in another upheaval and another change in the appearance of the island.

But volcanoes, terrible and impressive as they are, are hardly worthy of comparison with the great earthquakes. The volcanic effects are of limited area, while the "earth movers" frequently extend thousands of miles, marking their paths with destruction.

It has been observed that in certain portions of the South Pacific Ocean there are almost continuous eruptions of fire, water, and foreign bodies, forming considerable islands in inconceivably short periods, which quite as frequently vanish again beneath the waves.

The eruption of the volcano of Krakatoa was a most wonderful illustration of this hidden power. Ashes were projected 14 miles into the air and carried 600 miles, while the accompanying tidal wave swept the shores for immense distances, submerging all life.

THE HUMAN TOLL OF EARTHQUAKES

One appalling feature of earthquakes is the almost instant death of thousands of people. What wonder, then, that no other phenomenon of nature produces such unreasoning terror in all forms of life?

Tracing back, it is recorded that in 373 B. C. Burao Helico, called the Superb, was engulfed in the Sea of Corinth and over 100,000 inhabitants drowned.

In 13 A. D., 13 great and noble cities of Asia Minor were destroyed in one night. The destruction of Burao Helico was

paralleled November 4, 1799, at Cumana, a magnificent New World city, situated on the Venezuelan coast, where, almost in the twinkling of an eye, the city, with all its unhappy inhabitants, sank beneath the waves.

THE DESTRUCTION OF PORT ROYAL

The last earthquake at Kingston, Jamaica, almost sinks into insignificance when compared with that which destroyed the old city of Port Royal, practically on the same location, on June 7, 1692. Immense waves swept over the town, and in less than three minutes submerged 2,500 houses, drowning nearly all the inhabitants. The sea remained 33 feet above even the steeples of the town, and the large English frigate "Swan" was carried safely over the city and escaped to sea.

Lisbon was destroyed in 1755; when, it is computed, 60,000 people perished in less than two minutes.

The destruction of Sodom and Gomorrah, the wicked cities of the plain, by fire sent from heaven, is paralleled by the utter destruction of a small town in Ecuador by fires bursting through the ground.

I quote from a quaint account given by "a member of the Royal Academy" at Berlin concerning the birth of an island:

"At a place in the sea where fishermen used to fish every summer, called La Ferrera, 6 miles from Pico Della Caramine, upon the fifth Sunday in July, a subterranean fire—notwithstanding the weight and depths of the sea in that place, which was 120 feet by soundings, and the multitude of waters, which one would have thought sufficient to have quenched the fire—fire, I say, broke out with inexpressible violence, carrying with it up to the clouds water, sand, earth, stone, and other bulk of bodies, after which was formed an island in the main ocean, which was not, at first, over 5 furlongs; but in 13 days it had extended to 14 miles."

RIDING A TIDAL WAVE

It is the purpose of this article to record a thrilling experience in one of the modern earthquakes, in which a United States man-of-war was carried on the

crest of a tidal wave 5 miles down the coast, 2 miles inland, and set down, entirely unharmed, upon the beach, within 100 feet of the Andes (see page 70).

In 1868 I was attached to the U. S. S. "Waterloo," then on duty in the South Pacific—one of a class of boats built at the close of our Civil War to ascend the narrow, tortuous rivers of the South; she was termed a "double ender," having a rudder at each end, and was quite flat-bottomed—a conformation which, while it did not add to her seaworthiness, enabled her to carry a large battery and crew, and eventually saved our lives, in the catastrophe which was soon to come upon us.

We had about finished our cruise and, now that it was nearly over, were congratulating ourselves that we had passed safely through all the exciting phases of our station, such as northern revolutions, yellow fever, and even earthquakes, for we had experienced several shocks which sent the natives screaming to the squares, while we, with an ignorance soon to be enlightened, smiled calmly at their fears and made the usual remarks about "the cowardly Dagos."

AT ANCHOR AT ARICA

August, 1868, found us quietly at anchor off the pretty Peruvian town of Arica, whither we had towed the old United States store-ship "Fredonia" to escape the ravages of yellow fever, then desolating Callao and Lima. We had received preparatory orders to go up the coast to San Francisco, and had been at anchor for six weeks overhauling boilers and engines preparatory to the long trip. This unusually prolonged stay in one port had given us opportunities to form pleasant acquaintances and friends among the hospitable citizens, and we congratulated ourselves on the fact that our lines had been cast in such a charming place.

Arica was, for a Peruvian town, beautiful, having about 10,000 inhabitants, it was supposed—I say supposed, for the inquisitive census-taker had never made his rounds, and one arrived at population as the Jerseyman weighs his pig—by guessing.

Being the only port of entry for rich and prosperous Bolivia, behind her; con-

nected with Tacna, 40 miles distant, by what then was the only railroad in Peru, her inhabitants had grown rich and cultured on the imports and exports that crowded the large and imposing custom-house and the shipping that thronged the open roadstead.

THE SITUATION OF ARICA

The town was picturesquely situated in a cleft or valley running up into the seacoast range of the Andes. Through the valley ran a little stream, which furnished the water for irrigation, and caused the desert to blossom with a fertility that never ceased to surprise. It was blocked in, on the one hand, by the perpendicular cliffs of the Morro, 500 feet high, which, without a single break to mar its imposing front, was ever lashed by the waves of the mighty Pacific; on the other, by gradually sloping heights, rising one above the other until lost in the clouds.

The town was of unknown antiquity, there having been a large city of the Incas located there when the Spaniards overran the country, and tradition asserts that even the Incas found a people dwelling there when they, in their turn, had been conquerors.

Favored with a most charming climate, with a temperature varying from 70 to 80 degrees; the cloudless blue of the sky never darkened by storm or rain; fevers and epidemics unknown; it seemed an Eden until we found our "crumpled rose leaves" in the form of a myriad of the most active and voracious fleas that ever drove a human being distracted, and further discovered that a regular deluge would be necessary to remove the cause of a lively series of unsavory odors which would have thrown the famed city of Cologne into the background.

Behind these minor discomforts lurked the ever-present fear in the native mind of another earthquake, for Arica seemed a sort of "head center" for such seismic disturbances, having been twice before destroyed, with great loss of life.

OUT OF SYMPATHY WITH NATIVE FEARS

In blissful ignorance of what a *terremote* (earth mover) really was, we did not sympathize with their fears, and we



Photo from E. Todor Gries, Providence, R. I.

ONLY SURVIVOR OF ST. PIERRE

It is estimated that 3,000 people lost their lives when Mt. Pelée, on the island of Martinique, broke forth with a whirlwind of gas or steam that overwhelmed the city of St. Pierre, May 8, 1902. Only one ship, the "Rodam," escaped from the harbor, and the only person in the city to come through the ordeal alive was the Martinique negro in this picture, who was imprisoned in a dungeon.

had celebrated our National holiday, the 4th, and theirs, the 10th, of July with zeal and an abundant burning of gunpowder. We were not alone in the roadstead—our store-ship, the "Fredonia"; a large Peruvian man-of-war, the "America"; and several square riggers, together with quite a fleet of smaller merchantmen, being in our company.

While the anchorage at Arica was an open roadstead of almost unlimited extent, it was partly protected from the prevailing winds by Alacran Island, small and apparently a lump of rock broken off from the Morro by some prior convulsion. All the merchantmen were clustered rather closely under the lee of this island, near the Morro, maybe a quarter of a mile from the usual man-of-war anchorage, and about the same

distance from the shore. The men-of-war anchored more abreast of the town and possibly half a mile distant.

The vessels were about 200 or 300 yards apart and anchored in from 8 to 10 fathoms of water. The bottom was a somewhat sandy plateau, shelving gradually from 2 fathoms to 40 or 50 for a few miles, and then dropping off rather abruptly to great depths.

WHEN THE EARTH SHUDDERED

It was August 8, 1868, that the awful calamity came upon us, like a storm from a cloudless sky, overwhelming us all in one common ruin.

I was sitting in the cabin with our commanding officer, about 4 p. m., when we were startled by a violent trembling of the ship, similar to the effect produced

by letting go the anchor. Knowing it could not be that, we ran on deck. Looking shoreward, our attention was instantly arrested by a great cloud of dust rapidly approaching from the southeast, while a terrible rumbling grew in intensity, and before our astonished eyes the hills seemed to nod, and the ground swayed like the short, choppy waves of a troubled sea.

The cloud enveloped Arica. Instantly through its impenetrable veil arose cries for help, the crash of falling houses, and the thousand commingled noises of a great calamity, while the ship was shaken as if grasped by a giant hand; then the cloud passed on.

As the dust slowly settled we rubbed our eyes and looked again and again, believing they must be playing us a trick; for where but a few short moments before was a happy, prosperous city, busy with life and activity, we beheld but a mass of shattered ruins, hardly a house left standing; not one perfect; the streets blocked with debris, through which struggled frantically the least wounded of the unhappy wretches imprisoned in the ruins of their once happy homes; while groans, cries, and shrieks for help rent the air. Over all this horror the sun shone pitilessly from an unclouded sky; the sea rolled shoreward as steadily as before. How long did it last? No one took any note of time. It seemed a nightmare, from which we would presently awake; but the agony and suffering before us were too real and apparent to be the effects of imagination. The shock may have been four or five minutes in reaching us and passing.

With the fresh recollection in our minds of the tidal wave that followed the earthquake at Santa Cruz and stranded one of our proudest sloops-of-war, the "*Mimongahela*," in the streets, we anxiously scanned the sea for any unusual appearance betokening the coming of that dreaded accompaniment; but all was as calm and serene as before.

PREPARING FOR THE WORST

Our prudent commander, however, gave the necessary orders to prepare for the worst. Additional anchors were let go,

hatches battened down, guns secured, life lines rove fore and aft, and for a few moments all was the orderly confusion of a well-disciplined man-of-war preparing for action. Many hands make short work, and in a few moments we were prepared for any emergency.

Looking shoreward again, we saw the uninjured thronging the beach and crowding the little pier, crying to the vessels to aid them in digging their loved ones from the ruins and to transport them to the apparent safety of the vessels riding so quietly at anchor. This was more than we could witness unmoved, and orders were given to prepare a landing party of 40 men, duly equipped with shovels, etc. The gig, a large, double-banked whale-boat, with a crew of 13 men, shoved off at once. She reached the shore and landed her crew, leaving only the customary boat-keeper in charge.

WAVING A BRAVE FAREWELL

Our attention was now distracted from the formation of our working party by a hoarse murmur. Looking shoreward, to our horror we saw vacancy where but a moment before the pier had been black with a mass of humanity—all swallowed up in a moment. Amid the wreckage we saw the gig, bearing a single boat-keeper, borne by an irresistible tide toward the battlemented front of the Morro, with the gallant seaman struggling to stem the current. Finding his efforts vain and certain death awaiting him, he laid in his useless oar, and, running aft to the cockswain's seat, grasped the boat flag and waved a last farewell to his shipmates as the boat disappeared forever in the froth of the cruel rock at the foot of the Andes. Thus the "*Waterer*" lost the only one of her crew of 235 souls on that fateful day.

OTHER TROUBLES CAME UPON US

But our troubles then commenced. We were startled by a terrible noise on shore, as of a tremendous roar of musketry, lasting several minutes. Again the trembling earth waved to and fro, and this time the sea receded until the shipping was left stranded, while as far as seaward as our vision could reach, we saw the rocky bottom of the sea, never before exposed

to human gaze, with struggling fish and monsters of the deep left high and dry. The round-bottomed ships keeled over on their beam ends, while the "*Waterer*" rested easily on her floor-like bottom; and when the returning sea, not like a wave, but rather like an enormous tide, came sweeping back, rolling our unfortunate companion ships over and over, leaving some bottom up and others masses of wreckage, the "*Waterer*" rose easily over the tossing waters, unharmed.

THE SEAS DEFY ALL NATURE

From this moment the sea seemed to defy the laws of nature. Currents ran in contrary directions, and we were borne here and there with a speed we could not have equalled had we been steaming for our lives. At irregular intervals the earthquake shocks recurred, but none of them so violent or long-continued as the first.

The Peruvian man-of-war "*America*," said to be the fastest ship in the world at that time, had hastily gotten up steam and attempted to get to sea. She was well out when the receding water left her partly afloat and broke her back, of course destroying her engines. With her funnels still vomiting black smoke and apparently under full command of her people, she backed down toward the helpless "*Fredonia*," which was then rapidly settling in toward the Morro, as if intending to help her.

Lieutenant Commander Dyer, commanding the "*Fredonia*," saw the maneuver, and, thinking the "*America*" was coming to their aid, and that a nearer approach would only involve them both in destruction, ran on the poop and hailed the approaching ship, then but a few yards distant: "*America*, ahoy! You can do nothing for us; our bottom is crushed. Save yourselves. Good bye." Then down to his station among his silent, unshrinking crew he ran again. The next moment the "*Fredonia*" was crushed, and of that ill fated company not one was saved, while a counter-current catching the Peruvian ship drove her rapidly in another direction.

Facing the Morro, and a short distance away, a rocky islet rose some feet above

the sea. On it the Peruvians had hewn a fort from the solid rock and had mounted therein two 15-inch guns, the garrison numbering some 200 souls. We were but a short distance from this fort and were fearing to be cast against its rocky sides, when suddenly we saw it disappear beneath the waves. Whether it sank or the water rose we could not tell; we only knew it vanished; and when it reappeared, after a few moments, like a huge whale, not only were the unfortunate garrison gone, but the guns and carriages as well. Imagine, if you can, how the water lifted those immense masses of iron, weighing many tons and offering no holding surface from their resting places and tumbled them out of the 8-foot parapet. It is a problem never to be solved.

Before the earthquake Arica had one of the best and most modern machine-shops between Callao and Valparaiso. Many of the machines were ponderous and properly secured on cement foundations. There were also several locomotives, cars, and many heavy castings. These all disappeared; not a vestige was left. It seems impossible they could have been swept out to sea, but assuredly they could not be found on shore.

During the first of the disturbance we had lowered one of our large cutters and sent it, in charge of a midshipman, to rescue a number of persons drifting about on some wreckage. There was no sea on at this time, but to our astonishment we saw that, with all the efforts of the crew, the boat could make no headway, but went sailing about in the most erratic fashion.

The midshipman, finding it impossible to rescue the people he had been sent to save, attempted to return to the ship. That, too, was impossible, and presently his efforts were ended by having his boat dashed violently against the side of the "*America*" and crushed like an egg-shell. He and his crew managed to scramble to her deck.

There they found a scene which beggars description. A condition of panic prevailed. Officers and men in abject terror were running about, imploring all the saints in the calendar to help them.

Meantime the heavy guns, that had been cast adrift in a vain attempt to throw them overboard to lighten the ship when she grounded, were running riot. With every "send" of the sea the guns rushed madly from side to side, crushing everything, animate or inanimate, in their path, and strewn the deck with bloody victims. There is nothing more to be dreaded than a gun on an old-time mount adrift in a seaway; it seems possessed of a demon, and baffles ordinary means of control. Some of the "America's" spars had been carried away and still further lumbered her deck, and, worse than all, fire had broken out near the engine-room and threatened the after powder magazine.

A FEROIC MIDSHIPMAN

Finding the Peruvians so panic-stricken as to be of no use, our gallant young midshipman, only a lad of 18, quickly took command, with his crew of 13 men. Making a line fast around his waist, he was lowered into the burning hold and flooded the powder magazine; then by choking the rampant guns with masses of hammocks piled on them he soon had them secured, extinguished the fire, and, after quieting the natives, calmly awaited events.

No one born under our glorious flag could help feeling proud of the courage, discipline, and self-reliance displayed by our officers and men at this awful test of bravery and fidelity to duty. While the crew of the Peruvian ship was simply an ungovernable mob, whose cries pierced the air, our men stood in battle array, grouped around the guns, every man at his station, ready to obey any order given by the keen-eyed first lieutenant; not a word spoken or a movement made, except when a sharp command called for instant obedience!

When men are taught self-discipline and control, as were our sailors during the four years of battle and storm which we had just passed through in our Civil War, not even nature's greatest convulsions can shake their nerve, and in this awful test of courage they determined if they could not live they would at least emulate the example of the heroes of the

"Fredonia" and show how American sailors could die.

THE GRAVES GIVE UP THEIR DEAD

As the last rays of the setting sun fell on the heights of the Andes, we saw to our horror that the graves, where the ancients had entombed their dead, on the sloping side of the mountain, had opened, and in concentric rows, like chairs in an amphitheater, the mummies of the long-buried and forgotten aborigines rose to the surface. They had been buried in a sitting posture, facing the sea. The soil, impregnated with niter, had thoroughly preserved them, and the violent shocks disintegrating the dry earth was now exposing this long-buried, frightful city of the dead. Words cannot paint the ghastliness of the scene. In addition to what we had already experienced, to our excited imagination it seemed as if the day of judgment had come, the earth was passing away, and the bitterness of a death so full of terrors as no imagination can conceive was now to befall us.

It had now been dark for some time and we knew not where we were, the absence of the usual beacon and shore lights adding to our confusion. About 8.30 p. m. the lookout hailed the deck and reported a breaker approaching. Looking seaward, we saw, first, a thin line of phosphorescent light, which loomed higher and higher until it seemed to touch the sky; its crest, crowned with the death light of phosphorescent glow, showing the sullen masses of water below. Heralded by the thundering roar of a thousand breakers combined, the dreaded tidal wave was upon us at last. Of all the horrors of this dreadful time, this seemed the worst. Chained to the spot, helpless to escape, with all the preparations made which human skill could suggest, we could but watch the monster wave approach without the sustaining help of action. That the ship could ride through the masses of water about to overwhelm us seemed impossible. We could only grip the life-line and wait the coming catastrophe.

AT LAST THE TIDAL WAVE

With a crash our gallant ship was overwhelmed and buried deep beneath a semi-



Photo by Gay E. Mitchell

REMAINS OF A DRY-LAND HARDWOOD FOREST, REELFOOT LAKE, TENNESSEE, CAUSED BY SINKING OF THE LAND

One of the greatest earthquakes of which the modern world has knowledge took place within our own country. It occurred in the year 1811 in the West Tennessee-East Arkansas region, and the remains of the sunken forests, upheaved swamps, and uprooted trees tell an eloquent story of the devastating character of the quakes. The few inhabitants of that region were kept in terror for days. Such a quake in the same region today might destroy tens of thousands of people and do millions of dollars' damage (see page 67).

solid mass of sand and water. For a breathless eternity we were submerged; then, groaning in every timber, the staunch old "Waterloo" struggled again to the surface, with her gasping crew still clinging to the life-lines—some few seriously wounded, bruised, and battered; none killed; not one even missing. A miracle it seemed to us then, and as I look back through the years it seems doubly miraculous now.

Undoubtedly our safety was due to the design of the ship. Part of our battery was two 200-pound rifles; one forward the other aft; both mounted so they could be pivoted on either side. When not in battery, they were secured amidships.

The bulwarks, or pivot ports, in the side of the ship were arranged as a series of heavy ringed panels, which, when the guns were in use, could be lowered out-

ward, leaving an opening of about one-third of the side of the ship practically level with the deck. Expecting the tidal wave, they had been lowered early in the afternoon. This permitted the water to run off the deck—about as it would from a raft or floating plank.

The ship was swept on rapidly for a time, but after a while the motion ceased, and, lowering a lantern over the side, we found ourselves on shore, but where, we knew not. Smaller waves washed about us for a time, but presently they ceased. For some time we remained at quarters; but as the ship remained stationary, and nothing new occurring, the order was given to "Pipe down," followed by the welcome order, "All hands stand by your hammocks," and such of the crew as were not on watch quietly made their way through the reopened hatches to the sodden berth deck—to sleep. I know not

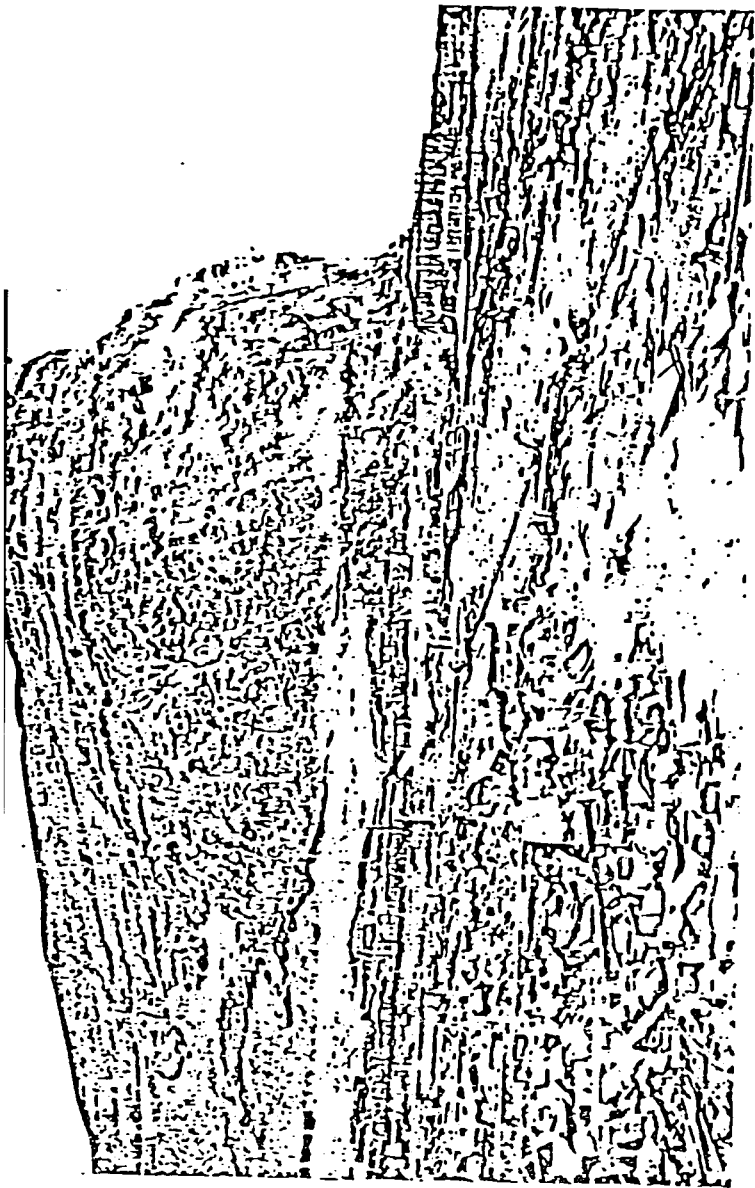


Photo from Rear Admiral L.G. Billings, U.S. Navy

MORRO HILL AND THE RUINS OF THE CITY OF ARICA, PERU

"The cloud enveloped Arica. Instantly through its impenetrable veil arose cries for help, the crash of falling houses, and the thousand commingled noises of a great calamity, while the ship was shaken as if grasped by a giant hand; then the cloud passed on. As the dust slowly settled we rubbed our eyes and looked again and again, believing they must be playing us a trick, for where but a few short moments before was a happy prosperous city, busy with life and activity, we beheld but a mass of shattered ruins, hardly a house left standing; not one perfect; the streets blocked with debris, through which struggled frantically the least wounded of the unhappy wretches imprisoned in the ruins of their once happy homes, while groans, cries and shrieks for help rent the air. Over all this horror the sun shone pitilessly from an unclouded sky; the sea rolled shoreward as steadily as before" (see page 63).

what dreams must have visited the pillows of these brave fellows on that eventful night, but to me one of the wonders of this wonderful experience was the matter-of-fact obedience to orders manifested by these sorely tried men.

FINDING OURSELVES HIGH AND DRY

The morning sun broke on a scene of desolation seldom witnessed. We found ourselves high and dry in a little cove, or rather indentation in the coast-line. We had been carried some 3 miles up the coast and nearly 2 miles inland. The wave had carried us over the sand dunes bordering the ocean, across a valley, and over the railroad track, leaving us at the foot of the seacoast range of the Andes. On the nearly perpendicular front of the mountain our navigator discovered the marks of the tidal wave, and, by measurements, found it to have been 47 feet high, not including the comb. Had the wave carried us 200 feet further, we would inevitably have been dashed to pieces against the mountain-side.

There we lay on as even a keel as if still afloat, with our flag flying and our port anchor and 100 fathoms of chain led out as carefully as we could have placed them there. Was it possible that this, our heaviest anchor and chain, could have drifted with us throughout all the mazes of our voyaging of the afternoon? And why was not the chain parted by the last shock, as were the others?

We found near us the wreck of a large English bark, the "Chanacelia," which had one of her anchor chains wound around her as many times as it would go, thus showing she had been rolled over and over; a little nearer the sea lay the Peruvian ship, the "America," on her bilges; and the sand was strewn with the most heterogeneous mass of plunder that ever gladdened the heart of a wrecker: Grand pianos, bales of silk, casks of brandy, furniture, clothing, hardware; everything imaginable was there. A rough estimate placed this emptying of the custom-house at \$1,100,000.

"WE SAVED THE FLAG, SIR!"

Our first work was to establish a cordon of sentries around the ship, while a

strong working party stove in the brandy casks and shattered the wine cases, for we did not propose having drunkenness added to the other horrors surrounding us. One of the incidents of the morning was the return of the midshipman and crew from the wrecked Peruvian ship and the laconic report of the youngster in command: "Returned on board, sir. I have to report the loss of the second cutter, 12 oars, and two boat-hooks; but we saved the flag, sir."

Most of the surviving Peruvians, when they discovered the "America" was on shore, deserted the ship, and were drowned by the next incoming wave, which, though not a breaker, was high enough to sweep them away, while our officer held his men until daybreak.

In a few days the savage Araucanian Indians from the mountains descended upon us with long trains of llamas, the camels of the Andes. They broke open boxes, cut the fastenings of bales, and started back to their retreats loaded down with plunder. We were not able to argue with them, but there was an invitation to stop in the shriek of our shells that all understood. By firing in front of them with one of our smaller guns we "love them to" and made them approach and unload their cargoes near us. Soon we had accumulated an assorted pile of merchandise much larger than our ship.

NUMMIES CARRIED TO WASHINGTON

The earthquake shocks continued at varying intervals, but none of them so violent or long-continued as at first; some of them, however, were severe enough to shake the "Waterloo" until she rattled like an old kettle, and caused us to abandon the ship and camp on a considerable plateau, some 100 feet high, and overlooking the ship and wreckage. Here we had an opportunity of seeing the disastrous results of the earthquake on land. We found in some places immense fissures, many of them over 100 feet wide and of unknown depths; others were mere cracks. Some of them proved the graves of the fleeing inhabitants. In one instance, I remember, we found the body of a lady sitting on her horse, both swallowed up while fleeing for their lives.

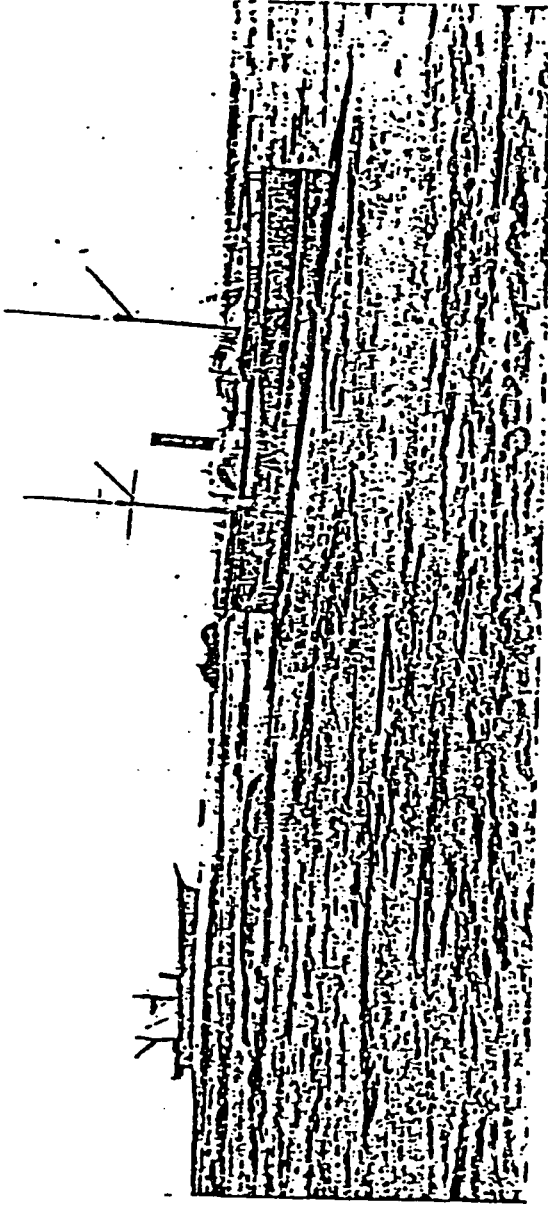


Photo from Rear Admiral L.G. Billings, U.S. N

THE "AMERICA", PERUVIAN MAN-OF-WAR, AND THE U.S.S. "WATEREE" ON SHORE AFTER THE EARTHQUAKE: ALSO WRECK OF THE ENGLISH MERCHANT VESSEL "CHANACELIA": ARICA, PERU

"Heralded by the thundering roar of a thousand breakers combined, the dreaded tidal wave was upon us at last. Of all the horrors of this dreadful time, this seemed the worst. Chained to the spot, helpless to escape, with all the preparations made which human skill could suggest, we could but watch the monster wave approach without the sustaining help of action. That the ship could ride through the masses of water about to overwhelm us seemed impossible. We could only grip the life-line and wait the coming catastrophe. . . The morning sun broke on a scene of desolation seldom witnessed. We found ourselves high and dry in a little cove, or rather indentation in the coast-line. We had been carried some three miles up the coast and nearly two miles inland". (see page 66).

SOME PERSONAL EXPERIENCES WITH EARTHQUAKES 71

Quite a number of the mummies were brought down to the ship and were ultimately sent to the Smithsonian Institution in Washington, where, I presume, the curious can inspect them at any time. It is now known that while Arica was probably the center of disturbance, the shocks were felt nearly 1,000 miles, and great destruction was occasioned in Bolivia. The beach line of the ocean was raised from 2 to 20 feet for over 600 miles. The tidal wave was felt at the Sandwich Islands, 5,580 nautical miles distant, only 12 hours and 37 minutes later than it had broke on the desolated shores of Peru.

DESOLATION AND DEATH

At Arica we found but desolation and death. Where once had stood that pretty little city, a flat, sandy plain stretched before us. Except on the outskirts, higher up on the mountain, not a house marked the spot. Built to withstand earthquake shocks, the houses were low—few boasting a second story—with light roofs and thick walls of "adobe brick" (sun-dried mud). The shocks first leveled them, then the waves dissolved and washed them away. On the higher slopes a few houses, part of a church, and a hideous mass of debris, composed of everything, including dead bodies, was piled 20 or 30 feet high. This was all that remained of Arica. The loss of life was proportionate to the destruction of property. We could not ascertain how great it was, but as all provisions, clothing, and even fresh water were destroyed, the pitiful remnant of the few hundred persons who gathered

about the "Waterer," living on our stores, in tents made of our sails, told the story as could no figures. Afloat, with the exception of the crew of the "Waterer," nearly all perished.

It was three weeks before relief came. Then can well be imagined the swelling of the hearts and the mist that dimmed the eyes of our sailor men as we looked across the water and hailed the stars and stripes floating from the mast-head of the old United States frigate "Powhatan" as she steamed majestically into that desolated harbor. Her decks were filled with all possible stores and supplies, which were soon distributed among the stricken and helpless who had sought our aid and succor.

Careful survey of the "Waterer" proved that while she was practically uninjured, it would be impossible to launch her; so, after removing the most valuable of her equipment, she was sold at auction to a hotel company. An epidemic of yellow fever broke up that enterprise, and the old ship was afterward used successively as a hospital, a store-house, and, lastly, a target for great guns during the Peruvian-Chilian war. But her gaunt iron ribs still rise above the shifting sands, a fitting monument to one of the greatest of modern earthquakes.*

* See "The World's Most Cruel Earthquake," by Charles W. Wright, NATIONAL GEOGRAPHIC MAGAZINE, April, 1909.
 "The Recent Eruption of Mount Katmai," by George C. Martin, NATIONAL GEOGRAPHIC MAGAZINE, February, 1913.
 "Taal Volcano and Its Recent Destructive Eruption," by Dean C. Worcester, NATIONAL GEOGRAPHIC MAGAZINE, April, 1912.



UNUSUAL ACCELEROGRAMS RECORDED AT LIMA, PERU

BY WILLIAM K. CLOUD AND VIRGILIO PEREZ

ABSTRACT

Accelerograms recorded in downtown Lima, Peru, appear to have two unusual characteristics in comparison with accelerograms recorded outside of Peru. First, the predominant period is approximately 0.1 sec, regardless of epicentral distance of earthquakes. Second, maximum accelerations are high in relation to epicentral distance of major earthquakes. For example, 0.40 g at an epicentral distance of over 160 km during the magnitude 7.5, October 17, 1966, earthquake, and 0.13 g at an epicentral distance of over 320 km during the May 31, 1970, earthquake, whose magnitude was rated by various agencies from 7.6 to 7.8. If the source of energy of Lima were closer than the earthquake epicenters, the accelerograms would appear less unusual, but there is no proof that this is the case.

INTRODUCTION

In 1944, the Coast and Geodetic Survey (now the National Ocean Survey) installed a C&GS standard strong-motion accelerograph in a two-story building in downtown Lima, Peru, in cooperation with the Geophysical Institute of Peru. In 1963, the accelerograph was moved to a small isolated hut in a nearby level park, and, in April 1970, the accelerograph was moved, again a short distance, to its present location, a one-story Institute building at 701 Arequipa Avenue.

At each of the three ground-level sites, soil conditions are probably similar to that reported by Lee and Monge (1968) for the excavation shown in Figure 1: coarse dense gravel and boulders to an unknown depth, possibly 100 ft or more, with a deep water table.

RECORDED EARTHQUAKES

Epicentral distance and direction of earthquakes (all offshore) recorded by the Lima accelerograph and, for sample comparison, similar data for an earthquake recorded at Ferndale, California, are listed in Table 1. Ferndale was selected for two reasons. First, the earthquake epicenter was offshore as in Peru. Second, the accelerograph is identical to the one in Lima.

In Table 1, the list of Peru earthquakes recorded at the first Lima site is incomplete, because of the lack of reported epicenters for several of the earthquakes. However, the table as a whole is adequate to show that practically all Lima accelerograms are characterized by short-period maximum accelerations, regardless of epicentral distance and direction. Furthermore, the table suggests that maximum accelerations recorded at Lima site 2 during the 1966 earthquake and at Lima site 3 during the 1970 earthquake are unusually high, considering epicentral distance.

After the October 17, 1966, earthquake was recorded at site 2, it was thought that the unusual record was perhaps due to some malfunction of the accelerograph. New accelerometers were installed, and those in the accelerograph during the earthquake were returned to United States. Two of the three accelerometers were broken in transit, but the third arrived in excellent condition. The results of shaking-table tests on this accelerometer are summarized in Table 2. Judged from the results there is no

reason to believe instrument malfunction was responsible for the unusual accelerograms recorded at Lima.

PREDOMINANT PERIODS

Lima accelerograms of the 1966 and 1970 earthquakes, Figure 2, show that short periods not only associate with maximum acceleration but also predominate. The Ferndale record, Figure 3, suggests that this is unusual.

The range of predominant periods is more clearly defined by Fourier acceleration amplitude spectra (Figure 4). For the spectra, the method was one used by Jenische

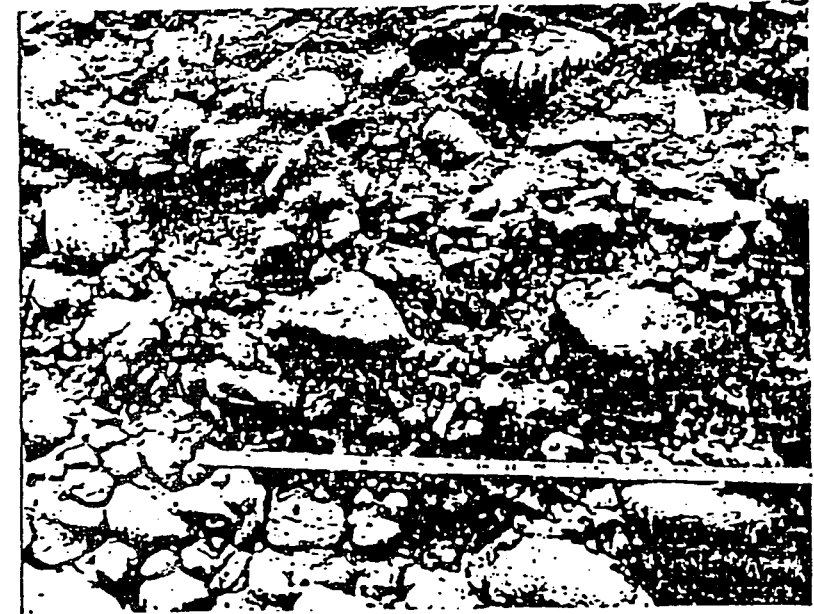


FIG. 1. Typical soil exposed in an excavation near the park site in downtown Lima. (Courtesy Kenneth L. Lee.)

et al. (1961), modified to take an unequally spaced data input. Programming also included corrections to the raw digital data for zero acceleration base line and for variation in length of time marks caused by nonuniform paper speed of the accelerograph.

In Figure 4, it is evident that predominant periods of the two Lima accelerograms are less than 0.15 sec. Discounting the numerous peaks, a reasonable approximation is 0.1 ± 0.03 sec. In comparison, although the Ferndale spectra have a peak in this period range, the more predominant period range is 0.13 to 0.5 sec.

The difference in predominant periods between the Lima and Ferndale accelerograms are of the same order as Lee and Monge (1968) obtained between the 1966 Lima accelerogram and several western United States accelerograms. By the method

of counting the number of times acceleration crossed the zero axis over the duration of strong shaking, they estimated an average predominant period of 0.1 to 0.125 sec for the Lima accelerogram and 0.25 to 0.5 sec for United States accelerograms from earthquakes such as El Centro, 1940; Kern County, 1952; and Washington, 1949.

TABLE I
EARTHQUAKES AND INSTRUMENTAL DATA

Earthquake	Epicenter		Accelerograph			Maximum Acceleration	
	Km	Direction	Component	Period (sec)	Damping (ratio)	Period (sec)	Amplitude (g)
Lima, Jan. 31, 1951, 12°S, 78°W, M < 6	106	N.86°W.	V	0.014	6	0.1	0.03
			L	0.014	8	0.1	0.07
			T	0.004	3	0.1	0.06
Lima, Aug. 3, 1952, 12.5°S, 78°W, M 6.3	115	S.66°W.	V	0.063	9	0.2	0.01
			L	0.063	8	0.2	0.02
			T	0.004	10	0.2	0.02
Lima, Feb. 15, 1953, 12°W, 77.5°W, M 4.9	50	N.81°W.	V	0.001	8	0.1	0.01
			L	0.063	9	0.1	0.03
			T	0.063	9	0.1	0.02
Lima, Apr. 29, 1954, 13°S, 77°W, M 5.7	106	S.02°W.	V	0.065	7	0.1	0.02
			L	0.061	7	0.1	0.03
			T	0.064	8	0.1	0.02
Lima, Oct. 17, 1966, 10.9°S, 78.5°W, M 7.5	206	N.51°W.	V	0.065	7	0.1	0.13
			L	0.004	8	0.1	0.20
			T	0.004	10	0.1	0.40
Lima, May 31, 1970, 9.2°S, 75.6°W, M 7.4-7.8	370	N.33°W.	V	0.065	8	0.1	0.10
			L	0.006	11	0.1	0.12
			T	0.005	8	0.1	0.13
Ferndale, Oct. 7, 1951, 40.28°N, 124.8°W, M 8.0	60	S.58°W.	V	0.006	12	0.4	0.02
			L	0.016	9	0.2	0.09
			T	0.008	10	0.2	0.07

TABLE 2
SHAKING TABLE TEST OF AN ACCELEROMETER THAT
RECORDED THE OCTOBER 17, 1966,
EARTHQUAKE IN LIMA, PERU

Shaking Table		Measured displacement (cm X 10 ²)	Accelerometer* Computed Displacement (cm X 10 ²)	Difference (%)
Sinusoidal motion (cps)	(sec)			
10	6.10	8.78	9.40	7
11	0.001	6.40	6.50	3
12	0.007	8.00	8.30	4
13	0.078	4.37	4.80	10
14	0.071	3.00	3.20	7
15	0.068	5.53	5.92	12
19	0.053	2.50	2.72	9

* Natural period 0.004 sec; damping about 60 per cent of critical.

† Double trace amplitude divided by magnification of spindle-mirror device (400).

‡ Double trace amplitude divided by lever magnification times dynamic magnification at given frequencies (256 M).

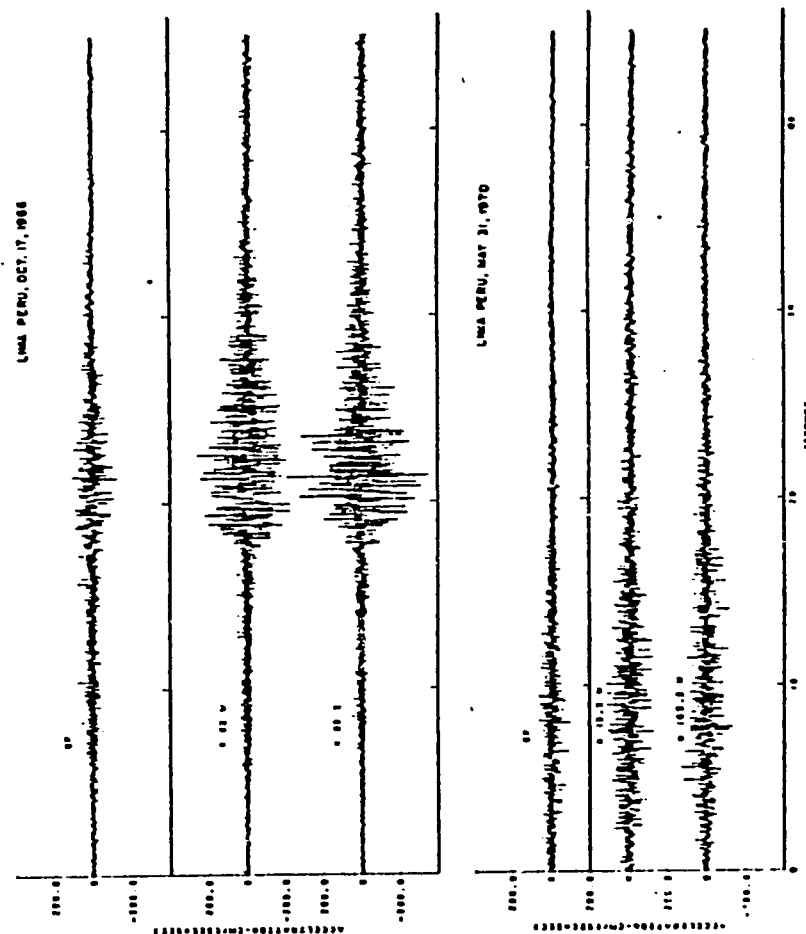


FIG. 2. Lima, Peru, accelerograms.

MAXIMUM ACCELERATIONS

Maximum accelerations recorded by accelerographs in the C&GS (now NOS) cooperative network at various distances are shown in Figure 5. In the few cases where surface faulting was observed, the accelerations are plotted at distance to the nearest point on the fault. In most cases no faulting was observed and accelerations are plotted at distance from reported epicenters. Considering epicentral distance, Lima maximum accelerations are much higher than any previously recorded. This would still be true if the few maximum accelerations plotted in Figure 5 at distance from faulting were replotted at distance from epicenter. The effect simply would be that Parkfield data would move to about 30 miles and El Centro data to about 7 miles.

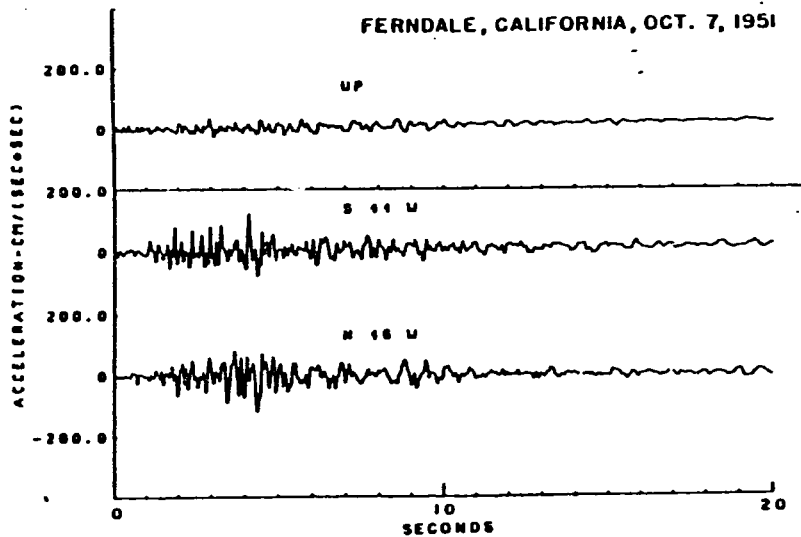


FIG. 3. Ferndale, California, accelerograms.

After the 1966 earthquake, Lee and Monge (1968) suggested that the origin of strong seismic energy might have been closer to Lima than the epicenter. The suggestion seems logical but proof is lacking.

RESPONSE SPECTRA

So far as damage to Lima is concerned, the most important earthquake recorded by the accelerograph is the one on October 17, 1966. Figure 6 shows the absolute acceleration response spectra from the accelerogram in the predominant period range. The zero damped spectra are almost the same as the Fourier spectra, except for amplitude, as would be expected from theory (Hudson, 1962). The effect of 2 per cent of critical damping, which is more than many buildings have at the start of an earthquake, is to reduce and smooth the spectra. However, even reduced, the response

of between 1,000 and 2,000 cm/sec^2 (1 and 2 g) is startling. From the response spectra, it appears that buildings with short natural periods should have suffered the most damage, and this is apparently what occurred, according to reports by Lee and Monge (1968), Lomnitz and Cabro (1968), and others.

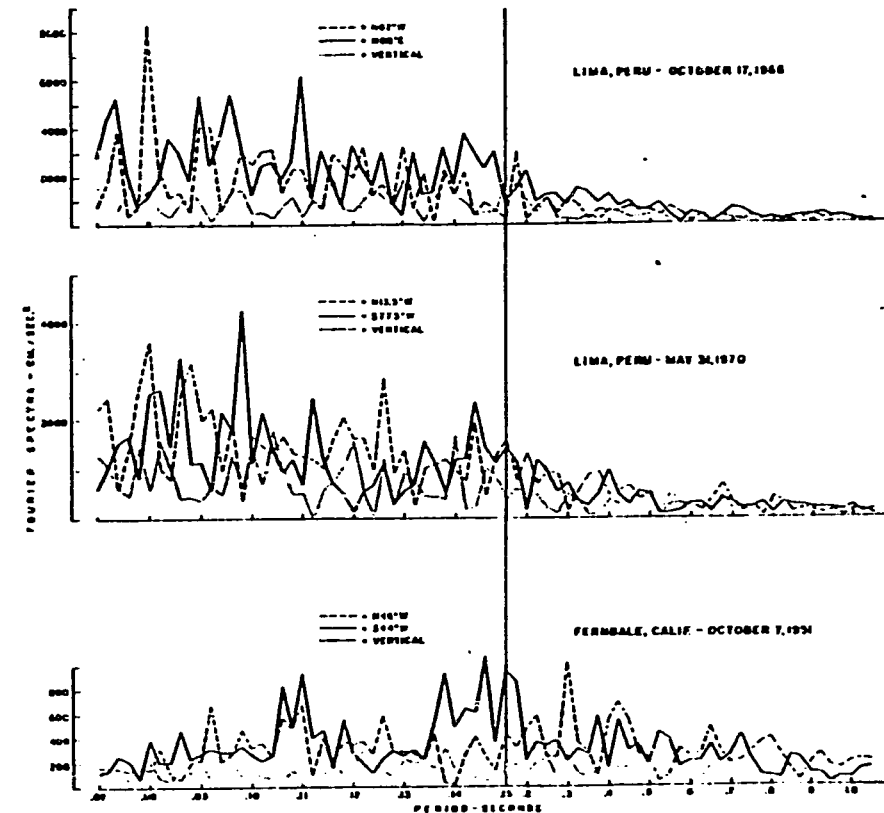


FIG. 4. Fourier acceleration amplitude spectra.

CONCLUSIONS

Accelerograms recorded at three sites in downtown Lima, Peru, on probably similar soils, are characterized by about 0.1-sec periods, regardless of distance and direction to earthquake epicenters. In addition, accelerograms from the major 1966 and 1970 earthquakes are characterized by unusually high maximum accelerations, considering epicentral distance. These characteristics make the Lima accelerograms unusual in comparison with accelerograms recorded to date in United States.

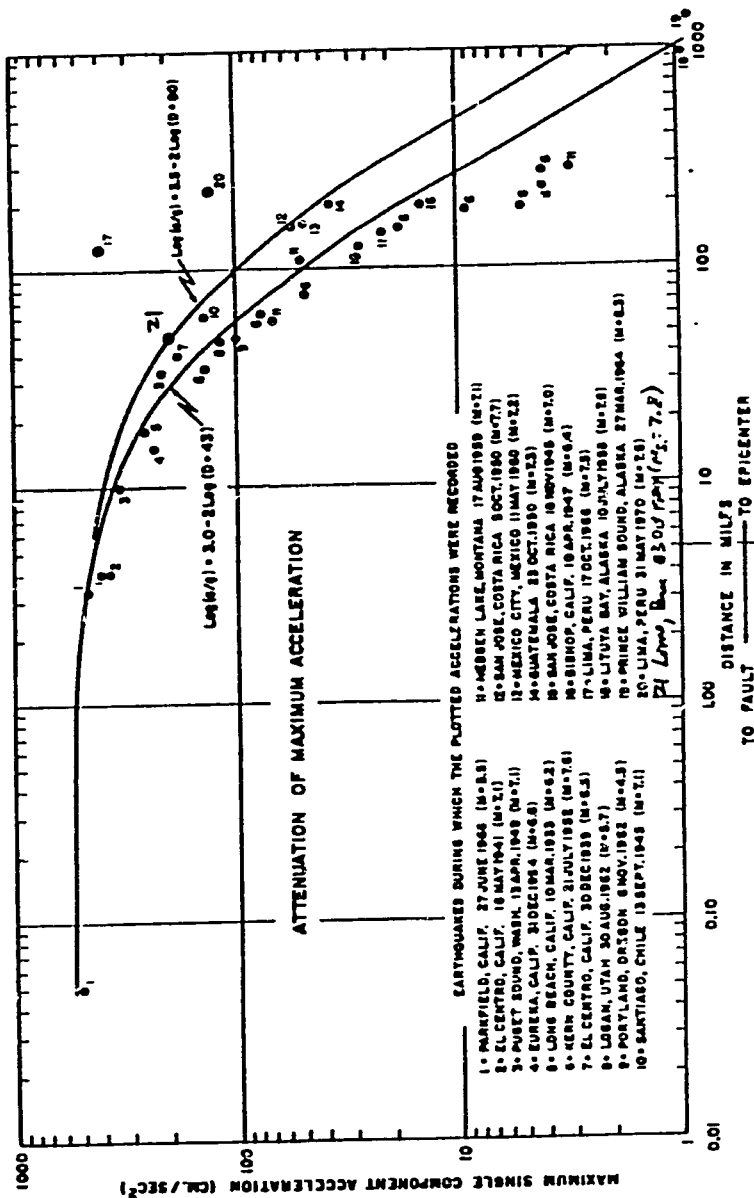


FIG. 5. Maximum accelerations recorded at various distances.

The question of whether or not the Lima accelerograms were properly recorded by the accelerograph cannot be completely answered. However, shaking-table tests of one accelerometer that was in the Lima accelerograph at the time of the 1966 earthquake make malfunction as a cause of the unusual Lima record seem very unlikely.

Perhaps during the 1966 and 1970 shocks the origin of strong seismic energy might have been closer to Lima than the epicenters. This would make the Lima accelerograms appear less unusual. However, it seems unlikely that the origin of seismic energy would be close to Lima during all of the recorded earthquakes.

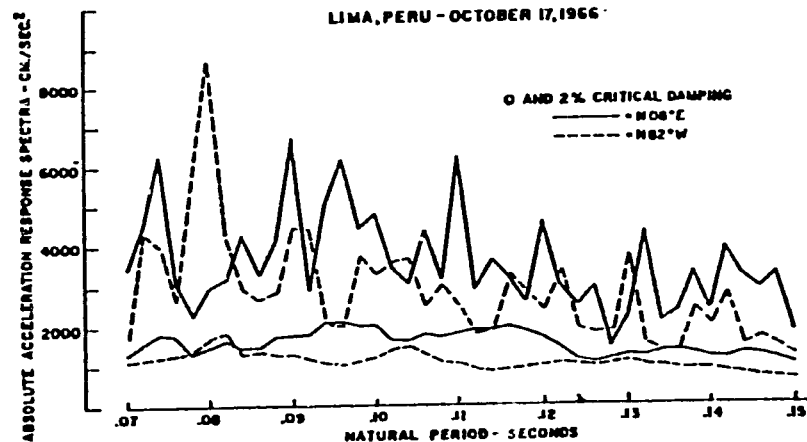


FIG. 6. Absolute acceleration response spectra.

Whatever the cause of the unusual accelerograms may be, the answer is important enough to warrant a stepped-up program in geophysical and geological research and the establishment of a strong-motion accelerograph network in Peru.

ACKNOWLEDGMENTS

The help of the California Institute of Technology and of Richard P. Maley in digitalization of accelerograms used for analysis is gratefully acknowledged.

REFERENCES

Hudson, D. E. (1962). Some problems in the application of spectrum techniques to strong-motion earthquake analysis, *Bull. Seism. Soc. Am.* 52, 417-430.
 Jenachke, V., R. W. Clough, and J. Pensen. (1961). *Analysis of earth motion accelerograms*, Institute of Engineering Research, University of California, Berkeley.
 Lee, Kenneth L. and Joaquin Monge (1968). Effect of soil conditions on damage in the Peru earthquake of October 17, 1966, *Bull. Seism. Soc. Am.* 58, 937-962.
 Lomnitz, Cinnia and Ramon Cabre, B. J. (1968). The Peru earthquake of October 17, 1966, *Bull. Seism. Soc. Am.* 58, 645-661.

SEISMOLOGICAL FIELD SURVEY
 NATIONAL OCEAN SURVEY
 NATIONAL OCEANIC AND ATMOSPHERIC ADMINISTRATION

Manuscript received February 20, 1971.

Mechanism and Spatial Distribution of Chilean Earthquakes with Relation to Subduction of the Oceanic Plate

WILLIAM STAUDER

Saint Louis University, St. Louis, Missouri 63103

The focal mechanisms for 61 earthquakes occurring in northern and central Chile during the years 1962-1970 indicate underthrusting of the oceanic plate for earthquakes with focal depth 30-60 km. The axis of tension for intermediate-depth earthquakes is parallel to the direction of dip of the plate. For deep-focus earthquakes the axis of compression is parallel to the axis of the plate. Together with the seismicity of the region, the focal mechanisms indicate that subduction of the oceanic plate under this part of the coast of South America takes place in discrete and localized episodes and that the lithospheric slab itself is broken into a series of tongues that are absorbed independently and quite differently from one latitude zone to the next or even at one depth as opposed to another. Near the Chile-Peru border, 18°S-25°S, the more principal present day activity is at intermediate focal depths. The motion of the plate is in the azimuth N85°E at shallow depths, veering to N65°E at intermediate depths. The zone 25°S-27°S is at present a silent zone at intermediate depths. The zone 27°S-34°S corresponds to underthrust of the oceanic plate but such that at depths of about 120 km this segment of the plate moves horizontally under the continent. The deep-focus zone, 19°S-23°S, overlaps the three zones just mentioned and is discontinuous with them. It more probably corresponds to an independent and earlier epoch of plate absorption. Under central Chile the plate motion appears to correspond to a current episode of subduction of relatively recent initiation. The motion is in the azimuth N80°E.

An important aspect of the hypothesis of plate tectonics, one about which seismology has had more to say than other disciplines, is the sink mechanism for absorbing crustal plates as these move outward from the mid-ocean ridges and encounter continents or island arcs [Isacks *et al.*, 1968; Isacks and Molnar, 1971]. The Fiji-Tonga-Kermadec arc has been studied extensively in this regard [e.g., Sykes, 1966; Oliver and Isacks, 1967; Isacks *et al.*, 1969; Barazangi and Isacks, 1971]. Similar studies illustrate the subduction of the oceanic plate in the New Guinea-Solomon Islands region [Johnson and Molnar, 1972], the Indonesia-Philippine region [Fitch and Molnar, 1970], the western Pacific [Katsumata and Sykes, 1969], Japan [Fitch and Scholz, 1971], the Kurile-Kamchatka arc [Sykes, 1966; Stauder, 1971], the Aleutians [McKenzie and Parker, 1967; Stauder, 1968a, b], and Middle America [Molnar and Sykes, 1969].

The present paper is a study of the subduction of a part of the Nazca plate under the coast of northern and central Chile as evidenced

by the general seismicity of the region and by focal mechanism solutions of the larger earthquakes occurring there in the interval 1962-1970. Some of the results presented here parallel and supplement studies reported earlier by Isacks [1970].

EARTHQUAKES SELECTED FOR STUDY

The region selected for study is the straight part of the west coast of South America, from the Chile-Peru boundary to the intersection of the Chile ridge with the Chilean coast. The dimensions of the region, and the relation of its seismicity to that of the eastern Pacific, are indicated in Figure 1. A break in the seismicity and a change in the character of the earthquake motion allow the region to be divided, in turn, into two subregions: northern Chile, 18°S-34°S, and central Chile, 34°S-46°S.

The northern region includes the deep part of the South American trench and a well-developed Benioff zone of shallow-, intermediate-, and deep-focus earthquakes. In this region, 47 earthquakes were selected for study: 25 earthquakes of normal focal depth, 14 intermediate, and 8 deep-focus earthquakes. This set con-

Earthquake prediction

Variations in physical properties such as electrical conductivity and elevation of benchmarks may fortell not just the place but also the time and magnitude of an earthquake.

Carl Kisslinger

Earthquake prediction entails the specification of the time, place and magnitude of an individual future event. All three of these parameters are poorly known and complicated functions of the relative motions of parts of the Earth's crust and mantle, the rate of strain accumulation in rocks and the strength of those rocks. Even if the processes by which the energy is accumulated and released were completely understood, the imprecise knowledge of the initial conditions, boundary conditions and relevant material properties would make the prediction of a particular seismic event very difficult.

Nevertheless, earthquake prediction has been a research goal of some seismologists and other geophysicists for about a decade. One approach is to base predictions on studies of the seismicity gaps and recurrence rates in a particular region. But the main thrust is the search for precursors, that is, phenomena that occur in a characteristic way prior to an earthquake. Most of the research to date has been empirical. Recently, however, a physical model of processes preceding a seismic event has been successful in explaining and unifying a number of independent observations. Although this theory, known as "dilatancy," is still being tested, it offers hope that at

least some earthquakes in some geological settings are predictable on the basis of easily observable phenomena.

A starting point in earthquake prediction is the determination of areas in which earthquakes are most likely to occur. Earthquakes are not located randomly over the earth but occur in distinct active belts, as illustrated by figure 1. This map displays the epicenters of 42 000 earthquakes that were located by the National Earthquake Information Service between 1961 and 1969. This figure outlines the main features of global seismicity but represents too short a time span to yield required parameters. With a more adequate data base, however, estimates can be made regarding the expected activity levels, recurrence rates, maximal expected magnitudes and maximal effects on the works of Man. This procedure is called by various names—"seismic probability estimation," "seismic risk mapping," "seismic regionalization" or "seismic zoning."

Reliable seismic probability estimation, coupled with sound engineering and construction of earthquake-resistant structures, is the primary means of reducing damage and minimizing loss of lives during an earthquake. But seismic probability estimation is not to be confused with earthquake prediction, as the term is commonly understood. A properly used, reliable earthquake-prediction system could reduce injuries and deaths substantially below the levels that would occur even with the best earthquake engineering. However, even if earthquake prediction is completely successful, it is not

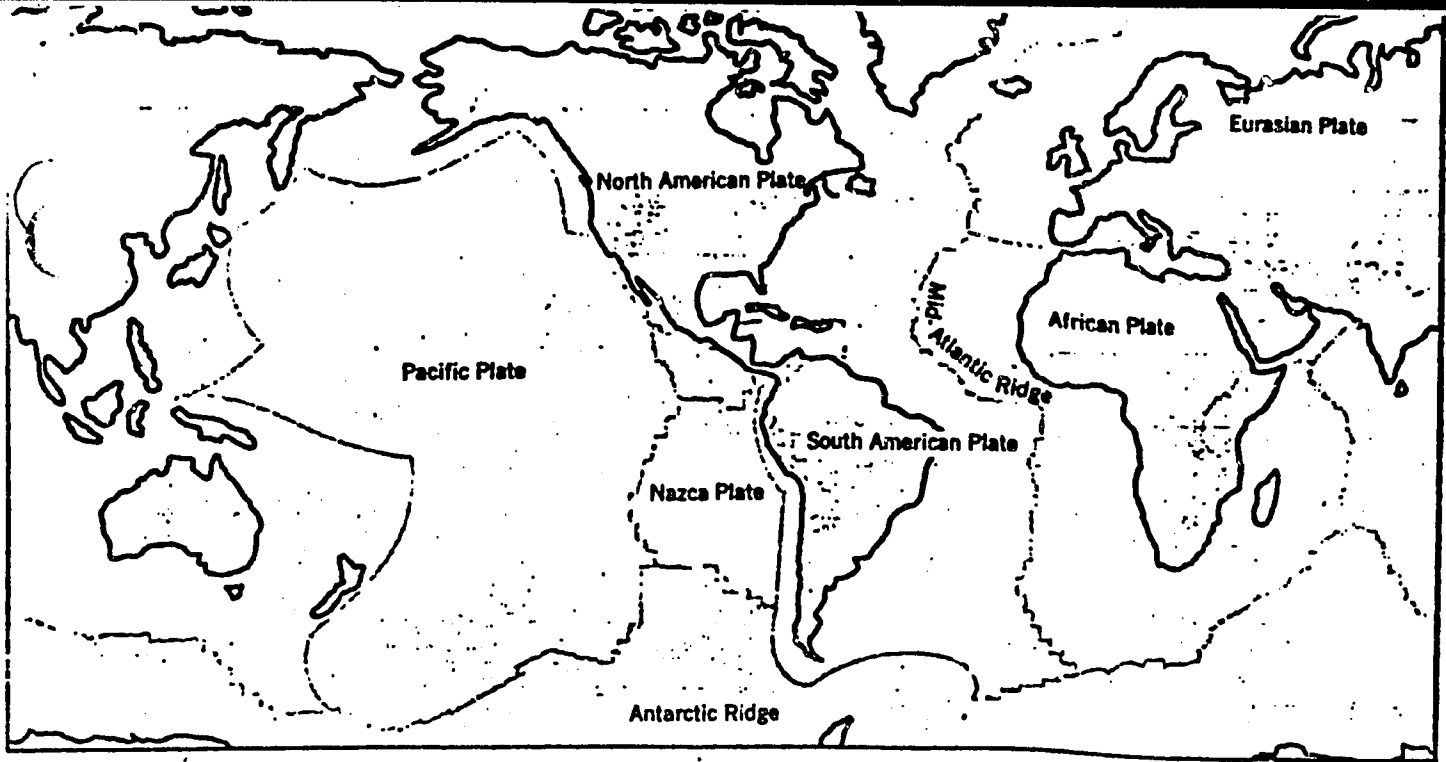
in any sense a substitute for long-range planning and adequate engineering.

Predictions from seismicity gaps

A careful examination of the seismicity distribution in figure 1 reveals that, although the epicenters tend to define long, continuous belts of activity, there were in fact portions of these active belts within which few earthquakes occurred during the nine years. At one time such seismic gaps were interpreted as being especially safe places relative to the surrounding regions. But now, as a result of the development of the plate-tectonics model and the consequent improved understanding of the ultimate causes of earthquakes, at least some of these places are viewed as likely sites for future big events.

The nature of seismicity gaps is illustrated by the data for the northwestern border of the Pacific basin, shown in figure 2. The occurrences of the great earthquakes in Kamchatka (November 1952), Andreanof Islands (March 1957), Kuril Islands (October 1963), Prince William Sound, Alaska (March 1964), and Rat Islands (February 1965) can all be seen as horizontal clusters of points. The data in figure 2 illustrate dramatically that the aftershock sequences of the great earthquakes are sharply bounded in longitude, defining distinct tectonic blocks with almost no overlap of activity in adjacent blocks. Furthermore, in each case the activity within the zone of a major event was relatively low beforehand. On this basis, one would speculate that the Alaskan peninsula (155°

Carl Kisslinger is professor of geophysics in the department of geological sciences, and director of the Cooperative Institute for Research in Environmental Sciences, at the University of Colorado, Boulder.



Earthquake belts and tectonic plates. The epicenters of some 42 000 earthquakes from 1961 to 1969 are concentrated in three main belts—the circum-Pacific, the Alpid (from the Azores to

Southeast Asia) and one along the undersea ridges. The colored lines on this map are the tectonic-plate boundaries. Note the occasional gaps in otherwise continuous earthquake belts. Figure 1

W to 165° W) and the Commander Islands (165° E to 170° E) are likely sites for large events in the future.

The concept of the seismicity gap as a predictive device was developed by a group at Lamont-Doherty Geological Observatory, Columbia University and by a group working in the Soviet Far East.^{1,2,3} The Lamont group has defined criteria for delineating zones of "special seismic potential." Their primary criteria are that the segment must be part of a major shallow seismic belt characterized predominantly by strike slip or thrust faulting and that the segment has not ruptured for at least 30 years. Their supplementary criteria, used to select the especially interesting zones from among the many that satisfy the primary criteria, are based on the seismic history of the region. Seismicity gaps have been used by S. A. Fedotov to provide a basis for successfully predicting the location of some major earthquakes near Kamchatka. Kunihiro Shimazaki⁴ has shown that the site of the great Kanto earthquake of 1923 has been very quiet since 1926, as seen from figure 3, and postulates that strain may be accumulating there for another big event. The seismic gap concept has also been applied on a more localized scale to microearthquake distributions in an attempt to identify portions of a particular fault system likely to slip soon.

Predictions from recurrence rates

The identification of a gap does not in itself give an indication of the time at which the event is to be expected.

Two approaches to the problem of projecting the approximate time have been suggested. The first, and more speculative, is based on the proposition that major earthquakes may migrate along the great seismic belts of the world.^{2,5} If great earthquakes do occur in a spatial sequence, a basis for identifying the next gap to be activated is available, even though the time of its activation remains uncertain.

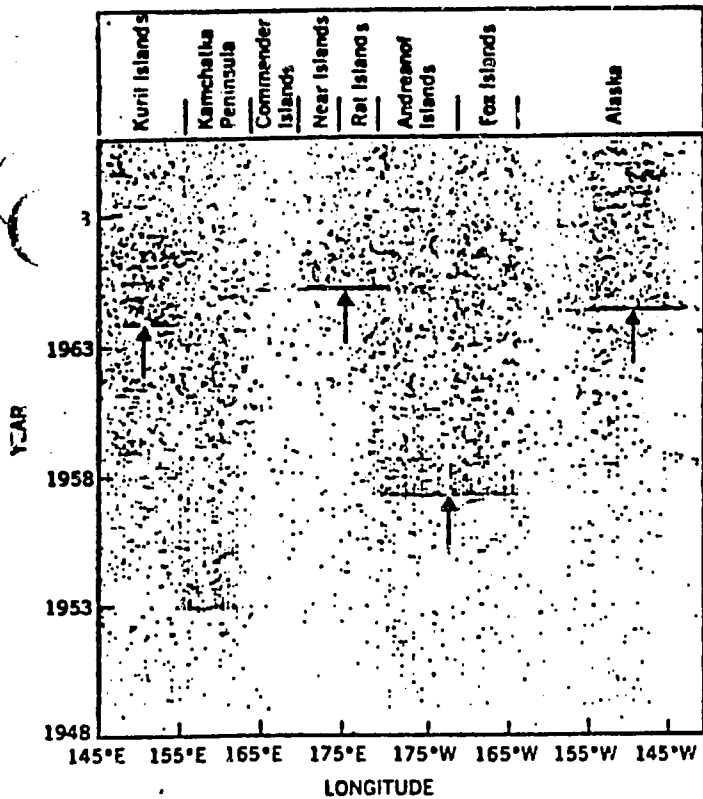
The second approach to fixing the time is to estimate earthquake recurrence rates, either from a statistical analysis of past activity or more deterministically from strain rates based on plate-tectonics theory. Many investigators have found that if the logarithm of the number of earthquakes, N , exceeding a given magnitude, M , is plotted against the magnitude, the data fall close to a linear trend, down to the smallest magnitude for which the data set is complete (a function of network sensitivity). This linear relation between $\log N$ and M is found on spatial scales ranging from global to very local. The slope of the line, called the "b-value," is always of the order of -1 , ranging from about -0.5 to -1.5 , implying that about ten times as many events exceeding magnitude M occur as for magnitude $M + 1$. The b value in a given region may not be stationary, but may vary with time in a way that is itself indicative of an impending large earthquake. If the recurrence data are normalized to unit time, an expected return time for an earthquake of a given magnitude may be estimated for the area covered.

The plate-tectonics model provides a

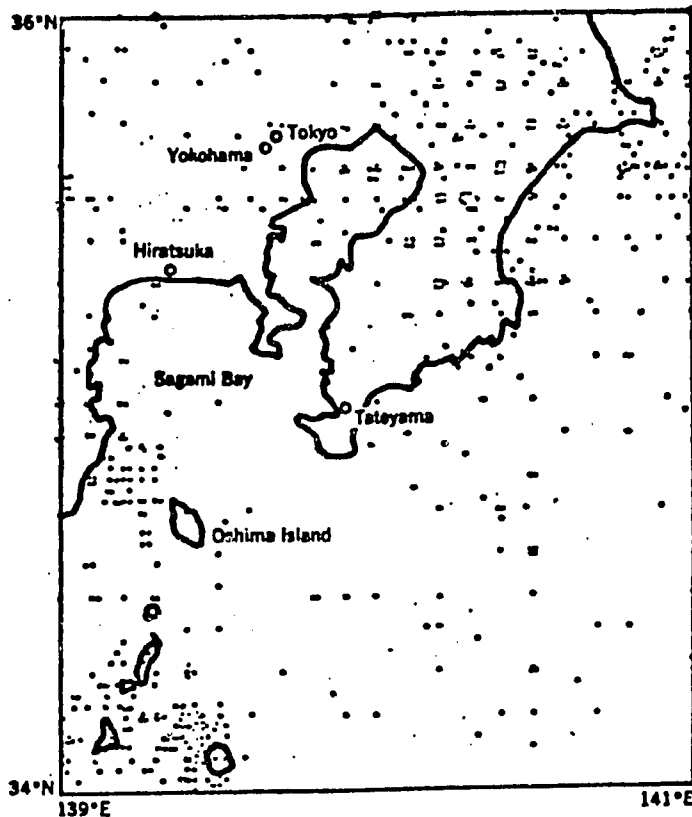
basis for estimating the rate of strain accumulation at plate boundaries, although major uncertainties arise as to the current rates of relative plate motions and the amount of the relative motion at a boundary that is taken up by seismic slip and the amount by aseismic creep. Tsuneji Rikitake⁶ has estimated both the critical value of strain at which great Japanese earthquakes occur and the rates at which strain is accumulating in some selected active zones. On the assumption that the last great earthquake reduced the strain energy in the rocks in the source volume to zero, he then estimates, for example, that the probability of a magnitude-8 earthquake in Sagami Bay, the site of the great 1923 event, before 1980 is only 0.2 and will not reach 0.5 until 2080.

The plot of $\log N$ against M provides valuable information about the level of activity and the return interval of earthquakes but does not tell what is the largest magnitude earthquake ever to be expected at the place. The assumption that no event in the future will be significantly more energetic than any in the past has proved to be a dangerous one. Yuri V. Ryznichenko and his coworkers⁷ have been seeking to establish a correlation between the level of activity in a region, as given by the normalized value of $\log N$ at a selected magnitude, and the maximal magnitude to be expected. The success of their technique, as applied to several active regions of the USSR, cannot be established until further data on large events are available.

Because of the uncertainties intro-



Space-time plot of earthquakes in northwest basin of the Pacific shows major events and aftershocks (arrows) preceded by gaps in seismic activity. The greater number of points in recent years reflects the improved density and quality of recording instruments. (Unpublished data from E. R. Engdahl.) Figure 2



Inactive area in Sagami Bay, Japan, may be the site of the region's next major earthquake. The points are epicenters in the south Kanto region of Japan during 1926-67. This bay was the location of a great earthquake in 1923 and of others as far back as 818 AD. (From K. Shimazaki, reference 4.) Figure 3

... by depending entirely on past experience, Igor E. Gubin⁸ suggests that a combination of geological and seismological data be used to judge the maximal possible earthquake. Careful geological mapping can determine the position and lengths of the faults in the region as well as the dimensions of geological structures that should be considered as single mechanical units. Seismological data can indicate the maximum depth at which slip occurs in the region. These data then enable one to estimate the largest mass of rock that can be expected to move in an earthquake, even though the entire unit has not moved within the historical record. Unfortunately there are few places in the world at which the mapping has been detailed enough to permit the application of this approach.

Premonitory phenomena

Earthquake prediction requires the discovery of localized anomalous behavior of one or more observable quantities that characteristically occurs prior to, and only prior to, an event to be predicted. In the best case, the size of the anomaly and/or the duration of anomalous behavior will scale in the same way with the magnitude of the impending earthquake and the length of the future time to its occurrence. To date, the search for such precursors

has been the primary objective of most prediction research. Several have been identified and they provide the basis for optimism that at least some large earthquakes are predictable.

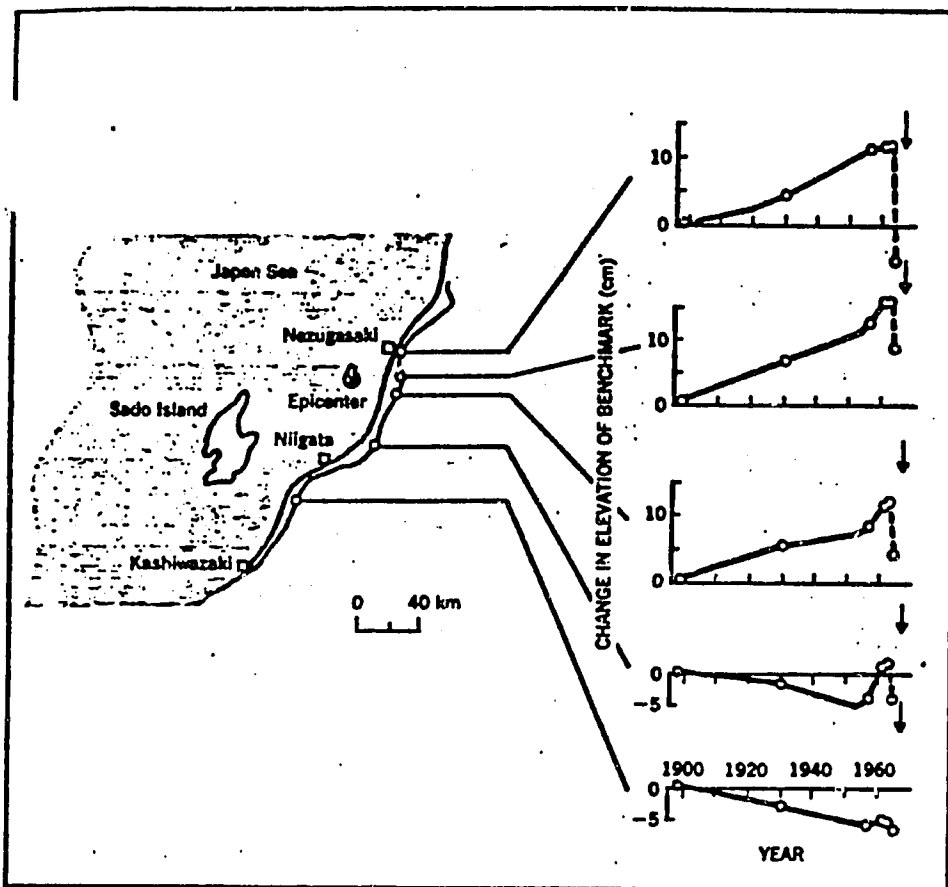
The search for earthquake precursors has been generally guided by the conceptual model of earthquake occurrence known as the "elastic rebound" theory. This theory, first proposed by H. Fielding Reid,⁹ states that the energy that is released at the time of an earthquake was present just before the event in the form of elastic-strain energy in the rocks forming the source volume and that the energy is released by slip on a fault when the shear stresses exceed the strength of the medium. The strain energy has been slowly accumulated as a result of deformations of the rocks, a process that we now hold is caused by the relative motions of lithospheric plates. Accordingly, to predict an earthquake we need to know that strain has accumulated to the point that the system of rocks is approaching failure by sudden slip.

Evidence that a volume of rock is in a highly strained state can come from two types of observations. In the more direct type, one looks for changes in the relative positions of points on the Earth's surface, either from geodetic measurements or from point measurements of strain and tilt. The second

technique is the determination of strain-dependent physical properties of the rocks *in situ*, either by direct measurement or by observation of local values of force fields that depend on these properties. Examples of some properties that have been explored are elastic-wave velocities, electrical conductivities and magnetic properties. Other observable parameters that have been interpreted as evidence of accumulating strain are temporal changes in the *b*-values, temporal changes in microearthquake counts and temporal changes in the concentration of a geochemical tracer, such as radon gas, in well water.

Changes in geodetic measurements

The observation of changes in the elevation of benchmarks was suggested as a premonitory device by the striking changes that occurred in such measurements near the city of Niigata, Japan, prior to an earthquake of magnitude 7.5 on 16 June 1964. Figure 4 displays the elevations observed over the period from 1898 to 1964;¹⁰ frequent releveling was undertaken after 1954 because of concern over land subsidence. The data show a rapid rise during 1955-59. As a result, one of the principal elements in the Japanese prediction strategy is detection of an area in which anomalous changes in elevation are taking place. They have



Data from leveling at four locations near Niigata, Japan, show a dramatic rise in elevation of benchmarks prior to 1964 earthquake (arrows). (From I. Tsubokawa, ref. 10.) Figure 4

established 20 000 km of first-order leveling routes which are to be resurveyed every five years and more frequently around Tokyo and other selected areas.¹¹

The following correlation between the size of the region of anomalous elevation change and the magnitude of the impending earthquake has been suggested:

$$M = 1.96 \log r + 4.45$$

where r is the radius of the region in kilometers. Thus, once an area of anomalous elevation change has been detected, the site and approximate magnitude of the future earthquake can be estimated.

Changes in the distances between points on the surface, as determined by trilateration measurements, should also reveal changes in the strain regime in a region. This technique was used to monitor strain accumulation during the great Matushiro earthquake swarm of 1965-67.¹² Systematic measurements along lines crossing the San Andreas fault in California since 1959 reveal changes in line length generally concordant with right-lateral movement along the fault, with some sections showing other types of behavior.¹³ No anomalous variations related to individual earthquakes have been detected, either prior to an event or accompanying it.

Numerous investigators have used strain meters and tilt meters in an effort to detect strain accumulation by measurements at discrete points. Both secular strain rates and tilts have been monitored and episodes of rapid change prior to earthquakes have been sought, with some reports of success.¹⁴ Although promising in principle, measurements of this kind are subject to at least two major difficulties. One is a large annual variation caused by thermal strains whose elimination requires extraordinary stability of the strain meter. This stability has apparently been achieved in recent years through the use of laser interferometry and by a new design based on the detection of volumetric strain changes. The second and more fundamental problem is the determination of the relation of near-surface strains and tilts to the processes at depth where the earthquakes originate. Surface measurements in or near an active fault zone may be modified by creep, tilt or deformation of blocks that are not mechanically an integral part of the materials that make up the source volume.

Changes in physical properties

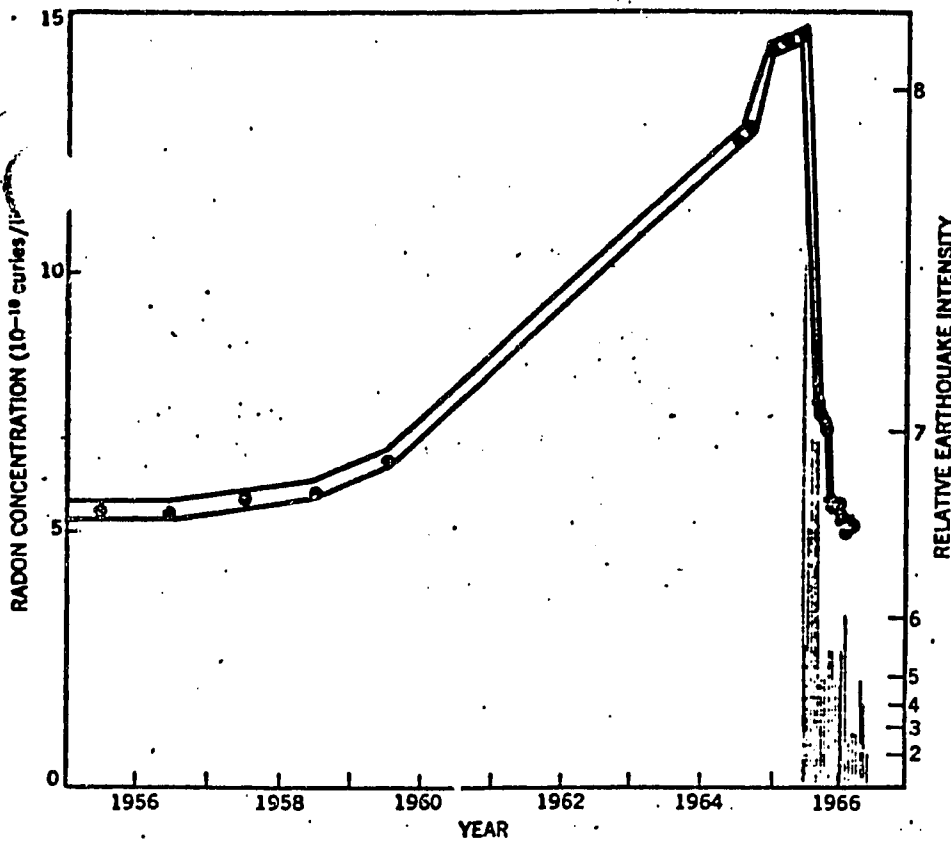
An early discovery of an earthquake precursor was V. I. Ulomov's recognition of the increase in the radon concentration in the mineral water of the

Tashkent Basin prior to the destructive earthquake of 1966.¹⁵ The chemistry of these waters, valued for their medicinal properties, had been monitored since 1956. As shown in figure 5, the radon content in mid-1965 was almost double the initial values, rose rapidly until October, 1965, and then stabilized until 26 April 1966, the date of the earthquake. The concentration fell sharply after the earthquake, but its behavior during the strongest aftershocks is unknown because of the lack of observations during three months after the main shock. Once frequent measurements were resumed, in the latter part of 1966, they revealed several clear cases of increase of radon prior to stronger aftershocks.

The radon is important only as a tracer, and not because it is thought to play any role in the tectonic process. Its short half-life, $3\frac{1}{2}$ days, makes it very suitable for the purpose of tracking current processes. The shape of the curve bears a general similarity to those in figure 3, showing the elevation changes near Niigata.

Another possible precursor is the variation of the parameters on a log $N-M$ plot. Both the slope and the intercept at a selected magnitude of the curve are characteristic of the seismicity of a region but detailed investigations show that they are not stationary in time and their variations may indicate an impending event. Shigeji Suyehiro¹⁶ first suggested that the b values during the period of foreshocks of a major event are abnormally low, as low as -0.35 to -0.5 , compared to normal values of -0.8 to -1.2 determined for background activity and aftershocks of the main event. Because the number of clearly identifiable foreshocks is usually small, the parameters describing these groups of earthquakes are not as reliable as for more general sequences. Recent studies¹⁷ give further support to the diagnostic value of this parameter when the data are treated carefully. Max Wyss and William H. K. Lee have found for four groups of California earthquakes that the b value is lower than the background value during an extended period before and after the main event, but drops very rapidly during the short interval of true foreshocks. Thus, Suyehiro's observations that the b value for aftershocks is higher than for foreshocks are not incompatible with these recent results.

A low b value implies a relatively small number of low-magnitude earthquakes. If one measures the activity level in a region by the number of earthquakes of a given magnitude, and chooses a fairly low magnitude, say 4.0 or smaller, in order to ensure a sufficiently large number of events, he will then note a drop in his index of activi-



Radon concentration in well water increased prior to earthquakes (colored vertical lines) of 1966 in the Tashkent Basin, USSR. On the relative-intensity scale, "8" corresponds to serious damage, "6" to minor damage. (From V. I. Ulomov, ref. 15.) Figure 5

ring the time prior to a major event. Considerable speculation exists, based in part on laboratory observations of rock failure, that the number of small events should decrease during the time of preparation for rupture and then increase markedly just prior to a major event. Furthermore, these small vents should tend to concentrate near the fault surface on which the major rupture will occur. Counting small events may be one means of sharpening the prediction of the occurrence time as it draws near.

Seismic wave velocities

The elastic constants, and therefore the elastic wave velocities, of solids have long been known to be stress dependent. Much research has been devoted to the stress dependence within the regime of elastic deformation of the materials, in which the velocity generally increases with increasing confining pressure and velocity anisotropy results from the effects of a deviatoric stress. More significant for prediction are the few observations of the behavior under loads sufficient to cause failure.¹⁸

Matsushima subjected samples of granite to successively greater axial compressive loads up to the value to cause rupture, at confining pressures up to about 4 kilobars. He measured the compressional wave velocity in the direction of the applied axial load and transverse to that direction. At small-

er loads the velocity in both directions increases as the pore spaces and fractures in the sample close, an effect that disappears at high confining pressures.

At confining pressures above about 1 kbar, the velocity in the direction of the load remains almost constant, or at most show a small decrease (less than 3%) all the way to failure. On the other hand, the velocity normal to the axis of maximal compression begins to drop dramatically at a load roughly half that required to produce rupture. At rupture the velocity has dropped approximately 38% for a confining pressure of 400 bars or 20% at a confining pressure of 3.5 kbars. These confining pressures correspond roughly to depths within the earth of 1 and 10 km, respectively.

Indra Gupta extended these earlier observations in two ways. First he confined the sample only along one axis normal to the applied compressive load, thereby defining axes of maximal, minimal and intermediate compression. Second, he measured both the compressional and shear wave velocities along all three axes for all values of the applied load. He found that as the system approached failure both velocities decreased along all three directions, but by significantly different amounts. Expressed in terms of the ratio of compressional-to-shear wave velocities, V_p/V_s , the ratio hardly

changed in the direction of maximal compression, dropped about 2% in the direction of the intermediate stress and about 12% in the direction of minimal compressive stress. Because of the anisotropy of the effect, its detectability is sensitive to the geometry of the stress system and the position of the source volume relative to the observing network; thus, the effect will be more easily observed for some types of faulting than for others.

Much of the current optimism that a successful scheme of prediction is ultimately achievable stems from the discovery that systematic temporal variations in the ratio of the two seismic wave velocities do occur within the vicinity of an impending earthquake. The discovery was first reported for small-to-moderate earthquakes in the Garm district of the Soviet Union and has since been confirmed for small earthquakes in northern New York state and for relatively shallow, moderate earthquakes in the central Aleutian Islands.¹⁹ James H. Whitcomb and his colleagues²⁰ found that the destructive San Fernando earthquake of February 1971 was preceded by a well defined anomaly in V_p/V_s and could have been predicted on this basis.

The nature of the anomaly is illustrated by A. N. Semyenov's original data from the Garm district, part of which is reproduced in figure 6. From seismograms of small earthquakes in the selected source region, a value of the ratio V_p/V_s is determined for each event.²¹ A normal value of the ratio, usually around 1.75, is measured during time intervals in which the processes leading to a strong event are not active. Before an earthquake, the ratio drops to a minimum and then returns to its normal value, with perhaps a small overshoot, just about the time that the large event occurs.

Duration of the anomaly

The magnitude of the predicted event appears to be independent of the size of the anomaly but does correlate with its duration: approximately 30 days for a magnitude-4 event, 90 days for magnitude 5.5, 3½ years for the 6.5 San Francisco event and about 10 years for magnitude 7.5. The data reported all appear to fit a linear trend on a plot of the logarithm of time, in days, against magnitude, with a slope of about 0.7. No data are available yet to support an extrapolation to magnitude 8 or greater.

Whitcomb²⁰ found that this effect was caused by changes in the compressional-wave velocity, V_p , as one would expect from the laboratory studies, rather than the shear-wave velocity. Wyss and David Holcomb have developed a technique for monitoring changes in the compressional-wave ve-

locity under seismograph stations in seismically active areas from routinely reported earthquake observations.²² No special regional instrument networks or observations of local activity are required; the data for predicting major events that will occur in the next few years may already be in the files.

Most likely, even with measurements closely spaced in time, the onset of the anomaly would not be recognized until it was well developed. The time at which the values begin to return to normal is the earliest time at which an estimate of the time of occurrence and the magnitude can be made. The anomalies are not symmetric about the minimum; thus, predictions of the time of occurrence must be revised as the return to normal approaches.

The determination of the width of the time window during which the event is to be expected after the anomaly ends is a critical unsolved problem. The present limited data suggest that this uncertainty is of the order of 10% of the total anomaly duration. This has important implications for large, potentially disastrous events, for which the forecast time will be of the order of years. Whether or not government authorities can respond to the forecast in a meaningful way to reduce losses will depend strongly on both the reliability of the forecast and the duration of the period of the alert.

A final set of properties that are sensitive to stress are the electrical and magnetic properties of crustal rocks. Field studies to seek temporal variations in either the electrical conductivity or the local geomagnetic field give results that offer promise but are not definitive. The conductivity of crustal rocks is largely governed by the porosity of the rock, the degree of saturation with fluids and the electrolytic properties of those fluids. If the period of preparation for a large earthquake is marked by microfracturing of the mass of rock in the source volume, changes in conductivity will result, depending on the availability of fluids to fill newly created crack porosity. The work in the Garm district suggests that the larger events occur at times of minimal resistivity, or maximal saturation of pore spaces with fluid. This result is in general agreement with laboratory findings. However, the laboratory studies show that a very strong effect, with decreases of resistivity by an order of magnitude, occurs in low-porosity rocks that are stressed to failure, but that the effect is much smaller if the load is reapplied to cause slip again along an existing fracture surface. Thus, the proper field observations should be made with electrodes on one side of the active fault surface rather than with an array that crosses the

fault in order to observe changes in the highly stressed but unbroken material near the fault. Additional research concerns a piezomagnetic effect, in which the susceptibility varies with stress, and a possible correlation of stress changes with geomagnetic field.

Physical basis of prediction

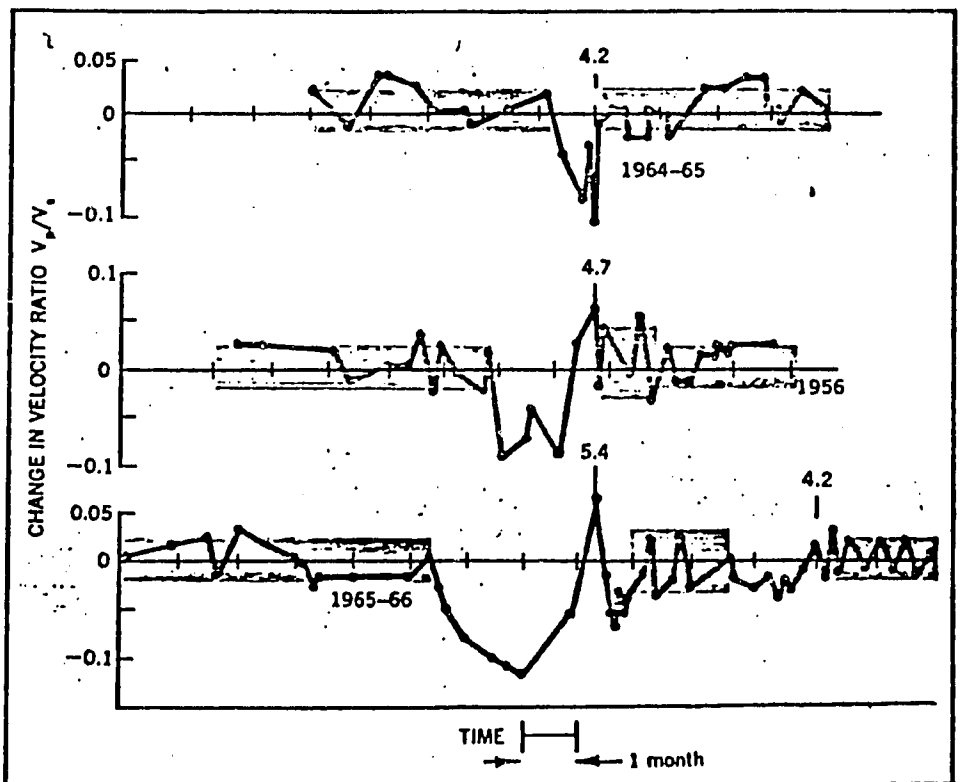
Although the original search for earthquake precursors was almost entirely empirical, the discovery of a number of promising promonitory phenomena has led to the formulation of working hypotheses concerning the underlying physics. Each data set in figures 4-6 suggests that the preparation of a region for a large earthquake occurs in a number of distinct stages. From the *re* data, Ulomov postulated a four-stage process. In the first stage, a prolonged, slowly increasing elastic-plastic deformation is accompanied by the compression of large volumes of rock, through the closing of pore spaces and the deformation of soft inclusions. The second stage is marked by rapid elastic deformation; the volume decreases further and the deformation of mineral grains occurs. His third stage is one of plastic deformation with almost no volume change; the material is under large stress and this stage culminates in the earthquake. The final stage is an interval of strain relaxation, during which the aftershocks characteristic of major crustal events occur.

Laboratory studies of rock fracture

reveal that this model fails to take into account the phenomenon of dilatancy, which has been discovered to play an essential role in rock failure. First discovered experimentally by Osborne Reynolds²³ in 1886 and investigated in detail by William Brace²⁴ and his co-workers, dilatancy is an inelastic volume increase caused by the formation of microcracks oriented parallel to the axis of maximal compression and opening up in the direction of least compression. The axial load at which dilatancy begins depends on the confining pressure and the material, but it is somewhat in excess of 50% of the load to produce failure. Most of the evidence that dilatancy occurs has been developed in the laboratory, but Brace has interpreted certain ore bodies as the result of deposition from solutions that filled cracks opened by dilatancy.

Amos Nur²⁵ suggested that the behavior of the seismic wave velocities prior to earthquakes can be explained on the basis of dilatancy in low-porosity rocks that are initially saturated with water. As new cracks and additional porosity develop during dilatancy, the rock becomes less than totally saturated. Because the compressional-wave velocity is more sensitive than the shear velocity to the degree of saturation, the ratio V_p/V_s will drop.

Two mechanisms have been suggested to explain the return of the ratio to normal and the occurrence of failure at about the time this recovery is complete. Nur suggests that ground water



Large earthquakes in the Garm district, USSR, were preceded by drops in the ratio of compressional- to shear-wave velocity. Significant changes are those outside the region (shaded) bounded by one standard deviation. The duration of anomalous values scales with the magnitude of the event (numbers above arrows). Figure 6

from the surrounding region will slowly percolate into the newly formed cracks, with a consequent return of the compressional wave velocity to its original value. Because the resistance of a fault to slip depends strongly on the pressure of the fluids in the pores, especially when that pressure is near the confining pressure, the resaturation of the medium will weaken it and result in an earthquake about the time of the return to the fully saturated state.

In an alternative model developed by Brian Brady, the interval of widespread dilatancy throughout the volume of rock is followed by a period of very strong dilatancy in the immediate neighborhood of the incipient fracture. The nascent source zone acts as an inhomogeneity in the medium, with corresponding strong stress concentrations around it and a reorientation of the principal stress axes in the immediate neighborhood. The substantial volume increase in the neighborhood of the fault surface is accommodated by a closing of the cracks in the region into which the fracture will extend next, causing the velocities in this zone to return to their predilatancy values. Once again, failure is expected at about the time of the return to normal, although the details are not worked out quantitatively. Brady's model in no way rules out the presence of water as a lubricative agent but it does not depend

An encouraging aspect of either model is that the false-alarm rate should be very low, if not zero. That is, it appears that a mass of rock cannot go through the entire sequence of behavior without failing in the end. It is not known whether the converse is true, that is, whether every earthquake must be preceded by this sequence of events; limited evidence indicates that earthquakes on the critically important San Andreas fault are not preceded by detectable dilatancy.²⁶

Chris Scholz and his colleagues²⁷ have pointed out that the dilatancy-migrating fluids model can explain not only the characteristic variations of V_p/V_s , but also a number of the other premonitory phenomena. Crustal deformation (at least for thrust faulting), radon concentration, electrical conductivity and local seismicity will all be affected in ways that are in at least qualitative agreement with the model. Whitcomb and Don Anderson point out that under the ambient conditions, the drop of pressure accompanying dilatant volume increase should vaporize the fluid; thus, both the changes in the physical properties of the fluid and the resulting changes in the medium as a whole will be large.

The role of fluids in faulting has received much attention since it was suggested some years ago. The studies

devoted to the earthquakes associated with the deep disposal well at the Rocky Mountain Arsenal²⁸ greatly advanced knowledge of this subject and formed the basis for concepts of earthquake control. If migrating fluids do play an essential part in natural earthquakes, then the physical basis of prediction and of control may be closely related. Since both of these are in their early stages of research, the general feasibility of either is far from established.

Outlook for the future

The first formal program of prediction research in the US will begin in 1974. As part of a broader national program on the reduction of earthquake hazards, the prediction studies will be funded and monitored by the US Geological Survey. The US is also cooperating in prediction research with two other nations—Japan and the USSR. Only one other nation—the People's Republic of China—is known

References

1. J. A. Kelleher, *J. Geophys. Res.* 75, 5745 (1970); L. R. Sykes, *J. Geophys. Res.* 76, 8021 (1971).
2. J. A. Kelleher, L. Sykes, J. Oliver, *J. Geophys. Res.* 78, 2547 (1973).
3. S. A. Fedotov, N. A. Dolbilkina, A. N. Morozov, V. I. Myachkin, V. B. Preobrazhensky, G. A. Sobolev, *Tectonophysics* 9, 249 (1970); S. A. Fedotov, *Trudy Inst. Fiz. Zemli, Akad. Nauk SSSR* 36, 66 (1965).
4. K. Shimazaki, *Tectonophysics* 11, 305 (1971).
5. K. Mogi, *Bull. Earthquake Res. Inst. Tokyo Univ.* 46, 53 (1968).
6. T. Rikitake, "International Association of Seismology and Physics of the Earth's Interior," in *Comptes Rend.* 18, 142 (1973).
7. Yu. V. Riznichenko, *Doklady Akad. Nauk SSSR* 157, 6 (1964); Yu. V. Riznichenko, A. I. Zakharova, *Izv. Akad. Nauk SSSR* 3, 178 (English Edition) (1971).
8. I. E. Gubin, *Bull. Int. Inst. Seismology and Earthquake Eng.* 4, 107 (1967).
9. H. F. Reid, "The Mechanics of the Earthquake; The California Earthquake of April 18, 1906," Report of the State Investigation Commission, Vol. 2, Carnegie Institution of Washington, Washington, D.C. (1910).
10. I. Tsubokawa, Y. Ogawa, T. Hayashi, *J. Geodetic Soc. Japan* 10, 165 (1964).
11. T. Rikitake, *Geophysical Surveys* 1, 4 (1972); T. Dambara, *EOS—Trans. Amer. Geophys. Union* 55 (to be published 1974).
12. K. Kasahara, A. Okada, M. Shibano, V. Sasaki, S. Matsumoto, *Bull. Earthquake Res. Inst. Tokyo Univ.* 45, 225 (1967).
13. J. C. Savage, W. H. Prescott, W. T. Kinoshita, *Proceedings of the Conference on Tectonic Problems of the San Andreas Fault System*, Stanford University Publications in the Geological Sciences 13, 44 (1973).
14. M. D. Wood, R. V. Allen, *Bull. Seis. Soc. Amer.* 61, 1801 (1971).
15. V. I. Ulomov, *Zemlya i Vselennaya* 3, 23 (1968).
16. S. Suyehiro, T. Asada, M. Ohtake, *Papers in Meteorology and Geophysics* 15, 71 (1964); S. Suyehiro, *Bull. Seis. Soc. Amer.* 56, 185 (1966).
17. L. Gedney, J. Van Wormer, *EOS—Trans. Amer. Geophys. Union* 55 (to be published, 1974); M. Wyss, W. H. K. Lee, *Proceedings of the Conference on Tectonic Problems of the San Andreas Fault System*, Stanford University Publications in the Geological Sciences 13, 24 (1973).
18. S. Matsushima, *Bull. Disaster Prevention Research Institute, Kyoto University*, 32 (1960); I. Gupta, *Bull. Seis. Soc. Amer.* 63, 1157 (1973).
19. A. N. Semvenov, *Izv. Akad. Nauk SSSR* 4, 245 (English edition) (1969); Y. P. Aggarwal, L. R. Sykes, J. Armbruster, M. L. Sbar, *Nature* 241, 101 (1973); C. Kisslinger, E. R. Engdahl, *Tectonophysics* (to be published, 1974).
20. J. H. Whitcomb, D. L. Anderson, *Science* 180, 632 (1973).
21. C. Kisslinger, E. R. Engdahl, *Bull. Seis. Soc. Amer.* 63, 1723 (1973).
22. M. Wyss, D. Holcomb, *Nature* 245, 139 (1973).
23. O. Reynolds, *Nature* 33, 429 (1886).
24. W. F. Brace, B. W. Paulding Jr., C. H. Scholz, *J. Geophys. Res.* 71, 3939 (1966).
25. A. Nur, *Bull. Seis. Soc. Amer.* 62, 1217 (1972).
26. T. V. McEvilly, L. R. Johnson, *Science* 182, 581 (1973).
27. C. H. Scholz, L. R. Sykes, Y. P. Aggarwal, *Science* 181, 803 (1973).
28. J. H. Healy, W. W. Rubey, D. T. Griggs, C. B. Raleigh, *Science* 151, 1301 (1968).

Subduction of the Nazca Plate Under Peru as Evidenced by Focal Mechanisms and by Seismicity

WILLIAM STAUDER

Department of Earth and Atmospheric Sciences, Saint Louis University, St. Louis, Missouri 63103

The focal mechanisms of 40 earthquakes in Peru and Ecuador, together with the seismicity of the region, indicate particular features of the subduction of the oceanic plate beneath this portion of South America. At shallow depths near the coast and at foci along the contact between the subduction zone and the continental plate the focal mechanisms indicate an underthrust of the continent by the oceanic plate on a thrust plane dipping 10° - 15° beneath the continent. Near this same depth but at foci within the oceanic plate, normal faults occur that correspond both to flexure of the plate and to downward axial tension. At intermediate depths the plate continues to act as a stress guide, the axis of tension being down about 30° from the horizontal and trending to the ENE. The dip of the Benioff zone steepens notably in southern Peru near the Peru-Chile corner, and the motion of the descending slab relative to the continental plate is in a direction $N40^{\circ}E$. Deep-focus earthquakes indicate a vertical segment of plate under axial compression at depths of 550-600 km. Numerous earthquakes also occur interior to the continent and within the continental lithosphere at depths down to 90 km. Both strike slip and reverse-type faults are found, but in either case the stress system corresponds to an E-W horizontal compression. Comparison with the seismicity is consistent with the model of an oceanic plate moving almost horizontally under the continental lithosphere in northern and central Peru and a separate, more steeply plunging segment of plate moving normal to the coast under southern Peru.

In a recent paper *Stauder* [1973] presented focal mechanism solutions for 61 earthquakes occurring in northern and central Chile. Since present-day earthquakes are manifestations of plate tectonics in process, the relative directions of motion and the orientation of principal stresses indicated by these solutions have thrown light on the characteristics of the subduction of the oceanic plate under this portion of South America. The present paper extends these studies to earthquakes of Peru and Ecuador.

EARTHQUAKES SELECTED FOR STUDY

The overall seismicity of Peru and Ecuador for the years 1961-1968 is indicated in the epicenter map in Figure 1. It is noted that normal-focus earthquakes are confined chiefly to the coastal region, although normal-focus earthquakes are also located within the continental plate (interior to the coast) and are more numerous within the continental plate than they are, say, in Chile. Intermediate-depth earthquakes tend to lie in a broad band beneath central Peru and, except in southern Peru, are relatively disconnected laterally from the normal-focus earthquakes. Deep-focus earthquakes are confined to a narrow N-S strip in western Brazil extending from only $7^{\circ}S$ to $11^{\circ}S$. A second very minor locale of deep-focus earthquakes occurs offset to the east and to the south from the first and extends from $13^{\circ}S$ to $14^{\circ}S$.

Against this background of seismic activity, 40 of the larger earthquakes of 1963-1972 were selected for study. These earthquakes lie within the latitude range 0° - $18^{\circ}S$. All are of magnitude $m_b = 5.7$ or greater, and the suite of these events constitutes virtually all of the earthquakes occurring within the space and time frame in question that are large enough to study by the methods applied.

Hypocenter information is given in Table 1, where for ease of identification the earthquakes are listed in chronological order. Later discussion will be in geographic order according to class groupings, as indicated by the identification number N given in the last column of the table. The relative locations and

the identification by classes of all of these earthquakes are indicated in Figure 2. There are 14 normal-focus earthquakes with foci near the coast or beneath the trench. There are 10 intermediate-depth shocks and six deep-focus shocks. There are also 10 earthquakes identified as occurring within the continental block. The depth of focus of these latter events varies from 1 to 89 km.

The data source for the study consisted of 70-mm film copies of the records of selected World-Wide Standard Seismograph Network stations. Observations of the P and S waves were made on the long-period records only. Focal mechanisms were determined from both P wave first motions and S wave polarization angles.

The focal mechanisms so determined are given in Table 2. In this table the earthquakes are listed by the identification number N defined above. In addition to date, origin time, and location, the table presents the trend and plunge of the X and Y axes (poles of the nodal planes) and of the P , T , and B axes (axes of pressure and tension and the null axes, or axes of greatest, least, and intermediate compressional stress, respectively). Half these solutions were determined for this particular study; one solution is taken from the work of *Chandra* [1970], one is taken from *Stauder and Bollinger* [1966], and the remaining solutions are from *Wagner* [1972], as is indicated by the reference in the last column of the table. Graphic solutions, with the P and S wave data on which the individual solutions are based, are available upon request.¹

EXAMINATION OF SOLUTIONS

The focal mechanism solutions in Table 2 are ordered from north to south and according to four groupings. We consider them in order.

Normal-focus earthquakes. Earthquakes 1-15 (Table 2) are of normal focal depth. The focal mechanisms for all these

¹ Equal-area projections are available with entire article on microfiche. Order from American Geophysical Union, 1909 K Street, N.W., Washington, D. C. 20006. Document J75-003; \$1.00. Payment must accompany order.

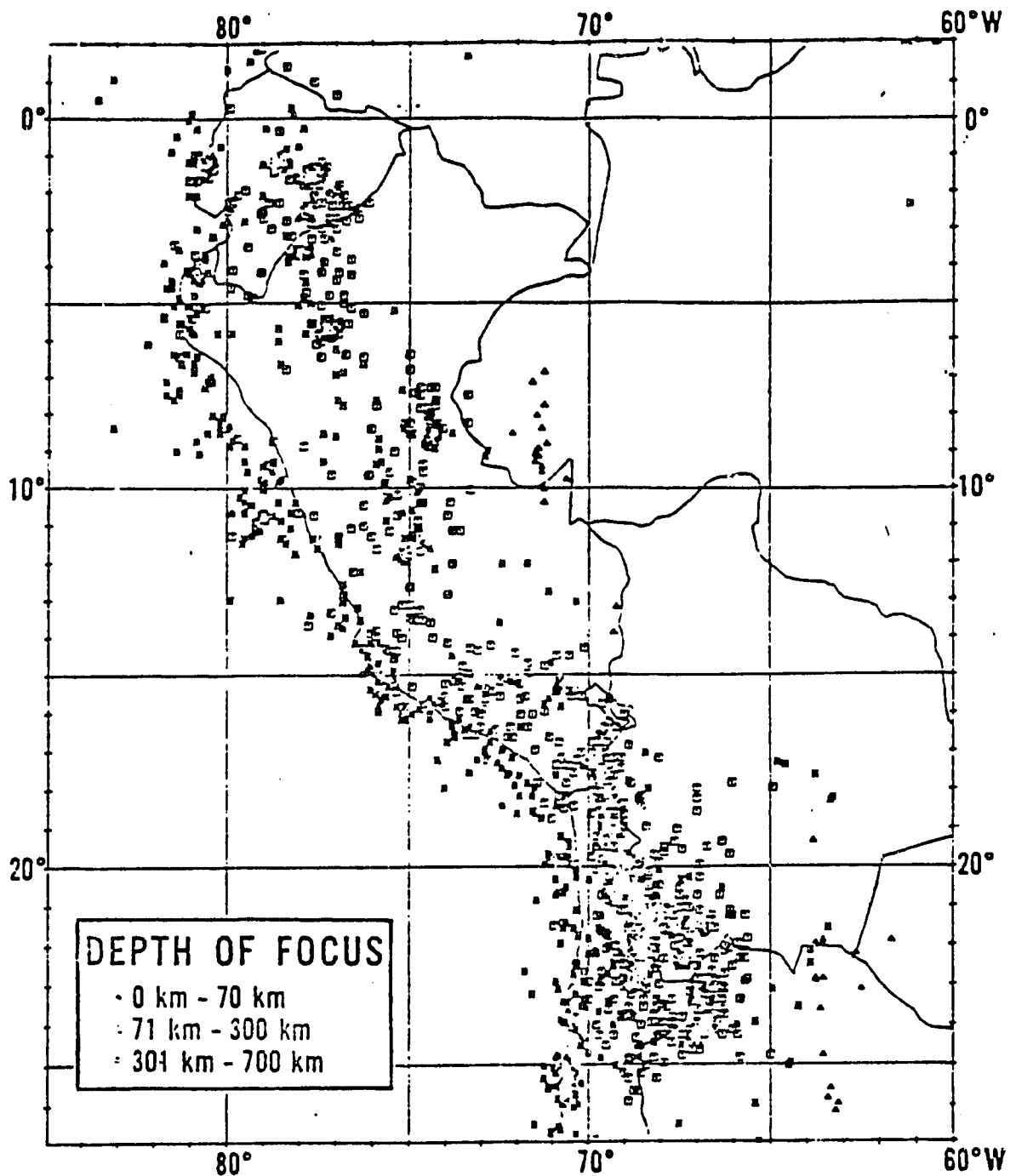


Fig. 1. Seismicity of Peru and Ecuador for the years 1961-1968. (Taken from Map NEIC 3014, U.S. Department of Commerce.)

earthquakes are indicated in Figure 3, which presents a mechanism diagram for each individual earthquake together with the identification of its epicentral location, a comparison of the focal mechanisms with one another thus being allowed. The shaded quadrants in the mechanism diagrams represent the quadrants of rarefaction first motion of the *P* wave. The centers of these quadrants are the *P* axes. The centers of the unshaded quadrants are the *T* axes.

The mechanisms themselves can be considered in three groupings: (1) those of the earthquakes clustering at about 10°S, which are related to the zones active in the two larger earthquakes of October 1966 and May 1970 (earthquakes 2-7); (2) those of isolated foci occurring near or under the coast but separated from the first group (earthquakes 1, 8, 9, and 10); and (3) those of earthquakes occurring under or near the trench (earthquakes 11-14).

Beginning with the middle group, each mechanism (see Figure 3) involves one nodal plane that dips steeply to the west or southwest. The second nodal plane in each case dips gently under the continent. If the latter is taken as the fault plane, the signs of the first motion quadrants are such as to correspond to an underthrusting of the continent by the oceanic plate at the depth of focus. The direction of underthrust is to the east in earthquakes 1 and 8 and to the northeast and on a slightly steeper thrust surface nearer the Peru-Chile corner in earthquakes 9 and 10.

The mechanisms in the vicinity of the earthquakes of 1966 and 1970 are more complicated. The two major earthquakes in question have been studied by Abe [1972]. The result of the present study serve to confirm his findings and to extend the study of the earthquake motion to some of the large aftershocks of the 1970 earthquake. The shaded regions ir

Figure 3 outline the area active in the two earthquakes as identified by Abe from the zone of aftershocks. The mechanism given in Table 2 for the major shock of 1966 is virtually identical to that determined by Abe from *P* first motion and from the spectra of surface waves. The motion is interpreted as an underthrust of the oceanic plate along an elongated surface normal to the coast, as identified by the aftershocks, and dipping gently (only 10°–15°) under the continent. Earthquake 6 (1963) occurred at a greater depth, 63 km, at the inward extent of this zone and corresponds to extension within the subducted plate parallel to the dip of the plate. Earthquake 15, deeper still (*h* = 80 km) and included among the intermediate-depth shocks below, carries this same axial extension further downward along the plate and in the same ENE direction.

The mechanism of the main shock of 1970 (earthquake 2) as given in Table 2 is again in close agreement with that of Abe. The two solutions differ by only 3° in the dip of the nodal planes. As Abe remarks, the aftershocks of this earthquake are located over a range of depth from 40 to 100 km. The elongation of the aftershock zone corresponds to the strike of the nodal planes. Either of the nodal planes may be taken as the fault plane, and in either case the faulting is normal faulting. It is concluded that the fracture occurred within the plate and is related to flexure as the plate begins to descend or to axial tension under gravitational stress.

The three aftershocks studied here (earthquakes 3, 4, and 5),

however, are more difficult to interpret. All of these correspond to reverse faulting, the axis of compressive stress being located approximately along the dip of the plate. The listed focal depths of these shocks are comparable to or only slightly greater than the focal depth of the main shock. It is possible that these represent a stress condition in the lower portion of the plate as the plate bends or as it adjusts to the condition of the stress after the initial major fracture.

Earthquakes 11–14 are those that occur under the trench. The mechanisms of 11 and 12 indicate horizontal tension normal to the tectonic trend. These foci are located in the upper portion of the oceanic plate and at the point of flexure of the plate as it begins to converge beneath the continental plate. This interpretation is in agreement with the condition found previously by Stauder [1968] for foci beneath the Aleutian trench.

In earthquakes 13 and 14 one of the principal stresses is again horizontal and normal to the trend of the trench, but in this case the horizontal stress is compressive. The focal depth and location of earthquake 13 indicate that the focus of this shock may be in the continental plate near its leading edge, where reverse faulting might be expected. No explanation is offered for the mechanism of earthquake 14 (reverse faulting within the upper portion of the oceanic plate). Similar mechanisms were found for foci under the trench off the coast of Chile [Stauder, 1973]. Mendiguren [1971] has shown that the

TABLE 1. Chronological List of Earthquakes Studied

Date	Origin Time	Latitude, deg	Longitude, deg	<i>h</i> , km	<i>m_s</i>	<i>N</i>
Apr. 13, 1963	02h 20m 58s	6.2	76.5	125	7.0	19
May 10, 1963	22h 22m 42s	2.2	77.6	33	6.7	31
Aug. 15, 1963	17h 25m 06.0s	13.8	69.3	543	8.0	30
Aug. 29, 1963	15h 30m 31s	7.1	81.6	23	6.5	11
Sep. 17, 1963	05h 54m 34s	10.6	78.2	61	6.7	6
Sep. 24, 1963	16h 30m 16s	10.6	78.0	80	7.0	22
Nov. 3, 1963	03h 10m 13s	3.5	77.8	33	6.7	33
Nov. 9, 1963	21h 15m 30.0s	9.0	71.5	600	7.0	26
Nov. 10, 1963	01h 00m 39.0s	9.2	71.5	600	6.7	27
Aug. 3, 1965	02i: 01m 52.0s	7.7	81.3	49	5.8	12
Sep. 17, 1965	11h 13m 56.0s	1.4	77.6	190	6.0	16
Nov. 3, 1965	01h 39m 03.1s	9.1	71.3	593	6.2	29
May 1, 1966	16h 22m 56s	8.5	74.3	165	5.7	20
June 7, 1966	00h 59m 46s	14.9	75.8	48	6.5	8
Oct. 17, 1966	21h 41m 56s	10.7	78.7	38	7.5	7
Feb. 9, 1967	15h 24m 47.2s	2.9	74.9	58	6.3	32
Feb. 15, 1967	16h 11m 11.8s	9.0	71.3	597	6.2	28
Mar. 2, 1967	02h 49m 31.7s	0.3	78.7	121	5.8	15
Sep. 3, 1967	21h 07m 30.8s	10.6	79.8	38	6.5	14
June 19, 1968	08h 13m 35.0s	5.5	77.15	89	6.4	35
July 30, 1968	20h 38m 42.0s	6.9	80.45	37	5.8	1
Sep. 9, 1968	00h 37m 43.2s	8.7	74.5	120	6.0	21
Sep. 28, 1968	13h 53m 35.4s	13.2	76.4	70	6.4	23
Oct. 31, 1968	09h 15m 46.9s	16.4	73.4	67	5.7	9
Feb. 4, 1969	14h 10m 13.3s	8.2	80.2	16	6.0	13
July 19, 1969	04h 54m 54.1s	17.3	72.5	4	5.9	10
July 24, 1969	02h 59m 21.0s	11.9	75.1	1	5.9	38
Oct. 1, 1969	05h 05m 43.2s	11.9	75.1	4	5.9	39
Feb. 14, 1970	11h 17m 16.1s	9.9	75.6	35	5.9	37
May 31, 1970	20h 33m 27.3s	9.2	78.8	43	6.6	2
June 2, 1970	01h 37m 27.7s	9.8	78.8	58	5.7	3
June 4, 1970	04h 09m 26.3s	9.8	78.6	57	5.8	4
June 17, 1970	04h 44m 20.9s	15.8	71.8	91	5.9	24
July 2, 1970	00h 45m 02.0s	10.1	78.6	62	5.8	5
Dec. 10, 1970	04h 34m 59.8s	4.0	80.7	25	6.3	34
May 17, 1971	11h 04m 07.1s	1.6	77.7	176	5.7	17
July 27, 1971	02h 02m 49.6s	2.7	77.4	135	6.3	18
Oct. 15, 1971	10h 33m 46.7s	14.1	73.3	54	5.7	40
Jan. 12, 1972	09h 59m 10.3s	6.9	71.8	580	5.9	25
Mar. 20, 1972	07h 33m 49.6s	6.8	76.8	64	6.1	36

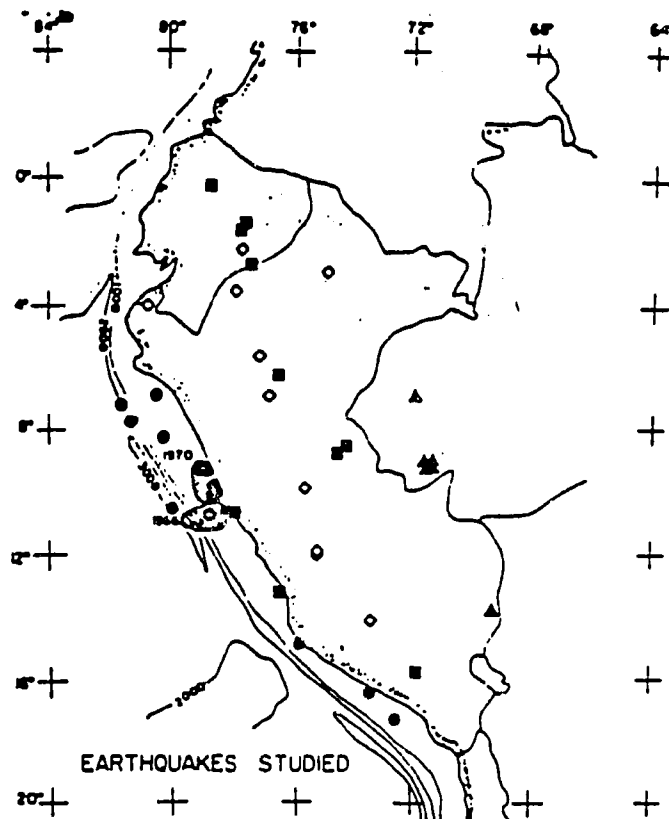


Fig. 2. Earthquakes selected for study. Solid circles represent normal-focus earthquakes occurring near the coast, solid squares indicate shocks of intermediate focal depth, solid triangles indicate deep foci, and open diamonds represent the foci occurring interior to the continent within the continental lithosphere.

Nazca plate itself is being compressed in the direction of plate motion, this compression possibly influencing the release of stress in earthquakes near the trench.

Earthquakes of intermediate focal depth. The mechanism diagrams for the earthquakes of intermediate focal depth (15–24 in Table 2) are presented in Figure 4. A twofold classification suggests itself. The first classification concerns earthquakes in Ecuador and in northern to central Peru versus those in central and southern Peru. The latter are shallow and have their foci under or near the coast. If it is assumed, as was suggested by *Elsasser* [1967] (see *Isacks et al.* [1968]) and amply documented by *Isacks and Molnar* [1971], that the descending slab acts as a stress guide, the axial stress in these earthquakes and at depths of 70–90 km in southern Peru is tensional and to the northeast. This represents failure under gravitational sinking relatively high in the slab and along a zone descending more steeply under the continent than to the north.

A second classification concerns the direction of motion or direction of principal stresses active at the foci of the northern group. Examination of the symbols in Figure 4 shows two categories: (1) squares with the solid upper portion, which indicate foci whose axes are oriented in a manner similar to that of those just discussed (that is, with the tension axis down 30° from the horizontal and dipping to the northeast), and (2) squares with the solid lower portion, which indicate foci with N-S trending nodal planes and axes of tension that are nearly horizontal and oriented E-W. An equal-area projection presents the *P*, *B*, and *T* axes of the two groups in the upper and lower insets of Figure 4, respectively. A depth difference (depths are indicated by the number near the symbol for each earthquake in Figure 4) separates the two classes, at least in

Ecuador and northern Peru. The shallower foci ($h = 120$ – 135 km) have horizontal E-W tension axes, and the deeper foci ($h = 175$ – 190 km) have a trend that seems to correspond to the dominant trend of the axis of least stress under both Chile [*Stauder*, 1973] and Peru. Again on the assumption that the slab acts as a stress guide, this indicates that the general current motion of subduction, whatever its differences in character from point to point, is downward at an angle of about 30° and to the northeast at the level of the intermediate focal depth earthquakes investigated.

Earthquakes 20 and 21 reverse the depth relationship of the E-W versus northeast trending axes of tension. The deeper of the two, earthquake 20, has the E-W tension axis, and the shallower, earthquake 21, has the NE trending axis. These two foci are near the southern extremity (see Figure 1) of the band of intermediate focal depth earthquakes extending from Ecuador to near the Peru-Brazil border and probably mark a change in the character of subduction south of this latitude.

Deep-focus earthquakes. Earthquakes 25–30 (Table 2) are deep-focus shocks. The first five of these shocks belong to the main, very narrow trend of deep-focus shocks between 7°S and 11°S. The first occurs at the northern extremity, and the next four group toward the southern extremity of the zone. The focal depths are all remarkably uniform, varying from 580 km for the first to 593–600 km for the remaining four.

The focal mechanisms for these earthquakes are indicated in Figure 5. The similarity of the mechanisms for earthquakes 25–29 is clear. The strikes of the possible fault planes are aligned closely along the trend N10°W (see Figure 1) of the epicenters of deep-focus earthquakes. The central quadrant in all cases is a rarefaction quadrant corresponding to normal faulting in the conventional sense. But the geometric configuration with relation to a descending slab is such as to correspond to shortening or to compressional stress in the vertical direction.

The inset on the left of Figure 5, the equal-area projections of the *P*, *B*, and *T* axes, illustrates the similarity of mechanisms more quantitatively. The *P* axes are nearly vertical, the *B* or intermediate-stress axes are horizontal and oriented N10°W, and the *T* axes are almost horizontal and N100°W. If it is assumed that the trend of the hypocenters in Figure 1 corresponds to the orientation of a segment of plate and that the plate acts as a stress guide, three conclusions follow: (1) the *P* and *B* axes lie in the plate and indicate a segment of plate descending vertically in this locality under South America, (2) the segment of plate in question is limited in dimension and is oriented N10°W, and (3) the concentration of deep-focus earthquakes at a 600-km depth and the compressional stress along the axis of the plate at this depth indicate the lower terminus of this segment of subducted plate as the plate encounters more resistive rock material at this depth within the mesosphere.

The mechanism of earthquake 30 requires some difference in interpretation. This earthquake is one of the small concentration of foci at 13°S–14°S. The *P* axis dips steeply (65°) to the northeast, the *T* axis is nearly horizontal and trends N60°W (parallel to the coast), and the *B* axis dips gently (23°) to the southwest. Again assuming that the descending plate acts as a stress guide, and for other cumulative reasons to be developed below, we conclude that in this case the *P* and *T* axes lie within and define the orientation of a segment of plate and that the plate in this locality and at this depth is descending in the direction N30°E.

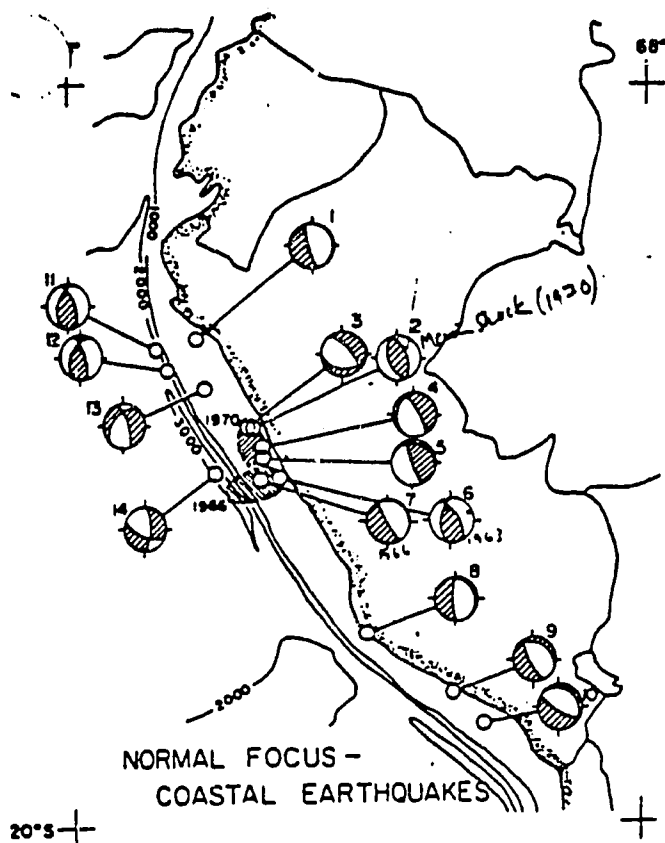
Foci within the continental plate. Earthquakes 31–40 all oc-

TABLE 2. Focal Mechanism Parameters

N	Date	Time	Latitude, deg	Longitude, deg	A, km	X		Y		P		T		B		Reference
						Trend	Plunge									
1	July 30, 1968	2038	6.9	80.4	37	256	75	73	15	254	30	72	60	163	1	
2	May 31, 1970	2033	9.3	78.8	49	250	40	70	50	250	85	70	05	340	0	Wagner [1972]
3	June 2, 1970	0137	9.3	79.0	49	230	25	5	57	33	17	267	63	130	21	
4	June 4, 1970	0409	9.8	78.6	57	100	70	24	16	70	28	223	59	334	12	
5	July 2, 1970	0045	10.1	78.6	62	180	79	68	4	79	48	239	40	337	10	
6	Sep. 17, 1963	0554	10.6	78.2	61	238	37	97	46	76	5	180	69	344	20	Wagner [1972]
7	Oct. 17, 1966	2141	10.7	78.7	38	60	12	220	77	236	33	66	57	329	4	
8	June 7, 1966	0059	14.9	75.8	48	90	17	240	71	252	27	104	61	357	9	
9	Oct. 31, 1968	0915	16.4	73.4	67	225	50	25	38	214	6	336	78	123	10	
10	July 19, 1969	0454	17.3	72.5	54	225	72	35	18	217	27	30	63	125	3	
11	Aug. 29, 1963	1530	7.1	81.6	23	247	36	460	49	82	7	193	72	350	17	Wagner [1972]
12	Aug. 3, 1965	0201	7.7	81.3	49	250	30	117	50	201	63	90	11	355	24	
13	Feb. 4, 1969	0410	8.2	80.2	16	140	47	254	21	101	15	210	50	360	36	Wagner [1972]
14	Sep. 3, 1967	2107	10.6	79.8	38	270	30	23	34	57	2	325	49	150	41	Wagner [1972]
15	Mar. 2, 1967	0247	0.3	78.7	121	72	35	312	36	12	55	282	0	192	35	Wagner [1972]
16	Sep. 17, 1965	1113	1.4	77.6	190	18	74	225	14	234	59	39	30	133	7	Wagner [1972]
17	May 17, 1971	1104	1.6	77.7	176	220	19	60	70	45	26	209	63	312	6	
18	July 27, 1971	0202	2.7	77.4	135	253	36	118	44	194	65	94	4	2	24	
19	Apr. 13, 1963	0220	6.2	76.5	125	290	59	79	27	270	16	48	68	176	14	Stauder and Bollinger [1966]
20	May 1, 1966	1622	8.5	74.3	165	279	15	157	63	117	27	251	54	15	22	Wagner [1972]
21	Sep. 9, 1968	0037	8.7	74.5	120	7	74	249	8	57	36	265	51	157	14	Wagner [1972]
22	Sep. 24, 1963	1630	10.6	78.0	80	0	65	235	15	251	56	39	27	139	20	
23	Sep. 28, 1968	1353	13.2	76.4	70	31	75	246	12	59	32	257	57	154	8	Wagner [1972]
24	June 17, 1970	0444	15.8	71.8	91	220	10	45	80	219	55	41	35	310	1	
25	Jan. 12, 1972	0959	6.9	71.8	580	70	28	275	60	43	70	259	16	166	11	
26	Nov. 9, 1963	2115	9.0	71.5	600	80	44	262	46	180	89	261	1	171	1	Wagner [1972]
27	Nov. 10, 1963	0100	9.2	71.5	600	87	46	275	44	339	86	91	1	181	4	Wagner [1972]
28	Feb. 15, 1967	1611	9.0	71.3	597	77	35	257	55	77	80	257	10	347	0	Wagner [1972]
29	Nov. 3, 1965	0139	9.1	71.3	593	105	50	89	39	136	81	263	5	353	7	Wagner [1972]
30	Aug. 15, 1963	1725	13.8	69.3	543	98	37	322	44	37	66	299	4	207	24	Chandra [1970]
31	May 10, 1963	2222	2.2	77.6	33	295	16	27	7	250	6	341	16	140	73	Wagner [1972]
32	Feb. 9, 1967	1524	2.9	74.9	58	290	28	23	6	243	15	340	24	123	61	Wagner [1972]
33	Nov. 3, 1963	0310	3.5	77.8	33	256	37	82	53	79	8	239	81	348	3	Wagner [1972]
34	Dec. 10, 1970	0434	4.0	80.7	25	175	35	338	54	348	9	209	78	79	8	
35	June 19, 1968	0813	5.5	77.2	89	95	36	267	54	272	9	115	80	2	4	Wagner [1972]
36	Mar. 20, 1972	0733	6.8	76.8	64	265	65	80	25	262	20	76	70	171	2	
37	Feb. 14, 1970	1117	9.9	75.6	35	95	27	245	60	264	17	124	68	358	13	
38	July 24, 1969	0259	11.9	75.1	1	138	45	250	20	99	15	206	48	357	38	
39	Oct. 1, 1969	0505	11.9	75.1	4	130	45	242	20	91	15	198	48	349	38	
40	Oct. 15, 1971	1033	14.1	73.3	54	130	15	225	18	268	2	177	24	2	66	

899 - *for near field*
deep-focus
in transition focus
shallow, converted

STAUDER: NAZCA PLATE SUBDUCTION



3. Focal mechanism diagrams for earthquakes of normal focal mechanism. Shaded areas indicate quadrants of rarefaction first motion.

occur within the continental plate. About half of these are quite shallow, but others extend down to depths of 50-90 km. The focal mechanism diagrams for these earthquakes are presented in Figure 6.

Three of the diagrams (earthquakes 31, 32, and 40) indicate predominantly strike slip faulting. The remainder are high-angle reverse faults. The former are indicated by the diamond symbols with the solid upper portion in Figure 6, and the latter, with the exception of earthquake 34, by the symbols with the solid lower portion. The projections of the *P*, *B*, and *T* axes of the two groups are given in the upper and lower insets of the figure, respectively. It is seen that both groups correspond to a horizontal E-W pressure.

Earthquake 34 is close to the leading edge of the continental plate and near, in fact, to the westernmost limit of South America. The motion in this earthquake represents a N-S compression and is probably a result of the reaction within the continental slab to small differences in the direction of subduction of the oceanic plate in response to its contact with the sharply convex boundary here of the continental slab.

Earthquakes 38 and 39 were destructive earthquakes that occurred near Huancayo on July 24 and October 1, 1969. Both were of very shallow focus. As was reported by Ernesto Dega of the Instituto Geofísico del Perú, Lima [Lander, 1970], the first was accompanied by a surface fracture with a vertical displacement of 0.4 m. In the second earthquake the same fault

is again activated with up to 1.6 m of vertical displacement and around 0.70 m of horizontal displacement. The fault had a northwest strike, the motion being up on the northeast block and down on the southwest.

When this information is used as a guide in selecting the fault plane from the two nodal planes for the earthquake of October 1, the focal parameters in Table 2 give a fault with a

strike N28°W, dipping 70° to the northeast. The first motion indicates up on the northeast side, in conformity with the field observations. The motion vector gives 0.77 as the dip slip component of displacement and 0.64 left lateral as the strike slip component.

RELATION TO THE SEISMICITY

The number of earthquakes large enough to yield a determination of the focal mechanism is, unfortunately, relatively small. A fuller picture of the overall flow of the subduction process, however, may be obtained by correlating these few individual foci with the general seismicity of the region. For this purpose the National Ocean Survey hypocenter file for the years 1961-1972 was searched to obtain the subset of hypocenters occurring within the region 2°N-18°S, 65°W-85°W. These are plotted (Figure 7) in a series of projections A-A to F-F on a vertical plane by 4° intervals of latitude. The sections are identified on the index maps indicated in sections A-A and E-E. The position of the Peru trench is indicated by the small inverted solid triangle at the top of each section.

The shallow dip of the zone of intermediate-depth earthquakes is immediately apparent, as is the silent zone below about a 300-km depth, or even below a 200-km focal depth in northern Peru. But for more detailed examination, attention is first called to sections D-D, E-E, and F-F. The first two are E-W sections, approximately in the direction of motion of the Nazca plate as it approaches the coast. Section F-F overlaps the other two and has a strike N45°E, approximately perpendicular to the coast. The steeper dip and the well-defined character of the Benioff zone indicate that this section is much closer to the gradient of the zone of hypocenters than either of the other two.

The conclusion is that the Benioff zone, and by assumption the dip of the oceanic slab and its direction of motion under southern Peru, is N30°-40°E (normal to the coast) and down from the horizontal about 30°, in keeping with the motion found above in earthquakes 9 and 10 (underthrust to the northeast) and in earthquake 24 (axial tension N42°E, down 35°).

The contrast between section F-F and sections D-D and E-E, with the graphic information that it gives about the subduction under southern Peru, suggested trying sections normal to the coast along remaining portions of the coast of Peru. Some minor improvement was found in the definition of the zone of intermediate-focus earthquakes in the section normal to the coast of central Peru, but no other significant changes were found. This finding is in keeping with a very shallow dip or even a shoaling of the oceanic slab under the continent.

On this basis, for the purpose of further discussion, the hypocenter sections are re-presented in Figure 8 with a proposed slab configuration drawn in. Also indicated are the positions on the sections of the intermediate-depth and continental plate earthquakes whose mechanisms were presented above.

DISCUSSION

In previous related studies Sykes and Hayes [1971] reported that in Peru the oceanic lithosphere may not descend at a moderate dip under the continent as it does in northern Chile but may move almost horizontally under the continent. Isacks and Anar [1971] showed that for earthquakes of magnitude 5 and larger the seismic zone is slablike under central Peru and has a dip of only 10°-15°. The focal mechanisms of this study

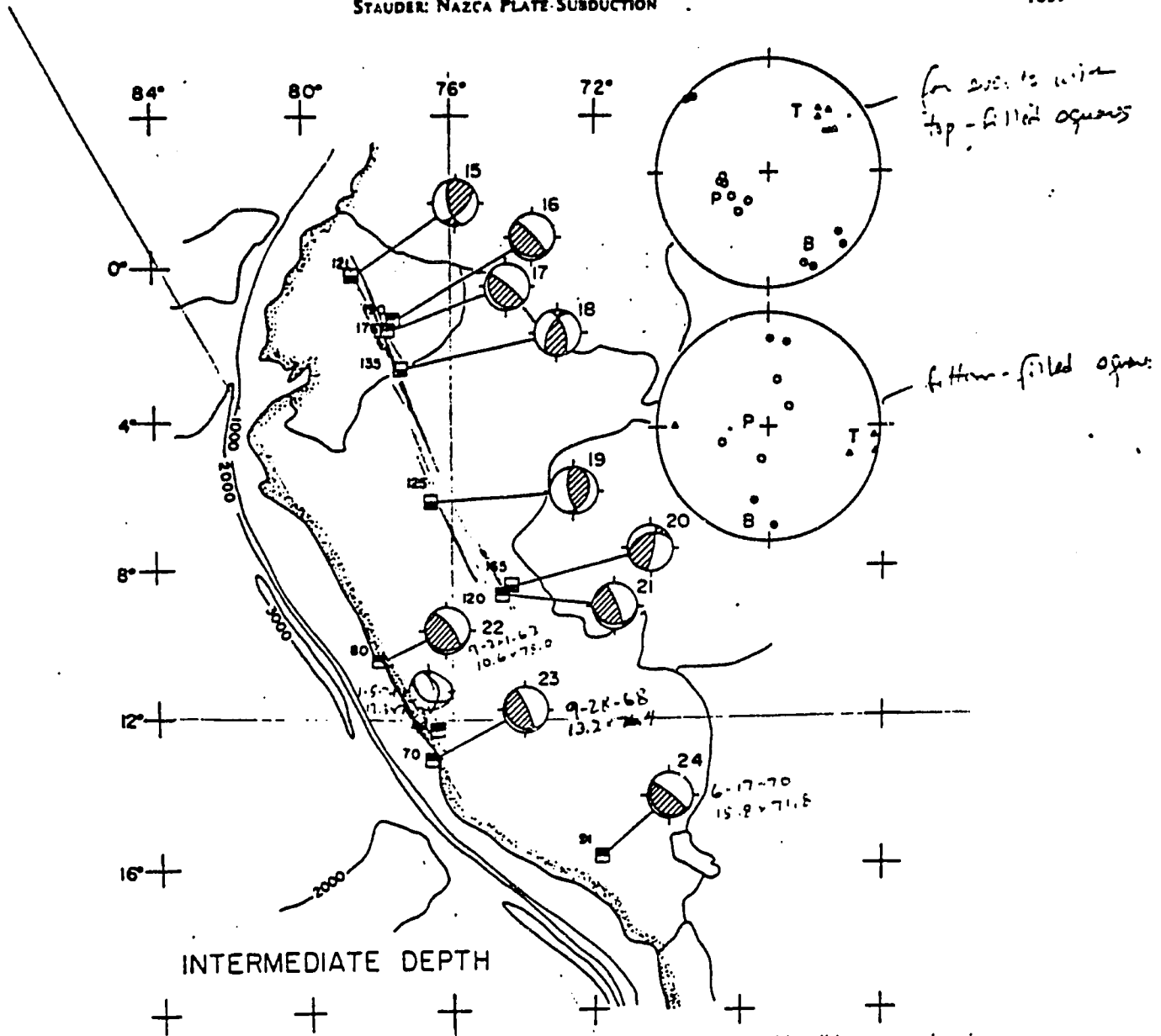


Fig. 4. Focal mechanism diagrams for earthquakes of intermediate focal depth. Squares with solid upper portions indicate foci with tension axes dipping 20° to the northeast. Squares with solid lower portions indicate foci with tension axes horizontal and oriented E-W.

and the hypocenter sections in Figure 8 allow further specifications of the slab and of the slab motion.

A comparison of sections A-A and B-B (Figure 8) shows the convergence motion of the plate under Ecuador and northern Peru to be influenced by the configuration of the continental boundary. Section B-B includes the westernmost promontory of the continent. The dip of the oceanic slab is least under this portion of South America. Immediately to the north both the coast of Ecuador and the axis of the trench verge to the east; descent of the slab begins at a more easterly point, with a consequent steeper dip and an attendant contortion of the slab. Intermediate-depth foci show that at a depth of about 200 km (see section A-A) and near the leading edge, or at least the edge of the seismically active portion of the plate, the direction of subduction as indicated by the tension axes is northeast and down at about 30°.

Section C-C is the least well defined. There is some indication (see section C-C, Figure 7) that the Benioff zone may descend more steeply, divorced from the cluster of intermediate-depth foci that occur 500-600 km interior from the border of the continent. This hypothesis has been proposed, in fact, by Okada [1973], who found the depth of conversion from ScS to

an ScSp phase, which he identified with a plate boundary, to be below the gently dipping slab model of Isacks and Molnar [1971], Sykes [1972], and others but along a line continued downward from the ocean side shallow seismic activity. In this event the slab itself is virtually aseismic at intermediate depths. This would be in keeping with the high Q reported by Sacks and Okada [1973] beneath the continent and interpreted as implying that the underthrust mantle in western South America is lithospheric rather than asthenospheric and hence capable of supporting earthquakes. That is, the continental lithosphere has a thick (350 km) high-rigidity root. Encounter with this root forms the shape of the subduction zone.

On the basis of the fault motion in normal-focus earthquakes off the coast of Peru (shallow underthrust plus axial extension within the plate) reported above and on the basis of the difference that we have found in the type of earthquakes occurring within the continental plate down to a 100-km depth versus those below this level, in what we have inferred to be the oceanic slab, we prefer the interpretation of Sykes and Hayes [1971] and Isacks and Molnar [1971] cited above. This, too, allows for a lithosphere of double thickness under Peru but one of continental composition and one of oceanic. It also

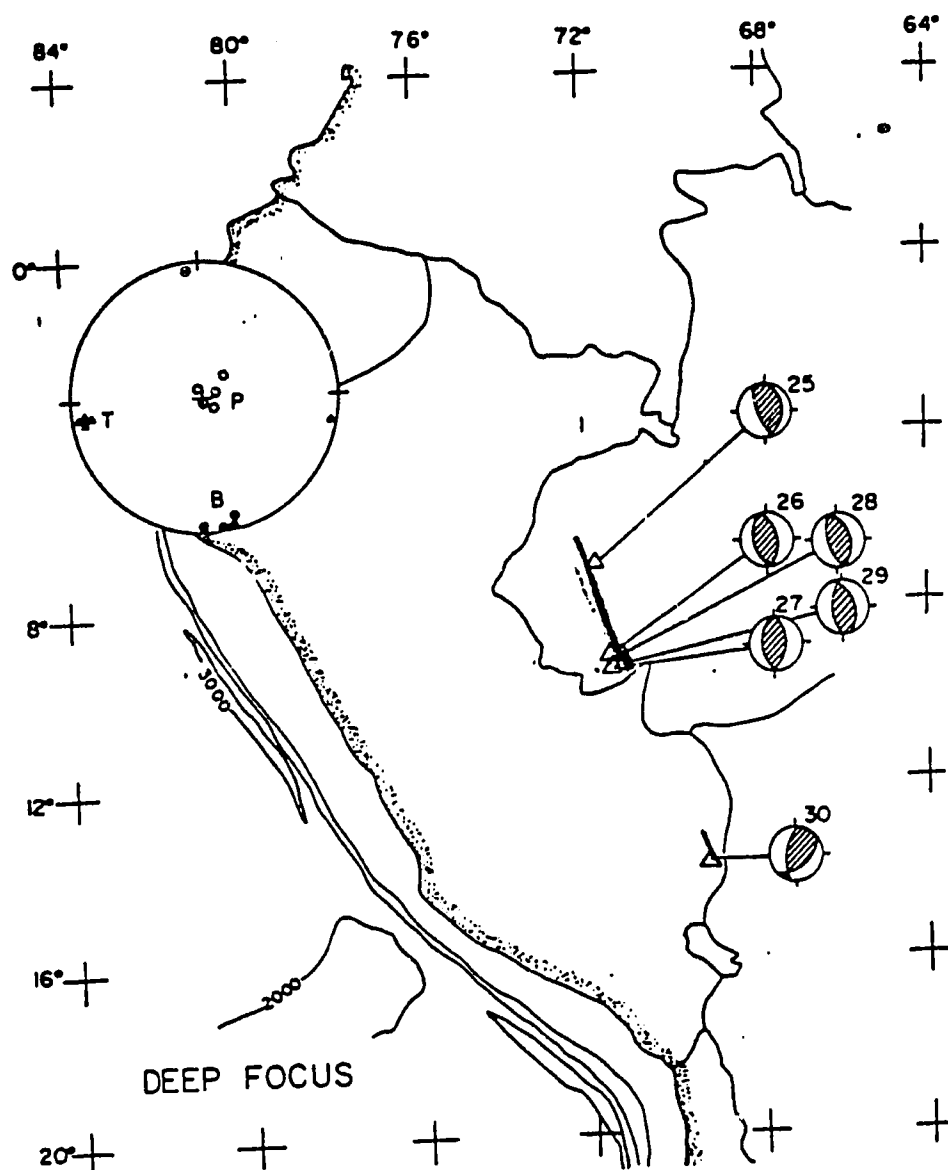


Fig. 5. Focal mechanism diagrams for deep-focus earthquakes.

allows for a laterally homogeneous low- Q zone below a 350-km depth as found by Sacks and Okada [1973] under Peru.

Model studies by Jacoby [1973] suggest that such a subduction configuration might result if, in addition to motion of the oceanic plate, the arc or continent side plate advances toward the descending plate with respect to the deeper mantle, as is the case in South America.

Accordingly, section C-C (Figure 8) proposes a slab of shallow dip extending almost horizontally under the continent. The evidence from the several normal-focus earthquakes, especially those associated with the coastal earthquakes of 1966 and 1970, shows that the direction of underthrust is normal to the coast, that is, about $N60^{\circ}E$. The motion of the plate at intermediate depths is presumed to be the same as that in sections B-B and A-A, although foci 20 and 21, as mentioned above, may imply some change at the latitude of these epicenters. We associate this indication of change with a boundary of a segment of the plate and infer that to the south the plate is descending more steeply, independently of the segment that we have been considering, and in a direction $N30^{\circ}-40^{\circ}E$. In fact, the segment of plate indicated in C-C or in D'-D' below may partially override the one indicated in E'-E'.

Section D'-D' presents a section 6° in width that is normal to the coast of central Peru and overlaps the previous section at the interior extreme of the hypocenter zone. This section is

regarded as being along the gradient of the slab rather than oblique to it, as was the preceding section. No additional comment is required concerning the motion of the oceanic slab at shallow to intermediate depths. Attention is drawn, however, to the deep-focus earthquakes and to the silent zone from depths of 250 to 550 km.

There is much discussion about whether in South America, both under Peru and under Chile, the descending oceanic slab is continuous through the silent zone with the zone of deep-focus earthquakes or whether the shallow and intermediate seismicity defines a present segment of plate and the deep seismicity defines the remnant of an earlier epoch of subduction. We have already seen that the deep-focus earthquakes define a zone (segment of vertically descending slab) oriented $N10^{\circ}W$. The greater diffusion of deep-focus hypocenters in section D'-D' versus that in C-C is consistent with this but also illustrates that a slab whose dip direction is along the cross section D'-D' is not likely to be continuous with the zone of deep-focus earthquakes. That is, the trend of the gradient of a segment of plate defined by the deep-focus earthquakes is not the same as that of the slab at intermediate depth. The choice, then, of the shallow slab under Peru favors two distinct epochs of spreading and discontinuity of the slab between depths of about 250 and 550 km.

Section E'-E' is a vertical section 6° in width in the direction

N40°E, approximately normal to the coast of southern Peru. As was remarked above, the Benioff zone in this region clearly defines the dip and direction of the descending slab under this portion of Peru. The focal mechanisms agree with this configuration and direction of subduction. The marked difference between the dip of this segment and that of central Peru implies severe contortion or, more likely, separate tongues of the oceanic slab, which is the interpretation here proposed.

Given a steepening of the dip of the slab from 30° to 60° below a depth of 300 km, the zone just mentioned has the same trend as that defined by the *P* and *T* axes of earthquake 30 discussed above. The segment of plate at this depth (543 km) is of small lateral dimension, and the horizontal *T* axis, assumed to define the orientation of the plate, implies lateral extension. Given the steeper dip of the slab at depths shallower than those in other regions under Peru and the similarity of trend of segments of slab and of slab motion at intermediate- and deep-focus depths, the probability of continuity of the slab may be argued more forcefully here than in section D'-D'. Although there is no reason to believe that the plate should be continuous here but not under central Peru or under Chile, the present study offers no evidence favoring one position rather than the other in southern Peru.

It is variously argued that anomalous high-frequency

arrivals following the normal *S* wave arrival on seismograms at Naña, Peru (NNA), Arequipa, Peru (ARE), Antofagasta, Chile (ANT), and other stations support continuity of the slab [Sacks and Barazangi, 1973] under western South America or that they are converted waves that imply no continuity [Snook et al., 1973]. The question is still an open one and seems most likely to yield to further studies of the anomalous high-frequency arrivals and of the *Q* structure.

SUMMARY

The focal mechanisms of earthquakes and the seismicity of Peru are interpreted as evidencing an underthrust of the oceanic plate along a thrust surface of small dip (10°-15°) under northern and central Peru and for a continuing subduction of the plate almost horizontally under the continental lithosphere in the direction N60°E. Under southern Peru a separate tongue of the plate descends more steeply, at a dip of about 30° and in the direction N30°-40°E. Under central Peru the zone of deep-focus earthquakes is more probably not a segment of slab that is continuous with the slab at intermediate depths. Within the continental lithosphere the focal mechanisms that occur at depths from 1 to 100 km indicate an E-W horizontal compression.

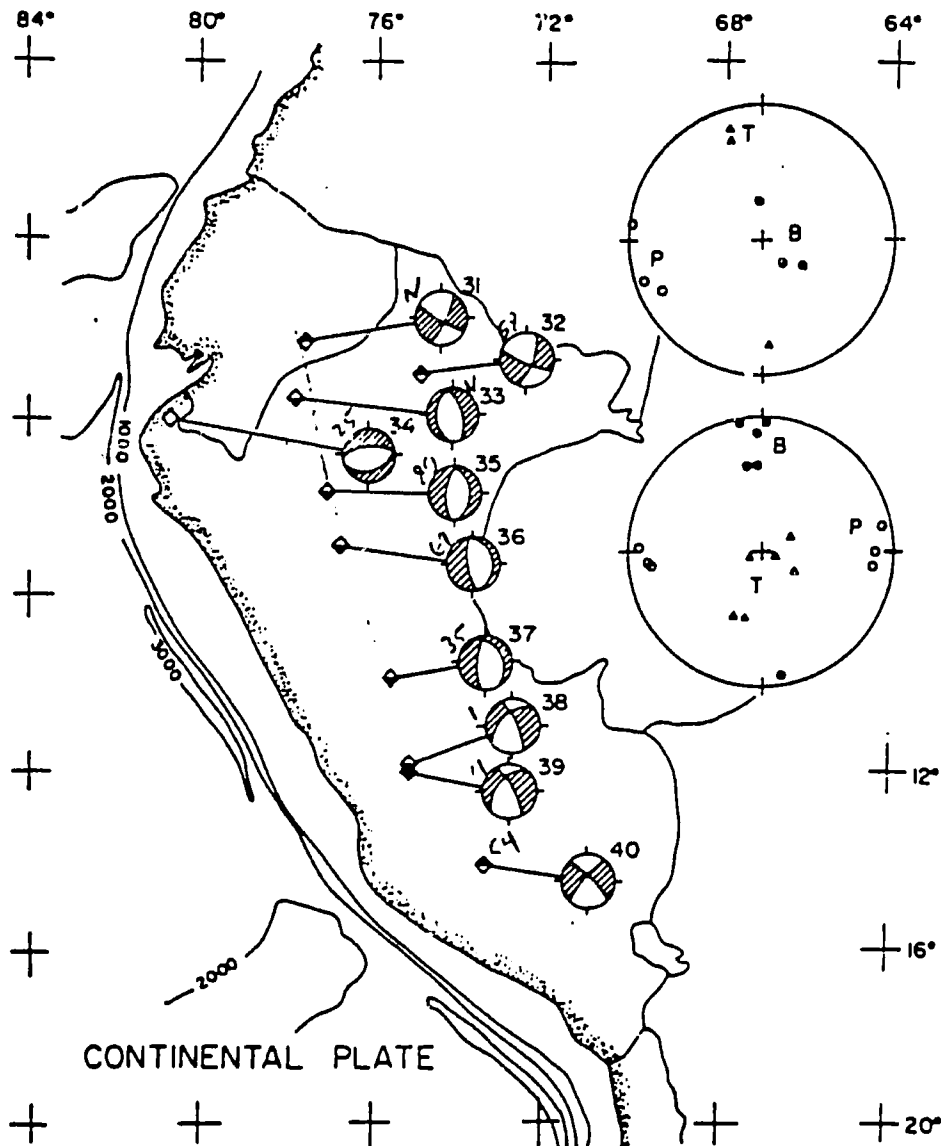


Fig. 6. Focal mechanism diagrams for foci interior to the continent within the continental lithosphere.

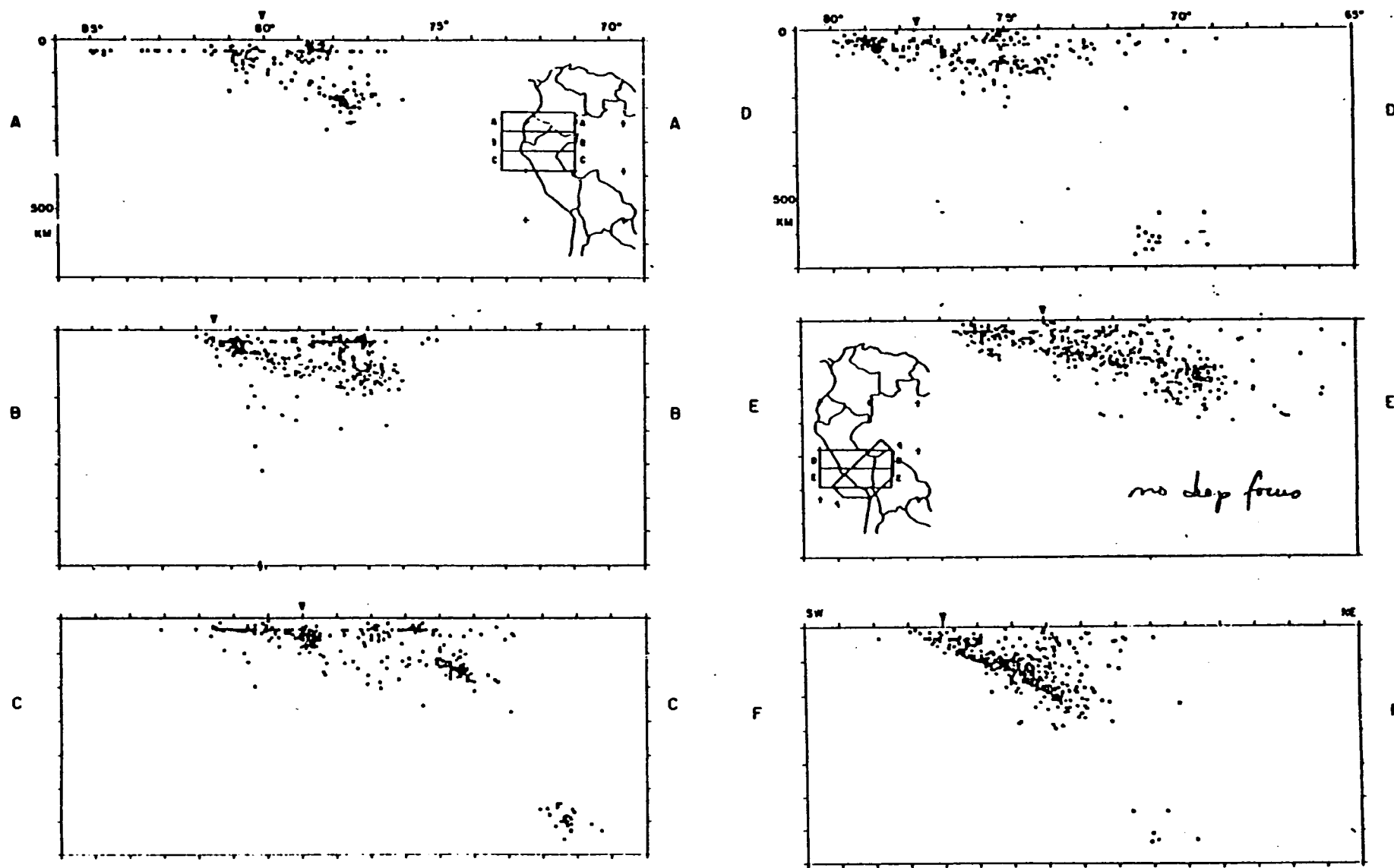
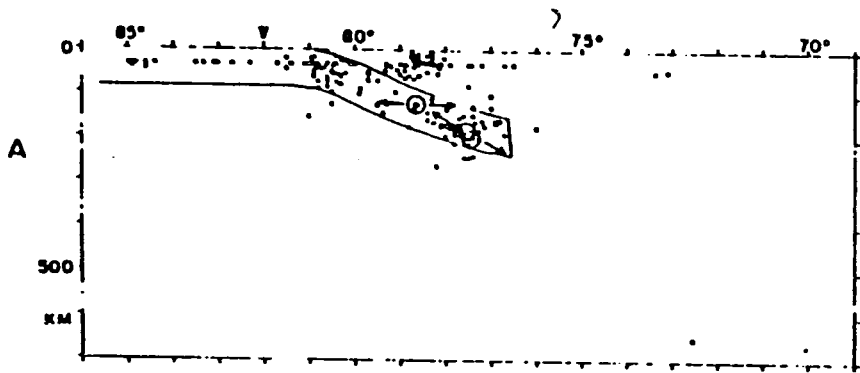
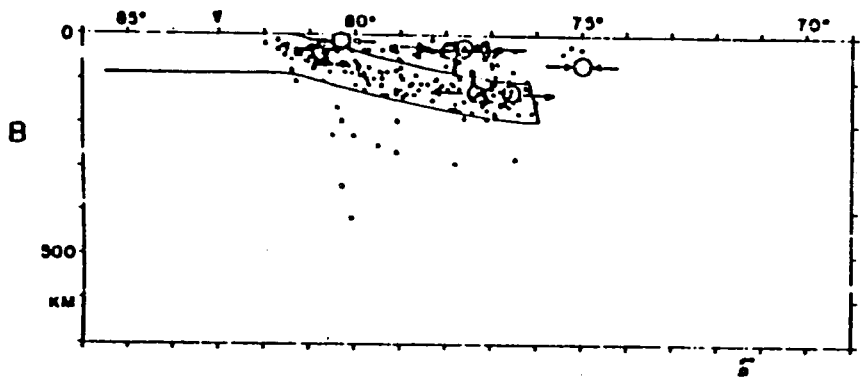


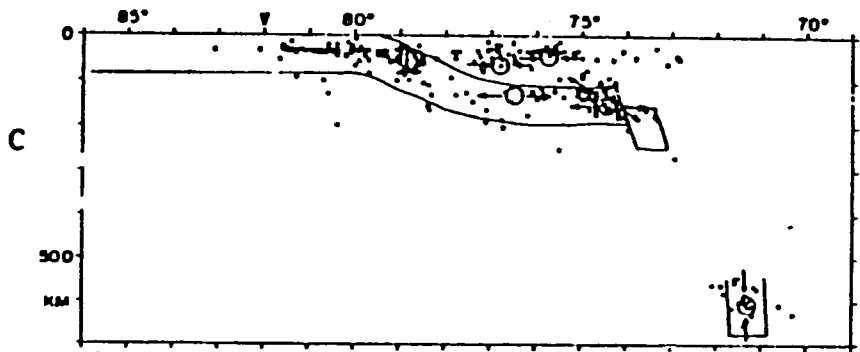
Fig. 7. Vertical sections showing the seismicity at 4° intervals of latitude along sections A-A to F-F, according to the index maps indicated in sections A-A and E-E.



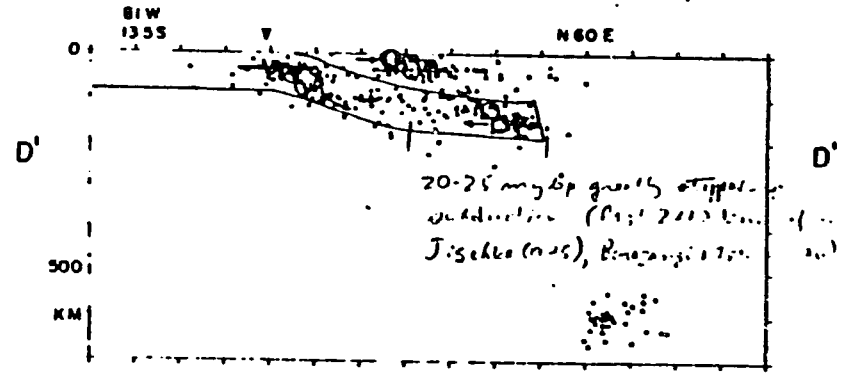
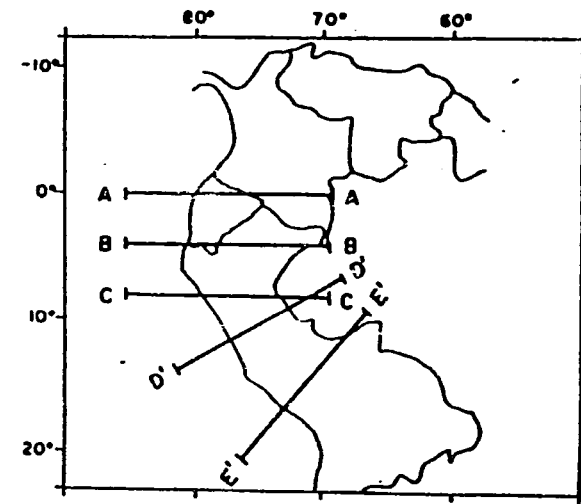
A



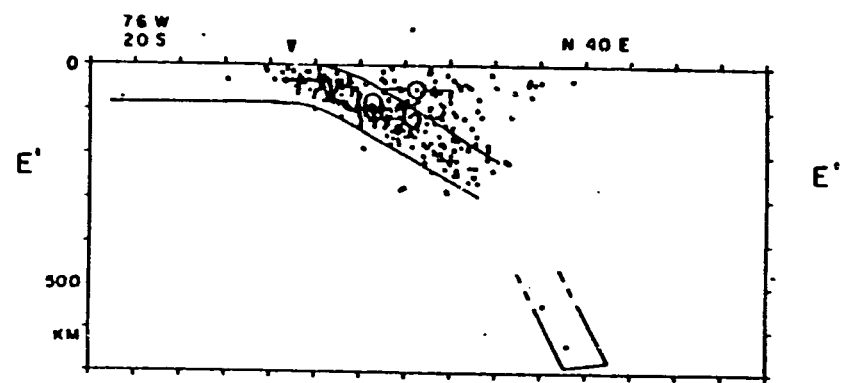
B



C



D'



E'

STAUDER: NAZCA PLATE SUBDUCTION

Fig. 8. Vertical sections showing the seismicity but with reference to an assumed slab configuration. Open circles indicate the positions of hypocenters studied in this work and located within the continental lithosphere or at intermediate depths within the assumed oceanic plate.

Acknowledgments. This research was supported by the National Science Foundation under grant GA-15816. The assistance of Shiang-ho Cheng and Robert Herrmann in the preparation of some of the illustrations is gratefully acknowledged.

REFERENCES

- Abe, K., Mechanisms and tectonic implications of the 1966 and 1970 Peru earthquakes, *Phys. Earth Planet. Interiors*, 5, 367-379, 1972.
- Chandra, U., The Peru-Bolivian border earthquake of August 15, 1963, *Bull. Seismol. Soc. Amer.*, 60, 639-646, 1970.
- Elsasser, W. M., Convection and stress propagation in the upper mantle, *Tech. Rep. 5*, Princeton Univ., Princeton, N. J., June 15, 1967.
- Isacks, B., and M. Barazangi, High frequency shear waves guided by a continuous lithosphere descending beneath western South America, *Geophys. J. Roy. Astron. Soc.*, 33, 129-139, 1973.
- Isacks, B., and P. Molnar, Distribution of stresses in the descending lithosphere from a global survey of focal mechanism solutions of mantle earthquakes, *Rev. Geophys. Space Phys.*, 9, 103-174, 1971.
- Isacks, B., J. Oliver, and L. R. Sykes, Seismology and the new global tectonics, *J. Geophys. Res.*, 73, 5855-5899, 1968.
- Jacoby, W. R., Model experiment of plate movements, *Nature*, 241, 130-134, 1973.
- Lander, J., Seismological notes—September and October 1969, *Bull. Seismol. Soc. Amer.*, 60, 685-693, 1970.
- Mendiguren, J. A., Focal mechanism of a shock in the middle of the Nazca plate, *J. Geophys. Res.*, 76, 3861-3879, 1971.
- Okada, H., Converted *F* phase from the *ScS* phase at the inclined deep seismic zone, *Carnegie Inst. Washington Yearb.*, 72, 238-245, 1973.
- Sacks, I. S., and H. Okada, A comparison of the anelastic structure between western and South America and Japan, *Carnegie Inst. Washington Yearb.*, 72, 226-233, 1973.
- Snoke, A., I. S. Sacks, and H. Okada, Empirical models for anomalous high-frequency arrivals from deep-focus earthquakes in South America, *Carnegie Inst. Washington Yearb.*, 72, 233-248, 1973.
- Stauder, W., Tensional character of earthquake foci beneath the Aleutian trench with relation to sea floor spreading, *J. Geophys. Res.*, 73, 7693-7701, 1968.
- Stauder, W., Mechanism and spatial distribution of Chilean earthquakes with relation to subduction of the oceanic plate, *J. Geophys. Res.*, 78, 5033-5061, 1973.
- Stauder, W., and G. A. Bollinger, The *S*-wave project for focal mechanism studies, earthquakes of 1963, *Bull. Seismol. Soc. Amer.*, 56, 1363-1371, 1966.
- Sykes, L. R., Seismicity as a guide to global tectonics and earthquake prediction, *Tectonophysics*, 13, 393-414, 1972.
- Sykes, L. R., and D. Hayes, Seismicity and tectonics of South America and adjacent oceanic areas (abstract), *Geol. Soc. Amer. Abstr. Program*, 3, 206, 1971.
- Wagner, D., Statistical decision theory applied to the focal mechanisms of Peruvian earthquakes, Ph.D. dissertation, 176 pp., St. Louis Univ., St. Louis, Mo., 1972.

(Received July 30, 1974;
revised October 21, 1974;
accepted November 8, 1974.)

Theory of Earthquakes

I. A Scale Independent Theory of Rock Failure

By B. T. BRADY¹⁾

Summary - A scale independent failure theory governing the initiation and subsequent growth of the shear fault in rock is presented in this article. Four distinct phases of behavior in this theory are known to precede fault growth in rock. 1) *Dilatant Phase*: Cracks form in the rock in response to the applied stresses. This phase begins at a maximum principal stress whose magnitude is usually well below the ultimate strength of the rock. 2) *Inclusion Phase*: Clusters of cracks develop in the rock at a point in time when the rock is within a few per cent of its ultimate strength. The clusters behave physically as low modulus elastic inclusions embedded within a host material of higher modulus. As a result of this 'elastic' contrast, there is a rotation of the principal stress axes and a decrease in the magnitude of the principal stress difference in the focal region of the inclusion; that is, the region into which the inclusion will grow at failure. 3) *Closure Phase*: In this phase, there is closure of cracks in the focal region in response to the decrease in the magnitude of the principal stress difference due to the formation of the inclusion. As a result of crack closure in the focal region, the stress concentration in the focal region increases and becomes a maximum once all cracks which opened during the dilatant phase are closed. At this time, the transverse tensile stress in the interior of the inclusion also reaches a maximum. Macrocrack growth within the inclusion begins. 4) *Growth Phase*: Fault growth commences during this phase. Reopening of previously closed cracks occurs due to the increase in the principal stress difference in the focal region resulting from macrocrack growth within the inclusion. New cracks form and rapid growth of the macrocrack (in its own plane) occurs once the length of the macrocrack exceeds a critical value. The fault represents the portion of the macrocrack which has closed.

Introduction

An understanding of the causes and mechanisms of earthquakes is one of the most basic problems in geophysics today. The cause of an earthquake must be the creation at some location within the earth of a stress condition sufficient to cause failure of rock. Large horizontal stresses whose magnitudes often exceed the vertical stress are known to be present in the crust and, possibly, the upper portion of the earth's mantle. Direct evidence of high excess horizontal stress has been found from static stress measurements in deep mines in the crust and from seismic studies (OBERT and DUVAL [1], WYSS and MOLNAR [2]). It is clear that these high stresses are related to plate motions and that

¹⁾ Physicist, U.S. Dept. of the Interior, BuMines, Denver Mining Research Center, Denver, Colo., U.S.A. (present address).

failures (or earthquakes) result at or near boundaries where collision or slip between plates is occurring. However, the most difficult and least understood parts of the earthquake problem are the processes involved in the focal region; that is, the region where failure occurs prior to the earthquake and, in particular, the mechanism or mechanisms which allow the stresses in the crust or upper mantle to be concentrated so as to produce the earthquake. An understanding of the processes leading to failure of rock cannot help but be of major importance to the geophysicist in his understanding of earthquake occurrence. Without this understanding, it is difficult to interpret premonitory effects observed prior to earthquakes, such as anomalous velocity and ground tilt behavior to mention a few. Without this understanding, the application of these data in developing possible methods of earthquake control becomes at best a matter of guesswork.

La
dition
portic
or tri

Background

It has been established experimentally in the laboratory that dilatancy, or the opening of cracks whose major axes are oriented in a direction parallel to the axis of maximum principal stress, commences in brittle rock at stress levels on the order of two-thirds the rock's ultimate strength (BRACE *et al.* [3]). There is some field evidence suggesting that dilatancy is an active mechanism in earthquake prone areas (CHERRY and SAVAGE [4]). Observations at Garm, U.S.S.R., the New York Adirondacks, and for the San Fernando, California, earthquake have shown that prior to these earthquakes the ratio of longitudinal (V_p) and shear (V_s) seismic velocities, V_p/V_s , decreased to anomalously low values and that earthquakes occurred shortly following the return of V_p/V_s to its normal value (SCHOLZ *et al.* [5], SEMENOV [6], WHITCOMB *et al.* [7]). Some investigators have explained the premonitory decrease in V_p/V_s in terms of dilatancy of rocks in the focal region of the impending earthquake (NUR [8], SCHOLZ *et al.* [5], WHITCOMB *et al.* [7]). Although there may be some disagreement with a dilatancy mechanism for earthquakes, the model proposed for the subsequent increase in V_p/V_s to its predilatant value; that is, diffusion of fluids into the dilatant region, prior to the earthquake, has generated considerable controversy. A major reason for this controversy is the absence of a realistic physical theory describing the processes leading to the failure of rock.

Fra:

Mc

This paper is the first part of a three-part series concerned with the physical processes responsible for producing earthquakes. In this paper, a scale independent failure theory, termed the inclusion theory, governing the initiation and growth of shear faulting in dry rock is presented. Shear faulting refers to growth of a fault in its own plane. Scale independence in the context used here requires that the fracturing characteristics of rock in the laboratory (small scale), mine (intermediate scale) and the earth (large scale) are governed by identical equations and principles. Thus laboratory studies of rock failure can provide valuable information and guidelines for understanding rock failure on the large scale and, as a result, will be found to have direct applicability to large-scale phenomena such as earthquakes. The application of the scale independent theory of rock failure to the earthquake problem will form the subject matter of Parts II and III.

Laboratory study of fault growth in rock

Laboratory tests conducted by the author on rock fracture under stiff loading conditions have shown that load carrying ability of rock begins to diminish once the proportional limit is reached (Fig. 1). These tests showed that fault growth in either uniaxial or triaxial compression did not occur until point *F* in Fig. 1(A, B) was reached. At

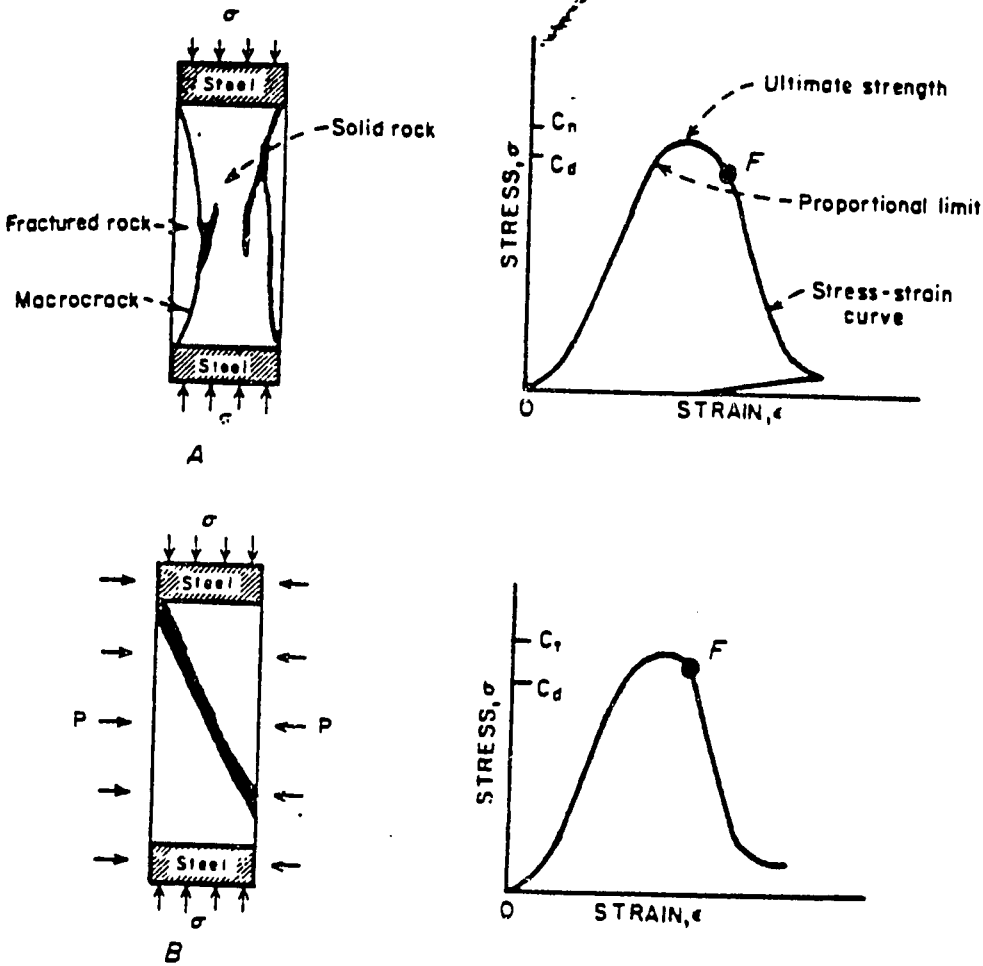


Figure 1

Stress-strain behavior of rock in pre-failure and post-failure region; A—uniaxial compression, B—triaxial compression

point *F* a sudden change was observed in the deformation rate of the sample at which time the slope of the unloading curve became equal to the testing machine stiffness; that is, there appeared to be little or no contribution due to the sample. It was as if the rock was not present in the testing system. This observation led to the series of tests discussed below.

678

Experimental procedure

Uniaxial and triaxial compression tests were made on cylindrical specimens of a marble and granite by deforming the specimens in a conventional hydraulic loading system which was artificially stiffened to 2.4×10^{12} dynes/cm by placing high strength steel columns in parallel with the specimen. Specimens were 5.39 cm diameter size with length-to-diameter values of 2.00 for uniaxial and 2.50 for triaxial tests. All specimens were compressed between hardened steel end plates whose diameter and length were 5.39 cm and 3.00 cm, respectively. Confining pressure was approximately 100 bars in the triaxial tests. Strain rate was 10^{-4} /sec. All specimens were loaded to preselected points along their respective stress-strain curves. Each specimen was then unloaded, cast in hydrostone, cut in half parallel to the core axis, polished and impregnated with a fluorescent dye to delineate the cracks. Ultraviolet light was used to delineate crack zones.

Data and data analysis

Figures 2, 3, and 4 show test results for representative samples of marble and granite deformed under uniaxial and triaxial compression. The location on the force (F)-displacement (u) curve where each sample was unloaded is indicated under each photograph. Large cracks (macrocracks) are clearly illustrated. Note that zones of small cracks (microcracks) extend well beyond the macrocracks. 'Microcrack' and 'macrocrack' as employed here are not absolute but relative terms. As a consequence of the scale independence principle to be proved later, their sizes increase as specimen size increases. However, for simplicity, I have chosen these terms in describing failure on the small (laboratory) scale.

Microscopic examination of these samples shows extensive microcrack concentration within the 'light' zones. Microcrack development within the 'dark' zones is small in comparison. The fluorescent dye did not penetrate the microcracks in the 'dark' zone. These microcracks appear to have closed during unloading of the specimen, a result suggesting the *total* dilatancy strain is composed of both a reversible and irreversible component. The irreversible component probably represents those microcracks whose stress fields are influenced by the close proximity of other microcracks. These microcracks are located in zones where the microcrack density is large. The other microcracks which are located in regions of the specimen where the microcrack density is less tend to close as the applied load is reduced. Other laboratory studies have been performed which show some of the dilatant strain is recoverable as the applied stress is reduced (SCHOLZ and KRANZ [9]).

Examination of these test specimens showed the following important observations: 1) Rock failure in compression is not due to the development of uniform microcracking (or dilatancy) but is a consequence of clustering of microcracks within certain zones in the rock; 2) The microcrack clusters in rock develop when the rock is within a few per cent of its ultimate strength; 3) The microcrack density in the cluster zone is significantly

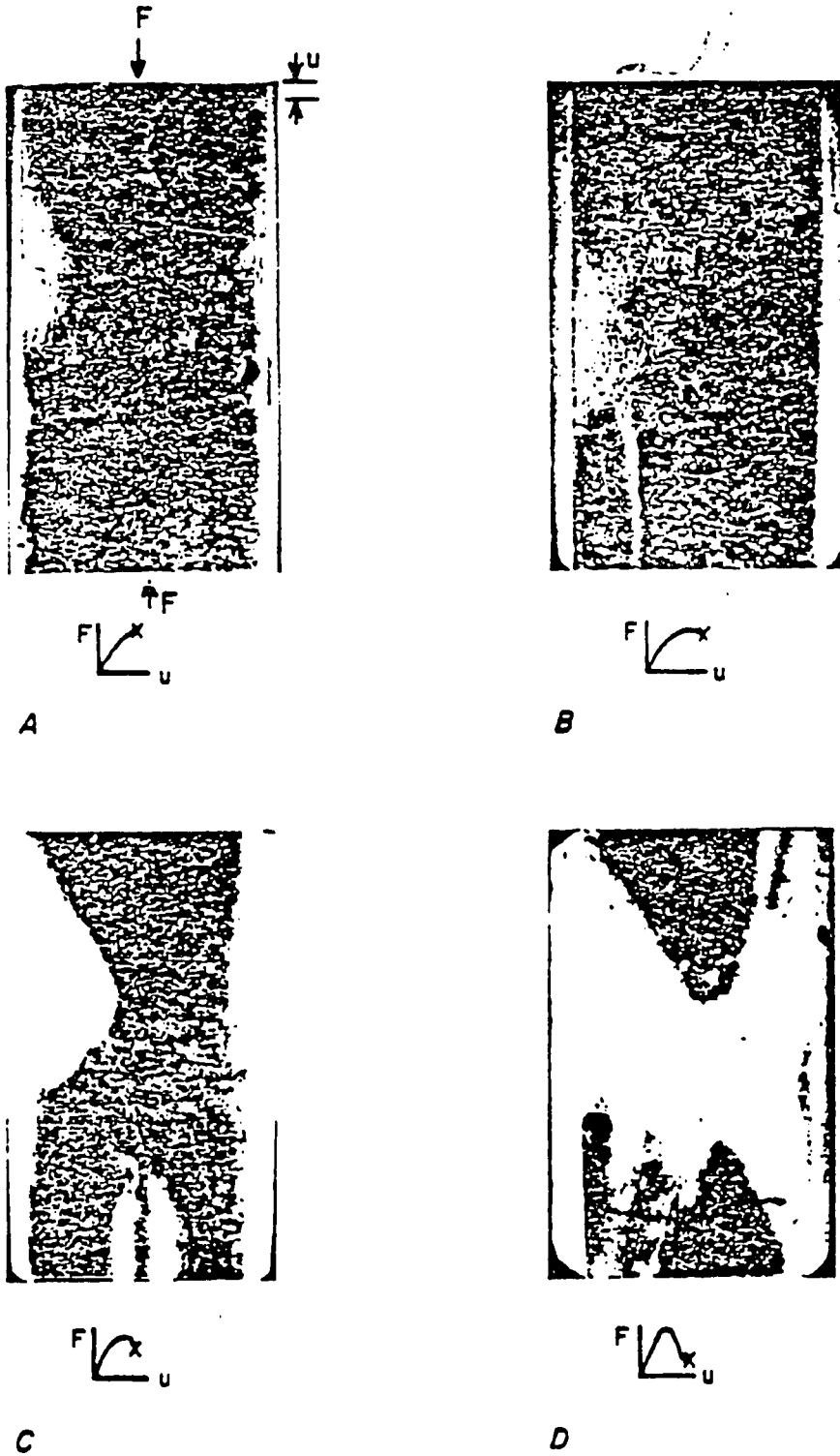
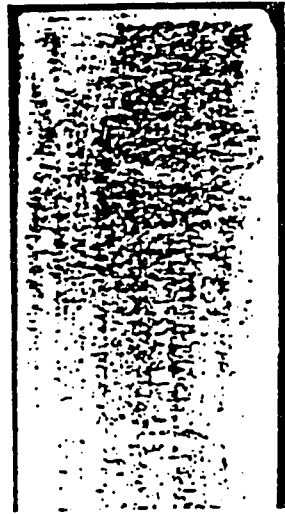
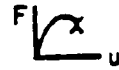


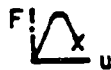
Figure 2
Fault growth in marble under uniaxial compression



A



B



C



D

Figure 3

Fault growth in marble under triaxial compression ($P = 100$ bars)

greater than the 'background' (dark) microcrack density which formed throughout the rock at a time prior to cluster formation; 4) Slabbing failure; that is, growth of macrocracks parallel to the axis of maximum applied compression, a common observation in

1081

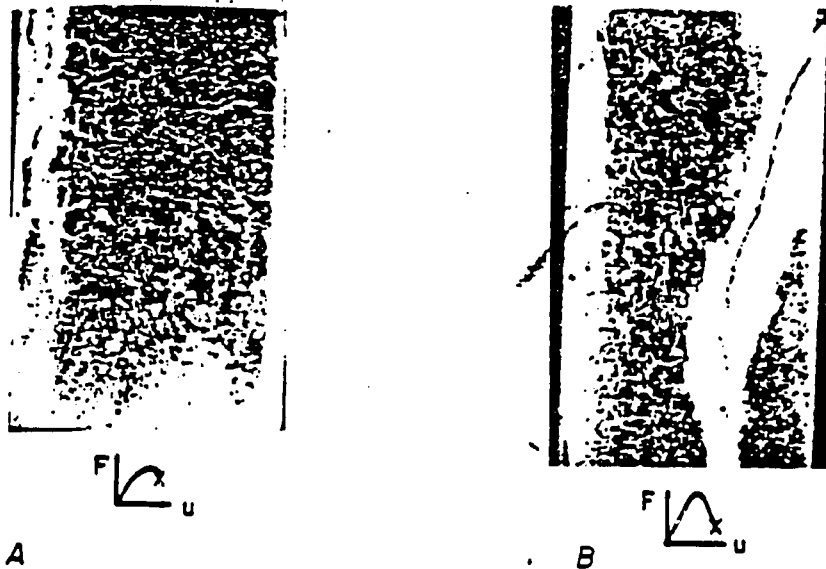


Figure 4

Fault growth in granite under uniaxial (A) and triaxial (B) compression ($P = 100$ bars)

uniaxial compression (Fig. 2), is inhibited with confining pressure (Figs. 3, 4). WAWERSIK and BRACE [10] reported a similar observation on the effect of confinement on slabbing failure in rock.

Numerical simulation of the failure process in rock

These observations suggest that the cluster zones may be treated mathematically as low modulus inclusions which are embedded within a higher modulus 'host' material. This approach should be clearly recognized and understood to be a mathematical simplification of the real problem, since inelastic strains associated with the introduction of the inclusion into the rock structure are neglected. In this simplification the zone of intense microcrack growth is replaced by an inclusion whose effective elastic properties are obtained by neglecting the inelastic strains associated with its introduction. I have studied this problem using the finite element method and have found that this idealization does not result in any significant differences in the stress distribution within or in the immediate vicinity of the inclusion.

To obtain a preliminary semiquantitative understanding of the effect of inclusions, a three-dimensional finite element analysis using approximately 1200 elements (Fig. 5) was made of an inclusion geometry similar to that shown in Fig. 3A. For calculation purposes, inclusion modulus was taken to be one-third of the host modulus. The Young's modulus and Poisson's ratio of the steel end plates were taken to be 2 Mb ($1 \text{ Mb} = 1 \times 10^6 \text{ bars}$) and 0.24, respectively. This particular finite element model physically approximates the state of the system just prior to failure. This point will become clear later in the article.

It is recognized that numerical results obtained by using the above finite element technique are only approximate, since in addition to the above limitations, the variation in microcrack density within the inclusion is not considered. In this analysis, the elastic properties of the inclusion are taken to be average properties of the inclusion zone. This method of replacing microcrack clusters by an elastic inclusion implies loading path independence since knowledge of the intermediate states of the rock system is not

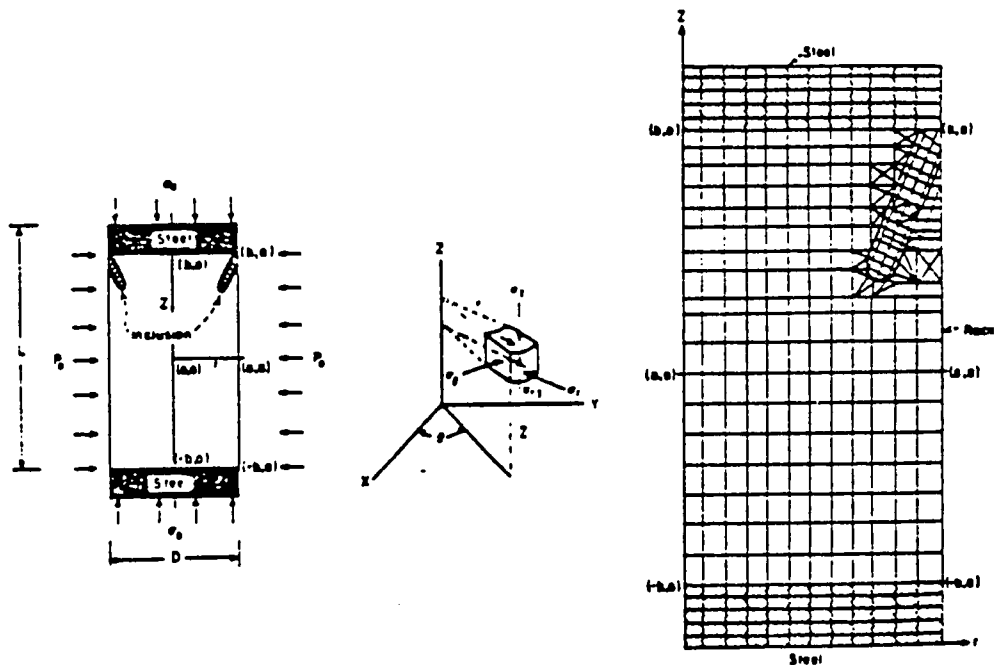


Figure 5

Specimen end plate, shear fault geometry, coordinate system nomenclature and finite element idealization of inclusion

required. Experimental laboratory evidence suggests rock failure is path independent (BROWN *et al.* [11], BRADY [12]). With this in mind, some typical results for uniaxial and triaxial compression ($P_0 = 0.10\sigma_0$, where σ_0 and P_0 are the applied axial stress and confining pressure, respectively), are shown in Figs. 6 and 7, respectively. In these figures, principal stress distributions $[(\sigma_1^*, \sigma_2^* = \sigma_3^*)$ where σ_1^* , σ_2^* , and σ_3^* represent the local maximum, intermediate and least principal stresses, respectively], and their angular relationship (Figs. 6D, 7D) to the applied principal stress system (σ_0, P_0, P_0) are shown. The following results are apparent: 1) The axes of principal stress rotate about the intermediate principal stress ($\sigma_2^* = \sigma_3^*$) axis and change in magnitude in immediate vicinity of the inclusion (hereafter referred to as 'focal volume'). As defined in this article, focal volume refers to the volume of material whose stress state outside the inclusion is affected by the presence of the inclusion. *The focal region of the inclusion is defined as the zone into which the inclusion and its associated faults will grow.* 2) In uniaxial compression, a tensile crack exists on the underside of the inclusion. The magnitude

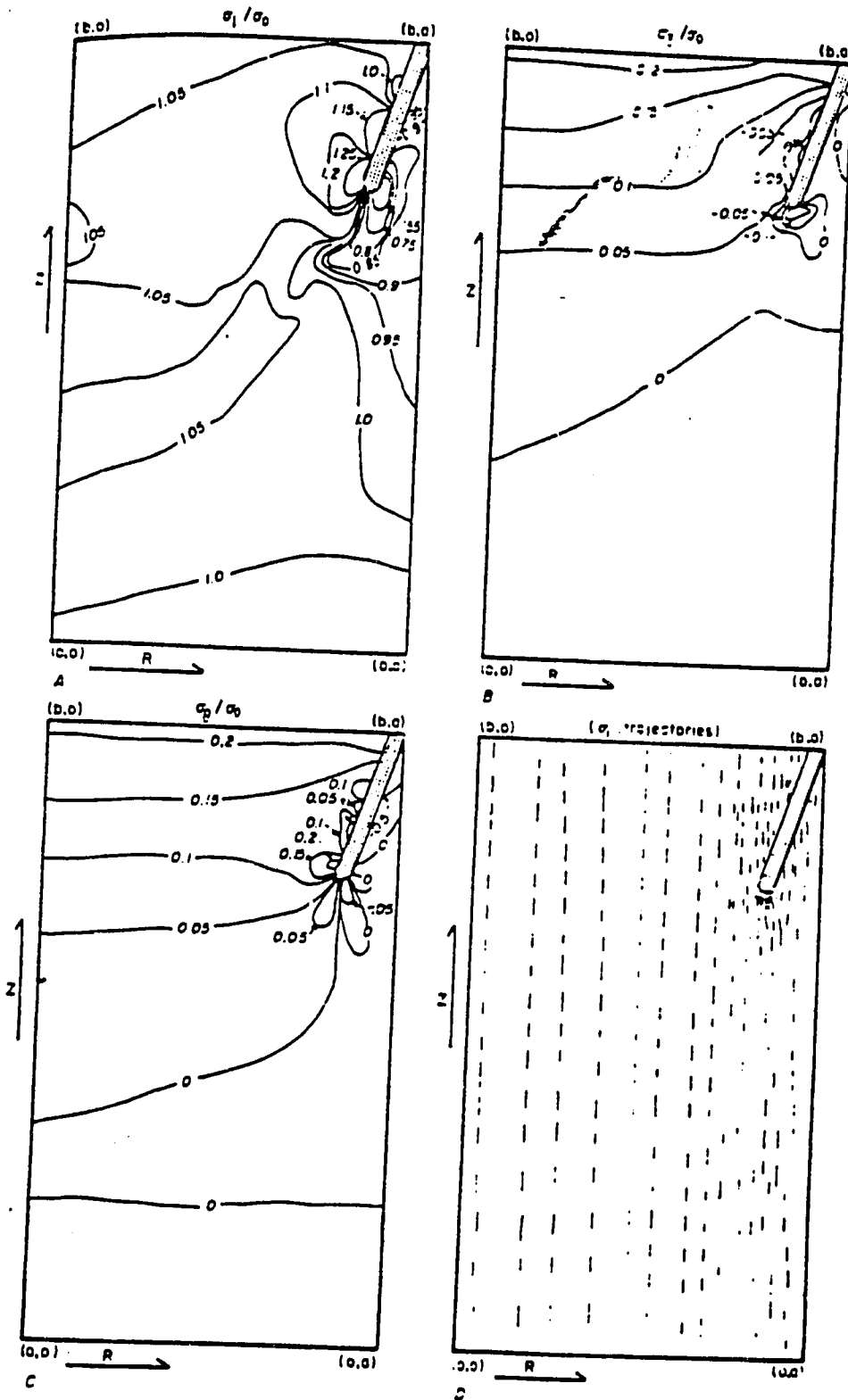


Figure 6
stress analysis of inclusion development in rock. ($P_0 = 0$, $E_0 = 0.24$ Mb, $E_1 = 0.08$ Mb, $\nu_0 = \nu_1 = 0.24$,
1 Mb = 1×10^8 bar)

uniaxial compression; a slabbing failure mode: that is, growth of microcracks and its associated macrocrack(s) in a direction parallel to σ_0 should be favored, and microcrack growth will tend to be parallel to σ_0 as was the case before the inclusion formed.

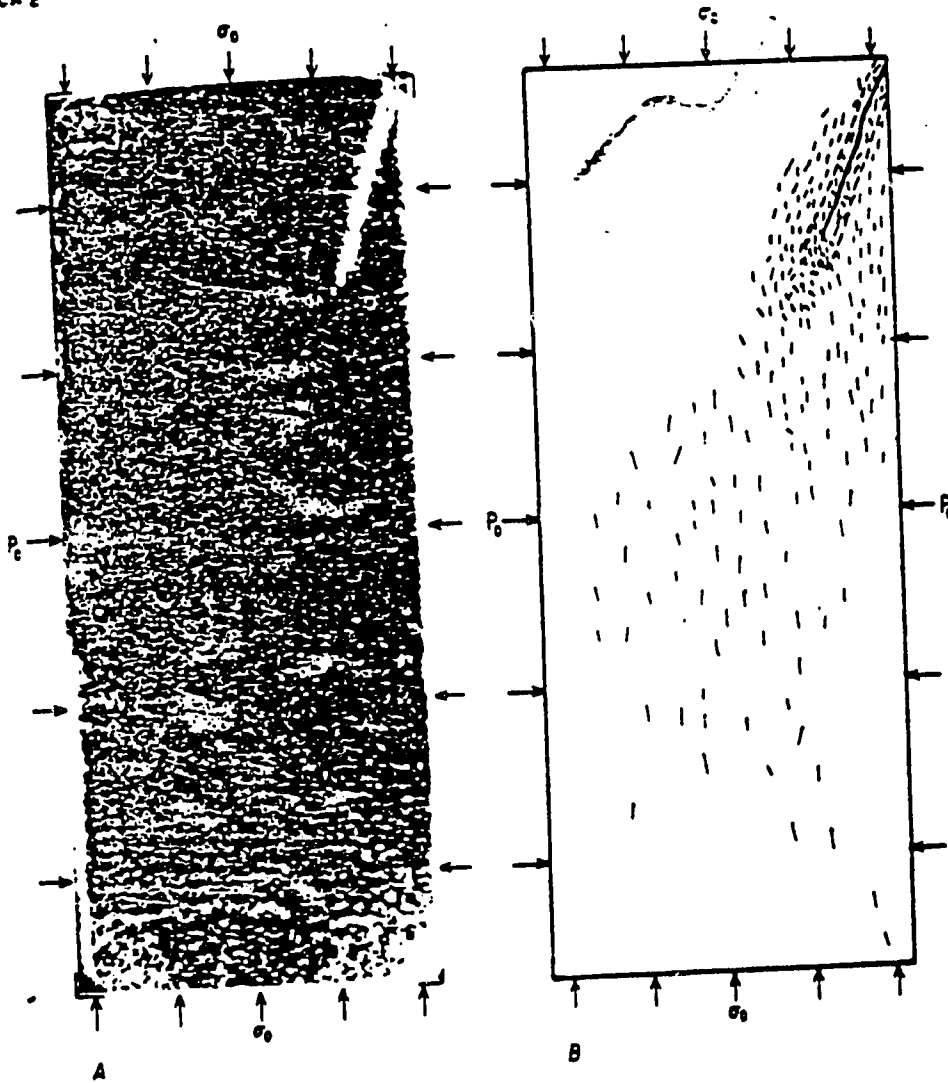


Figure 8

Fault and inclusion growth in marble showing microcrack distribution in vicinity of the macrocrack ($P_0 = 100$ bars)

As confinement pressure on the specimen increases, slab thickness, defined as radial thickness of the fractured rock segments, should increase and conditions favoring shear fault growth; that is, growth of the macrocrack in its own plane will occur, since tensile stress on the underside of the inclusion decreases. When the tensile stress on the underside is negligible, further microcracking in the focal region will be in response to the local compressive stresses. 3) The least principal stress within the inclusion is tensile and is oriented in a direction approximately normal to the major (long) axis of the inclusion.

Figure 8 is a photograph of a marble specimen ($P_0 = 100$ bars) showing inclusion geometry and microcrack distribution in the vicinity of the macrocrack. Note microcracks in the vicinity of the inclusion are oriented subparallel to the long axis of the inclusion, a result that is in qualitative agreement with the finite element predictions. In the inclusion phase, stress distortion in the vicinity of the inclusion causes new microcracks to form at a small angle ($\sim 10^\circ$) to σ_0 ; that is, subparallel to the inclusion long axis when the confining pressure is sufficient to inhibit microcrack formation on the underside of the inclusion. Microscopic examination of the microcrack distribution in the inclusion shows a larger microcrack density exists near the upper portions of the inclusion than near the inclusion tip. As a result of the microcrack density gradient within the inclusion, it would be expected that the macrocrack in the inclusion will extend in the plane of the inclusion just prior to shear failure, since the tensile stress at the tip of the macrocrack is normal to the long axis of the inclusion. Our tests show macrocrack growth is governed by the inclusion direction this adding support to this observation. The reader should observe that the inclusion and its focal region are not separated by a distinct boundary. This point is discussed at length later in the paper.

The inclusion failure theory on this small scale gives qualitative predictions regarding rock failure in uniaxial and triaxial compression in qualitative agreement with experimental laboratory observations. This model is now used to develop a failure criterion governing shear fault growth in laboratory rock specimens under triaxial compression. Failure in rock specimens under applied tension and combined tension-compression is not explicitly considered at this time.

Failure criterion for shear fault growth

These and other experimental studies of rock failure suggest three distinct phases of behavior occur before or slightly after the ultimate strength of rock is reached. 1) *Pre-Dilatant Phase*: This phase begins with closure of open cracks throughout the rock volume due to the application of compressive stresses to the rock. Once most of the open cracks have closed, the axial stress-strain curve becomes linear. Frictional sliding occurs along favorably oriented closed cracks in this phase (BRACE *et al.* [3]). 2) *Dilatant Phase*: Formation of new cracks (microcracks) occurs uniformly throughout the rock and the microcracks grow in a direction roughly parallel to the axis of applied maximum compression. This phase begins at stresses typically on the order of one-half to two-thirds the rock ultimate strength (BRACE *et al.* [3]). However, there are some rocks, such as fine-grained Solenhofen limestone, where the fracture initiation stress; that is, the stress required to initiate dilatancy and ultimate strength, are observed to be nearly equal. Rocks of this type usually fail violently in either uniaxial or triaxial compression. 3) *Inclusion Phase*: Clusters of microcracks develop within the rock, usually within a few per cent of ultimate strength; that is, near or slightly after the proportional limit stress has been reached. These zones can be represented physically as low modulus inclusions embedded within a host material of higher modulus. As a result of this

'elastic' contrast, there is both a rotation and change in magnitude of the principal stresses in the focal region of the inclusion.

Two further phases are now postulated to be necessary and sufficient conditions in initiating fault growth. 1) *Closure Phase*: In this phase there is closure of microcracks in the focal volume and, in particular, the focal region of the inclusion due to the decrease in magnitude of the local principal stress difference. Laboratory studies have clearly shown that addition of confining pressure to rock deformed into the dilatant phase can result in closure of previously open microcracks (BROWN and SWANDON [13]). Tests performed at our laboratory support this observation. The finite element results in Fig. 7 indicate there is a considerable increase in local ($\sigma_1^* \approx 1.35\sigma_0$, $\sigma_2^* = \sigma_3^* \approx 3P_0$) mean pressure in the material on the upper side of the inclusion due to the presence of the low modulus inclusion; that is, the ratio of σ_3^* to σ_1^* in the focal region ranges from 0.12 to almost 0.20 for a modulus reduction in the inclusion of only one-third. Note that on the under side of the inclusion (Fig. 7) the local maximum principal stress decreases. Closure of previously open microcracks should also occur here. As a result of crack closure in the focal volume, the stress concentration in the focal region of the inclusion increases and becomes a *maximum* once all cracks are closed. At this point in time, the transverse tensile stress in the interior of the inclusion also reaches a maximum value. Macrocrack growth within the inclusion due to microcrack formation in response to tensile stress in the inclusion begins. As a result of macrocrack formation within the inclusion, the stress concentration throughout the focal volume and the tensile stress component within the inclusion increase. New microcracks may also form at the inclusion tip in response to local high stress conditions during this phase. 2) *Growth Phase*: Fault growth commences during this phase. (Some phases of 'growth' are slow and others catastrophic. The relative stiffnesses of the loading system and the failing region determine which type of 'growth' process prevails. For example, if the post-failure stiffness of the failing region exceeds or equals the loading system stiffness, growth will be catastrophic.) Reopening of previously closed microcracks occurs. The system becomes unstable and rapid growth of the macrocrack (in its own plane) occurs once the length of the macrocrack exceeds a critical value. Note this model explains the observed break in the stress-strain curve shown at point *F* in Fig. 1. Sliding on the fault surface occurs once the macrocrack has traversed the specimen. In the inclusion theory of failure, the fault refers to that portion of the macrocrack which has closed. Thus the inclusion and its associated macrocrack precede the fault.

Analysis

The above test results suggest that failure of rock in shear is in actuality failure in tension, since the macrocrack within the inclusion grows because of tensile stress. The inclusion, however, accretes (or grows) by compression generated microcracks. This process is in turn enhanced by growth of the macrocrack within the inclusion suggesting that shear failure occurs once the length of the macrocrack within the inclusion

exceeds some critical value. Consequently, shear fault growth may be governed by a maximum tensile stress failure criterion.

Let the inclusion shown in Fig. 9 be approximated by an isotropic ellipsoidal shaped material of Young's modulus E_i , embedded within a host material of modulus E_h . The host material is subjected to applied maximum and minimum principal stresses, σ_{10} and σ_{30} , respectively, at distances far removed from the inclusion boundary.

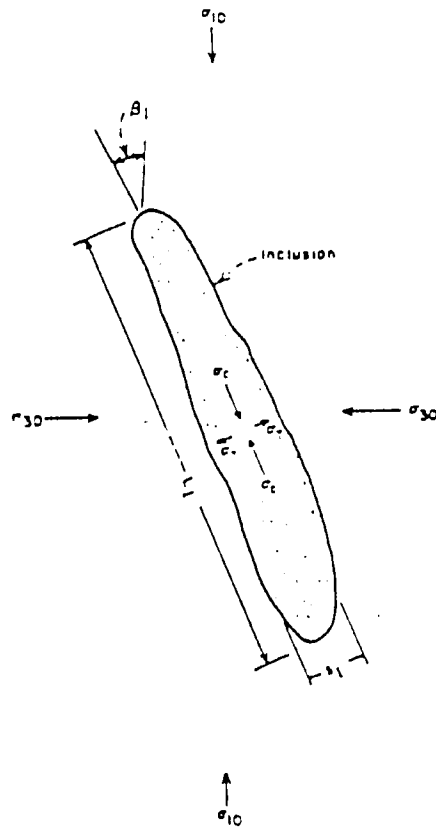


Figure 9

Schematic illustration of inclusion and associated nomenclature

The inclination of the major axis of the inclusion to the direction of the maximum principal compression stress (σ_{10}) is β_i . The aspect ratio of the inclusion is $\alpha_i (=s_i/L_i)$, where s_i and L_i are the average thickness and length of the inclusion, respectively). When the Poisson's ratio of the inclusion and host are equal, the stress distribution within the inclusion for the case of plane strain is (DONNELL [14]).

$$\sigma_c = b_{13} \sigma_{10} + b_{11} \sigma_{30} \quad (1)$$

$$\sigma_n = b_{33} \sigma_{10} + b_{31} \sigma_{30}$$

where σ_c and σ_n denote the principal stresses parallel and normal, respectively, to the major axis of the inclusion. There will be also a shear stress component which is a

function of position within the inclusion. However, this stress is of second order and can be safely neglected when the aspect ratio of the inclusion is small. The coefficients b_{ij} ($i, j = 1, 2, 3$) in equation (1) are (DONNELL [14])

$$\begin{aligned} b_{11} &= \frac{1}{2}(1 - \cos 2\beta_i) a_{11} + \frac{1}{2}(1 + \cos 2\beta_i) a_{13}; \\ b_{13} &= \frac{1}{2}(1 + \cos 2\beta_i) a_{11} + \frac{1}{2}(1 - \cos 2\beta_i) a_{13}; \\ b_{31} &= \frac{1}{2}(1 - \cos 2\beta_i) a_{31} + \frac{1}{2}(1 + \cos 2\beta_i) a_{33}; \\ b_{33} &= \frac{1}{2}(1 + \cos 2\beta_i) a_{31} + \frac{1}{2}(1 - \cos 2\beta_i) a_{33}, \end{aligned} \tag{2}$$

where

$$\begin{aligned} a_{11} &= \frac{3K}{D} [3(K + \alpha^2) + (1 + 5K)\alpha_i]; & a_{13} &= \frac{3K}{D} [(1 - K)(1 - \alpha_i)] \\ a_{31} &= -\frac{3K}{D} [(1 - K)\alpha_i(1 - \alpha_i)]; & a_{33} &= \frac{3K}{D} [3(1 + K\alpha_i^2) + \alpha_i(1 + 5K)] \end{aligned} \tag{3}$$

$$D = 9K(1 + \alpha_i^2) + 2\alpha_i(2 - K + 8K^2).$$

The K value is E_i/E_n . The process of macrocrack formation is illustrated in Fig. 10A.

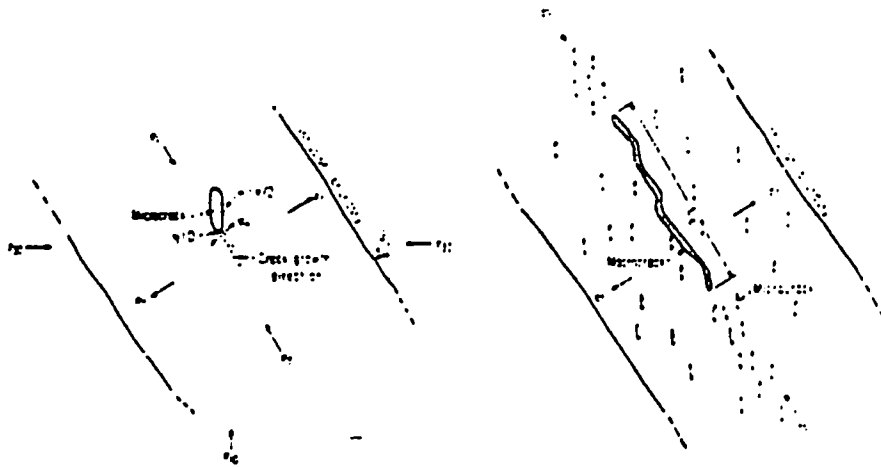


Figure 10
Sequence of macrocrack growth within the inclusion

This figure shows an elliptical microcrack of aspect ratio α within the inclusion. Applied to this geometry, the analytical expression for the tangential stress, σ_η , along the boundary of this microcrack is approximately (JAEGER [15])

$$\sigma_\eta \approx \frac{(\sigma_c + \sigma_i) \sinh 2x + (\sigma_t - \sigma_c) [e^{2x} \cos 2(\beta_i - \eta) - \cos 2\beta_i]}{\cosh 2x - \cos 2\eta} \tag{4}$$

Equations (2), (3) and (4) show that σ_n is a function of α_i , β_i , η , K and the applied stress σ_{10} and σ_{30} ; that is,

$$\sigma_n \approx F(\beta_i, \eta, \alpha_i, K, \sigma_{10}, \sigma_{30}). \quad (5)$$

To find where σ_n is an extremum, the condition $d\sigma_n = 0$ is imposed on equation (5). This condition requires solving the equations

$$\frac{\partial \sigma_n}{\partial \eta} = 0 \quad (6a)$$

$$\frac{\partial \sigma_n}{\partial \beta_i} = 0 \quad (6b)$$

$$\frac{\partial \sigma_n}{\partial \alpha_i} = 0 \quad (6c)$$

for the critical values of $\eta (= \eta_c)$, $\beta_i (= \beta_{ic})$ and $\alpha_i (= \alpha_{ic})$ and substituting these results into equation (4). The maximum value of the resulting tangential stress, σ_n , is then found by letting K approach its minimum value. This value occurs when all microcracks which were originally open during the dilatant phase close in the focal region of the inclusion. The variables in equation (5) are related to each other in such a way as to maximize the tangential stress, σ_n , along the surface of each microcrack within the inclusion. For example, equations (4) and (6a) can be combined to give

$$\eta = \eta_c \approx \frac{\alpha[\sigma_i \cos^2 \beta_i + \sigma_c \sin^2 \beta_i - \sqrt{\sigma_i^2 \cos^2 \beta_i + \sigma_c^2 \sin^2 \beta_i}]}{(\sigma_i - \sigma_c) \sin \beta_i \cos \beta_i}, \quad (7)$$

and substituting equation (7) into equation (4) gives

$$\sigma_n \approx \frac{1}{\alpha} [\sigma_i \cos^2 \beta_i + \sigma_c \sin^2 \beta_i + \sqrt{\sigma_i^2 \cos^2 \beta_i + \sigma_c^2 \sin^2 \beta_i}]. \quad (8)$$

The solution of equations (6b) and (6c) and imposing the constraint that K becomes a minimum at failure is involved but can be accomplished numerically.

Two important results follow from equations (6b), (6c), and (8). 1) The equations reduce to the Griffith equations when $K = 1$; that is, when there is no elastic contrast between the inclusion and host materials. *This illustrates the important result that the Griffith theory is a limiting case of the inclusion failure theory.* 2) Figure 10A shows the trajectory of the macrocrack growing from the microcracks based on this analysis. It is important to note that the direction of new growth will be parallel to the major axis of the inclusion. Thus the macrocrack within the inclusion (Fig. 10B) should exhibit a step-like pattern. Therefore the process by which the macrocrack is formed is due to the formation of additional inclined microcracks in response to the tensile stress existing within the inclusion. *Since the major axes of the microcracks comprising the*

inclusion tend to cluster parallel to the direction of the maximum principal compressive stress axis, the value of applied stress when rapid unstable shear failure occurs is approximately equal to the value required to initiate new microcrack growth within the inclusion. Consequently, the reasoning advanced that the criterion for shear failure, namely, that the length of the macrocrack must exceed a critical value, say L_c , is given theoretical justification. The failure criterion is given by the condition

$$b_{33}\sigma_{1f} + b_{31}\sigma_{3f} = \sigma_f, \quad (9)$$

where subscript 'f' refers to the magnitude of the principal applied stresses at failure. The coefficients b_{33} and b_{31} , given by equations (2) and (3), are used with the appropriate values of β_{1c} and α_{1c} determined from equation (6).

The value of the critical tension stress at failure (σ_f) can be derived directly from the energy considerations used by Griffith. The result is (JAEGER [15])

$$\sigma_f = -T_0 = -\sqrt{\frac{E_0\gamma_c}{L_c}}, \quad (10)$$

where E_0 is the value of the intrinsic Young's modulus of the rock specimen when all cracks in the rock are closed ($E_h = E_0$), γ_c is the surface energy of the macrocrack per unit area and L_c is the length of the macrocrack when unstable fault growth occurs. The value of K to be used in equation (9) has been derived elsewhere and is (BRADY [12])

$$K = \frac{E_1}{E_h} (1 + \frac{1}{2} E_h \Delta\beta), \quad (11)$$

where $\Delta\beta = \beta - \beta_h$ and E_h and β_h are the values of Young's modulus and compressibility, respectively, in the focal region of the inclusion when all cracks which opened during the dilation phase are closed. β is the compressibility of the focal region at a time, say Δt , into the closure phase. The compressibility difference, $\Delta\beta$, in equation (11) is a time-dependent function not only because closure of cracks involves sliding on crack surfaces which is a time-dependent process but also because the rate of the closure is a function of the loading rate existing in the focal region of the inclusion.

There are a number of consequences of the inclusion failure theory. 1) Curvature of the failure envelope in $(\sigma_{1f}, \sigma_{3f})$ space is a function of σ_{3f} , since E_h in rocks is known to be a function of confining pressure. The non-linearity of the failure envelope decreases as the confining stress σ_{3f} increases and the envelope becomes linear when $E_h = E_0$. 2) The rock specimen will exhibit a tendency for a more violent failure as confining stress increases, since the 'elastic' contrast between the inclusion and host material increases; that is, the effective post-failure stiffness of the specimen (see Fig. 1) increases relative to the loading system stiffness. Both these observations have been observed experimentally (WAWERSIK and BRACE [10], BRADY *et al.* [16]). 3) The inclusion failure criterion is a general failure theory in that it becomes possible to predict the fracturing characteristics of the material under any loading state once the failure conditions has been

determined from a simple loading state such as uniaxial compression or uniaxial tension. The only restriction is that the material behavior remain the same under the loading states considered. Consequently, in the inclusion theory, rock failure is described by the general function

$$G\left(\sigma_{1f}, \sigma_{3f}, \alpha_{1f}, \beta_{1f}, \frac{E_f}{E_h}, \Delta\tau, -T_0\right) = 0, \quad (12)$$

where $\Delta\tau$ refers to the total time required to close cracks in the focal region of the inclusion. This time, defined as the precursor time, is discussed below.

Relationship of precursor time to focal region conditions

Precursor time, $\Delta\tau$, will be defined to be the time interval between the initiation of the microcrack closure phase and the occurrence of failure. The functional relationship of $\Delta\tau$ to the physical and geometrical characteristics of the focal region and inclusion is found as follows. Consider a volume element, dV_{fr} , of the total focal region volume V_{fr} . Let E_{fr} denote the value of the Young's modulus at a time, t , into the closure phase of the rock material in the vicinity of dV_{fr} . The inelastic strain increment, $d\epsilon$, in dV_{fr} resulting from closure of microcracks in response to an increment in pressure, dP , is proportional to the density of microcracks in dV_{fr} (BRADY [12]); that is,

$$d\epsilon \approx \frac{3A_1 \rho}{E_{fr}} dP, \quad \Delta\epsilon = \frac{3A_1 \rho \Delta P}{E} \quad (13)$$

where A_1 is a constant and ρ is the microcrack density ($\rho = n/dV_{fr}$, where n is the number of microcracks within dV_{fr}). Let \dot{P} represent the rate of pressure increase occurring within dV_{fr} during the closure phase. Then

$$dP = \dot{P} dt. \quad (14)$$

The total inelastic strain, ϵ , in dV_{fr} , due to microcrack closure is

$$\epsilon \approx \int_0^{\Delta\tau} \frac{3A_1 n \dot{P}}{E_{fr} dV_{fr}} dt \approx \frac{3A_1 n \dot{P}}{E_{fr} dV_{fr}} \Delta\tau \quad \epsilon = \frac{3A_1 \rho \Delta P \dot{P} \Delta\tau}{E} \quad (15)$$

where the change in E_{fr} during the time dt produced by microcrack closure in dV_{fr} is neglected. If $\bar{\epsilon}$ denotes the average strain within dV_{fr} due to closure of an average size microcrack, $\epsilon \approx n\bar{\epsilon}$, and equation (15) can be written

$$\Delta\tau \approx \frac{\mu \bar{\epsilon} E_{fr}}{\dot{P}} dV_{fr} \quad \epsilon' \dot{P} = \frac{3A_1 n \dot{P} \Delta\tau}{E} \quad (16)$$

↑
this is wrong.

$$\Delta\tau = \frac{\mu \bar{\epsilon}}{\dot{P}} E'$$

where $\mu (= 1/3A_1)$ is a constant. The precursor time, $\Delta\tau$, defined as the time required to close all microcracks in V_{fr} is

$$\Delta\tau \approx \int_{V_{fr}} \frac{\mu \bar{E} E_{fr}}{\dot{P}} dV_{fr} \tag{17}$$

where the integration is performed throughout the focal region volume. It is important to observe that both \dot{P} and E_{fr} in equation (17) are variables whose magnitudes depend not only on their position in the focal region but also on time. This result should not be surprising since the microcrack density within the focal region is variable; that is, the microcrack density gradually diminishes in magnitude away from the inclusion and is zero in the uncracked rock volume, the Young's modulus of which is E_n .

If we let $\langle \dot{P} \rangle$ and E_n denote the average values of the loading rate and the Young's modulus in the focal region just prior to failure, respectively, equation (17) can be approximated by

$$\Delta\tau \approx \frac{\mu \bar{E} E_n V_{fr}}{\langle \dot{P} \rangle} \tag{18}$$

The focal region volume can be approximated by $V_{fr} \approx A_{fr} s_i$, where A_{fr} is the area of the focal region and s_i is the inclusion thickness which is approximately the same as the focal region thickness. If L represents an effective length of the focal region, $A_{fr} \approx L^2$, and the precursor time can be expressed

$$\Delta\tau \approx \frac{\mu \bar{E} (E_n s_i)}{\langle \dot{P} \rangle} L^2, \tag{19}$$

or simply, precursor time as defined in this article is proportional to the square of the focal region length. It should be noted that this type of relationship; that is, $\Delta\tau \sim L^2$, has been used to justify the assumption that a diffusion-like process is operative in the focal region since $L \sim \sqrt{\Delta\tau}$ behaves formally as a diffusion length. However, this type of relationship arises from the inclusion theory for entirely different reasons.

Equation 19 can be rewritten as

$$\Delta\tau \approx m K_{fr} A_{fr} \tag{20}$$

where $m = \mu \bar{E} / \langle \dot{P} \rangle$ and $K_{fr} = E_n s_i$ is the stiffness of the focal region in the direction parallel to the long axis of the inclusion just prior to failure. Equation (20) shows that a stiff focal region (K_{fr} large) will be characterized by a long precursor time when both A_{fr} and m are constant. This relationship implies that more strain energy can be stored within the focal volume as A_{fr} increases. It follows from this result that the logarithm of precursor time is linearly related to earthquake magnitude. This type of relationship has been observed for earthquakes (SCHOLZ *et al.* [5]) and for mine failures (READY [17]).

Principle of scale independence in failing rock

Figure 11 shows precursor time as a function of earthquake dimension L which is estimated from the aftershock area. Two additional data points are included with the earthquake data in this figure, one point from a rock burst in northern Idaho and the other from a coal mine roof fall in Pennsylvania (BRADY [17]). Precursor time (approximately one to two days) for the rock burst was determined from V_p and rock

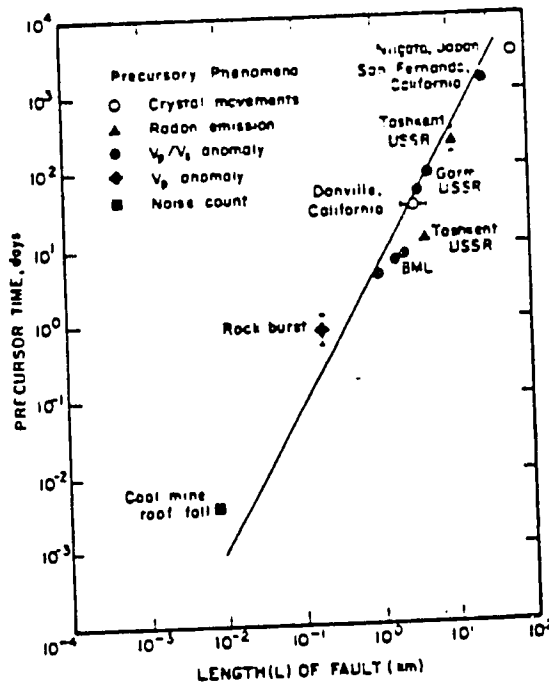


Figure 11
Precursor phenomena prior to earthquakes and mine failures

noise count anomalies prior to the burst. Precursor time for the coal mine roof fall (~15 minutes) was found from a significant noise count decrease prior to the roof fall. Volumes of rock affected by these failures were accurately determined in both cases. The data in Fig. 11 show that to a good approximation

$$\frac{d(\Delta\tau)}{dA_{fr}} \approx \text{constant}, \tag{21}$$

for a wide range of earthquake sizes including the intermediate scale earthquake (or rock burst) in northern Idaho and a coal mine roof fall in Pennsylvania. [The reader should note that the precursor times used for the mine failures in Fig. 11 are measured (approximately) from the initiation of crack closure to the time of failure. The use of a precursor time measured from dilatancy initiation to failure would result in a slight

increase (10-20%) of the mine failure precursor times]. A consequence of the closure phase portion of the inclusion theory is that the precursor time, or the time required to close all cracks in the focal region, will be proportional to the focal region area. Thus the result predicted by equation (19) should not be surprising. What is of importance, however, is that the data in Fig. 11 clearly suggest that some form of scale independence is operative in rock failure. The inclusion theory is by its very nature a scale independent theory: that is, given two systems, each containing an inclusion scaled in size in proportion to the relative dimensions of the two systems, the stress and displacement distributions in each system will be identical when the same boundary conditions are applied to each system. Therefore, it should be possible to determine whether the basic postulates of the inclusion theory; namely, closure of cracks in the focal region and the existence of a critical aspect ratio (thickness-to-length) of the inclusion at failure, follow from equations (17) and (21). This proof would furnish a strong test of the applicability of the inclusion theory to rock failure on any scale. This problem is considered below.

When the inclusion modulus, E_i , is much less than the focal region modulus E_{tr} , the pressure concentration factor, k , in the focal region near the inclusion is approximately (DONNELL [14])

$$k \approx \gamma \frac{L_i}{s_i}, \quad (22)$$

where γ is a constant and L_i is the length of the inclusion. Similarly, when the inclusion modulus, E_i , is less than the focal region modulus, E_{tr} , the stress concentration factor, k , in the focal region of the inclusion is approximately E_{tr}/E_i . Therefore, to a first approximation,

$$k \approx E_{tr}/E_i \quad (23)$$

Combining equations (22) and (23) gives the relationship between the elastic and geometrical properties of the inclusion and focal region to be

$$\frac{E_{tr}}{E_i} \alpha_i \approx \gamma. \quad (24)$$

Equation (24), together with the data in Fig. 11, suggest that scale independence is operative in rock failure; that is, the fracturing characteristics of rock are similar regardless of specimen size. A functional relationship that is similar in form to equation (24), only much more complex, can be derived by using equations (2), (9) and (10). However, the essential functional interrelationship of α_i and E_{tr}/E_i is not changed by the above approximate analysis.

The parameters in equation (24) can now be interpreted in terms of the inclusion failure theory outlined in the previous section. Equations (17) and (21) can be combined to give

$$(\mu \bar{e}) \frac{E_{tr} s_i}{\rho} \approx \text{constant}. \quad (25a)$$

Substituting equation (24) into (25a) gives

$$\gamma(\mu\bar{\epsilon}) \frac{E_i L_i}{p} \approx \text{constant.} \quad (25b)$$

The elastic contrast between the focal region and inclusion increases during the closure phase; that is, the stress concentration at any point in the focal region increases and reaches its maximum value just prior to failure. Accordingly the average value of the loading rate increases during this time and also reaches a critical maximum value just prior to failure. Equation (25a) shows that focal region modulus must also reach a maximum value at this time. Furthermore, since the inclusion modulus does not vary significantly during this time interval, the length of the inclusion must approach a critical value, say L_{ic} , before failure can occur. Therefore, failure occurs when the aspect ratio of the inclusion approaches the value α_{ic} ($= s_i/L_{ic}$). At the instant of failure, equation (25) can then be written

$$\frac{E_h}{E_i} \alpha_{ic} \approx \gamma. \quad (26)$$

This analysis, together with the theoretical and experimental basis that $d(\Delta\tau)/dA_i \approx \text{constant}$, gives support not only to the scale independence principle advanced earlier in the paper but also tends to confirm the basic postulates of the inclusion failure theory; namely that failure occurs in rock when 1) the elastic contrast between the inclusion and host approaches a maximum, and 2) the aspect ratio of the inclusion approaches a critical value. Once these conditions are met, tension stress within the inclusion becomes a maximum and failure occurs.

Discussion

Equations (25) and (26) illustrate mathematically that what has been referred to in this paper to represent the inclusion and the focal region should be considered to be zones of varying microcrack densities. This result is not surprising since while microcracks may tend to form uniformly throughout the dilatant volume during the early portions of the dilatant phase, there will be a time in this phase when some of these microcracks will begin to interact with one another. This interaction is the result of a statistical fluctuation(s) occurring within the dilatant volume which will cause microcracks to form in close proximity to one another. At this time the inclusion(s) begins to form within the dilatant volume. The effect of this interaction will be to produce a distortion and change in the magnitude and direction of the principal stresses. This interaction allows strain energy to be stored in the vicinity of the inclusion(s). Further microcrack development will be then in response to the local values of the principal stresses. Consequently, the postulate advanced earlier in the paper that inclusions form prior to failure in rock can be theoretically as well as experimentally justified.

This concept of the evolution of the inclusion and focal region zones shows that the microcrack density in the inclusion zone is greater than the microcrack density in the focal region zone. Also, the microcrack density within the focal region is variable and will decrease to zero as the undilated rock volume is approached. As the local principal stress difference in the focal region volume decreases in response to the presence of the evolving inclusion zone, microcrack closure in the focal region will occur and the tensile stress within the inclusion will increase. In the transition zone between the inclusion and focal region, the least principal stress changes in some prescribed manner from tension near the inclusion zone to compression as the focal region zone is approached. As microcrack closure continues in the focal region, the transition zone will decrease in size as the inclusion zone lengthens in the manner prescribed by equation (25). Consequently, the physical contrast between the inclusion and its associated focal region increases during the closure phase and the boundary between the two zones becomes distinct at the instance of failure. This physical reasoning was used in constructing the finite element simulation of the failure process discussed earlier in the paper. It should be noted that dilation will continue to occur within the transition zone during the closure phase.

A remaining question to be considered is the effect of sample size on the geometrical characteristics of the microcracks comprising both the inclusion and the dilated focal region. For example, are the microcrack sizes within the inclusion on the small or intermediate scales the same as those existing within an earthquake zone or, as is more likely, do these microcracks increase in size as the scale dimension increases and, if so, how do these microcracks increase in size; that is to say, what is the scaling law?

Consider a dilated volume of rock, V , containing an inclusion of volume V_i with thickness s_i and cross-sectional area A_i . Let the Young's modulus of this volume prior to dilation be E_n . During the closure phase, the total pressure increase, ΔP , required to close all cracks in the focal region can be approximated by (BRADY [12])

$$\Delta P \approx E_n \sum_{i=1}^N \epsilon_i, \tag{27}$$

where ϵ_i is the volumetric strain associated with closure of the i th crack. If ΔP_0 denotes the total change in pressure applied to the volume V during the closure phase, then equation (27) can be written

$$k \Delta P_0 \approx N \bar{\epsilon}_{tr} E_n, \tag{28}$$

where $\bar{\epsilon}_{tr} (= (1/N) \sum_{i=1}^N \epsilon_i)$ is the strain associated with closure of an average size crack in the focal region. Combining equations (22) and (28) gives

$$N \bar{\epsilon}_{tr} \approx \gamma \epsilon_0 \frac{L_i}{s_i}, \tag{29}$$

where $\epsilon_0 \sim (\Delta P_0/E_s)$ denotes volumetric strain in the sample due to the change in mean pressure applied to the boundaries of the sample. Equation (29) can be written as

$$\Delta V_c \approx \frac{\gamma \epsilon}{\alpha_i} V_{fr} \quad (30)$$

where ΔV_c represents the volume change in the focal region of volume V_{fr} due to crack closure.

Equations (25) and (30) represent the scale independent properties of the inclusion theory. Equation (25) describes the physical properties and geometrical characteristics of the inclusion and focal region while equation (30) specifies the geometrical characteristics of the cracks within the inclusion, or equivalently, the focal region. Equation (30) shows that average crack volume is directly proportional to focal region volume. Thus, as the sample and inclusion increase in size, what has been called 'microcrack' and 'macrocrack' on the laboratory scale increase in size in accordance with the 'scaling law' specified by equation (30).

Conclusions

A scale independent theory of rock failure, referred to as the inclusion theory, has been presented in this article. The key hypothesis of the inclusion theory is that the intense crack concentrations which develop within localized regions in rock near its ultimate strength can be replaced by low modulus inclusion(s). The inclusion theory rests on the postulates that catastrophic failure occurs in rock when all cracks in the focal region of the inclusion which opened during the dilatant phase close and when the aspect ratio; that is, the thickness-to-length value of the inclusion, reaches a critical value. These postulates can be shown to satisfy the constraint that they minimize the energy required to fail rock.

Direct laboratory examination of these postulates has not been made at this time. However, recent field studies on rock failure in the intermediate and large scale such as mine failures and earthquakes (Fig. 11), respectively, add support to the scale independent properties of the inclusion theory. These studies also suggest that precursor times in standard size laboratory specimens (obtained by extrapolating the curve in Fig. 11 to a 'length' of 10 cm) will be of the order of a few milliseconds. The small time interval during which crack closure occurs suggests for these specimens that the closure phase would go undetected and, as a result, the laboratory investigator could incorrectly infer that dilatancy would peak at failure and that dilatancy is the only phenomenon which preceded failure. While direct laboratory tests of the inclusion theory has not been made at this time, this should not be taken to imply that the theory is not testable. An indirect test of the theory can be made by applying the postulates to recent observations on precursor phenomena reported to occur prior to earthquakes. This subject is examined in Parts II and III.

Lastly, the significance of the scale independent principle for failing rock cannot be overemphasized. If this principle is verified and shown to be applicable to all classes of rock failure, then equations describing the mechanical behavior of rock on the laboratory scale (see for example, BRADY [12]) under comparable conditions will be directly applicable to intermediate and large-scale rock behavior provided methods to evaluate the material constants in these equations are made available.

REFERENCES

- [1] L. ORERT and W. I. DUVAL, *Rock Mechanics and the Design of Structures in Rock* (John Wiley and Sons, New York 1968), 650 pp.
- [2] M. WYSS and P. MOLNAR, *Source parameters of intermediate and deep-focus earthquakes in the Tonga arc*, *Phys. Earth Planet. Interiors* 6 (1972), 279-292.
- [3] W. F. BRACE, B. W. PAULDING and C. SCHOLZ, *Dilatancy in the fracture of crystalline rocks*, *J. Geophys. Res.* 71 (1966), 3939-3953.
- [4] J. T. CHERRY and J. C. SAVAGE, *Rock dilatancy and strain accumulation near Parkfield, California*, *Bull. Seism. Soc. Am.* 62 (1972), 1343-1347.
- [5] C. H. SCHOLZ, L. R. SYKES and Y. P. AGGARWAL, *The physical basis for earthquake prediction*, *Science* 181, No. 4102 (1973), 803-810.
- [6] A. M. SEMENOV, *Variations in the travel time of transverse and longitudinal waves before violent earthquakes*, *Isv. Earth Physics*, No. 4 (1969), 245-248.
- [7] J. WHITCOMB, J. GARMAN and D. ANDERSON, *Earthquake prediction: Variation of seismic velocities before the San Fernando earthquake*, *Science* 180 (1973), 632-635.
- [8] A. NUR, *Dilatancy, pore fluids and premonitory variations of t_s , t_p travel times*, *Bull. Seism. Soc. Am.* 62 (1972), 1217-1222.
- [9] C. H. SCHOLZ and R. KRANZ, *Notes on dilatancy recovery*, *Jour. Geophys. Res.* 79, No. 14 (1974), 2132-2136.
- [10] W. R. WAWERSIK and W. F. BRACE, *Post-failure behavior of a granite and diabase*, *Rock Mechanics J.* No. 2 (1971).
- [11] W. S. BROWN, S. R. SWANDON and W. R. WAWERSIK, *Further Studies of Dynamic and Biaxial Loading of Rock*, Final Report, University of Utah Mechanical Engineering Department, Contract #DASA 01-71-C-0017, 99 pp., 1972.
- [12] B. T. BRADY, *A mechanical equation of state for brittle rock*, Part I, *International J. Rock Mech. Min. Sci.* 7 (1970), 385-421; Part II, *International J. Rock Mech. Min. Sci.* 10 (1973a), 291-309.
- [13] W. S. BROWN and S. R. SWANDON, *Influence of Load Path and State of Stress on Failure Strength and Stress-Strain Properties of Rocks*, Technical Report No. AFWL-TR-70-53, Kirtland Air Force Base, New Mexico, 1971.
- [14] L. H. DONNELL, *Stress Concentrations Due to Elliptical Discontinuities in Plates Under Edge Forces*, Theodore V. Karman Anniversary Volume, California Institute of Technology, Pasadena, Calif., pp. 293-309, 1941.
- [15] J. C. JAEGER, *Elasticity, Fracture and Flow* (2nd ed.) (John Wiley and Sons, New York 1962).
- [16] B. T. BRADY, W. I. DUVAL and F. G. HORINO, *An experimental determination of the true, uniaxial stress-strain behavior of brittle rock*, *Rock Mechanics* 5 (1973b), 107-120.
- [17] B. T. BRADY, *Seismic precursors prior to rock failures in underground mines*, *Nature* (1974), in press.

(Received 21st June 1974)

Theory of Earthquakes

II. Inclusion Theory of Crustal Earthquakes

By B. T. BRADY¹⁾

Summary – The scale independent inclusion theory of rock failure developed in Part I is applied to the problem of crustal earthquakes and, in particular, to the problem of premonitory phenomena reported to precede such earthquakes. Several well-known premonitory effects such as anomalous variation in the ratio of longitudinal (V_p) and shear (V_s) seismic velocities, V_p/V_s , tilt, regional and local crustal movements and stress axis rotation, to mention a few, are shown to be a natural consequence of the physical processes leading to failure in dry rock. The effects of fluids on failure in the focal region of a potential earthquake are considered in terms of the scale independent inclusion theory.

1. Introduction

Observations at Garm, USSR, the New York Adirondacks, and the San Fernando, California, earthquake have shown that prior to these earthquakes the ratio of longitudinal (V_p) and shear (V_s) seismic velocities, V_p/V_s , decreased to anomalously low values and that earthquakes occurred shortly following the return of V_p/V_s to its normal value (SEMENOV, 1969; AGGARWAL *et al.*, 1973; WHITCOMB *et al.*, 1973). A variety of other effects premonitory to earthquakes have also been reported. These include stress axis rotation and anomalous crustal movements and tilt, to mention a few (NERSESOV and SIMBIREVA, 1968; SADOVSKY *et al.*, 1972; SASSA and NICHIMURA, 1956).

These data suggest that a reevaluation of our concepts of what constitutes an earthquake is required. The approximation of an earthquake by a model in which the sudden formation of a shear discontinuity in rocks occurs is an oversimplification in view of these observations. The occurrence of the earthquake following the return of V_p/V_s to its normal value prior to the earthquake further suggests that this and related premonitory phenomena must be related in a causal manner to the processes leading up to and responsible for producing the earthquake. Thus a theory of failure that is applicable to describe failure of rock on the large scale, such as an earthquake, is required. Such a theory must provide not only an explanation of the processes leading up to and including failure but also *all* the precursor phenomena occurring prior to the failure.

¹⁾ U.S. Dept. of the Interior, BuMines, Denver Mining Research Center, Denver, Colo. (present address).

In this paper, the inclusion theory is extended by invoking the scale independent principle to the problem of crustal earthquakes. The paper begins with a recapitulation of the essential concepts of the inclusion theory. This is followed by the application of the theory to earthquake premonitory effects. The subject of earthquake prediction and or control is considered in terms of the inclusion theory.

2. Inclusion theory - a recapitulation

A theory of rock failure, termed the inclusion theory, was formally developed in Part I. The key hypothesis of the inclusion theory is that the intense crack concentrations that develop within localized regions in rock near its ultimate strength (BRADY, 1975) can be mathematically modeled and physically replaced by elastic inclusions whose modulus are lower than the surrounding material. The results of this theory show that there is a three-fold effect of the inclusions. 1) The principal stress axes rotate and change in magnitude both within and outside the inclusion. 2) The least principal stress within the inclusion is tensile and is oriented in a direction normal to the major (long) axis of the inclusion. 3) The magnitude of the least principal stress increases in the focal region of the inclusion; that is, the region into which the inclusion and its associated fault(s) will grow. As the magnitude of the least principal stress in the focal region of the inclusion increases in compression, cracks in the immediate vicinity of the inclusion that opened during the dilatant phase close as the rock begins to store strain energy. As these cracks close, the tensile stress (oriented in a direction normal to the long axis of the inclusion) within the inclusion increases due to the increased elastic contrast between the inclusion and the surrounding rock. Cracks within the inclusion begin to coalesce in response to the increasing tensile stress and a macrocrack(s) forms.

The inclusion theory rests on the postulates that catastrophic failure occurs when all cracks in the focal region of the inclusion that opened during the dilatant phase close and when the aspect ratio of the inclusion, that is, the thickness-to-length ratio of the inclusion, reaches a critical value. When these conditions occur, the length of the macrocrack(s) within the inclusion reaches a critical value. Failure occurs and growth of the fault results from closure of the macrocrack as the inclusion advances into its focal region. In this theory, all faults terminate in an inclusion zone or, simply, a zone of concentrated dilatancy.

The inclusion theory is a scale independent theory. This scale independence in failing rock provides a simple explanation of why the precursor time-magnitude-length relationships hold for both mine failures and a wide range of earthquake magnitudes (see BRADY, 1975, Fig. 11). In the inclusion theory, precursor time ($\Delta\tau$), measured between the initiation of crack closure and the time of failure, depends both on the loading rate in the focal region and on the size of the focal region which in turn is governed by the size of the inclusion. Consequently, the duration of the closure phase is a function of the size of the earthquake that follows it.

3. Application of inclusion theory to earthquake premonitory effects

Premonitory effects have been reported to occur prior to earthquakes. These effects include, for example, regional and local crustal movements, anomalous variations in V_p/V_s , tilt, changes in resistivity, changes in microearthquake frequency and stress axis rotation in the focal region of an impending earthquake. Vigorous programs to monitor some of these effects, particularly in Japan and the USSR during the past decade, suggest these effects are real and that they occur together, although not necessarily at the same time (SASSA and NICHIMURA, 1956; NERSESOV and SIMBIREVA, 1968; SADOVSKY *et al.*, 1972; SCHOLZ *et al.*, 1973; WHITCOMB *et al.*, 1973).

Ratio of seismic compressional velocity to seismic shear velocity, V_p/V_s

Figure 1 is a schematic illustration of the variation with time of the ratio of seismic compressional velocity to seismic shear velocity, V_p/V_s , in the focal region of a rock satisfying the constraints of the scale independent inclusion theory. In the following discussion, the behavior of V_p/V_s is considered to represent an average value of V_p/V_s for typical ray paths that pass through the whole focal region. The temporal and spacial variation of V_p/V_s in any small volume of the focal region is considered later.

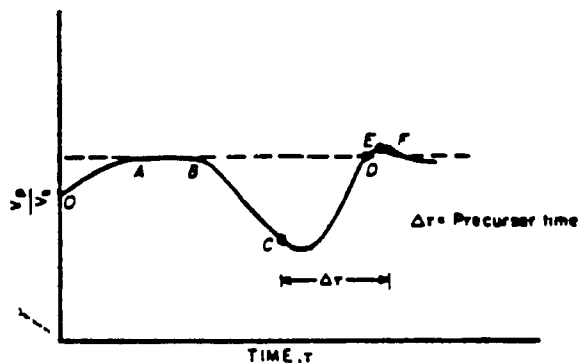


Figure 1

Predicted behavior of V_p/V_s in focal region and characterization of stress-strain behavior

The predilatant phase (\overline{OA}) is characterized in Fig. 1 by a gradual increase in V_p/V_s (due to an increase in the far-field tectonic stress) to a stable value resulting from closure of open cracks initially present in the focal region. The period of constant V_p/V_s is denoted by \overline{AB} . A decrease in V_p/V_s (\overline{BC}) characterizes the dilatant phase. During this phase, new cracks open in the focal region in response to the applied principal stresses. The axes of principal stress begin to rotate both in the focal region and within the region that is to eventually become the inclusion as the inclusion forms. The V_p/V_s value increases during the closure phase (\overline{CD}) up to its predilatant value. During this phase, the magnitude of the difference between the maximum and least principal stress (principal stress difference) in the focal region decreases. The least principal stress increases in

compression and, as a result, cracks which opened during the dilatant phase (\overline{BC}) in response to the applied stresses begin to close or 'heal'. Along pre-existing crack surfaces, the decrease in principal stress difference reverses the shear stress direction and the cracks begin to close in the focal region (Fig. 2). Once all cracks have closed in the focal region (D , Fig. 1), macrocrack growth begins and the stress concentration factor or, equivalently, the principal stress difference in the focal region begins to increase due to transfer of stress into the focal region in response to macrocrack growth within the inclusion. The macrocrack length approaches a critical value and unstable growth occurs (F).

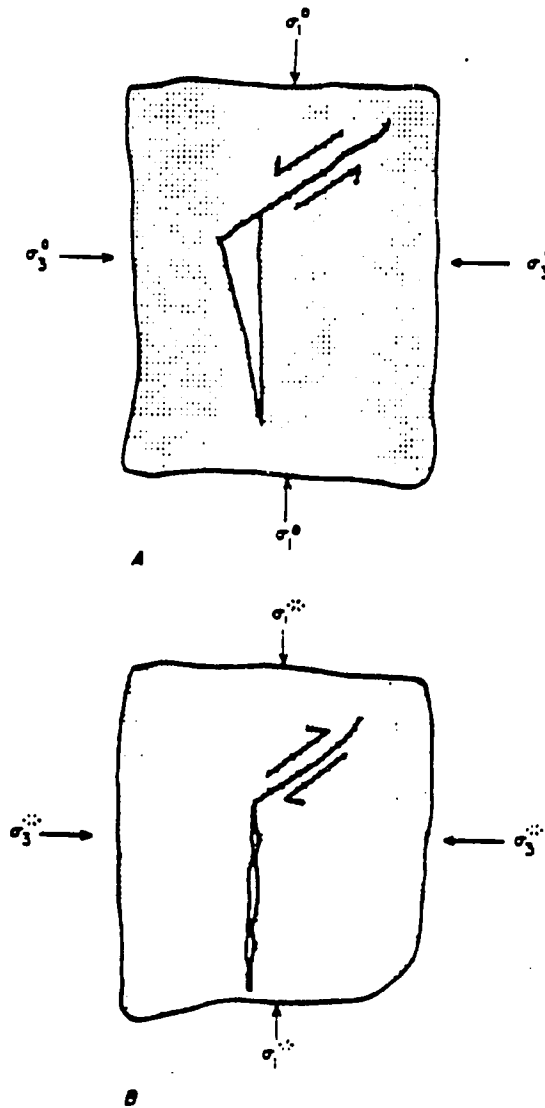


Figure 2
Illustration of crack closure in focal region resulting from a decrease in stress-difference

Since the r values of the l phase, the ave failure if not initiation of t. Fig. 1); that i the inclusion between inclu (F, Fig. 1).

Field obser observed unus: pressional wa have since be WHITCOMB er

It is impo: explained by t gion since the fying effect of the inclusion) paper.

Stress axis ro

A predict: terminated stre rotation occu reported that in the Garm results can be stress axes in approximate: to an earthqu relationship axes were ob same positio: an approxim

Exactly t rotation of t closure of cr increase in th that the orie: the main she crack closur:

Vol. 113, 1975)

Since the mean pressure, \bar{P} ($\bar{P} = \frac{1}{3}(\sigma_1 + \sigma_2 + \sigma_3)$, where σ_1 , σ_2 , and σ_3 denote the values of the local principal stresses), increases in the focal region during the closure phase, the average V_p/V_s value may exceed its predilatant value (D , Fig. 1) before failure if not all the cracks originally present in the rock were closed prior to the initiation of the dilation phase. If failure is preceded by a foreshock sequence (E , Fig. 1): that is, the formation of new cracks in response to the tension stress within the inclusion zone, the average V_p/V_s value may decrease until the elastic contrast between inclusion zone and focal region is a maximum. Failure occurs at this time (F , Fig. 1).

Field observations similar to these were first reported by SEMENOV (1969), who observed unusual variations of the travel-time ratio, t_s/t_p , of shear waves (t_s) to compressional waves (t_p) in the Garm area of the Tadzhik Soviet Socialist Republic. They have since been reported in the United States by AGGARWAL *et al.* (1973) and by WHITCOMB *et al.* (1973).

It is important to note that the anomalous V_p/V_s behavior prior to failure can be explained by the inclusion theory without requiring diffusion of fluids into the focal region since the theory is based entirely on the failure properties of dry rock. The modifying effect of fluids and fluid diffusion (resulting from crack closure in the vicinity of the inclusion) and their effect on the failure process in rock is considered later in the paper.

Stress axis rotation in the focal region

A prediction of the inclusion theory developed in Part I is that the seismically determined stress axes rotate in the focal region prior to an earthquake, and that this rotation occurs during the formation of the inclusion. NERSESOV and SIMBIREVA (1968) reported that stress axis rotation in the focal region occurred prior to an earthquake in the Garm area. The stress axes were determined from fault plane solutions. Their results can be summarized as follows: 1) There is a change in orientation of the seismic stress axes in the foci of weak earthquakes prior to a strong earthquake. 2) A period of approximately 1.5–2.0 months was observed during which the stress axes turned prior to an earthquake of magnitude 4.5 and 2.0 months for a magnitude 5 earthquake. The relationship was nearly linear: that is, the larger the magnitude the earlier the stress axes were observed to turn. 3) The intermediate stress axis remained practically in the same position with the compressional and tensional axes turning about it. 4) There was an approximate 90° rotation of the stress axes in the focal region.

Exactly this behavior is predicted from the inclusion theory. For example, the 90° rotation of the seismically determined stress axes in the focal region corresponds to closure of cracks in the closure phase. Here the shear direction is reversed due to an increase in the magnitude of the least principal stress in the focal region (Fig. 2). Note that the orientation of the seismically determined stress axes responsible for producing the main shock will be similar in orientation to the principal stress axes that produce crack closure (CD , Fig. 1).

Microearthquake frequency anomalies prior to major earthquakes

The magnitude-frequency relations of earthquakes in any given place are observed to satisfy an empirical relation of the form

$$\log N = a + bM, \quad (1)$$

where N is the number of earthquakes whose magnitudes are in the range M to $M + \delta M$ and a and b are constants. Laboratory studies and recent field observations (SCHOLZ *et al.*, 1973; WYSS, 1973) suggest b is a function of applied stress.

During the closure phase, the incremental change in seismic activity, dN , and the volumetric inelastic strain associated with this decrease, $d\epsilon$, can be shown to be proportional to the number of open cracks, N , remaining in the focal region of the inclusion at any time t into the closure phase; that is,

$$dN \approx -AN d\epsilon, \quad (2)$$

where A is a constant of proportionality. Let β denote the average compressibility of the focal region at some time, t , into the closure phase. Let β_0 represent the compressibility of the focal region when all cracks which opened during the dilatant phase are closed. The relationship between the volumetric closure strain, $d\epsilon$, and β and β_0 is (BRADY, 1973)

$$d\epsilon \approx c\Delta\beta \dot{\beta} dt, \quad (3)$$

where c is a constant, $\Delta\beta = \beta - \beta_0$ and $\dot{\beta}$ denotes the loading rate averaged throughout the focal region.

The seismicity, $n(t)$, or dN/dt , is found from equations (2) and (3) to be

$$n(t) \approx B \Delta\beta N_0 \exp\left[-\int_0^t B \Delta\beta dt\right], \quad (4)$$

where $B = Ac\dot{\beta}$ and N_0 is the number of open cracks in the focal region prior to initiation of the closure phase. Since $\Delta\beta$ decreases during the closure phase, equation (4) shows that the seismicity must also decrease during the time interval that closure occurs.

The b -value for events occurring during the closure phase is found from equations (1), (2) and (3)

$$b \approx b_0 - \frac{1}{M} \int_0^t B \Delta\beta dt, \quad (5)$$

where b_0 is the b -value prior to initiation of the closure phase. Equation (5) shows the b -value will be positively correlated with the seismicity rate in the focal region; that is, when the seismicity rate decreases the b -value also decreases. Similarly, it can also be shown that when the seismicity rate increases the b -value increases.

WYSS (1973, Table 1) observed that the b -values for the foreshock sequence, $b_{f.s.}$ of a major earthquake are lower than the b -values of the aftershock sequence, $b_{a.s.}$ which follows the main earthquake. If the inclusion theory is applied to this problem.

it is clear that the compressibility, β_n^a , of the fractured focal region (of the main shock) where the aftershocks occur must be greater than the compressibility, β_n^f , of the material where the foreshocks occur. Therefore, equation (5) can be used to give the b-value difference of the aftershock and foreshock sequences,

$$b_{a.s.} - b_{f.s.} \approx \frac{1}{M} \int_0^t B(\Delta\beta_{f.s.} - \Delta\beta_{a.s.}) dt \approx \frac{1}{M} \int_0^t B[\beta_n^a - \beta_n^f] dt \geq 0, \quad (6)$$

where t represents the time into the closure phase of either the foreshock or aftershock whose magnitude is M . In equation (6), β_n^a and β_n^f denote the compressibilities of the focal regions of the aftershock and foreshock sequences, respectively, prior to the initiation of the dilatant phase for these events. Consequently, b-values for the aftershock sequence after the main shock will be greater than the b-values for the foreshock sequence occurring prior to the main shock. Wyss (1973) has interpreted the b-value difference as implying higher tectonic stress for foreshocks than aftershocks. This interpretation is consistent with the inclusion theory, since more strain energy can be stored in the focal region of the main shock than in the focal region of each individual aftershock. The compressibility difference, $\beta_n^a - \beta_n^f$, is simply a reflection of the energy difference.

Electrical resistivity

Electrical resistivity anomalies have been observed prior to earthquakes. As a case in point, consider the results of a long baseline (6 km) resistivity profile made at Garm, USSR (SADOVSKY *et al.*, 1972). The resistivity data, together with the times of all earthquakes of magnitude greater than 3.0 that occurred within 10 km of the baseline, is shown in Fig. 3. While there may be an obvious correlation between the resistivity profile and the earthquakes that group at the minima of the profile curve, it is difficult

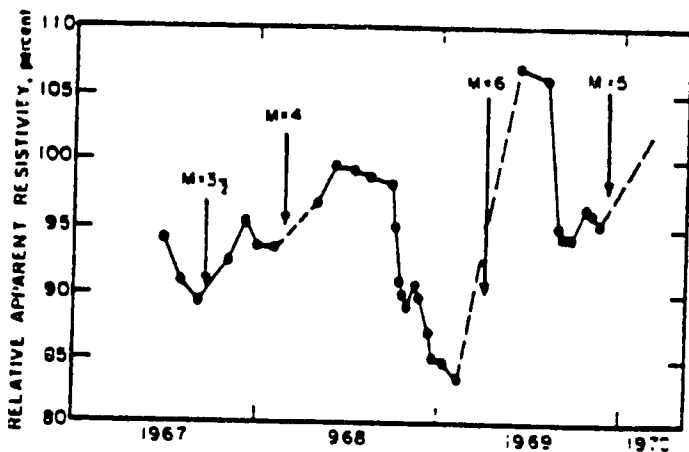


Figure 3
Electrical resistivity anomalies observed prior to earthquakes at Garm, USSR (after SADOVSKY *et al.*, 1972)

to arrive at a unique interpretation of this data without additional information. For example, the resistivity anomalies in Fig. 3 may be interpreted using the inclusion theory and 'dry' rock by invoking the argument that the apparent resistivity decrease is correlated with crack closure in the focal region. 'Dry' rock in the context used here means that the crack volume is not filled with water. Decrease of resistivity with closure of cracks has been reported to occur in 'dry' rock in the laboratory (PARKHOMENKO and BONDARENKO, 1963). This resistivity behavior is believed to be due to the existence of a thin film of water along the crack surfaces. Under these conditions, the formation of cracks parallel to the direction of maximum principal stress during the dilation phase will produce an increase of resistivity that is greatest in the direction normal to crack growth. Closure of these same cracks during the closure phase will produce a corresponding decrease of resistivity along this direction. However, an alternative explanation of the anomalies in Fig. 3 can be made by postulating that water is present in the dilatant volume that contains both the inclusion and its associated focal region. Crack closure in the focal region prior to the earthquake will produce a migration of water away from the focal region into both the inclusion zone and the dilatant volume. This process would produce an increase in pore pressure in these zones. The overall effect that would be produced by this diffusion is a decrease of the apparent resistivity in the dilatant volume.

Regional crustal movements

Anomalous crustal movements are known to precede earthquakes. One well-documented case is the 1964 Niigata earthquake. The magnitude of the main shock was 7.5. Repeated geodetic measurements were made in the vicinity of the main shock. Vertical movements are shown in Fig. 4. The vertical movements had been occurring in the vicinity of the epicenter at a slow, steady rate from 1898 to 1955. Rapid uplift

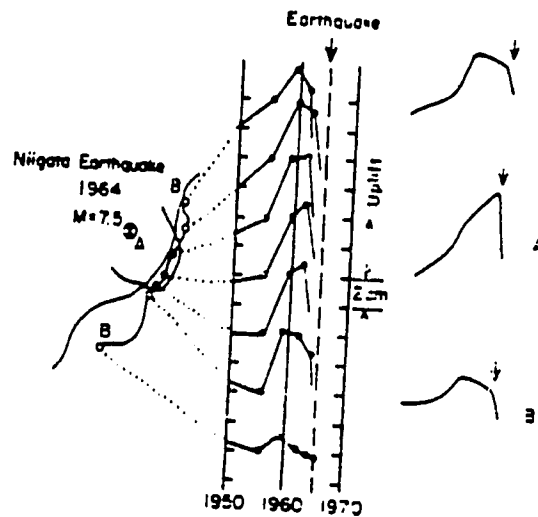


Figure 4
Crustal uplift anomalies in the vicinity of Niigata, Japan, prior to the Niigata 1964 earthquake (after MOGI, personal communication, 1974)

vol. 113, 1975.

began in 1955; uplift continued 3. located on elevation began and B will c

Tilt anomalies

Rapid changes in major earthquakes; 1971; LATYNS models of the earthquake and an of these changes

A key process correspond to deformation of open cracks attained (or not) of macrocracks produces an inclusion the volumetric stress present) in the increase may of this effect, with A and B respectively. normal fault failure although events will occur during the closure. However, A and B are closing between the time when 3) At a time just zone. At this time will then tilt to resulting from occur shortly after inclusion theory the surface out

began in 1955. The data in Fig. 4 show that in region A, located near the main shock, the uplift continued unabated until the occurrence of the earthquake. However, in regions B, located on either side of A, the period of rapid uplift was followed by a decrease in elevation beginning in 1959. If the inclusion theory is applied to this problem, regions A and B will correspond to the inclusion and its associated focal volume, respectively.

Tilt anomalies

Rapid changes in tilt direction are known to occur shortly before the occurrence of major earthquakes (SASSA and NICHIMURA, 1956; HOSOYAMA, 1952; WOOD and ALLEN, 1971; LATYNINA and KARMAKYEVA, 1970). These changes place severe constraints on models of the physical processes occurring in the focal region of an impending earthquake and any successful theory of earthquakes must provide a satisfactory explanation of these changes.

A key prediction of the inclusion theory is that anomalous displacements that may correspond to what has been referred to by some investigators as premonitory 'creep' deformation will occur in the focal region prior to the earthquake. For example, closure of open cracks in the focal region of the inclusion at a time when the V_p/V_s value has attained (or nearly so) its dilatant value will be followed by a period of rapid growth of macrocracks to a critical length within the inclusion. The growth of these cracks produces an increase in the stress concentration factor in the immediate vicinity of the inclusion that results in an elastic volumetric compression and possibly an inelastic volumetric strain component due to closure of any additional open cracks (if they are present) in the focal region during this time. The deformations produced by this stress increase may be detected by both tilt and vertical crustal movements. As an example of this effect, consider the behavior of two tiltmeters, A and B, located on the surface with A and B positioned directly above and outside of the focal region of the inclusion, respectively. The reader will note the following discussion applies only to thrust and normal fault earthquakes. Similar behavior will be observed prior to strike-slip failure although the effect will be much less pronounced. The following sequence of events will occur prior to the earthquake. 1) Both A and B will tilt away from the inclusion or the region which will become the inclusion during the dilatant phase. 2) During the closure phase, B will always tilt in a direction where closure is occurring. However, A will tilt toward the inclusion zone during the time interval when open cracks are closing between A and the inclusion zone. The tilt direction of A will reverse during the time when open cracks are closing between A and the boundary of the dilatant zone. 3) At a time just prior to the earthquake macrocrack growth occurs within the inclusion zone. At this time both A and B will tilt away from the inclusion zone. 4) Both A and B will then tilt toward the inclusion zone due to compaction of rock within the focal region resulting from stress transferral due to growth of the macrocrack. The earthquake will occur shortly following the tilt reversal. This example illustrates two predictions of the inclusion theory for thrust and normal fault earthquakes. 1) Tiltmeters (B) located on the surface outside the focal region will exhibit S-bend behavior a short time prior to the

earthquake. Tiltmeters (A) located on the surface directly over the focal region will not exhibit S-bend behavior. However, if the tiltmeters are located directly above the inclusion zone, S-bend behavior will be observed. 2) All tiltmeters, with the exception of those located above the inclusion zone, will tilt toward the epicenter (inclusion zone) just before the earthquake.

Tiltmeter behavior similar to the above predictions has been observed. Tiltmeters have recorded several cases of precursor crustal movements. A well-documented case is a magnitude 6 earthquake which occurred at Odaigahara, Japan (SASSA and NICHIMURA, 1956), where six months prior to the earthquake rapid tilting in a direction away from the epicenter was recorded at two locations 40 km and 100 km respectively from the epicenter (closure phase). This tilting continued for three months and then ceased, at which time a station further to the south began tilting. One month before the earthquake, these three stations begin tilting rapidly in a direction toward the epicenter. WOOD and ALLEN (1971) reported anomalous tilting one month prior to the Danville ($M = 4.5$) earthquake. In this earthquake, a short-term precursor tilt occurred toward the epicenter for 10 hours before the main shock. Additional examples of tilt anomalies showing behavior similar to that predicted by the inclusion theory are on record (LATYNINA and KARMAKYEVA, 1970; HOSOYAMA, 1952; SASSA and NICHIMURA, 1956). For instance, tilt measurements in Japan and the Garm region have sometimes shown the "S-bend" a day, or a few hours, prior to an earthquake. In most cases the tiltmeters tilt in a direction toward the epicenter prior to the earthquake.

Electrical and magnetic precursors

In addition to S-bend tilt behavior, other short-term precursors may result from the extreme compression occurring within the focal region near the inclusion just prior to the earthquake. Precursors of this class may, under certain conditions, include changes in the polarization and/or magnetization vectors in the rock volume being compressed. Stress is known to modify the magnetocrystalline anisotropy of magnetic minerals so that an anisotropy of magnetic susceptibility of the rock in the vicinity of the inclusion would appear just before the earthquake (STACEY, 1969). This effect may be particularly pronounced in basic rocks such as basalt. The stress intensification in the focal region would distort and increase the magnitude of the geomagnetic field in this region. Stress is also recognized to effect the piezoelectric properties of rock. These effects, amounting to 0.1 to 1.0% of the piezoelectric effect produced in single quartz crystals, have been shown to occur in rocks such as granites, gneisses and quartzites (IIDA and KUMAZAWA, 1961).

Anomalous electrical and magnetic phenomena similar to those discussed above have been observed prior to major crustal earthquakes. For example, during the most violent stage of the Matsushiro seismic activity, RIKITAKE (1972) observed the magnetic intensity increased approximately 10 gammas. There are some instances (RIKITAKE, 1972) where no geomagnetic changes exceeding the overall instrument accuracy were

observed prior to large earthquakes ($M \geq 6.0$). However, the time interval between the readings for this case during which the earthquake occurred was 40 days. Geomagnetic anomalies resulting from a stress-induced mechanism would become detectable a short time (~few hours) before the earthquake and would dissipate rapidly after the earthquake. KATO and UTASHIRO (1949) found a magnetic declination increase of approximately 25 gammas just prior to the 1946 Nankado earthquake. They noted that the field intensity changed dramatically just before the main shock and reverted to normal a few months later. MOORE (1964) observed a geomagnetic field disturbance with an amplitude of approximately 100 gammas at Kodiak, Alaska, an hour before the 1964 earthquake.

Anomalies in the atmospheric-electric potential (on the order of 120 volts/meter) which were characterized by an abrupt onset a few hours prior to an earthquake whose epicenter was 120 km from the observation station have been reported by CHERNYAVSKIY (1963). YOSIMUTSU and NAGATA (SOBOLEV and MOROZOV, 1970) have reported cases of anomalous variations in the telluric current potential several hours before major earthquakes. SOBOLEV and MOROZOV (1970) observed a sharp change in the electric potential gradient three hours before a magnitude 4.5 earthquake in Kamchatka. The electrical disturbance stopped after the earthquake at which time the field resumed its normal behavior.

The above examples suggest a general behavior of electrical and magnetic disturbances just prior to earthquakes that would be expected from the inclusion theory. The inclusion theory requires an increase in the magnitude of the electric polarization vector in the highly stressed rocks of an acidic composition approximately normal to the fault growth direction just prior to the earthquake. It is important to note that the high potential differences produced by the stresses in the focal region would develop only upon an abrupt change in the magnitude and orientation of the local principal stresses, since current leakage would dissipate the polarization effect over a period of time longer than a day, or few days at most. The magnetization effect, on the other hand, if conditions favoring its existence are present, would dissipate more slowly since it is less sensitive to stress changes. The magnetization effect would vanish completely only when all areas of high stress in the fractured focal region are removed.

Precursor phenomena such as electrical resistivity, anomalous crustal movements, tilt and anomalous electrical and magnetic effects are difficult to quantify. At the present time, the best that can be expected is to determine whether these phenomena are qualitatively consistent with any one theory. While these effects are consistent within the framework of the inclusion theory the need for additional data which could be obtained from a comprehensive field test program designed to measure all the above precursors is obvious. It is important to note that the inclusion theory predicts that all of the precursor phenomena discussed above bear a fixed relation in time to one another, and further that these phenomena result *only from definite physical processes* related to failure and preparation for failure in the focal region and in the inclusion zone of an impending earthquake.

4. Prediction and possible control of crustal earthquakes

The inclusion theory and its associated scale independence principle suggest that the earthquake problem is truly deterministic. Implicit in this concept is the applicability of the theory to the dual problems of earthquake prediction and, possibly, earthquake control. However, the development of possible methods of earthquake prediction and/or control requires an understanding of 1) the effect of fluids on the earthquake process, and 2) the applicability of the inclusion theory to the occurrence of earthquakes within existing fault zones. These subjects are considered before the problem of earthquake prediction and/or control is discussed.

Effect of fluids on inclusion growth

In the inclusion theory, fluids are not required to be present in the focal region to produce most of the precursory effects observed prior to an earthquake. The inclusion theory implies that the effect of fluids in the focal region is that of a modifying agent, an effect discussed at length in rock mechanics literature.

The presence of fluid pressure in the interstices or pores of rock affects the stress state in the solid rock matrix. The fluids within the cracks or pores can be under pressure. The effect of this pressure, P_p , is to cause the cracks to remain open and is conveniently included in the analysis when the total pressure, P , is replaced by the effective pressure $P^* = P - \gamma^* P_p$, where $\gamma^* \approx 1.0$ for most practical problems. Failure of rock containing fluids with pore pressure is then determined in the inclusion theory only by the effective stresses ($\sigma_1 - P_p$, $\sigma_2 - P_p$, $\sigma_3 - P_p$, where σ_1 , σ_2 , σ_3 denote the applied principal stresses) acting on the rock.

Assume fluids are present in both the inclusion and dilatant volumes of an impending earthquake. During the closure phase, fluids in the focal region must diffuse out from that part of the focal region where closure is occurring. Fluid will also diffuse into the inclusion zone. Thus, pore pressure in the inclusion zone will increase during this phase. As a result of the increased pore pressure in the inclusion zone, the tensile stress, σ_{11} , within the inclusion will increase to a value $\sigma_{11} + P_p$. This increase in tension in the inclusion zone produces a concurrent increase in stress concentration in the focal region.

When the scale independent principle is applied to this situation, it is clear that diffusion and increased pore pressure in the inclusion zone have a much larger influence on focal region modulus than on inclusion modulus. Consequently, inclusion thickness must decrease due to elastic deformation resulting from increased tension in the inclusion and increased compression in the focal region. Therefore, the effect of fluids in the potential earthquake region and fluid diffusion produced by closure is merely to enhance failure: that is, the system, primary inclusion - focal region, tends toward a condition of instability earlier than it would if the rock were completely dry. Once the main earthquake has occurred, the fluid will tend to diffuse into the fractured secondary inclusion zone in response to the stress transferral resulting from the earthquake. The effect of fluid diffusion in the secondary inclusion zone on aftershock sequences will be similar to its effect on the main shock.

BOOKER ()
to result in
rock activit
rock. Howe
without fluid
and fluid diff
Earthquakes

Figure 5 s
including a r
BRADY, 1974

Prec

dry unjointed
listed in Fig. :
Fig. 5 sugge
pre-existing fa
and the fact t
again, suggest
either a reorie
from high ten
quake.

BOOKER (1972) showed that the effect of fluid diffusion on aftershock sequences is to result in a $1/t$ type decay law for the aftershocks. This result suggests some aftershock activity may be caused by transient pore pressure change induced by the main shock. However, it is possible to show that a $1/t$ aftershock decay law can also occur without fluid diffusion. This result strengthens the hypothesis that the effect of fluids and fluid diffusion on the earthquake process is only one of a modifying agent.

Earthquakes within existing fault zones

Figure 5 shows precursor time (Δt) versus failure length (L) for several earthquakes, including a rock burst from northern Idaho and a coal mine roof fall in Pennsylvania (BRADY, 1974). Both the rock burst and roof fall were fresh failures that occurred in

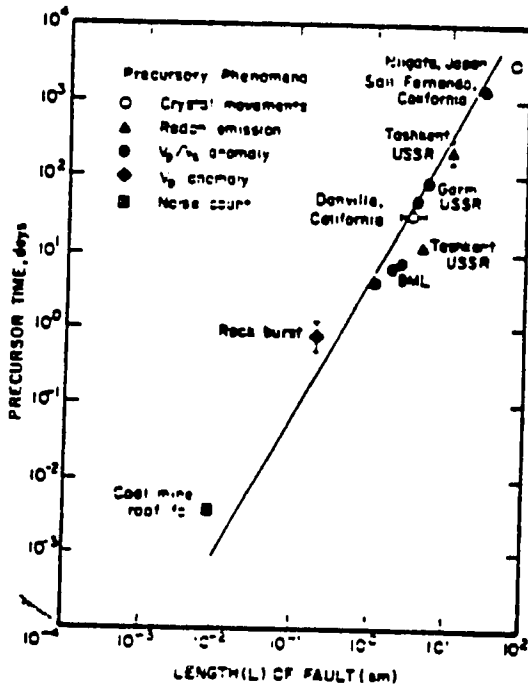


Figure 5
Precursor time-failure length relationships for earthquakes and mine failures

dry unjointed rock. Most major earthquakes in the world, including the earthquakes listed in Fig. 5, are known to occur within pre-existing fault zones. However, the data in Fig. 5 suggest a similar mechanism of failure must be operative both for failures along pre-existing fault zones and failures in fresh unfaulted rock masses. This observation, and the fact that earthquakes re-occur in basically the same locations time and time again, suggest that old faults may 'heal' with time resulting from crack closure due to either a reorientation of the applied principal stresses or to crack cementation resulting from high temperature fluids depositing minerals within these cracks after an earthquake.

The inclusion theory is directly applicable to describe earthquakes for the case where effective healing of any kind has occurred. In addition, the inclusion theory obviously has application to earthquakes generated along 'old' fault surfaces where 'lock' points or asperities are present. Effects similar to this are known to occur in laboratory-size rock specimens (SCHOLZ *et al.*, 1973; BYERLEE, 1966). These studies have shown that sliding along pre-existing surfaces in rock can be characterized as either stable or unstable (stick-slip). BYERLEE (1966) has proposed that whenever two surfaces of a brittle material are brought together, the asperities on the surfaces in contact become locked together. If the stiffness of the system normal to the surfaces is large enough, the asperities must be sheared off before stable sliding can occur. The application of this type of failure mechanism to an existing fault surface implies that during sliding some asperities become locked along the fault and must be broken before sliding can resume. In terms of the inclusion theory, the asperities or 'lock' points become nuclei for inclusion formation and growth. Failure in the vicinity of these inclusions follows the same process discussed in Part I.

There are some consequences of failure of 'lock' points within pre-existing fault zones. For example, the method of estimating what has been called 'effective fault length' in the literature (Fig. 5) from the aftershock region and relating this to the precursor time for the main shock is, in general, consistent with the inclusion theory. However, there may be situations where the calculated 'fault length' is too large. For example, consider the problem where a major 'lock' zone exists along a pre-existing fault. This zone must be destroyed before slippage along the fault can occur. Therefore this zone becomes the nucleus for the inclusion and its associated focal region. Thus, the focal region or, alternatively, the aftershock region, will be contained within the 'lock' zone. When the earthquake occurs, there will be slippage along the fault in the vicinity of the 'lock' zone. Failure of additional smaller 'lock' zones in the vicinity of the major 'lock' may occur due to the rapid stress transferral from the earthquake. As a consequence, the aftershock area will include the aftershock areas of the major 'lock' zone and the additional smaller zones along the fault and appear somewhat larger than it really is. Consequently, care must be exercised in interpreting the numerical relationship between $\Delta\tau$ and the 'effective fault length' L .

Precursor time as an earthquake predictor

Precursor time, $\Delta\tau$, should be used with caution as a possible prediction of earthquake magnitude, because in addition to being dependent on focal region volume it is also functionally related to boundary conditions applied to the focal region of an impending earthquake. Thus, if loading rate suddenly increases or decreases in the focal region, precursor time will be shortened or lengthened in proportion to the excess rate of load increase or decrease, respectively, in the focal region. As a practical example, recent studies by the author in northern Idaho by the U.S. Bureau of Mines have demonstrated that a rock burst in one mine pillar can result in rapid stress transferral to neighboring portions of the pillar or adjacent pillars, resulting in secondary rock bursts.

precursor times for
increased over and
example of
sequences that appe
may be shortened in
region resulting fro
Caution must a
individuals (WYSS and
of an impending ea
served by monito
of an impending ea
travel time from ar
some earth model.
Caution decreases te
ation will arrive
communication, 19
increased for a time
earthquake. Consec
earthquake to follo
occurs when the V_p
processes that woul
independent inclusi
zones at various tin
in both cross-section
directly above the d
increase in V_p -resid
at time t_2 by a decr
However, the earthc
had occurred at po
additional velocity :

Methods of earthqua

Water injection :
earthquake control
parallel to and withi
drawn from the two
the fault at these po
released sequentially
It is of interest to co
Consider first th
inclusion. Assume c
Two possibilities ar

quakes for the case of the inclusion theory. Fault surfaces where known to occur (1966). These studies be characterized as that whenever two on the surfaces in al to the surfaces is ing can occur. The surface implies that st be broken before es or 'lock' points ne vicinity of these

pre-existing fault led 'effective fault elating this to the i sion theory. is too large. For ng a pre-existing occur. Therefore cal region. Thus, tained within the g the fault in the s in the vicinity from the earth- ock areas of the ppear somewhat ng the numerical

fiction of earth- region volume cal region of an ecreases in the on to the excess ctical example, s have demon- ferral to neigh-) ck bursts.

Precursor times for the secondary bursts were thereby shortened, because loading rate increased over and above that which existed prior to the secondary bursts. A large scale example of stress transferral may be the occurrence of multiple earthquake sequences that appear to be causally connected. Precursor times for the secondary shock may be shortened in proportion to the amount of stress transferral to the second shock region resulting from the main event.

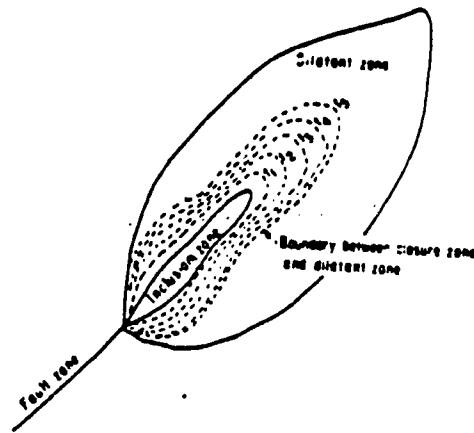
Caution must also be exercised in using velocity anomalies such as V_p , V_s or V_p -residuals (WYSS and HOLCOMB, 1974) to predict the time of occurrence and the magnitude of an impending earthquake. P -wave velocity decreases prior to earthquakes have been observed by monitoring the average V_p -residual at seismic stations near the focal region of an impending earthquake. The V_p -residual is the difference between the observed travel time from an epicenter to a station and that computed theoretically based on some earth model. Thus, if the P -velocity in the crustal material underneath a seismic station decreases temporarily before an earthquake, each seismic wave reaching this station will arrive somewhat later during the premonitory period. Wyss (personal communication, 1974) observed that prior to the Sitka earthquake the V_p -residual increased for a time and then decreased back to zero well before the occurrence of the earthquake. Consequently, both the 'precursor time' as well as the magnitude of the earthquake to follow would be underestimated if it were assumed that the earthquake occurs when the V_p -residual returns to zero. Figure 6 is a schematic illustration of the processes that would be expected to occur in an earthquake region based on the scale independent inclusion theory. The boundary between the closure and the dilatant zones at various times, t_1, t_2, \dots, t_3 ($t_1 > t_2 > t_3$), into the closure phase are shown in both cross-section (A) and plan view (B). If a seismic station is located on the surface directly above the dilatant zone at point C in Fig. 6B, an observer would first detect an increase in V_p -residual due to the formation of the dilatant zone. This would be followed at time t_2 by a decrease to its normal value due to crack closure beneath the station. However, the earthquake would not occur until some later time, say t_3 , well after closure had occurred at point C. To accurately determine the precursor time and magnitude, additional velocity measurements throughout the dilatant zone are required.

Methods of earthquake control

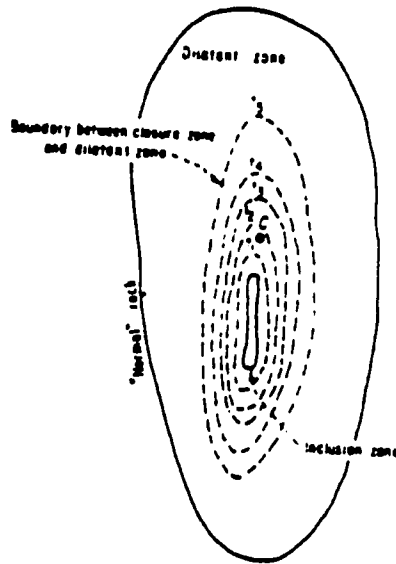
Water injection and withdrawal in high stress zones has been considered a method of earthquake control (HEALY *et al.*, 1972). One procedure consists of drilling three wells parallel to and within an active fault zone where natural water is present. Water is withdrawn from the two outlying wells, increasing normal stress and thus theoretically locking the fault at these points. Water is pumped into the central well and the stored energy is released sequentially by increasing the pore pressure in the vicinity of the central well. It is of interest to consider this technique in terms of the inclusion theory.

Consider first the case where no water is present in either the focal region or in the inclusion. Assume crack closure has occurred or is occurring within the focal region. Two possibilities arise. This first case involves 1): Direct water injection into the focal

series of small c
method of contr
are not present,
Now consid
clusion. Assum
use, as shown
enhances instab
focal region ne:



A - Cross Section View



B - Plan View

Figure 6
Spatial and temporal variation of crack closure in focal region of the primary inclusion

region. The effective pressure decreases in the focal region and tensional stress in the inclusion decreases. This procedure locally destresses the system and prevents failure until possibly some later time. The method should probably be rejected on the grounds that if conditions responsible for producing instability prevail, namely high stress, this method could only serve to cause a larger shock in the focal region at some later time. 2) The second case is direct injection of water into the inclusion. This produces an increase in tensional stress in the inclusion and an increase of the effective pressure in the focal region. This technique tends to produce instability, and there is a distinct possibility of undesirable side-effects, such as triggering a large earthquake where only a

Plan view of pr

2) Two wells in th
pressure decreas
system tends to
and injection wel
region and tensi
instability. 4) Al
outlying wells de
develops between
dangerous becau

series of small quakes was desired. Since the fault or focal region is not 'locked', this method of control should also be tentatively rejected. Consequently, when natural waters are not present, the injection and withdrawal method of control is unsatisfactory.

Now consider the case where water is present in both the focal region and the inclusion. Assume for simplicity the system is in the dilatant phase. Four possibilities arise, as shown in Fig. 7. 1) *All three wells in the focal region* (Fig. 7A): This procedure enhances instability as withdrawal increases the effective pressure in that part of the focal region nearest to the inclusion. The tension stress increases in the inclusion.

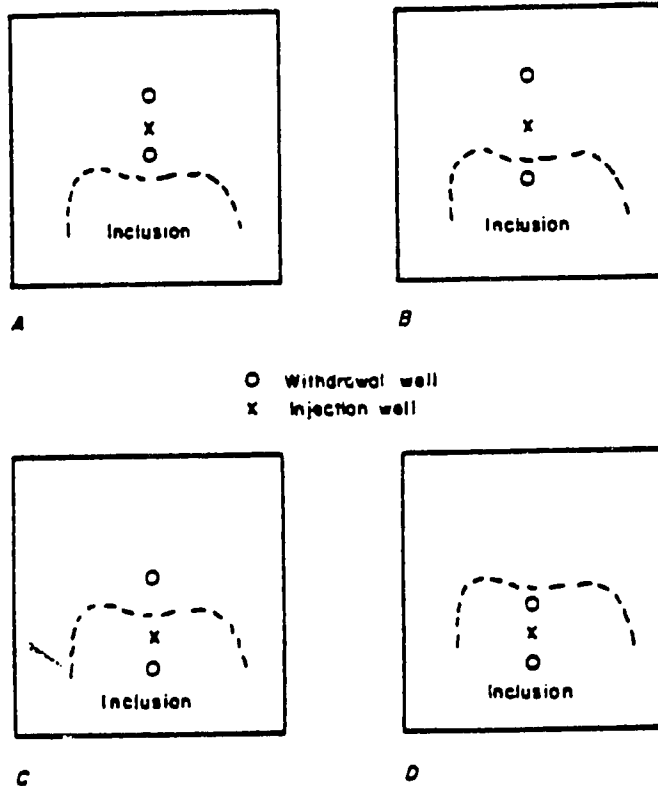


Figure 7

Plan view of possible injection-withdrawal sequences in the vicinity of the primary inclusion

2) *Two wells in the focal region, one withdrawal well in the inclusion* (Fig. 7B): The effective pressure decreases in the focal region and tension stress in the inclusion decrease. The system tends towards stability. 3) *One withdrawal well in the focal region, withdrawal and injection wells in the inclusion* (Fig. 7C): The effective pressure increases in the focal region and tension stress in the inclusion increases. The system tends toward a state of instability. 4) *All three wells in the inclusion* (Fig. 7D): Tension stress in the inclusion at outlying wells decreases and the tension stress increases in the central region. Instability develops between the two withdrawal wells. Methods 1 and 3 should be rejected as dangerous because of the possibility of triggering a large earthquake. A modification

ion
ess in the
its failure
e grounds
gh stress.
ome later
roduces an
ure in the
not possi-
nly a

method 2 is discussed in the following paragraph. Method 4 produces the desired effect of destressing the inclusion. If the inclusion represents a 'lock' point along an active fault, this method could be successful provided water is initially present and the location of the 'lock' point is known beforehand.

A third control possibility not considered is a modification of method 2 above. Assume the inclusion is saturated with water of pore pressure P_p and that the system is in the dilatant phase. If wells are drilled into the inclusion zone and water withdrawn, P_p will decrease. The inclusion will begin to 'tighten' up or close as the water is withdrawn. The effective inclusion modulus increases and the stress difference decreases in the focal region as tension stress in the inclusion decreases. The system behaves as if the inclusion is vanishing. If the tectonic stresses are large enough by themselves to close all the cracks in the inclusion when the water is completely withdrawn, this method of control could prove to be '100%' effective in destressing both the inclusion and focal region. If the tectonic stresses in the absence of the inclusion are not large enough to initiate further crack formation and/or growth, this method of control could permanently eliminate an earthquake in this region provided the boundary stresses remain fixed. However, if the tectonic stresses continue to increase, a condition will again eventually be reached where a larger magnitude earthquake may occur where only a smaller one would have taken place had the zone been left alone.

Destressing by using high explosives in high stressed zones is a proven method in many instances of rock burst control (BLAKE, 1968). If the scale independence principle is applied to this problem, then methods used to control rock bursts may apply in earthquake control problems. Very simply, destressing removes a high stress on a small area and redistributes it over a larger area. The inclusion theory provides an explanation of why destressing is a valuable control tool for earthquakes. Destressing of the focal region results in a decrease in focal region modulus. Since inclusion modulus is less affected by destressing, the inclusion length must decrease due to crack closure produced by the decrease in tensile stress within the inclusion. Thus destressing has the effect of decreasing both the tensile stress within the inclusion and the stress concentration factor at any point in the focal region. Aside from numerous practical problems involved in destressing focal regions of potential earthquakes, this approach may prove of some value in either preventing or controlling low magnitude earthquakes.

5. Conclusions

The scale independent inclusion failure theory has been applied in this paper to the problem of crustal earthquakes and, in particular, to the precursory phenomena that precede these earthquakes. In this theory, fluids are not required to be present in the focal region of an impending earthquake to produce either the precursor effects or the earthquake. Short-term precursors, such as S-bend tilt behavior and changes in the electric polarization and magnetization vectors in the focal region occurring shortly before some crustal earthquakes, were also shown to be qualitatively consistent with the inclusion theory.

My friend
constructive
ANDERSON,
drafts of thi

- AGGARWAL, Y.
Seismic tectonics
BLAKE, W., RC
Report, TPR
BOOKER, J. R.
(14), 2037-20
BRADY, B. T. (1
10, 291-309.
BRADY, B. T. (15
BRADY, B. T. (16
appl. Geophys.
BYERLEE, J. D.,
Technology,
CHERMYAVSKY,
Telonika, Tas
HEALY, J. H., L
Earthquake pr
HUSOYAMA, K. (1
quake of Mar
JIDA, K., and F
high temperat
KATO, Y., and L
Nankaido ear
LATYNTINA, L. A
strains before
MOORE, G. W. (1
NERSESOV, I. L.,
Earthquakes in
Seismic Region
PARKHOMENKO,
at pressures up
1106-1111.
RIKITAKE, T. (19
SADOVSKY, M. A
A. N., SIMBIRI
some regions o
SASTA, K., and N
Inst., Kyoto U
SCHOLZ, C. H., S
Science 181 (4)
SILVERNOV, A. M.,
earthquakes, Is
SMOLEV, G. A.,
relation to earth
Ed. 1970.

Acknowledgements

My friend and colleague, G. FITZPATRICK, has offered valuable insight and constructive criticism throughout this study. K. MOGI, M. S. PATTERSON, D. ANDERSON, C. KISSLINGER, J. DEWEY, M. WYSS, W. SPENCE, AND W. SILL read early drafts of this work and offered valuable criticism.

REFERENCES

- AGGARWAL, Y. P., SYKES, LYNN R., ARMBRUSTER, J., and SBAR, M. L. (1973), *Premonitory changes in seismic velocities and prediction of earthquakes*, Nature 241.
- BLAKE, W., *Rock Burst Research at the Galena Mine, Wallace, Idaho, USA*, BuMines Tech. Progress Report, TPR 39, 1971.
- BROKER, J. R. (1974), *Time dependent strain following faulting of a porous medium*, Geophys. Res. 79, (14), 2037-2044.
- BRADY, B. T. (1973), *A mechanical equation of state for brittle rock, Part II*, Int. J. Rock Mech. Min. Sci. 10, 291-309.
- BRADY, B. T. (1974), *Seismic precursors prior to rock failures in underground mines*, Nature 252, 549-552.
- BRADY, B. T. (1974) *Theory of earthquakes - Part I - A scale independent theory of rock failure*, Pure appl. Geophys. 112, 701-725.
- BYERLEE, J. D., *The Fractional Characteristics of Westerly Granite*, Ph.D Thesis, Mass. Institute of Technology, 1966.
- CHERMAYVSKY, A. *Atmospheric-Electric and Electrotelluric Phenomena in Earthquakes*, Cots Nauka I Telonika, Tashkent, 1963.
- HEALY, J. H., LEE, W. H. K., PAKISER, L. C., RAYLEIGH, C. B., and WOOD, M. D. (1972), *Prospects for earthquake prediction and control*, Tectonophysics 319-332.
- HUSOYAMA, K. (1952), *Characteristic tilt of the ground that preceded the occurrence of the strong earthquake of March 7, 1952*, J. Phys. Earth 1, 75-81.
- IIDA, K., and KUMAZAWA, M. (1961), *Measurements of elastic wave velocities in volcanic rocks at high temperatures by means of ultrasonic impulse transmission*, J. Earth Sci. 9.
- KATO, Y., and UTASHIRO, S. (1949), *On the changes of terrestrial magnetic field accompanying the great Nankaido earthquake of 1946*, Sci. Rep. Tohoku Univ., Series 5, Geophysics 1.
- LATYNINA, L. A., and KARMALEYEVA, R. M. (1970), *On certain anomalies in the variations of crustal strains before strong earthquakes*, Tectonophysics 9, 239-247.
- MOORE, G. W. (1964), *Magnetic disturbances preceding the 1964 Alaska earthquake*, Nature 203.
- NERSESOV, I. L., and SIMBIREVA, I. G., *Regularities in the Distribution of Stresses in the Foci of Weak Earthquakes in the Garm Area and Their Relationship to Seismicity*, Third All-Union Symposium of the Seismic Regime, June 3-7, 1968, Part I, pp. 147-181.
- PARKHOMENKO, E. I., and BANDARENKO, A. T. (1963), *Investigation of the electric resistivity of rocks at pressures up to 40,000 kg/cm² and temperatures up to 400°C*, Izv. Akad. Nauk SSSR, Geofiz. Ser. 12, 1106-1111.
- RIKITAKE, T. (1972), *Earthquake prediction studies in Japan*, Geophys. Surv. 1, 4-26.
- SADOVSKY, M. A., NERSESOV, I. L., NIGMATULLAEV, S. K., LATYNINA, L. A., LUKK, A. A., SEMENOV, A. N., SIMBIREVA, I. G., and ULOMOV, R. I. (1972), *The processes preceding strong earthquakes in some regions of Middle Asia*, Tectonophysics 14, 296-307.
- SASSA, K., and NICHIMURA, E. (1956), *On phenomena forerunning earthquakes*, Bull. Disast. Prev. Res. Inst., Kyoto Univ. 13, (1), 1-8.
- SCHOLZ, C. H., SYKES, L. R., and AGGARWAL, Y. P. (1973), *The physical basis for earthquake prediction*, Science 181 (4102), 803-810.
- SEMENOV, A. M. (1969), *Variations in the travel time of transverse and Longitudinal waves before violent earthquakes*, Izv. Earth Physics 4, 245-248.
- SUBOLEV, G. A., and MOROZOV, V. N. *Local disturbances of the electrical field on Kamachika and their relation to earthquakes*, in *Physical Bases of Seeking Methods of Predicting Earthquakes*, M. Sadovskii, Ed. 1970.

- STACY, F. D., *Physics of the Earth* (John Wiley and Sons, Inc., New York 1969), 324 pp.
- WHITCOMB, J., GARMAN, J., and ANDERSON, D. (1973), *Earthquake prediction: Variation of seismic velocities before the San Fernando earthquake*, *Science* 180, 632-635.
- WOOD, M. D., and ALLEN, R. V. (1971), *Anomalous Microtilt preceding a local earthquake*, *Bull. Seism. Soc. Am.* 61, 1801-1811.
- WYSS, MAX (1973), *Towards a physical understanding of the earthquake frequency distribution*, *J. Geophys. Res.* 78, 341-359.
- WYSS, M., and HOLCOMB, D. J. (1973), *Earthquake prediction based on station residuals*, *Nature* 243

(Received 14th August 1974)

Geophys.
vol. 113 (1975)

By V. I.

Summary -
... the Sovi
... these phenome
... diffusion mode
... expansion. Diff
... seismic velocity
... of cracks is also
... model, the earth
... here is due to c
... precursor form,
... earthquake. A
... study of post-er
... occurrence of p
... anomalous peri

In 1969 s
... velocities pri
... precursors ar
... earthquakes
... during the 15
... similar chang
... the United S
... changes in ve
... changes were
... prior to smal

There are
... cursors. One
... the Earth, Me
... resembles in
... by STUART (4)

- ¹) Institute
²) MIT Earth
³) US Geol

Theory of Earthquakes. Part III: Inclusion Collapse Theory of Deep Earthquakes

By B. T. BRADY¹⁾

Abstract

A theory of deep earthquakes, termed the inclusion collapse theory, is proposed in this paper. In the inclusion theory of crustal (or shallow) earthquakes, faults were shown to terminate within an inclusion zone. This zone represents a region within the brittle portion of the lithospheric plate that contains open cracks (voids) of varying sizes that, to a first order approximation, are uniformly distributed throughout the inclusion zone. When the lithospheric plate containing these faults and their associated inclusions is subducted into the mantle, the stress normal to the fault planes must increase. A depth is eventually reached where slippage along the fault planes is no longer possible. Earthquakes are postulated to occur at a specified depth within the mantle as a result of processes leading to collapse of these voids.

When the long-term modulus of the plate is much greater than the long-term modulus of the mantle, large pressures are shown to develop within the plate during periods of active subduction. These pressures are shown to be sufficient to initiate partial collapse of voids of similar geometry throughout the inclusion zone.

The inclusion collapse theory and the concentration of pressure within the plate lead to four results. (1) Earthquakes that are produced by a void collapse mechanism will not occur below a subduction depth calculated to be between 350 and 1000 km. (2) The physical process most likely responsible for producing void collapse is the formation of shear melt zones whose thicknesses are the order of 1 to 10 cm in the immediate vicinity of the voids. This mechanism is shown to produce a 'precursor' time on the order of a few hundred seconds during which there is a release of shear strain prior to the earthquake. (3) The maximum energy released by void collapse is independent of the source depth. (4) The number of earthquakes produced by this process will decrease hyperbolically with source depth. Source depth, in the context used in this article, refers to the depth in the mantle to the inclusion zone where voids of similar geometry are undergoing partial collapse. The maximum source depth refers to the depth where all voids have closed.

Introduction

Earthquakes have been observed to occur at depths ranging from the surface to 700 km (GUTENBERG, 1951). GUTENBERG and RICHTER (1942) determined that of the total energy released in earthquakes, nearly 15% comes from deep earthquakes. Observational data show that the frequency of occurrence of deep earthquakes decreases hyperbolically with depth and that the maximum magnitude of these earthquakes is essentially independent of depth (RICHTER, 1959). Seismic source studies also

¹⁾ Physicist, United States Department of the Interior, BuMines, Denver Mining Research Center, Denver, Colorado, USA.

suggest that the strength of rock at depths in the mantle down to 700 km is not significantly different than the strength of the rock in the vicinity of crustal earthquakes (BULLEN, 1959; WYSS and MOLNAR, 1972).

A number of different mechanisms such as faulting and/or phase changes, for example, have been proposed as possible causes of deep earthquakes. Laboratory studies have shown that sudden slip on a fault surface can only occur when the shear stress along the fault exceeds the frictional stress (BYERLEE, 1966). However, the existence in the mantle of confining pressures of 300 kb at a mantle depth of 700 km in the vicinity of the subducted plate is evidence against a shear faulting mechanism for deep earthquakes. Yet seismic signatures suggest that the mechanism producing deep earthquakes is similar to the faulting mechanism displayed by shallow crustal earthquakes (GRIGGS and HANDIN, 1960; OROWAN, 1960; ISACKS and MOLNAR, 1971). There is also some evidence that suggests the cause of deep earthquakes may be due in part to rapidly running phase transitions such as would occur in response to shear melting and/or the occurrence of polymorphic phase changes such as the pyroxene-garnet transformation and the inversion of orthorhombic enstatite to monoclinic clinoenstatite (GRIGGS and HANDIN, 1960; RINGWOOD, 1970; RIECKER and ROONEY, 1966; KNOPOFF and RANDALL, 1970; RAYLEIGH and PATERSON, 1965). Laboratory studies suggest that phase transitions, while they may be somewhat accelerated in the presence of shear stress, are much too slow to produce the observed violent characteristics of these earthquakes. Yet deep earthquakes also appear to exhibit some of the characteristics expected of a phase change mechanism; namely, volumetric compression (KNOPOFF and RANDALL, 1970). To date, no theory of deep earthquakes has been proposed that can account for these apparent paradoxes.

Inclusion collapse theory of deep earthquakes

A postulate of the inclusion theory of shallow earthquakes is that all faults must terminate within an inclusion zone. The inclusion zone creates an environment favorable for the continuation of fault growth; namely, the existence within the inclusion of a tensile stress whose axis is oriented in a direction normal to the long (major) axis of the inclusion zone. This stress eventually produces catastrophic macrocrack formation within the inclusion. Once the inclusion grows beyond a critical size, a portion of the macrocrack near the fault zone closes and becomes part of the fault. The primary inclusion zone illustrated in Fig. 1 can be considered to be a collection of smaller secondary inclusion zones each with their associated macrocracks. The collective behavior of these secondary inclusions and macrocracks is modeled by a single primary inclusion (BRADY, 1975).

With increasing depth in the earth, both the confining pressure and the ratio of the least principal stress to the maximum principal stress increase. Thus, a depth must be eventually reached where slippage within the fault zone becomes impossible (Fig. 1b).

Growth
least p
Howe
tines

(vo
im:
str:
po
vo
ma
of

Growth of the inclusion in the sense discussed in parts I and II cannot occur since the least principal stress within the inclusion zone changes from tension to compression. However, as the pressure within the lithospheric plate that contains these zones continues to increase, earthquakes in the plate may be induced by closure of macrocracks

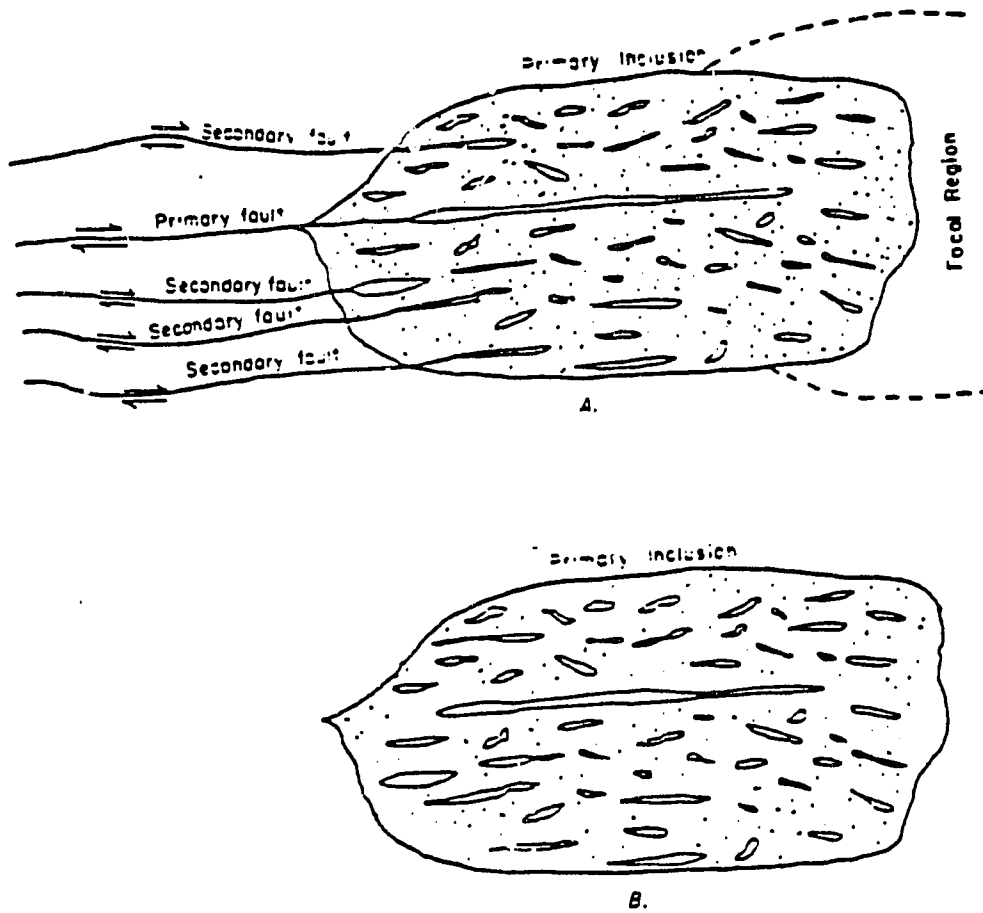


Figure 1
Effect of confining pressure on inclusion growth.

(void collapse) of successively larger aspect ratios (thickness-to-length ratio). It is important to note that void collapse will occur only near the ends of the void where the stress concentration is highest. Collapse will proceed sequentially towards the central portions of the void as the applied pressure is increased; that is, the aspect ratio of the void that remains will increase following each phase of collapse and will approach a maximum value of 1.0. Collapse of voids of aspect ratio 1.0 will signify the termination of deep earthquakes produced by this process.

Pressure required to produce collapse of spherical cavities

An estimate of the pressure required to initiate partial collapse can be made. Assume that the macrocracks, referred to hereafter as cracks, can be modeled by ellipsoidal cavities of aspect ratio α . WALSH (1965) has shown that the magnitude of the upper limiting pressure required to close cracks of aspect ratio α is αE_1 , where E_1 is the Young's modulus of the material containing the crack. The pressure (or depth within the mantle) required to close spherically-shaped cracks is of particular importance to the deep earthquake problem, since their collapse signifies the termination of all deep earthquakes caused by a void collapse process. A more refined method of calculating this pressure is presented below.

The tangential stress along the boundary of a spherical void contained within a lithospheric plate subjected to a far-field hydrostatic pressure of magnitude P , is $2P$. Let us assume that all voids whose aspect ratios are less than 1.0 have closed under the existing stress field. Since shear induced crack formation in the immediate vicinity of the spherical void is impossible (they will close unless spherical), I will postulate that the physical process by which shear induced collapse begins is by the formation of thin (low aspect ratio) platelets of melt material that are oriented in a direction parallel to the axis of local maximum compression: that is, parallel to the direction of $2P$. These regions represent the nuclei of the shear failure zones. The regions that contain the melt platelets can be modeled as inclusion zones of aspect ratio α_1 and relative 'elastic' contrast K_1 ($= E_m/E_1$, where E_m and E_1 are the moduli of the melt zone and plate, respectively). The magnitude of the tensile stress, C_1 , that is developed within this region is approximately (BRADY, 1974)

$$\frac{C_1}{2P} = \frac{3K_1(1 - K_1)\alpha_1(1 - \alpha_1)}{9K_1(1 + \alpha_1^2) + 2\alpha_1(2 - K_1 + 8K_1^2)} \quad (1)$$

where the effects due to the preferred orientation of the melt platelets is neglected. Note that the orientation of C_1 is normal to the direction of eventual shear failure. The maximum value of C_1 (C_1^{max}) will occur along the boundaries of the void and can be calculated from equation 1. The result is

$$C_1^{max} = 0.05(2P) \quad (2)$$

The theoretical tensile strength, σ_1 , of crystalline materials is known to lie between the values (COTTRELL, 1964)

$$\frac{E_1}{30} \leq \sigma_1 \leq \frac{E_1}{10} \quad (3)$$

Shear failure begins once the tensile stress, C_1 , in the melt zone equals σ_1 . The magnitude of the pressure, P_m , required to initiate collapse of the spherical crack is found from equations 2 and 3 to be

$$0.33E_1 \leq P_m \leq 1.00E_m \quad (4)$$

when the app
is much great
to initiate co

The value
collapse of c

where γ is a
Equation
spherical voi
sures in the
great depths
mately 700 k
mechanism,
present can
problem is c
in the paper.
earthquakes
mantle and
plates (ENGI

S.

Assume
disturbed st
rock in the i
of the plate.
tion, the pr
which the e
reader will
entire subd
associated v
the melt ze
impending

Two pl
subduction
plate is ass
variable su
'hung' up
mantle can

when the applied far-field stresses are hydrostatic. When the maximum far-field stress is much greater than the least stress, the range of the maximum principal stress required to initiate collapse is

$$0.22E_r \leq P_r \leq 0.66E_r \quad (5)$$

The value of the maximum applied principal stress, P_r , required to initiate partial collapse of cracks of aspect ratio α is

$$P_r = \gamma \alpha E_r \quad (6)$$

where γ is a numerical constant specified by equations 4 and 5.

Equations 4, 5, and 6 show that the pressure required to produce collapse of the spherical void is on the order of the modulus of the lithospheric plate. However, pressures in the mantle on the order of E_r ($\sim 2 \times 10^{12}$ dynes/cm²) are present only at great depths (~ 5000 km). Yet deep earthquakes have not been observed below approximately 700 km in the mantle. Thus, if deep earthquakes are induced by a void collapse mechanism, it is necessary to determine how pressures well in excess of those normally present can be concentrated in the upper mantle so as to produce collapse. This problem is considered below. The detailed physics of void collapse is analyzed later in the paper. The following analysis begins with the well-known observations that deep earthquakes occur only within lithospheric plates that are being subducted into the mantle and that these earthquakes occur only within the upper 10-to-20 km of these plates (ENGDAHL, 1973; WYSS, 1973).

Subducting lithospheric plates as manifestations of stiff inclusions

Assume that the lithospheric plate is subducted into mantle rock that in the undisturbed state is subject to hydrostatic loading. The long-term strength of the mantle rock in the immediate vicinity of the plate is assumed to be small in comparison to that of the plate. Physical justification for this assumption is presented later. In this situation, the problem reduces to that of a 'hard' inclusion; that is, the region (plate) in which the earthquakes occur, embedded within a 'softer' host material (mantle). The reader will note that the notion of an inclusion is now being extended to include an entire subducted plate. This inclusion is *not* to be confused with the primary inclusion associated with an impending crustal earthquake or with the inclusion associated with the melt zone postulated earlier to be the nucleus of the shear failure zone of an impending deep earthquake.

Two plate model motion schemes are considered. The first is the steady-state subduction model. In this scheme the entire length of the subducted portion of the plate is assumed to be in uniform motion within the mantle. The second scheme is the variable subduction rate model. In this model, the plate is assumed to be locally 'hung' up at lock zones that must be broken before motion of the plate into the mantle can occur.

Steady-state subduction model

Consider an elliptically-shaped inclusion zone (subducted plate model) of average thickness d , and length L , with average modulus E , embedded within a host material (mantle) of modulus E_m . This inclusion zone represents the brittle portion of the lithosphere in which the earthquakes occur. Let the composite system (plate and mantle) be subjected to an applied far-field hydrostatic pressure of magnitude P_0 . When the system is in mechanical equilibrium and the Poisson's ratios of the plate and mantle are equal, the stresses $\sigma_{||}$ and σ_{\perp} [where $\sigma_{||}$ and σ_{\perp} denote the principal stresses parallel to, and normal to, respectively, the length, L , of the plate] within the plate are constant and equal to (BRADY, 1974)

$$\begin{aligned}\sigma_{||} &= 3K[3(K + \alpha_1^2) + (1 + 5K)\alpha_1]N + 3K(1 - K)\left(\frac{1}{\alpha_1^2} - \frac{1}{\alpha_1}\right)N^* \\ \sigma_{\perp} &= 3K(1 - K)(\alpha_1^2 - \alpha_1)N + 3K\left[3\left(K - \frac{1}{\alpha_1^2}\right) - (1 + 5K)\frac{1}{\alpha_1}\right]N^*,\end{aligned}\quad (7)$$

where α_1 ($\alpha_1 = d/L$) is the aspect ratio of the plate, $K = E_p/E_m$ and

$$\begin{aligned}N &= \frac{P_0}{9K(1 + \alpha_1^2) + 2(2 - K + 3K^2)\alpha_1} \\ N^* &= \frac{P_0}{9K\left(1 + \frac{1}{\alpha_1^2}\right) + 2(2 - K + 3K^2)\frac{1}{\alpha_1}}\end{aligned}\quad (8)$$

The ratio of the principal stresses normal to (σ_{\perp}) and parallel to ($\sigma_{||}$) the length L , of the plate is

$$\frac{\sigma_{\perp}}{\sigma_{||}} = R = \frac{(3 + \alpha_1)K\alpha_1 + \frac{1}{2}(3 + \alpha_1^2)}{(1 + 3\alpha_1)K + \frac{1}{2}(1 + 3\alpha_1^2)}.\quad (9)$$

When the plate is 'elastically stiffer' ($E_m \ll E_p$) than the host material,

$$\begin{aligned}R &> 1, & \alpha_1 &> 1 \\ R &= 1, & \alpha_1 &= 1 \\ R &< 1, & \alpha_1 &< 1.\end{aligned}\quad (10)$$

Equations 9 and 10 show that down-dip compression must exist within the plate at depths greater than the plate thickness (d). The down-dip direction, in the context used in this paper, refers to the direction of plate descent: that is, parallel to the direction of plate motion.

The transition depth from down-dip extension ($\sigma_{\perp} > \sigma_{||}$) to down-dip compression ($\sigma_{||} > \sigma_{\perp}$) in equation 10 should be considered to be a lower limit in this subduction model for two reasons. (1) Equations 7 and 8 are only valid when the applied pressure is constant. The use of an applied pressure, P_0 , that increases with depth in the mantle, while complicating the analysis, will tend to increase the depth that the plate will have

to be s
the pla
The as
of the
numer
the ver
to a su
K is 5.
pressic
ence c
subduc
eviden
and th

It s
been s
The ex
that sa
a trans
a plate
motion

Variab

The
ductio:
is repr
(2) The
quakes
viscosi
lower
subduc
The b
no mc
The ve
the ap
actual
not be
the as
analy:

As
length
the di:

to be subducted into the mantle before down-dip compression would exist throughout the plate. This correction can be shown to produce only a 10-20% depth increase. (2) The assumption that the far-field pressure is hydrostatic in the upper 200 to 300 km of the mantle is not realistic. For example, it can be shown using equation 9 and the numerical results in the appendix that if the horizontal stress is only 20% larger than the vertical stress in the upper mantle, down-dip extension can exist within the plate to a subduction depth on the order of three times the plate thickness when the ratio K is 5.0. However, once the plate is subducted beyond this depth, down-dip compression will predominate in that part of the plate beyond this depth. Thus, the existence of down-dip extension in a plate (satisfying the constraints of the steady-state subduction model) subducted beyond a depth on the order of its thickness would be evidence that the pressure distribution within the upper mantle is nonhydrostatic and that the horizontal pressure is larger than the vertical.

It should be noted that down-dip extension has been observed in plates that have been subducted to depths on the order of 200-300 km (ISACKS and MOLNAR, 1971). The existence of down-dip extension at such depths is incompatible with a plate model that satisfies the constraints of the steady-state subduction scheme. At the maximum, a transition depth from down-dip extension to down-dip compression is 100 km when a plate thickness of 15 km is assumed. This problem does not arise in the variable motion subduction model.

Variable plate motion subduction model

The following definitions are required to develop the variable plate motion subduction model. (1) The brittle portion of the lithosphere in which the earthquakes occur is represented as an elastic plate of Young's modulus E , and average thickness d_e . (2) The mantle rock and the lower portions of the crustal lithosphere in which no earthquakes occur are both modeled as a viscous medium of average thickness d_v and linear viscosity η . The viscous zone is defined to represent that portion of the mantle and the lower viscous portions of the lithosphere whose physical state is affected by the subduction of the brittle portion of the lithosphere (referred to hereafter as the 'plate'). The base of the viscous zone is defined to be that portion of the mantle where no motion occurs. The viscous zone will be referred to as the asthenosphere. (3) The velocity-depth relationship in the asthenosphere is assumed to be linear. While the approximation of the asthenosphere as a Newtonian solid is a simplification of actual behavior (POST and GRIGGS, 1974), the general results derived below should not be significantly affected. The effect of return flow in the upper portions of the asthenosphere due to plate subduction will be neglected in the following analysis.

Assume that the plate is compressed under a compressive stress parallel to its length and that the resulting deformations of the plate are purely elastic. If u denotes the displacement of a point in the plate as it is subducted into the mantle, the local

horizontal stress parallel to the direction, s , of motion is approximately $\sigma_s = E_s(\partial u/\partial s)$ and the horizontal force per unit thickness of the plate is $d_s(\partial\sigma_s/\partial s)$. The shear stress at the bottom and top of the plate is $\eta_a d_s(\partial u/\partial t)$. Balance of the forces parallel to the direction of plate motion with the shear forces on the plate gives

$$\frac{\partial u}{\partial t} = K_s \frac{\partial^2 u}{\partial s^2}, \quad (11)$$

where $K_s = d_s d_s \bar{E}_s / 2\eta_a$. This equation has the form of the simple diffusion equation whose solutions are well-known.

The average velocity that a disturbance applied to the upper near surface portions of the plate propagates in a time t is approximately (ELSASSER, 1969)

$$v = \frac{2d_s d_s \bar{E}_s}{s\eta_a}, \quad (12)$$

where $v (=s/t)$ represents the 'propagation velocity' of the disturbance averaged over a specified time interval, t , and s denotes the distance traveled by the disturbance during this time. The average plate thickness, d_s , will be taken to be 15 km and is based on recent estimates of the source dimensions of deep earthquakes (WYSS, 1973; ENGDAL, 1973). The average asthenosphere thickness, d_a , will be taken to be 300 km and is based on calculations by ARTYUSHKOV (1971). A reasonable range for E_s for shallow depths (~ 100 km) is 0.50×10^{12} dynes/cm² to 1.0×10^{12} dynes/cm² (GRIGGS and HANDIN, 1960). NUR and MAVKO (1973) and ARTYUSHKOV (1971), using independent methods, calculated asthenosphere viscosities of 5.0×10^{19} P and 1.0×10^{20} P, respectively, where P denotes viscosity units in poise. Substituting these values into equation 12 [$\eta_a = 7.5 \times 10^{19}$ P, $E_s = 0.75 \times 10^{12}$ dynes/cm²] gives an average propagation velocity of the pressure pulse to be

$$v = 53 \text{ km/yr.} \quad (14)$$

This velocity is in close agreement with observations by MOGI (1973) on earthquake occurrence rates versus depth following major underthrust earthquakes.

Now consider the response of the plate to an underthrust earthquake that occurs near the boundary between two lithospheric plates. Assume that the plate is being compressed by horizontal forces and that the plate is locally 'hung' up on a 'lock' point(s) between the continental and oceanic plates. The following sequence of events will occur during the subduction process. (1) An underthrust earthquake destroys the 'lock' point, thereby freeing a portion of the plate to move under the existing force system. A pressure pulse whose magnitude can be estimated from equations 7 and 8 (where α , now refers to the aspect ratio of the moving portion of the plate) begins to propagate down the subducted portion of the plate at an average velocity of 50 km/yr. (2) Motion of the plate begins at a velocity estimated to be a few centimeters per year and downward migration of earthquake activity at an average velocity of 50 km/yr begins. (3) The pressure in that portion of the asthenosphere located on the underside

of the plate will decrease and this decrease will cause an extension of the trench. (4) The contrast between the upper (brittle) portion of the plate and the lower (ductile) portion will cause a reduction in the plate's resistance to compressional stress pulses following an underthrust event. (5) The effect of this extension will be to locally destress an area and this will be required for the stress to occur again [assumed from equation

where A_c is measured as 1.5×10^8 cm². A typical value of A_c from shock area measurements is approximately 66×10^8 cm² (1974) observations should also be noted as the 1964 Alaska earthquake for pressure buildup and aftershock area. In summary, the subduction model at (1) There will be a sp... plate; that is, seismic region within the plate of 50 km/yr. (2) There will be a pressure pulse in the plate when the pressure distribution collapses and down-dip extension begins. (4) The subduction process will be followed by thrusting followed by earthquake activity and 'healing' of the loc

of the plate will decrease in response to the increase in plate pressure. Stress equilibrium will cause an extensional stress state to develop within the plate on the oceanic side of the trench. (4) This physical process and the possibility of a positive density contrast between the plate and the asthenosphere in the leading portions of the moving portion of the plate will lead to conditions that tend to favor normal faulting in the upper (brittle) portions of the oceanic lithosphere. Furthermore, to this pressure reduction in the plate must be added the pressure reduction resulting from the extensional stress pulse that propagates up the plate from the initial location of the underthrust event. Thus, the plate, so to speak, slides down into the mantle.

The effect of the underthrust and normal fault sequence discussed above is to locally destress an area, A_c , of the plate between these two locations. The time, T_c , required for the stress within this area to build up and for failure (underthrusting) to occur again [assuming that the lock point(s) has been reestablished] can be calculated from equation 11. The result is

$$T_c = \frac{2\eta_a A_c}{d_a d_a E_s} = 2.11 \times 10^{-3} A_c \text{ years}, \quad (15)$$

where A_c is measured in km^2 and where $\eta_a = 7.5 \times 10^{19} \text{ P}$, $d_a = 30 \times 10^3 \text{ cm}$, $d_s = 1.5 \times 10^6 \text{ cm}$ and E_s (= surface plate modulus) is equal to $0.50 \times 10^{12} \text{ dynes cm}^{-2}$. A typical value of A_c for an underthrust event is $30,000 \text{ km}^2$ [determined from after-shock area measurements (MOGI, 1973, 1974)]. The time required for pressure build-up is approximately 66 years. This time interval is in good agreement with MOGI's (1973, 1974) observations on earthquake recurrence relationships in the western Pacific. It should also be noted that equation 15 predicts that for large underthrust events, such as the 1964 Alaska earthquake [$A_c \approx 200,000 \text{ km}^2$ (PLAFKER, 1965)], the time required for pressure buildup is on the order of 500 years. Equation 15 also shows that the pressure build-up time should increase with earthquake magnitude since magnitude and aftershock area are known to be proportional to one another.

In summary, the following five results are predicted by the variable plate motion subduction model and the associated inclusion collapse theory of deep earthquakes. (1) There will be a spatial and temporal variation in earthquake occurrence within the plate; that is, seismic activity will progress in time from a shallow region to a deep region within the plate that is calculated to occur at an average velocity on the order of 50 km/yr . (2) There will be no earthquakes induced by a void collapse mechanism in the plate when the plate is stationary or in the process of deceleration, since void collapse cannot occur in the absence of pressure overloads within the plate. (3) If the pressure distribution within the upper 200 to 300 km of the mantle is nonhydrostatic, down-dip extension can exist within the moving portion of the plate to these depths. (4) The subduction process is quasi-periodic: that is, it has a definite beginning (underthrusting followed by the migration of a pressure pulse down the plate and perhaps earthquake activity) and an end [reduction in the horizontal stress in the plate and a 'rehealing' of the lock zone(s)] and that the process may recur after a time interval

that depends on the magnitude of the earthquake and the viscosity of the asthenosphere. (5) The overall plate motion is of an oscillatory nature. An entire plate segment pulses its way down into the mantle. It is important to note that this type of motion minimizes the power required for subduction to take place.

These theoretical results are in agreement with recent observations of shallow and deep seismic events in the seismically active regions of the world (FEDOTOV, 1965; MOGI, 1968, 1973, 1974; SAVAGE, 1970; SPENCE, 1975). It is also important to note that the assumptions required to develop the variable motion subduction model are incompatible with the convection (world-wide) theory of plate motions.

Inclusion collapse as a function of depth

When the elastic contrast between the plate and asthenosphere is large; that is, $K = E_p/E_m \gg 1$, the ratio $R(= \sigma_{\perp}/\sigma_{\parallel})$ is approximately

$$R = \frac{3 + \alpha_1}{1 + 3\alpha_1} \alpha_2 \quad (16)$$

This relationship shows that in the steady-state subduction model the down-dip compression stress will be nearly ten times the normal stress (σ_{\perp}) in the plate when the total length of subducted plate is 500 km ($d_s = 15$ km). It should be noted that R will be greater than the value specified by equation 16 when nonhydrostatic stresses exist in the upper mantle (horizontal stress is assumed to be larger than the vertical). In the variable motion subduction model, the value of R will also be larger than the value specified by equation 16 since the aspect ratio of the moving portion of the plate must be greater than the aspect ratio of the total subducted portion of the plate. For example, let the length of plate freed by an underthrust event be 75 km. This gives an aspect ratio of the moving portion of the plate to be 0.20 ($d_s = 15$ km), or equivalently, a down-dip compression stress nearly two and one-half times the stress normal to the direction of plate descent. This calculation assumes that the far-field stresses are hydrostatic.

In the derivation of equation 16, attention has not been given to the additional compressive stresses that will arise from the thermal contrast between the cooler plate and the hot mantle material. These stresses will increase slightly the value of R specified by equation 16. Thus, the value of R in equation 16 should be considered to be a lower limiting value. This result suggests that brittle fracture, in the sense observed in shallow earthquakes; that is, fault-primary inclusion-focal region growth, will be unlikely unless a triggering mechanism is available for producing decreases in the local values of the principal stress difference (maximum principal stress - minimum principal stress) within the plate. It will be shown shortly that the existence of voids (cracks) in the plate that were themselves produced by shallow earthquakes prior to plate subduction can act as triggers for producing shear instabilities (melting) within the

brittle portions of the lithospheric plate. These instabilities will be shown to initiate adjacent to the void(s) and then propagate across the brittle plate, thus producing the earthquake as well as partial collapse of the void.

The preceding analysis and the two plate motion schemes and, in particular, the variable motion subduction model, show that the plate can behave both as a stress guide and as a vehicle that can produce anomalous *local* pressure concentrations within the upper mantle. Consequently, collapse of spherically- or cylindrically-shaped cracks within the primary inclusion zones produced earlier by shallow earthquakes prior to subduction may occur in the mantle as is shown by the following analysis.

Let α_i be the aspect ratio of the i th crack and c_i , its concentration, within the primary inclusion (Fig. 1b). For simplicity, a uniform distribution of crack sizes will be assumed to exist throughout the volume of the primary inclusion. The pressure P_{ci} , required to initiate partial closure of the i th crack set is approximately

$$P_{ci} = \gamma \alpha_i (1 - c_i) E_p \quad (17)$$

where E_p is the average plate modulus and γ is a parameter shown earlier to depend on the stress state existing within the plate. The average pressure, \bar{P} , within the plate is ($E_p \gg E_m$)

$$\bar{P} = \frac{1}{2} (2\sigma_{11} + \sigma_{33}), \quad (18)$$

where the intermediate principle stress within the plate is assumed to be equal to σ_2 . Equations 7, 8, and 18 combine to give

$$\begin{aligned} \sigma_1 &= \frac{6}{16\alpha_i} (1 + 3\alpha_i) P_0 \\ \sigma_2 &= \frac{6}{16} (3 + \alpha_i) P_0, \end{aligned} \quad (19)$$

where α_i is the aspect ratio of the moving portion of the plate, $P_0 = \rho_m g h$ and ρ_m and h are the average mantle density and depth below the mantle surface, respectively. The average pressure within the moving portions of the plate is found from equations 18 and 19

$$\bar{P} = \frac{1}{2} \left[9 + \alpha_i + \frac{2}{\alpha_i} \right] P_0. \quad (20)$$

The critical depth, h_i , required to initiate partial collapse of the i th crack set is

$$h_i = \frac{\gamma \alpha_i (1 - c_i) E_p}{m k_i}, \quad (21)$$

where $k_i = \bar{P}/P_0$ and $m = \rho_m g$. Equations 20 and 21 combine to give

$$h_i = \frac{8\alpha_i (1 - c_i) E_p \alpha_i \gamma}{m (2 + 9\alpha_i)}, \quad (22)$$

where terms on the order of α_1^2 are neglected. The critical depth that will be required to close all cracks; that is, the depth beyond which there will be no earthquakes that can be induced (or triggered) by a void collapse mechanism occurs when $\alpha_1 = 1.0$,

$$h_{\max} = \frac{8(1-c)E_1\alpha_1\gamma}{m(2+9\alpha_1)} \quad (23)$$

where c is the concentration of spherically-shaped cracks within the primary inclusion.

An estimate of this depth can be made. Consider first the steady-state plate motion model. Let the length (L_1) and thickness (d_1) of the plate be 800 km and 15 km, respectively. The aspect ratio of this plate is approximately 0.018. Let the average density of the mantle in the vicinity of the plate be 3.75 gm/cm^3 . A reasonable value of the plate modulus at a subduction depth of 700 km is $2.00 \times 10^{12} \text{ dynes/cm}^2$ (GRIGGS and HANDIN, 1960). Substituting these values into equation 23 gives

$$h_{\max} = 350\gamma \text{ km}, \quad (24)$$

where a nominal spherical crack concentration of 5% is assumed.

It was shown earlier that the parameter γ ranges in value from 0.33 to 1.00 for hydrostatic ($\sigma_1 = \sigma_2$) and 0.22 to 0.66 for uniaxial ($\sigma_1 \gg \sigma_2$) loading within the plate. Focal mechanism studies suggest that deep focus earthquakes are characterized by down-dip compression (ISACKS and MOLNAR, 1971). This result suggests a reasonable range of γ to 0.22 to 0.66. Thus, the maximum depth range for deep earthquakes induced by a void collapse mechanism in a plate satisfying the constraints of a steady-state subduction model is

$$77 \text{ km} \leq h_{\max} \leq 230 \text{ km}. \quad (25)$$

Now consider the variable motion subduction model. Let the length of the plate freed by an underthrust event be 75 km. The aspect ratio of the moving portion of the plate is 0.20 for a plate thickness of 15 km. Let the plate modulus and average mantle density at the critical depth be $2.00 \times 10^{12} \text{ dynes/cm}^2$ and 4.50 gm/cm^3 , respectively. The maximum depth is

$$h_{\max} = 1650\gamma \text{ km}. \quad (26)$$

In this case the maximum depth range for deep earthquakes induced by a void collapse mechanism is

$$360 \text{ km} \leq h_{\max} \leq 1090 \text{ km}. \quad (27)$$

The exact cut-off depth for either the steady-state or variable motion subduction model depends critically on parameters such as α_1 and γ that are not known with precision at this time. It is important to note that the variable motion subduction model is a physically more realistic model since the power required to subduct a plate satisfying this model is approximately three-fourths the power required to subduct a plate satisfying the constraints of the steady-state model. If the observed cut-off depth of

700 km.
the req
lated e:

Wh
require
whethe
that pro
The sol
in this c
the coll

It h.
material
is great
system (c
adjacent
plate m
zone the
the mech
able (~

The
crack ca
material
energy,
stress is
between

The s
(1928) ar
tion nor
parallel t
 L_1 and w

where v_1
and $O(\alpha)$
crack is l

700 km for the occurrence of deep earthquakes is used in the variable motion model, the required value of γ is 0.42 ($\alpha_1 = 0.20$). This value is well within the bounds calculated earlier in the paper.

Physics of inclusion collapse

While the equation $P_{cr} = \gamma\alpha E_1$ may signify the magnitude of the plate pressure required to initiate collapse of cracks of aspect ratio α , this equation gives no indication whether collapse proceeds rapidly (\sim few seconds) or what the physical processes are that produce the observed characteristics of the earthquakes associated with collapse. The solution of these two problems requires knowledge of both the loading system, in this case, the mantle, and the physical process(es) that are responsible for producing the collapse.

It has been demonstrated experimentally that failure of either brittle or ductile materials can be controlled only when the post-failure stiffness of the loading system is greater than the post-failure stiffness of the material contained within the loading system (for example, see BRADY, 1974). The low pressures within the mantle material adjacent to the subducting plate suggest that the loading system is less stiff than the plate material (see appendix). Thus, failure of cracks within the primary inclusion zone that is contained within the plate will probably be of a violent nature provided the mechanism(s) that initiate collapse can be shown to occur a time interval comparable (\sim few seconds) to that observed in shallow crustal earthquakes.

The elastic strain energy stored in a material that contains an elliptically-shaped crack can be calculated once the difference between the strain energy, W , of the material containing the crack under a specified state of applied stress and the strain energy, W_0 , of the same material without the crack under the same state of applied stress is known. The strain energy of the crack, W_c , is defined to be the difference between these two quantities: that is,

$$W_c = W - W_0. \quad (25)$$

The strain energy due to the presence of the crack has been calculated by STARR (1928) and SACK (1946) for two cases: namely, a normal stress, σ_n , applied in a direction normal to the major axis of the crack and a shear stress, τ , applied in a direction parallel to the major axis of the crack, respectively. The result for a crack of length L_c and width t contained within a plate subject to a condition of plane strain is

$$W_c = \frac{(1 - \nu_1^2)\pi L_c^2 t}{4E_1} [\sigma_n^2 + \tau^2 + O(\alpha)], \quad (29)$$

where ν_1 and E_1 are the Poisson's ratio and Young's modulus of the plate, respectively, and $O(\alpha)$ refers to terms that are on the order of the aspect ratio of the crack. If the crack is long and narrow, $O(\alpha) \approx 0.0$, and

$$W_c = \frac{(1 - \nu_1^2)\pi L_c^2 t}{4E_1} [\sigma_1^2 \cos^2 \beta + \sigma_2^2 \sin^2 \beta], \quad (30)$$

where σ_1 and σ_2 denote the principal stress (maximum and minimum respectively) and β is the angle between the major axis of the crack and σ_1 .

Equation 30 represents the energy that will be released during crack closure. For example, let the energy released by a deep earthquake at a depth of two hundred kilometers be 1×10^{23} ergs. Let the Young's modulus and Poisson's ratio of the plate segment in motion be 2.00×10^{12} dynes/cm² and 0.30, respectively. Substituting these values into equations 7, 8, and 30 gives a maximum value of the crack length (letting $l = L_c$ and $\beta = 0^\circ$) to be 175 meters for an aspect ratio of the moving plate segment equal to 0.20. Thus, to an order of magnitude, the maximum lengths of the cracks contained within the primary inclusion that are undergoing partial collapse are on the order of a few hundred meters. It should be clearly noted that this length value does not necessarily equal the source dimensions of deep earthquakes. Source dimensions of deep earthquakes are observed to be on the order of 10 km (Wyss, 1973). The cracks that are undergoing partial collapse act as triggers for the propagation of shear instabilities (melting) in a direction away from the collapsing void for reasons discussed below.

The physical process by which partial void collapse develops will be postulated to be shear failure that occurs only near the end portions of the crack (Fig. 2). Collapse of the crack will proceed sequentially toward the central portions of the crack as the inclusion zone that contains these cracks is subducted to increasing depths in the mantle.

It is important to determine whether these shear failure zones can be propagated by melting. Let H denote the heat energy required to melt a unit mass of material near the ends of the crack. The increment of energy required to melt n zones of thickness δ and lateral extent $\frac{1}{2}dL_c$ in the immediate vicinity of the crack is

$$dW_m = \frac{1}{2}n(\delta dL_c)\rho_s H. \quad (31)$$

The increment of energy released by closure of the crack by an amount dL_c is

$$dW_r = \frac{(1 - \nu_s^2)\pi t L_c dL_c}{2E_s} \sigma_1^2, \quad (32)$$

where $\beta = 0^\circ$ for purposes of calculation. Equations 31 and 32 combine to give

$$\frac{L_c}{n\delta} = \frac{E_s}{(1 - \nu_s^2)} \frac{\rho_s H}{\sigma_1^2}. \quad (33)$$

Equation 33 gives the magnitude of the crack length when the energy released by crack closure of an amount dL_c is equal to the energy that is absorbed by melting. Typical values of H , ρ_s , E_s , ν_s , α_s are 100 cal/gm = 4.2×10^9 ergs/gm, 4 gm/cm³, 2.00×10^{12} dynes/cm², 0.30 and 0.20 for a mantle depth of 700 km (GRIGGS and HANDIN, 1960) and for a plate motion model satisfying the constraints of the variable motion subduction scheme. Substituting these values into equation 33 gives

$$\frac{L_c}{n\delta} = 0.04. \quad (34)$$

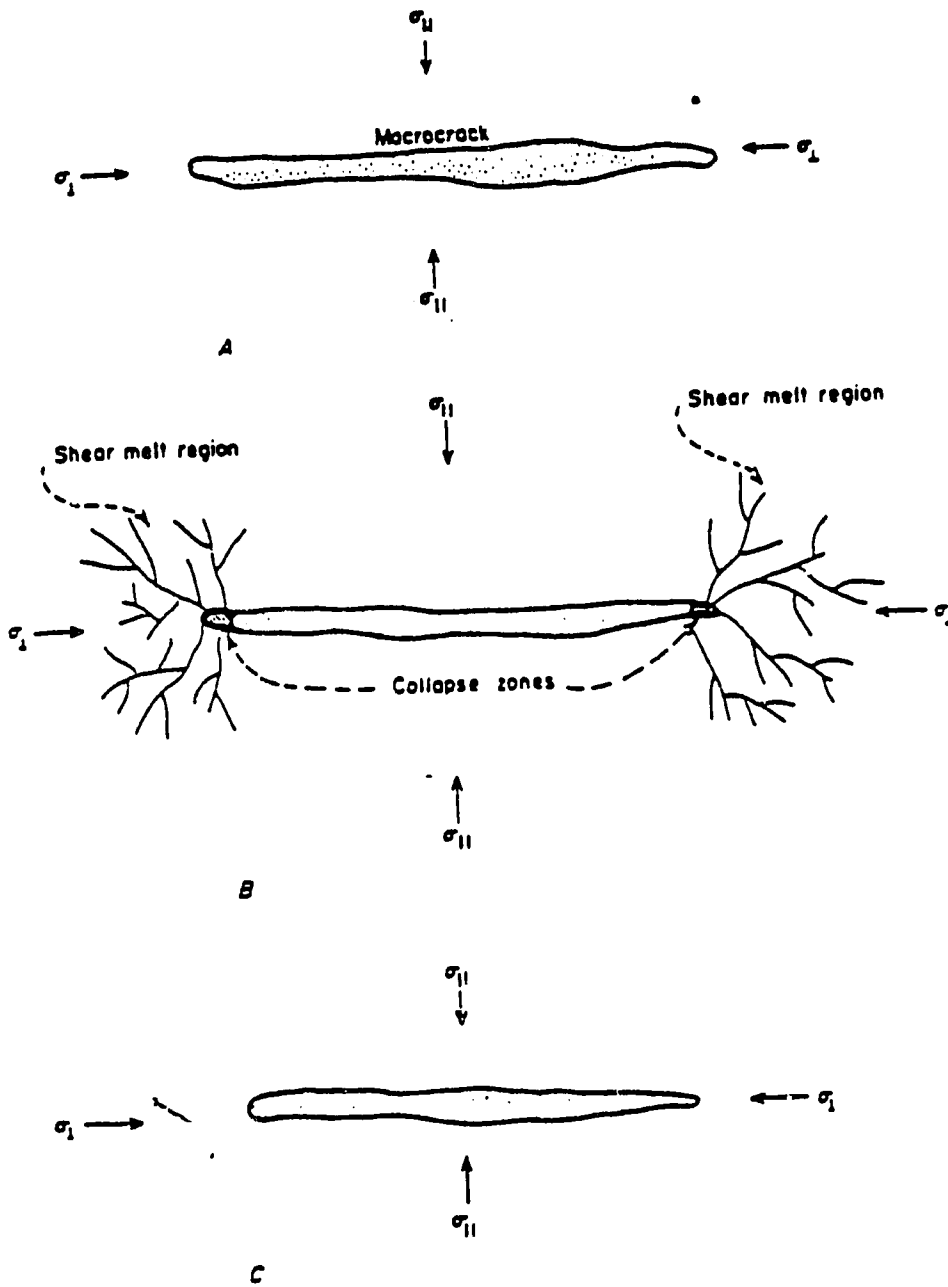


Figure 2

Process of void collapse by formation of shear melt zones in the vicinity of the void.

As an example, let $L_c = 5 \times 10^2$ cm. The number, n , of melt zones is found from equation 34 to be nearly 1×10^4 for $\bar{s} = 1$ cm and 1×10^3 for $\bar{s} = 10$ cm. Equation 35 shows that the energy released by a collapse mechanism will be at least several orders of magnitude greater than the energy required to initiate shear melting in the vicinity of the crack (Fig. 1b). This calculation suggests that the shear failure zones may propagate by a shear melting mechanism once a shear crack zone(s) has formed in

the immediate vicinity of the crack. It is to be noted that the effect of this propagating shear melt zone will be to increase the magnitude of the *local* principal stress difference in the brittle portion of the lithospheric plate. Thus, conditions become favorable for shear faulting within the plate. *It is this process that will give rise to the earthquake.*

The time required to melt a zone of thickness \bar{s} in the vicinity of the crack can be calculated. Consider a zone of thickness s^* subjected to a shear stress of magnitude τ such that the upper surface is displaced parallel to the lower surface at a velocity v . In the absence of heat flow, the time required to heat this zone to a temperature above ambient is (GRIGGS and HANDIN, 1960)

$$t_c = \frac{T_0 C_p s^*}{\tau v} \quad (35)$$

where C_p is the specific heat of the material. To obtain an order of magnitude estimate of t_c , let $T = 700^\circ\text{C}$, $\rho_s = 4 \text{ gm/cm}^3$, $C_p = 0.30 \text{ cal/gm}$, $\tau = \frac{1}{2}(\sigma_1 - \sigma_2) = 2.0 \times 10^{12} \text{ dynes/cm}^2$ and $s^* = 10 \text{ cm}$. A reasonable value of v is approximately 50 km/yr ($= 1.59 \times 10^{-1} \text{ cm/sec}$). This value of v denotes the average velocity that a pressure pulse propagates down the plate following the release of the upper near-surface portions of the plate by an underthrust and/or normal faulting sequence. Substituting these values into equation 35 gives

$$t_c \approx 400 \text{ seconds.} \quad (36)$$

The time t_c represents the period during which there will be a release of shear strain energy in the plate, after which, violent failure (shear faulting in the plate followed by partial void collapse) takes place.

The time t_c is in satisfactory agreement with the 'precursor' time observed by DZIEWONSKI and GILBERT (1974) for two deep earthquakes during which they calculated a hypocentral compression 80 seconds prior to each earthquake. This agreement also supports the hypothesis that void collapse initiating shear melting may be a viable mechanism operative in deep earthquakes.

The reader will note that the inclusion collapse theory of deep earthquakes combines both the features of shear failure and volumetric compression. It will also be noted that a shear failure mechanism aided by a shear melting scheme is not necessarily a process that will belong exclusively to deep earthquakes that are produced by a void collapse model. It is likely that a similar process will be operative in the deeper ($\sim 50 \text{ km}$) portions of shallow earthquakes characterized predominately by faulting. This hypothesis could be tested by determining whether such earthquakes exhibit a 'precursor' time during which there is a 'slow' release of strain energy a few minutes prior to the main shock. The energy released by melting would be comparable to the energy released by the main shock itself.

Discussion

Detailed studies of the focal mechanisms producing deep earthquakes will readily determine the applicability of the model proposed in this paper. For example, the mechanism of void collapse must involve two distinct processes. The first is the formation of shear melt zones that will first develop adjacent to the void and will then propagate outward from the void into the plate. The source dimensions produced by this process will be comparable to the thickness of the plate ($\sim 10-20$ km). The orientation of the shear planes will be determined by the direction of maximum compression within the plate. The second process will involve collapse of a portion of the void itself and will include the attendant volume increase of the fractured material as it is relieved of high stress. This volume increase is large and is theoretically on the order of 10% (TAKEUCHI, 1966) due to the high pressures generated within the plate during periods of motion in the mantle. Thus, if the shear failure mode generates down-dip compression as would be expected in deep focus shocks, the collapse phase, probably occurring within a few seconds after the main shock, would produce a down-dip extension component to the radiation pattern of the main shock. These two processes should produce two distinct seismic signatures: the first representing shear failure, the second representing the partial collapse of the void itself. These two effects will be observed irrespective of the position of the earthquake within the plate. It should also be noted that the expansion phase that will accompany partial collapse, ensures that aftershock sequences of deep earthquakes produced by this mechanism will either be nonexistent or else exhibit temporal characteristics of much shorter duration than their shallow counterparts. However, collapse of one void may trigger the collapse of nearby voids of similar geometry due to stress transferral. This process would give the appearance of aftershocks.

The frequency of occurrence of deep earthquakes is observed to drop off in a nearly hyperbolic pattern with depth (SYKES, 1966). In the inclusion collapse theory, the number of deep earthquakes that occur is inversely proportional to the crack length. If the distribution of crack lengths is assumed to be uniform within the primary inclusion zone prior to its subduction into the mantle, a hyperbolic frequency decay law will result since the pressure within the plate is very nearly proportional to the depth of subduction.

Equation 29 shows that the energy released by crack collapse is proportional to $P^2 L_c^3$, where L_c is the crack length and P is the pressure in the plate at the instant of collapse. This pressure is inversely proportional to L_c (equation 6). Thus, neglecting terms on the order of $O(\alpha)$ in equation 29, the energy released from deep earthquakes that are produced by a void collapse process is independent of source depth. This result is in agreement with seismic magnitude studies of deep earthquakes (RICHTER, 1958).

Lastly, an important consequence of the inclusion collapse theory is that the energy released by deep earthquakes is small in comparison to the total energy released by the descent of the plate that contains the primary inclusion zones. It was suggested that the

energy will be released in a sequential manner not only parallel to the direction of plate descent but also parallel to the strike of the plate (trench). The energy release will also be of a quasi-periodic nature with a mean period that depends on the area of plate distressed by the earthquake. These results suggest that the spatial and temporal nature of the energy released by plate motions may be sufficient to produce cumulative changes in the rotation of the earth, such as the excitation and maintenance of the Chandler wobble. Accordingly, large-scale plate motions that indirectly produce the earthquakes may also be responsible for maintaining the wobble. Earthquakes, while they may be correlated with the wobble, would clearly not be the source of this phenomenon.

Conclusions

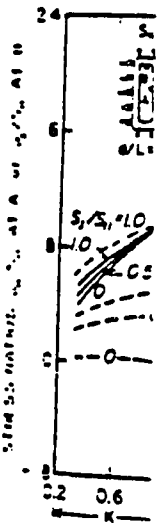
A theory of shallow and deep earthquakes with a physical basis in the scale invariant properties of rock failure has been proposed in this set of papers. Deep earthquakes were proposed in this paper to be initiated by the closure of the voids that were formed in the brittle portions of the oceanic lithosphere by large underthrust earthquakes and independently by normal earthquakes associated with the pre-trench rise. The physical process by which void collapse is initiated was shown to be consistent with the formation of shear zones by melting adjacent to the void. The large pressures required to initiate void collapse were shown to result from subduction of the plate into a material (asthenosphere) whose strength is much less than that of the plate. It was also shown that high pressures generated within the plate must be counterbalanced by lower than normal pressures in the mantle rock adjacent to the plate. If the mantle rock adjacent to the plate is near its melting point, this pressure reduction may be sufficient to produce partial melting adjacent to the plate. Thus, the plate may create an environment favorable for its subduction; namely, the formation of a low viscosity melt zone (asthenosphere) in the vicinity of the plate-mantle boundary.

Acknowledgements

Discussions with G. Fitzpatrick and W. Spence are gratefully acknowledged. Max Wyss was instrumental in improving the editorial quality of the original manuscript.

Appendix

Figure A1 illustrates the stress distribution at selected locations within and in the vicinity of a rectangular-shaped elastic inclusion of variable aspect ratio. The inclusion is contained within a material that is deformed by stresses S_1 and S_2 applied at distances far removed from the inclusion boundary. The curves in this figure were obtained by using a two-dimensional finite element method (OUDENHOVEN *et al.*



Stress ratios (σ_1/σ_2) of aspect ratios a/b : ($S_1 \geq S_2$) ap

1972). In Fig. A1 within (Fig. A1) relative stiffness shown for rectangular stress value negligible (Only with value substantiate th

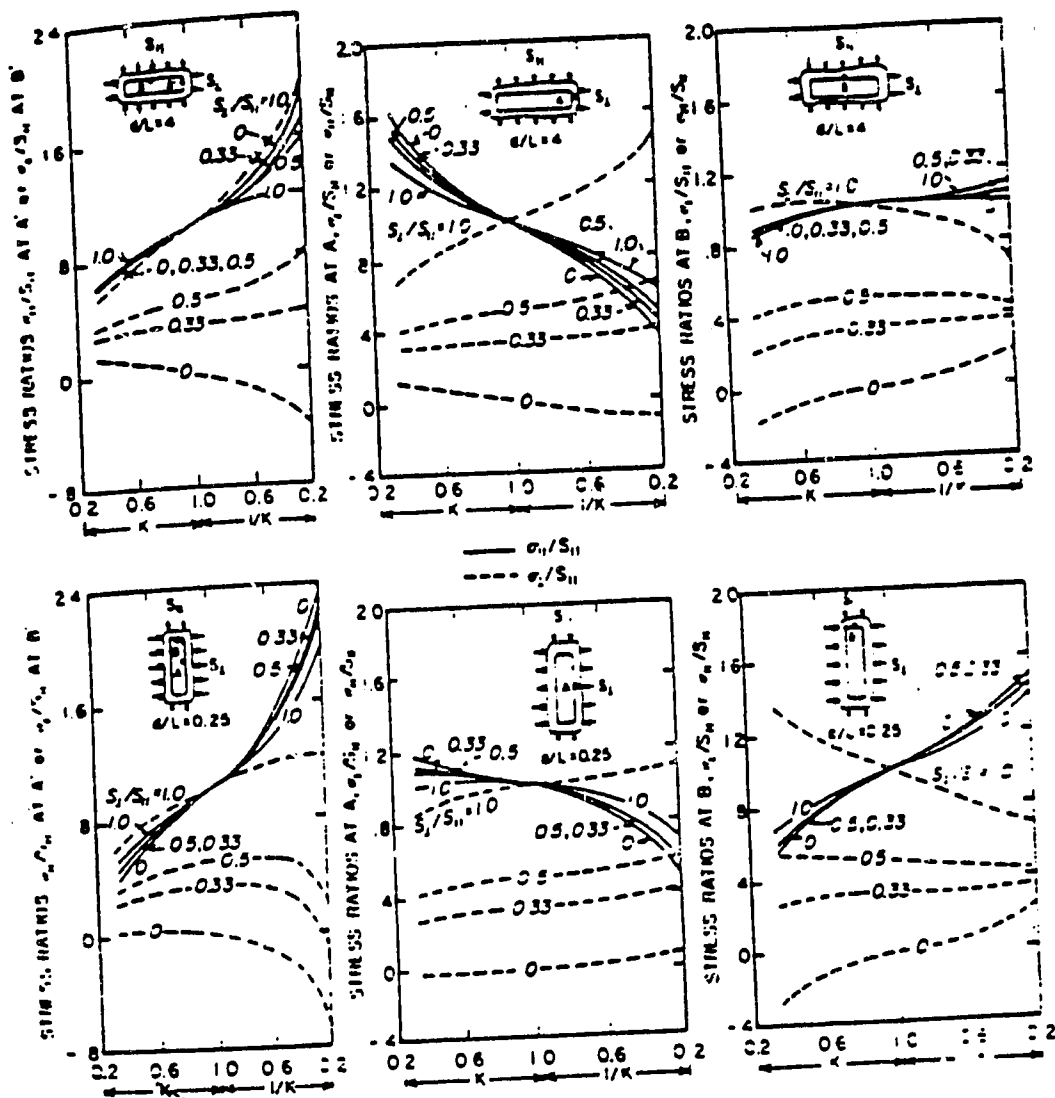


Figure A1

Stress ratios (σ_x/S_1 and σ_y/S_2) at selected points within and outside a rectangular shaped inclusion of aspect ratios 4.0 and 0.25 centrally contained within an elastic plate deformed by stresses S_1 and S_2 ($S_1 \geq S_2$) applied at distances far removed from the inclusion boundary (after OUDENHOVEN *et al.*, 1972).

1972). In Fig. A1, the stress concentrations at selected points along the boundary both within (Fig. A1a,d) and outside the inclusion (Fig. A1b,c,e,f) are shown for values of relative stiffness $K (= E_s/E_m)$ ranging in value from 0.20 to 5.00. The solutions are shown for rectangular-shaped inclusions of aspect ratios 0.25 and 4.00. The difference in stress values between this geometry and the ellipsoidally-shaped inclusion are negligible (OUDENHOVEN *et al.*, 1972). For our current application, we are concerned only with values of K greater than 1.0. Note that the numerical results in this figure substantiate the results discussed earlier in the paper and further, for values of $K > 1.0$,

the high pressures within the inclusion must be counterbalanced by low pressures outside the inclusion. Note that if the material outside the inclusion cannot support shear; that is, its relaxation constant is zero, the effective elastic contrast between the inclusion and host material vanishes. The pressure concentration within the inclusion and plate becomes equal to the applied far-field pressure.

REFERENCES

- [1] E. V. ARTYUSKOV, *On the isostatic equilibrium of the earth's crust*, Geophys. J. R. Astr. Soc. 14, 251-260, 1967.
- [2] M. BARAZANGI and B. ISACKS, *Lateral variations of seismic-wave attenuation in the upper mantle above the inclined earthquake zone of the Tonga Island Arc: deep anomaly in the upper mantle*, J. Geophys. Res. 76, no. 35, 8493-8516, 1971.
- [3] B. T. BRADY, *Theory of earthquakes - Part I, a scale independent theory of failure*, Pure and Applied Geophysics (in press), 1975.
- [4] K. E. BULLEN, *An Introduction to the Theory of Seismology*, 2nd Edition, Cambridge Press, 256 pp., 1959.
- [5] J. D. BYERLEE, *The frictional characteristics of westerly granite*, Ph.D thesis Massachusetts Institute of Technology, 1966.
- [6] A. H. COTTRELL, *The Mechanical Properties of Matter*, John Wiley and Sons, New York, New York, 430 pp., 1964.
- [7] A. M. DZIEWONSKI and F. GILBERT, *Temporal variation of the seismic moment tensor and the existence of precursive compression for two deep earthquakes*, Nature 247, 1974.
- [8] W. M. ELSASSER, *Convection and stress propagation in the upper mantle*, in S. K. Runcorn (editor), *The Application of Modern Physics to the Earth and Planetary Interiors*, Wiley, New York, New York, pp. 223-246, 1969.
- [9] E. R. ENGDALH, *Relocation of intermediate depth earthquakes in the Central Aleutians by seismic ray tracing*, Nature 245, 23-25, 1973.
- [10] T. J. FITCH and P. MOLNAR, *Focal mechanisms along inclined earthquake zones in the Indonesia-Philippine region*, J. Geophys. Res. 75, no. 8, 1431-1444, 1970.
- [11] D. T. GRIGGS and J. HANDIN, *Observations on fracture and a theory of earthquakes*, GSA Memoir 79, 1960.
- [12] B. GUTENBERG, *Internal Constitution of the Earth*, Dover Publications Inc., 2nd Edition, 439 pp., 1951.
- [13] B. ISACKS and P. MOLNAR, *Distribution of stresses in the descending lithosphere from a global survey: of focal mechanism solutions of mantle earthquakes*, Rev. Geophys. Space Phys. 9, no. 1, 103-174, 1971.
- [14] K. MUGI, *Active periods in the world's chief seismic belts*, Tectonophysics 22, 265-282, 1974.
- [15] K. MUGI, *Development of aftershock areas of great earthquakes*, Bull. Earthquake Res. Inst. 46, 175-203, 1968.
- [16] K. MUGI, *Relationship between shallow and deep seismicity in the western Pacific region*, Tectonophysics 17, 1-22, 1973.
- [17] A. NUR and G. MAVKO, *Postseismic viscoelastic rebound*, Science, 183, 204-206, 1973.
- [18] R. L. POST and D. T. GRIGGS, *The earth's mantle: Evidence of non-Newtonian flow*, Science 181, 1974.
- [19] E. OROWAN, *Mechanism of seismic faulting*, GSA Memoir 79, 1960.
- [20] A. E. RINGWOOD, *Phase transformations and the constitution of the mantle*, Upper Mantle Project Scientific Report No. 26, North Holland Publishing Company, pp. 109-156, 1970.
- [21] J. B. WALSH, *The effect of cracks on the compressibility of rock*, J. Geophys. Res. 70, 381-389, 1965.
- [22] M. WYSS and P. MOLNAR, *Source parameters of intermediate and deep focus earthquakes in the Tonga Arc*, Phys. Earth Planet. Interiors 6, 279-292, 1972.

[23] R. E. olivine
Enviro
[24] L. KNO deep ec
[25] M. S. C an isor
7645, 3
[26] J. C. S 76, no.
[27] S. A. F Islands
[28] W. SPE (in pres
[29] R. A. S London
[30] A. T. S 1928.
[31] G. PLAI 1675-16
[32] B. GUTTI Edition.
[33] C. B. R implicat
[34] L. R. SY
[35] MAX W

- [23] R. E. RIECKER and T. P. ROONEY, *Shear strength, polymorphism, the mechanical behavior of olivine, enstatite, diopside, laboradorite, and pyrope garnet, tests to 920°C and 60 kb*, AFCRL Environ. Res. Rep. 216, 1966.
- [24] L. KNOPOFF and R. RANDALL, *The compensated linear-vector dipole: A possible mechanism for deep earthquakes*, J. Geophys. Res. 75, no. 26, 4957-4963, 1970.
- [25] M. S. OUDENHOVEN, C. O. BABCOCK, and W. BLAKE, *A method for the prediction of stresses in an isotropic inclusion or orebody of irregular shape*, U.S. BuMiner Report of Investigations 7645, 36 pp., 1972.
- [26] J. C. SAVAGE, *A theory of creep waves propagating along a transform fault*, J. Geophys. Res. 76, no. 8, 1954-1967, 1971.
- [27] S. A. FEDOTOV, *Regularities of the distribution of strong earthquakes in Kamchatka, the Kurile Islands and Northeastern Japan*, Trudy Inst. Fiz. Zemli. Akad. Nauk. SSR 36, 66-93, 1965.
- [28] W. SPENCE, *The Aleutian Arc: Fracture zone, tectonic block, subduction, and magma generation* (in preparation), 1975.
- [29] R. A. SACK, *Extension of Griffith's Theory of Rupture to Three Dimensions*, Proc. Phys. Soc., London 58, 729-736, 1946.
- [30] A. T. STARR, *Slip in a crystal and rupture in a solid due to shear*, Camb. Phil. Soc. 24, 489-500, 1928.
- [31] G. PLAFKER, *Tectonic deformation associated with the 1964 Alaska earthquake*, Science 148, 1675-1687, 1965.
- [32] B. GUTENBERG and C. F. RICHTER, *Seismicity of the Earth and Associated Phenomena*, 2nd Edition, Princeton University Press, 1954.
- [33] C. B. RAYLEIGH and M. S. PATERSON, *Experimental deformation of serpentinite and its tectonic implications*, J. Geophys. Res. 70, 1965.
- [34] L. R. SYKES, *The seismicity and deep structure of island arcs*, J. Geophys. Res. 71, 1967.
- [35] MAX WYSS, *The thickness of deep seismic zones*, Nature 242, 255-256, 1973.

(Received 22nd October 1974)

Theory of Earthquakes – IV. General Implications for Earthquake Prediction

By B. T. BRADY¹⁾

Abstract – The scale invariant inclusion theory of failure is applied to the general problem of precursors that precede failure. A precursor is defined to be an effect produced within a physical system which indicates that the process leading to failure of the system has begun. Precursors are grouped into three classes. *Class I* precursors refer to long-term indicators of impending failure. These may include v_p/v_s , long-term tilt, and crustal uplift anomalies observed to precede some major shallow earthquakes by a few years. *Class II* precursors refer to short-term indicators of failure and include: S-bend tilt, electromagnetic radiation, radon emanations, and seismicity changes that have been reported to precede major earthquakes by a few hours. *Class III* precursors refer to very short-term phenomena such as long-period (strain) waves, rapid changes in surface ground tilts, and seismicity increase in the hypocentral region that are predicted by the inclusion theory to precede major shallow earthquakes by a few seconds.

The physical processes that occur within the inclusion zone of an impending failure that indirectly produce the class II precursors are used with the scale invariant properties of failure to show that their time duration is a direct measure of the average length of the cracks that comprise the inclusion zone. This result is used to derive the precursor time–'fault' length relationship that has been observed to hold for class I precursors of shallow earthquakes, mine failures, and laboratory size failures of rock. The physical model proposed for producing class I, class II, and indirectly, the class III precursors leads to six results when both the Utsu relationship between aftershock area and earthquake magnitude and the Gutenberg–Richter energy–magnitude relationship are satisfied. (1) The seismic efficiency factor for failures satisfying the constraints of the inclusion theory is approximately 0.40%. (2) The energy radiated by aftershocks will be at least 1.0% of the energy radiated by the mainshock. (3) An upper limiting magnitude of any aftershock in the aftershock sequence is $M - 1.6$, where M is the mainshock magnitude. (4) The time durations of all three precursor classes are shown to be shortened (or lengthened) by a factor inversely proportional to the rate of increase (or decrease) of the far-field stresses during the time duration of the precursor. Changes in far-field stresses, such as might occur to tidal effects, are shown to be of particular importance in initiating class II precursors, and it is shown that tidal stresses provide a mechanism for triggering large earthquakes ($M \geq 6.0$) in regions that are at the point of incipient failure. Thus, class II precursors may give the appearance of being independent of magnitude for large earthquakes. (5) When fluids are present in the focal volume of the mainshock, the predicted magnitude, calculated by class I precursors, will always be larger than the observed magnitude. (6) Seismic events that produce the inclusion zone of the impending mainshock will not be followed by aftershocks. These events are predicted to be characterized by anomalously long rupture lengths.

The inclusion theory is shown to provide a physical basis for criteria required to predict failure. The implications of the inclusion theory to the problem of earthquake prediction are discussed. The theory is applied to existing earthquake-prone regions.

A precursor is defined in this article to be an effect produced within a physical system which indicates that the process leading to failure of the system has begun. Precursors of failure will be grouped into three distinct classes. *Class I* precursors refer to the long-term indicators of impending failure and may include v_p/v_s , long-term tilt, b -value, and crustal uplift anomalies that are often observed to precede major shallow earthquakes by a few years [3, 13, 14, 19, 28, 29, 34, 35, 39, 43].² A physical model that explains many of the essential features of this precursor class has been described elsewhere [6, 7]. *Class II* precursors will be defined to represent short-term indicators of failure. For example, there is some evidence that tilt changes, in addition to the tilt anomaly of the class I type, develop several hours prior to major shallow earthquakes ($M \sim 7.0$). These tilt changes are termed S-bend tilt and are characterized by two reversals in the tilt direction in the vicinity of the earthquake epicenter shortly (\sim few hours) before the mainshock [28, 29]. Similarly, in addition to S-bend tilt, there are other class II precursors that have been reported. These include anomalous short-term vertical and horizontal crustal displacements, electrical and magnetic effects, change in water level, and in some instances, increased seismicity in the hypocentral region of the mainshock [16, 19, 28, 29, 33, 47]. There is experimental and theoretical evidence suggesting that class II precursors may be causally related to physical processes that occur in the hypocentral region prior to the mainshock [6, 7]. *Class III* precursors will be defined to represent very short-term phenomena of impending failure and include phenomena such as long-period (strain) waves, rapid changes in surface ground tilts, and seismicity increase in the hypocentral region predicted by the inclusion theory to precede major shallow earthquakes by a few seconds [10].

The study of precursors of failure and, in particular, class II precursors, their general implications for earthquake prediction, and their importance to the understanding of the physical processes involved in the preparation of a region for failure forms the subject matter of this article. The article is divided into two sections. The first section is concerned with the mathematical development of the inclusion theory. A problem of special importance examined in this section is determining the criteria for recognizing that a region has approached a condition that it will experience a failure. The second section is concerned with the application of these criteria to existing shallow earthquake zones in the earth.

Physics of failure

In order to understand the physical processes that produce the precursors of failure, a detailed physical model of the failure process in an impending failure zone

¹⁾ Physicist, U. S. Department of the Interior, BuMines, Denver Mining Research Center, Denver, Colorado, 80225 USA.

²⁾ Numbers in brackets refer to references listed at the end of this article.

is required. This subject is examined in this section. For convenience, the reader is referred to Appendix A for a glossary of symbols and terms used in the article.

Class I precursors of failure: their physical basis

Four distinct phases have been postulated and experimentally demonstrated to precede fault growth in rock on a small scale (laboratory) [6, 9]. These behavioral phases have been shown to be scale invariant over a wide range of sample sizes and are, therefore, fully applicable to the earthquake process [7, 8, 11, 12]. These phases are also applicable to describing failures that occur within lock point regions along preexisting fault zones (Figs. 1d, 2). The characteristics of these phases are clarified and summarized here as the basis for later arguments.

Dilatant phase: Cracks form within the rock mass in response to the applied far-field stresses. The far-field stresses refer to the stresses that exist within the rock mass

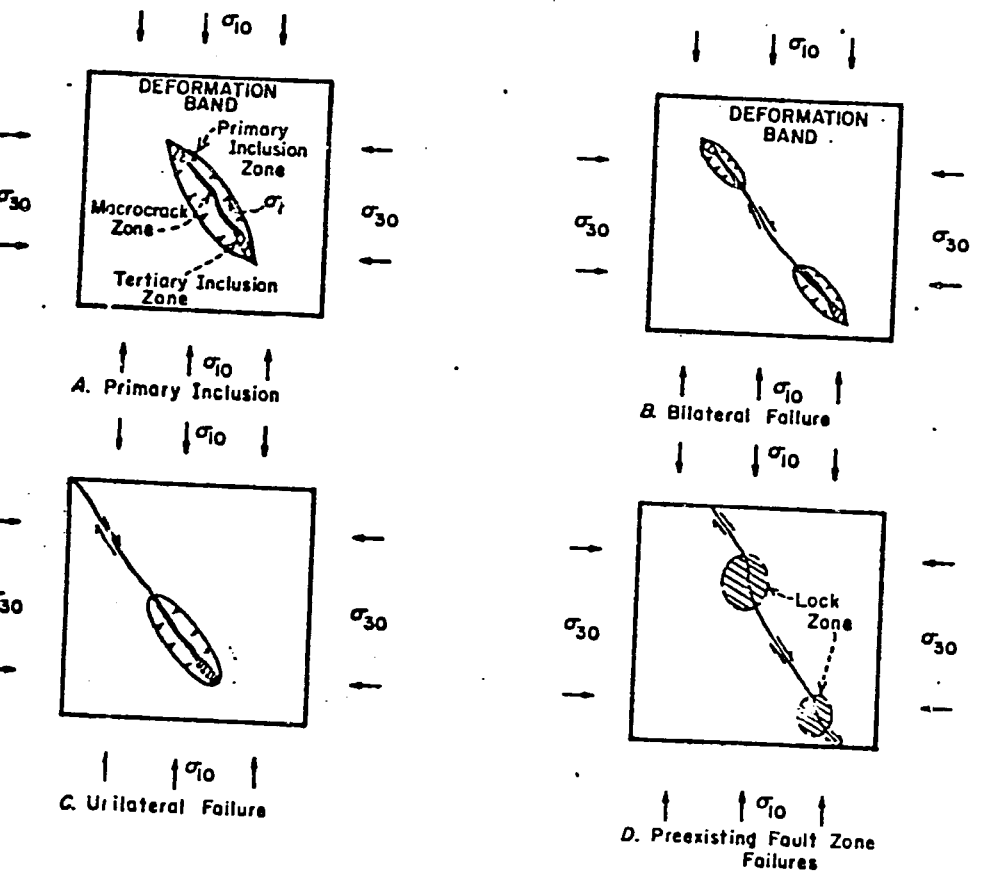


Figure 1

Classification scheme for shear failure illustrating the formation of the primary inclusion zone within the deformation band (A). Bilateral and unilateral failure classes are shown diagrammatically in B-C. Failure along a preexisting fault zone is illustrated in D.

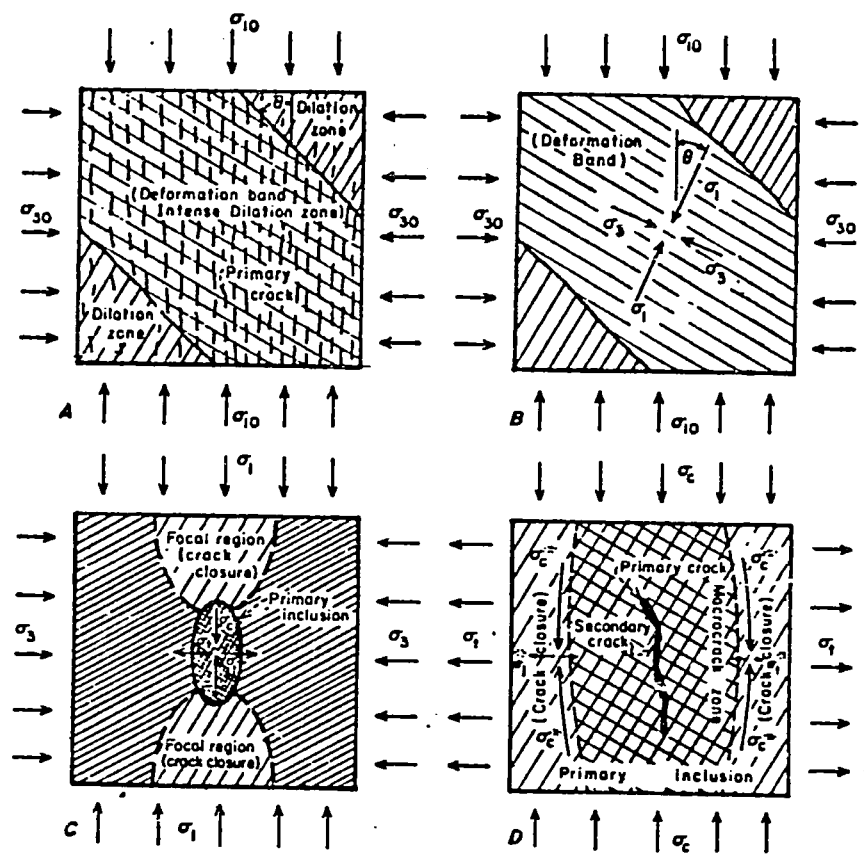


Figure 2

Sequence of macrocrack growth prior to failure. This figure illustrates the formation of the primary inclusion zone within the deformation band (anomalous region) (A-C). The formation of the secondary cracks within the primary inclusion zone and their coalescence with the primary cracks to form a macrocrack is illustrated in D.

at a distance far-removed from the dilatant zone (hereafter referred to as the anomalous region). In Figs. 1 and 2, the maximum and minimum far-field principal applied stresses are denoted by σ_{10} and σ_{30} . The intermediate principal stress, σ_{20} , is assumed equal to σ_{30} for the sake of argument. The dilatant or anomalous phase begins at a maximum far-field principal stress whose magnitude is usually well below the ultimate strength of the rock mass. This phase culminates in the formation of crack clusters [deformation band(s) (Fig. 2a)] within the anomalous volume when the rock mass is within a few percent of its ultimate strength. The deformation band(s) behaves physically as a low modulus elastic inclusion(s) that is embedded within a host material (dilatant and uncracked volume) of higher elastic modulus. This elastic contrast produces a rotation, θ , and change in magnitude ($\sigma_{10} \rightarrow \sigma_1, \sigma_{30} \rightarrow \sigma_3$) of the principal stresses both within and in the vicinity of the deformation band. The

magnitude of σ_3 decreases in compression within the deformation band as the deformation band softens. The amount of stress axis rotation and the change in the stress values depend on the relative elastic contrast between the deformation band and the surrounding material [6]. An example and brief discussion of this behavioral phase is presented in Appendix B.

Inclusion phase: Additional cracks will develop in response to local stress conditions existing within the deformation band as the applied far-field stresses (σ_{10} , σ_{30}) continue to increase. Cracks may also develop along the boundaries of the deformation band due to stress concentrating effects of the deformation band and as the deformation band continues to soften in response to continuing crack growth within the band. At a point in time before failure, an *inclusion zone*, termed *the primary inclusion zone* will develop within the deformation band (Figs. 1, 2c). In the context of this article, the primary inclusion zone represents a region of highly concentrated dilatancy that forms at a time before failure that is dependent only on the size (magnitude) of the failure that is to follow and the time rate of change of the far-field applied stresses [6, 7].

Once the primary inclusion zone has formed, compressive (σ_c) and tensile (σ_t) stresses are induced within the zone parallel to and normal to, respectively, the eventual direction of fault growth (Fig. 2c). These stresses are a result of the elastic contrast between the primary inclusion zone and the surrounding material. It is important to observe that the primary inclusion zone exists, or begins to evolve, only when the *least principal stress within the deformation band in the vicinity of where the primary inclusion zone will form changes from compression to tension*. The formation of the primary inclusion zone causes the local principal stress difference $\sigma_1 - \sigma_3$ to decrease in the focal region of the primary inclusion, that is, the region into which the primary inclusion will grow at the instant of failure (Figs. 1, 2c). Class I precursors, such as tilt and seismicity rate, will begin to exhibit deviations from their 'normal' pre-earthquake values as the primary inclusion zone forms. The seismic velocities v_p and v_s will decrease for seismic ray paths that pass through the primary inclusion zone. There will be no change for ray paths passing only through the focal region. Note also that b -values will decrease from their 'normal' background level for the seismic events that form the deformation band. The physical cause for the b -value decrease is that the local least principal stress decreases during the formation of the deformation band. Thus, some of the energy that normally would have been dissipated by frictional sliding for these events will now be available to power the growth of these events into their respective focal regions where the value of the least principal stress is σ_3 ($\sigma_3 < \sigma_{30}$). Hence, the effective magnitudes of the seismic events will tend to increase as the deformation band softens, that is, as σ_3 decreases in compression. The largest b -value decreases will be for the events that form the primary inclusion zone of the forthcoming mainshock since the value of σ_3 in the vicinity of where the primary inclusion zone will form is approximately zero.

in magnitude of the local shear stress and the corresponding increase (in compression) of the least principal stress (σ_3). The seismically determined stress axes that produce crack closure will be rotated 90° from the stress axes that produced the cracks that comprise the anomalous volume and the primary inclusion zone. Thus, the strain energy density increases throughout the focal region and approaches its *maximum possible value* when all cracks that formed during the dilatant phase are closed. Consequently, the focal region will become elastically stiffer than its surroundings and, as such, will behave physically as a *stress guide* for the direction of fault growth during the growth phase of the failure. *Therefore, focusing of the strain energy, some of which will be released during the mainshock, is predicted to occur in a direction parallel to the rupture propagation direction.*

Shortly before failure, when the focal region of the primary inclusion zone has become elastically stiffer than the surrounding anomalous volume, the stress difference will increase outside the focal region in the direction of eventual fault growth. Thus, increased seismicity is predicted by the model to occur outside the focal region prior to the mainshock. The seismically determined stress axes of these seismic events will exhibit an orientation similar, though not identical, to the stresses that produced cracks during the dilatant phase within the anomalous zone.

It is not a necessary and sufficient condition for cracks to be physically present in the focal region of the primary inclusion to produce failure. The presence of the primary inclusion zone produces both a reversal in the local principal stress difference and an increase in the mean pressure in the focal region. These two conditions give rise to an increasing value of σ_1 within the primary inclusion zone as this zone evolves toward its final pre-failure state. Thus, v_p , v_s , and/or v_p/v_s anomalies need not exist within the focal region prior to the failure. Therefore, when the focal region of the impending failure is 'dry', that is, when effects due to fluid diffusion away from the primary inclusion zone can be neglected, the seismic velocities v_p and v_s will both increase during the closure phase for ray paths passing through the focal region. There will be no increase in v_p and v_s from their 'normal' background values during the formation of the primary inclusion zone. However, when the focal region is wet, fluid diffusion away from the primary inclusion zone (in response to crack closure) may produce small fractures within the focal region, causing both v_p and v_s to locally decrease for ray paths through the focal region. These velocities will recover to their pre-dilatant values only when the closure front has passed.

Just prior to failure, the tensile stress, σ_t , in the interior of the primary inclusion approaches its maximum possible value when all cracks in the focal region have closed. If the ratio of the applied stresses (σ_1 and σ_3), σ_1/σ_3 , is sufficiently small [≤ 0.10], secondary cracks (Fig. 2d) (termed *primary* foreshocks of the impending mainshock) will form in the primary inclusion zone. Coalescence of the primary and secondary crack occurs and macrocrack growth begins within the macrocrack zone (Figs. 2c,d). It is important to observe that both the shear stress and shear strain will decrease within the focal region prior to the mainshock, that is, during the class I

precursor phase. Similarly, both the mean pressure and volumetric strain will increase during this phase. In addition, both the shear stress and strain will increase within the focal region just prior to the mainshock in response to crack growth within the primary inclusion zone. This predicted behavior is in marked distinction from other 'dry' failure models [44, 48] where the shear strain increases as the shear stress decreases prior to failure.

Class II precursors of failure: their physical basis

The scale invariant inclusion theory has been used successfully to explain class I precursors, such as anomalous tilt and seismicity to mention a few, observed to occur a few years prior to major shallow earthquakes [7, 28, 29]. This theory also provides a physical basis for class II precursors, such as S-bend tilt, and several results of particular physical importance follow.

S-bend tilt. Figure 2d illustrates the formation of secondary cracks in response to an increasing magnitude of the tensile stress, σ_n , within the primary inclusion zone as the focal region of the primary inclusion begins to store strain energy. The secondary cracks lead to the formation of the macrocrack (macrocrack zone, Fig. 2d) by their coalescence with previously formed (primary) cracks whose lengths are comparable with the secondary cracks. Finite element modeling of this problem [8] has shown that the compressive stress, σ_c^* , increases along the boundary of the macrocrack zone as the macrocrack zone 'softens' in response to the generation of the cracks within the secondary inclusion zones that will lead to the formation of the secondary cracks. Thus, as the relative elastic contrast increases between the macrocrack zone and its surroundings, the local values of the stress difference and the mean pressure decrease and increase, respectively. Hence, cracks that formed earlier within the primary inclusion zone outside the macrocrack zone begin to close as the secondary inclusion zones that are contained within the macrocrack zone (Fig. 2d) evolve to their respective failure initiation points. Therefore, the thickness, or equivalently, the aspect ratio of the primary inclusion zone, defined as the zone that contains open cracks, must decrease as failure becomes imminent.

Figure 3 illustrates the fault-primary inclusion zones, the focal region of the primary inclusion zone, and the idealized behavior of a tiltmeter located on the surface above the focal region. The physical situation depicted in Fig. 3 would be that of a thrust fault earthquake-type geometry. Similar, though not as pronounced, tilt behavior will also be observed for a strike-slip fault earthquake type geometry [7]. The tiltmeter will exhibit the following sequence of events in response to physical processes occurring within the focal region and the primary inclusion zone prior to the failure. (1) Tilting is in a direction away from the primary inclusion zone as this zone evolves in response to the applied principal stress within the deformation band. This time interval will be evidenced by decreasing v_p/v_s values within the primary

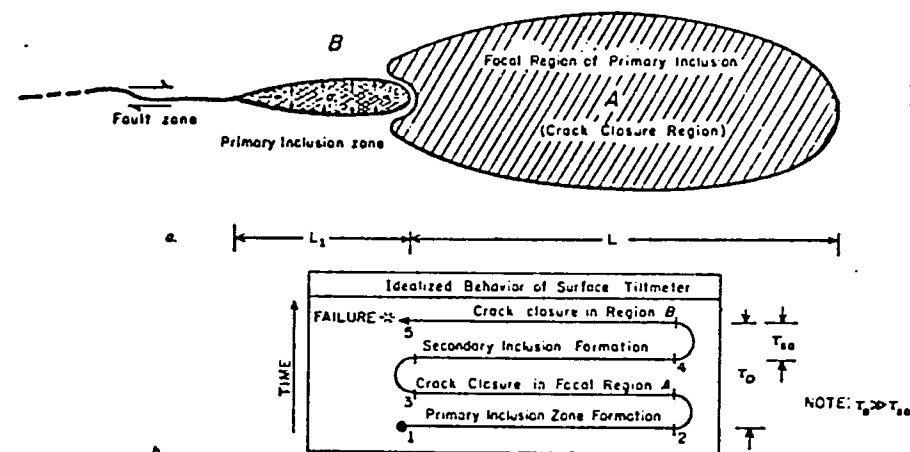


Figure 3

Fault zone—primary inclusion zone—focal region idealization of a thrust-fault geometry (a) and the idealized behavior of a hypothetical tiltmeter location on the surface above the focal region (b).

rotation within the focal region of the impending failure [7]. (2) Crack closure in the focal region of the primary inclusion will eventually dominate the deformation, causing a reversal in the tilt direction. Recovery of v_p/v_s may occur in the focal region, and other class I precursors, such as tilt, will return to their 'normal' predilatant values during this time interval. (3) Crack growth within the secondary inclusion zones that are themselves contained within the primary inclusion zone (macrocrack zone, Fig. 2d) eventually leads to the formation of the secondary cracks. Crack growth within the secondary inclusion zone produces tilting in a direction away from the primary inclusion zone. Note that the increased stress levels in the focal region of the primary inclusion may produce 'overshoot' of v_p/v_s above its pre-dilatant level; that is, its value prior to the formation of the primary inclusion zone, as additional cracks that were present prior to the anomalous phase close. (4) As cracks continue to form within the macrocrack zone, the stresses σ_c^* and σ_t^* increase and decrease, respectively, causing the closure of cracks outside the macrocrack zone. This closure will produce a reversal in the tilt direction. As these cracks close, the elastic contrast between the macrocrack zone and its surroundings approaches a maximum. The tensile stress in the primary inclusion zone, the stress concentration within its focal region, and the shear stress along the fault zone all approach their maximum pre-failure values. When the stress conditions within the primary inclusion zone are favorable to produce secondary crack growth, that is, those cracks that will coalesce with the primary cracks in the macrocrack zone, the failure must occur at this point in time as the principal stress difference within the focal region of the primary inclusion begins to increase during the class II precursor time [7]. Note that the predicted tilt direction will be toward the epicentral region just prior to the mainshock. Note also that this model predicts that the time duration of S-bend tilt

is a direct measure of the length of the secondary cracks that comprise the macrocrack zone. This time duration will also provide a direct measure of the average length of the cracks that initially formed the primary inclusion zone. In addition, the lengths of the secondary cracks are, in turn, directly related to the size (magnitude) of the failure that will be produced.

Other class II precursors. Other short-term precursors resulting from the physical processes that occur in the primary inclusion of the impending failure are also predicted to develop during the time duration of the S-bend tilt phase. For example, when the impending failure will be of a thrust-like geometry, these precursors will include the following phenomena. (1) The regional uplift displacement rate above the primary inclusion will increase in response to crack formation within the secondary inclusion zone during the early phases of S-bend tilt. The rate of uplift will begin to decrease in response to crack closure within the volume outside the macrocrack zone during the latter portions of the S-bend tilt phase. Thus, regional subsidence may occur above the primary inclusion zone just prior to the mainshock. Similarly, the rate of regional subsidence above the focal region of the primary inclusion will increase during the S-bend tilt phase in response to the increased stress levels during this phase. (2) Seismic velocities will increase as cracks close within the volume outside the macrocrack zone. (3) Seismicity will increase within the macrocrack zone as cracks form within the macrocrack zone. The energy released by this process is shown shortly to be at least five orders of magnitude less than the energy that will be released during the mainshock.

Direct field observations of some of these predicted precursors have been reported [19, 28, 29, 36]. For example, MATUZAWA [36] has reported evidence of rapid elevation changes a few minutes prior to the 1923 Kanto earthquake. Increased radon content shortly before earthquakes has been detected in wells far removed from the hypocentral region of impending large earthquakes [19]. Increased stress in these regions, resulting from crack growth within the macrocrack zone, may be responsible for this effect, thus suggesting that radon emission and increased stress levels prior to earthquakes are positive correlated quantities. Electromagnetic phenomena, if conditions favoring their existence are present [7], that may be stress induced have been reported to precede major earthquakes. Anomalous animal behavior prior to these earthquakes may also be a result of these same stress-induced electromagnetic effects. Such anomalies are consistent within the framework of the inclusion theory [7].

Class III precursors of failure: their physical basis

The inclusion theory rests on the postulate that failure occurs when all cracks in the focal region of the primary inclusion are closed, or equivalently, when the strain energy density throughout the focal region is a maximum. At this point in time, the physical contrast between the primary inclusion and its focal region becomes a maximum. The tension stress within the primary inclusion and the strain energy

density throughout its focal region reach a maximum just prior to the initiation of the mainshock. Crack growth occurs within the secondary inclusion zones, leading to the formation of secondary cracks, coalescence of these secondary cracks with the primary cracks occurs, and the macrocrack forms within the primary inclusion zone. This sequence of events marks the termination of the class II precursor stage. Growth of the macrocrack, or alternatively, the initiation of the mainshock sequence, begins at this point in time.

Growth of the macrocrack into its focal region, termed the tertiary inclusion zone (Fig. 4), will be evidenced by a decrease in the magnitude of the tensile stress within the primary inclusion to a value, say σ_i , that is below its maximum pre-failure value σ_{i0} . Closure of the macrocrack in the immediate vicinity of the fault zone will

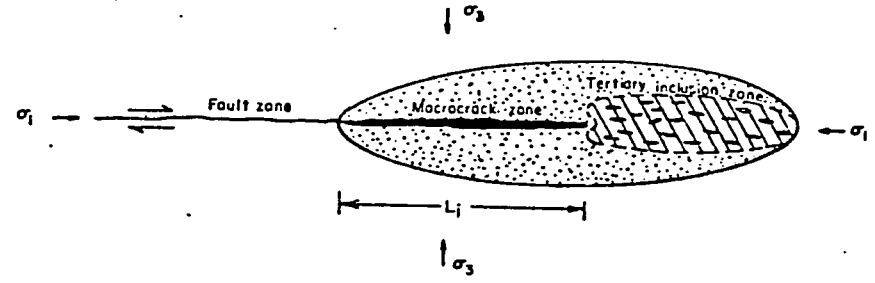


Figure 4
Illustration of the tertiary inclusion zone within the primary inclusion zone.

occur as the normal stress at the fault-primary inclusion zone boundary increases as the tensile stress within the primary inclusion zone increases. In the inclusion theory, failure can continue only when the tension stress within the primary inclusion equals its maximum pre-failure value (σ_{i0}), that is, the tensile stress that exists in the immediate vicinity of the macrocrack tip (tertiary inclusion zone, Fig. 4) must be sufficient to initiate new crack growth.

This model of macrocrack growth predicts a number of precursory phenomena that will result from the physical processes that occur within the tertiary inclusion zone. These precursors will include the following: (1) The displacement rate above the primary inclusion zone will increase dramatically as cracks form within the tertiary inclusion zone. (2) Seismicity increase in the tertiary inclusion zone and electromagnetic phenomena in the epicentral region (assuming conditions favoring their existence are present), will become pronounced during the time duration of the class III precursor in response to the rapid increase in load and loading rate in the focal region of the primary inclusion [7, 49]. These increases will be in addition to those that developed during the class II precursor phase. (3) There will be a release of strain energy produced by macrocrack growth within the primary inclusion just prior to the initiation of catastrophic fault growth ('strong motion'). The time duration of this release is on the order of L_i/v_p , where L_i is the length of the primary inclu-

inclusion zone and v_p is the longitudinal wave velocity in the material just prior to the mainshock. Thus, the model predicts that there will be a release of 'low' frequency elastic energy prior to the initiation of strong motion (fault growth). The time duration of this energy release will be shown shortly to be a function of the magnitude (M) of the mainshock.

A detailed model of the dynamics of fault growth during the mainshock sequence and its role in aftershock formation has been discussed elsewhere [10].

Direct field observations of these predicted class III precursors are scanty, although there is some evidence of low frequency waves occurring before some strong earthquakes [41]. There is also evidence of low frequency waves recorded on long-period seismometers shortly before (~few seconds) the initiation of strong motion of some shallow earthquakes [S. T. HARDING, personal communication, 1975]. The phenomena of 'earthquake lights' and atmospheric electrical discharges have been documented to occur a few minutes or seconds prior to some strong earthquakes [49]. There is also some evidence of very short-term anomalous tilt prior to moderate earthquakes. For example, HARDING and KIRBY [personal communication, 1975], using long-period seismometers in the epicentral region of the August 1975 Yellowstone earthquake sequence, observed a tilt-like precursor approximately 0.2 sec prior to a number of aftershocks in the magnitude $M4$ range.

Lastly, there are three additional observations of the inclusion theory that deserve mention. (1) The direction of fault growth will be parallel to the direction of the local maximum principal stress at all times during the growth phase of the failure. Thus, while shear faulting would appear to violate the requirement that failure satisfy a minimum energy principle, that is, the fault forms at an angle to the applied stresses (σ_{10}, σ_{30}), this difficulty does not arise in the inclusion theory. The fault always grows parallel to the direction of the local maximum applied principal compressive stress (σ_1). (2) The Griffith theory is a limiting case of the inclusion theory since the equations reduce the Griffith equation when there is no elastic contrast between the inclusion and its surroundings [6]. However, the Griffith theory is strictly applicable only to describe the formation of the *first crack*, usually considered to form on the molecular level [23]. Once this crack(s) has formed, crack interaction effects must be considered to describe the further evolution of failure. (3) The inclusion theory predicts the existence of a critical confining stress when the behavior of the material changes from a brittle to a ductile deformation mode. This transition will occur when the ratio of the least principal far field stress, σ_{30}/σ_{10} , attains a value ($\sim 0.07 \rightarrow 0.10$) such that the tensile stress within the inclusion zone cannot attain the value σ_{10} .

Precursor time-length relationship of failure

A diffusion-like functional relationship between precursor time and focal region area is predicted by the scale invariant properties of the inclusion theory [7]. Thus,

relationship between the class I precursor time (τ_0) and the focal area (A), the primary inclusion zone of the impending failure can be written,

$$\tau_0 = \alpha A, \quad (1a)$$

where α is a proportionality constant. Once the primary inclusion zone has formed, the process leading to the formation of the secondary cracks which will, in turn, coalesce with the primary cracks at the instant of the mainshock, begins. If A_c denotes the cross-sectional area of an average size crack within the primary inclusion zone, then the relationship between τ_0 and A_c can be written by virtue of the scale invariant properties of the inclusion theory

$$\tau_0 = \beta A_c, \quad (1b)$$

where β is a constant whose magnitude and relationship to α are determined below.

For simplicity, we shall assume that the average size crack which forms within the secondary inclusion zone just prior to failure can be modeled by a narrow penny-shaped geometry, that is, $A_c = (\pi/4)L_c^2$ where L_c denotes an average linear dimension of the secondary inclusion zone. Let us also assume that the scale invariant properties of the theory are applicable to some minimum average length, say $L_c = l_c$, that is on the order of a few molecular bond lengths. On this scale, l_c denotes the fundamental secondary inclusion length within which a crack of length l_c will form at the instant of failure. This crack may be nucleated at dislocations and/or other stress raisers, such as point defects (impurity atoms, vacancies). The energy required to form such a crack on this scale is of the order of a few electron volts ($1 \text{ eV} = 1.6 \times 10^{-12} \text{ ergs}$) [23]. Thus, an order of magnitude estimate of l_c is $1 \times 10^{-7} \text{ cm}$ (see equation 10). Let v_p represent the longitudinal wave velocity in a physical system of this dimension. Major structural changes, in this instance, crack formation, cannot be predicted within this system in a time interval that is shorter than the characteristic time, l_c/v_p , of the system. Therefore, the relationship $l_c/v_p = (\pi/4)\beta l_c^2$ must be satisfied, or simply, the proportionality constant β is $(\pi/4)/l_c v_p$. Reasonable values of v_p and l_c on this length scale are $1 \times 10^6 \text{ cm/sec}$ and $1 \times 10^{-7} \text{ cm}$, respectively. Hence, an order of magnitude estimate of the class I precursor time-crack area relationship is

$$\tau_0 \approx 10 A_c \quad (A_c \geq 10^{-14} \text{ cm}^2), \quad (2a)$$

where τ_0 and A_c are measured in seconds and square centimeters, respectively.

Equation (2a) can be used to derive the functional relationship between τ_0 and what has been referred to in the literature as 'fault' length, L . 'Fault' length will be defined to be the average dimension of the aftershock region (focal region) whose area is denoted by A [2, 5, 11]. Let $L = \mu L_i$, where μ (≥ 1.0) is a scale invariant quantity relating the ratio of focal region length to primary inclusion length. Let γ denote the ratio of the average crack length (L_c) within the primary inclusion zone to the length of the primary inclusion zone (L_i). Equation (2a) can be written

$$\tau_0 \approx 10(\gamma/\mu)^2 L^2. \quad (2b)$$

A reasonable estimate of μ is 3.0, since the range of influence of an ellipsoidal-shaped inclusion is of the order of three times its length [22]. Experimental investigations by the Bureau of Mines of tilt and seismicity precursors in a wide variety of rock types indicate that in standard size laboratory specimens (5 cm in diameter, 10 cm in length), τ_0 and L are approximately $(1 \pm 3) \times 10^{-3}$ sec and 1 ± 3 cm, respectively [9]. Substituting these values into equation (2b) gives $\gamma = 1 \times 10^{-2}$, in good agreement with other independent measurements of crack size within the primary inclusion (see Fig. B1, Appendix B). Thus, an order of magnitude estimate of class I precursor time—focal region area relationship in rock materials is approximately $\tau_0 \approx 1.0 \times 10^{-4} A$, where τ_0 and A are measured in seconds and square centimeters, respectively.

It will be shown in the application section and Appendix C that rockbursts in northern Idaho, where the primary inclusion zone length, magnitudes, and class I precursor times are known, give an upper limiting value of the relationship between τ_0 and A . The result is

$$\tau_0 = 2.43 \times 10^{-4} A. \tag{3}$$

It is also shown that (for materials whose porosity is approximately zero) the ratio of focal region area to primary inclusion area is $A/A_i = 21.8$. According to the postulated scale invariant properties for failure, the evaluation of these parameters for a known failure is sufficient to describe the characteristics of all other failures.

Figure 5a illustrates the precursor time—'fault' length relationships that are observed for selected earthquakes, mine failures, and laboratory size rock failures [1, 9, 11, 34]. The fit of equation (3) to these data is shown for comparison. The relationship between precursor time and calculated average crack length ($L_c = (\gamma/\mu)L = 5.28 \times 10^{-3}L$) for these data is shown in Fig. 5b. Note that the predicted average crack lengths associated with the rock bursts are in the order of 10^2 cm. These length estimates also agree with independent calculations of crack lengths associated with the energy radiated by individual cracks in rockbursts ($\sim 10^{10}$ ergs). Note also that average crack lengths predicted to be associated with the dilatant zones of major crustal earthquakes, such as might occur at sites of major underthrusts and/or normal-faulting earthquakes along subduction zones, are of the order of a few tens of meters to a few hundred meters. These length predictions agree closely with crack lengths calculated elsewhere [8] that induce deep earthquakes by a void collapse mechanism.

The relationship between the time duration for the class II precursor time, τ_{10} , focal region area (A), and average crack area (A_c) within the primary inclusion zone is readily determined from equations (2a) and (3). The result is

$$\tau_{10} = 2.43 \times 10^{-4} A_c = 1.11 \times 10^{-9} A, \tag{4}$$

where τ_{10} is measured in seconds and both A and A_c ($A_c = 10^{-4} A_i = 10^{-4} A/21.8$) are measured in square centimeters. It is assumed that no changes occur in the far-

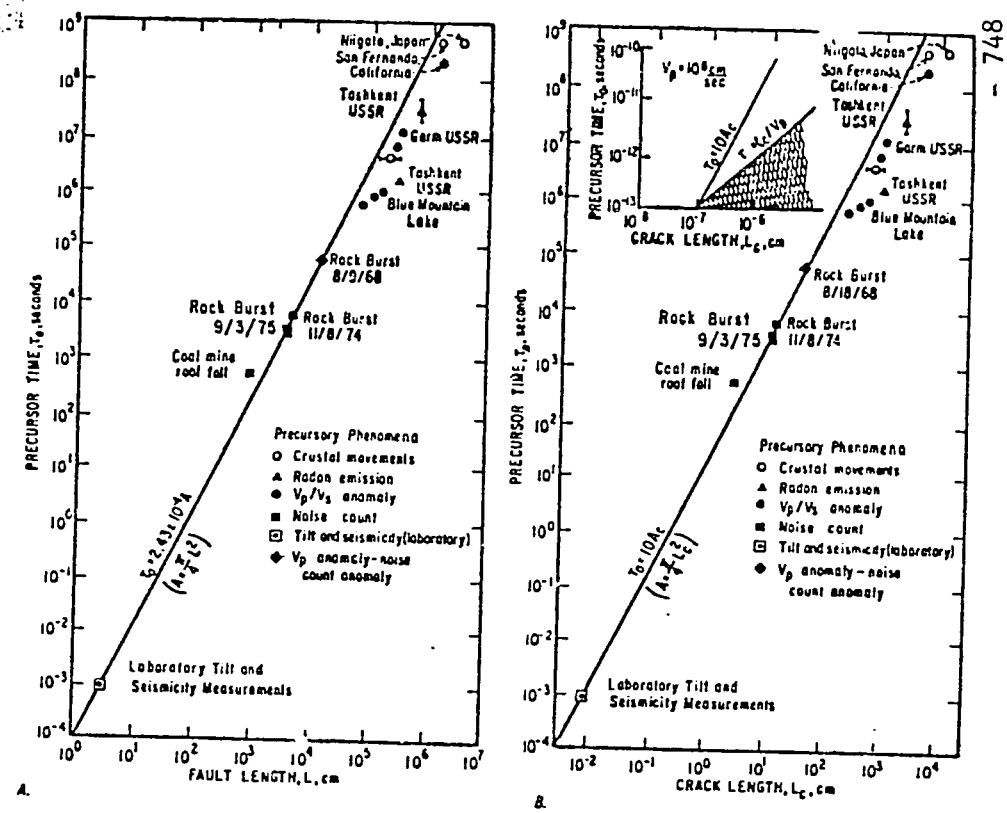


Figure 5 Precursor time—fault length (A)—Crack length (B) relationships of failure.

It is of value to express the class I and II precursor times in terms of the energy released as seismic radiation during the mainshock, or alternatively, the magnitude, M , of the mainshock. UTSU and SEKI [31] and MOGI [18] have observed that the aftershock area (A) of Japanese earthquakes can be related to magnitude by the relationship [recently revised by UTSU, 46, 53]

$$\log_{10} A = M + 6.3 \tag{5}$$

where A [$= (\pi/4)L^2$] is measured in square centimeters. Equations (3), (4), and (5) can be combined to give

$$\log_{10} \tau_0 = M + 2.68 \quad \log_{10} \tau_{10} = M - 2.65 \tag{6}$$

Table I lists predicted precursor times for class I and class II precursors for a range of magnitudes varying from $M(-)$ 5 to $M8$ failures. It is of interest to note S-bend tilt precursor times of nearly 0.6 hr, 6.2 hr, and 2.6 d are predicted to occur for mainshock magnitudes in the $M6$, $M7$, and $M8$ class, respectively. SASSA and NISHIMURA [28, 29] observed S-bend precursor time durations comparable to those predicted

Table 1

Predicted precursor times as a function of magnitude

(Note: no changes are assumed to occur in the far-field boundary conditions during the times τ_0 and τ_{r0})

Magnitude	τ_0	τ_{r0}	Comment
-5	4.8 m	0.02 μ s	Typical laboratory size failure
2	13.3 hr	0.2 s	Typical mine failure
4	55.4 d	20.0 s	Earthquake
5	1.5 yr	6.5 m	Earthquake
6	15.2 yr	0.6 hr	Earthquake
7	152 yr	6.2 hr	Major earthquake
8	1520 yr	2.6 d	Great earthquake

by equation (6) prior to several major underthrust events in Japan. In addition, an S-bend tilt time of the order of 20 seconds is predicted to occur prior to a magnitude $M4$ earthquake. This value is large enough to suggest the use of S-bend tilt (and other class II precursors) as a possible indicator of impending moderately sized ($\geq M4$) earthquakes.

The relationship between the predicted class III precursor time, τ_{r0} , and an average dimension (L_i) of the primary inclusion zone is

$$\tau_{r0} = \frac{L_i}{v_p} \quad (7)$$

where v_p is the longitudinal wave velocity in the focal volume just prior to the mainshock. The relationship between τ_{r0} and magnitude is found from equations (5) and (7a)

$$\log_{10} \tau_{r0} = 0.5M + 2.8 - \log_{10} v_p \quad (7b)$$

Thus, for a typical longitudinal velocity of 3×10^5 cm/sec, the predicted class III precursor times for earthquakes magnitudes of $M4$, $M5$, $M6$, and $M7$ are 0.2 s, 0.6 s, 2 s, and 6.2 s, respectively. These times represent the minimum time interval between the initiation of macrocrack growth and the initiation of fault motion at the fault-macrocrack zone. Note also that the predicted polarities of these motions will be opposite to one another.

HARDING and KIRBY (1975, personal communication) observed low frequency 'tilt' precursors, recorded on long period seismometers, whose time durations were of the order of 0.2 s prior to aftershocks in the $M4$ range in the August 1975 Yellowstone mainshock ($M6.2$). The observed polarities of these precursory events were opposite to the seismic event they preceded. SPENCE (personal communication, 1976) has also observed precursory events occurring at intervals of the order of 1 s prior to subterrace normal faulting events following the 1965 Rat Island mainshock. The body wave magnitudes of these events were in the range of 5.2 to 5.6. The precursory events were also of opposite polarity to the event they preceded.

Relationship of the class I precursor time to mainshock magnitude

In the inclusion theory of failure, a macrocrack zone that contains an open void of cross-sectional area A_i forms within the primary inclusion zone prior to the mainshock. The total change in the elastic potential energy, Ψ , of the system provides the energy required for the failure. When the boundaries far removed from the primary inclusion zone are rigidly fixed, no work can be done by the far-field stresses (σ_{10} , σ_{20} , σ_{30}). Thus, the change in the elastic potential energy is equal to the decrease in the strain energy of the system. If, on the other hand, the far-field stresses are constant during the mainshock, work will be done by these stresses and the strain energy of the system will decrease. However, the change in the elastic potential energy of the system is the same as in the case where the boundaries are rigid. Consequently, the total potential energy change, Ψ , is the difference between the total strain energy for the medium with and without the void. The result of this calculation is [4, 27, 26, 32]

$$\Psi = \frac{(1 - \nu_0^2)}{\pi E_0} \sigma_0^2 L_i^3, \quad (8)$$

where ν_0 and E_0 are the intrinsic values of Poisson's ratio and Young's modulus of the medium, σ_0 ($\sigma_0^2 = \sigma_c^2 \sin^2 \beta + \sigma_i^2 \cos^2 \beta$) denotes the 'effective' stress existing within the primary inclusion zone, and β is the angle between the major axis of the macrocrack and the axis of the maximum principal compressive stress (σ_c). As this angle is zero (Fig. 2), the 'effective' stress is $\sigma_0 = \sigma_c$.

Equations (3) and (10) can be combined to give

$$\Psi = 1.19 \times 10^3 \frac{1 - \nu_0^2}{E_0} \sigma_i^2 \tau_0^{3/2}, \quad (9)$$

where $L_i = L/4.67$. The relationship between Ψ and the magnitude of the mainshock is found by combining equation (6) and (9). The result is

$$\log_{10} \Psi = 7.10 + \log_{10} \frac{1 - \nu_0^2}{E_0} \sigma_i^2 + 1.50M, \quad (10)$$

where Ψ is measured in ergs. The appropriate value of σ_i to be used in equation (10) must be the theoretical tensile strength of the material because this is the stress required to form a void of length L_i . This strength is estimated to lie between the limits $\frac{1}{30}E_0 \leq \sigma_i \leq \frac{1}{10}E_0$ [23]. We shall use an average value of $\sigma_i = \frac{1}{20}E_0$ in the following calculations. Appropriate values of E_0 and ν_0 for brittle materials are 1×10^{12} dynes/cm² and 0.30, respectively. Thus, the average change in the total potential energy of a system within which a void of length L_i forms prior to failure is approximately

$$\log_{10} \Psi = 16.5 + 1.5M. \quad (11)$$

The energy provided by the decrease in the potential energy, Ψ , will be partitioned during the failure in the form of heat generated by friction along the fault(s), crack closure, plastic deformation, and seismic wave radiation. Thus, the total change in potential energy of the system can be written

$$\Psi = \Psi_p + \Delta\Psi, \quad (12)$$

where $\Psi_p (= \Psi_r + \Psi_d)$ represents the energies radiated by seismic waves and dissipated by inelastic processes as the fault(s) and its associated inclusion(s) advances into the focal region of the primary inclusion and $\Delta\Psi$ denotes the reversible component of Ψ required to complete the failure preparation process. Ψ_p denotes the energy required to form the primary inclusion zone of the impending failure. *This energy must be supplied by the seismic events that form the primary inclusion zone.*

The energy radiated by the mainshock will be assumed to be given approximately by the Gutenberg-Richter relationship

$$\log_{10} \Psi_r = 11.8 + 1.5M. \quad (13)$$

This relationship should be considered to represent only the average energy that can be radiated by an earthquake since the radiated energy will obviously be dependent on both the material properties and the stress conditions persisting in the hypocentral region of the mainshock.

The energy, Ψ_d , required in the formation of the primary inclusion zone of the mainshock represents a maximum value of the energy available for aftershocks, assuming of course, that the system approaches an equilibrium state following the mainshock. To determine the functional relationship of Ψ_d to Ψ_p , we shall require an understanding of the processes required to form the primary inclusion. First, recall that one of the more distinguishing characteristics of the primary inclusion zone of an impending failure is the existence within this zone of a tensile stress that is oriented normal to the direction of eventual rupture propagation. This direction is parallel to the direction of the local maximum principal stress axis (σ_1 , Fig. 2b) within the deformation band that is itself contained within the anomalous or dilated volume. Thus, shear failure, as defined in this article, *cannot* occur within the primary inclusion zone. Consequently, seismic events that produce the primary inclusion zone *will not be followed by aftershocks*, or at the very least, will exhibit a severely curtailed aftershock sequence. These events will be characterized by anomalously long rupture lengths. The regions fractured by these seismic events form the volume of the primary inclusion zone of the forthcoming mainshock. Of course, the energy, $\Psi_d (= \Psi_p - \Psi_r)$ that would normally have been available for frictional dissipation and aftershocks for each of these events becomes available to fracture a region much larger than the individual focal regions of the individual events.

Equations (11) and (13) can be combined to give the equivalent magnitude of each seismic event that forms the primary inclusion zone. The result is

$$M^* = M_n + 3.1 \quad (14)$$

where M_n represents the magnitude of the event had it not been involved in forming the primary inclusion zone. Since $\Delta\Psi^* = \Psi^* - \Psi_p^* \approx \Psi^*$, it can be assumed that *all* the energy that would have normally been dissipated by frictional sliding and aftershocks is available to fracture a portion of the evolving primary inclusion zone. Thus, M^* in equation (14) represents an upper limiting value to the equivalent magnitude. The effective area, A^* , fractured by these events is found by equation (5) to be

$$A^* = 10^{3.1} A_n \quad (15)$$

Let A_i denote the area of the primary inclusion zone of the forthcoming mainshock. If n denotes the number of seismic events, of average equivalent magnitude M^* , then $nA^* = A_i$, where the areas of the individual primary inclusion zones that give rise to each of the n events are neglected. The scale invariant properties of failure and experimental data (see Appendix B) give an order of magnitude estimate of the ratio of A_i and A_n , A_i/A_n , to be 1×10^4 . Thus, an upper limit to the required number of events, of equivalent magnitude M^* , predicted to form the primary inclusion zone is

$$n \approx 1 \times 10^4 \frac{A_n}{A^*} \approx 10. \quad (16)$$

This value is shown to be close to values observed prior to moderate rock bursts and moderate earthquakes in the application section. Equations (15) and (16) can be combined to give

$$\begin{aligned} \log_{10} n &= \log_{10} A_i - \log A^* \\ &= \log_{10} A - \log A_n - 4.3 \end{aligned} \quad (17)$$

where $A (= 21.8A_i)$ represents the focal region area of the primary inclusion zone. Equation (17) provides an estimate of the upper limiting value of the difference in magnitude between the impending mainshock, M , and the average magnitude, M_n , of the 'background' seismic events that occur prior to the formation of the deformation band within which the primary inclusion zone,

$$\Delta M = M - M_n = 5.3. \quad (18)$$

In addition, note that equation (18) can be interpreted as indicating that if M_{\max} denotes the maximum value of the average 'background' seismicity, then an *upper limiting value* of the magnitude of an earthquake that this region can sustain is $M_{\max} + 5.3$.

The energy, Ψ_p , required to form the primary inclusion zone is simply

$$\begin{aligned} \log_{10} \Psi_p &= \log n + 16.5 + 1.5M^* \\ \log_{10} \Psi_p &= 14.2 + 1.5M, \end{aligned} \quad (19)$$

where for calculation purposes it is assumed that each of the n events that form the primary inclusion zone is equivalent. Thus, the energy partitioning of failure predicted by the inclusion theory is approximately

$$\begin{aligned} \Psi_r &= 0.004\Psi_p \\ \Psi_d &= 0.996\Psi_p \\ \Psi_p &= 0.005\Psi \end{aligned} \quad (20)$$

Equation (20) shows that the seismic efficiency factor, η ($\eta = \Psi_r/\Psi_p$), for failures satisfying the constraints of the inclusion theory and the Gutenberg-Richter relationship is only 0.40%. Similarly, of the total energy available for aftershocks, only 0.40% will be available for seismic radiation. Thus, the model predicts that, at the very minimum, approximately 0.5% of the total energy radiated by the mainshock will be radiated by all of its aftershocks. In addition, the functional relationship between the total energy radiated by the aftershock sequence, $\Psi_r^{(as)}$, and Ψ_p can be written

$$\log_{10} \frac{\Psi_r^{(as)}}{\Psi_p} = 1.5 \delta M, \quad (21)$$

where $\delta M = M - \bar{M}$ and \bar{M} denotes an upper limiting magnitude to the largest possible aftershock. Equations (20) and (21) give this value of \bar{M} to be $M - 1.6$, or simply, the predicted maximum value of the magnitude of any aftershock within the aftershock sequence is the magnitude of the mainshock less 1.6. This result is close enough to and thus lends theoretical support to the well-known empirical relationship referred to as Bath's law, that the largest magnitude of an aftershock within an aftershock sequence is $M - 1.2$ [50].

The above analysis suggests a method of determining the average linear dimensions, l_0 , of the anomalous zone within which a shock of magnitude M can occur. The modified Utsu relationship can be written for the mainshock as

$$\begin{aligned} \log_{10} A &= M - 3.7 \\ &= M_n + 1.6, \end{aligned} \quad (22)$$

where M_n denotes the 'average background' seismicity and A is the minimum area in km^2 that can support this level of seismicity. Thus

$$A = 35.8 \times 10^{M_n}, \quad (23)$$

and if l_0 denotes an average linear dimension of the anomalous region, equation (23) leads to the relationship

$$l_0 \leq 8.9\sqrt{(2/\pi)} \times 10^{0.5M_{\max}}, \quad (24)$$

Equation (24) should be considered as specifying the *minimum average* linear dimension of an assumed circularly-shaped anomalous region that can sustain an average 'background' seismicity of maximum value M_{\max} . By way of example of equation

Table 2
Typical minimum dimensions of anomalous region and earthquake magnitude
($M = M_{\max} + 5.3$; $\log_{10} A = M_{\max} - 3.7$; $A_i = A/21.8$)

M_{\max}	M	A , km^2	A_i , km^2	l_0 km	Remarks
-5	0	2×10^{-9}	9×10^{-11}	2×10^{-2}	Typical laboratory size failure
-2	3.3	2×10^{-6}	9×10^{-8}	0.80	Typical mine failure
1	6.3	2×10^{-3}	9×10^{-5}	25.0	Earthquake
2	7	2×10^{-2}	9×10^{-4}	80	Earthquake
3	8.3	0.20	9×10^{-3}	250	Earthquake
3.3	8.6	0.64	3.0×10^{-2}	450	Earthquake

(24), Table 2 lists several typical values of l_0 against M_{\max} as well as the value *maximum* allowable magnitude, M , of an earthquake that can occur within this region.

Geodetic investigations in seismically active regions indicate that the spatial extent of the anomalous region is often much larger than the focal volume of the earthquake itself. For example, premonitory changes were detected as far as 100 km from the epicenter of the 1964 Niigata earthquake ($M7.5$) [38] and nearly 25 km prior to magnitude 3 events in the Garm region [39]. AGGARWAL *et al.* [2] observed the size of an anomalous zone to be at least 10 km prior to a magnitude 3.6 event in the Blue Mountain Lake region of New York state. Equation (24) shows that the calculated minimum dimension (l_0) for the Niigata mainshock must be at least 90 km ($M7.5$). The calculated range of l_0 is approximately 20 km to 200 km for 'background seismic events' in the magnitude range of $M_{\max} = 1.0$ to 3.0 in the Garm region. The calculated size of the anomalous region at Blue Mountain Lake is in the range of 10 km. The typical magnitude of the 'background' seismicity is in the order of 1.0 in this region [2].

Factors affecting the precursor time focal region area-magnitude relationships of failure

The functional relationship between the class I precursor time (τ_0) and focal region area (A), where $A = (\pi/4)L^2$, can be written

$$v_0 = \frac{L}{\tau_0} = 5.24 \times \frac{10^3}{L} \text{ cm/sec}, \quad (25)$$

where v_0 denotes the average velocity of the crack closure front in the focal region of the primary inclusion zone when the far-field stresses (strains) remain constant during the time duration of the class I precursor. Equations (5) and (25) show that this velocity is magnitude dependent, that is, the larger the magnitude, the smaller the closure front velocity. For example, typical values of L on the laboratory scale [$M(-)5$] and major shallow earthquakes ($M8$) are calculated from equation (5) to

e in the order of 1 cm .07 cm, respectively. These length values suggest closure front velocities in the order of 10^3 cm/sec and 10^{-3} cm/sec, respectively. Note that an upper limiting value of v_0 must be v_p .

When a condition arises such that changes (increases) in the far-field stresses (trains) can occur at a velocity v , where $v \geq v_0$, then the crack closure front will proceed at the higher velocity v in the focal region. In this instance, the correct class I precursor time, τ , is $\tau = L/v$. The precursor time-focal region area relationship becomes

$$\tau = \tau_0 \frac{v_0}{v} = 2.43 \times 10^{-4} \left(\frac{v_0}{v} \right) A. \quad (v \geq v_0) \quad (26)$$

As an example of equation (26), consider a magnitude $M7.5$ earthquake. Equations (3), (5), and (25) give τ_0 , A , and v_0 to be approximately 244 yr, 3.16×10^3 km², and 0.26 km/yr, respectively, for this event. However, when changes in the far-field stress (or strains) are occurring at a velocity, say of the order of 50 km/yr, as is observed and predicted to occur in major shallow earthquake zones [8, 18], then the predicted actual class I precursor time for this hypothetical event becomes $\tau = \tau_0 (26/50) = 1.27$ yr, a reduction in what would have been the predicted time by nearly two orders of magnitude. This example serves to illustrate that the class I precursor time-area relationship, as specified by equation (3), must be used with extreme caution. However, this relationship can be modified to take into account changes in the far-field boundary conditions once it has been determined how the boundary conditions are changing.

Observational data for large earthquakes ($\geq M6$) suggest that there is little or no relation between earthquake magnitude and what has been referred to as the class II precursor time (τ_{s0}) in this article [46]. Yet equation (6) suggests that τ_{s0} and M are functionally related to one another. It is of interest, therefore, to consider whether changes in the far-field boundary conditions, such as might occur owing to tidal strains, can influence or possibly trigger earthquakes. Earthquakes that would be triggered by such short-term changes in the far-field boundary conditions would have the appearance of exhibiting little or no positive correlation between τ_{s0} and magnitude. This will be particularly true for those large earthquakes where the phase of secondary crack growth within the primary inclusion begins or is occurring during the time interval when tidal effects are increasing the value of σ_1 within the primary inclusion zone.

The lunar tidal stress is known to have a peak amplitude of approximately 1×10^4 dynes/cm², cycled every 13 h, in the crust. The peak rate of change of the tidal stress is about 7 dynes/cm²/sec [49]. Let us assume that the average Young's modulus of the primary inclusion zone is in the order of 1×10^{11} dynes/cm². Thus, the peak volumetric strain, ϵ , that can be induced within the primary inclusion zone is in the order of $\epsilon \approx 5 \times 10^{-7}$. The problem of resolving whether the lunar tidal stress can trigger an earthquake rests with a determination of whether this stress can initiate

accelerate the formation of cracks that will eventually lead to the formation of the secondary cracks that, in turn, will coalesce with the primary cracks (Fig. 2d) and thus produce the earthquake.

Theoretical and experimental results discussed earlier in this article have shown that an order of magnitude estimate of the area, A_c , of the secondary cracks is $A_c \approx 1 \times 10^{-4} A_i$, where A_i is the area of the primary inclusion. Since the cracks that produce the secondary cracks form in a tensile stress field, the area of these cracks is approximately $a_c \approx 1 \times 10^{-3} A_c \approx 1 \times 10^{-7} A_i$ by equation (15). The relation of a_c to the area, a_{ci} , of the primary inclusion zone that produces this crack is $a_{ci} \approx 1 \times 10^{-7} A_i / 21.8 \approx 4.6 \times 10^{-9} A_i$. If l_{ci} denotes the length of this inclusion zone, then $l_{ci} \approx 6.8 \times 10^{-5} L_i$. It is shown in Appendix D that an order of magnitude estimate of the thickness, t_{ci} , of these cracks is αl_{ci} , where α , of the order of 1×10^{-3} , is their aspect ratio. Consequently, an order of magnitude estimate of the volumetric strain, ϵ^* , that will be induced within the primary inclusion zone as a result of crack growth within the secondary inclusion zone is $\epsilon^* = t_{ci}^*/L_i \sim 6.8 \times 10^{-8}$. This value compares with the peak strain of $\epsilon \sim 5 \times 10^{-7}$ that can be induced within the primary inclusion zone by tidal strains, and is suggestive that induced tidal strains are of sufficient magnitude to initiate crack growth within the primary inclusion zone once this zone has approached a critical state. In addition, these calculations show that the tidal strains can induce strains within the secondary inclusion zones that are several orders of magnitude greater than the strains required to induce the level of crack growth that will, in turn, lead to the development of those cracks that form the secondary inclusion zone. Therefore, those earthquakes whose size is sufficiently large that their secondary inclusion zones begin to form during the time interval that the tidal stresses are increasing may be triggered by this stress increase. Such earthquakes, particularly those of large magnitude, may give the misleading appearance of exhibiting class II precursory phenomena whose time durations (τ_{s0}) appear to be independent of magnitude. Thus, the apparent lack of a significant correlation between τ_{s0} and M [46] may be explained by changes induced within the far-field boundary conditions resulting from the influence of lunar tides. This hypothesis could be treated by monitoring class II precursors of small shocks whose magnitude is small, say $\leq M4$, and determining the relationship of τ_{s0} to M for these events. Detailed monitoring of rockbursts may be useful in this respect.

The effect of changes in the applied far-field stresses (σ_{10} , σ_{30}) will produce no change in the amount of energy released by the failure. However, the same cannot be said when fluids under a pressure, P_f , are present in the focal volume. For example, when fluids are present within the anomalous volume, the principal stresses (σ_1 , σ_3) within this volume will each be reduced by an amount approximately equal to P_f . Consequently, less strain energy can be stored within the anomalous volume and subsequently released during the mainshock. Thus, the predicted magnitude, say M_p , of a failure occurring within a volume containing fluids under pressure will be greater than the observed magnitude M .

Equation (9) can be readily applied to this situation to give the total potential energies for the 'dry' (Ψ_0) and 'wet' (Ψ) cases

$$\log_{10} \Psi_0 = 3.08 + \log_{10} \frac{1 - \nu_0^2}{E_0} \sigma_0^2 + 1.50 \log_{10} \tau_0 \quad \text{'Dry'}$$

$$\log_{10} \Psi = 3.08 + \log_{10} \frac{1 - \nu_0^2}{E_0} \sigma_{eff}^2 + 1.50 \log_{10} \tau_0, \quad \text{'Wet'}$$

where $\sigma_{eff}/\sigma_0 = (\sigma_3 - P_f)/\sigma_3$, σ_3 is the least principal stress existing within the anomalous zone, and *no* changes are assumed to occur in the far-field tectonic stresses (strains) during the time duration of the class I precursor. Equations (10) and (27) can be combined to give the discrepancy between the predicted and observed magnitudes to be

$$M = M_p + \frac{4}{3} \log_{10} \frac{\sigma_{eff}}{\sigma_0} \quad (M \leq M_p) \quad (28)$$

As an example, assume the difference between the predicted and observed magnitudes is 1.0. Equation (28) predicts that the magnitude discrepancy can be readily explained by the presence of a pore fluid in the focal volume of the mainshock with a pressure P_f equal to approximately 80% of the local far-field minimum principal stress. Local, in the context used here, refers to the stresses existing within the anomalous volume in which the failure occurs.

Two important practical results arise from equation (28). (1) The existence of pore fluids in an earthquake zone will produce a discrepancy between the predicted (M_p) and observed magnitudes (M) of the earthquake ($M \leq M_p$). There will be *no* discrepancy in the predicted precursor time τ_0 provided the far-field tectonic stresses remain constant during the precursor time duration τ_0 . (2) The decrease in observed magnitude M as P_f is increased will be evidenced by a transition from unstable to stable formation. This predicted behavior has been observed experimentally by MARTIN [1975, personal communication]. *This result suggests that earthquake prone regions exhibiting swarm activity may be characterized by high values of P_f/σ_3 .*

Application to existing earthquake regions

The application of the seismic conditions discussed above that are required to predict earthquakes is made in this section. The seismic conditions include the magnitude, seismicity, and the spatial and temporal distribution of seismicity in and near the pending rupture zone. Five earthquake sequences are investigated and have been chosen so as to illustrate the predictive capability of the inclusion theory and, in particular, to point out some of the difficulties that can and will occur in the development of any reliable predictive capability for earthquakes. These examples

include: (1) The 3 September 1975, Rockburst, Star mine, Burke, Idaho; (2) The Garm Earthquake of 22 March 1969; (3) The 9 February 1971, San Fernando, California, Earthquake; (4) The August 1973, Earthquake at Blue Mountain Lake, New York; (5) The 3 October and 9 November 1974, Peru Earthquake sequence.

The 3 September 1975, rockburst, Burke, Idaho

A moderate rockburst occurred on the 7500 level of the Star mine, Burke, Idaho, at 10:09 a.m. (18:09 UTC) on 3 September 1975. The burst was preceded by a dramatic increase of seismic activity that was followed by a distinct decrease prior to the burst. Miners were evacuated from an active mine stope located in the immediate vicinity of the eventual burst hypocenter. Detailed information of the Star mine and the mining method used in this mine are available elsewhere [12]. Location accuracy of the seismic events in this mine is ± 4 m.

Table 3
Seismic event number and time prior to burst

Event number	Time (a.m.)	Event number	Time (a.m.)	Event number	Time (a.m.)
1*	9:00:32	11	9:02:32	21	9:30:40
2	9:00:38	12*	9:02:40	22	9:44:52
3*	9:00:48	13*	9:03:00	23	10:01:03
4*	9:00:53	14*	9:03:38	24	10:01:58
5	9:00:55	15	9:05:53	25	10:02:08
6*	9:00:57	16	9:06:09	26	10:02:24
7	9:01:11	17	9:06:46	27	10:02:42
8*	9:01:38	18	9:10:44	28	10:05:10
9*	9:01:39	19	9:22:27		
10	9:02:29	20	9:24:32		

Burst was event number 29 and occurred at 10:09:04 a.m.
* Refer to seismic events that formed the primary inclusion zone.

Table 3 lists the seismic event numbers and their corresponding times of occurrence prior to the burst. Figure 6a shows the event location numbers as well as the seismic events, termed aftershocks, that followed the burst. Figure 6(a,b,c) illustrate the seismic events as projected onto the horizontal plane (a), the projection of the aftershocks onto the vertical plane along sections A-A' (b) and B-B' (c). There are a number of results that are noteworthy from this data. First, the rapid increase of seismic activity prior to the burst was essentially associated with events 1 through 14 (Table 3). The seismicity increase was associated with the formation of the circularly shaped zone (shaded region, Fig. 6a) whose area, A_i , is approximately $7.86 \times 10^5 \text{ cm}^2$. The total time required to form this zone was 188 s. Second, the seismic events that followed the formation of this zone were concentrated outside this zone, and were primarily located near and outside the boundaries of what was to be the aftershock

region. There was a increase in seismicity in the hypocentral region (events 24 and 25) approximately ten minutes prior to the burst. Third, the burst occurred at 10:05:10 a.m. (18:05:10, UTC) and was followed by 22 aftershocks that defined an elliptically shaped zone of approximately area, A , equal to $1.74 \times 10^7 \text{ cm}^2$. The total time to the burst, measured from the initiation of growth (9:00:32 a.m.) of the primary inclusion zone, was 68.5 m. Fourth, the cross-sections of the aftershock zone reveal an elliptically shaped zone (Fig. 6b) whose major axis is parallel to the inferred rupture propagation direction as well as a circularly-shaped zone (Fig. 6c) normal to this direction. The observed geometry is remarkably similar to the aftershock zone geometry that is predicted by the inclusion theory when the local least and intermediate principal stresses are equal. This observation is also consistent with stress measurements on the 7300 level by S. CHAN [personal communication, 1976]. Chan's measurements show that the intermediate (σ_2) and least (σ_3) principal stresses are equal (Table 4). The major horizontal stress (σ_1) is probably of tectonic origin. Fifth, the inferred rupture propagation direction, that is, the direction where most of the energy was released (section A-A', Fig. 6a), was approximately normal to the vein

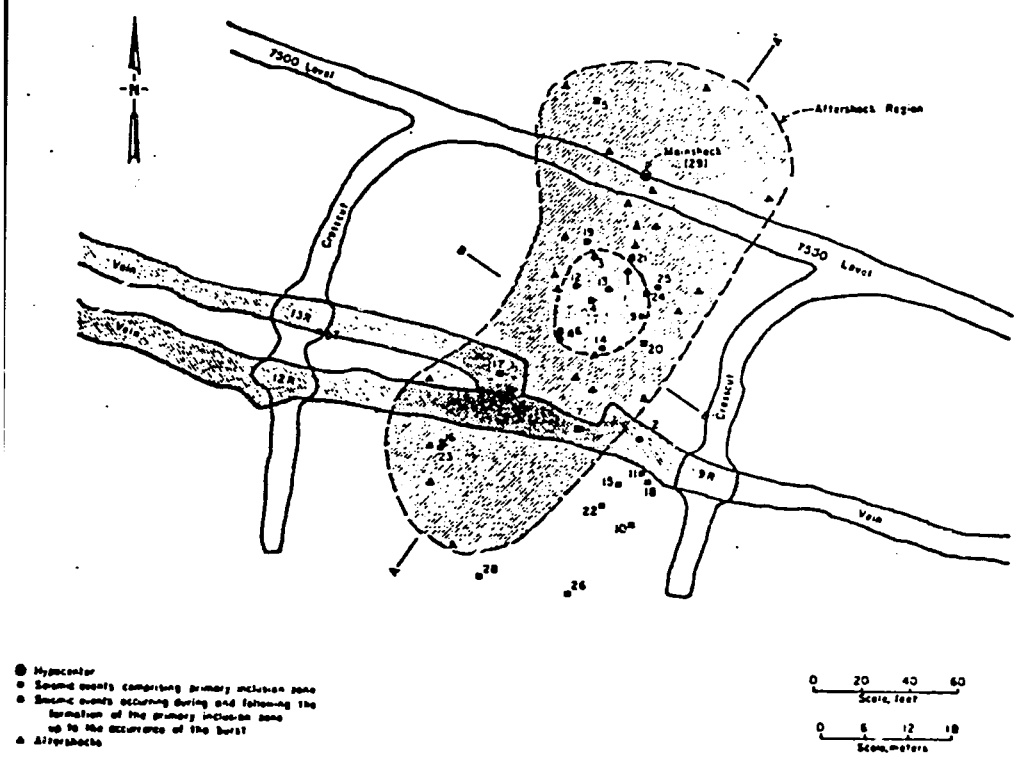


Figure 6a

Plan view of the 7500 level of the Star Mine, Burke, Idaho. A. Plan view of aftershock region, primary inclusion zone and burst hypocenter. B-C. Vertical sections of aftershock region along sections A-A' (B) and B-B' (C). D. Seismic count versus time in 4 September 1975 rockburst.

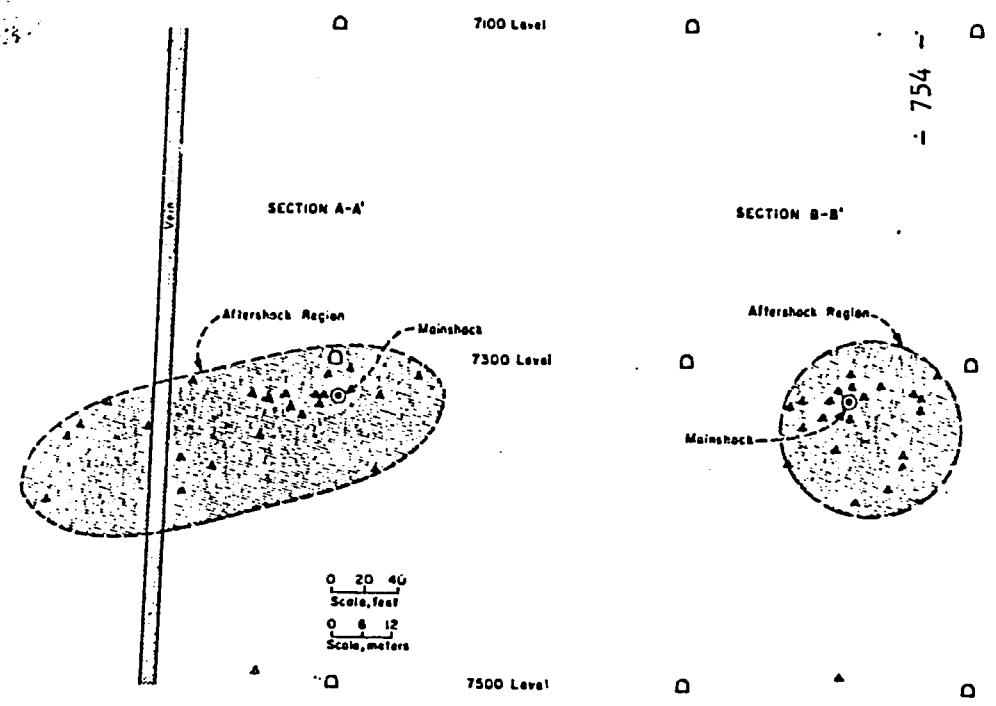


Figure 6b

Figure 6c

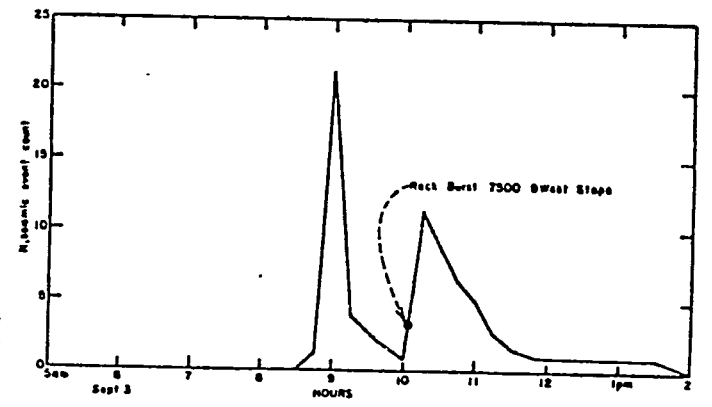


Figure 6d

Table 4
In-situ stress distribution at east lateral drift
7300 level—star mine
(CHAN, personal communication, 1976)

Stress	Magnitude	Bearing
Major horizontal (σ_1)	0.66 kb	N 14° W
Major horizontal (σ_3)	0.42 kb	N 76° E
Vertical (σ_2)	0.43 kb	—

(1 kb = 1×10^3 b, 1 b = 15 psi)

and, in particular, normal to the region where active mining was in progress. Major structural damage to the mine workings was observed in this area following the occurrence of the burst. Sixth, the burst hypocenter in Fig. 6 appears to be displaced approximately 6 m from the edge of the circularly-shaped zone, termed the primary inclusion zone. However, the burst is located using velocity surveys taken prior to the burst. Thus, as the focal volume of the primary inclusion zone begins to store strain energy, the seismic velocities in this volume will increase, thus giving rise to an apparent displacement of the burst hypocenter from the theoretically predicted location on the boundary of the primary inclusion zone.

Independent studies (reported in Appendix C) by the Bureau in the Galena mine, Wallace, Idaho, have shown that a lower limit to the ratio τ_0/τ_{d0} is 12.5. Consequently, once τ_d is known, a *minimum* predicted time to the burst is possible. The calculated time to the 3 September burst is 40 m, where the observed value of 188 sec is used for τ_d . This value compares favorably with the observed value of 68.5 m. However, based upon the observed areas A_i and A_0 , the calculated times τ_{d0} and τ_0 are 191 sec and 70.3 m, respectively, in good agreement with the observed times of 188 sec and 68.5 m. Thus, not only was this burst predicted, the analysis admits a more realistic estimate of the ratio τ/τ_d (=21.8) required for future accurate prediction times. This analysis provides the physical basis for using this ratio in this article.

Lastly, this rockburst was not detected by the Newport, Washington, seismic station. The Newport station is capable of detection of events of magnitude $M1.5$ in the Coeur d'Alene district [KERRY, personal communication, 1976]. The functional relationship between aftershock area, A , and magnitude, M , is $\log_{10} A = M + 6.3$, where A is measured in square centimeters. Substituting the observed area of 1.74×10^4 cm² into this relationship gives a calculated magnitude for the 3 September burst of $M0.9$. This value is well below the threshold value of $M1.5$.

The 22 March 1969, M5.7 Garm earthquake

This earthquake was located 25 km from the Garm seismic station at a depth of 15 km [19]. All precursor observations were obtained within a radius of 25 km of

epicenter and outside the 6 km by 10 km aftershock zone. NERS. *et al.* [19] have suggested that the precursor volume exceeded the source dimensions by a factor of five for this seismic event.

NERSESOV *et al.* and WYSS [19, 35] have summarized five independent precursor observations of this earthquake. (1) The seismicity decreased outside the epicentral region 1.7 to 1.5 yr prior to the mainshock. (2) The compression axes, obtained from fault plane solutions of small earthquakes located within the precursor volume, showed evidence of rotation approximately 1.7 yr before the mainshock; this re-orientation of the compression axis was then followed by another rotation of 90°, approximately 3 months before the event. (3) The P-residual increased 0.4 sec at 1.2 yr prior to the mainshock [35]. (4) The resistivity began to decrease about simultaneously with the return to normal of v_p approximately 6 months before the earthquake. This change was measured at 10 km to the north of the epicenter. The calculated source radius for this shock was approximately 3 km. (5) The rate of uplift near the Garm station began to increase 1.7 yr prior to the mainshock.

The calculated magnitude for an event producing an aftershock area of 60 km², assuming the Utsu relationship (equation (5)) is applicable to this region, is found from equation (5) to be $M_p 5.5$ as compared with the observed value of $M5.7$. The calculated minimum diameter (l_0) of the anomalous region, within which the mainshock occurred, is approximately 125 km. This calculation is based on observational data suggesting that this region sustains an average *maximum background* seismicity of magnitude $M_{max} = 2.5$ [19]. Thus, the calculated ratio of l_0/L for this seismic event ($M_p 5.5$) is approximately 12.5 for a source dimension, L , of 10 km. This value compares with the observed value of 5.0 [19].

In the *absence* of changes in the far-field stresses (strains) during the preparation time required for this event, the calculated precursor time, τ_0 , for a mainshock of calculated magnitude $M_p 5.5$ is 4.8 yr. The observed precursor time, τ , for this earthquake is estimated to be 1.7 yr [19, 35]. Because most major earthquakes occur in active tectonic zones, such as the Garm region, it is doubtful that the tectonic boundary conditions would remain constant during the predicted precursor time τ_0 , and the corrected precursor time is now given by equation (26). However, once it is determined how these changes affect the predicted precursor time, the theoretical relationship between τ_0 and A (or M_p) can be appropriately modified and used to provide more accurate long-range prediction of future seismic events of comparable magnitude that might occur in this region. For example, equation (26) shows that the ratio between the velocity (v_0) of the crack closure front when the boundary conditions are changing is $v_0/v = \tau/\tau_0 = 0.35$ ($v_0 = 10$ km/4.8 yr = 2.08 km/yr) for the Garm region. Thus, for earthquakes of comparable magnitude in this region, the calculated precursor time-focal area relationship is $\tau = 8.60 \times 10^{-5} A$, where τ and A are measured in seconds and square centimeters.

The calculated time, τ_{d0} , required to form the primary inclusion zone of the 22 March 1969 mainshock is found from equation (C.5) and the experimentally

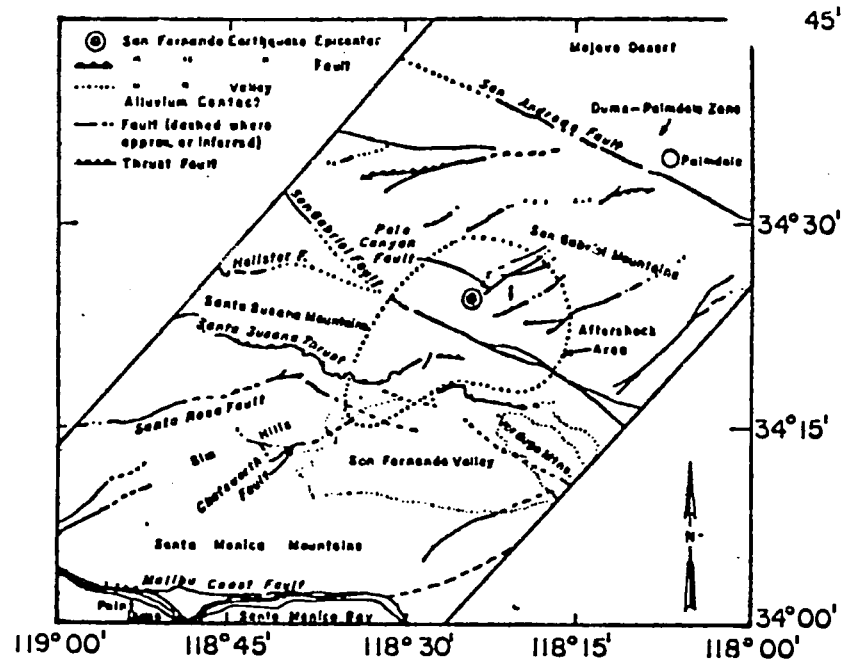
determined ratio of ν_p and A ($A/\nu_p = 1/21.8$). The result is 4.3 months. The predicted times required to form the individual seismic events, whose predicted magnitudes, M_p , are determined from equation (18) to be approximately 0.4 are only 0.3 hr. Since this time interval is short enough that changes in the far-field stresses are negligible, the predicted time of 4.3 months is probably a reasonable estimate for the formation of the primary inclusion zone. It is important to note that this time interval will represent the time required for the seismic compression axes to change over to their new orientation. This calculated time is in reasonable agreement with the observed time (~6 months, see Fig. 2, reference 35).

It is noted that in the context of the inclusion theory, the focal region of an impending failure must become elastically stiffer than the surrounding anomalous volume during the latter portions of the earthquake preparation process. Thus, the stress difference will increase both within the focal region and throughout the anomalous volume in the plane of the primary inclusion and focal region zones. If the increase in stress difference is sufficient to initiate seismic events, then their compression axes will be rotated 90° to those associated with the seismic events that were produced by crack closure. The compression axis of the mainshock will be identical in orientation to the axes of those events that occurred in the pre-primary inclusion phase. This predicted behavior is in agreement with Soviet observations [19].

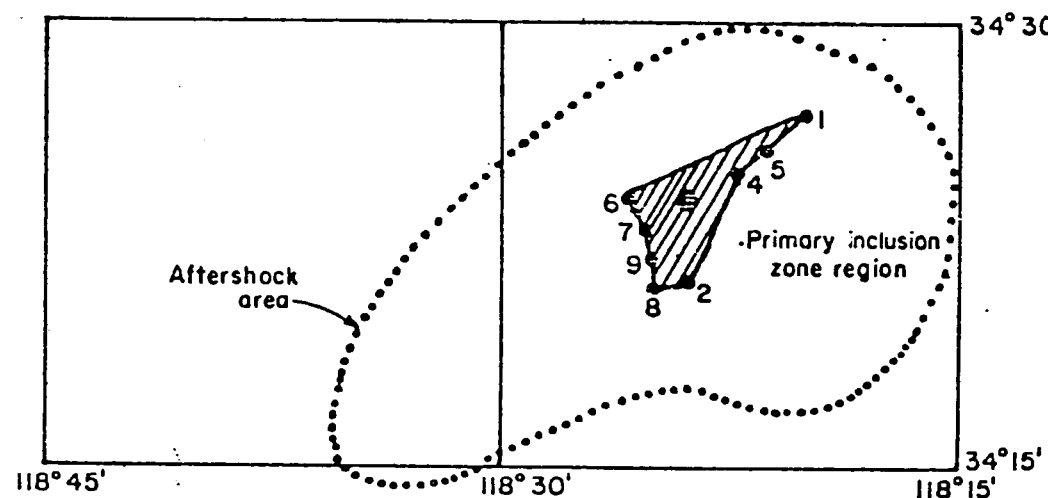
The San Fernando, California, earthquake of 9 February 1971

WHITCOMB *et al.* [34] have proposed that the dilatancy-diffusion model may be applicable to the San Fernando, California, earthquake ($M_{6.4}$) of 9 February 1971. According to their interpretation, a large precursory change in the seismic body-wave velocities occurred approximately 3.5 yr prior to the mainshock. It is of interest to examine this earthquake from an alternative point of view.

Figure 7a illustrates the major tectonic features in the region surrounding the mainshock and its associated aftershock area [51]. The aftershock area was estimated to be approximately 400 km² [34]. Equations (3) and (5) give a calculated precursor time, τ_0 , and mainshock magnitude, M_p , to be 30.4 yr and 6.3, respectively, assuming that (1) no changes occurred in the far-field tectonic stresses (strains) and (2) the Utsu relationship is applicable to this region. Table 5 lists the seismic events that occurred in the epicentral region beginning with the $M_{2.4}$ event of 7 June 1961. A seismic search (data provided by the USGS and included all seismic data contained in the Caltech catalogue) in the region 37°N \pm 35°N and 118°W \pm 119°W for the time period of 1955-1974 shows no events occurred in the epicentral region from January 1955 to 7 June 1961. The data also show that following 11 February 1964, most of the seismic activity developed in the northwest, west, and southern regions that were outside the aftershock region. There was little activity within the aftershock region.



A.



B.

Figure 7
Major tectonic features in the region surrounding the San Fernando mainshock of 9 February 1971, and aftershock area (A) and the hypothesized location of the primary inclusion zone [Fig. 7a is reproduced from reference 5].

Table 5
Seismic events in the epicentral region of the 9 February 1971, San Fernando, California, earthquake

Event	Date	Latitude	Longitude	Magnitude
1*	7 June 1961	34.45°	118.33°	2.4
2*	15 September 1961	34.45°	118.40°	2.0
3	6 October 1961	34.33°	118.48°	3.0
4*	8 December 1961	34.42°	118.37°	2.2
5*	3 February 1962	34.43°	118.35°	2.1
6*	17 March 1962	34.40°	118.43°	2.6
7*	3 May 1962	34.42°	118.38°	2.6
8*	17 September 1963	34.35°	118.41°	2.5
9*	11 February 1964	34.37°	118.40°	2.3
10	9 February 1971	34.40°	118.40°	6.4

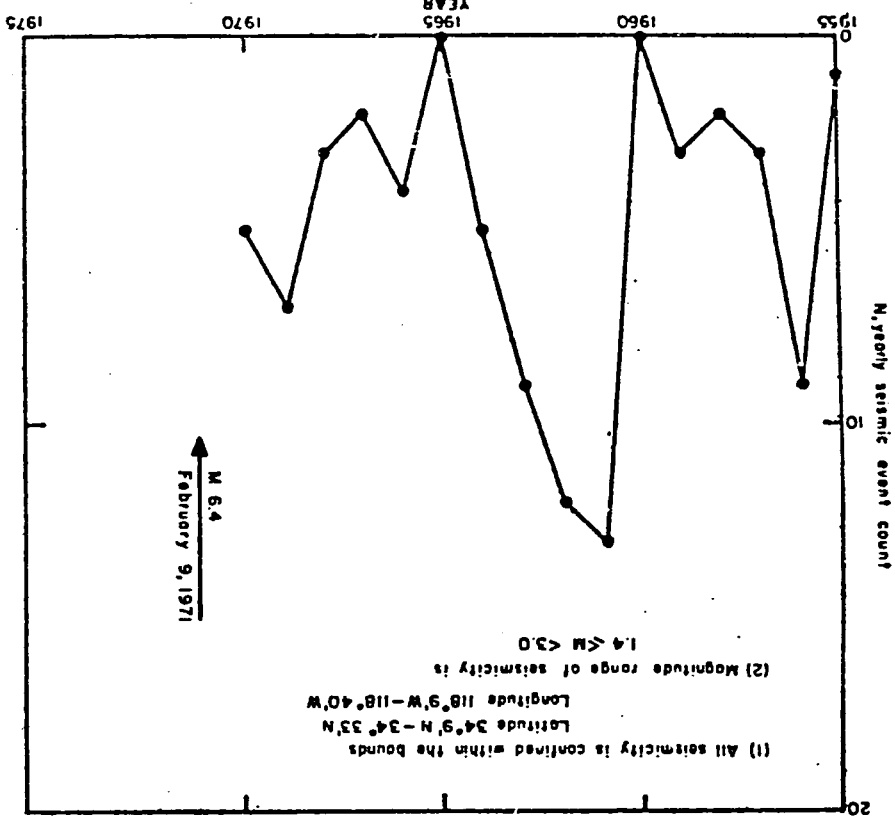


Figure 8
Yearly seismic event count in the San Fernando region from 1955-1971

A prediction of the inclusion theory of failure is that the seismicity will increase dramatically as the primary inclusion zone of the impending failure forms and that the seismicity within the area surrounding the primary inclusion zone will decrease once this zone has formed. Figure 8 depicts the yearly seismic event count from 1955 to 9 February 1971. The seismicity examined in this figure was confined to the region $34^{\circ}9'N \pm 34^{\circ}33'N$ and $118^{\circ}9'W \pm 118^{\circ}40'W$. Note the pronounced peak in seismic activity beginning in 1961 and terminating early in 1964. This activity was then followed by a slight increase beginning in 1966 and ending in the $M6.4$ mainshock of 9 February 1971. Figure 7b shows the aftershock area and the locations of the seismic events 1 through 9. Thus, the peak of activity during 1961-1964 was primarily associated with the formation of the shaded zone depicted in Fig. 6b.

The data in Figs. 7b and 8 suggest that the primary inclusion zone that gave rise to the $M6.4$ mainshock may have formed between 1961 and 1964. There are additional data supporting this hypothesis. For example, CASTLE *et al.* [13] observed that a major episode of uplift occurred in the epicentral region of the San Fernando mainshock during the 1961-1964 time interval. Such uplift is required when the primary inclusion zone is developing. As the seismic events that form the primary inclusion zone will be characterized by anomalously long rupture lengths, the theory requires that surface displacement will be anomalously large for both the number and magnitude of the seismic events. Thus, the interpretation of the data in Table 5 is consistent with observation. In addition, analysis of the time variation of v_p and v_s [reference 34, Fig. 1b] shows that there is a definite tendency for these velocities to decrease from early 1962. The velocity data are also consistent with the hypothesis that fluids were present within the focal volume. Once the primary inclusion zone has formed, the fluids will be expelled from the focal region of the impending mainshock. Thus, at shallow depths the cracks in the focal region will expand and the cracks will become undersaturated. The compressional velocity, v_p , and to a lesser extent, the shear velocity, v_s , will decrease at this point because of the high compressibility of the rock containing dry or unsaturated cracks. Once the crack closure front has passed, the velocity anomalies will disappear. Consequently, the velocity anomalies can be interpreted as being consistent with the hypothesis that the primary inclusion zone formed in the 1961-1964 time interval and that this zone developed within a region that was fluid saturated.

The calculated time, τ_{10} , to form the primary inclusion zone is found from equation (C.5) to be approximately 22 months, using the observed mainshock magnitude of $M6.4$. The seismic events 1 through 9 in Table 5 give an observed time duration of nearly 32 months (2.6 yr) required to form this zone. Seismic event 3, of magnitude $M3$, in Table 5 has been excluded from representing part of the primary inclusion zone. Thus, the seismic events hypothesized to have formed the zone are all in magnitude range of 2.0 to 2.6. It is of interest to note that the number of events, 8 in total, compares favorably with the predicted value of 10 (equation (16)). The area of the hypothesized primary inclusion zone in Fig. 7b is approximately

40 km². The calculated value is $A_i = \tau_d/\alpha = 33 \text{ km}^2$, where $\alpha = 2.43 \times 10^{-4}$, using the 'observed' value of $\tau_d = 31$ months. The precursor time for the mainshock was reduced nearly 300% from 30 yr to approximately 10 yr. This result suggests, not surprisingly, that changes are developing in the far-field boundary conditions during the time duration (τ_0) required for the mainshock to develop. Equation (26) gives the corrected precursor time-focal region area for earthquakes of comparable magnitude in this region, assuming the boundary conditions change in the same prescribed manner to be $\tau = 5.70 \times 10^{-5}A$, where τ and A are measured in seconds and square centimeters, respectively.

The formation of the primary inclusion zone of an impending shock of magnitude M was shown earlier to be represented by a decrease in gravitational potential energy of amount Ψ_p (equation (19)). This process occurs over a time interval during which the far-field tectonic stresses can be assumed constant. Thus, the energy decrease, Ψ_p , must be manifested by a corresponding increase of gravitational potential energy in the region surrounding the primary inclusion zone. For the San Fernando shock, equation (19) gives Ψ_p to be approximately 6.30×10^{23} ergs. This energy compares with the energy of 2.5×10^{21} ergs radiated by the mainshock and is sufficient to vertically displace a volume of rock, V , by an amount $\Psi_p/\rho Vg$, where ρ is mass density, g , the gravitational constant (10^3 cm/sec^2). Let V be Ah , where A and h denote the vertical thickness and A the cross-sectional area of the rock mass. If $A \sim 20,000 \text{ km}^2$, $h \sim 10 \text{ km}$, then $\delta h \sim 1.50 \text{ cm}$ for $\rho = 3.5 \text{ g/cm}^3$. Thus, the theory predicts that anomalous uplift should be associated with the formation of the primary inclusion zone of an impending shock, and further, the greatest rate of uplift will occur during the time interval τ_d (~ 31 months for the San Fernando earthquake). The above calculations are consistent with recent observations reported by CASTLE *et al.* [52] on the uplift in the Palmdale-Dume region, near the epicentral region of the 1971 San Fernando shock. An estimate of the average stress increase, $\delta\sigma$, associated with the formation of the primary inclusion zone of the 1971 shock, assuming the uplift is 'elastic' is $\delta\sigma \sim (\delta h/h)E_0/\nu_0 \sim 9$ bars, where E_0 and ν_0 are taken to be $1 \times 10^{12} \text{ dynes/cm}^2$ and 0.30, respectively. These order of magnitude calculations are suggestive that the observed uplift (covering approximately 12,000 km² [51]), while being of a tectonic nature, should not be confused with the processes leading to an impending earthquake, rather, the result of physical processes that led to the formation of the San Fernando mainshock on 9 February 1971. If event 9 in Table 5 marks the termination of the primary inclusion phase, then v_p and r_s should begin to decrease in the focal region as fluids diffuse away from the primary inclusion zone. This behavior would be evidenced by earthquakes in the focal volume tending to migrate with time away from the primary inclusion zone. This behavior is observed. Lastly, the predicted minimum dimension of the anomalous region, assuming an average maximum 'background' seismicity of $M_{\max} = 2.5$, is 25 km, respectively. This value compares favorably with the value of 80 km quoted

The August 1973, earthquake at Blue Mountain Lake, New York

A magnitude $M2.6$ earthquake occurred at Blue Mountain Lake at a depth of approximately 1 km on 3 August 1973. This earthquake was preceded by approximately 5 days by decreases in v_p and v_s of approximately 22% and 12% below normal. The anomalous zone (region of low v_p) for this earthquake was about 3 km \rightarrow 5 km radius. According to AGGARWAL *et al.* [2], the anomalous zone had a radius of at least 6, but probably less than 10 times the radius of the aftershock zone. AGGARWAL *et al.* [2] observed that the P -wave delays were a maximum in the hypocentral region of the earthquake and decreased away from this region. The earthquake occurred approximately one day following a return of v_p/v_s to its pre-anomaly value. Both these results are consistent with the existence of pore fluids within the focal volume of this earthquake for reasons discussed earlier in this article.

The aftershocks of this event were observed to occur within an elliptically shaped zone whose dimensions were slightly less than 1 km by 0.3 km, giving an aftershock area of 0.24 km². Equation (3) gives a calculated precursor time, τ_0 , for this event of approximately 6.8 d. The observed time, measured from the onset of v_p/v_s decrease, was approximately 5 d. Note that the time of onset of the v_p/v_s decrease must be considered to represent a *minimum* value for τ_0 . The average maximum magnitude of the background seismicity, M_{\max} , in this region is approximately 1.0 [1, 2], giving a calculated minimum diameter of the anomalous volume of approximately 22 km. These values are well within the bounds calculated by AGGARWAL *et al.* [2]. AGGARWAL *et al.* also observed that the future rupture zone was seismically quiet during the time of the low v_p/v_s values preceding the 3 August event. Nearly all the seismic events studied occurred in an area surrounding the aftershock zone. This result is in agreement with the behavior predicted by the inclusion theory. However, the calculated magnitude of the 3 August shock, assuming that the aftershock area (A) magnitude (M) satisfies the Utsu relationship is $M3.1$, a discrepancy in magnitude of nearly 0.5. This result may possibly be interpreted as indicating that pore fluids were present within the hypocentral region of the 3 August event. The magnitude of this pressure is found from equation (28) to be approximately $0.60\sigma_3$, where σ_3 for this event is the vertical stress and is approximately 0.2 kb. Thus, P_f in the hypocentral region of the 3 August shock is predicted to be in the order of 0.12 kb.

The 3 October and 9 November 1974, Peru earthquake sequence

An earthquake sequence that may have important seismological and sociological implications occurred approximately 60 km off the coast of central Peru between 3 October and 9 November 1974 and within a well-documented seismic gap. The 3 October ($m_b = 6.3$, $M_s = 7.6$, USGS) and 9 November ($m_b = 6.0$, $M_s = 7.2$, USGS) shocks were shallow (~ 20 km depth), complex multiple ruptures that began with a low energy episode followed by higher energy ruptures [30]. The subsequent

Table 6
Precursory seismicity in the immediate epicentral region prior to the 3 October–9 November 1974, Peru earthquake sequence (after SPENCE and LANGER, 1976)

Date	Latitude °S	Longitude °W	Depth (km)	m_b	M_s
1. 7 October 1963	12.9	76.8	69	5.4	—
2. 22 August 1967	12.5	76.8	57	4.8	—
3. 5 August 1968	12.8	76.8	78	4.4	—
4. 9 February 1970	12.8	77.2	40	4.6	—
*5. 28 May 1971	12.5	67.8	56	4.9	—
*6. 1 August 1971	12.9	76.8	64	5.2	—
*7. 1 October 1971	12.8	77.1	43	4.7	—
*8. 3 October 1971	12.7	77.2	—	4.6	—
*9. 3 October 1971	12.8	77.4	42	5.2	—
*10. 3 October 1971	12.6	77.6	—	4.2	—
*11. 19 June 1972	12.1	77.5	72 (?)	5.2	—
*12. 29 January 1973	12.1	77.3	63	4.5	—
*13. 24 December 1973	12.6	77.5	—	5.4	—
*14. 31 August 1974	12.7	77.0	61	4.4	—
*15. 27 September 1974	12.4	77.6	41	5.0	—
16. 3 October 1974	12.3	77.7	20	6.3	7.6
17. 10 October 1974	12.4	77.6	27	5.3	—
				(largest aftershock)	
18. 9 November 1974	12.5	77.7	10	6.0	7.2
19. 14 November 1974	12.8	77.1	shallow	5.4	—

Table 6 summarizes the date, focal depth, and magnitude data for the seismic events that preceded the 3 October 1974 event. Location accuracy of these events is ± 15 km [SPENCE, personal communication, 1975]. These data show that no seismic event occurred in the immediate hypocentral zone between 1962 and 1970. The precursory seismicity data, however, suggest a peak of activity on 3 October 1971, followed by a period of relative quiescence in the epicentral region. Seismic events 5 through 10, beginning on 28 May and terminating on 3 October 1971, a time span of approximately 4 months, map out an area, A_1 , of approximately 1.5×10^{13} cm². These events migrated in time toward the epicentral regions of the 3 October and 9 November shocks, and as such, appear to be causally related to these shocks. There was *no* further activity within this zone until the mainshock of 3 October 1974. It should be noted that events 1–4 developed within the E–SE portions of this zone several years prior to, and may have been instrumental in, its formation.

Figure 9d illustrates the yearly seismic event count within the bounds $11.5^\circ\text{S} \approx 14.0^\circ\text{S}$ and $76^\circ\text{W} \approx 79^\circ\text{W}$. The body-wave magnitude range of the seismicity in this figure is $4.0 \leq m_b \leq 5.5$. Note the pronounced peak in seismic activity that occurred during 1971, followed by a period of relative quiescence that terminated with the 3 October 1974 mainshock. Figure 9c shows the aftershock area and the locations of

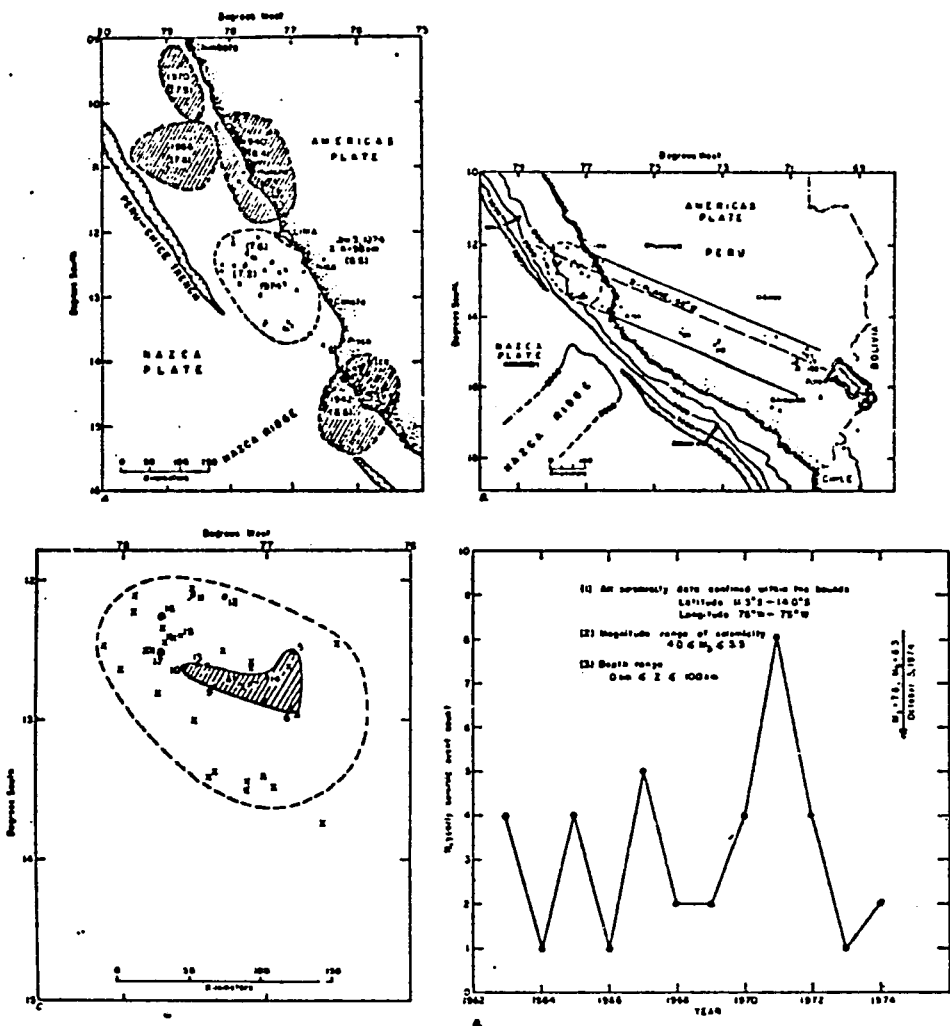


Figure 9

Location of mainshock and aftershock region of the 3 October–9 November 1974 Peru earthquake sequence. A. Relationship of 3 October 1974 aftershock region to previous earthquakes in the immediate epicentral region. B. Rupture propagation direction of the 3 October mainshock. C. Location and dimensions of the hypothesized primary inclusion zone of the 3 October mainshock. D. Yearly seismicity count versus time in the epicentral region of the 3 October–9 November mainshocks. [Figures A–B are reproduced with permission of SPENCE and LANGER, 1975].

aftershock sequence of the 3 October event, occurring within an elliptical zone some 250 km by 150 km, partially filled the seismic gap and was essentially terminated by the 9 November 1974 mainshock (Figs. 9a,b). The primary aftershock region of the 3 October event since 14 November 1974 is now very near to the normal background level of seismic activity. Subsequent activity has shifted to the north-northeast of this region [SPENCE, personal communication, 1975].

ismic events 5 through 15. The peak of seismic activity in 1971, like the peak of seismic activity associated in the San Fernando region and the rockburst discussed earlier, was associated with the formation of the shaded zone depicted in Fig. 9c. Thus, the data in Figs. 9c,d suggest that the primary inclusion zone associated with the 3 October 1974 mainshock may have formed during the time interval between 28 May 1971 and 3 October 1971.

The 3 October and 9 November shocks occurred within a well-documented seismic gap that is of a size to suggest that it could have supported a much larger magnitude earthquake sequence than what did actually occur (Fig. 9a). There is also some seismic evidence that suggests that the earthquakes in the sequence were 'anomalous' events in that the actual shock could have been of a much larger magnitude ($\leq M8$). The estimated aftershock area, A , of the 3 October 1974 event was approximately $3.0 \times 10^{14} \text{ cm}^2$ [30]. The calculated magnitude of an event having an aftershock area of this dimension is calculated from equation (5) to be approximately $M_p 8.2$, where it is assumed that the modified Utsu relationship between A and M_p is applicable to this region. If the seismic event sequence (5 \rightarrow 10) in Table 6 can be assumed to denote the formation of the primary inclusion zone of this shock, then the calculated aftershock area A ($A = 21.8A_0$), of this event is approximately $1.3 \times 10^{14} \text{ cm}^2$, in good agreement with the observed aftershock area. The class I precursor time, τ_0 , for the calculated mainshock ($M_p 8.2$) and the time, τ_{d0} , required to form the primary inclusion zone of this event would have been 2405 yr and 113 yr, respectively, in the *unlikely* situation of there being no changes in the far-field boundary conditions due, for example, to plate motions during the time τ_0 and the predicted time required to form the primary inclusion zone. Thus, assuming that (1) the Utsu relationship is applicable to this region and (2) the time, τ_d , to form the inclusion zone required only 4 months, the calculated time to the mainshock becomes $\tau = \tau_0(\tau_d/\tau_{d0}) = 7.1 \text{ yr}$, a reduction from the theoretical value by a factor of nearly 300. Substituting these values into (26) gives a predicted velocity, v , at which changes are occurring in the far-field boundary conditions equal to 28 km/yr. This value is in close agreement with observational and theoretical treatments of the average velocity of strain pulses in the lithosphere along major subduction zones [8, 45, 46].

The calculated precursor time for an event of this magnitude ($M_p 8.2$) would have required approximately 7 yr. This time is measured from the 28 May 1971 event. However, the actual earthquake sequence occurred 3 yr from that time. The observed partial filling of the aftershock region of the 3 October 1974 mainshock could be interpreted as indicating that this region may not have had the time required for the preparation of the larger magnitude shock. In addition, it should be noted that events 11, 14, and 15 (Table 6) occurred within the epicentral region of the 3 October and 9 November mainshocks. In particular, events 13, 14, and 15 appear to migrate toward the hypocenters of these shocks. These events were of significant magnitude to have acted as possible 'destressing earthquakes' in the region of what could have

only a large failure could have occurred in the absence of destressing. Similar behavior has been reported to occur in mines experiencing rockbursts [12]. It is conceivable, therefore, that both the 3 October and 9 November shocks may have been 'triggered' by events 11, 14, and 15. Thus, according to these arguments, it is theoretically possible that the mainshock should have been much larger ($M8.2$) than what was actually observed ($M_p 7.6$).

There is some evidence that suggests this region may have again approached a critical state. For example, the multiple rupture characteristics of the 3 October and 9 November events, taken in context of the inclusion theory, may signify a low compression level of the least local principal stress in the hypocentral region. Similarly, the relatively high M_p values of these events may be an indication that this stress is nearing or has attained a tensile value in the hypocentral region. Necessary and sufficient conditions for an impending failure include the condition that σ_3 become tensile within the inclusion zone. As discussed above and elsewhere [11, 12], destressing seismic events, such as may have occurred in events 13, 14, and 15, merely postpone the total release of the energy that is stored in the region. In addition, the magnitude of the event that may occur, assuming no additional destressing-type events occur during the earthquake preparation process, may be larger than the event that would have occurred had the destressing shocks not occurred, that is, the magnitude of the impending shock will be at least $M8.2$, and possibly higher.

These arguments and the observational data that the 9 November 1971 shock terminated the earthquake sequence with only one additional aftershock (event 19, Table 6) nearly 5 days later are consistent with the theoretical conditions discussed earlier in this article that this region may now be in the process of being prepared for an earthquake whose magnitude will be at least $M8.2$. The 14 November 1974 shallow focus event occurred within and near the eastern end portions of the zone that may have been the postulated primary inclusion zone of the 3 October and 9 November mainshocks. According to SPENCE [personal communication, 1975], this shock produced a radiation pattern characteristic of deep earthquakes, that is, small rupture length but high energy release. Thus, the location of the 14 November event may mark the eastern termination of the inclusion zone of the impending mainshock.

If the hypocentral regions affected by the 3 October and 9 November events are now contained within this inclusion zone, then the total area of the 'new' primary inclusion zone is of the order of $3 \times 10^{13} \text{ cm}^2$. The *predicted* magnitude and class I precursor time, τ , is measured from the 14 November 1974 event. However, without more reliable information on the dimensions of the hypothesized new primary inclusion zone, the best estimate that can be made at this time of the magnitude of the impending shock is that it will be at least $M8.2$. Accordingly, if there are no further destressing seismic events and the far-field boundary conditions in this region change in the same prescribed manner as for the 3 October 1974 shock, then the predicted class I precursor times for a range of predicted magnitudes of 8.2, 8.3, and 8.5 are

7.1 yr, 8.9 yr, and 10.7 yr, respectively. The predicted location and preferred fault plane for this event should be similar to those of the 3 October 1974 shock (Fig. 9b). This earthquake, like the 3 October–9 November 1975 sequence, will be an under-thrust event.

In this interpretation of the Peru sequence, I have assumed that the Utsu relationship is applicable to this region. Thus, the anomalously large size of the aftershock region for the 3 October 1974 event and the relatively small magnitude ($m_b = 6.3$, $M_s = 7.6$) of the earthquake that produced the aftershock region may be evidence that the region may not have been relieved of the available stored energy. However, as discussed earlier in the text, it is possible that the existence of fluids under pressure in the hypocentral region of the 3 October shock may be partially responsible for lowering the 'predicted' magnitude, based on the observed aftershock area, from 8.2 to 7.6. Yet, neighboring regions, such as shown in Fig. 9a, have also experienced great earthquakes ($\geq M8$) in the recent past. Thus, there is no obvious reason to assume that the epicentral region of the 3 October 1974 event is any different. Similarly, historical records indicate that this region has experienced large earthquakes (and their accompanying tsunamis) in the historical past (28 October 1746; $M \sim 8.4$, SPENCE and LANGER, personal communication, 1976).

The hypothesis that the primary inclusion zone of an impending great earthquake may have formed approximately 75 km off the coast of central Peru on 9 November 1974 can be tested by detailed monitoring of sea level changes (sea level should decrease as the focal region begins to store energy), anomalous v_p , v_s , and/or v_p/v_s behavior if fluids are present in the focal region, radon emanations, possible secular variations in the geomagnetic field, and other class I precursors that have been reportedly observed prior to major earthquakes. If the measurements support this interpretation, then detailed monitoring of the region for the class II type precursor is in order. Detection of the class II precursors may give a few hours warning of the impending shock.

Discussion

Theoretical arguments and supporting data presented in this article suggest that the inclusion theory of failure and its associated scale invariant properties may have important applications to earthquake seismology and, in particular, to the problem of earthquake prediction. It was shown that to have a predictive capability, detailed knowledge of both when the primary inclusion forms and its geometrical characteristics are essential. Knowledge of the dimensions of the primary inclusion zone and the time duration required for its formation provides an estimate of both the magnitude and the class I precursor time for the impending failure. In addition, it was shown that there are features characteristic of earthquake prone regions which indicate that accurate prediction of both the class I precursor time and the magnitude of an

impending earthquake is difficult. Changes in the far-field tectonic boundary conditions due, for example, to plate motions occurring during the usual class I precursor time interval as well as the existence of pore fluids under pressure in the focal volume of an impending shock are both factors that influence the precursor time-magnitude relationship. However, once it has been determined how these parameters affect the class I precursor time-focal region area-magnitude relationships in a given region, then it is possible to adjust the theoretical relationships so as to accurately predict these parameters for other earthquakes in the same region, *providing*, of course, that the boundary conditions change in the same prescribed manner. These difficulties, however, do not arise for the class II precursors since their time durations are short enough that changes in the far-field boundary conditions are, for all practical purposes, constant during the class II time duration. Thus, monitoring of this precursor class in the epicentral region of an impending earthquake may provide an accurate indicator of when the mainshock will occur.

The criteria required to determine when a region is approaching or has approached a condition that it will experience an earthquake are readily provided by the inclusion theory. These criteria include the following: (1) A determination of the b -value variation of the seismic events occurring within the anomalous (or dilated) volume. The b -values are predicted to decrease as the deformation band, within the primary inclusion zone will form, develops within the anomalous volume. (2) Once a candidate region has been found, detailed monitoring of this region is required to determine where and when the primary inclusion zone forms. The events that form this zone are predicted to be relatively few in number (≤ 10). Each event will be characterized by anomalously large rupture lengths since they are forming within a stress field characterized by a tensile value of the local least principal stress. The b -values of these events are predicted to be low. In addition, since these events are predicted to have long rupture lengths, anomalous uplift and/or anomalous horizontal expansion, depending upon the focal mechanism of the impending mainshock, both within and outside the epicentral region are predicted. The overall level of background seismicity will decrease once the primary inclusion has formed. (3) The epicentral region of the impending earthquake should be instrumented at this time so as to detect the onset of the class II precursor.

It is of particular importance to note that the numerical calculations, such as the energy budget of a failure, that have been performed in this article are subject to revision as more reliable data on the functional relationship between the aftershock area and magnitude are available. This relationship may be dependent upon the location and physical characteristics of the rock materials in the focal volume. *This relationship represents the 'calibration factor' in applying the inclusion theory to given earthquake prone zones.*

It should also be clearly understood that the inclusion theory is directly applicable to failures along existing fault zones as the physical processes responsible for 'lock zone' failure and 'fresh' failures are identical. However, when applying the theory

to the prediction of earthquakes along existing fault zones, it is possible that considerable underestimation of the magnitude of an impending shock, even when factors due to pore fluids have been taken into account, can result since failure of the lock zone may also result in the sudden release of stored strain energy along the fault zone outside the lock point. Thus, it is theoretically possible that a large magnitude shock could occur only when a much smaller magnitude shock has been predicted. We have found evidence supporting this prediction from certain classes of rockbursts in northern Idaho, that is, rockbursts that develop along pre-existing fault zones that are activated by mining.

The inclusion theory requires the existence of low magnitude foreshocks, termed primary foreshocks, whose magnitudes are approximately $M-5.3$, where M is the mainshock magnitude, to form in the hypocentral region during the time duration of the class II precursor phase. This class of foreshocks should not be confused with secondary foreshocks which may occur in the focal volume of the mainshock as a result of strength variations in the rock mass comprising the focal volume. Secondary foreshocks can serve to prematurely 'trigger' the mainshock. It is to be noted that the spectral characteristics of secondary foreshocks will be considerably different than primary foreshocks for reasons discussed earlier in the text. It is also important to note that the inclusion theory requires that the probability of occurrence of secondary foreshocks will increase as the magnitude of the mainshock increases. The reason for this behavior is that as the size of the primary inclusion zone increases, the greater the probability that this region will include rock materials of greater strength disparity. Thus, as the focal region of the impending shock approaches a critical state, that part of the primary inclusion zone containing rock of the lowest strength will fail first. Failure of this zone will then load the adjacent stronger region and thereby trigger the mainshock.

Lastly, it is of interest to observe that the deviation of the observed class I precursor time, τ , from the predicted time, τ_0 , which is obtained when no changes are occurring in the far-field boundary conditions must provide a relative indication of how the boundary conditions that indirectly produce the earthquake are changing in the region where the earthquake is occurring. Thus, the deviation of τ_0 and τ in Fig. 5 should provide quantitative information of relative plate velocities, or alternatively, the relative magnitude of how the far-field strains induced within a given earthquake prone region are changing in response to these relative plate motions. Evidence presented in this article lends support to this hypothesis. Clearly, this aspect of the earthquake problem warrants further attention.

Acknowledgments

William Spence kindly provided me a preprint of his results on the 3 October and 1 November 1974 Peru earthquake sequence. Discussions with Dr. Spence on this

sequence are gratefully acknowledged. In addition, I would extend my appreciation to Max Wyss and the anonymous reviewers of this sequence of papers. Their conscientious reviews have been of considerable value to me in improving the final manuscripts.

REFERENCES

- [1] Y. P. AGGARWAL, L. R. SYKES, J. ARMBRUSTER, and M. L. SBAR (1973), *Prennitory changes in seismic velocities and prediction of earthquakes*, Nature, 241, 101-104.
- [2] Y. P. AGGARWAL, L. R. SYKES, D. W. SIMPSON, and P. G. RICHARDS (1975), *Spatial and temporal variations in τ_0 and in P-wave residuals at Blue Mountain Lake, New York: application to earthquake prediction*, J. Geophys. Res. 80, No. 5, 718-732.
- [3] D. L. ANDERSON and J. H. WHITCOMB (1975), *Time-dependent seismology*, J. Geophys. Res. 80, No. 11, 1497-1503.
- [4] C. ARCHAMBEAU and S. SAMMIS (1970), *Seismic radiation from explosions in prestressed media and the measurement of tectonic stress in the earth*, Rev. of Geophys. Space Phys. 8, No. 3, 473-499.
- [5] M. BÄTHI, *Handbook on Earthquake Magnitude Determinations* (Seismological Institute, Uppsala, Sweden, 1969), 158 pp.
- [6] B. T. BRADY (1974), *Theory of earthquakes—I. A scale independent theory of failure*, Pure appl. Geophys. 112, 701-726.
- [7] B. T. BRADY (1975), *Theory of earthquakes—II. Inclusion theory of crustal earthquakes*, Pure appl. Geophys. 113, 149-169.
- [8] B. T. BRADY (1976), *Theory of earthquakes—III. Inclusion theory of deep earthquakes*, Pure appl. Geophys. 114, 119-139.
- [9] B. T. BRADY (1976), *Laboratory investigation of tilt and seismicity anomalies in rock before failure*, Nature, 260, No. 5547, 108-111.
- [10] B. T. BRADY (1976), *Dynamics of fault growth: A physical basis for aftershock sequences*, Pure appl. Geophys. (in press).
- [11] B. T. BRADY (1975), *Seismic precursors prior to rock failures in underground mines*, Nature 252, 549-552.
- [12] B. T. BRADY and F. W. LEIGHTON (1976), *Seismicity anomaly prior to a moderate rock burst: A case study*, to be presented and published in the *Proceedings of the 17th Rock Mechanics Symposium, Snowbird, Utah, August 25-27, 1976*.
- [13] R. L. CASTLE, J. N. ALT, J. C. SAVAGE, and E. J. BALAZA (1974), *Elevation changes preceding the San Fernando earthquake of February 9, 1971*, Geology 2, 61-66.
- [14] W. L. ELLSWORTH (1975), *Bear Valley, California, earthquake sequence of February-March, 1972*, Bull. Seis. Soc. Am. 65, No. 2, 483-586.
- [15] T. C. HANKS (1974), *Constraints on the dilatancy-diffusion model of the earthquake mechanism*, J. Geophys. Res. 79, No. 20, 3021-3025.
- [16] J. KELLEHER and J. SAVINO (1975), *Distribution of seismicity before large strike-slip and thrust-type earthquakes*, J. Geophys. Res. 80, No. 2, 260-271.
- [17] A. MCGARR (1971), *Violent deformation of rock near deep-level, tabular excavations—Seismic events*, Bull. Seis. Soc. Amer. 61, No. 5, 1453-1466.
- [18] K. MOGI (1968), *Development of aftershock areas of great earthquakes*, Bull. Earthquake Res. Inst. 46, 175-203.
- [19] I. L. NERSESOV, A. A. LUKK, V. S. PONOMAREV, T. G. RAUTAIN, B. G. RULEV, A. N. SEMENOV, and I. G. SIMBIREVA, *Possibilities of Earthquake Prediction, Exemplified by the Garm Area of the Tadzhik S.S.R.*, in *Earthquake Precursors*, ed. M. A. SADOVSKII, I. L. NERSESOV, and L. G. LATYNINA (Academy of Science of the USSR, Moscow, 1975), pp. 79-99.
- [20] J. C. JAEGER, *Elasticity, Fracture and Flow* (2nd Ed.) (John Wiley and Sons, New York, 1962).
- [21] R. J. O'CONNELL and B. BUDIANSKY (1974), *Seismic velocities in dry and saturated cracked solids*, J. Geophys. Res. 79, No. 35, 5412-5426.

- [22] L. OBERT and W. I. DUVALL, *Rock Mechanics and the Design of Structures in Rock* (John Wiley and Sons, New York, 1968), 650 pp.
- [23] E. OROWAN (1938), *The mechanical strength properties and the real structure of crystals*, Z. Kristallographie 89, 327-343.
- [24] H. F. REID (1911), *The elastic rebound theory of earthquakes*, Bull. Dept. Geol., Univ. of Calif. 6.
- [25] N. J. PETCH, *Metallographic aspects of fracture*, in *Fracture: An Advanced Treatise* (ed. H. Liebowitz) (Academic Press, 1968), pp. 351-390.
- [26] F. PRESS and C. ARCHAMBEAU (1962), *Release of tectonic strain by underground nuclear explosions*, J. Geophys. Res. 67, No. 2, 335-343.
- [27] R. A. SACK (1946), *Extension of Griffith's theory of rupture to three dimensions*, Proc. Phys. Soc., Lon. 58, 729-736.
- [28] K. SASSA (1944), *Tilting motion of ground observed before and after the destructive Tottori earthquake*, Kagaku, Science 14, No. 6, 220-221.
- [29] K. SASSA and E. NISHIMURA (1951), *On phenomena forerunning earthquakes*, Trans. Amer. Geophys. Union 32, No. 1, 1-6.
- [30] W. C. SPENCE, C. J. LAGER, and J. N. JORDAN, *A tectonic study of the Peru earthquakes of October 3 and November 9, 1974* (in preparation).
- [31] T. UTSU and A. SEKI (1955), *A relation between the area of the aftershock region and the radius of the sensibility circle* (in Japanese), Zisin 3, No. 34, 1955.
- [32] J. B. WALSH (1968), *Mechanics of strike-slip faulting with friction*, J. Geophys. Res. 73, No. 2, 761-776.
- [33] R. WESSON and W. ELLSWORTH (1973), *Seismicity preceding moderate earthquakes in California*, J. Geophys. Res. 78, 8527-8546.
- [34] J. WHITCOMB, J. GARMANY, and D. L. ANDERSON (1973), *Earthquake prediction: Variation and seismic velocities before the San Fernando earthquake*, Science 180, 632-635.
- [35] M. WYSS (1975), *Precursors to the Garm earthquake of March 1969*, J. Geophys. Res. 80, No. 20, 2926-2930.
- [36] T. MATUZAWA, *Study of Earthquakes* (UNO Shoten, Tokyo, Japan, 1964), 213 pp.
- [37] T. UTSU (1969), *Aftershocks and earthquake statistics (I)*, J. Fac. Sci., Hokkaido Univ. Ser. 73, 129-195.
- [38] T. HAGIWARA and T. RIKITAKI (1967), *Japanese program on earthquake prediction*, Science 157, 761-762.
- [39] A. M. KONDRATENKO and I. L. NERSESOV (1962), *Some results of a study of changes in the speeds of longitudinal and transverse waves in the focal zone, physics of earthquakes and explosion seismology*, Tr. Inst. Fiz., Zomli Akad. Nauk, USSR, 25.
- [40] J. B. SMALL and E. J. PARKIN, *Horizontal and Vertical Crustal Movement in the Prince William Sound, Alaska, Earthquake of 1964*, paper presented to the Fifth United Nations Regional Cartographic Conference for Asia and the Far East, Canberra, Washington, E.S.S.A., U.S. Dept. of Commerce, March 1967.
- [41] A. E. OSTROVSKY, *Long-Period Waves and Tilts of the Earth's Surface Before Strong Earthquakes* (abstract) (International Union of Geodesy and Geophysics, Grenoble, 1975).
- [42] M. WYSS (1974), *Will there be a large earthquake in Central California during the next two decades?* Nature 253, 126-128.
- [43] R. ROBINSON, R. L. WESSON, and W. L. ELLSWORTH (1974), *Variation of P-wave velocity before the Bear Valley, California, earthquake of February 24, 1972*, Science 184, 1281-1283.
- [44] V. I. MIACHKIN, W. F. BRACE, G. A. SOBOLEV, and J. H. DIETERICH (1974), *Two models for earthquake forerunners*, Pure appl. Geophys. 113, No. 1/2, 169-183.
- [45] K. MOGI (1973), *Relationship between shallow and deep seismicity in the Western Pacific region*, Tectonophysics 17, 1-22.
- [46] T. RIKITAKE (1975), *Earthquake precursors*, Bull. Seismo. Soc. Amer. 65, No. 5, 1133-1162.
- [47] F. R. GORDON (1970), *Water level changes preceding the Meckering, Western Australia, earthquake of October 14, 1968*, Bull. Seismo. Soc. Amer. 60, No. 5, 1739-1740.
- [48] W. D. STUART (1974), *Diffusionless dilatancy model for earthquake precursors*, Geophys. Res. Lett. 1, 261-264.
- [49] F. D. STACEY, *Physics of the Earth* (John Wiley and Sons, Inc., New York, 1969).

- C. F. RICHTER, *Elementary Seismology* (Freeman and Sons, San Francisco, 1958).
- [51] J. H. WHITCOMB, C. A. ALLEN, J. D. GARMANY, and J. A. HILLMAN (1973), *The February 9, 1971 San Fernando earthquakes and aftershocks*, Rev. Geophys. 11, 1-10.
- [52] R. O. CASTLE, J. P. CHURCH, and M. R. ELLIOTT (1976), *Aseismic uplift in Southern California*, Science 192, 251-253.
- [53] T. UTSU (1969), *Aftershocks and Earthquake Statistics (I)*, J. Fac. Sci., Hokkaido Univ. Ser. 73, 129-195.

(Received 22nd December 1975)

Appendix A

Glossary of Terms and Symbols

Terms

- (1) *Anomalous Zone*: This zone refers to the dilation zone within which a deformation band will form prior to a major failure.
- (2) *Deformation Band*: This band denotes the portion of the anomalous zone within which the principal stress axes rotate as the region is being prepared for a major failure.
- (3) *Primary Inclusion Zone*: This zone forms within the deformation band at a time prior to failure that is dependent on the magnitude of the failure that will occur. The formation of this zone marks the initiation of the class I precursor phase.
- (4) *Secondary Inclusion Zone*: This zone represents the inclusion from which secondary crack growth occurs within the primary inclusion zone. This crack growth leads to the coalescence of cracks within the primary inclusion to form the macrocrack. The formation of this zone marks the initiation of the class II precursor phase.
- (5) *Tertiary Inclusion Zone*: This zone denotes the inclusion from which macrocrack growth occurs during the growth phase of the mainshock. The formation of this zone marks the initiation of the class III precursor phase.
- (6) *Macrocrack Zone*: The zone containing the macrocrack within the primary inclusion zone.
- (7) *Focal Region*: The region into which the failure is propagated. This region

represents the zone where strain energy storage occurs during the preparation stage of the mainshock and where the aftershocks occur.

- (8) **Hypocenter:** The contact between the fault zone and the primary inclusion zone. The hypocenter denotes the location where closure of the macrocrack first occurs.
- (9) **Fault Zone:** Represents the faulted region that precedes the primary inclusion zone. The fault represents that part of the macrocrack that has closed.
- (10) **Lock Point Zone:** A zone along a pre-existing fault zone where movement is prohibited. This zone represents the region within which a primary inclusion that will lead to its failure is nucleated.

Symbols

σ_{10}, σ_{30}	Far-field maximum (σ_{10}) and least (σ_{30}) principal stresses. These represent the principal stresses that exist outside and are far removed from the anomalous region within which the mainshock occurs.
σ_1, σ_3	Local values of the maximum and least principal stresses within the deformation band.
θ	The angle between σ_{10} and σ_1 .
σ_e, σ_t	Principal stresses parallel (σ_e) and normal (σ_t) to the major axis of the primary inclusion zone.
σ_{i0}	The magnitude of σ_t at the inception of failure.
$\sigma_d (= \sigma_1 - \sigma_3)$	Principal stress difference within the focal region.
σ_c^*, σ_t^*	Compressive and tensile stresses existing in the region outside the macrocrack zone during the time duration of the class II precursor.
v_p, v_s	Longitudinal and transverse wave velocities.
L_i, A_i	Length and area of the primary inclusion zone.
L, A	Average dimension and area of the focal region of the primary inclusion zone.
A_c	Area of the average-sized cracks within the primary inclusion zone.
l_c	Fundamental inclusion length ($\sim 10^{-7}$ cm).
τ_0, τ	Predicted and observed times of the class I precursor.
τ_{10}, τ_s	Predicted and observed times of the class II precursor.
τ_{r0}, τ_r	Predicted and observed times of the class III precursor.
τ_{d0}, τ_d	Predicted and observed times required to form the primary inclusion zone.
$v_0 (= L/\tau_0)$	Average predicted and average observed velocity of the crack

 t_0 M_p, M M_{max} Ψ_0, Ψ Ψ_r Ψ_d Ψ_{as} \bar{M} $\sigma_{eff} (= \sigma_3 - P_f)$ P_f $\eta \left(= \frac{\Psi_r}{\Psi_p} \right)$

Average linear dimension of the deformation band. This length also denotes the average minimum dimension of the anomalous zone.

Predicted and observed magnitudes of the mainshock.

Predicted background value of the average maximum magnitude of seismic events within the anomalous zone.

Total potential energy changes of the system due to presence of the primary inclusion zone when fluids are not present (Ψ_0) or present (Ψ) in the focal volume of the primary inclusion zone.

Energy radiated by the mainshock.

Energy dissipated by frictional sliding, plastic flow, etc., during the mainshock.

Total energy radiated by aftershocks.

Predicted maximum magnitude of any aftershock during the aftershock sequence.

Effective value of the local least principal stress.

Pore pressure within the focal volume of the primary inclusion zone.

Seismic efficiency factor.

Appendix B

An example of the dilatant or anomalous phase in rock is shown in Fig. B.1. This figure is a photograph of a corner section of an oil shale sample that illustrates the process of fault (F) growth. The initial length and diameter of this specimen were 10 cm and 5 cm, respectively. This specimen recovered nearly 10% of the total initial deformation (~ 0.25 cm) within one day following the test. Note the orientation of the deformation band (D), whose width is approximately one centimeter and the tensile cracks (t_0) that developed within the band in a direction nearly normal to the predicted direction of σ_1 , that is, normal to the direction of eventual fault growth [6]. Microscopic examination of this deformation band, as well as other deformation bands within this specimen, shows the existence of numerous (apparently closed) small cracks (whose average lengths are approximately 0.01 cm) that are slightly inclined to the fault direction. Residual tensile and compressive stresses in the deformation band (following unloading) in directions parallel and normal to σ_1 , respectively, are predicted by the inclusion theory [6]. The tensile strength of oil shale normal to the bedding plane is small (~ 50 bars, V. E. HOOKER, personal communication, 1975), and is suggestive that a major contributing factor to the post-test recovery of the specimen was the formation of the tensile cracks within the deformation band(s).

Appendix C

Experimental determination of the precursor time-fault length relationship of failure

When there are *no* changes in the far-field tectonic stresses (strains) during the precursor time interval (τ), the relationship between τ and the focal region area (A) can be written [7]

$$\tau = \alpha A, \quad (\text{C.1})$$

where α is a constant to be determined by experiment. Rockbursts, whose class I precursor times are small enough (≤ 24 hr) so to satisfy the constraints imposed by (C.1), can be used to evaluate the parameter α . Assume that the Utsu relationship (equation (7)) between magnitude (M) and aftershock area (A) is applicable to the rockburst failure. Equations (5) and (C.1) give

$$\log_{10} \tau_0 = 6.3 + \log_{10} \alpha + M, \quad (\text{C.2})$$

where τ_0 is the class I precursor time and is measured in seconds. A major rockburst occurred in the Galena Mine, Wallace, Idaho, on 9 August 1968 (see reference 11 for details). The magnitude and precursor time of this burst were determined to be approximately $M2.3$ and 21.6 hr, respectively. Substituting these values into (C.2) gives $\alpha = 2.43 \times 10^{-4}$ sec/cm². Thus, equation (C.2) becomes

$$\tau_0 = 2.43 \times 10^{-4} A, \quad (\text{C.3})$$

τ_0 and A are measured in seconds and square centimeters.

The relationship between the primary inclusion area (A_i) and A must be determined. A moderate rockburst occurred on 8 November 1975 (1:10 am) at the Galena Mine. Seismic data obtained from this burst allows a determination of the relationship of A_i and A as well as other critical parameters applicable to the scale invariant properties of the inclusion theory. Briefly, the following sequence of events preceded the burst. (1) Blasting in a nearby stope (mining zone), located approximately 75 m from the burst hypocenter, occurred at 2:23 pm on 7 November. No apparent seismic activity was triggered in the hypocentral region as a result of this blasting sequence. (2) At 11:20 pm on the same day, blasting occurred in another stope, located approximately 25 m from the hypocentral region. The time required for blasting was 8 min, during which time a length segment of approximately 15 m of rock was removed from the stope. (3) The burst occurred at 1:10 am, nearly 100 min after blasting.

Experimental studies by the Bureau of Mines in the Galena Mine have shown that the majority of rockbursts are apparently 'triggered' by blasting in stopes that are located in the immediate vicinity of the burst hypocenter. There are theoretical

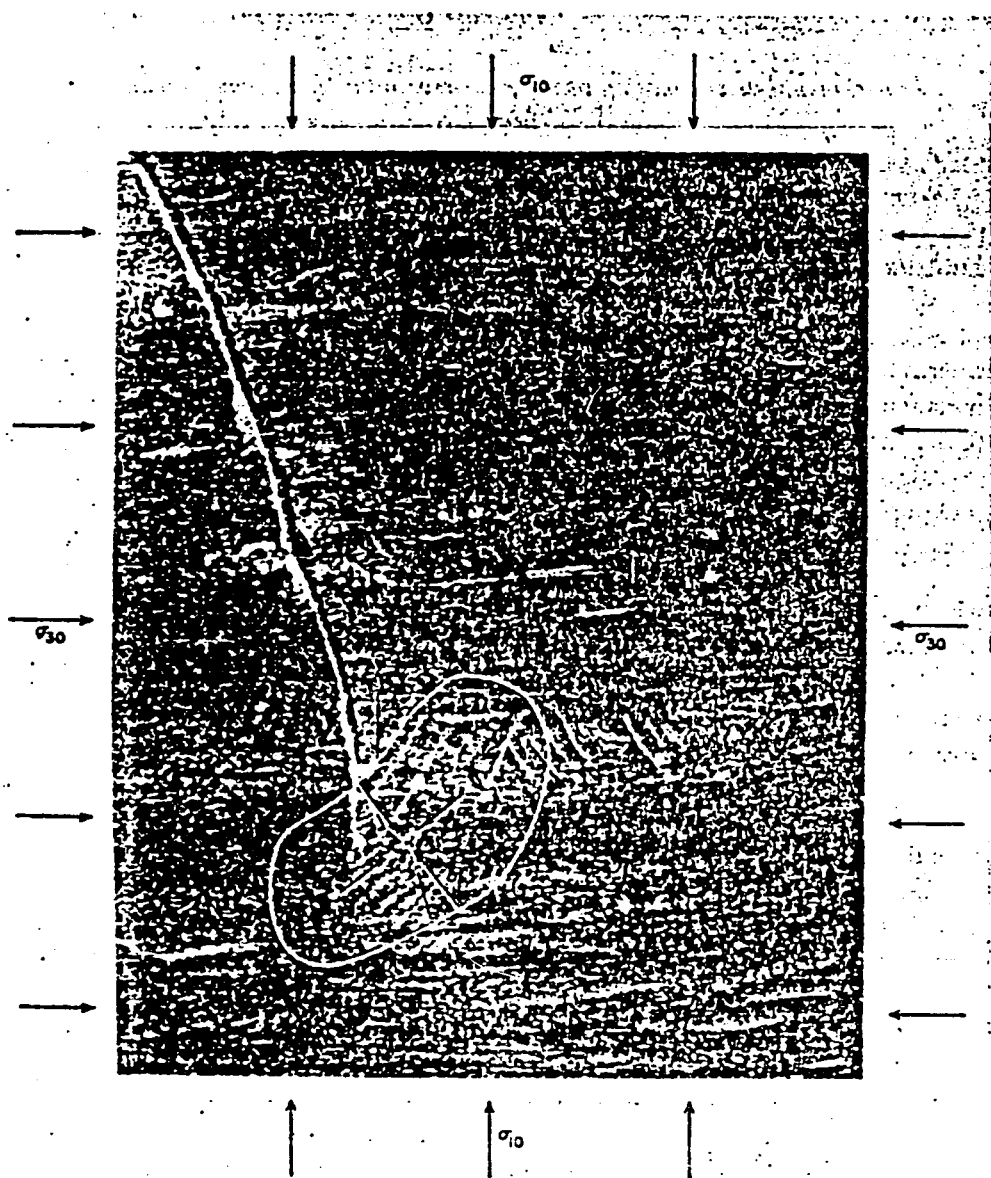


Figure B.1

Polished section of oil shale sample deformed under 100 bars confining pressure, illustrating the deformation band within which the fault developed.

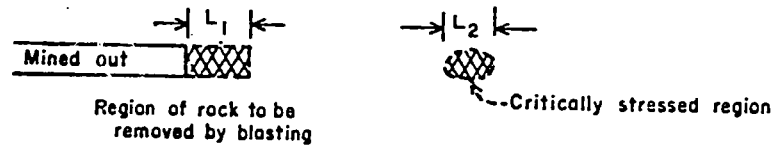
arguments that support this observation. For example, using equations (C.1) and (C.3), the time τ_{d0} , required to form the primary inclusion zone of an impending burst is $\tau_{d0} = 2.43 \times 10^{-4} A_i$. Combining this relationship with the revised Utsu relationship ($\log A = M + 6.3$ [46])

$$\log_{10} \tau_{d0} = M + 2.69 + \log_{10} \mu \tag{C.4}$$

where $\mu = A_i/A$. The observed value of μ , as calculated from the 3 September 1975 Star burst is 0.046. Equation (C.4) becomes

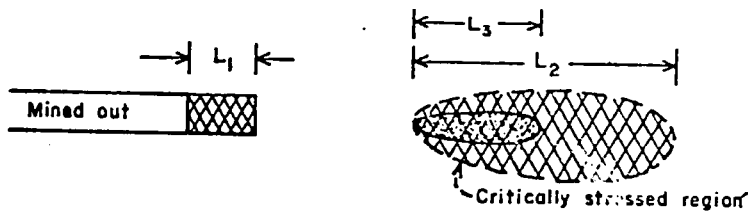
$$\log_{10} \tau_{d0} = M + 1.35 \tag{C.5}$$

Thus, for a typical burst magnitude of $M1.5$, the time, τ_{d0} , required for the formation of the primary inclusion zone is nearly 6 min. However, the time required to form the individual seismic events whose magnitudes are of the order of $M(-3)$, that comprise the primary inclusion zone of an $M1.5$ burst are only a second. Therefore, the seismic signature of these events will be included within the signatures of the individual events. As a result, the primary inclusion zone of the impending burst will be formed by the stress transferrals to the critically stressed region (Fig. C.1) due to blasting. Consequently, the time interval required for blasting provides a maximal value of τ_{d0} (and A_i) for the impending burst.



CASE I

$L_1 > L_2$ Blast-Burst (Burst occurs during blasting)



CASE II

$L_1 < L_2$ Blast-Burst (Burst occurs at time t after blasting)
 $L_1 \leq L_3 < L_2$ Length of Primary Inclusion Zone of Impending Burst.

Figure C.1

Influence of blasting in triggering rockbursts. The critically stressed region represents the zone where the stresses have approached a critical state such that an increase in the maximum principal stress (resulting from blasting in a nearby region) will produce a burst.

The ratio of τ_{d0} (=8 min) and τ_0 (=100 min) for the 8 November 1974 burst gives a minimum estimate of τ_{d0}/τ_0 (= A/A_i) equal to 12.5. This value compares with the observed value of 21.8 calculated for the 3 September 1975 Star rockburst discussed earlier in the test.

Appendix D

Geometrical characteristics of the primary inclusion zone at the instant of failure

Theoretical and experimental arguments suggest that the length of the primary inclusion zone (L_i) and the average length (L_c) of the cracks that comprise this zone are proportional to each other with a proportionality constant, or equivalently, scaling factor γ ($= L_c/L_i$), experimentally observed to be approximately 0.01 (Appendix B). The scaling factor, γ , denotes the relationship by which the length (L_c) and thickness (t_c) of these cracks with respect to the length (L_i) and thickness (t_i), respectively, of the primary inclusion zone. Thus, the scaling law for the inclusion theory can be expressed as

$$L_c = \gamma L_i \tag{D.1}$$

$$t_c = \gamma t_i$$

In the inclusion theory, failure, or equivalently, growth of the primary inclusion zone occurs only when the tensile stress within the primary inclusion zone equals its maximum possible value σ_{i0} . This physical situation develops only when the aspect ratio of the inclusion zone approaches a value that is of the order of 0.20 [5]. Several recent finite element investigations have shown that this aspect ratio is insensitive to the relative stiffness of the primary inclusion zone and the surrounding host material (BABCOCK, USBM, in press, 1976). Substituting this ratio in (D.1) gives

$$t_c = 2.0 \times 10^{-3} L_i \tag{D.2}$$

Thus, the condition for failure can also be stated that the ratio of the thickness of the crack zone to the length of the primary inclusion zone must equal approximately 2.0×10^{-3} at the instant of failure. This condition is also equivalent to the criterion that the tensile stress within the macrocrack zone becomes a maximum at failure.

To a first-order approximation, the crack zone thickness (t_c) will also equal the thickness of the macrocrack zone, say t_g , at the instant of failure. This thickness will also correspond to the thickness of the fault gouge zone. Consequently, when the focal region of the primary inclusion is circular ($A = (\pi/4)L^2$, $A_i = A/21.8$), the functional relationship between t_g and the class I precursor time τ_0 can be written

$$t_g = 0.03 \sqrt{\tau_0} \tag{D.3}$$

where t_g and τ_0 are measured in centimeters and seconds, respectively.

Equation (D.3) states that a knowledge of the fault zone thickness along either active or inactive faults may be an indication of the magnitude of the earthquake(s) that produced the fault zone. The functional relationship of t_g to M , σ_3 , and P_f is found from equations (5), (27), (28), and (D.3).

$$\log_{10} t_g = 0.50M + 0.66 \log_{10} \frac{\sigma_3 - P_f}{\sigma_3} - 0.18 \quad (D.4)$$

where M is the predicted magnitude of the mainshock when $P_f = 0$ and t_g is measured in centimeters.

Table D.1 lists the typical value of fault zone thickness for magnitudes ranging from $M(-)5$ to $M8$. The pore pressure is zero in these calculations. As an example,

Table D.1
Fault zone thickness-magnitude relationship
($P_f = 0$)

L_i km	L km	M	t_g km	Comments
1×10^{-5}	5×10^{-5}	-5	4.8×10^{-8}	Laboratory failure scale
1×10^{-3}	5×10^{-3}	-1	4.8×10^{-6}	Laboratory failure scale
1×10^{-3}	5×10^{-3}	1	4.8×10^{-5}	Mine failure scale
0.03	0.16	2	1.5×10^{-4}	Mine failure scale
0.10	0.5	3	4.8×10^{-4}	Mine failure scale
0.34	1.6	4	1.5×10^{-3}	Earthquake scale
1.1	5	5	4.8×10^{-3}	Earthquake scale
3.4	16	6	1.5×10^{-2}	Earthquake scale
10.6	50	7	4.8×10^{-2}	Earthquake scale
34	160	8	1.5×10^{-1}	Earthquake scale

a magnitude $M8$ earthquake corresponds to a fault zone thickness of nearly 60 m, while the thickness on the scale of major rock bursts ($M = 2 \rightarrow 3$) is only predicted to be in the range of 15 \rightarrow 48 cm.

These values appear to be in good agreement with measurements taken in rock-burst prone mines in South Africa [17]. Also, note that t_g on the laboratory scale [$M(-)5$] is predicted to range in value from 10^{-5} cm, in reasonable agreement with measurements taken in our laboratory. Lastly, note that in real fault zones in the earth, where fluids under pressure are probably present, gouge zone thickness will be less than if the zone were 'dry' at the time of its formation.

If (D.4) is found by experiment to be applicable to real fault zones, it may become possible to predict the spacial distribution of earthquake magnitude along either active or inactive faults of known geologic age as a function of geologic time. Such a method may, in some instances, be of value in assessing seismic risk for engineering structures proposed or currently in operation in these regions.

The preceding calculations can be used to estimate the fault displacement that occurs during an earthquake of magnitude M . Let θ denote the angle between the major axis of the macrocrack zone (Fig. 1) and the maximum applied far-field principal stresses σ_{10} . In the inclusion theory of failure, the shear displacement that can occur during the mainshock sequence is due only to closure of the cracks that developed during the dilatant phase. These cracks formed under the applied far-field stresses, σ_{10} , σ_{20} , and σ_{30} (Fig. 2a). Thus, to a good first-order approximation, the total shear displacement, s_0 , that will occur as the fault grows into the hypocentral region is

$$s_0 = t_g \cot \theta \quad (D.5)$$

As an example of (D.5), MCGARR [17] observed that following a $M3$ rockburst, which produced violent crushing of supports in the vicinity of the burst, shear displacements of 30 \rightarrow 50 cm were observed along the fault. Equation (D.4) gives $t_g = 48$ cm, where $P_f = 0$. The predicted relative shear displacement for a failure of this magnitude, assuming $\theta \approx 30^\circ$, is 83 cm, in reasonable agreement with observation.

Lastly, it is important to observe that (D.1) suggests that the component of volumetric strain, ϵ ($\equiv \gamma$) due to the formation of the primary inclusion zone and its associated macrocrack zone at the *instant of failure* is approximately 1×10^{-2} . This result suggests that current theoretical methods of modeling shear dilatancy in rock by linear classical models may be unsatisfactory [21].

Spatial distribution of earthquakes and subduction of the Nazca plate beneath South America

Muawia Barazangi,* Bryan L. Isacks
Department of Geological Sciences, Cornell University
Ithaca, New York 14853

ABSTRACT

A detailed study of the spatial distribution of precisely located hypocenters of South American earthquakes that occurred between lat 0° and 45° S shows that the data can be explained by the simple model of a descending oceanic plate beneath a continental plate and that the following conditions obtain: (1) The hypocenters clearly define five segments of inclined seismic zones, in each of which the zones have relatively uniform dips. The segments beneath northern and central Peru (about lat 2° to 15° S) and beneath central Chile (about lat 27° to 33° S) have very small dips (about 10°), whereas the three segments beneath southern Ecuador (about lat 0° to 2° S), beneath southern Peru and northern Chile (about lat 15° to 27° S), and beneath southern Chile (about lat 33° to 45° S) have steeper dips (25° to 30°). No clear evidence exists for further segmentation of the descending Nazca plate beneath South America. If the two flat segments are in contact with the lower boundary of the continental plate, the thickness of that plate is less than approximately 130 km. This is in marked contrast to the reports of thicknesses exceeding 300 km for the South American continental plate. (2) There is considerable seismic activity within the upper 50 km of the overriding South American plate. This seismic activity is well separated from the inclined seismic zones and probably occurs in the crustal part of the South American plate. Thus, hypocenters in South America are not evenly distributed through about a 300-km-thick zone as previously described. (3) A remarkable correlation exists between the two flat segments of the subducted Nazca plate and the ab-

sence of Quaternary volcanism on the South American plate. (4) The transition from the flat Peru segment to the steeper Chile segment is abrupt and is interpreted as a tear in the descending Nazca plate. The tear is located approximately beneath the northern limit of the Altiplano (a high plateau in the Andes), and about 200 km south of the projection of the oceanic Nazca ridge down the subduction zone. (5) A gap in seismic activity exists between depths of 320 and 525 km.

INTRODUCTION

South America is a part of one of the major lithospheric plates. Study of the subduction zone along the western margin of this plate provides the opportunity to examine whether the simple model of the descending of oceanic plates beneath an oceanic or small continental block (as developed primarily for the northern and the western Pacific) is also a working model for the subduction of an oceanic plate beneath a continental plate. In this study we show that the simple model of subduction is essentially a valid one for the subduction process beneath South America. However, some features of the interactions and geometries of the descending Nazca plate and the overriding South American plate are quite different from those observed in the northern and western Pacific.

We present here a detailed study of the spatial distribution of South American earthquakes. Previous studies have used, for the most part, the hypocenter file of the United States Geological Survey (USGS) for different time periods (see, for example, Santo, 1969; Isacks and Molnar, 1971; James, 1971; Stauber, 1973, 1975; Sacks and Okada, 1974; Swift and Carr, 1974). Sykes and Hayes (1971) reported results of relocations of South American earthquakes

occurring between 1950 and 1964. Some of the studies mentioned above used very much the same data but the authors came to quite different conclusions regarding the tectonics of South America. This is partly a result of contamination of the data set with poor-quality data. In this study we analyzed mainly the data provided by the International Seismological Summary (ISS) and the International Seismological Centre (ISC). We established criteria for selecting good-quality data out of the hypocenter file and rejected all but about 30 percent of the events as a result. This severe rejection procedure is compensated for by considering the entire sample of high-quality data that have accumulated since the late 1950s. We are thus able to resolve features more clearly than is possible with a smaller set of data or one with a large number of poorly located events.

DATA

The earthquakes analyzed in this study are mainly all those located between lat 0° and 45° S and long 60° and 85° W reported by the ISS from 1959 to 1963, by the ISC from 1964 to August 1973, and by the USGS (Earthquake Data Report) from September 1973 to April 1975. However, because few deep earthquakes occur beneath South America, the final data set also includes all the well-located deep events (deeper than 500 km) located by the ISS for the period 1953 to 1958. Data for events located within the Nazca plate or along the Chile Rise are not included.

The ISC data represent the most complete compilation of data on hypocenter locations available on a world-wide basis. These data, however, include a large number of imprecisely located events, mainly because the events of small size, and especially those in areas far from any local seismic stations, are reported by only the very sensitive teleseismic stations. Thus, a selection of the better quality data from the ISS, ISC, and the USGS data file can be made. A selection based on the elimination of events that are located by less than a certain number of stations is often used but will still include poorly located events, even though many of the worst locations are thereby eliminated.

A selection procedure based on the control of depth by local stations, pP depth control, and the azimuthal control of the epicenter is used in this study. In this procedure all events reported by the ISS and ISC and the large events of the USGS are examined and either rejected or selected

* Present address: Department of Geology, University of Petroleum and Minerals, Dhahran, Saudi Arabia.

depending on (1) the distances and the number of local stations that recorded the events, (2) the consistency and the number of *pP* readings, and finally (3) the azimuthal distribution of the teleseismic stations. The latitude and longitude of the hypocenters as reported by the ISS, ISC, and USGS are used for the selected events; however, we used the depths as obtained from *pP* readings if provided by the ISS, ISC, or USGS.

Of a total of about 5,700 events, only 1,700 events (about 30 percent) were selected for this study. A computer program was used in plotting the selected events on maps and cross sections. The sphericity of the Earth is shown on the sections, and all the sections are plotted without any vertical exaggeration.

GENERAL CHARACTERISTICS OF SEISMICITY

An outstanding and well-known feature of the spatial distribution of hypocenters along South America is the gap in seismic activity between depths of 320 and 525 km (Fig. 1). The deep earthquakes (deeper than 525 km) define two relatively narrow belts of activity, and the number of small-magnitude events relative to the number of large-magnitude events is very low (Joyehiro, 1968; Lomnitz, 1973).

The intermediate-depth activity tends to cluster in space. There is a peak in activity between depths of about 100 and 130 km; most of these events occur between about lat 17° and 24°S near the bend in the coastline between Peru and Chile. This is also the region that has lacked large shallow earthquakes for about the past 100 yr (Kelleher, 1972). The gap in seismic activity at intermediate depths between about lat 25.5°S and 27.0°S is evident; however, this region experienced many large shallow events (Santo, 1969).

SEGMENTATION OF INCLINED SEISMIC ZONE AND APPROXIMATE THICKNESS OF CONTINENTAL SOUTH AMERICAN PLATE

A careful examination of a large-scale map of the seismicity of South America shows that major regional differences exist in the spatial distribution of events with depths greater than about 70 km. It is important to find out how coherent the spatial distribution of events within any region is and whether a single transverse cross section can be made to include all the events within any region and still show a well-defined inclined seismic zone.

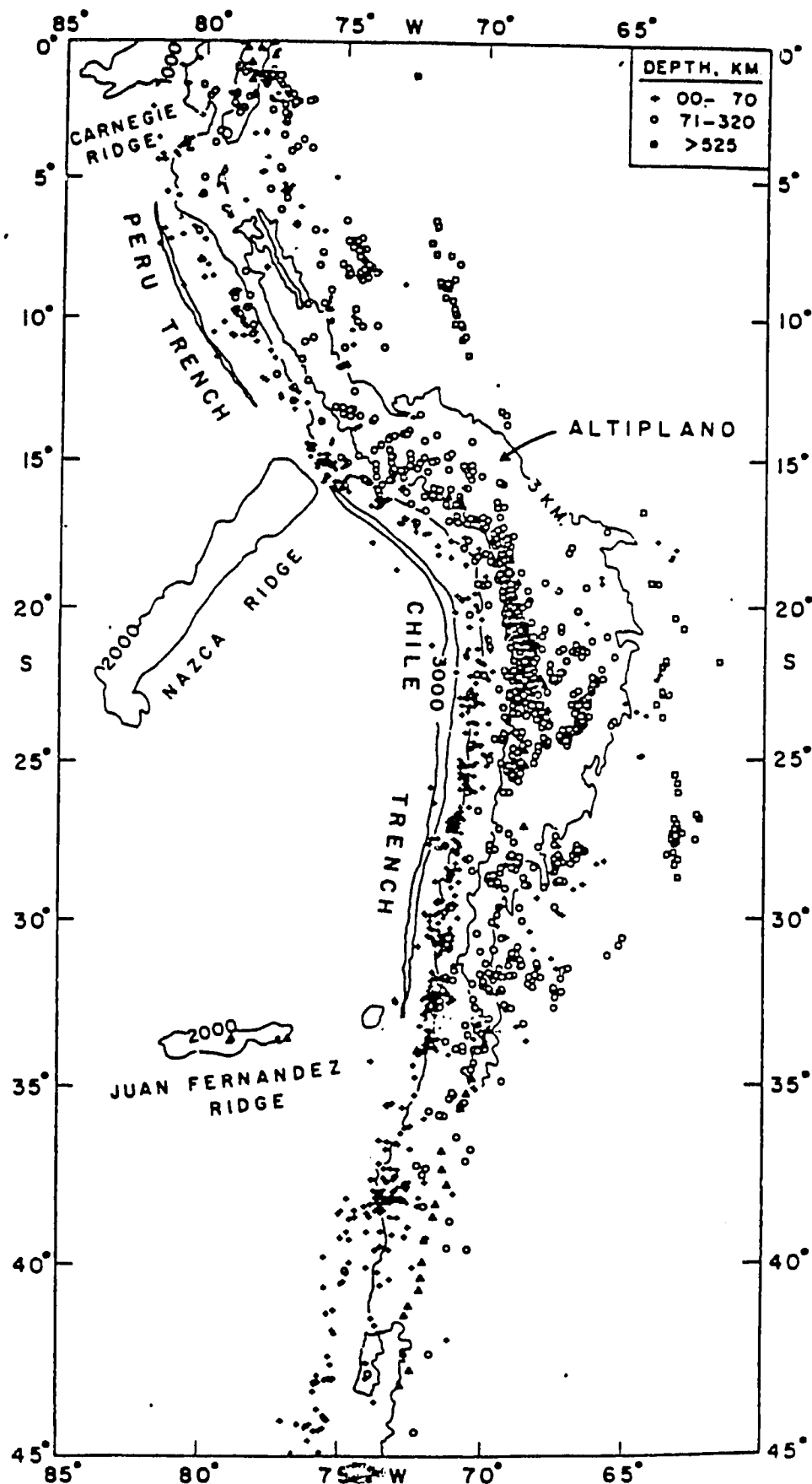


Figure 1. Seismicity map of South America. Bathymetry (in fathoms) from Mammerickx and others (1974). Historical volcanoes (solid triangles) from Casertano (1963), Richards (1962), and Hantke and Parodi (1966). Altiplano, a high plateau in central Andes, is approximately represented by a 3-km contour.

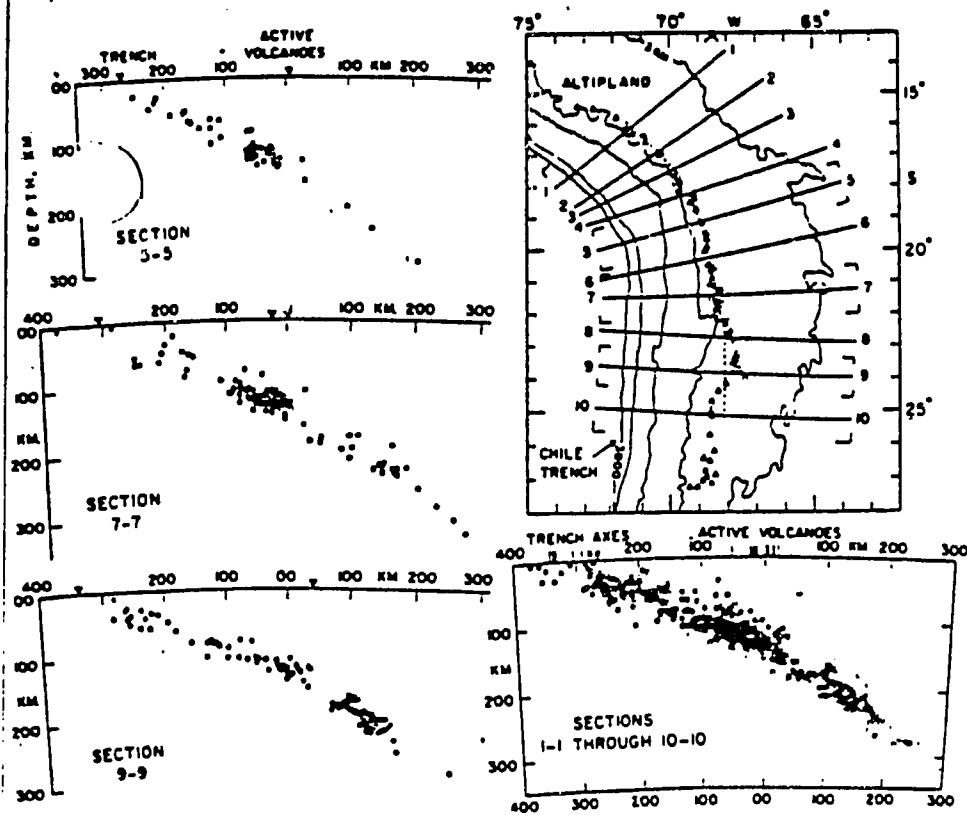


Figure 2. Map of southern Peru-northern Chile region, showing location of 10 cross sections superimposed to obtain composite section shown in lower right-hand corner. Projection of volcanoes and trench axes shown by vertical lines on composite section. Three representative sections are shown on left side. Solid triangles = historical volcanoes; open triangles = Quaternary volcanoes (from Bullard, 1964; Bullard, 1962).

I. The region of southern Peru and northern Chile (about lat 15° to 27°S) has the following characteristics: (1) A major bend in the Chile Trench and in the coastline occurs in this region. (2) The Quaternary volcanoes are well developed (Fig. 2). The volcanoes define a reasonably smooth curve (the volcanic line) in the northern part of the region, with variations that do not exceed about 20 km. However, near lat 22°S the volcanoes start to make a bend that deviates from the volcanic line by about 50 km. (3) The distance between the trench axis and the volcanoes varies from about 250 km in the north to a maximum of about 370 km near lat 24°S. An important question is whether the inclined seismic zone (which is taken to define the descending Nazca plate) beneath this region is reasonably coherent and can be represented by a single transverse cross section or whether abrupt segmentations of the inclined seismic zone are required (as suggested, for example, by Swift and Carr, 1974).

Ten transverse cross sections, each with a total width of about 100 km, were made for this region. The azimuths of the seismic sections are approximately perpendicular to the trench, the volcanic line, and the trend

of seismicity (Fig. 7). An important point is that the inclined seismic zone seems to have a thickness of about 30 km. This is not a result of the projection procedure; the "seismic thickness" is very clear on the large-scale map of hypocenters. This apparent thickness probably reflects fault zones within the descending plate (Isacks and Barrzangi, 1977). The 10 sections can be superimposed in a way that produces the least amount of scatter in the hypocenters, but at the same time does not have large scatter in the relative positions of the projected volcanoes and the trench axes (Fig. 2). If we choose the center position of the projected volcanoes to represent the zero position for the composite section, then it is clear that the location of this zero position on the map (dashed line in Fig. 2) very much coincides with the volcanoes except near the bend of the volcanoes between about lat 22° and 25°S. However, the seismic sections of events located beneath this bend do match very well with the rest of the sections and do not require any recognizable offset from the other sections.

Thus, the seismicity of the region of southern Peru and northern Chile can be represented by a single transverse compos-

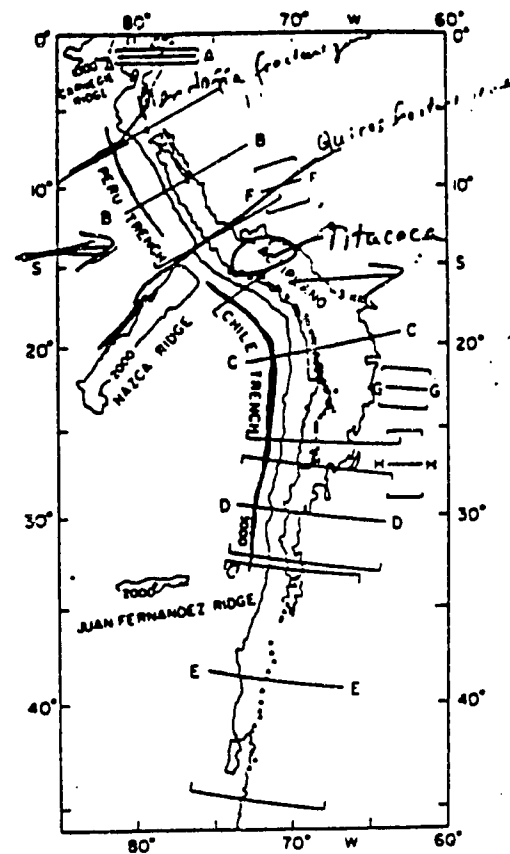


Figure 3. Map showing locations and limits of the cross sections that define five segments of inclined seismic zone (secs. A, B, C, D, E) as well as deep seismic zone (secs. F, G, H) (see Fig. 4). Symbols as in Figures 1 and 2.

ite cross section and still shows a well-defined inclined seismic zone. If we keep in mind the thickness of the seismic zone, then the data do not require any segmentation of the inclined seismic zone (and hence the descending Nazca plate) along the total length of this region. Furthermore, the volcanic line is a better reference for projecting seismic sections than the trench axis, and the variations in the distance between the trench axis and the volcanoes in this region may be a manifestation of accretionary phenomena (Karig and Sharman, 1975).

In the other regions, the projection of seismic cross sections is more straightforward, mainly because the geologic structure (trench, volcanoes, and coastline) and the seismicity trend are less complicated than those of the region discussed above. Tens of seismic cross sections were made for every region with different widths and azimuths to determine the final composite section for any particular region. The results are shown in Figure 3 and Figure 4, sections A through E. The transition from the type of spatial distribution of events in section A to that of B is reasonably well determined (see Figs. 3, 5); the transition from B to C is also well determined and

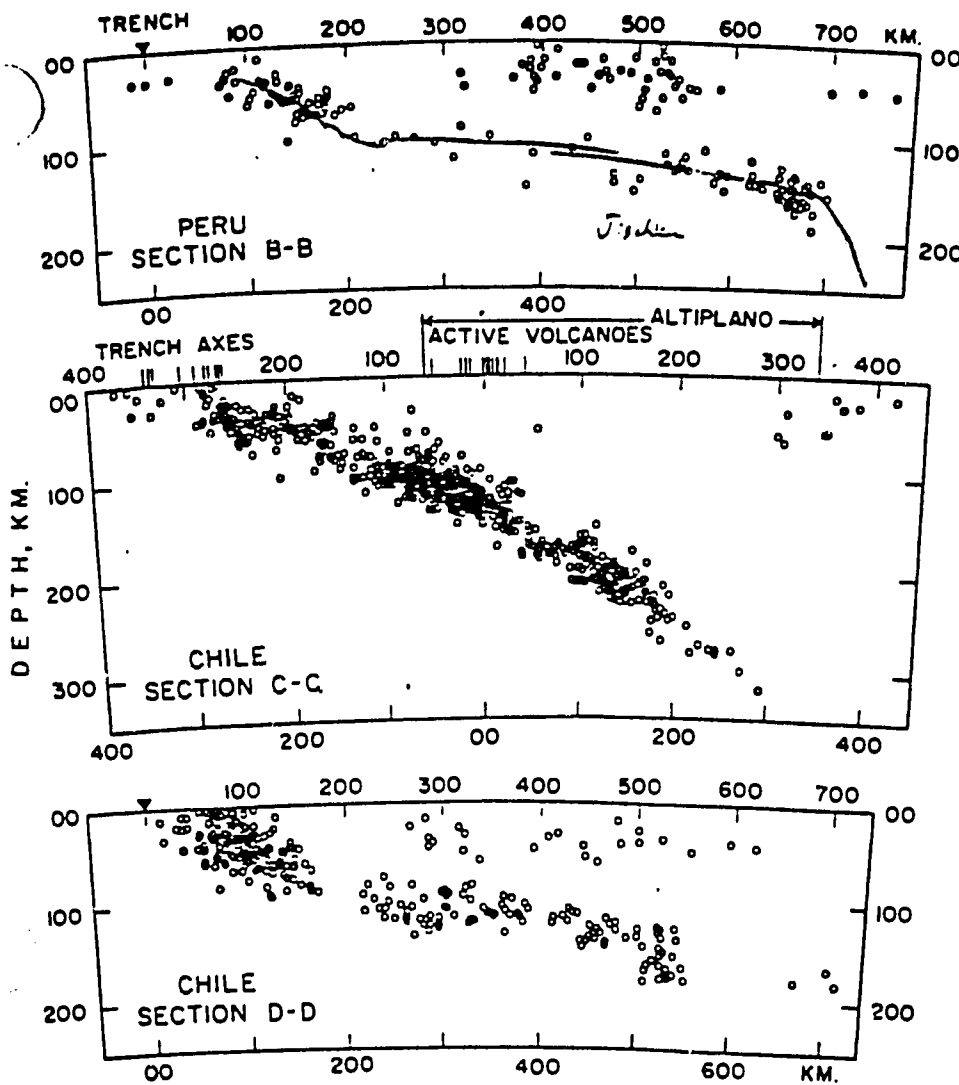


Figure 4. Cross sections showing segments of inclined seismic zone (A, B, C, D, E) and deep seismic zone (F, G, H). See Figure 3 for locations and limits of sections.

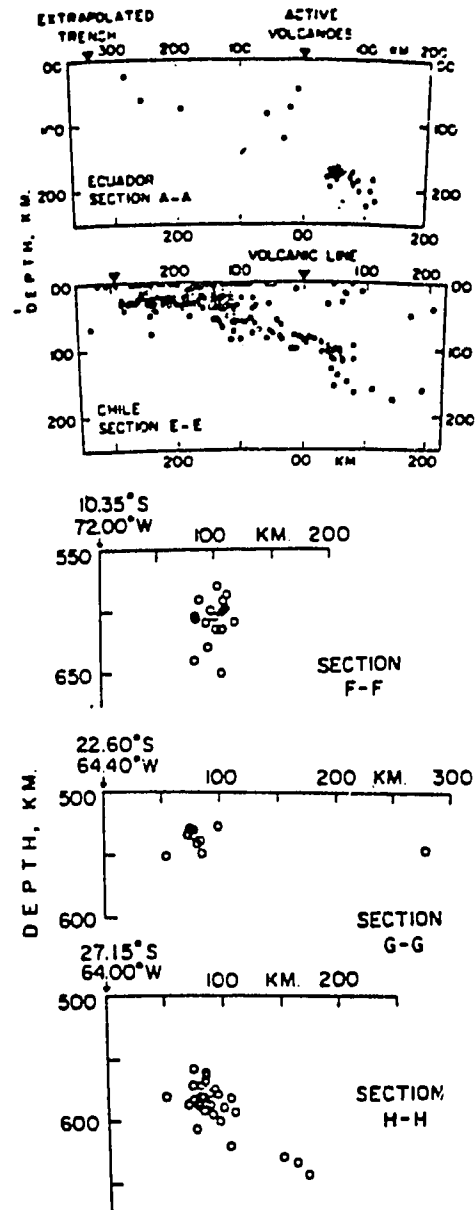
will be discussed in detail in a section below; the transition from C to D is poorly determined because of the lack of intermediate-depth events between about lat 25.5° and 27°S; and the transition from D to E is not well determined because of the scarcity of mantle events to the south of about lat 33°S.

Figure 4 shows that cross sections B and D are very similar. For both sections the dip of the inclined seismic zones is about 10°, and for both sections an upward bending of the zones (and hence the descending Nazca plate) near 80 km of depth is suggested by the data; both of these features are unique to South America (see Isacks and Barazangi, 1977). For section B, note that although the number of events at depths of about 100 km and distances of about 200 to 500 km from the Peru Trench are relatively few, the available data strongly suggest the continuity of the inclined seismic zone.

Figure 4 also shows that section C has an inclined seismic zone with a dip of about 25° to 30°, and that sections A and E appear to be similar to section C. Quaternary volcanoes are located in the South American plate above these three sections (A, C, and E). However, the depth to the seismic zones beneath the volcanoes is noticeably different from section C to section E: about 130 km for C and about 90 km for E.

In summary, five segments of inclined seismic zones are defined beneath the western margin of the South American plate. The available seismic data show no evidence for any further segmentation. It is also important to note that any mixing of data between sections B and C or sections C and D will produce a much thicker seismic zone and will give the false impression that seismic activity occurs in the wedge above the inclined seismic zone.

The two flat segments of the subducted



Nazca plate provide a unique opportunity to measure an approximate thickness of the continental South American plate along its western margin. If the flat segments are in contact with the lower boundary of the continental plate and since the intermediate-depth events associated with the two flat segments occur within the descending Nazca plate (Isacks and Molnar, 1971), then it is possible from geometrical considerations to obtain an estimate of the thickness of the overriding South American plate in these two regions of less than about 130 km (see Fig. 8). This result is in marked contrast to recent reports (for example, Jordan, 1975) of thicknesses exceeding 400 km for continental plates.

The widths and the azimuths of the cross sections of deep earthquake zones (Fig. 4, secs. F, G, H) were chosen to produce the least scatter in the seismic zones. Section F (western Brazil) shows a vertical seismic zone about 80 km long, section H

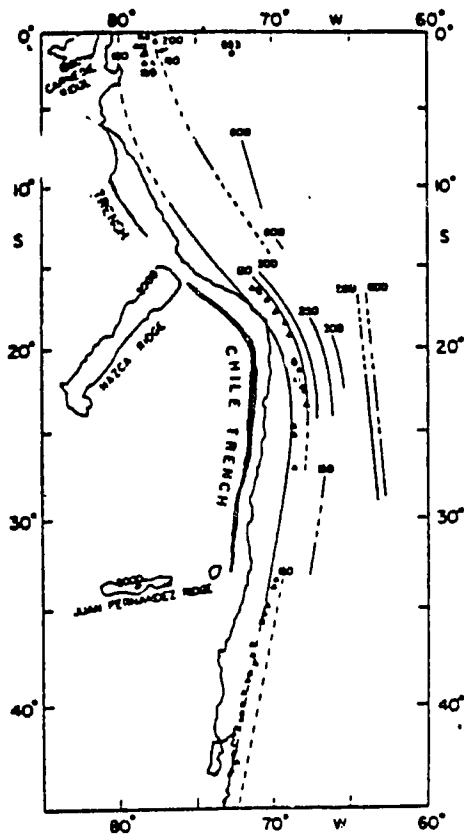


Figure 5. Map showing contours of hypocentral depth to top of inclined seismic zone. Dashed lines indicate that contours are based on fewer data than those shown by solid lines.

(western Argentina) shows a dipping (about 40°) inclined seismic zone about 130 km long, and the events in section G (western Argentina) do not define a clear pattern. Note that the spatial distribution of deep earthquakes overlaps with that of the different segments of the inclined seismic zones at intermediate depths (Figs. 1, 5). Whether the descending Nazca plate is continuous across the gap in seismic activity between 320 and 525 km is not clear. We have suggested (Isacks and Barazangi, 1973) the continuity of the plate for the deep events in western Argentina. However, Snoke and others (1974) showed that our results do not require the continuity of the descending plate.

CORRELATION OF DIP OF DESCENDING NAZCA PLATE WITH VOLCANOES

There is a remarkable correlation between the two flat segments of the inclined seismic zones (secs. B and D, Fig. 4) and the absence of Quaternary volcanoes on the overriding South American plate (Fig. 5). The descending Nazca plate beneath these two regions has a small dip and may follow the trend of the lower boundary of the South American plate. This could leave

little or no room for asthenospheric material between the overriding and descending plates. This may explain the absence of volcanism as well as the observed absence of high attenuation of seismic waves in the uppermost mantle beneath these two regions (Molnar and Oliver, 1969; Barazangi and others, 1975; Chinn and others, 1976). In effect, the continental South American plate and the oceanic Nazca plate form a double thickness of lithosphere (Sykes, 1972; Barazangi and others, 1975; Stauder, 1975) of about 200 km; such thickness is in approximate agreement with the results of Sacks and Okada (1974).

In the other three regions where the inclined seismic zones have a steeper dip (25° to 30°), Quaternary volcanism is well developed (Figs. 3, 4, 5). A wedge of asthenospheric material appears to separate the descending Nazca plate from the overriding South American plate. The existence of asthenospheric material seems to be a requirement for the development of active volcanism. The Altiplano, a high plateau in the Andes, closely coincides with the southern Peru-northern Chile region, and an asthenospheric material of extremely high attenuation exists above the inclined seismic zone and beneath most of the Altiplano (Barazangi and others, 1975; Chinn and others, 1976). However, for the Ecuador and southern Chile regions, the nature of the asthenospheric wedge is currently under study (Chinn and others, 1976).

MAJOR TEAR IN DESCENDING NAZCA PLATE

Fortunately, enough data are available to study in some detail the nature of the transition between the gently dipping Peru segment and the more steeply dipping zone beneath southern Peru and northern Chile. The seismicity map in Figure 6 shows that at about the same distance from the trench, events with depths of about 200 km in southern Peru are located adjacent to events with depths of only about 100 km (see also Fig. 5). This indicates that the descending Nazca plate, as defined by these mantle events, has an abrupt vertical offset. The two cross sections shown in Figure 6 clearly illustrate the geometry in this region. The transverse cross sections show that the inclined seismic zone of central Peru coincides with that of southern Peru at depths less than about 100 km. At greater depths, the central Peru zone remains flat at a constant depth of about 100 km, whereas the southern Peru zone has a steeper dip and reaches depths of

about 240 km. The longitudinal section also shows the relative sharpness of the transition between the two regions.

The location of the inferred tear in the descending plate is near the northern end of the volcanic line; two Quaternary volcanoes are located about 50 and 100 km northwest of the tear. The inland projection of the aseismic oceanic Nazca ridge beneath the South American plate is located about 200 km northwest of the tear, as are the northern limits of the Altiplano. The exact extent of the northern limits of the high-attenuation zone that exists beneath the Altiplano is not yet determined and is currently under study. There thus may be some genetic relationship between all of the above features and the tear. The Nazca ridge may represent a dormant transform fault (Anderson and others, 1976), and hence it is a major zone of weakness in the descending Nazca plate along which the plate may tear. Although the location of the tear is offset from the offshore location of the Nazca ridge, it is tempting to speculate that the ridge had an offset along its trend. Moreover, it is possible that the tear in the descending Nazca plate affects the asthenospheric material adjacent to it and hence contributes to the formation of the high-attenuation zone and the uplifted plateau of the Altiplano.

Another remarkable correlation also seems to exist between the location of the oceanic Juan Fernandez ridge and the transition from the Chilean flat seismic zone (between about lat 27° and 33°S) to the steeper seismic zone in southern Chile (Figs. 1, 5). Active volcanoes are located on the Juan Fernandez ridge. The ridge intersects the Chilean coastline near lat 33°S, where the coastline has a major bend and where the trench becomes increasingly sediment filled. Moreover, the inland projection of the ridge beneath the South American plate closely coincides with the northern limit of the active volcanoes of southern Chile as well as with the end of the Central Valley of Chile (see also Sillitoe, 1974; Vogt and others, 1976). In this case, it is tempting to suggest that the Juan Fernandez ridge forms a zone of weakness in the Nazca plate along which the plate tears as it descends beneath the South American plate.

SHALLOW SEISMIC ACTIVITY WITHIN CONTINENTAL SOUTH AMERICAN PLATE

The shallow seismic zone within the overriding South American plate is proba-

bly the most active of all subduction zones on Earth. Figures 1 and 4 show that most of the activity occurs within the upper 100 km of the South American plate, and most of it takes place between depths of about 30 and 50 km. These depths are within the South American crustal thickness as reported, for example, by James (1971) and Ocola and Meyer (1972). As Figure 4 shows, the shallow seismic activity is separated from the well-defined inclined seismic zones. Thus, there is no evidence for any seismic activity within the mantle part of the South American plate.

A striking observation is that although the shallow seismic activity is relatively dispersed, most of the activity is near the eastern flanks (sub-Andean zone) of the Andes regardless of the distance of the sub-Andean zone from the trench (Figs. 1, 4). Moreover, it appears that most of the large events are located above the two shallow-dipping seismic zones (secs. B and D, Fig. 4). This could be the result of the strong interaction between the South American plate and the descending Nazca plate in these two regions. The observed high compressive stresses in the Peru region (Stauder, 1975) could contribute to the lack of volcanism in the region (Sykes, 1972).

LINEAR FEATURES IN SPATIAL DISTRIBUTION OF CHILEAN INTERMEDIATE EARTHQUAKES

The distribution of intermediate earthquakes in South America tends to cluster in space. A strikingly linear distribution of events occurs between about lat 17° and 23°S and has a trend of about N18°W, and most of the events are between 110 and 130 km deep (Fig. 7). In fact, at a closer look, this linear feature seems to be formed of two approximately parallel linear features. Figure 7 also shows the compression, tension, and null axes of seven focal mechanisms obtained by Isacks and Molnar (1971) and Stauder (1973) for events located along the linear feature. Isacks and Molnar and Stauder interpreted these mechanisms to indicate extensional stresses parallel to the inclined seismic zone. In each case, one of the nodal planes of these mechanisms closely coincides with the trend of the linear feature, and hence these planes could possibly represent fault planes (Fig. 7). Failure accompanied by these large intermediate events could occur along a zone of weakness associated with the linear feature within the subducted Nazca plate. Moreover, the linearity and continuity of the spatial distribution of events within the linear feature is evidence

that there is no segmentation of the inclined seismic zone in this region.

Two other clusters of activity are shown in Figure 7. Both have an approximate strike of northeast-southwest, and both represent linear pencil-shaped zones that dip obliquely to the overall dip of the inclined seismic zone. The first cluster begins near lat 24.5°S, long 67°W with events of about 170-km depth and ends toward the northeast with events of about 220-km depth. Note that this linear activity is approximately parallel to the contorted part of the volcanic line in central Chile (Figs. 2, 7). The second cluster begins near the end of the first one at about 200-km depth and ends at about 270-km depth. Again, these two dipping "lines" of activity may represent relatively narrow zones of weakness within the descending Nazca plate.

SUMMARY

The data presented show that the oceanic Nazca plate is divided into five distinct segments as it descends beneath the continental South American plate. Two of the segments (one beneath central and northern Peru and the other beneath central Chile between lat 27° and 33°S) are relatively flat and may follow the contours of the lower boundary of the South American plate, with little or no asthenospheric material in between them. The regions above these two segments are characterized by the lack of Quaternary volcanism (Fig. 8). The other three segments (beneath Ecuador, beneath southern

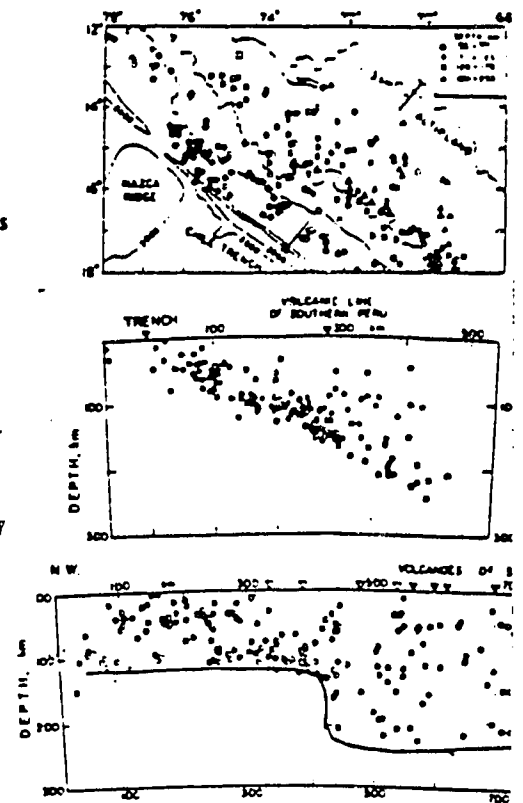


Figure 6. Map view, cross section, and longitudinal section of distribution of earthquakes in southern Peru and northern Chile, showing abrupt increase in hypocenter depth in passing from flat Peru segment to more steeply dipping northern Chile segment. Filled and open circles in middle cross section are for events to northwest and southeast, respectively, of line indicated in map view. Longitudinal section is perpendicular to that line. Solid triangles = historical volcanoes; large open triangles (and divided triangles in map view) = Quaternary volcanoes.

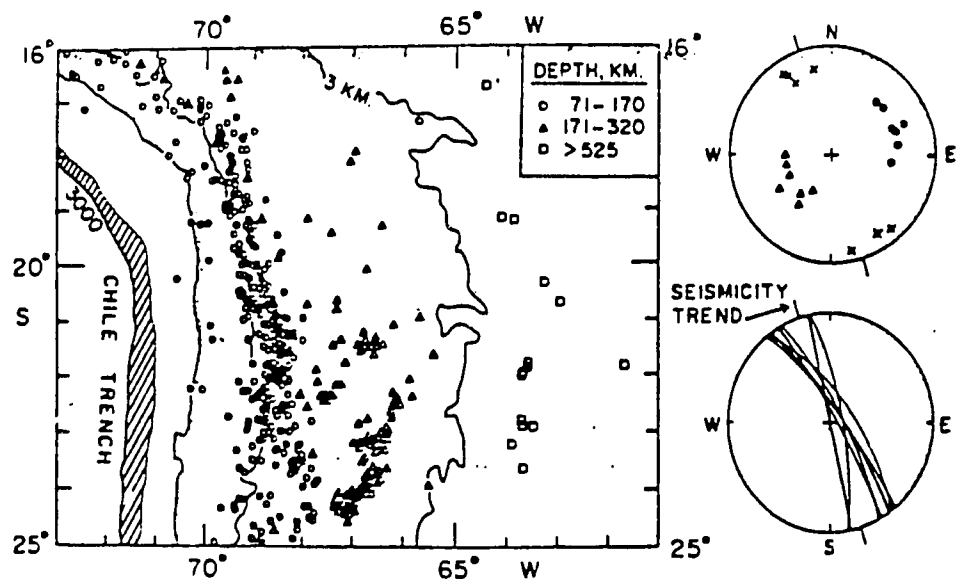


Figure 7. Seismicity map of northern Chile, showing earthquakes deeper than 70 km. Equal-area projection (upper right) of lower hemisphere of a focal sphere shows compression axes (open triangles), tension axes (open circles), and null axes (crosses) of seven focal mechanisms of intermediate-depth events (filled circles on map). Focal plot (lower right) shows one of the nodal planes for each of the seven focal mechanisms.

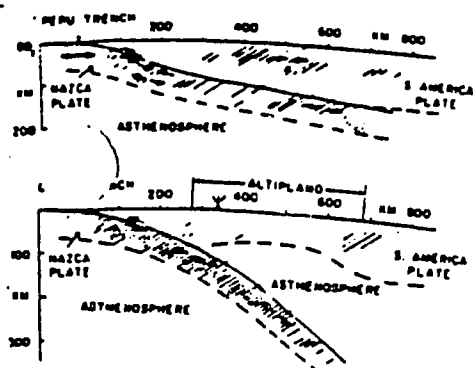


Figure 8. Two cross sections showing inferred geometries of descending Nazca plate and continental South American plate in central Peru and in northern Chile. Inclined thin lines schematically represent distribution of hypocenters. Results obtained from focal-mechanism data by Isacks and Molnar (1971), Stauder (1973, 1975), and Isacks and Barazangi (1977) indicate thrusting of Nazca plate beneath South America (thin arrows), downdip compression or tension within descending Nazca plate, horizontal tension beneath trench, and horizontal compression within South American plate (heavy arrows). Thickness of South American plate to east of Altiplano in Chile is taken to be same as that found in Peru.

Peru-northern Chile, and beneath southern Chile) are steeper (25° to 30°) than the two flat segments, and asthenospheric material appears to separate them from the overriding South American plate. The regions along these three segments have abundant active volcanism. The transition from the flat Peru segment to the steeper segment to the south occurs along a major tear in the descending Nazca plate. A thickness of less than about 130 km is estimated for the continental South American plate along its western margin.

Recently, Jischke (1975) proposed a model for the dynamics of the descending plates that may be applicable, in particular, to the South American arc. He argued that if the region between the descending and overriding plates is narrow and varies with depth, hydrodynamic forces arise that can balance the gravitational forces acting on the descending plate, and hence the plate will have a tendency to adhere to the lower boundary of the overriding plate. The geometry of the two flat segments of the descending Nazca plate in Peru and Chile can be explained by Jischke's model.

Although there has been no volcanism in central and northern Peru during Quaternary time, the region had considerable volcanism during Miocene and Pliocene time (Gilotti and Day, 1968; Noble and Chinn, 1974). If the lack of active volcanism is directly related to the flat geometry of the descending Nazca plate beneath the region, then we infer that the present-

day geometry is not a steady-state process and that the descending plate must have had a steeper dip during Pliocene time (that is, similar probably to the present situation in northern Chile). One can speculate that in the future the gravitational forces acting on the flat segment of Peru will overcome the hydrodynamic forces that are holding the plate flat, leading to the separation of the descending Nazca plate from the South American plate and the flow of asthenospheric material into the wedge between the two plates. This would result in an episode of volcanism. It is possible that the present geometry of plates in northern Chile is a result of such a mechanism.

REFERENCES CITED

- Anderson, R., Langseth, M., Vacquier, V., and Francheteau, J., 1976. New terrestrial heat flow measurements on the Nazca plate: *Earth and Planetary Sci. Letters*, v. 29, p. 243-254.
- Barazangi, M., Pennington, W., and Isacks, B., 1975. Global study of seismic wave attenuation in the upper mantle behind island arcs using pP waves: *Jour. Geophys. Research*, v. 80, p. 1079-1092.
- Bullard, F., 1962. Volcanoes of southern Peru: *Bull. Volcanol.*, v. 24, p. 443-453.
- Casertano, L., 1963. Catalogue of the active volcanoes of the world. Pt. XV, Chilean continent: Rome, Internat. Assoc. Volcanology, Editing Office, *Ist. Geologia Applicata*, 55 p.
- Chinn, D., Isacks, B., and Barazangi, M., 1976. Tectonic features of western South America inferred from variations in travel times and attenuation of the seismic phases S_n and L_g : *EOS (Am. Geophys. Union Trans.)*, v. 57, p. 334.
- Gilotti, B., and Day, H., 1968. Potassium-argon ages of igneous intrusive rocks in Peru: *Nature*, v. 220, p. 570-572.
- Hantke, G., and Parodi, A., 1966. Catalogue of the active volcanoes of the world. Pt. XIX, Colombia, Ecuador and Peru: Rome, Internat. Assoc. Volcanology, Editing Office, *Ist. Geologia Applicata*, 73 p.
- Isacks, B., and Barazangi, M., 1973. High frequency shear waves guided by a continuous lithosphere descending beneath western South America: *Royal Astron. Soc. Geophys. Jour.*, v. 77, p. 129-139.
- , 1977. Geometry of Benioff zones: Lateral segmentation and downwards bending of the subducted lithosphere, in *Proceedings of Ewing symposium: Am. Geophys. Union Geophys. Mon. (in press)*.
- Isacks, B., and Molnar, P., 1971. Distribution of stresses in the descending lithosphere from a global survey of focal mechanism solutions of mantle earthquakes: *Rev. Geophysics and Space Physics*, v. 9, p. 103-174.
- James, D., 1971. Plate tectonic model for the evolution of the central Andes: *Geol. Soc. America Bull.*, v. 82, p. 3325-3346.
- Jischke, M., 1975. On the dynamics of descending lithospheric plates and slip zones: *Jour. Geophys. Research*, v. 80, p. 4809-4813.
- Jordan, T., 1975. The continental tectosphere: *Rev. Geophysics and Space Physics*, v. 13, p. 1-12.
- Karig, D., and Sharman, G., 1975. Subduction and accretion in trenches: *Geol. Soc. America Bull.*, v. 86, p. 377-389.
- Kelleher, J., 1972. Rupture zones of large South American earthquakes and some predictions: *Jour. Geophys. Research*, v. 77, p. 2087-2103.
- Lomnitz, C., 1973. A statistical argument for the existence of a discontinuity in some subduction zones: *Jour. Geophys. Research*, v. 78, p. 2612-2615.
- Mammerickx, J., Smith, S., Taylor, I., and Chase, F., 1974. Bathymetry of the South Pacific: Charts 15 and 21: Scripps Inst. Oceanography Tech. Repts. 48A, 54A.
- Molnar, P., and Oliver, J., 1969. Lateral variations of attenuation in the upper mantle and discontinuities in the lithosphere: *Jour. Geophys. Research*, v. 74, p. 2648-2682.
- Noble, D., McKee, E., Farrar, E., and Petersen, U., 1974. Episodic Cenozoic volcanism and tectonism in the Andes of Peru: *Earth and Planetary Sci. Letters*, v. 21, p. 213-220.
- Ocola, L., and Meyer, R., 1972. Crustal low-velocity zones under the Peru-Bolivia Altiplano: *Royal Astron. Soc. Geophys. Jour.*, v. 30, p. 199-209.
- Richards, A. F., 1962. Catalogue of the active volcanoes of the world. Pt. XIV, Islas Juan Fernandez: Rome, Internat. Assoc. Volcanology, Editing Office, *Ist. Geologia Applicata*, 50 p.
- Sacks, S., and Okada, H., 1974. A comparison of the anelasticity structure beneath western South America and Japan: *Physics Earth and Planetary Interiors*, v. 9, p. 211-219.
- Santo, T., 1969. Characteristics of seismicity in South America: Tokyo Univ. Earthquake Research Inst. Bull., v. 47, p. 635-672.
- Sillitoe, R., 1974. Tectonic segmentation of the Andes: Implications for magmatism and metallogeny: *Nature*, v. 250, p. 542-545.
- Snoke, A., Sacks, S., and Okada, H., 1974. A model not requiring continuous lithosphere for anomalous high frequency arrivals from deep focus South American earthquakes: *Physics Earth and Planetary Interiors*, v. 9, p. 199-206.
- Stauder, W., 1973. Mechanism and spatial distribution of Chilean earthquakes with relation to subduction of the oceanic plate: *Jour. Geophys. Research*, v. 78, p. 5033-5061.
- , 1975. Subduction of the Nazca plate under Peru as evidenced by focal mechanisms and by seismicity: *Jour. Geophys. Research*, v. 80, p. 1053-1064.
- Suyehiro, S., 1968. A search for small, deep earthquakes in the Andes: *Carnegie Inst. Washington Year Book* 66, p. 35-36.
- Swift, S., and Carr, M., 1974. The segmented nature of the Chilean seismic zone: *Physics Earth and Planetary Interiors*, v. 9, p. 183-191.
- Sykes, L. R., 1972. Seismicity as a guide to global tectonics and earthquake prediction: *Tectonophysics*, v. 13, p. 393-414.
- Sykes, L., and Hayes, D., 1971. Seismicity and tectonics of South American and adjacent oceanic areas: *Geol. Soc. America Abs. with Programs*, v. 3, p. 206.
- Vogt, P., Lowrie, A., Bracey, D., and Hey, R., 1976. Subduction of aseismic oceanic ridges: Effects on shape, seismicity, and other characteristics of consuming plate boundaries: *Geol. Soc. America Spec. Paper* 172, 59 p.
- Zeil, W., 1964. *Geologie von Chile*: Berlin, Gebruder Borntraeger, 210 p.

ACKNOWLEDGMENTS

Reviewed by Jack Oliver.
Supported by National Science Foundation Grants DES75-14815 and DES74-03647.
We thank G. Cole, D. Chinn, J. Ni, S. Billington, and N. Fitzpatrick for assistance on different aspects of the paper.

MANUSCRIPT RECEIVED JULY 6, 1976
MANUSCRIPT ACCEPTED AUG. 17, 1976

The Energy Release in Great Earthquakes

HIROO KANAMORI

Seismological Laboratory, California Institute of Technology, Pasadena, California 91125

The conventional magnitude scale M suffers saturation when the rupture dimension of the earthquake exceeds the wavelength of the seismic waves used for the magnitude determination (usually 5–50 km). This saturation leads to an inaccurate estimate of energy released in great earthquakes. To circumvent this problem the strain energy drop W (difference in strain energy before and after an earthquake) in great earthquakes is estimated from the seismic moment M_0 . If the stress drop $\Delta\sigma$ is complete, $W = W_0 = (\Delta\sigma/2\mu)M_0 \sim M_0/(2 \times 10^4)$, where μ is the rigidity; if it is partial, W_0 gives the minimum estimate of the strain energy drop. Furthermore, if Orowan's condition, i.e., that frictional stress equal final stress, is met, W_0 represents the seismic wave energy. A new magnitude scale M_w is defined in terms of W_0 through the standard energy-magnitude relation $\log W_0 = 1.5M_w + 11.8$. M_w is as large as 9.5 for the 1960 Chilean earthquake and connects smoothly to M_s (surface wave magnitude) for earthquakes with a rupture dimension of about 100 km or less. The M_w scale does not suffer saturation and is a more adequate magnitude scale for great earthquakes. The seismic energy release curve defined by W_0 is entirely different from that previously estimated from M_s . During the 15-year period from 1950 to 1965 the annual average of W_0 is more than 1 order of magnitude larger than that during the periods from 1920 to 1950 and from 1965 to 1976. The temporal variation of the amplitude of the Chandler wobble correlates very well with the variation of W_0 , with a slight indication of the former preceding the latter. In contrast, the number N of moderate to large earthquakes increased very sharply as the Chandler wobble amplitude increased but decreased very sharply during the period from 1945 to 1965, when W_0 was largest. One possible explanation for these correlations is that the increase in the wobble amplitude triggers worldwide seismic activity and accelerates plate motion which eventually leads to great decoupling earthquakes. This decoupling causes the decline of moderate to large earthquake activity. Changes in the rotation rate of the earth may be an important element in this mechanism.

INTRODUCTION

The energy release in earthquakes is one of the most fundamental subjects in geophysics. In most cases the amount of energy E released in seismic waves is estimated from the earthquake magnitude M through the magnitude-energy relation $\log E = 1.5M + 11.8$ developed by Gutenberg and Richter [Gutenberg, 1956a]. While this relation was very carefully calibrated through repeated revisions and is considered to give a reasonably accurate estimate of seismic wave energy for most earthquakes, the validity of this relation is questionable for great earthquakes. Here great earthquakes are those with a very large, 100 km or greater, rupture length. This arises from the fact that for such a great earthquake the magnitude M which is determined at the period of 20 s (or converted from m (body wave magnitude) determined at shorter periods) does not represent the entire rupture process of an earthquake. In fact, there is little correlation between M and the rupture length for great earthquakes. Thus the energy E estimated from M is very uncertain for great earthquakes. Yet it is such great earthquakes that contribute most to the seismic energy budget. In order to circumvent this difficulty we estimate in this paper the energy involved in great earthquakes on the basis of static source parameters such as the seismic moment and the area of the fault plane. Since the absolute level of stress involved in faulting is unknown, it is not possible to determine the change in the strain energy before and after an earthquake. However, it is possible to estimate the minimum strain energy drop which, under reasonable conditions, approximates the seismic wave energy. Since the static source parameters are very accurately determined for many great earthquakes, this method gives accurate estimates of energy for great earthquakes, which have the greatest contribution to the seismic energy budget. It is hoped that this method provides a more

meaningful basis for various studies pertaining to global processes such as heat flow, Chandler wobble, and plate motions.

COMPILATION OF SEISMIC MOMENTS OF GREAT EARTHQUAKES

The seismic moment M_0 , which is defined by μDS (μ is the rigidity; D is the average offset on the fault; and S is the area of the fault), is one of the most accurately determined seismic source parameters. For many great earthquakes, M_0 has been determined by using long-period body waves, surface waves, free oscillations, and geodetic data. A partial list is found in the work by Kanamori and Anderson [1975b]. For earthquakes for which no direct determination of M_0 has been made, we estimate it from the area of the fault plane S and/or the 100-s magnitude determined by Brune and Engen [1969].

A remarkable linearity between $\log M_0$ and $\log S$ has been noted by Aki [1972], Thatcher and Hanks [1973], Kanamori and

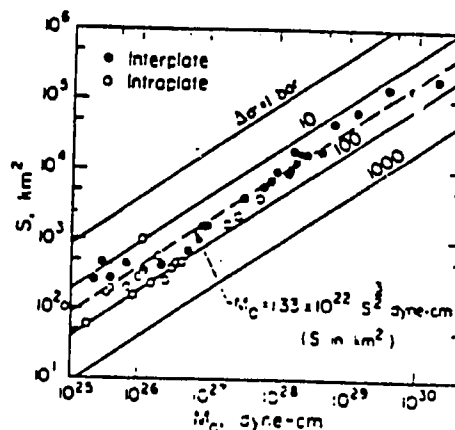


Fig. 1. The relation between the fault area and the seismic moment — 775 — (modified from Kanamori and Anderson [1975b]). The dashed line gives the average M_0 versus S relation suggested by Abe [1975a].

TABLE 1. Great Earthquakes

Date	Region	M_s	M_w , 10^{27} dyn cm	M_w	Source for M_s Value*
June 25, 1904	Kamchatka	8.0			
June 25, 1904	Kamchatka	8.1			
April 4, 1905	East Kashmir	8.0			
July 9, 1905	Mongolia	8.1	50	8.4	Okal [1977].
July 23, 1905	Mongolia	8.1	50	8.4	Okal [1977].
Jan. 31, 1906	Ecuador	8.6	204	8.8	From the aftershock area.
* April 18, 1906	San Francisco	8.1	10	7.9	Estimated from fault length of 500 km, width of 15 km, and dislocation of 5 m.
* Aug. 17, 1906	Rat Islands	8.0			
* Aug. 17, 1906	Central Chile	8.4	29	8.2	From the aftershock area.
* Sept. 14, 1906	New Britain	8.1			
April 15, 1907	Mexico	8.1			
Oct. 21, 1907	Afghanistan	8.0			
Jan. 3, 1911	Turkestan	8.4	4.9	7.7	Chen and Molnar [1977].
May 23, 1912	Burma	8.0			
* May 1, 1917	Kermadec	8.0			
* June 26, 1917	Samoa	8.3			
* Aug. 15, 1918	Mindanao	8.1			
* Sept. 7, 1918	Kurile	8.1			
* April 30, 1919	Tonga	8.3			
* June 5, 1920	Taiwan	8			
* Sept. 20, 1920	Loyalty Islands	8			
Dec. 16, 1920	Kansu, China	8.5	6.6	7.8	Chen and Molnar [1977].
* Nov. 11, 1922	Central Chile	8.3	69	8.5	From the aftershock area.
* Feb. 3, 1923	Kamchatka	8.3	37	8.3	From the aftershock area.
* Sept. 1, 1923	Kanto	8.2	8.5	7.9	
* April 14, 1924	Philippine	8.3			
May 22, 1927	Tsinghai, China	8.0	3.0	7.6	Chen and Molnar [1977].
* June 17, 1928	Guerrero, Mexico	7.8	12	8.0	From the aftershock area.
* Dec. 1, 1928	Central Chile	8.0	3	7.6	From the aftershock area.
* March 7, 1929	Fox Islands (Aleutian)	8.1	6.7	7.8	Kanamori [1972b].
Aug. 10, 1931	Sinkiang, China	8.0	12	8.0	Chen and Molnar [1977].
* May 14, 1932	Molucca	8.0	1.5	7.4	From the 100-s magnitude.
* June 3, 1932	Jalisco, Mexico	8.1	15	8.1	Average of value from the aftershock area and value from the 100-s magnitude.
* March 2, 1933	Sanriku	8.5	43	8.4	
Jan. 15, 1934	India-Nepal	8.3	16	8.1	Chen and Molnar [1977].
July 18, 1934	Santa Cruz Islands	8.2	0.8	7.2	From the 100-s magnitude based on one station.
* Feb. 1, 1938	Banda Sea	8.2	70	8.5	From the 100-s magnitude.
* Nov. 10, 1938	Alaska	8.3	28	8.2	Average of value from the aftershock area and value from the 100-s magnitude.
* April 30, 1939	Solomon Islands	8.0			
Dec. 26, 1939	Turkey	8.0			
* May 24, 1940	Peru	8.0	25	8.2	From the aftershock area.
June 26, 1941	Andaman Islands	8.1	3	7.6	From the 100-s magnitude.
Nov. 25, 1941	North Atlantic	8.3			
* Aug. 24, 1942	Peru	8.1	27	8.2	From the aftershock area.
April 6, 1943	Chile	7.9	28	8.2	From the aftershock area.
* Dec. 7, 1944	Tonankai	8.0	15	8.1	
* Nov. 27, 1945	West Pakistan	8.1			
Aug. 4, 1946	Dominican Republic	8.1			
* Dec. 20, 1946	Nankaido	8.2	15	8.1	
Jan. 24, 1948	Philippine	8.2			
* Aug. 22, 1949	Alaska	8.1	15	8.1	From the aftershock area.
Aug. 15, 1950	Assam	8.6	100	8.6	Average of values from Ben-Menahem et al. [1974], Chen and Molnar [1977], and G. S. Stewart (personal communication, 1977).
Nov. 18, 1951	Tibet	8.0	1.9	7.5	Chen and Molnar [1977].
* March 4, 1952	Tokachi-oki	8.3	17	8.1	
* Nov. 4, 1952	Kamchatka	8.1	350	9.0	Kanamori [1976b].
* March 9, 1957	Aleutian Islands	8.1	585	9.1	From the aftershock area.
Dec. 4, 1957	Mongolia	8.3	18	8.1	Okal [1976].
* July 10, 1958	Alaska	7.9	29	8.2	From the aftershock area.
* Nov. 6, 1958	Kurile Islands	8.7	40	8.3	Y. Fukao (personal communication, 1977).
* May 4, 1959	Kamchatka	8.1	26	8.2	From the aftershock area.
* May 22, 1960	Chile	8.3	2000	9.5	
* Oct. 13, 1963	Kurile Islands	8.1	67	8.5	
* March 25, 1964	Alaska	8.4	820	9.2	
Feb. 4, 1965	Aleutian Islands	7.1	125	8.7	
Oct. 17, 1966	Peru	7.5	20	8.1	
* May 16, 1968	Tokachi-oki	7.9	28	8.2	
Feb. 28, 1969	North Atlantic	8.0	6	7.8	
* Aug. 11, 1969	Kurile Islands	7.8	22	8.2	

TABLE 1. (continued)

Date	Region	M_s	$M_0, 10^{21}$ dyn cm	M_w	Source for M_0 Value*
May 31, 1970	Peru	7.8	10	7.9	
Jan. 10, 1971	West New Guinea	8.1			
Oct. 3, 1974	Peru	7.6	15	8.1	G. S. Stewart (personal communication, 1977).
May 26, 1975	North Atlantic	7.9	5	7.7	Hadley and Kanamori [1975].
July 27, 1976	China	8.0	2	7.5	Revised from Stewart et al. [1976].
Aug. 16, 1976	Mindanao	8.2	19	8.1	G. S. Stewart (personal communication, 1977).

The values of M_0 not referenced are taken from Table 1 of Kanamori and Anderson [1975b].

Anderson [1975b], Abe [1975a], and Geller [1976]. This linearity is interpreted in terms of constant average stress drop in earthquakes [Chinnery, 1964]. Figure 1 demonstrates this linearity for large and great earthquakes. Abe [1975a] and Geller and Kanamori [1977] suggest a relation

$$M_0 = 1.23 \times 10^{22} S^{1.75} \text{ dyn cm}$$

where S is in square kilometers, to represent the overall relation between S and M_0 . In many cases the aftershock area defined at a relatively early stage of the aftershock sequence, usually 1 day after the main shock, is used for S . This procedure involves some ambiguity but is adequate for the present purpose. Utsu and Seki [1954], Fedotov [1965], Mogi [1968a, b], Sykes [1971], Kelleher [1972], and Kelleher et al. [1973] mapped aftershock areas and rupture zones of many large and great earthquakes, including those for which no direct determination of M_0 has been made. We estimate M_0 of these earthquakes by using (1) and the size of the rupture zones determined by these authors. Although not very essential, one adjustment is made. The rupture zones determined by these authors are based on the aftershock area at a relatively later stage, usually several months, after the main shock, while S used in (1) is determined from the aftershock area at a relatively early stage, usually 1 day. Comparison between these two sets of data suggests that the former is, on the average, 75% larger than the latter. Therefore in using (1) we divided the size of the published rupture zones by 1.75. The results of moment determinations by this method are listed in Table 1.

Brune and Engen [1969] determined 100-s magnitude M_{100} for 21 great earthquakes. Since M_{100} is determined from the spectral amplitude of 100-s mantle surface waves, it can be used to estimate M_0 if the corner period is shorter than 100 s. In fact, there is a very good correlation between M_{100} and $\log M_0$. For 7 out of the 21 events of Brune and Engen [1969], direct determination of M_0 is available. Comparison of M_{100} and $\log M_0$ for these events leads to a relation

$$\log M_0 = 2.83 M_{100} + 4.83 \quad (2)$$

where M_0 is in dyne centimeters. This relation is used to estimate M_0 for the remaining 14 events. The results are listed in Table 1. Table 1 includes all shallow earthquakes of $M_s \geq 8.0$ since 1904 (when the magnitude refers specifically to the 20-s surface wave magnitude, it is denoted by M_s). These earthquakes are taken from Gutenberg and Richter [1954] for the period from 1904 to 1952, from the Science Almanac [Tokyo Astronomical Observatory, 1975, 1977] for the period from 1953 to 1975 and from the Preliminary Determination of Epicenters (PDE) cards of the U.S. Geological Survey for

1976. Nine earthquakes of $M_s < 8.0$ for which M_0 is known are included.

For the period from 1921 to 1976 the data are fairly complete; there are eight earthquakes for which M_0 is unknown, but only four of them have M_0 larger than 8.1. It is notable that in terms of M_0 , four earthquakes, the 1960 Chilean, 1964 Alaskan, 1957 Aleutian Islands, and 1952 Kamchatka earthquakes, dominate. For the period prior to 1920, Table 1 is very incomplete, except around 1905 and 1906.

MOMENT M_0 , MINIMUM STRAIN ENERGY DROP W_0 , AND A NEW MAGNITUDE SCALE M_w

The seismic moment M_0 is a very important earthquake parameter that measures the overall deformation at the source. In particular, it has a very important bearing on global phenomena such as plate motion [Brune, 1968; Davies and Brune, 1971; Kanamori, 1977], polar motion, and rotation of the earth [Smylie and Mansinha, 1968; Dahlen, 1973; Anderson, 1974; Press and Briggs, 1975; O'Connell and Dziewonski, 1976].

The seismic moment can be also interpreted in terms of the strain energy released in earthquakes. In the framework of the elastic stress relaxation model of an earthquake [Knopoff, 1958] the difference in the elastic strain energy W before and after an earthquake can be written as

$$W = \bar{\sigma} \Delta S \quad (3)$$

where $\bar{\sigma}$ is the average stress during faulting. If the stress drop is complete, the stress drop $\Delta\sigma$ is equal to $2\bar{\sigma}$, and

$$W = W_0 = \frac{1}{2} \Delta\sigma \Delta S = (\Delta\sigma/2\mu) M_0 \quad (4)$$

Since $\Delta\sigma$ is nearly constant at 20–60 bars = $2-6 \times 10^9$ dyn/cm² for very large earthquakes (Figure 1) and $\mu = 3-6 \times 10^{11}$ dyn/cm² under crust-upper mantle conditions, $(\Delta\sigma/\mu) \sim 10^{-4}$ and (4) becomes

$$W_0 \sim M_0 / (2 \times 10^4) \quad (4')$$

Thus one can estimate W_0 by dividing the seismic moment by 2×10^4 .

When the stress drop is partial, the situation becomes more complicated. We let σ_0 and σ_1 be the initial and final stresses, respectively. Then

$$W = \bar{\sigma} \Delta S = (\Delta\sigma/2) \Delta S + \sigma_1 \Delta S = W_0 + \sigma_1 \Delta S \quad (5)$$

Unless a substantial overshoot occurs, σ_1 is usually positive, so that W_0 gives the minimum estimate of the strain energy drop. We can attach more significance to W_0 if we introduce a model proposed by Orowan [1960]. We let σ_f be the frictional stress during faulting. Then

$$W = H + E$$

TABLE 2. Earthquakes of Large M_w

Event	Year	M_w
Chile	1960	9.5
Alaska	1964	9.2
Aleutian	1957	9.1
Kamchatka	1952	9.0
Ecuador	1906	8.8
Aleutian	1965	8.7
Assam	1950	8.6
Kurile Islands	1963	8.5
Chile	1922	8.5
Banda Sea	1938	8.5
Mongolia	1905	8.4
Mongolia	1905	8.4
Sanriku	1933	8.4
Kamchatka	1923	8.3
Kurile Islands	1958	8.3
Chile	1906	8.2
Alaska	1938	8.2
Kamchatka	1959	8.2
Tokachi-oki	1968	8.2
Peru	1940	8.2
Peru	1942	8.2
Alaska	1958	8.2
Chile	1943	8.2
Kurile	1969	8.2
Mexico	1932	8.1
Tonankai	1944	8.1
Nankaido	1946	8.1
Alaska	1949	8.1
Tokachi-oki	1952	8.1
Mongolia	1957	8.1
Peru	1966	8.1
India-Nepal	1934	8.1
Peru	1974	8.1
Mindanao	1976	8.1
Mexico	1928	8.0
China	1931	8.0
San Francisco	1906	7.9
Kanto	1923	7.9
Peru	1970	7.9

where $H = \sigma_f \delta S$ is the frictional loss and E is the wave energy. Using (3), we have

$$E = \bar{\sigma} \delta S - \sigma_f \delta S = (\Delta\sigma/2) \delta S + \delta S(\sigma_1 - \sigma_f) \\ = W_0 + \delta S(\sigma_1 - \sigma_f) \quad (6)$$

Thus if *Orowan's* [1960] condition $\sigma_1 = \sigma_f$ is met, W_0 is not only the minimum estimate of W but also is equal to the wave energy [see also *Savage and Wood*, 1971].

Whether the earthquake stress drop is complete or partial is presently unresolved. *Brune et al.* [1969] argued, on the basis of lack of heat flow anomaly along the San Andreas fault, that frictional stress is very small. In this case the stress drop is nearly complete, and W_0 represents the actual strain energy drop. On the other hand, evidence for a very high (~ 1 kbar) tectonic stress has been suggested primarily from the analysis of the deformation of the oceanic lithosphere [*Hanks*, 1971; *Watts and Talwani*, 1974; *Caldwell et al.*, 1976]. If this high stress is representative of the tectonic stress that causes earthquakes, then the stress drop may be partial. Although this problem remains unresolved, W_0 is still a useful parameter in that it gives the minimum strain energy drop in earthquakes.

Furthermore, results of *Trifunac* [1972], *Kanamori* [1972a], *Abe* [1975b], *Kanamori and Anderson* [1975b], and *Geller* [1976] suggest that the stress drop is approximately equal to the effective stress; i.e., *Orowan's* [1960] condition $\sigma_1 = \sigma_f$ is

satisfied. Then (6) means that W_0 determined by (4') is equal to the wave energy E .

For a more conventional measure of the 'size' of great earthquakes it is convenient to use a magnitude scale. To this end, we define a new magnitude scale for great earthquakes in terms of W_0 by using the Gutenberg-Richter magnitude-energy relation, $\log E = 1.5M + 11.8$. We use W_0 calculated from M_0 for E in this equation, calculate M_s , and denote it by M_w . The results are listed in Table 1. Table 2 lists the 39 largest earthquakes on this scale. The 1960 Chilean earthquake has the largest M_w , 9.5. The 1964 Alaskan ($M_w = 9.2$), 1957 Aleutian Islands ($M_w = 9.1$), and 1952 Kamchatka ($M_w = 9.0$) earthquakes follow. It is interesting to note that M_w agrees very well with M_s for many earthquakes with a rupture length of about 100 km (e.g., 1944 Tonankai, 1946 Nankaido, 1952 Tokachi-oki, 1966 Peru, 1923 Kanto, and 1970 Peru). This agreement may suggest that the Gutenberg-Richter magnitude-energy relation, $\log E = 1.5M + 11.8$, gives the correct value of seismic wave energy for earthquakes up to this size, i.e., a rupture dimension of ≤ 100 km. Thus the M_w scale can be used as a natural continuation of the M_s scale for great earthquakes. The saturation of the M_s scale for great earthquakes [*Kanamori and Anderson*, 1975b; *Geller*, 1976; *Chinnery and North*, 1975] has been an inconvenient and sometimes a confusing element in the conventional magnitude scale. The use of M_w eliminates this saturation.

TEMPORAL VARIATION OF ENERGY RELEASE IN EARTHQUAKES

As shown in the previous section, $W_0 = (\Delta\sigma/2\mu)M_0$ represents the minimum strain energy drop in an earthquake, and under the condition $\sigma_1 = \sigma_f$ (i.e., *Orowan's* [1960] condition, or the condition that effective stress equal stress drop) it is equal to the seismic wave energy. The condition $\sigma_1 \sim \sigma_f$ has been verified experimentally for several earthquakes.

Figure 2 shows W_0 for great earthquakes as a function of year plotted from Table 1. The solid curve shows the annual average of W_0 obtained by taking a 5-year running average (taken at the center of the interval) of the data in Table 1. In the computation of the annual release curve, earthquakes for which the seismic moment M_0 is not known are inevitably

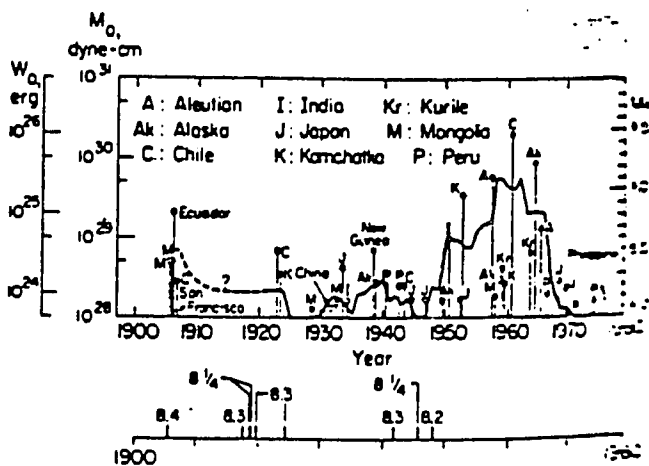


Fig. 2. The minimum strain energy drop W_0 (equal to the wave energy if *Orowan's* [1960] condition is met) in great earthquakes as a function of year. The solid curve shows unlagged 5-year running average (in ergs per year) taken at the center of the interval. The ordinate is given in three scales, the seismic moment M_0 , W_0 , and M_w . Large earthquakes for which M_0 has not been determined are plotted at the bottom with the surface wave magnitude M_s .

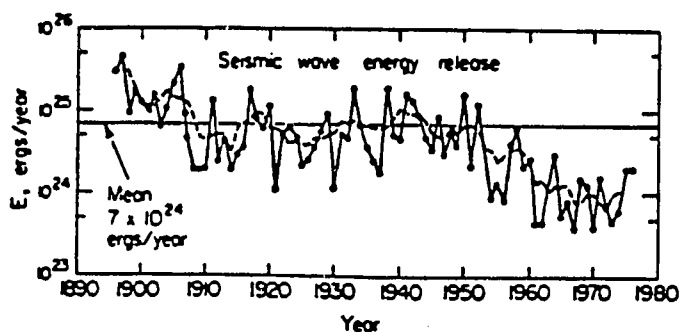


Fig. 3. Seismic wave energy released in earthquakes computed from the surface wave magnitude M_s , through the Gutenberg-Richter energy versus magnitude relation. The dashed curve shows the unlagged 5-year running average.

ignored. However, since 1921, only four events of $M_s \geq 8.2$ are missing, and it is unlikely that the omission of these events affects the energy release curve drastically. For the period prior to 1920, Table 1 is very incomplete except around 1906. The annual average of W_0 for the period from 1920 to 1976 is 4.5×10^{24} ergs/yr.

It is remarkable that during the 15-year period from 1950 to 1965 the annual average of W_0 is more than an order of magnitude larger than that during the periods from 1920 to 1950 and from 1965 to 1976. Another peak is suggested around the turn of the century, but its confirmation must await further studies.

As mentioned earlier, W_0 represents the minimum strain energy drop, and the actual strain energy drop can be larger than this, if the stress drop in great earthquakes is only partial. Even then, if the fractional stress drop is about the same for all earthquakes, Figure 2 still gives the correct trend of the relative strain energy release.

CORRELATION BETWEEN W_0 , GUTENBERG-RICHTER ENERGY, NUMBER OF EVENTS, AND POLAR MOTION OF THE EARTH

It is instructive to compare the temporal variation of W_0 with the conventional energy release curve computed from the magnitude. Gutenberg [1956b] calculated the annual energy release for the period from 1896 to 1955 by using the earthquake magnitude and the energy versus magnitude relation $\log E = 1.5M + 11.8$. We extended this calculation to 1975 by using the catalog of earthquakes listed in the *Science Almanac* [Tokyo Astronomical Observatory, 1975, 1977] and to 1976 by using the PDE cards of the U.S. Geological Survey and Caltech determinations. The energy E calculated by this method, here called the Gutenberg-Richter energy, refers to the seismic

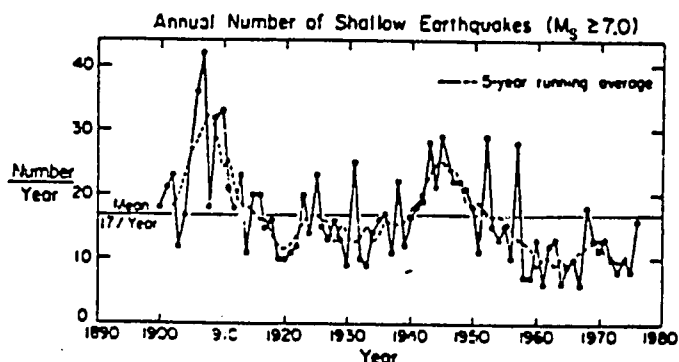


Fig. 4. The annual number of earthquakes of $M_s \geq 7.0$. The dashed curve shows the unlagged 5-year running average.

wave energy radiated by earthquakes. As was discussed earlier, however, because of the saturation of the ordinary magnitude scale this relation tends to underestimate the wave energy of great earthquakes. Thus the annual energy curve computed by this method can be considered to approximate the wave energy radiated by earthquakes of up to moderate to large size. Figure 3 shows the variation of E as a function of year.

Another measure of seismic activity is the number of earthquakes. Figure 4 shows the annual number N of earthquakes of $M_s \geq 7.0$ taken from the catalog of the *Science Almanac* [Tokyo Astronomical Observatory, 1975, 1977]. Since 96.7% of these earthquakes have M_s between 7 and 8, the temporal variation of N is more representative of the activity of moderate to large earthquakes.

Since the estimate of the Gutenberg-Richter energy E based on the magnitude-energy relation can be greatly affected by errors in the magnitude of the few larger earthquakes, the number of events N is more representative of the global activity of moderate to large earthquakes.

Despite the large uncertainty in E (Figure 3) the general trends of the curves of E and N are very similar to each other. In particular, both E and N show a very steady decrease since the middle 1940's. It is quite remarkable that during this period there was a very pronounced increase in W_0 . The correlation is shown in Figure 5. Although the energy release curve itself may be subject to considerable uncertainty, it is certain that the number of earthquakes of $M_s \geq 7.0$ decreased very sharply during the period when many great earthquakes with a very large rupture dimension (500–1000 km) occurred from 1952 to 1965. This complementary occurrence of great earthquakes and moderate to large earthquakes is a very intriguing feature, suggestive of a causal relationship between these two groups of earthquakes.

In Figure 5 is also plotted the temporal variation of the amplitude (envelope) of the Chandler wobble taken from Anderson [1974] (for the period from 1900 to 1960) and O'Connell and Dziewonski [1976] (for the period from 1960 to 1970). The variation of the wobble shows a trend very similar to that of W_0 for the period from 1920 to 1970. A peak in the wobble curve around 1910 may be correlatable to a peak in W_0 suggested around the turn of the century. Although the data presented in this paper are not complete for this period, it is notable that many large earthquakes occurred all over the world around the turn of the century, e.g., Alaska, Tibet, the

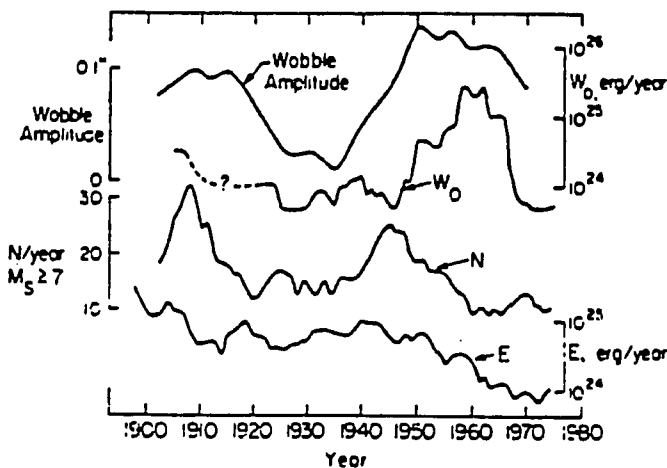


Fig. 5. Correlation between the amplitude (envelope) of the Chandler wobble, W_0 (5-year running average), annual number N of earthquakes of $M_s \geq 7.0$ (5-year running average), and the Gutenberg-Richter energy E (5-year running average).

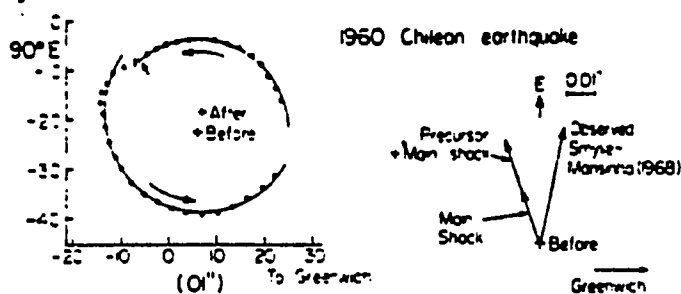


Fig. 6. The polar motion before and after the 1960 Chilean earthquake (left) inferred by Smylie and Mansinha [1968]. The center of the polar motion before and after the earthquake is shown by a plus sign. Comparison of the observed and computed polar shift is shown on the right. The computation is made by using Dahlen's [1973] expression for the source parameters determined by Kanamori and Cipar [1974].

Philippines, Mexico, New Zealand, Santa Cruz Island, Russia, the Caribbean, Loyalty Island, Guatemala, and Java.

DISCUSSION AND CONCLUSION

As shown in the previous section, W_0 represents the energy release in great earthquakes, while E or N represents that in moderate to large earthquakes. Therefore if there is a causal relation between the wobble and earthquake activity at all, it is more reasonable to compare the wobble with W_0 than with N or E .

Anderson [1974] discussed several possible mechanisms that would explain such a correlation. The first possibility is that the deformation caused by a great earthquake excites the Chandler wobble. The second is that a change in the polar motion caused by other factors, such as atmospheric changes, affects the plate motion, thereby triggering great earthquakes and other major earthquakes. Combination of these two mechanisms is also possible. Regarding the first possibility, many investigations have been made, those by Smylie and Mansinha [1968], Dahlen [1973], Israel et al. [1973], Press and Briggs [1975], and O'Connell and Dziewonski [1976] to mention a few. One problem is that the deformation caused by even a great earthquake is not large enough to excite the Chandler wobble unless a large aseismic slip is assumed [Dahlen, 1973; O'Connell and Dziewonski, 1976; Kanamori, 1976a]. Only the 1960 Chilean earthquake, the largest of all in M_w , can account for the shift of the pole position when the preseismic anelastic deformation reported by Kanamori and Cipar [1974] and Kanamori and Anderson [1975a] is included (Figure 6). Existence of large aseismic deformation has been suggested for very large tsunami earthquakes such as the 1896 Sanriku earthquake and the 1946 Aleutian Islands earthquake [Kanamori, 1972b], for the 1906 San Francisco earthquake [Thatcher, 1974], for the 1952 Kamchatka earthquake [Kanamori, 1976b], and for a Japanese earthquake [Fukao and Furumoto, 1975]. Also, disparity between seismic slip and plate motion provides evidence for such aseismic deformation [Kanamori, 1977]. Thus the first possibility still remains valid.

The second possibility is very intriguing. Recent analysis of Wilson [1975] suggests that atmospheric motions can maintain the Chandler wobble. In this context, Anderson [1975] notes that the temporal variation of global temperatures, one climatic indicator, is very similar to that of the wobble. It is quite possible that the increase in the amplitude of the Chandler wobble caused by such effects accelerates global plate motions, thereby triggering great earthquakes at plate boundaries. Figure 5 indicates that the sharp increase in W_0 around 1960

began very shortly after the amplitude of the wobble became maximum in 1950. This coincidence may be suggestive of the second possibility. It is remarkable that the annual number of earthquakes N increased toward 1945 and then decreased very sharply since then. One possibility is that when the wobble amplitude increases, the world seismic activity increases, and plate motion may be accelerated. However, once major plate boundaries are decoupled in great earthquakes, moderate to large earthquake activity declines owing to decrease in intraplate and interplate stresses as a result of plate decoupling.

It is equally possible that changes in the rotation rate of the earth are responsible for accelerated plate motions which in turn cause the variation in the Chandler wobble and great earthquakes. The change in the rotation rate of the earth correlates very well with the Chandler wobble [Anderson, 1974]. Since the rotational energy of the earth is so much greater than the energy involved in plate motions and earthquakes, even a small perturbation in the rotation can have a significant effect on earthquakes and plate motion.

The conclusions are as follows: (1) The minimum estimate of the strain energy drop in earthquakes, W_0 , which can be estimated from the seismic moment M_0 , can be considered to represent, under Orowan's [1960] condition, the seismic wave energy release. (2) Since W_0 can be estimated accurately for great earthquakes, it provides a more accurate picture of the seismic energy budget. (3) A new magnitude scale M_w is defined in terms of W_0 . It is as large as 9.5 for the 1960 Chilean earthquake and connects smoothly to M_s for moderate to large earthquakes. Therefore M_w provides a convenient magnitude scale which does not saturate. (4) The temporal variation of W_0 , the energy release in great earthquakes, is very different from that in moderate to large earthquakes. The activity of moderate to large earthquakes was very low when W_0 was largest during the period from 1950 to 1965. (5) The amplitude of the Chandler wobble seems to correlate very well with W_0 , with a slight indication of the former preceding the latter. (6) One possible mechanism that accounts for the correlation between the wobble, W_0 , and the activity of moderate to large earthquakes is that an increase in wobble amplitude triggers worldwide seismic activity and accelerates plate motion, which eventually leads to great decoupling earthquakes. This decoupling causes the decline of moderate to large earthquake activity.

Acknowledgments. I have benefited greatly from stimulating discussions with and helpful comments by Don Anderson, Bob Geller, and Yoshio Fukao. The idea of using static parameters to estimate the minimum energy involved in great earthquakes emerged from conversations held with Don Anderson and Tom Hanks. Yoshio Fukao and Gordon Stewart kindly made available some of their results prior to publication. This research was supported by the Earth Sciences Section of the National Science Foundation, grants EAR76-14262 and EAR74-22489. Contribution 2867 of the Division of Geological and Planetary Sciences, California Institute of Technology, Pasadena, California 91125.

REFERENCES

- Abe, K., Reliable estimation of the seismic moment of large earthquakes, *J. Phys. Earth*, 23, 381-390, 1975a.
 Abe, K., Static and dynamic fault parameters of the Suitama earthquake of July 1, 1968, *Tectonophysics*, 27, 223-238, 1975b.
 Aki, K., Earthquake mechanism, *Tectonophysics*, 13, 423-428, 1974.
 Anderson, D. L., Earthquakes and the rotation of the earth, *Science*, 186, 49-50, 1974.
 Anderson, D. L., Frontiers of geophysics: Earthquakes, volcanism, climate, and the rotation of the earth (abstract), *Eos Trans. Am. Geophys. Union*, 56, 346, 1975.
 Ben-Menahem, A., E. Aboodi, and R. Schild, The source of the great

- Assum earthquake—An interplate wedge motion, *Phys. Earth Planet. Interiors*, 9, 265-289, 1974.
- Brune, J., Seismic moment, seismicity, and rate of slip along major fault zones, *J. Geophys. Res.*, 73, 777-784, 1968.
- Brune, J. N., and G. R. Engen, Excitation of mantle Love waves and definition of mantle wave magnitude, *Bull. Seismol. Soc. Amer.*, 39, 923-933, 1969.
- Brune, J. N., T. L. Henyey, and R. F. Roy, Heat flow, stress, and the rate of slip along the San Andreas fault, California, *J. Geophys. Res.*, 74, 3821-3827, 1969.
- Caldwell, J. G., W. F. Haxby, D. E. Karig, and D. L. Turcotte, On the applicability of a universal elastic trench profile, *Earth Planet. Sci. Lett.*, 31, 239-246, 1976.
- Chen, W. P., and P. Molnar, Seismic moments of major earthquakes and the average rate of slip in central Asia (abstract), *Eos Trans. AGU*, 58, 182, 1977.
- Chinnery, M. A., The strength of the earth's crust under horizontal shear stress, *J. Geophys. Res.*, 69, 2085-2089, 1964.
- Chinnery, M. A., and R. G. North, The frequency of very large earthquakes, *Science*, 190, 1197-1198, 1975.
- Dahlen, F. A., A correction to the excitation of the Chandler wobble by earthquakes, *Geophys. J. Roy. Astron. Soc.*, 32, 203-217, 1973.
- Davies, G. F., and J. N. Brune, Regional and global fault slip rates from seismicity, *Nature*, 229, 101-107, 1971.
- Fedotov, S. A., Regularities of the distribution of strong earthquakes in Kamchatka, the Kuril Islands and northeastern Japan (in Russian), *Izv. Akad. Nauk SSSR Fiz. Zemli*, 36(203), 66-93, 1965.
- Fukao, Y., and M. Furumoto, Mechanism of large earthquakes along the eastern margin of the Japan sea, *Tectonophysics*, 24, 247-266, 1975.
- Geller, R. J., Scaling relations for earthquake source parameters and magnitudes, *Bull. Seismol. Soc. Amer.*, 66, 1501-1523, 1976.
- Geller, R. J., and H. Kanamori, Magnitude of great shallow earthquakes from 1904 to 1952, *Bull. Seismol. Soc. Amer.*, 67, in press, 1977.
- Gutenberg, B., The energy of earthquakes, *Quart. J. Geol. Soc. London*, 112, 1-14, 1956a.
- Gutenberg, B., Great earthquakes 1896-1903, *Eos Trans. AGU*, 37, 608-614, 1956b.
- Gutenberg, B., and C. F. Richter, *Seismicity of the Earth*, 2nd ed., 310 pp., Princeton University Press, Princeton, N. J., 1954.
- Hadley, D. M., and H. Kanamori, Seismotectonics of the eastern Azores-Gibraltar Ridge (abstract), *Eos Trans. AGU*, 56, 1028, 1975.
- Hanks, T. C., The Kuril trench-Hokkaido rise system: Large shallow earthquakes and simple models of deformation, *Geophys. J.*, 23, 173-189, 1971.
- Israel, M., A. Ben-Menahem, and S. J. Singh, Residual deformation of real earth models with application to the Chandler wobble, *Geophys. J. Roy. Astron. Soc.*, 32, 219-247, 1973.
- Kanamori, H., Determination of effective tectonic stress associated with earthquake faulting—Tottori earthquake of 1943, *Phys. Earth Planet. Interiors*, 5, 426-434, 1972a.
- ★ Kanamori, H., Mechanism of Tsunami earthquakes, *Phys. Earth Planet. Interiors*, 6, 346-359, 1972b.
- ★ Kanamori, H., Are earthquakes a major cause of the Chandler wobble?, *Nature*, 262, 254-255, 1976a.
- Kanamori, H., Re-examination of the earth's free oscillations excited by the Kamchatka earthquake of November 4, 1952, *Phys. Earth Planet. Interiors*, 11, 216-226, 1976b.
- Kanamori, H., Seismic and aseismic slip along subduction zones and their tectonic implications, in *Island Arcs, Deep Sea Trenches, and Back-Arc Basins, Maurice Ewing Ser.*, vol. 1, edited by M. Talwani and W. C. Pitman III, AGU, Washington, D. C., in press, 1977.
- ★ Kanamori, H., and D. L. Anderson, Amplitude of the earth's free oscillations and long-period characteristics of the earthquake source, *J. Geophys. Res.*, 80, 1075-1078, 1975a.
- Kanamori, H., and D. L. Anderson, Theoretical basis of some empirical relations in seismology, *Bull. Seismol. Soc. Amer.*, 65, 1073-1095, 1975b.
- Kanamori, H., and J. J. Cipar, Focal process of the great Chilean earthquake, May 22, 1960, *Phys. Earth Planet. Interiors*, 9, 128-136, 1974.
- Kelleher, J. A., Rupture zones of large South American earthquakes and some predictions, *J. Geophys. Res.*, 77, 2087-2103, 1972.
- Kelleher, J., L. Sykes, and J. Oliver, Possible criteria for predicting earthquake locations and their application to major plate boundaries of the Pacific and the Caribbean, *J. Geophys. Res.*, 78, 2547-2585, 1973.
- Knopoff, L., Energy release in earthquakes, *Geophys. J.*, 1, 44-52, 1958.
- Mogi, K., Development of aftershock areas of great earthquakes, *Bull. Earthquake Res. Inst. Tokyo Univ.*, 46, 175-203, 1968a.
- Mogi, K., Some features of recent seismic activity in and near Japan, 1, *Bull. Earthquake Res. Inst. Tokyo Univ.*, 46, 1225-1236, 1968b.
- O'Connell, R. J., and A. M. Dziewonski, Excitation of the Chandler wobble by large earthquakes, *Nature*, 262, 259-262, 1976.
- Okal, E. A., A surface-wave investigation of the rupture mechanism of the Gobi-Altai (December 4, 1957) earthquake, *Phys. Earth Planet. Interiors*, 12, 319-328, 1976.
- Okal, E. A., The July 9 and 23, 1905 Mongolian earthquakes: A surface-wave investigation, *Earth Planet. Sci. Lett.*, 34, 326-331, 1977.
- Orowan, E., Mechanism of seismic faulting, *Geol. Soc. Amer. Mem.*, 79, 323-345, 1960.
- Press, F., and P. Briggs, Chandler wobble, earthquakes, rotation, and geomagnetic changes, *Nature*, 256, 270-273, 1975.
- Savage, J. C., and M. D. Wood, The relation between apparent stress and stress drop, *Bull. Seismol. Soc. Amer.*, 61, 1381-1388, 1971.
- Smylie, D. E., and L. Mansinha, Earthquakes and the observed motion of the rotation pole, *J. Geophys. Res.*, 73, 7661-7663, 1968.
- Stewart, G. S., R. Butler, and H. Kanamori, Surface and body wave analysis for the February 4, 1975, Haicheng and July 27, 1976, Tangshan Chinese earthquakes (abstract), *Eos Trans. AGU*, 57, 953, 1976.
- Sykes, L. R., Aftershock zones of great earthquakes, seismicity gaps, and earthquake prediction for Alaska and the Aleutians, *J. Geophys. Res.*, 76, 8021-8041, 1971.
- Thatcher, W., Strain release mechanism of the 1906 San Francisco earthquake, *Science*, 184, 1283-1285, 1974.
- Thatcher, W., and T. Hanks, Source parameters of southern California earthquakes, *J. Geophys. Res.*, 78, 8547-8576, 1973.
- Tokyo Astronomical Observatory, *Science Almanac*, Maruzen, Tokyo, 1975.
- Tokyo Astronomical Observatory, *Science Almanac*, Maruzen, Tokyo, 1977.
- Trifunac, M. D., Stress estimates for the San Fernando, California, earthquake of February 9, 1971; Main event and thirteen aftershocks, *Bull. Seismol. Soc. Amer.*, 62, 721-750, 1972.
- Utsu, T., and A. Seki, A relation between the area of aftershock region and the energy of main shock (in Japanese), *J. Seismol. Soc. Jap.*, 7, 233-240, 1954.
- Watts, A. B., and M. Talwani, Gravity anomalies seaward of deep-sea trenches and their tectonic implications, *Geophys. J.*, 36, 57-90, 1974.
- Wilson, C. R., Meteorological excitation of the earth's wobble, Ph.D. thesis, Univ. of Calif., San Diego, 1975.

(Received January 31, 1977;
revised March 21, 1977;
accepted March 22, 1977.)

THE 3 OCTOBER AND 9 NOVEMBER 1974 PERU EARTHQUAKES:

SEISMOLOGICAL IMPLICATIONS

by B.T. Brady¹⁾

SYNOPSIS

An earthquake sequence that may have significant seismological and sociological implications occurred approximately 65 km off the coast of central Peru between 3 October and 9 November 1974. Both earthquakes occurred within a well-documented seismic gap. The 3 October ($m_b = 6.3$, $M_S = 7.8$) and 9 November ($m_b = 6.0$, $M_S = 7.1$) shocks were shallow-focus (~ 20 km depth), complex multiple-ruptures which began with a low-energy episode followed by higher amplitude multiples. The subsequent aftershock sequence of the 3 October event, however, only partially filled the seismic gap and, with the exception of one event (14 November 1974), was terminated by the 9 November shock. The areal extents of the seismic gap and of primary aftershock region are approximately 32,000 km² and 9,000 km², respectively.

The primary aftershock region of the 3 October mainshock and, in particular, a substantial part of the total area ($\sim 32,000$ km²) of the known seismic gap have been seismically quiescent since 14 November 1974. Subsequent seismic activity (teleseismically reported) has shifted to the north, west, and southeast along the boundaries of this seismic gap. These data, combined with additional results discussed in this report, indicate that this region may be now in the preparation stage

¹⁾ Physicist, U.S. Dept. of the Interior, BuMines, Denver Mining Research Center, Denver, Colorado.

for an earthquake whose estimated epicenter, magnitude, and minimum preparation time measured from 14 November 1974 are approximately 12.5°S , 77.7°W , $M_S = 8.4 (\pm 0.2)$, and 5.9 years (circa, October 1980) respectively. A program to test this hypothesis and to determine the onset of very short-term (\sim several days) precursors that may precede this event is presented.

TECTONIC SETTING

The relative velocity between the Nazca and Americas plates (figure 1), at the Peru continental margin, is approximately 10 cm/yr in an east-west direction (12)²⁾. This direct collision between these plates is recognized as producing a very high level of seismicity. This region is known to be capable of sustaining large underthrust earthquakes in Peru such as, for example, 24 May 1940 ($M_S \sim 8.0$) near Huacho, 24 August 1942 ($M_S = 8.1$) near Nazca, 17 October 1966 ($M_S = 7.6$), offshore the Huacho region, 31 May 1970 ($M_S = 7.8$) offshore Chimbote-Huaras, and the 3 October 1974 event ($M_S = 7.8$) about 65 km southwest of Lima. These large events are included in Figure 1.

The 1974 earthquake sequence formed within a well-known seismic gap (6). Such gaps are now believed to result from the episodic and non-uniform nature of the physical processes by which oceanic lithosphere is underthrust beneath continental lithosphere. In particular, this gap was recognized as being well-defined and consequently this region was believed to be of high earthquake expectancy. A first-order estimate

²⁾ Underlined numerals refer to references listed at the end of this report.

of the 3 October 1974 mainshock rupture area is shown in figure 1. This area is approximated by the teleseismically determined preliminary aftershock locations, generally for aftershocks of $m_b \geq 4.2$ (7).

The Nazca ridge is a dominant oceanic structural feature off central Peru. The Peru-Chile trench loses definition as this east-northeast trending topographic high underthrusts continental Peru. The 1974 earthquake sequence occurred immediately to the north of this tectonic junction.

PRECURSORY SEISMICITY ASSOCIATED WITH THE 3 OCTOBER 1974 MAINSHOCK

Table 1 summarizes date, focal depth, and body-wave magnitude data for all teleseismically reported seismic events which occurred within the coordinates $11.9^{\circ}\text{S}-14.0^{\circ}\text{S}$, $76.5^{\circ}\text{W}-79.0^{\circ}\text{W}$ (that is, the approximate geographical boundaries of the seismic gap recognized by Kelleher (6)) prior to the 3 October 1974 mainshock, hereafter referred to as the Kelleher gap. All events listed in Table 1 have source depths less than 100 km. This depth is taken to be the boundary between shallow and intermediate depth activity. Figure 2 illustrates the yearly seismic event count within these geographical boundaries. Figure 3 lists the symbol for magnitude range of the earthquakes shown in figures 4-8. Figures 4-8 show longitude vs latitude (a), longitude vs depth (b), and latitude vs depth (c) of all teleseismic reported events prior to 3 October 1974 which occurred within and immediately surrounding the seismic gap. There are several features of these data that warrant close attention. First, there is an indication of a relative peak of seismic activity within the gap zone during 1967 (figure 2). This peak was followed by an apparent "quieting"

period in the gap zone which was terminated on 28 May 1971. Second, these data show that no seismic events occurred within the immediate epicentral zone of the 3 October 1974 mainshock between 1962 and 1970. This tentative observation is also substantiated by seismic data obtained from the local Peruvian seismic network between 1965 and 1969 (Silgado, written communication, 1976). Third, the precursory seismicity data suggest a distinct peak of activity on 3 October 1971. This peak was then followed by a period of relative quiescence in the epicentral region. Fourth, seismic events 18, 21, 22, 23, and 24 (table 1), beginning on 28 May 1971 and terminating on 3 October 1971, a time span of approximately four (4) months, delineated an area, A_1 , of approximately $2,200 \text{ km}^2$ (figure 4a). In particular, these events migrated in time toward the epicentral regions of the 3 October 1974 and 9 November 1974 shocks and, as such, appear to be causally related to their occurrence. Fifth, there was no further activity within this zone until 24 December 1973 (event 1, figure 5). This was followed by three additional events (2, 3, and 4; figure 5a) and culminated with the 3 October 1974 mainshock. These foreshocks clearly appear to be related to the geometry of the zone mapped out by events 18, 21, 22, 23, and 24 during 1971. Of particular importance, event 29(1) may have been instrumental in triggering events 2-4 (figure 5).

ANALYSIS OF THE PRECURSORY SEISMICITY

A familiarity by the reader of the essential features of the inclusion theory of failure is assumed in this section. Specific concepts and essential equations used in analyzing the central Peru seismicity data can be found in earlier work (2, 3, 4). A brief qualitative discussion of the theory is given in the appendix to this report.

The increased level of seismic activity, beginning on 28 May 1971 and terminating on 3 October 1971, similar to peaks of seismic activity associated with other earthquakes and rock bursts (2, 3, 4), was associated with the formation of an irregularly-shaped zone (open circles in dashed region, figure 4). The interpretation of these data in terms of the inclusion theory of failure is suggestive that the primary inclusion zone (PIZ) associated with the 3 October 1974 mainshock may have formed off the coast of central Peru during a four (4) month period in 1971. Two other additional results support this hypothesis. First, local aftershock data shown in figure 7(a,b,c) (7) clearly exhibit a concentration and symmetry that is remarkably similar to the geometry of the PIZ. The aftershock concentrations near Chilca and parallel to the coastline, that is, the aftershocks "parallel" to the two orthogonal branches of the PIZ, map out an area of approximately $9,500 \text{ km}^2$ extent. Several aftershocks in the northeastern and southeastern portions of the seismic gap are not included in this area estimate. Second, foreshocks which preceded the 3 October 1974 mainshock (events 29-32, table 1; figure 5(a,b,c)) appear to be intimately associated with the geometry of the PIZ. It has been shown elsewhere .

(3,4) that an irregularly-shaped PIZ will have a much greater probability of exhibiting secondary foreshock activity which may serve to prematurely trigger a large earthquake. These secondary foreshocks are to be distinguished from primary foreshocks which occur as a result of crack coalescence within the PIZ shortly prior to the mainshock. These secondary foreshocks occur in response to the high stress concentrations induced on the material as a result an irregularly-shaped PIZ. In this respect, we note that following event 29(1), which occurred at the location where one would expect the greatest stress concentration (the joining of the two limbs), events 30(2) (near Chilca), 31(3) and 32(4) migrated sequentially toward the epicentral regions of the 3 October and 9 November 1974 mainshocks.

Table 2 lists the proposed PIZ forming events, their m_b and M_S values, and the calculated anomalous areas, $A_{o(n)}$, associated with each event. The functional relationship between M_S and m_b for M_S values less than 5.73 is taken to be

$$M_S = 1.05 m_b - 0.02 \quad , \quad (M_S < 5.73) \quad (1)$$

as observed by Nagamune (10) and discussed at some length by Geller (5). The anomalous area, $A_{o(n)}$, refers to the total area that is "shut-down" seismically and is associated with an impending large seismic event. The anomalous area, $A_{o(n)}$, of each event is related to the aftershock area, $A_{(n)}$, of the event by the equation $A_{(n)} = \eta A_{o(n)}$, where η is the seismic efficiency factor ($\approx 0.24\%$ (3,4)) of the failure. It can be shown (4) that knowledge of $A_{o(n)}$ and N (=total number of seismic events associated with PIZ formation) allows a prediction of the aftershock

area, A , of the impending event,

$$A_{(\text{pred})} = \frac{1}{\phi_p} \sum_{n=1}^N A_{o(n)}, \quad (2)$$

where ϕ_p is the total fracture porosity of the PIZ. This quantity is related to the seismic efficiency factor and N by

$$\phi_p = \alpha_o \left(\eta \sqrt{N} \right)^{2/3} \quad (3)$$

where $\alpha_o \left[= \frac{1}{\sqrt{\eta}} \approx 20 \text{ (2,4)} \right]$ is the ratio of the aftershock area (A) of the impending event to the area of its PIZ (A_1). Thus for the five (5) events listed in table 2, $\phi_p \approx 0.63$, equation 2 gives a predicted aftershock area of approximately $36,000 \text{ km}^2$ for the impending mainshock. This compares with the "observed" Kelleher seismic gap area of $32,500 \text{ km}^2$. The predicted area, A_1 , of the PIZ associated with an event of area $A = 36,000 \text{ km}^2$ is $\frac{1}{\alpha_o} A \approx 1,800 \text{ km}^2$ and compares favorably with the observed area in figure 4 of approximately $2,200 \text{ km}^2$. The predicted magnitude of this event is $M_S = 8.6 (= \log_{10} A - 4.0)$, considerably greater than the observed value of $M_S = 7.8$. The predicted time to this event, measured from the time of initiation of PIZ growth (28 May 1971) is $\tau_o^{(\text{pred})} = \tau_o \gamma_o A_o = 6.7 \text{ yrs}$, where $\gamma_o = 2.43 \times 10^{-4} \text{ sec/cm}^2$ (2) and A_o is the total area of the seismic gap. The calculated time is nearly a factor of two (2) greater than the observed time of 3.3 yrs.

DISCUSSION OF SEISMICITY

The 3 October 1974 mainshock occurred within a seismic gap of sufficient size to suggest that the gap could have supported a much larger magnitude earthquake sequence than what actually occurred. The measured area of the gap is approximately $32,000 \text{ km}^2$ while the approximate aftershock area, determined by the USGS local network, is only $9,000 \text{ km}^2$. However, the actual aftershock area would be much greater if the outlying aftershocks are included (figure 7a). In fact, these outliers conform somewhat to the boundaries of the known seismic gap. This is also true for the teleseismically reported aftershocks (figure 6).

The geometry of the hypothesized PIZ and the remarkable geometrical similarity of its associated focal region (aftershock zone) coupled with the spacial distribution of the secondary foreshocks prior to 3 October 1974 must be considered as strong support for the hypothesis that the PIZ which produced the 3 October 1974 mainshock formed during a four (4) month time interval approximately 60 km off the coast of central Peru during 1971. In addition, these foreshock data indicate that the irregular PIZ geometry may have led to conditions which produced a premature triggering of the seismic gap; that is, the foreshocks formed in response to the "higher than normal" stress concentrations induced in the focal region of the irregularly-shaped PIZ. Thus, these foreshocks may have acted as possible "destressing" events in a region which could have supported a much higher-magnitude earthquake. Destressing is recognized as the occurrence of early, low-magnitude failures, where only a larger failure could have occurred in the absence of "destressing" (2,3). Similar behavior is known to occur

in mines experiencing rock bursts (2, 3). Therefore, these observational data can be viewed as suggesting that both the 3 October and 9 November 1974 events were prematurely triggered by the four (4) foreshocks which were, in turn, produced by an irregular-shaped PIZ.

The observed partial filling of the seismic gap by the 3 October 1974 aftershock is also suggestive that the gap region may not have had the time, theoretically estimated to be 7 yrs, required for the preparation phase of the hypothesized larger magnitude shock. In this regard, it is of interest to note that seismicity (events 25, 26, 27, 28 in figure 5a) was present in the seismic gap. However, no seismicity was occurring within the inner gap area, A_o^* , of approximately $20,000 \text{ km}^2$ delineated by these events. It is interesting that these events conform closely to the boundaries of the observed aftershock region shown in figures 6 (teleseismic) and 7 (local). These data, coupled with the observed precursory peak of seismicity in 1971, suggest that the seismic gap was not only in the preparatory stage for a major seismic event but that the gap was to be prematurely triggered. For example, if we chose the "new gap" area, A_o^* , of $21,000 \text{ km}^2$, then the new time to the shock is $\tau_o^{(pred)} = \eta \gamma_o A_o^* \approx 3.5 \text{ yrs}$, in good agreement with the observed time of 3.5 yrs. Lack of precision of the locations of northwest, west, and southwestern boundaries of A_o^* will produce a corresponding lack of precision in $\tau_o^{(pred)}$, although clearly this time will be less than the value of 6.9 yrs based on the original gap area. We could, however, have anticipated that the gap would be prematurely activated and that the mainshock would have been preceded by secondary foreshocks.

Lastly, a point of interest concerning the 1967 spacially-diffuse- "peak" of activity. This activity occurred within the Kelleher gap was followed by a period of relative quiescence. This behavior is predicted by the inclusion theory and is discussed in the appendix. Briefly, this behavior arises in response to the buildup of tensional stress within the zone which will shortly, in this case four (4) years, become the PIZ. As this tensile stress buildup occurs, force equilibrium requires that there be a corresponding increase in the average compression stress level existing within the large focal region that contains the incipient PIZ. The stress referred to here is the local least principal stress which is oriented normal to the eventual rupture propagation direction. In our case, the focal region corresponds to the seismic gap. As a result, conditions now become less favorable for failure within the gap region.

IMPLICATIONS OF THE 9 NOVEMBER AND 14 NOVEMBER 1974 EARTHQUAKES

In order of increasing importance, there are six observations which suggest that this region (seismic gap) may have again approached a critical state. First, the space-time patterns of the 3 October aftershock series exhibit a characteristic sequence of alternating between the two limbs of the proposed PIZ (Spence, personal communication, 1977). In context of the inclusion theory, this constitutes evidence of a very precarious stress condition throughout the aftershock zone (figure 7). Second, the 9 November 1974 shock terminated the high rate of aftershock activity associated with the 3 October mainshock. The 9 November shock was not followed by an aftershock series. This is a necessary and sufficient condition required by the inclusion theory for PIZ-formation.

The focal mechanism of the 9 November event is nearly identical to that for the 3 October mainshock (12). Third, the only event which followed the 9 November earthquake was on 14 November 1974 and occurred near the junction of the two limbs of what may have been the PIZ of the 3 October mainshock. There is a dramatic absence of aftershocks in the limb of the PIZ parallel to the coastline (figures 6 and 7). The 14 November event occurred at the southeastern terminus of this zone. Fourth, there are no known normal faulting earthquakes associated with the 1974 Peru earthquake. Moreover, no normal faulting earthquakes are known to have occurred in the immediate region of the 1974 Peru earthquake series. This implies that the oceanic lithosphere has not yet freely decoupled, locally, from the continental lithosphere and that a major episode of relative plate motion has yet to occur (11). The ^{31 May 1974}~~17 October 1966~~ Peru main shock (figure 1) was a normal-fault earthquake followed by thrust-faulting aftershocks (13). Isacks (see 14) has found normal faulting mechanisms for a number of earthquakes occurring seaward after the 1960 Chilean earthquake, which was predominantly a thrust-faulting event. Fifth, the irregular shape of the 1974 aftershock zone (7) implies that much of the interface between the Nazca and South American plates, which constituted the seismic gap of the 1974 main shock, did not rupture during the earthquake sequence. There is no evidence that these downslab sections have undergone failure prior to the 1974 earthquake series. The area of these sections is about 23,000 km², compared to a total 'gap' area of about 32,000 km². Sixth, there have been no teleseismically reported events within the

entire gap zone since 14 November 1974 (figure 8). All subsequent activity has shifted outside and along the boundaries of this seismic gap. This "donut" seismicity pattern has been observed prior to major Japanese earthquakes (8, 9) and is required by the inclusion theory (see appendix).

These arguments and observational data are consistent with the theoretical requirements that this region may now be in the process of being prepared for a major earthquake. The calculated average A_0 of the gap zone shown in figure 8 is $32,000 \text{ km}^2$. However, precise delineation of the eastern and western boundaries is not possible at this time, although the western boundary does conform closely to the western boundary of the 1974 aftershock series. The calculated minimum predicted time, using a gap area of $32,000 \text{ km}^2$, is $\tau_0^{(\text{pred})} = \eta \gamma_0 A_0 = 5.9 \text{ yrs}$, as measured from 14 November 1974. This calculation suggests that the event will not occur prior to about October 1980. This calculated time is contingent on (1) no secondary foreshocks occurring in the epicentral region, and (2) the anomalous area, A_0 (the seismic shut-down area), is equal to the aftershock area of the impending event, and (3) the gap area is $32,000 \text{ km}^2$. The predicted magnitude of this event is $M_S = 8.4 \pm 0.2$.

It is shown elsewhere (4) that the functional relationship between A and A_0 is

$$A = 0.50 v^2 \gamma_0^2 \eta^2 A_0^2, \quad (A \leq A_0) \quad (4)$$

where $v (= L/\tau_0)$ is the average velocity with which cracks of identical geometry within the focal region of the PIZ are closing. This velocity is simply the rate at which strain information can be propagated within the focal region. Mogi (8, 9) has observed that in major subduction

zones, values of v are typically in the range of 25 km/yr (=0.08 cm/sec) to 50 km/yr (= 0.16 cm/sec). Substituting these rates and $A_0 = 32,000 \text{ km}^2$ into equation 4 gives a typical range of A to be 10,500 km^2 to 42,000 km^2 for this region. This calculation suggests that both A and A_0 are probably comparable for this earthquake. This condition can only be met when the impending mainshock is of sufficient magnitude so as to involve substantial portions of the upper mantle (1, 4).

These calculations should be viewed with caution as there is clearly a definite lack of precision in certain critical parameters, such as A and v , required to accurately estimate both τ_0 and M_S . However, even in the absence of precise knowledge of these quantities, these data are consistent with the observations that A_0 ($\cong 32,000 \text{ km}^2$) is now considerably greater than the shut-down area of nearly 9,000 km^2 associated with the $M_S = 7.8$ 3 October 1974 event. If we assume that their aftershock areas scale linearly, then the predicted magnitude of the impending event is $M_S \cong 8.4$ ($=7.8 + \log_{10} \frac{32,000}{9,000}$). These calculations independently suggest the magnitude of the impending shock may be in the $M_S = 8.4-8.5$ range.

In this interpretation of the 3 October 1974 - 9 November 1974 Peru earthquake sequence, I have assumed that the Utsu relationship ($M_S = \log_{10} A + 4.0$, where A is measured in km^2) is applicable to the Lima region. There is possibly justification for this assumption. For example, using the observed aftershock area of approximately 9,000 km^2 for the 3 October mainshock, we calculate a magnitude of $M_S = 7.9$, in good agreement with the observed $M_S = 7.8$. Historical records indicate that earthquakes of estimated magnitudes (based on damage intensity)

8.2 and 8.4 occurred on 20 October 1687 and 28 October 1746 in the immediate region of Lima (15). Both events, in particular the 1746 shock, produced considerable damage and casualties; only 200 of Callao's 5000 inhabitants survived (15).

DISCUSSION

The hypothesis that the PIZ of an impending great earthquake may have formed within 65 km off the coast of central Peru on 9 November 1974 can be tested. This testing program would have to include: (1) detailed monitoring of sea level changes (sea level will decrease as the ocean bottom rises (~several meters in the epicentral region)) in response to upper mantle involvement in the earthquake preparation process (1); (2) anomalous v_p , v_s behavior if fluids are present within the focal region; (3) increased radon emanations in response to increased pressure within the focal region; (4) an increase of ground tilt in a direction away from the epicentral region; (5) increase of stress within the focal region, and (6) possible secular variations in the local geomagnetic field. In addition, there may be low magnitude seismic events occurring within the focal region (aftershock area of the impending mainshock) whose magnitudes will decrease with increasing time into the preparation phase as cracks within the focal region close. There should be an increase in seismic activity outside what will become the aftershock region of the impending event. Teleseismically reported data suggests this condition is present. Lastly, there may be an increase in deep focus earthquake activity down-dip from the focal region of the

impending shock as increasing volumes of the upper mantle are involved in the preparation process. In this respect, the 5 January 1974 ($m_b = 6.3$, $z = 98$ km) event could be considered as a "precursor" to the 3 October 1974 mainshock.

It will be particularly important to detect short-term precursors, such as discussed in reference 2, prior to this event. While knowledge of the geometry of the hypothesized "new" PIZ is not available at this time, the somewhat uniform geometry of the seismic gap shown in figure 8 is suggestive that this event may not be preceded by secondary foreshocks. However, there will be very-low-magnitude events ($M \sim 1$ (2)) as cracks within the PIZ coalesce several hours prior to the mainshock. This region (PIZ) will then "quiet" down just prior to the mainshock. Ocean bottom seismometers to detect these events in the epicentral region would be particularly useful.

APPENDIX: A RECAPITULATION OF THE INCLUSION THEORY OF FAILURE

Observational data of rock failure on the large, intermediate, and small scale suggest not only that work failure satisfies a scale invariant principle, but also the existence of a time interval, defined as precursor or preparation time, during which materials, such as rock, exhibit detectable anomalous behavior prior to the initiation of violent catastrophic failure. The preparation time, τ_0 , refers to the time interval between the initiation of the process leading to failure and the actual occurrence of the failure. This process, once begun, proceeds independently of any changes in the far-field boundary conditions or of material properties within the primary inclusion zone (PIZ) and its associated focal region. The PIZ denotes a zone of intense local deformation and serves the purpose of initiating the failure preparation process (2, 4). The preparation time has the distinguishing characteristics that its duration is a function of the total energy that will be radiated and dissipated during failure. A theory of failure, termed the inclusion theory, has been proposed elsewhere that explains this behavior (2). This theory provides both necessary and sufficient conditions for failure, a significant difference from the Griffith theory. This difference has been shown to provide a unique determination of the energy budget (4).

In the inclusion theory of failure, a region termed the primary inclusion zone (PIZ) forms in the immediate vicinity of the impending rupture nucleation zone. The PIZ is preceded by a region of intense dilation within which the local least principal stress (σ_3) attains a higher level of tension than its immediate surroundings. Thus the PIZ

exists only when necessary, critical steps to failure have occurred. Following PIZ formation the system will inevitably evolve to the failure condition. The PIZ is preceded by intense local dilation but is itself elastically stiff relative to the immediately surrounding region. The direction of σ_3 is normal to the eventual direction of fault growth. Figures A1, A2, and A3 illustrate diagrammatically the essential characteristics of this condition. Figure A1 depicts seismic event count per unit time, $n(t)$ against time, t , within the anomalous zone, a region that will be affected by a major failure. Figures A2 and A3 illustrate the PIZ (area A_1), the focal region of the PIZ (area A , the aftershock zone of the impending rupture and the anomalous region (area A_0). Both the focal region and anomalous region denote zones whose physical properties are affected by the formation of the PIZ. The areas A_0 , A , and A_1 are functionally related to each other by $A_0 = \frac{1}{\eta} A$, $A = \alpha_0 A_1$, where η is the seismic efficiency factor ($\approx 0.24\%$) and α_0 is a function of the intrinsic porosity of the region that will become the PIZ. When this porosity is negligible or of second order, $\alpha_0 \approx 20.0$. The preparation time, τ_0 , is $\tau_0 = \gamma_0 A$, where $\gamma_0 \approx 2.43 \times 10^{-4} \text{ sec/cm}^2$. Detailed derivations of these relationships are available elsewhere (2, 4).

Prior to the formation of the PIZ, the anomalous zone (A_0) will exhibit "normal" seismic behavior (a in figure A1). As A_0 softens with respect to its surroundings, the least principal stress (σ_3) within A_0 will decrease. Because the region which will be the PIZ is elastically stiffer than its immediate surroundings, the impending PIZ (A_1) will be characterized by aseismic behavior prior to PIZ

formation (fig. A2). As a portion of the anomalous zone, in particular the focal region of the impending PIZ, experiences a local buildup of tensile stress due to "softening" in response to the seismic events, the tensile stress in the PIZ will increase because A_1 is behaving like a "hard" inclusion. Thus, the impending PIZ will appear as an aseismic region surrounded by a seismically active region (fig. A2). This condition provides an explanation of why the boundary of the PIZ must be physically distinct from its surrounding focal region. Within the time interval $t_E \leq t \leq t_E + \tau_{do}$ the PIZ is forming, thus accounting for a relative increase in seismicity within the anomalous zone (δn , fig. A1). Time, τ_{do} , represents the total time required to form the PIZ. Figure 3A depicts the PIZ and the seismic events (assumed to be seven in number for illustrative purposes) required to form this zone. Seismic events forming the PIZ are characterized by long rupture lengths and will exhibit no aftershocks, as energy that normally would have been available for frictional dissipation from these events is now available to power their respective growth. The anomalous zone (A_c^*) of each event denotes the total area ($\gg A^*$) cracked. The focal region (A^*) of these events denotes the region within which aftershocks would have occurred had these events represented normal failures. Note that the scale invariant principles also apply to each of the events forming the PIZ. Once the PIZ has formed, the elastic contrast between the PIZ and the focal region increases, allowing the least principal stress to decrease in tension within the focal region. Therefore, the shearing stress decreases and the effective confining

pressure (\equiv sum of principal stresses) increases. Therefore, both the focal region and, to a lesser extent, the anomalous zone will be characterized by a period of relative seismic quiescence, as illustrated in fig. A1 and A2 (B,C). Figure A4 further illustrates the essential physics involved within the anomalous zone during the preparation time. Here, the normal behavior zone refers to material outside the anomalous zone. During the preparation time the existence of the PIZ initiates the conversion of distortional strain energy (decreasing shear stress) into volumetric (compressional) strain energy throughout the activation volume (V_0). Thus, matter within V_0 exhibits an implosion-like behavior during τ_0 . This preparation phase is terminated by seismic activity increase within the PIZ (fig. 2A); that is, the zone which appeared to exhibit aseismic behavior during τ_0 . During time τ_0 the PIZ acts as a soft inclusion within the anomalous volume. The next phase (\equiv class II precursory phase (2)) denotes the final expenditures of energy required for crack coalescence within the PIZ. As soon as the cracks coalesce in the PIZ, catastrophic failure occurs. It is especially important to note that some precursory effects, such as a decrease in seismicity, can occur only within the anomalous volume produced by the PIZ. By virtue of the St. Venant's principle, other precursory effects, such as tilt, accelerating "creep" deformation, and electromagnetic changes will not be detected outside a region whose average linear dimension is more than 2-to-3 times the average linear dimension, L_0 of the anomalous volume.

In the inclusion theory, the size of the anomalous volume is governed by the amount of strain energy stored within the volume of material which will experience failure. The size of the anomalous volume, in turn, governs the length of fault produced by the failure. For example, when there are no changes in the far-field boundary conditions during the failure preparation time, the precursor time (τ_0) is obtained from the expression given earlier as $\tau_0 = \gamma_0 \eta A_0$. The aftershock area is given by $A = \eta A_0$.

References

- 1.) Brady, B.T. Theory of Earthquakes. III. Inclusion Collapse Theory of Deep Earthquakes, Pure and Applied Geophysics, vol. 114, pp. 1-21, 1976.
- 2.) Brady, B.T. Theory of Earthquakes IV. General Implications for Earthquake Prediction, Pure and Applied Geophysics, vol. 114, pp. 1031-1082, 1976.
- 3.) Brady, B.T. Anomalous Seismicity Prior to Rock Bursts: Implications for Earthquake Prediction, Pure and Applied Geophysics, vol. 115, pp. 357-374, 1977a.
- 4.) Brady, B.T. Physics of Brittle Fracture: Geophysical Implications. I. Energetics of the Brittle Fracture Process, to be submitted to Geophysical Journal (1977b).
- 5.) Geller, R.J. Scaling Relations for Earthquake Source Parameters and Magnitudes, Bull. Seismol. Soc. Am., vol. 66, no. 5, pp. 1501-1523, 1976.
- 6.) Kelleher, J. Rupture zones of large South American earthquakes and some predictions, J. Geophys. Res., 77, 2087-2103, 1972.
- 7.) Langer, C.J., and W. Spence. The Peruvian Earthquake of October 3, 1974, Aftershock Distribution, to be submitted to Bull. Seismol. Soc. Am., 1977.
- 8.) Mogi, K. Relationship Between Shallow and Deep Seismicity on the Western Pacific Region, Tectonophysics, vol. 17, pp. 1-22, 1973.
- 9.) Mogi, K. Some Features of Recent Seismic Activity in and near Japan (2) Activity Before and After Great Earthquakes,

Bull. Earthquake Res. Inst., vol. 47, pp. 394-417, 1969.

- 10.) Nagamune, T. Magnitudes Estimated from Body Waves for Great Earthquakes (in Japanese), Quart. J. Seismol., vol. 47, pp. 1-8, 1972.
- 11.) Spence, W. The Aleutian arc: tectonic flocks, episodic subduction strain diffusion, and magma generation, J. Geophys. Res., 82, 213-230, 1977.
- 12.) Spence, W., C. J. Langer, and J. N. Jordan, A. Tectonic Study of the Peru Earthquakes of October 3 and November 9, 1976, to be submitted to Bull. Seismol. Soc. Am., 1977.
- 13.) Stauder, W. Subduction of the Nazca Plate Under Peru as Evidenced by Focal Mechanisms and by Seismicity, J. Geophys. Res., 80, 1053-1069, 1975.
- 14.) Sykes, L. Aftershock zones of great earthquakes, seismicity gaps, and earthquake prediction for Alaska and the Aleutians, J. Geophys. Res., 76, 8021-8041, 1971.
- 15.) Berninghausen, W.H. Tsunamis reported from the west coast of South America 1562-1960, Bull. Seismol. Soc. Am., 52, 915-921, 1962.

TABLE 1

Precursory Seismicity Within Seismic Gap

11.9°S-14.0°S
76.5°W-79.0°W
Depth < 100 km

Event	Date	Latitude °S	Longitude °W	Depth km	m_b	M_S
1	19 May 1962	13.40	76.70	70	-	
2	28 September 1962	13.80	76.70	61	-	
3	25 November 1962	11.90	77.30	33	-	
4	7 October 1963	12.90	76.80	69	5.4	
5	28 October 1963	13.60	76.90	38	4.1	
6	13 October 1964	13.20	76.50	75	4.6	
7	12 May 1965	13.90	77.10	20	4.6	
8	3 June 1965	14.00 13.10 13.64	76.54 76.80 76.66	33 82	4.2	
9	26 August 1966	13.70 17.92	76.80	50	4.4	
10	1 August 1967	13.00 12.70	76.80 76.80	66	5.5	
11	22 August 1967	12.50 15.8	76.80	57	4.8	
12	17 October 1967	13.70 17.2	76.50 76.8	78	4.4	
13	26 November 1967	13.30 15.2	77.20 76.8	33	4.5	
14	5 August 1968	12.82	76.80	78	4.4	
15	13 January 1969	13.60	77.75	93	4.3	
16	20 August 1969	13.35	77.71	35G	4.6	
17	9 February 1970	12.77 12.51	77.22 77.2	40	4.6	$M_S = 4.7$
18	28 May 1971*	12.53 16	76.83 77	56	4.9	

Handwritten notes on the left side of the table, including "PIZ" and "30m" written vertically.

Is this the event that possibly triggered an irregular PIZ? Is this a PIZ foreshock? (led to premature triggering of the 7.8 Naha An. ...)

TABLE 1 (continued)

Event	Date	Latitude °S	Longitude °W	Depth km	m_b	M_S
19	6h, 1am, 4h 1 August 1971*	12.91	76.83	64	5.2	
20	10h, 4am, 35s 20 September 1971	13.41	77.14	1633N	4.3	
21	21h, 8m, 35s 1 October 1971*	12.75	77.11	43 10	4.7	
22	10h, 27m, 26s 3 October 1971*	12.71	77.20	33N	4.6	
23	14h, 55m, 26s 3 October 1971*	12.76	77.36	48	5.2	
24	15h, 21m, 39s 3 October 1971*	12.62	77.59	31 33N	4.2	
25	12 November 1971	13.01	76.40	92	4.8	
26	23 January 1972	13.23	76.78	60	5.1	
27	19 June 1972	12.10	77.51	72	5.2	
28	29 January 1973	12.10	77.29	63	4.5	
29 (1)	18h, 12m, 10s 24 December 1973**	12.62	77.47	33N	5.4	
30 (2)	7h, 32m, 9s 26 July 1974**	12.59	76.68	48	4.4	
31 (3)	0h, 37m, 12s 31 August 1974**	12.72	76.72	56	4.4	
32 (4)	10h, 9m, 48s 27 September 1974**	12.43	77.59	16	5.0	
33	14h, 21m, 29s 3 October 1974	12.40	77.60	27	6.3	7.8
34	12h, 59m, 50s 9 November 1974	12.50	77.70	10	6.0	7.1
35	19h, 11m, 35s 14 November 1974	12.80	77.10	Shallow	5.4	

* indicates seismic event associated with primary inclusion zone (PIZ) formation

** indicates seismic foreshock

• TABLE 2

Seismic Events Associated with PIZ Formation

Event	Date	Latitude	Longitude	Depth km	Magnitude		A _{o(n)} km ²
		°S	°W		m _b	M _S	
18	28 May 1971	12.55	76.83	56	4.9	5.1	5,200
21	1 October 1971	12.75	77.11	43	4.7	4.9	3,300
22	3 October 1971	12.71	77.20	33N	4.6	4.8	2,600
23	3 October 1971	12.76	77.36	42	5.2	5.4	10,500
24	3 October 1971	12.62	77.59	33N	4.2	4.4	1,000

MS

~~12.77~~
12.39

~~77.3~~
77.66

FIGURE CAPTIONS

- Figure 1 - Location of mainshock and teleseismically reported aftershock region of the 3 October - 9 November 1974 earthquake sequence. The relationship of the 3 October 1974 aftershock region to previous earthquakes in central Peru is shown for comparison (12).
- Figure 2 - Seismicity versus time in the gap region within which the 3 October 1974 mainshock occurred.
- Figure 3 - Symbols used in figures 4-8 to delineate magnitudes of events reported within the seismic gap.
- Figure 4 - Teleseismically reported events within and immediately outside the seismic gap during January 1962 - October 1971. The hypothesized PIZ of the 3 October 1974 mainshock is delineated by the dashed line within the seismic gap.
- Figure 5 - Relationship of foreshocks, 29-32 (1,2,3,4), to the PIZ and the teleseismically reported events (25, 26, 27, 28) which occurred during the interval between 3 October 1971 and 3 October 1974.
- Figure 6 - Locations of teleseismically reported aftershocks of the 3 October 1974 mainshock. Note the lack of density within the SE and NE portions of the seismic gap.
- Figure 7 - Locations of local aftershocks occurring between 9 October 1974 and 27 October 1974 (7). All magnitudes listed are $M_L \geq 3.6$.
- Figure 8 - Teleseismically reported events since 14 November 1974.
- Figure A1 - Diagrammatic representation of seismicity in the anomalous zone as a function of time. Zone a denotes typical seismicity within and surrounding the impending failure region. Zone b represents the seismicity increase, δn , within a localized

1

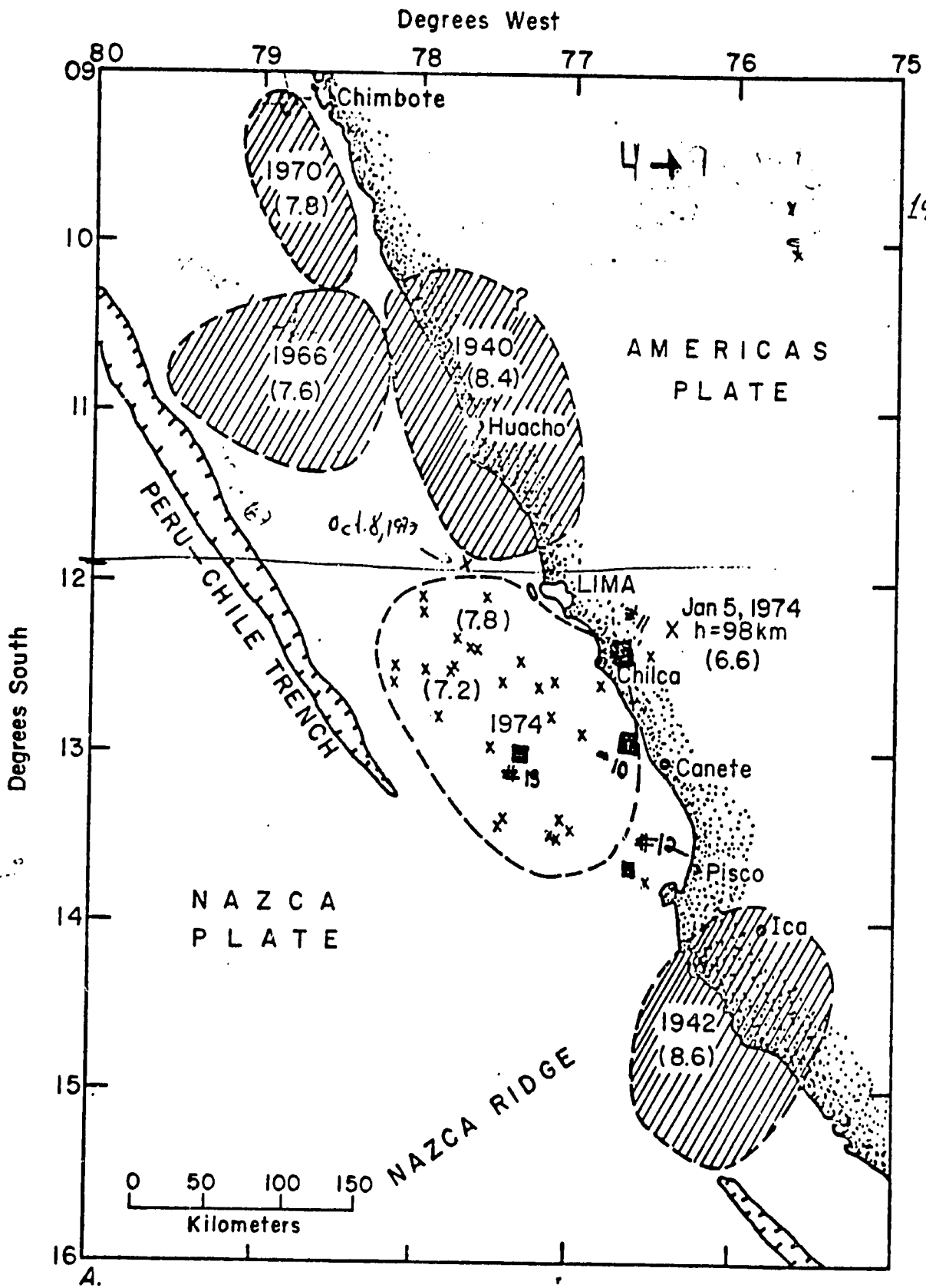
region, termed the primary inclusion zone (PIZ). Zone c denotes the decrease in seismicity (quiet period) within the anomalous region. The anomalous region, that region whose stress state is affected by the formation of the PIZ, is generally much larger than the subsequent aftershock zone. The time duration of the quiet period, τ_0 , refers to the preparation time required for the impending mainshock. τ_{d0} is the time required for PIZ formation.

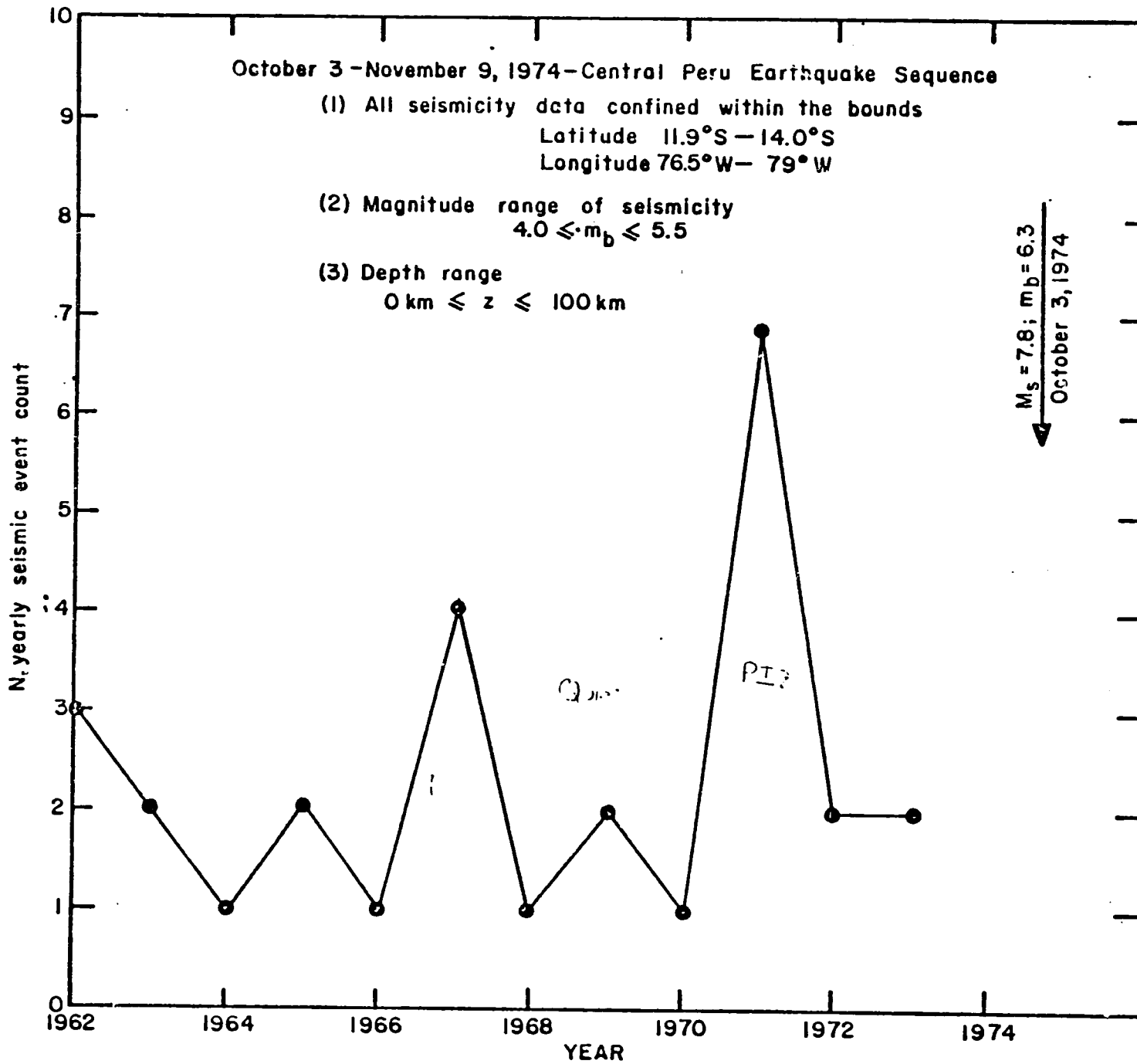
Figure A2 - Plan view of seismicity within a region that will experience a major failure. σ_{10} is the maximum far-field principal stress. A. Illustration of the region surrounding the impending PIZ. The impending PIZ refers to the "relatively" aseismic zone within which the local tensile stress is increasing to a level sufficient to initiate the PIZ formation. Areas A_1 , A, and A_0 denote areas of the PIZ, focal region of the PIZ, and the anomalous (\equiv activation) region of the PIZ. The anomalous region also contains the focal region. B. The PIZ has formed. The seismicity, $n(t)$, decreases as the effective pressure increases and the shear stress decreases throughout the anomalous region surrounding the PIZ. C. Illustration of primary foreshock activity within the PIZ just prior to the mainshock. This foreshock activity is in response to crack coalescence within the PIZ.

Figure A3 - A. Plan view of PIZ, focal region, and anomalous region.

B. Expanded view of PIZ illustrating the essential characteristics of the seismic events (seven in total for illustrative purposes) that formed the PIZ. The anomalous zone, A_o^* , of each event refers to the total area fractured by the event. These events are characterized by no aftershocks.

Figure A4 - Illustration of abnormal behavior induced within the anomalous region by the formation of the PIZ. Arrows depict motion of material as the anomalous region (activation volume) stores energy preparatory to the mainshock. Distortional strain energy is converted into volumetric strain energy within the focal region during the preparation time τ_o . Stress, strain, and strain rate will remain at their "normal" background at distances removed from the activation volume by 3-4 times the average linear dimension of the activation volume, by virtue of St. Venant's principle. Outside the affected region, no effects of the impending failure will be detected.





SYMBOLS

Magnitude (mb)

0 - 1.0	□
1.0 - 2.0	●
2.0 - 3.0	△
3.0 - 4.0	+
4.0 - 5.0	x
5.0 - 6.0	◇

Events forming PIZ ○

Mainshock (3 October, 1974) ⊕

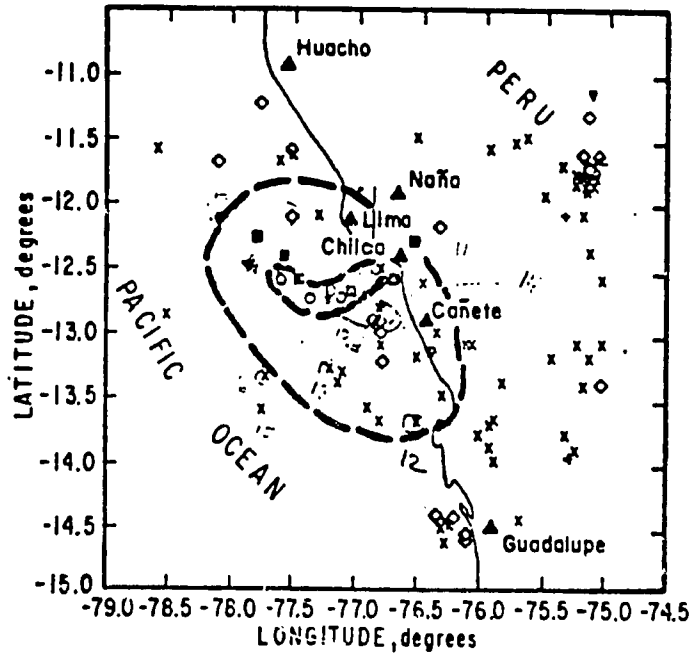
Foreshocks

24, December, 1973	}	⊗
26, July, 1974		
31, August, 1974		
27, September 1974		

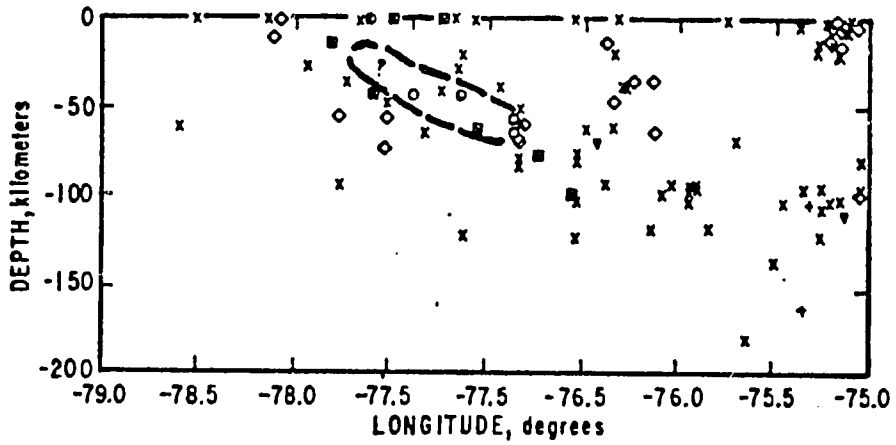
Other

5, January, 1974 ⊞

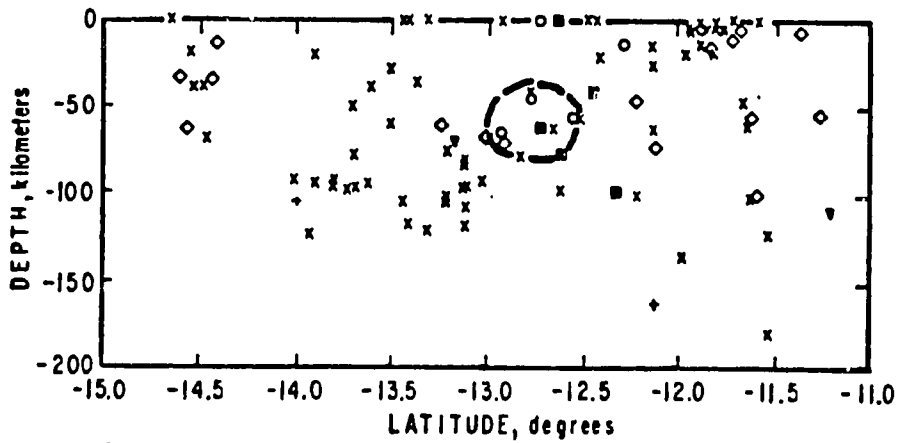
14, November, 1974 ⊠



A



B



C

FIGURE 4.

Handwritten notes or a stamp, partially illegible, located on the right side of the page.

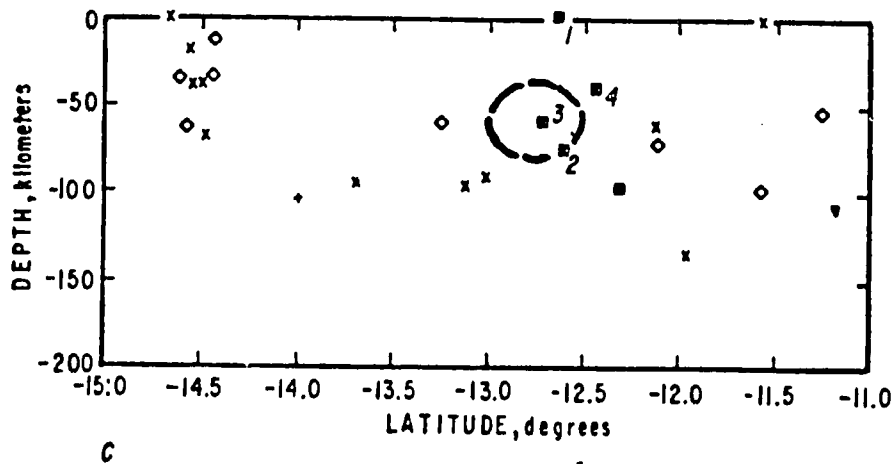
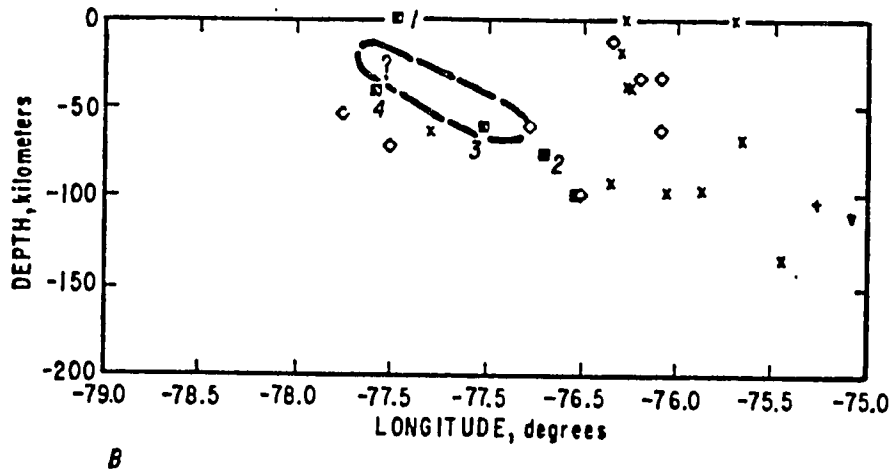
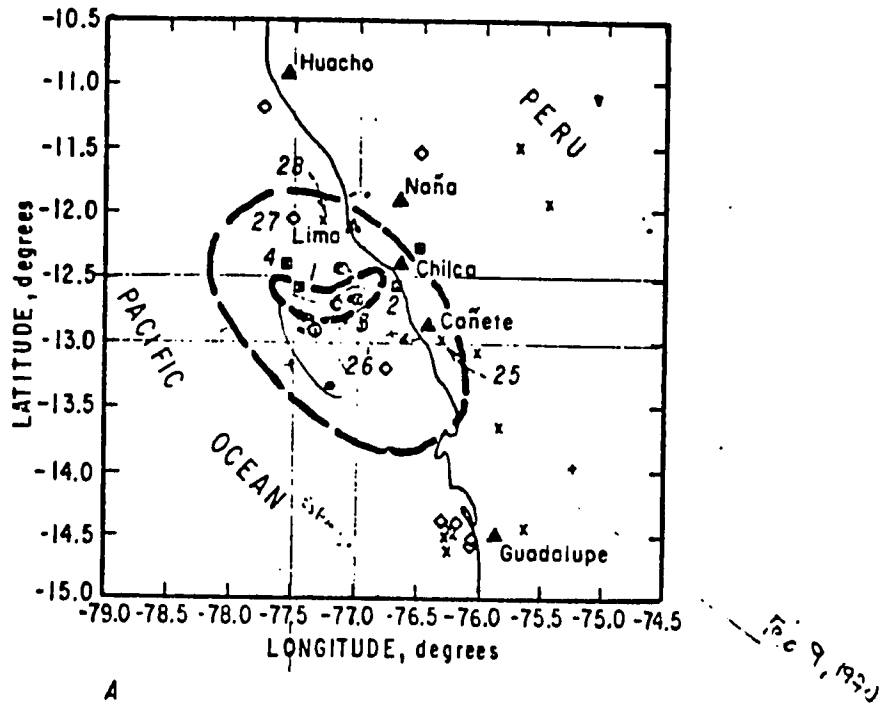
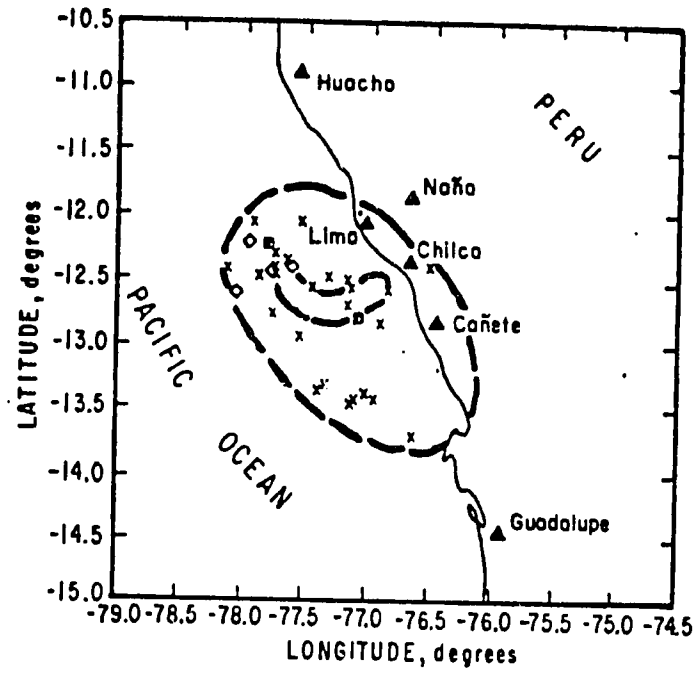
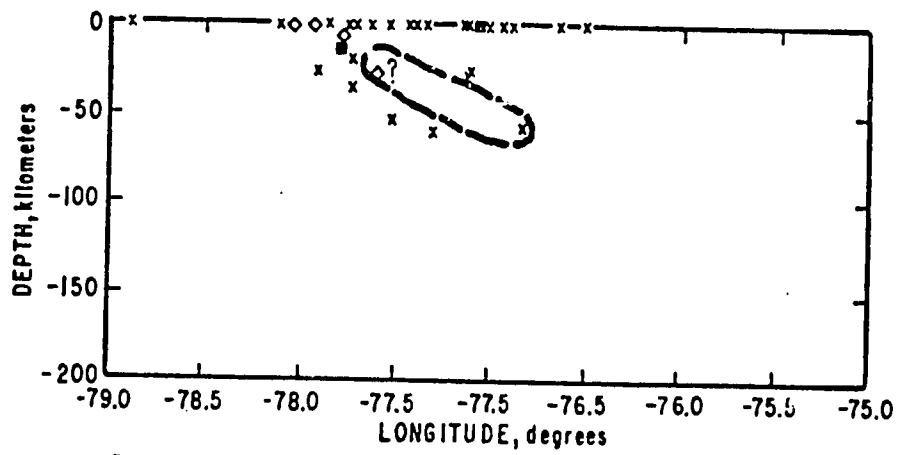


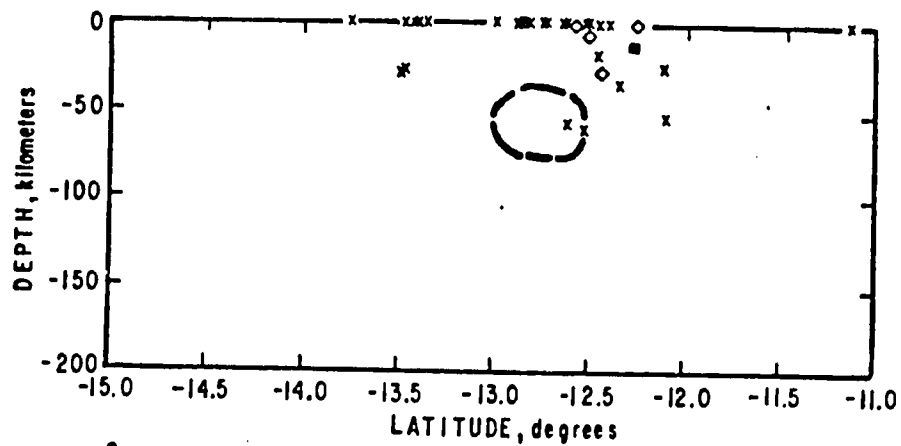
FIGURE 5.



A

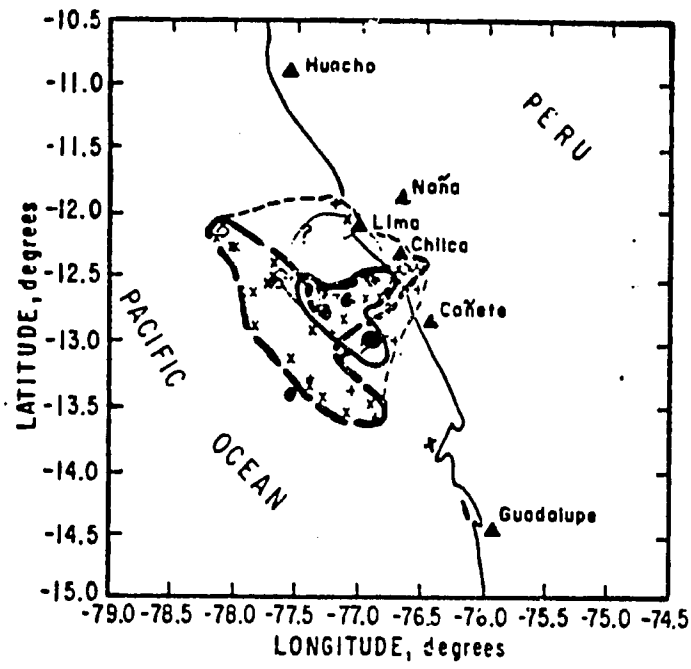


B

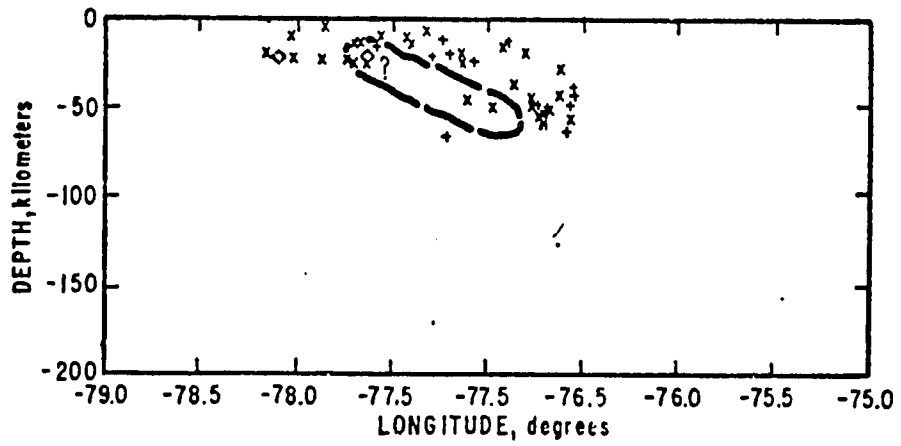


C

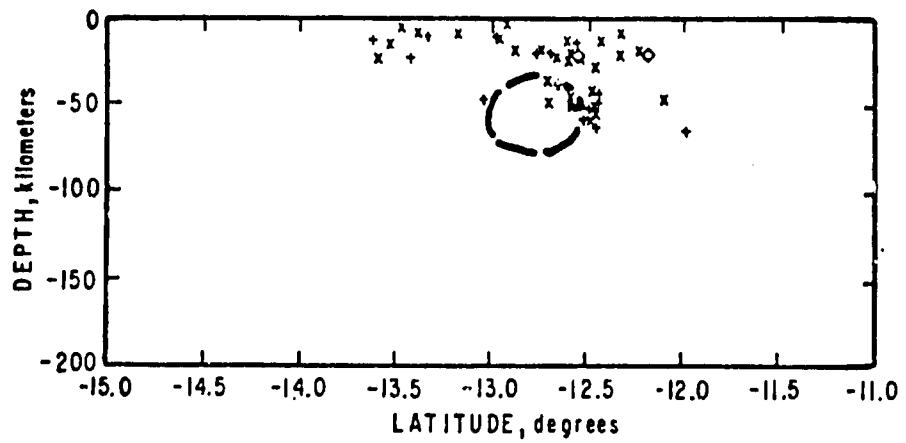
FIGURE 6.



A

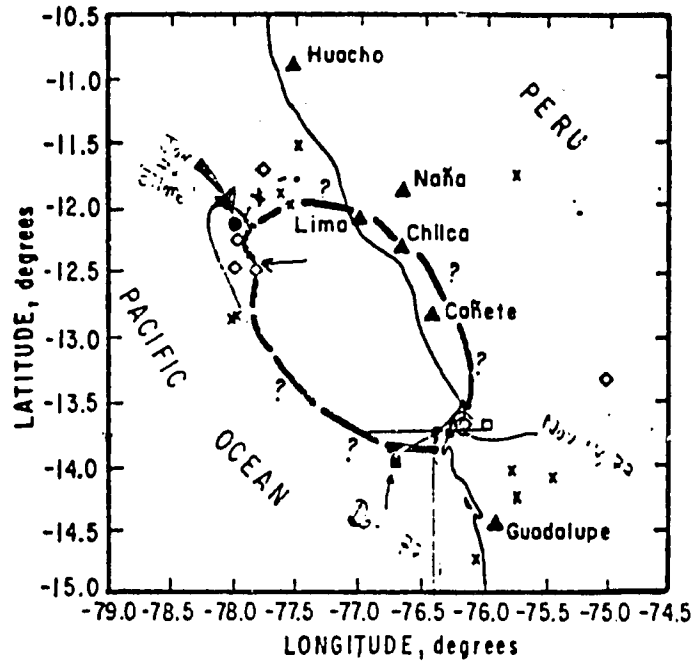


B

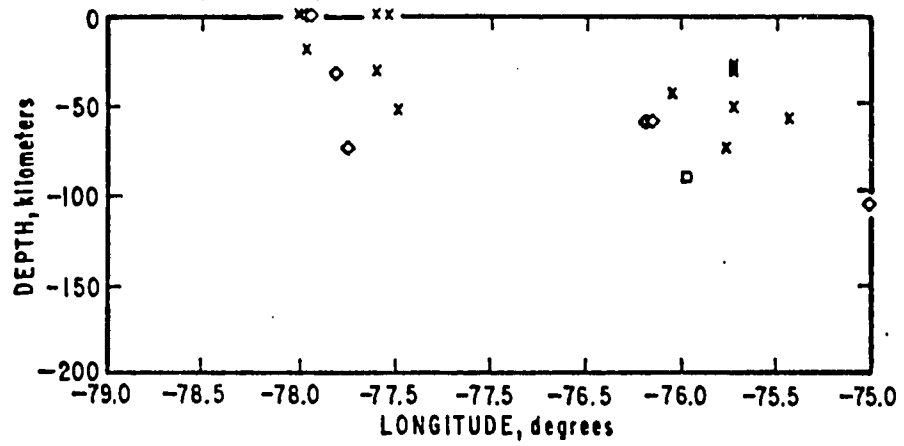


C

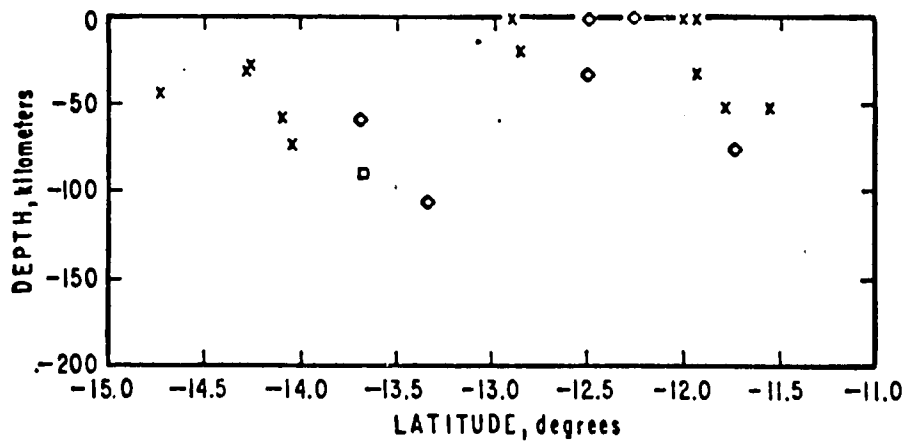
FIGURE 7.



A

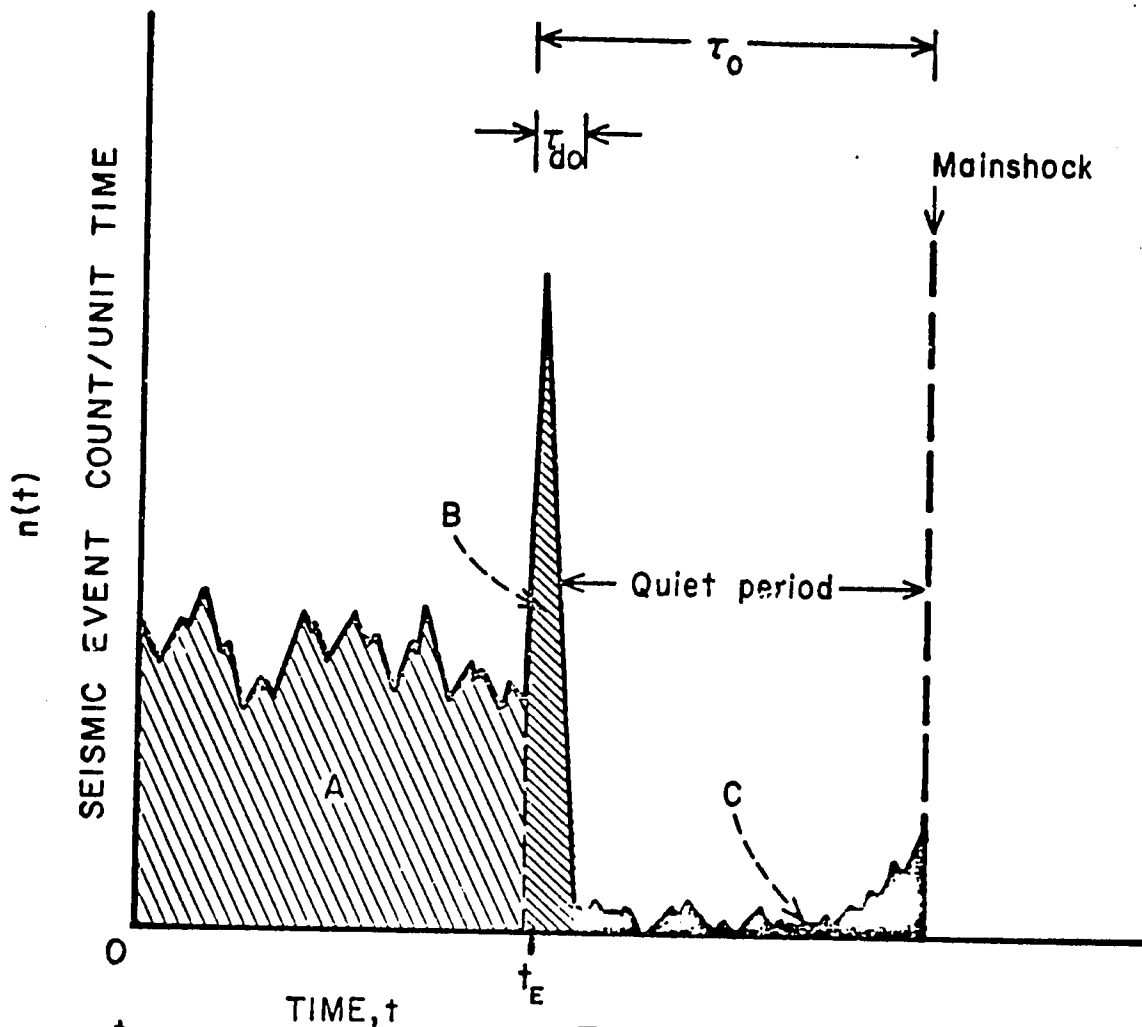


B



C

FIGURE 8.

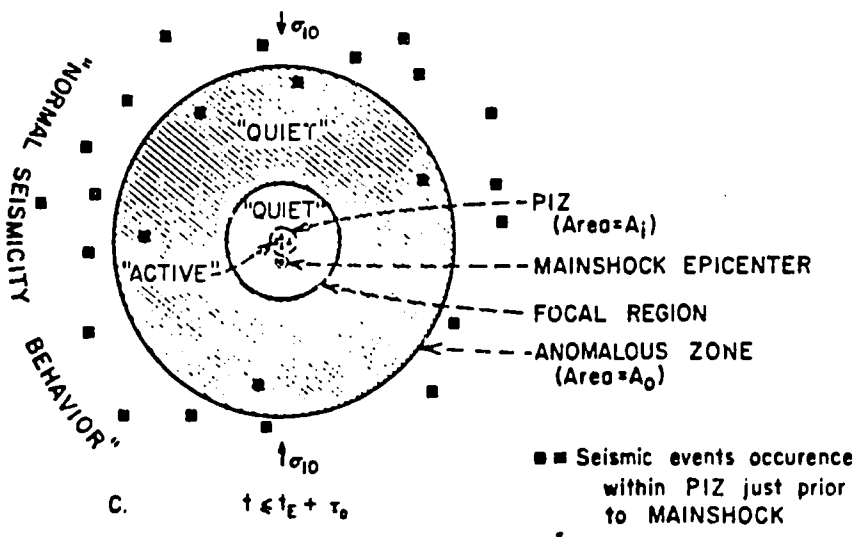
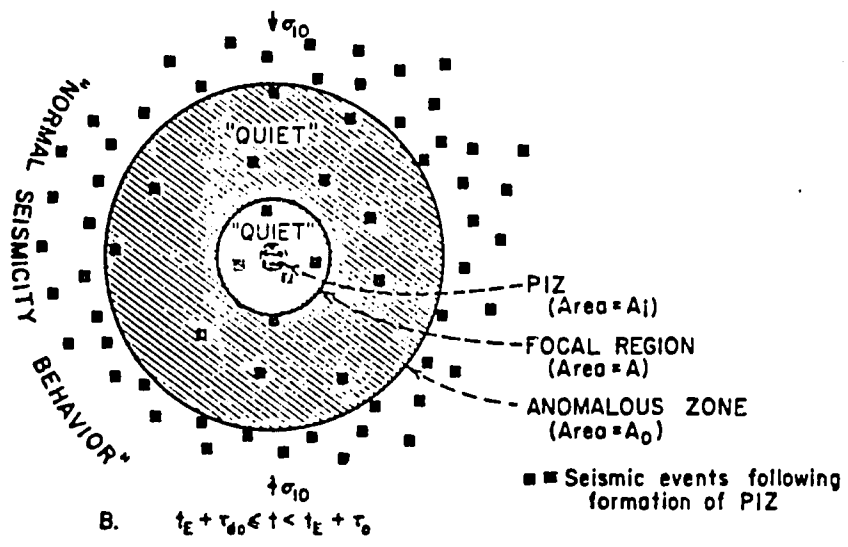
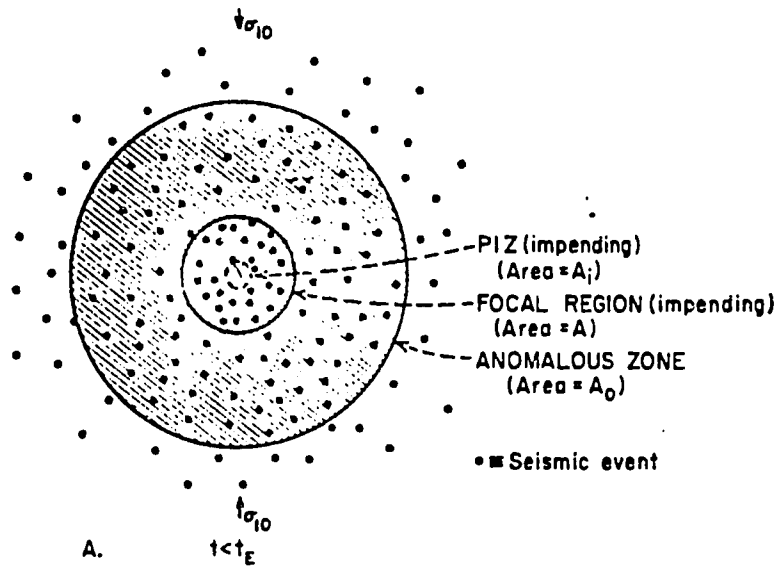


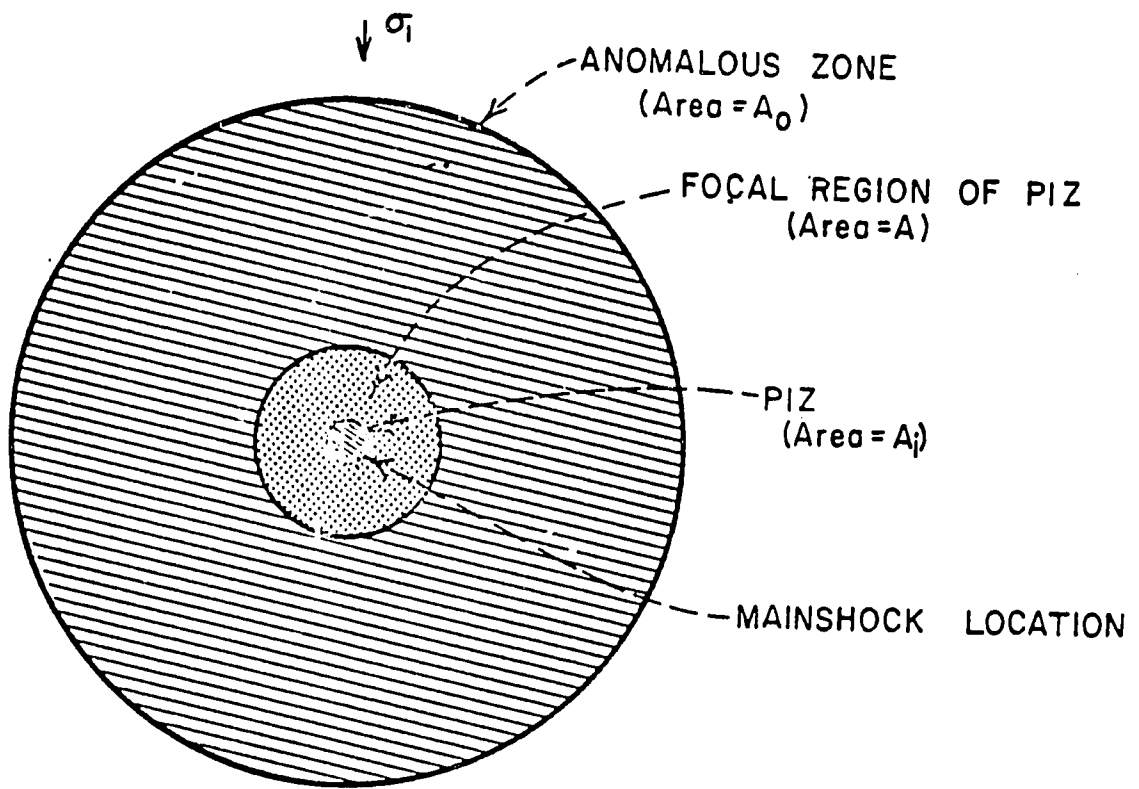
$$1. N_A = \int_0^{t_E} n(t) dt$$

$$2. N_B = \int_{t_E}^{t_{do}} n(t) dt$$

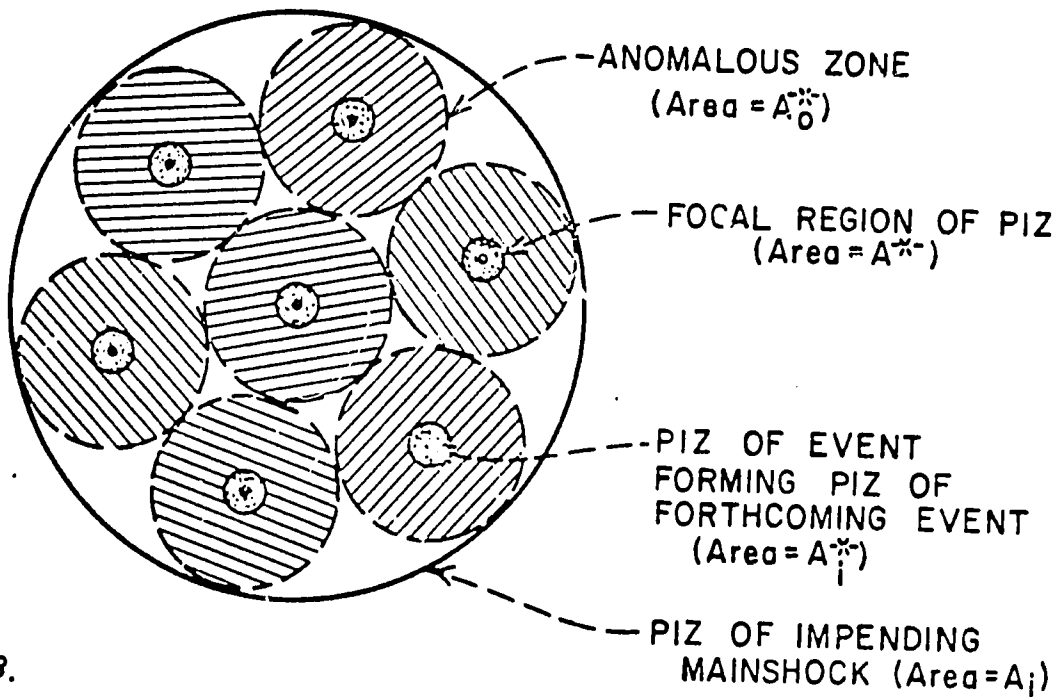
$$3. N_C = \int_{t_{do}}^{t_0} n(t) dt$$

$[n_B = n_A + \delta n; \delta n = \text{increment in seismic event count/unit time due to PIZ formation}]$

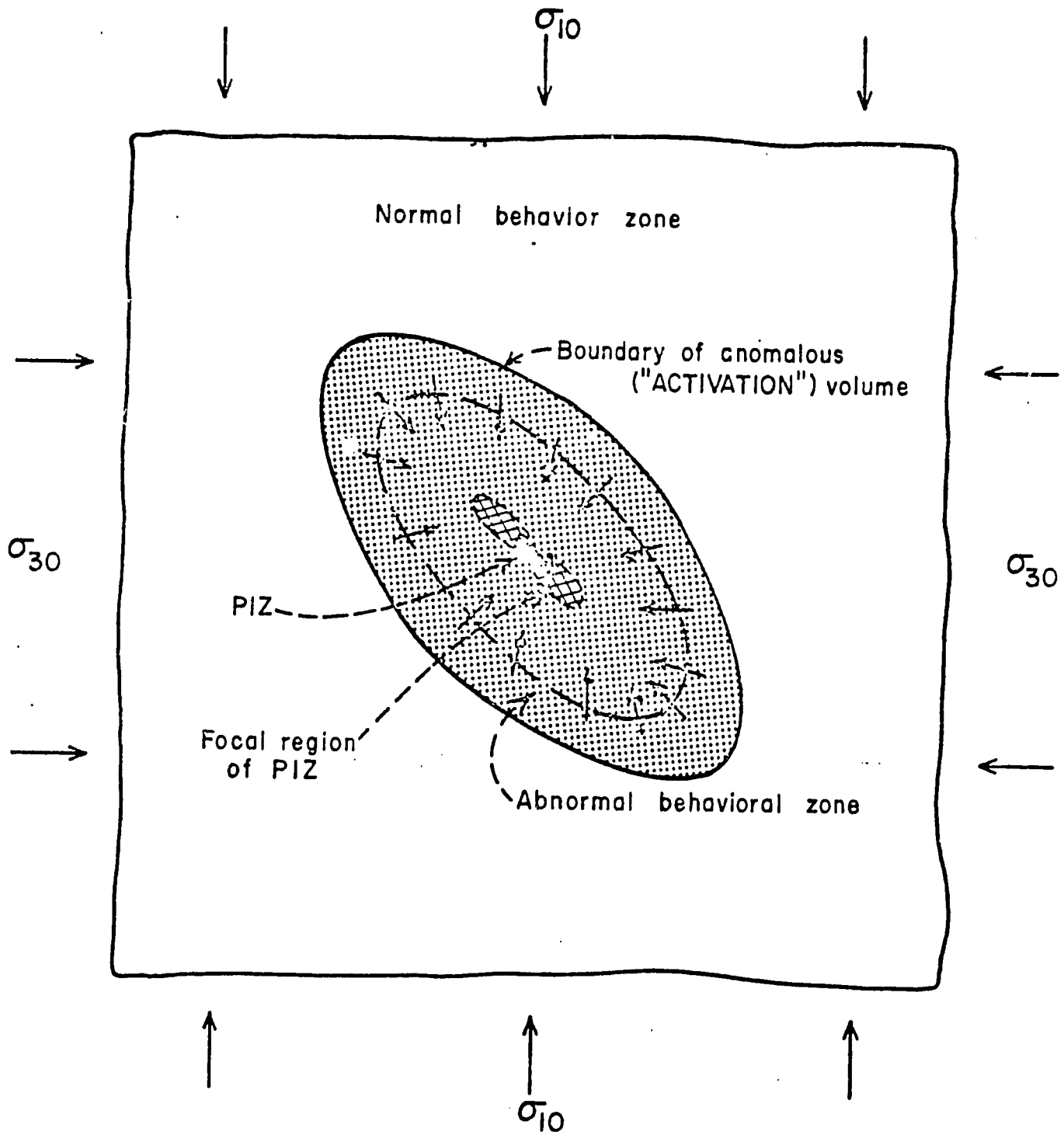




A.



B.



-  Aftershock region ("FOCAL REGION OF PIZ")
-  Implosion region ("STRAIN ENERGY STORAGE ZONE")
(Implosion region contains aftershock region)

THE LIMA EARTHQUAKE OF OCTOBER 3, 1974: INTENSITY DISTRIBUTION

BY A. F. ESPINOSA, R. HUSID, S. T. ALGERMISSEN, AND J. DE LAS CASAS

ABSTRACT

The epicenter of the October 3, 1974, earthquake was 80 km west of Lima at 12.2°S and 77.67°W. This earthquake caused severe damage in Lima and vicinity, producing a maximum Modified Mercalli intensity of IX in a few small scattered areas in Lima. The Modified Mercalli intensity in Lima varied from V to IX; in towns south of Lima the intensity exceeded VIII. The areas of high intensity, both in Lima and along the coast, appear to be related to unfavorable soil conditions or to a high water table, as is evident in the areas where large damage and/or differential settlement took place. Slumping was also observed along the coastal road south of Lima. In Callao differential earth settlement was associated with liquefaction of the soil. Pockets of high intensities, such as in the districts of La Molina and Chorrillos, are correlated with possible local ground-amplification effects. Subsidence of up to 35 cm took place in some areas along the wave-cut terrace in Miraflores, and 15 cm of subsidence was observed in Chorrillos. The isoseismal map constructed for Lima can be used in a preliminary zonation of Lima for potential earthquake effects.

INTRODUCTION

The earthquake of October 3, 1974 ($M_s = 7.6$) is one of many earthquakes that have been felt in Lima and vicinity, but this is the first to cause widespread damage to the city; others have caused slight or considerable damage. The definitions of slight, considerable, and severe damage used in this study conform with the definitions given by Medvedev (1968). The 1966 earthquake ($M_s = 7.5$) caused damage to Lima, but its epicentral distance was greater than that of the 1974 earthquake. A number of studies have been performed on previous earthquakes that have damaged Lima (Lomnitz and Cabre, 1968; Cluff, 1971; Lomnitz, 1970 and 1971; Berg and Husid, 1971; Cloud and Perez, 1971), but no attempt has been made to microzone the city for earthquake effects. The present study is an effort to evaluate the intensity distribution in Lima and its vicinity. The results of this investigation are given in a preliminary seismic zonation map of Lima. This map is similar to the seismic zoning maps prepared by the Russians (Medvedev, 1968).

REGIONAL SEISMICITY AND STRONG GROUND MOTIONS FELT IN METROPOLITAN LIMA

The October 3, 1974, earthquake epicenter was located 81 km west of Lima at 12.2°S. and 77.67°W. (U.S. Geological Survey, National Earthquake Information Service). This earthquake caused widespread damage in sections of metropolitan Lima and vicinity, and was felt over a wide area as far south as Arequipa. Prior to October 3, an earthquake occurred on January 5, 1974, which had a magnitude of 6.6 and an epicentral distance of 75 km. This earthquake caused some scattered damage and injuries and claimed several lives.

Other earthquakes in the past decade have been felt in Lima, but they have caused only slight or considerable damage to the city. Major earthquakes with focal depths ranging from the surface to nearly 90 km have occurred between the Peru-Chile trench and the coastal area of Peru. These earthquakes occasionally have produced

[NOTE: There is no page 822.]

tsunamis, landslides, and large-scale vertical deformations of the ground. The May 31, 1970, earthquake, for example, triggered a landslide that buried Yungay, a village in the valley of the Santa River (Plafker *et al.*, 1971; Silgado, 1973).

Strong-motion records of the October 3, 1974, earthquake were recorded at two sites, one in the central part of Lima and the other at the Huaco station southeast of the city. These recordings were made at epicentral distances of 81 and 83 km, and they show a number of interesting features: the long duration of shaking, the high accelerations, and high short-period energy. The predominant period determined from the response spectra for zero damping is about 0.38 sec. The predominant period in Lima, measured from the accelerograms of the earthquakes of October 17, 1966, May 31, 1970, and January 5, 1974, was in the range of 0.1 to 0.16 sec. The resultant maximum horizontal peak acceleration for the October 3, 1974, earthquake was 0.19 *g*. For comparison, the October 17, 1966, earthquake, with an epicenter located nearly three times farther from Lima than that of the October 3, 1974, earthquake, produced twice the maximum horizontal peak acceleration. The low attenuation of these signals at these distances implies a very high *Q* or low absorption of the seismic energy.

The predominant period of 0.38 sec (relatively long for Peruvian earthquakes) gives an indication of why single family dwellings and 1- or 2-story structures did not sustain more damage. Buildings in Lima with 3 to 5 stories have their fundamental period between 0.07 and 0.35 sec; those with 6 to 12 stories between 0.2 and 0.6 sec; and those with 12 to 22 stories between 0.6 and 1.4 sec (W. K. Cloud, written communication, 1975). Thus a predominant period of 0.38 sec will most likely affect those structures having 5 to 12 stories. Most of the structures that sustained severe damage (Husid *et al.*, 1977) were buildings of 3 or more stories and 1 or 2 stories of adobe and quincha-type construction. Many reinforced concrete structures sustained a high degree of damage. For example, northeast of Lima, in La Molina, several reinforced concrete structures sustained severe damage and partially collapsed. To the east, in Los Próceres, several 5-story frame reinforced concrete buildings sustained severe damage, and in La Campiña a 3-story reinforced concrete structure partially collapsed. To the northwest of Lima, in Callao, a 4-story reinforced concrete building collapsed. In this district there is a large amount of landfill, and the sediments are water saturated. One of the possible reasons for the collapse of this 4-story structure could have been a combination of poor construction and an amplification effect of seismic waves in the area. Similar amplification effects were found in Caraballeda, Venezuela (Espinosa and Algermissen, 1972), where several reinforced concrete structures were extensively damaged.

INTENSITY DISTRIBUTION IN LIMA AND VICINITY

A general surficial geology of Lima and vicinity (A. Martinez, written communication, 1974) is shown in Figure 1. Lima proper is on Quaternary alluvial deposits, and the depth to crystalline rock is shown in Figure 2 (A. Martinez, written communication, 1974).

A number of well logs give a general lithological description of the material underlying Lima, but no detailed description of the surficial geology is available.

Figure 3 shows a map of metropolitan Lima and some of its most important streets. The black dots in this figure represent the locations at which intensities were determined from questionnaires in a survey. The questionnaires used in the field were a Spanish translation of the U.S. Geological Survey "Earthquake Report," which pertains to intensities. The answers to the questionnaires were systematically ob-

tained throughout the city, which had been methodically divided into a number of sectors. These sectors were sampled for a period of 10 days and the questionnaires collected were used as the data base in this study. The questionnaires were rated using the version of the Modified Mercalli Intensity Scale of 1931 proposed by Richter (1958). A total of 400 observations was obtained in the city. Sixty-five observations of intensity were noted to the south along the coast to Cafete, to the north to Ancon, and to the east to Chosica.

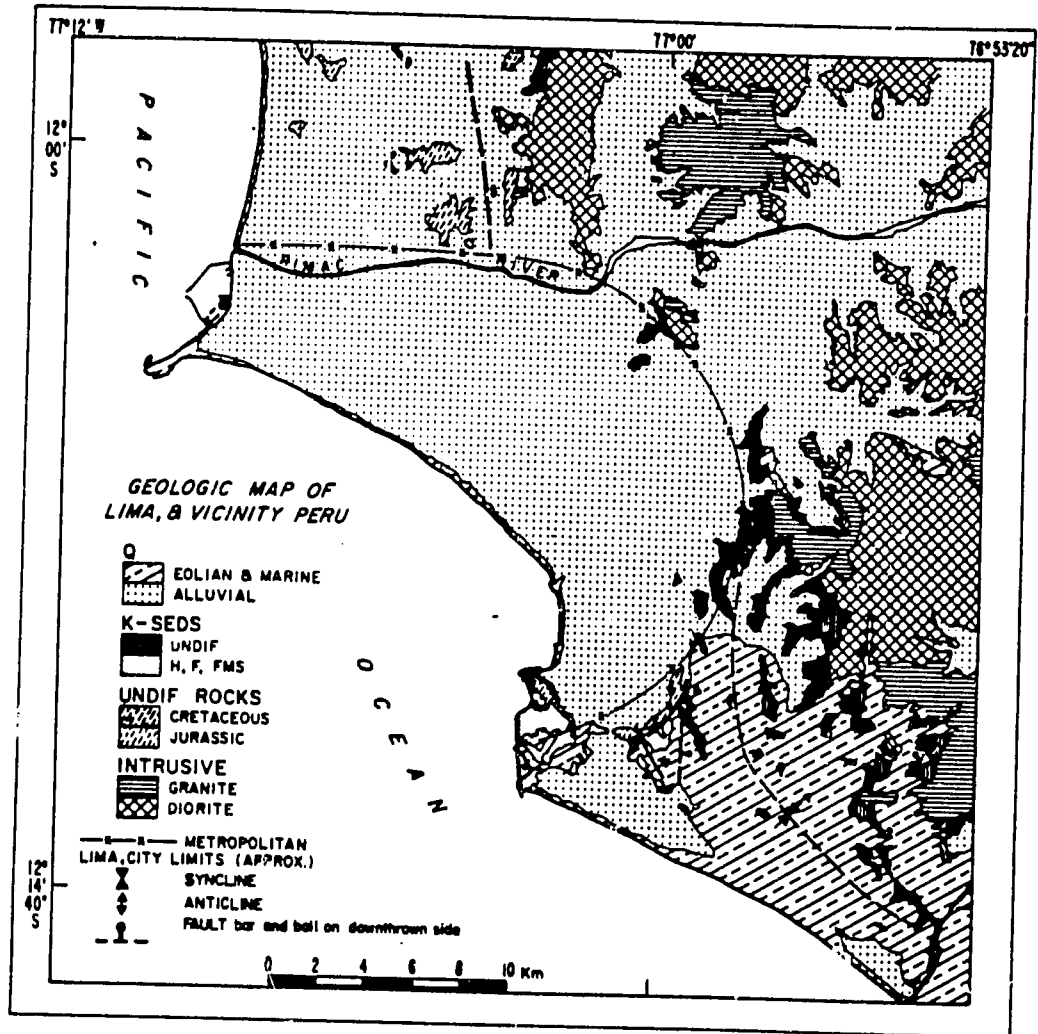


FIG. 1. Surficial geology map of Lima and vicinity. Modified from Martinez.

Metropolitan Lima was subdivided into a grid map of areas 200 by 200 m, and the intensity questionnaires of felt intensity IV or greater in each segment were recorded and plotted. This map was overlaid on a similar map, as shown in Figure 3. After the intensities were plotted, an isoseismal map was drawn, as shown in Figure 4. This map shows the intensity distribution in metropolitan Lima, and it could be used as a preliminary map for seismic zoning and land use planning. The highest MMI (Modified Mercalli intensity) in Lima was IX.

Intensity IX was observed in the districts of Callao, Barranco, La Molina, and Lima. The distribution of intensities in these districts is very diversified, and this

may be due in part to the different types of structures (Husid *et al.*, 1977) and to possible localized ground amplification effects found in metropolitan Lima. The intensity of shaking, shown in Figure 4, varies from V to IX. The overall picture shows high intensities in different districts of Lima.

High-rise structures are not distributed uniformly throughout the city. A number of the districts are residential with mixed type of construction; for example, in the Miraflores district there are a number of adobe, masonry, and reinforced concrete structures. In Callao there are adobe, quincha, masonry, frame reinforced concrete

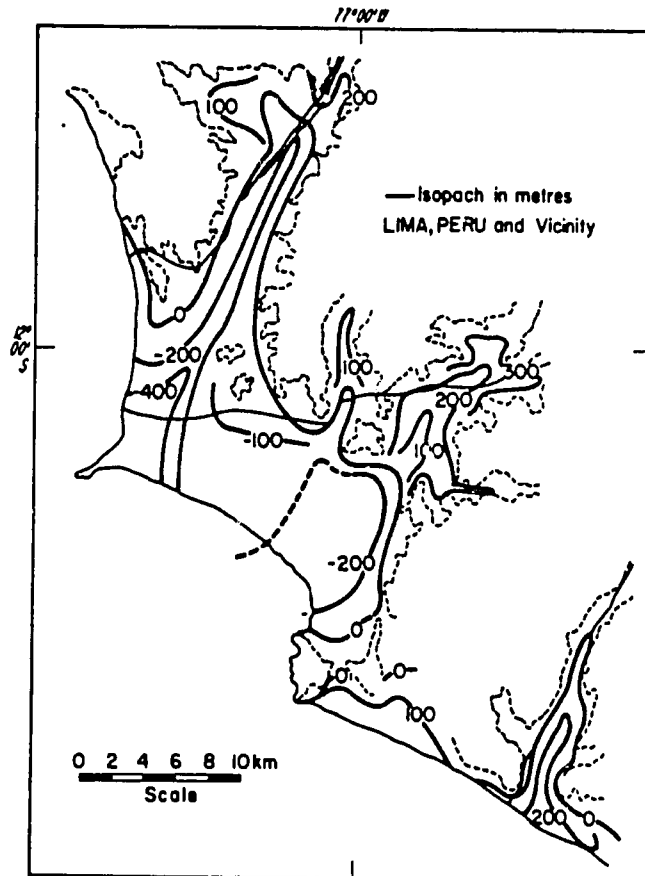


FIG. 2. Isopach contour map of Quaternary deposits of Lima. Contour interval, 100 and 200 meters. Modified from Martinez.

and frame brick-filled type of construction. Some of these structures sustained considerable damage. Other areas which sustained high intensities of shaking were in La Campiña, Los Proceres, and at the National University of Engineering in the Rimac district.

The procedure used in constructing the isoseismal map of Lima, described above, is similar to the seismic zoning maps prepared by some scientists of the Russian Academy of Sciences (Medvedev, 1968). However, Figure 4 is a larger scale map.

The intensity distribution map of metropolitan Lima (Figure 4) and the generalized damage contour map (Figure 26, Husid *et al.*, 1977) give an assessment of the seismic risk in Lima. The MMI distribution in Lima followed a pattern which can, in some instances, be correlated with the local surficial geology.

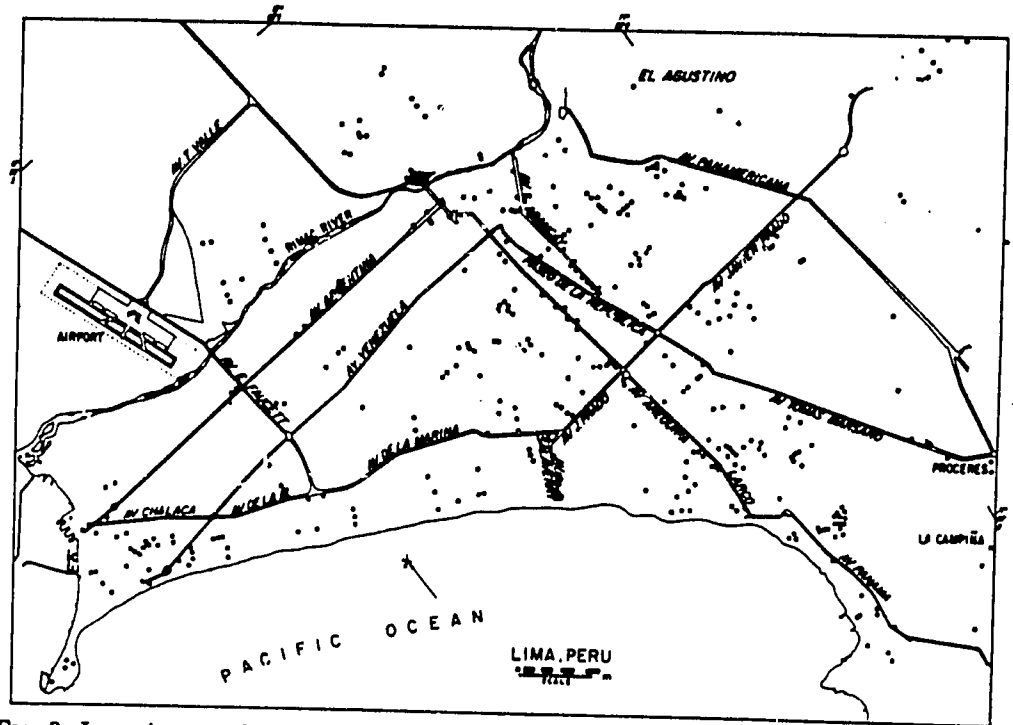


FIG. 3. Intensity sampling distribution. Each dot represents a questionnaire recorded from a survey taken in metropolitan Lima, Peru.

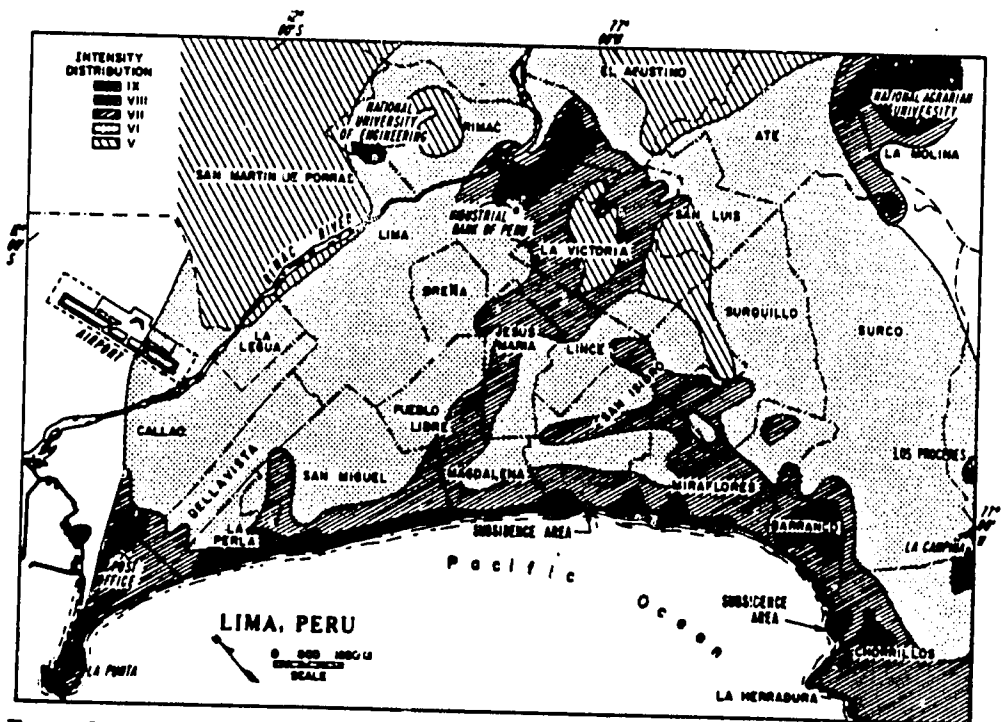


FIG. 4. Modified Mercalli Intensity distribution in Lima from October 3, 1974, earthquake.

The following sections describe the intensity observations by districts in metropolitan Lima and vicinity.

CHORRILLOS AND BARRANCO DISTRICTS

The coastal region of the city, from La Punta in Callao to the Chorrillos district in the southeast part of the city, was assigned an intensity rating of VIII. In this area, well-designed and constructed buildings were found to have negligible damage and well-built ordinary structures had only slight damage. In the Barranco and Chorrillos districts, there was a considerable amount of damage to adobe and quincha construction. This type of construction is inadequately built and/or badly designed.

A localized high-intensity effect was observed at the Colegio Chalet, a school in the Chorrillos district, where small landslides took place and a number of reinforced concrete structures sustained severe damage. Two reinforced concrete buildings in this school showed large, deep cracks and breaks in walls, collapsed walls, broken connections between buildings, fallen parapets, fallen plaster, collapse of inner walls, and cracks on the reinforced concrete beams. This school is located near the edge of wave-cut terraces in Chorrillos. These terraces are nearly 42 m above the beach and are bordered by steep slopes. There was also a large area in which a subsidence of 15 cm occurred.

In the school yard, one marble statue 180 cm high, standing on a pedestal 150 cm high and 90 cm wide, was displaced laterally 3.5 cm away from the coast. The statue weighed 1,000 kg. Another statue, 22 cm in diameter and 110 cm in height, weighing approximately 180 kg, which was set in a niche about 300 cm above the ground, was overthrown and fell to the ground. The 1965 and 1970 earthquakes did not move or overturn these statues, even though their epicentral distances were 160 and 360 km and their peak accelerations were 0.40 and 0.13 *g*, respectively. These accelerations were, respectively, higher than and similar to those of the October 3, 1974, earthquake.

The lower bound computation for the acceleration to slide an object weighing 1,000 kg is 0.7 *g*. This value was computed under static conditions (Krishna *et al.*, 1973). This acceleration is about three times the horizontal acceleration recorded in the center of Lima on a strong-motion accelerometer. Thus, there appears to have been an amplification of about three times at the school. The lithology of this area is not very well known; however, a few drillings show the depth of the water table to be less than 10 m. A number of springs in the Chorrillos and Barranco districts have been mapped (A. Martinez, written communication, 1975); they occur on the vertical side of the wave-cut terrace in these districts.

The amplification effect becomes very pronounced, especially when a low-rigidity layer (water table) allows some of the high-frequency energy to be trapped in the upper layers. This may explain the apparently very large strong motions experienced in the Chorrillos and Barranco districts.

SAN ISIDRO, LINCE, AND MIRAFLORES DISTRICTS

The area within the intensity VII isoseismal follows a trend from Miraflores into the San Isidro and Lince districts. This high-intensity distribution could possibly be correlated with the depth of the water table or with old irrigation channels that existed in this region. The colonial city of Lima used to be concentrated in what is today the Lima district. Callao, Miraflores, La Molina, Chorrillos, etc. were small villages, and the land between these towns remained farming areas until the first

quarter of this century. This area formerly had an old system of irrigation channels, which followed the geomorphological features of the valley, and some of these channels extended in the general direction of the maximum intensity VII rating in this region. Close examination of the hydrogeologic map of metropolitan Lima (Morales and Vancon, 1971) shows two channels; one of them is in the same general area where the intensity VII isoseismal is located. If one superimposes the intensity distribution map on the hydrogeologic map of Lima, it shows a close correlation with one of the water channels. The hydrogeologic map also shows the depth of the water table and springs in the region. There are a number of springs in the Chorrillos, Barranco, and



FIG. 5. Subsidence in the Miraflores District; scale being used shows 35-cm offset.

Miraflores districts. The water table in the Chorrillos and Barranco is shallow; in some areas it is less than 10 m deep.

Farther along the wave-cut terrace, between the Miraflores and San Isidro districts, subsidence of up to 3⁷ cm occurred (see Figures 4 and 5). Some slight damage was observed in brick construction; however, a wood-frame 1-story house, which was located at the inner part of the subsidence area, showed a great deal of deformation. Adjacent to this house, brick structures sustained slight damage.

LIMA DISTRICT

In downtown Lima the MMI rating was VIII. In this part of the city, a number of adobe and quincha structures sustained severe damage, and reinforced concrete structures were slightly or moderately damaged. There were a number of reports of overturned furniture, fallen plaster, and "felt observations" by persons driving automobiles. The earthquake was strongly felt in this localized central area; it caused people to run out-of-doors and frightened everyone in the community. A number of inade-

quately built houses on the banks of the Rimac River suffered moderate damage. The National University of Engineering in Lima sustained moderate damage to brick and reinforced concrete structures.

ATE AND LA MOLINA DISTRICTS

Other suburbs heavily damaged by this earthquake were Ate and La Molina. In particular, La Molina was damaged the most and was assigned a MMI rating of IX. Persons driving automobiles were disturbed and some panicked. The earthquake moved and overturned very heavy furniture, and there was severe damage to a number of well-constructed buildings.

As can be seen in Figure 4, there is a localized maximum of the intensity rating in the Chorrillos and La Molina districts. Other studies of ground amplification (Espinosa and Algermissen, 1972; Hays, 1972; Perkins *et al.*, 1972; Borchardt *et al.*, 1975) have shown, in some cases, a simple correlation between seismic-wave amplification and local geology. In particular, Espinosa and Algermissen (1972) have shown for the Caracas Valley that the observed amplification could be explained by a horizontal layered model without recourse to hysteretic or dissipative parameters. In that work, seismic-wave amplification for shear waves was of the order of 4 to 6 times. A significant effort has been directed toward understanding ground-amplification effects in non-dissipative surficial-earth models. Some of the results obtained thus far have shown, in the time- or frequency-domain, that surficial-earth layers cause an amplification effect when they have a mismatch of the "shear-impedance." This effect increases as the shear-impedance mismatch increases, and the layer thickness controls the dominant resonant frequency. By shear-impedance mismatch is meant the inequality between two units the value of which is the product of the shear-wave velocity times the density of the layers considered ($\beta_1\rho_1 \ll \beta_2\rho_2$). As the layer thickness increases, there is a relative shift of the amplification effect to lower frequencies (Espinosa and Algermissen, 1972).

La Molina district is located in a semi-elliptically shaped alluvial valley, and the soils are less competent than in other parts of Lima. They are composed of clays, soft clays, and loose sandy soils (Lee and Monge, 1968; A. Martinez, written communication, 1975). It is in this area that the intensity increases to IX, which could be due to a focusing effect that can cause a concentration of energy and to a constructive interference of seismic waves caused by the geometry of the valley.

SAN MARTIN DE PORRAS DISTRICT

The intensities in other districts in the city were V and VI. A curious effect was observed in the San Martin de Porras district, where a number of people reported only slight excitement and few ran outdoors. There were cracked windows; small objects were moved; buildings trembled; but there was no observed or reported damage, even to adobe houses. However, less than 2 km away in a northeast direction, there was moderate damage and excitement in the area; the intensity rating was VIII.

INTENSITY DISTRIBUTION IN VILLAGES AND COASTAL TOWNS AROUND LIMA

Figure 6 indicates the distribution of intensities in the coastal area of Peru, together with the epicenter reported by the National Earthquake Information Service of the U.S. Geological Survey. The number of intensity observations is shown in parenthesis after the name of the town, and the average intensity rating is shown in roman numerals. A field survey of intensity and damage was undertaken as far north

of Lima as Ancon, as far south of Lima as Cañete, and as far east of Lima as Chosica. Information for Chinchua, Paracas, and Ica were obtained in Lima from people who answered questionnaires and who were in those towns at the time of the earthquake.

The distribution of intensity ratings is variable owing to the sampling procedure and to the local conditions. For example, in San Luis, the intensity rating was VIII. In this town the people were frightened and alarmed; trees were shaken strongly; temporary changes in flow of spring water were reported; and considerable damage to quincha and reinforced concrete structures occurred. A large portion of the town's adobe houses were devastated. In the outskirts of San Luis, mud spouts and differential earth movement in cultivated fields due to liquefaction of the soil were reported.

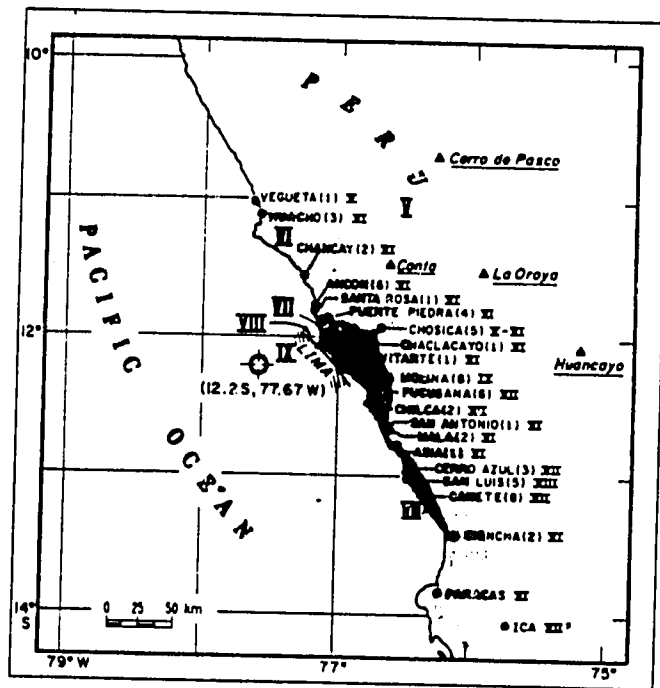


FIG. 6. Modified Mercalli Intensity distribution of the October 3, 1974, earthquake, shown by Roman numerals; number in parentheses indicates the number of observations at each indicated town. Circle with cross is the epicenter location of the October 3, 1974, earthquake.

The town of Turin and its surrounding areas, located about 12 km south of the Chorrillos district, were badly damaged. Between 80 and 90 per cent of the buildings collapsed or were severely damaged. Some reinforced concrete structures in Turin, such as the school buildings sustained severe damage (M. Corrao, written communication, 1976).

South in the town of Cañete, houses of adobe and quincha construction sustained serious damage, and a large number of them collapsed. In Cañete, well-built masonry and reinforced concrete structures were slightly damaged. There was general alarm, however. All the people ran out-of-doors; some people reported difficulty in standing; and a number reported that suspended objects were set in motion. The localized high-intensity ratings correlate with features of the local geology and with a high water table in some cases, such as occurred in the town of San Luis. Slumping was observed on the Pan American highway south of Lima on several places.

CONCLUSIONS

The October 3, 1974, earthquake presented the opportunity to conduct a field study of the distribution of intensity, damage, and strong motion in an area that has sustained slight and moderate damage from previous earthquakes. The results obtained from this field evaluation of the intensity and strong motions are as follows:

1. The intensity distribution in metropolitan Lima ranged from a MMI rating of V up to IX.

2. There is a definite correlation of high-intensity ratings with areas that have a high water table and springs such as occur in the southern part of Barranco and Chorrillos districts.

3. The isoseismal for an intensity VII in the Miraflores and San Isidro districts correlates with an area that once contained a large water irrigation channel.

4. The highest intensity outside Lima was VIII at San Luis, located about 160 km from the epicenter.

5. The general consensus of numerous individuals interviewed in the canvassing of Lima and vicinity is that this earthquake (October 3, 1974) was stronger and that the duration of shaking was longer than those of previous earthquakes (1940, 1966, 1970).

6. The highest intensity rating in Callao was IX at the Navy Yard in La Punta. Two other areas experienced an intensity of IX: Chorrillos and La Molina. It was reported that intensities are almost always higher in the La Molina district.

7. The results from the field canvassing conducted just after a destructive earthquake suggest that it is possible to microzone earthquake effects in a large city in a rather short period of time, provided the canvassing is systematic and the collected data is obtained homogeneously throughout the area.

8. The intensity amplification observed in greater Lima and vicinity is attributed to the amplification of incident seismic waves by the local surface-soil conditions and the depth of the water table. We recommend that detailed studies of some of the past destructive Peruvian earthquakes be carried out to properly document the intensity and damage distribution in Lima. This data will provide information on the dependence of intensity on magnitude and distance.

ACKNOWLEDGMENTS

We gratefully acknowledge the assistance and support given to us by the following individuals and institutions:

Prof. A. Martínez, head of the Geology Department, National University of Engineering (UNI), provided the authors with maps and information personally collected and unpublished at the time of the mission. Prof. L. Zapata, from the Civil Engineering Department (UNI), assisted the two senior authors during the intensity survey of Lima. Dr. E. Silgado from CERESIS provided information pertinent to intensities in Lima and vicinity. Mr. R. Brazee from EDS helped to rate a number of questionnaires obtained in Lima. Dr. J. Berrocal, Ing. E. Deza, and Ing. P. Huaco, from the Instituto Geofísico del Perú, gave us support at the beginning of our study in Lima, Peru. Ing. O. Maggiolo provided unpublished information about the soil conditions in Lima.

Dr. A. Quesada, from the Organization of American States, provided partial funds for our field study in Peru. Prof. G. Bollinger, Drs. A. Rogers, R. Page, W. W. Hays, and R. B. Mathiesen critically reviewed the manuscript and offered valuable comments and suggestions. Mr. W. K. Cloud provided us with his unpublished data which we have used in this study. Professors M. Corazao of the Catholic University of Peru, B. Arbulú of UNI, J. Roesset of Massachusetts Institute of Technology, A. Veletsos of Rice University, R. Hanson and G. Berg of the University of Michigan critically reviewed this manuscript and provided many suggestions.

REFERENCES

- Berg, G. and R. Husid (1971). Structural effects of the Peru earthquake; Special Papers on the May 31, 1970, Peru earthquake, *Bull. Seism. Soc. Am.* 61, 613-631.
- Borcherdt, R. D., D. M. Boore, E. E. Brabb, R. D. Brown, J. H. Dieterich, J. F. Gibbs, E. J. Helley, W. B. Joyner, K. R. Lajoie, D. R. Nichols, T. H. Nilsen, R. A. Page, R. E. Warrick, C. M. Wentworth, R. L. Wesson, and T. L. Youd (1975). A preliminary analysis of seismic zonation in the San Francisco Bay region, *U.S. Geological Survey Prof. Paper 841-A*.
- Cloud, W. K. and V. Perez (1971). Unusual accelerograms recorded at Lima, Peru, *Bull. Seism. Soc. Am.* 61, 633-640.
- Cluff, J. S. (1971). Peru earthquake of May 31, 1970, engineering geology observations, *Bull. Seism. Soc. Am.* 61, 511-534.
- Espinosa, A. F. and S. T. Algermissen, (1972). A study of soil amplification factors in earthquake damage areas—Caracas, Venezuela, *NOAA Tech. Report ERL 280-ESL 31*, U.S. Dept. of Commerce, 201 pp.
- Hays, W. W. (1972). Examples of the effect of source and recording site parameters on the seismic response observed from plowshare projects—GASBUGGY and RULISON, *Geophysics* 37, 288.
- Husid, R., A. F. Espinosa, and J. de las Casas, (1977). The Lima earthquake of October 3, 1974, damage distribution, *Bull. Seism. Soc. Am.* 67, 1441-1472.
- Krishna, J., A. A. Arya, and K. Kumar (1973). Determination of isoacceleration lines by sliding and overturning of objects, World Conference on Earthquake Engineering, 5th, Paper No. 158.
- Lee, K. L. and J. E. Monge (1968). Effects of soil conditions on damage in the Peru earthquake of October 17, 1966, *Bull. Seism. Soc. Am.* 58, 937-962.
- Lomnitz, C. (1970). The Peru earthquake of May 31, 1970, *Bull. Seism. Soc. Am.* 60, 1413-1416.
- Lomnitz, C. (1971). The Peru earthquake of May 31, 1970: Some preliminary seismological results, *Bull. Seism. Soc. Am.* 61, 535-543.
- Lomnitz, C. and R. Cabre (1968). The Peru earthquake of October 17, 1966, *Bull. Seism. Soc. Am.* 58, 645-661.
- Medvedev, S. F. (1968). *Seismic Zoning of the USSR*, Akad. Nauk. SSSR, 533 pp. (Translation available from U.S. Dept. of Commerce, 1976).
- Morales, A. A. and J. P. Vancon (1971). Hydrogeologic map of Lima, Ministerio de Agricultura, Direccion de Aguas y Distritos de Riego, Lima, Peru.
- Perkins, D. M., S. T. Harding, K. W. Campbell, and A. F. Espinosa (1972). Studies of site amplification in San Fernando, *Proceedings of the International Conference on Microzonation for Safer Construction*, 1, 911-928.
- Plafker, G., G. E. Ericksen, and J. Fernandez Concha (1971). Geological aspects of the May 31, 1970, Peru earthquake, *Bull. Seism. Soc. Am.* 61, 543-578.
- Richter, C. (1958). *Elementary Seismology*, Freeman, San Francisco, 768 pp.
- Silgado, E. (1973). Historia de los sismos mas notables ocurridos en el Peru 1555-1970, *Geofis. Panam.* 2, 179-243.

OFFICE OF EARTHQUAKE STUDIES
 U.S. GEOLOGICAL SURVEY
 DENVER FEDERAL CENTER
 DENVER, COLORADO 80225 (A.F.E., R.H., S.T.A.)

UNIVERSIDAD NACIONAL DE INGENIERIA
 DEPARTAMENTO DE INGENIERIA CIVIL
 LIMA, PERU (J.d.I.C.)

Manuscript received April 7, 1976

THE EFFECT OF STRESS ON RADON EMANATION FROM ROCK

by

R. F. Holub and B. T. Brady

Abstract

A uranium bearing granitic rock of known radon emanation has been deformed to failure under uniaxial stress. Radon emanation and micro-crack activity (seismicity) were recorded continuously during the test. Radon concentration in the closed system was measured by alpha detector. The system was designed with a large diffusion leak to optimize the sensitivity and response time. A decrease in emanation was observed during the initial loading of the sample and is interpreted as associated with the closure of pre-existing cracks within the rock. At a uniaxial stress equal to approximately one-half the ultimate strength, a temporary increase (30%) in the radon emanation is observed that is correlated with an increase in seismicity within the sample. When the stress is removed for several hours, the original emanation is restored. However, once the specimen failed a temporary emanation increase of 90% was observed. The emanation then decreased to a level nearly 5% greater than the pre-failed specimen emanation. Implications of these test results to failure related phenomena such as earthquakes are discussed.

Introduction

Radon emanation from rock has been extensively studied from many different aspects in recent years. A comprehensive review of this sub-

ject is available from the U. S. Bureau of Mines (Austin and Drouillard, 1978). As a rule, previous studies of radon emanation from rock have neglected the influence of stress on the emanation process. A notable exception is that of Newby (1973) who, using a high grade ore rock, investigated the effect of uniaxial stress on the radon emanation coefficient. Emanation coefficient is defined as a fraction of radon produced in the specimen that gets out of the specimen. Newby found that the application of uniaxial stress resulted in a temporary increase (500%) of the emanation coefficient. After a few days, the coefficient decreased to a value 30% lower than the initial one. He attributed the lowered rate to the closing of cracks already present within the rock. The stress levels attained in Newby's tests apparently were insufficient to initiate new crack growth within his rock specimens. The temporary increase was explained as due to the displacement of radon from nascent cracks within the rock structure.

An area of current active research is the monitoring of changes in radon concentrations in water wells and shallow dry holes in response to earthquake related processes (Sadovsky et al, 1972; Smith et al, 1976; O'Neil, 1977; Noguchi and Wakata, 1977; Li et al, 1975; King, 1978). Examination of these earthquake related radon investigations clearly implies the addition of further uncertainty, namely, the role of ground water and stress in radon emanation and transport, to the already very unpredictable phenomenon of radon emanation. The crucial, and as yet unproven, assumption made in these studies is that water carries any changes in radon emanation which might result from the failure prepara-

tion process. While no exhaustive studies have been made on the role of moisture content in radon transport, there is growing evidence that the effect is not very pronounced (Austin and Drouillard, 1973), except possibly at very low and very high moisture contents in rocks (below 5% and above 95% in relative humidity in pore spaces respectively). In such cases, there is a distinct decrease in emanation coefficient, usually not exceeding 20 - 30%. The mechanism suggested for the role of water in radon transportation is that at very low moisture content, there is a film of water which decelerates the recoil atoms. When the film is absent, the recoil atoms become enmeshed within the surrounding lattice, thereby leading to a lowered emanation coefficient (Shashkin and Prutkina, 1970). However, an equally attractive explanation is that in the dry case, there are simply more sites for the radon atoms to attach to, and thus, lower the emanation coefficient. In the water-saturated case, the decrease may be due to path clogging. However, it is possible that capillarity and water flow can contribute to offset the decrease of radon transport by high water content. Then, of course, there is the role of stress in radon emanation and in the transport processes. These considerations show that the problems associated with understanding radon emanation and its transport in rock are very complex.

There are certain characteristics of radon emanation which make such studies attractive. For instance, concentrations of radon can be easily detected by radioactive counting; radon is generated from atoms which are an integral part of the rock lattice and, being an inert gas, can travel through cracks, either nascent or induced. This provides a quanti-

tative information about both the nature of these cracks and the overall internal structure of the rock.

These considerations prompted our investigation on the physics of radon transport in rock and the effect of non-hydrostatic stresses on the radon emanation coefficient. In this article, we report on the basic characteristics of the effect of uniaxial stress on radon emanation from rock. In addition to monitoring radon emanation and stress, we also determined the effect of stress-induced microcracking (seismicity) on radon emanation rate and its transport. We shall argue that radon, as an indicator of impending failure (earthquakes), must be used with caution and then only with other independent indicators (e.g., seismicity, tilt). We shall also point out that the position of the radon detectors relative to the focus of an impending failure is crucial in whether an increase or decrease in radon background emanation rate will be observed prior to rupture.

Experimental Procedure

Uniaxial compression tests were conducted using a servo-controlled materials-testing-system (MTS Systems Corp. ^{2/}, 2.7 X 10⁶ N capacity). Tests were performed under deformation control with a displacement rate of 5.5 X 10⁻⁴ cm/sec during each loading and unloading cycle. Acoustic emission resulted from microcracking of the rock sample was detected with a Dunegan/Endevco piezo-electric transducer (Model 1229) and measured with a Dunegan/Endevco 3000 system that included a log convertor and a

^{2/}Reference to specific trade names is made for information only and does not imply endorsement by the Bureau of Mines.

reset clock. Two rock samples were cut and ground to a diameter and length of 4.7 cm and 7.3 cm, respectively. A length tolerance across any diameter of 0.002 cm was maintained. The perpendicular tolerance of the end planes to the specimen axis was less than 1.9°. The rock specimens are from a Wyoming granite impregnated with secondary (radioactive) mineralization and were collected early in 1975. The cores were preserved in a low humidity (Denver) environment for nearly 2 years. It is virtually certain that under these conditions (30% humidity) there is competition for sites between water molecules and radon atoms and where the emanation coefficient is practically independent of moisture content (Austin and Drouillard, 1978).

Data pertaining to the complexities of radon measurement for rock specimens under pressure are generally not available in the literature. Accordingly, we shall describe in detail here our experimental procedure and apparatus used in the testing program. Figure 1 is a schematic representation of the experimental arrangement. The radon circuit consists of two basic elements. 1) A cylindrical steel chamber for housing the specimen within the cylinder (excluding the specimen) during the test is 119 ml or 15% of the total volume of the closed radon system. The total volume of the system, including that of the tubing, is approximately 760 ml. ^(figures 4 and 5) 2) The radon detector was developed by the Bureau of Mines (Drouillard, 1976) and consists of a chamber whose walls are covered with a scintillator compound (ZnS). The volume of the chamber is 520 ml or 68% of the total system volume. The chamber is attached to a photomultiplier supplied with a high voltage source (HVPS) and a pre-

amplifier. Thus, any alpha particle arriving into the sensitive layer from the inner volume of the chamber or from a molecule deposited on the chamber walls produces a scintillation which is then counted. This condition gives rise to two types of limitations on radon counters. First, the radon detecting efficiency will depend on whether the measured species is in the gas phase or deposited on the chamber walls (plated out). Second, when the radioactive decay is in the form of radon daughters, no sudden decreases can be detected in the concentration of radon itself during the activity period of the daughters. The radon contribution will be obscured (see curve 1, figure 7). The efficiency of the detector has been determined experimentally to be approximately 65% for the three groups of alpha-particles produced by Rn, RaA, and RaC'. This efficiency was determined under static conditions; that is, no air flowing through the detector. This is similar to the situation prevailing in a Lucas flask (Lucas, 1957). The remaining portion of the system consists of a rotary pump and the tygon plus silicon tube system. The portion between the chamber and the detector has a volume of 68 ml (9% of the total system volume); the remainder of the system has a volume of 61 ml.

To ensure that the detection system is independent of the effect of barometric pressure and external humidity changes, considerable care must be taken to achieve a closed airtight system. To test our system, we applied an overpressure of approximately 1mm of mercury for a period of one day. No decrease in pressure was observed, implying the system was airtight.

The rotary pump produces an airflow velocity of approximately 0.234 l/min. The magnitude of the flow velocity was found to have a

negligible effect on the radon counting efficiency. When we increased the flow rate of 2.34 l/min by using a diaphragm pump, only about two percent decrease in efficiency was observed. This response was found to be due to the fact that the efficiency for the RaA and RaC' (which is somewhat higher than 2/3 of the total efficiency) depends primarily on the plate-out on the detector surfaces. The plate-out depends on the number of condensation nuclei per cm³, the diffusion coefficient, turbulence, particle charge, humidity, and the sticking coefficients.

The time duration of each cycle is 3.3 minutes (flow rate of 0.234 l/min), corresponding to approximately 10⁵ cycles for a ²²²Rn atom. The probability of detecting a radon atom decay is given approximately by the ratio of the sensitive volume of the detector to the total volume of the closed system. The probability in our system is 0.3.

The counting portion of our system is schematically shown in figure 1. Signals from the detector preamplifier are fed to a linear amplifier. The signal is then followed by a discriminator that, in turn, drives a counter timer and a ratemeter for both digital and analog output. Additional equipment, aside from the high voltage power supply for the detector, includes a chronometer and a teletype scanner. All nuclear instruments used in our laboratory are standard commercial units.

Data were recorded with a strip chart recorder (analog output) and a serial line printer output (digital output). The time duration of the counting (10, 30, or 200 minutes) was determined by the desired fineness of the response. It is particularly important to realize that the longer the counting time, the lower the counting error and, therefore,

the smoother the response.

The duration of the experiment for both specimens reported in this article was more than 14 days with continuous recording except when power failed. No apparent dependence on barometric pressure was observed during this period. It is important to recognize that a principal advantage of closed detection systems is that small changes be measured without resorting to laboratories with completely controlled environments. For example, there is extensive evidence in both buildings and mines showing that the radon emanation coefficient is quite sensitive to changes in barometric pressure and humidity (Jonassen, 1975; Schroeder, Evans, and Kraner, 1966). In these studies, deviations up to several hundred percent have been observed.

Data and Data Analysis

The overall view of our experimental results is given in figure 4. There is an indisputable correlation between the applied stress and the changes in the continuously measured radon concentration in the detector. There were two samples used in this experiment. Their characteristics are given in table 1. The radon emanation coefficient was determined using the closed can gamma-ray method (Austin and Drouillard, 1978). The closed can method consists of measuring two activities by means of NaI crystal gamma-ray detector, one of a sample open to air, the other of a sample closed in a can which prevents radon escape after equilibrium is established. The ratio of these two activities gives the emanation coefficient. The data shown in figure 4 were obtained using sample 1. The four repeated application of stress are labeled

1 to 4. The interruptions in the radon counts per minute line in this and some other figures are caused by power failures.

Prior to discussing and analyzing these data in detail several theoretical and experimental points should be discussed. First, either an open or a closed system (see figure 1) can be used to measure the effect of stress on radon emanating rock. In order to make an open system one simply disconnects the tubing, shown in figure 1, at an appropriate location so that fresh air can be constantly pumped into the crushing chamber which is then measured in the detector and released into the atmosphere. This is the way Nowby (1973) performed his experiment. The two disadvantages of any open system are: (1) The system is subject to barometric pressure variations; and (2) The system lacks sufficient sensitivity to measure low radium concentration rocks. This follows because no radon build-up is allowed; depending slightly on the mean radon stay in the detector (say one minute) the closed system can be orders of magnitude more sensitive. In a closed system the response time (the time required for a change in radon concentration to be detected as a response to a change in radon emanation) is consequently as many orders of magnitude longer. Because most rocks contain only trace amounts of uranium (and hence radium), the closed system is preferable for rocks other than high grade ores.

Closed systems, however, have an inherent disadvantage, for example, by building up the radon concentration in the specimen chamber they diminish the radon flux from specimen. Thus, changes in the flux due to stress loading are made less easily detectable. The system used in

Table 1

	Sample 1	Sample 2
Total Weight	222.9 g	292.1 g
Weight of U	0.242 g	0.0605g
Weight of Th	<0.0001g	negligible
²²² Rn Activity	1.81 X 10 ⁵ pci	4.53 X 10 ⁴ pci
Emanation Coefficient (X)	35-40X	30-35X

our study was airtight. The barometric variations had no effect on the radon concentration, even though our system had a designed 95% radon leak (see curve 2, figure 5), accomplished through a special silicon tubing for a rotary pump. This is due to the fact that radon is an inertial (noble) gas and it penetrates readily through membranes. This is a well known case, for instance, in helium transport studies. The response time was shortened nearly 20 times with respect to the totally closed system.

With the above considerations, one may safely assume that a leaking system is a necessary compromise between a slow and small response radon-proof closed system and the quick response open system. In the remainder of this report, all the air-proof systems will be called closed. The total air volume is the interstitial volume in the rock plus the air volume of the tubing, detector, and chamber.

The nature of radon release from the rock from the point of view of two basic responses is shown in figure 5. Note that this illustration is not a theoretical concept describing the mechanism of radon release from lattice. Assume a system where there are two possibilities for freshly formed radon atoms; those which make it to the surface and those which decay in the lattice. Assume that we start with a 50% emanation coefficient (see figure 5). Shortly before time T_0 an equilibrium is reached when 50% of all radon atoms make it out of the rock and are registered in the detector with the given efficiency. At time T_0 let stress be applied for an instant to the sample. Two situations can arise. First, the radon gas entrapped in the rock and which decays

before reaching the surface is instantaneously (let's assume it for the sake of simplicity) flushed out. The coefficient increases to 100% and then decays with the radon half-life (curve 1) until again 50% is reached. Second, all the paths leading from radium atoms to the surface are instantaneously and permanently opened while entrapped radon remains where it was; (this unlikely case is discussed again for the sake of simplicity to illustrate the nature of response of radioactive substances). The coefficient grows (curve 2) until it reaches 100% - an ordinary radon buildup in a closed system. When conditions 1 and 2 both occur at the same time, that is when both flushing of the existing trapped radon and subsequent buildup in the detection system are taking place simultaneously, we obtain the sum of both curves (the solid curve).

Closed systems build up the radon concentration approximately according to the equation:

$$\frac{dn}{dt} = k(t) - \lambda_{Rn} N, \quad (1)$$

where

N = number of radon atoms

λ_{Rn} = radon decay constant (sec^{-1}),

$\lambda_{Rn} = \lambda_{Rn} + \lambda_{leak}$,

λ_{leak} = leak constant (sec^{-1}),

$k(t)$ = radon flux (number of atoms sec^{-1}),

t = time.

The radon flux, $k(t)$, is a complicated function of time, diffusion constant, permeability, porosity, the dimensions of the sample, and the

radon changing concentration in the closed system. It is based on time-dependent solutions of the standard mass transport equation (which are not analytical). The time-independent solutions ($\frac{dC}{dt} = 0$, $k(t) = k$) are analytical, however, and any detailed descriptions of either type is not within the scope of this presentation.

Examination of Figure 6, where four experimental radon concentration buildup curves are shown, (curves 1 and 2 for sample 1, curves 3 and 4 for sample 2) suggests that a possible approximation is $k(t) = k$. After solving equation (1), and rearranging terms, we find:

$$C = k \frac{\lambda_{Rn}}{\lambda_{Rn} - \lambda_{Pb}} (1 - e^{-\lambda_{Rn} t}), \quad (2)$$

where C = CPM / eff. (number of decayed atoms sec⁻¹ liter⁻¹),

CPM = counts per minute,

eff = efficiency of the detector.

The time dependence of the curves in Figure 6 fits quite closely

(15%) the time dependence of equation (2). Equation (2) contains two

unknowns, k and λ_{leak} . The second equation needed to calculate these

two quantities can be obtained from equation (2) by expanding the exponent

to the first term (for small t):

$$C(t + 0) = k \lambda_{Rn} t \quad (3)$$

This equation describes slopes which are shown in Figure 6. Note they

are independent of leaks and that each sample has its own slope (or

radon flux, k).

For large t , equilibrium is reached and equation (2) becomes time

independent (curve 2 in Figure 6). The leak can now be calculated exactly.

The calculated leaks are given in Figure 6.

The response of the system to a sudden shut off of the radon supply is illustrated in Figure 7. The detector part was closed off about half-way between the crushing chamber and the pump, and the decay measured in the detector itself. The crushing chamber was allowed to build up more radon concentration. The decay rate (from 92 hours of R_n to 70 hours) indicates a 25% leak in the detector and the adjacent tubing (note the total leak is 45%). Once the radon supply was reintroduced into the system (pump switched on and the tubing opened), there was a sharp rise of activity over the equilibrium value (~ 7400 cpm). This is due to the concentration build-up in the crushing chamber which has only 20% leak and, consequently, has higher equilibrium concentration according to equation (2). There is a corresponding build-up in the rock itself. The decrease of this build-up had a half-life of approximately 33 hours (see Figure 7). A decay governed purely by 45% leak would have a half-life of about 50 hours. In addition to having the radon build-up, there is (on reintroduction of radon into the detector) a radon diffusion due to sudden increase of the total volume. The equilibrium is very fast in the gas phase because the pump circulates the air continuously. In the rock itself the equilibrium takes of the order of hours because the diffusion coefficient for radon in rock is much lower than in air. In this manner, the superposition of the diffusion delayed equilibrium and the 45% leak radon decay yields the observed "half-life" of 33 hours. To obtain a more comprehensive view, five experimental curves describing the decay, diffusion delay and the role of leaks are shown

in figure 8. Curve 1 is the decay of radon daughters plated out in the detector. This curve represents the fastest time response to an instantaneous removal of radon from the system. An identical curve, but plotted upside down, is the response of the detector to a sudden arrival of radon. Curve 2 is the decay in the 95% leaking system. This is similar to the decay shown in figure 7, where the detector is closed off from the pump and the radon source (the rock). Curve 4, the 33 hours decay from figure 7, is replotted in the figure for comparison. Curve 3 shows an analogous situation to curve 4, except here the additional radon slowly being released into the detector comes from the application of load rather than from a sudden decrease of the concentration of the radon gas surrounding the rock. Finally, curve 5 illustrates the decay of pure radon.

The difference in slopes in figure 6 and half-lives in figure 8 is not only due to the different leaks, but also to the different radon fluxes. The fluxes are dependent on the concentration gradients at the surface of the rock. This can be easily checked, for instance, by comparing the slopes in figure 6 with the slopes one should obtain from radon emanation coefficients (see table 1) measured by the closed can method.

A radon emanating rock has radon concentration on the surface of the rock equal to zero. Inside the rock the concentration has a certain gradient which (at steady state) is not changing with time. When the sample is placed into a closed system, the build-up immediately removes the condition that the radon concentration on the surface is zero. This

new condition changes the concentration gradient so that the radon flux, $k(t)$, is now a complicated function of time, and, when compared with the 35% - 40% emanation coefficient given in table 1, we find a 60% reduction in the slopes in figure 6 in comparison to the slopes corresponding to 35-40% coefficient. In other words it appears as if the slopes corresponded only to approximately 14% emanation coefficient.

A similar case was calculated by Clements, 1977. He shows that the reduction is due to a radon counterflow, from the space surrounding the rock into the rock. While in Clement's work this counterflow is convective and described by Darcy's flow, in our case the counterflow is diffusive and described by Fick's Law. Mathematically, however, these cases are identical.

With these preliminary discussions behind us, we are in a position to proceed with the analysis of the data proper.

It is possible to estimate, using the slopes of the peaks in figure 4, the increase in the "flush" release (or the magnitude of k from equation (2), of radon atoms during the duration of applied stress. In the first peak (see also figures 9a and 10), the increase is 30 to 40% of the slope of the curves 1 and 2 in figure 6, while in the case of the last peak (see also figures 9f and 13), the increase is approximately 80% of the same slope. Note that Neuby (1973) observed a load induced increase in radon emanation which was higher than 500%. All these increases are described basically by curve 1 in figure 5, the "flushing" or temporary stage. The same comparison can be made for the dip in radon activity shown before the first peak in figure 4 (see

also (figures 9a and 10). The decrease in radon flux is about 13% when compared to curve 2 in figure 8.

Figure 9 (a-g) shows how the measured radon concentration response can be explained in terms of the diffusion, leaks and decay described earlier. The last four figures 10-13 show correlation of the radon measured emanation with the integrated microcracking activity.

The analysis of figures 9a - 9g can be simplified by assuming that the dependence on stress of the growth and decay of the radon concentration can be approximated by exponential curves (dash, dash-dot, and dash-dot-dot) with half-lives of approximately 10 hours (see also curve 3 in figure 7). Incidentally, Newby (1973) also observed diffusion delay half-life of about 10 hours. Note that in the cases in figure 9, the response is time-dependent, although with the additional complications discussed earlier. The reasonable fit with the data indicate we are justified in using the above simplifying assumption.

The radon concentration in figure 9a (dated Feb. 23, 1977) is remarkable in showing that after applying the stress there was a decrease in radon concentration (the standard deviation for a 10 minute count is shown for comparison). The temporary decrease may be due to closure of radon pathways by applied stress as was first suggested by Newby (1973). However, Newby's results were obtained after "flushing" (curve 1, figure 4) rather than prior to "flushing" as it is the case in figure 9a. It is safe to say, with respect to

842

the complexity of the radon emanation process, that under some circumstances the radon flux can be diminished in response to applied stress, or simply, prior to "squeezing" (radon) out, there is "closing off" of radon paths. As additional pressure was applied, the response was positive.

A decomposition of the growth and decay is shown by the dashed curve in figure 9a. Note that the half-life is lower than 10 hours. As noted earlier, because the decay is governed by diffusion, it is possible that small changes in the diffusion coefficient, or permeability, occurred during the course of the repeated stress application. This condition would be reflected in the later experiments (see the second, third, and fourth peak in figure 8) by the sample exhibiting a slower diffusion rate.

Figure 9b shows that on the following day the radon concentration returned to its original value -- an indication that no additional paths to radium atoms were opened. When the load was re-applied at about midday for about 5 hours, a notable increase took place closer to the end of the loading period. The next day (figure 9c) shows a similar behavior, and even though there was an increase related to loading, at the end of the loading period there was an additional increase. The decomposition, in all cases, is done with 10 hours half-life. It is difficult to make any firm conclusion, except that these radon concentration changes are related to closing and opening cracks in response to applied stress. It should be noted that in all these cases the original value of the radon concentration was restored after the load

was removed. This is in contrast to Newby's (1973) finding where, after the 500% temporary increase in radon coefficient, the steady state radon coefficient decreased by 30% from pre-load value with the load on. The possible explanation is that at our lower concentration changes, the relative decrease in radon concentration changes, the relative decrease in radon concentration could not be observed.

All of the above phenomena can be described as the flushing stage and, as in the case of Newby's (1973) measurements, a partial and relatively low closing of some paths. It is only in the figures 9f and 9g where there is also a permanent opening of new paths recorded as evidenced by the higher steady state radon emanation. The reason for the permanent openings is apparent; increased surface area due to the development of microcracks within the rock structure.

The decomposition into growth (dash-dot-dot curve), decay (dash-dot curve) and the total (dash curve) in figures 9f and 9g is accomplished in the usual manner. The permanent increase of the emanation coefficient after the steady state was reached for the crushed rock system was approximately 5%.

The relationships between the stress (dashed line), seismicity (full line) and radon concentration (histogram above, full line) are shown in figures 10 to 13. Note the improvement of the standard deviation if counts of 10 minutes duration are replaced by 30 minute ones.

In figure 13 the response is unmistakably related to seismicity. The crushing of the sample, represented when the sample entered a

post-failure state (decrease in stress at fixed displacement rate), resulted in orders of magnitude increased microcracking activity (seismicity) and massive radon release. Once the seismicity declined (full curve), the increase in radon release slowed down.

Discussion and Conclusions

picture which emerges from these data is that complicated changes within the rock sample occur in response to applied stress. The role of creep, for instance, can easily explain the difference in behavior between the first and following peaks in figure 4. It is apparent that long before the sample enters a post-failure state, there are irreversible changes such as crack induced changes or permeability that modify the way radon is travelling through the rock.

The apparent most striking difference between our findings and those of Newby (1973) is that the increase in the emanation coefficient in the case of Newby was, nearly an order of magnitude higher. It would require detailed knowledge of Newby's experimental arrangement as well as an exact time-dependent calculation of the radon emanation process in our tests in order to uniquely determine why the radon increases in his experiment so much higher than ours. However, we believe the disagreement is only apparent. For example, the dynamics of the counterflow are different in our arrangement and its net result must be substantial lowering of the radon flux in comparison to no counterflow case. In addition, the rock samples used in Newby's tests were high grade uranium ore whereas our samples were a granite impregnated with secondary mineralization with probably an order of

magnitude lower uranium concentration. That is, the radon atoms in our specimens were enmeshed in a more compact crystallographic structure and are probably held in position or, at least, have to travel much farther and possibly slower through the interstitial space to deliver the same amount of radon to outside the specimen. It appears that small interferences with the lattice, radon concentration, subsequent gradient changes and numerous other parameters, such as surface porosity (as opposed to the deeper porosity) seem to have effect on radon emanation. Three conclusions can be drawn from this study. First, closure of nascent cracks by small increases in compressive stress can significantly decrease the radon emanation coefficient (13%). Second, the radon emanation will increase once the applied stress is sufficient to initiate crack growth within the rock structure. Third, when the method of α and γ measurements are used quantitatively, it should be possible to distinguish exactly the amount of radon that does not emanate from the rock structure and, in particular, how much radon is "permanently" entrapped within the sample. Thus, it should be possible to use radon emanation as a probe of the internal structure, such as microcrack distribution and surface vs. internal porosity of rock masses.

Our experimental results have implications for the use of radon as a precursor of imminent failures, such as earthquakes. Clearly the stress state in the immediate vicinity of radon source (well) is critical in determining whether an increase or a decrease is observed in the radon emanation coefficient. Based on our test results,

we anticipate that the emanation coefficient will decrease with any increase in the far-field stresses, such as might occur just prior to the mainshock (Brady, 1976) if the local stresses are insufficient to initiate microcracking. Similarly, the emanation coefficient should increase if these stress changes can initiate microcracking in the vicinity of the well-bore. Radon emanation prior to seismic activity (Sultanxodjaev, et al., 1976; O'Neill, 1976). Also, a most unusual feature of the above studies is the vast distances (400 km to 800 km from events) from the epicenters that these phenomena are occurring. These observations are certainly consistent with our observation that small changes in applied stress can produce significant changes in the radon emanation coefficient. However, based on our studies and experience, the use of radon or any other radioactive gas as a predictor of imminent failure must be used with caution. There are simply too many parameters which affect emanation rates, aside from stress, that can produce apparent anomalies which could be incorrectly identified as harbingers of imminent failure.

Figure Captions

1. Schematic view of the experimental setup. The total air volume, excluding specimen, of the system is about 750 ml. The detector volume is approximately 520 ml (68%).
2. Schematic of the crushing chamber. The chamber air volume around the rock is approximately 119 ml.
3. Further details of the crushing chamber.
4. Overall view of the data for sample 1. Note that the first three pressure applications did not result in a noticeable permanent change in the emanation.
5. Illustration of the "flushing" and "newly opened paths" parts of the system response to pressure applied at time T_0 .
6. Experimentally determined radon concentration rises when the sample is put into the system. Curve 2 corresponds to the system with 95% leak (mostly through the silicon tubing). This system was used to make the measurements. Other curves (3 and 4) are for sample 2. Curve 1 is for sample 1 with a much smaller leak.
7. This curve is an extension of the experimentally determined curve 2 from figure 6. At $t = 0$ an air pump was shut off and the radon in the detector, after isolating it from the rest of the system, was allowed to decay and leak (25%). When the detector was opened and the pump switched on, the build-up of radon was decaying--diffusion slowed--with half-life 33 hours. Note that no new paths were generated in this experiment.
8. Overall view of various experimentally measured decays (curve 1, radon daughters; curve 5, radon) and diffusion slowed decays (curves 2 and 3).
9. Summary view of test results. Upward arrows indicate the beginning and end of stress loading. The occasional interruptions of the experimental lines were caused by power failures.
 - a) A detailed view of the first peak from figure 4. The dashed line is calculated on the assumption that there is a 10-hour half-life in the build-up and the diffusion delayed decay.
 - b) A detailed view of the second peak. The dashed-dot line is for 10-hour half-life.
 - c) A detailed view of decomposition of the third peak. The dash-dot-dot line, when added to the dashed line, gives the total observed activity.
- d) and e) A detailed view of the restoration of the original level of activity.
- f) A detailed view of the last peak from figure 4. The slow radioactive growth owing to the opening of new paths is given by the dash-dot-dot curve. The "flush" growth and decay is given by the dash-dot curve. The total is given as the dashed curve.
- g) A continuation of the previous day. A permanent increase above the non-stressed level can be seen.
10. Complete load (dashed line), seismic (full line), and concentration (full line histogram) data are given for the first peak. The standard deviations for 10 and 30 minute counts are also given.
11. Complete load (dashed line), seismic (full line) and concentration (full line histogram) data are shown for the second peak. Note the increase clearly takes place at the end of the loading period.
12. A complete load (dashed line), seismic (full line) and concentration (full line histogram) data are shown for the third peak. Note that after the load application there was a delay of about 20 minutes before an increase took place. A second increase appears to take place after the termination of the loading period.
13. A complete load (dashed line), seismic (full line), and radon concentration (full line histogram) data for the fourth peak are shown. The high seismicity seems to account for this strong positive correlation between the seismicity and radon emanation coefficient. The sample was crushed into several pieces after this load was applied.

References

Albert, R. E. Thorium, Its Industrial Hygiene Aspects, Academic Press, New York, 1966.

Austin, S. Ralph, and Robert F. Drouillard. Radon Emanation from Domestic Uranium Ores Determined by Modifications of the Closed Can, Gamma-Only Assay Method, U. S. Bureau Rept. of Investigations 8264, pp. 1-74, 1978.

Brady, B. T. Theory of Earthquakes IV. General Implications for Earthquake Prediction, Pure and Applied Geophysics, vol. 114, pp. 1031 - 1082, 1976.

Clements, W. E. The Effect of Atmospheric Pressure Variation on the Transport of ²²²Rn from the Soil to the Atmosphere, Ph.D. Thesis, New Mexico Institute of Mining and Technology, Socorro, New Mexico, pp. 1-104, 1977.

Drouillard, R. F., private communication.

Jonassen, N. On the Effect of Atmospheric Pressure Variations on the Radon-222 Concentration in Unventilated Rooms, Health Phys., vol. 29, p. 216, 1975.

King, C. Y. Radon Emanation on San Andreas Fault, Nature, vol. 271, pp. 516-519.

Li, L. P., W. D. Kun, and W. T. Min. Studies on Forecasting Earthquakes in the Light of the Anormal Variations of Rn Concentration in Groundwater, Acta. Geophys. Sinica, vol. 18, pp. 279-288, 1975.

Lucas, H. F. Improved Low-Level Alpha Scintillation Counter for Radon, Rev. Sci. Instr., vol. 28, p. 680, 1957.

Newby, I. J. W. A Practical Investigation of the Parameters Controlling Radon Emanations from an Impermeable Uraniferous Ore, Master's Thesis, Queen's University, Kingston, Ontario, Canada, pp. 1-149, 1973.

Noguchi, H., and H. Wakita. A Method for Continuous Measurement of Radon in Groundwater for Earthquake Prediction, J. Geophys. Res., vol. 82, pp. 1353-1358, 1977.

O'Neil, J. R. Geochemical Methods of Earthquake Prediction in the U.S.S.R., Report of an Exchange Visit, Unpublished, 1976.

Sadovaky, M. A., I. L. Mersesov, S. K. Nigmatullaev, L. A. Latynina, A. A. Lukk, A. N. Semenov, I. G. Sumbireva, and R. I. Vlovov. The Processes Preceding Strong Earthquakes in Some Regions of Middle Asia, Tectonophysics, vol. 14, pp. 296-307, 1972.

Schroeder, C. L., R. D. Evans, and H. W. Krarner. Effect of Applied Pressure on the Radon Characteristics of an Underground Mine Environment, Trans, AIME, vol. 91, pp. 91-98, 1966.

Shashkin, V. L., and M. I. Prutkinn. Mechanism Underlying the Emanation of Radioactive Ores and Minerals, Atomn. Energ. vol. 29, pp. 724-726.

Smith, A. R., H. R. Bowman, D. F. Mosier, F. Asaro, H. A. Wollenberg and C. Y. King. Investigation of Radon-222 in Subsurface Waters as an Earthquake Predictor, IEEE Transactions on Nuclear Science, vol. NS-23, no. 1, pp. 694-698, 1976.

Sultanxodjaev, A. N., I. G. Chernov, and T. Zakirov. Hydroseismic Precursors to the Gzali Earthquake, Reports of the Academy of Sciences of Uzbekistan, no. 7, pp. 51-53, 1976.

Best Available Document

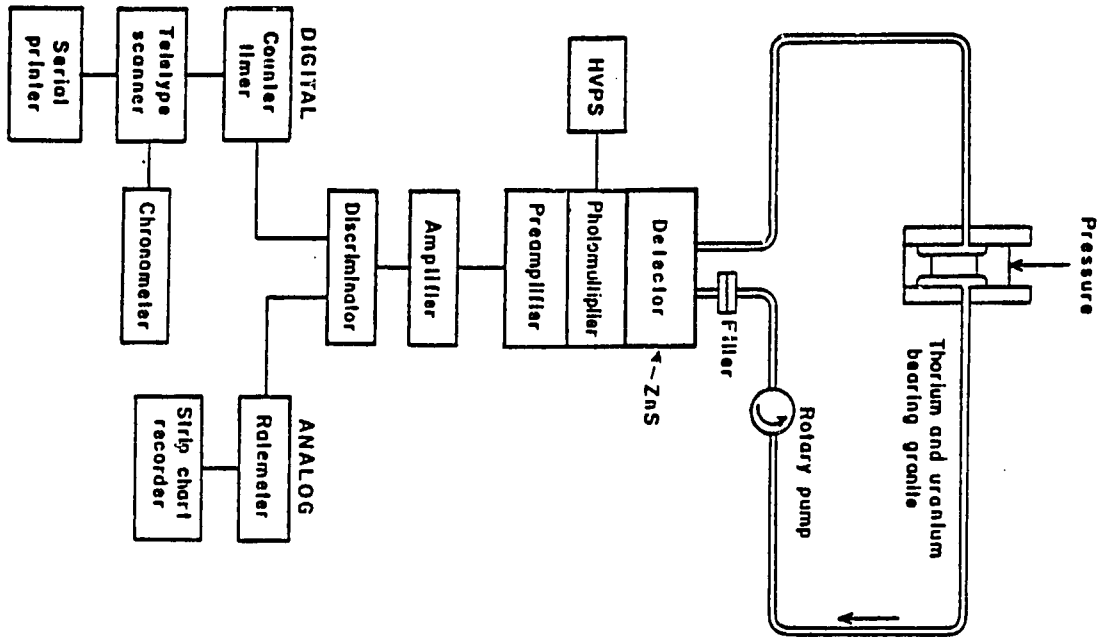
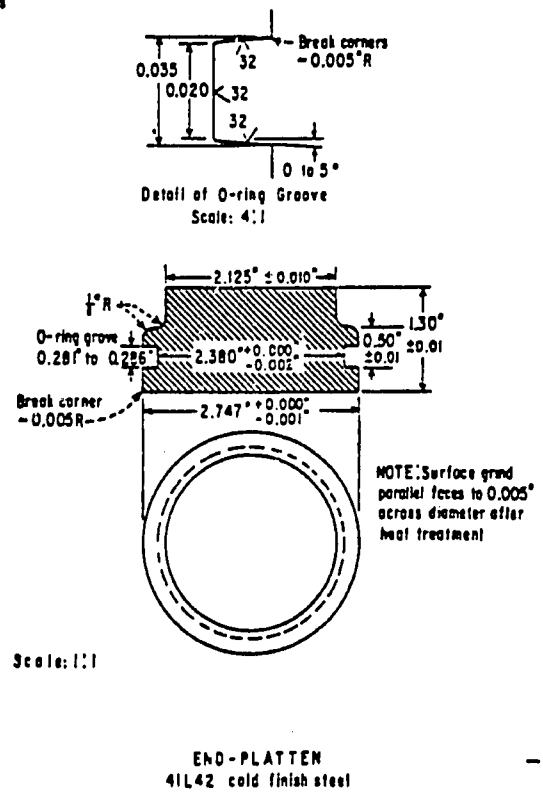
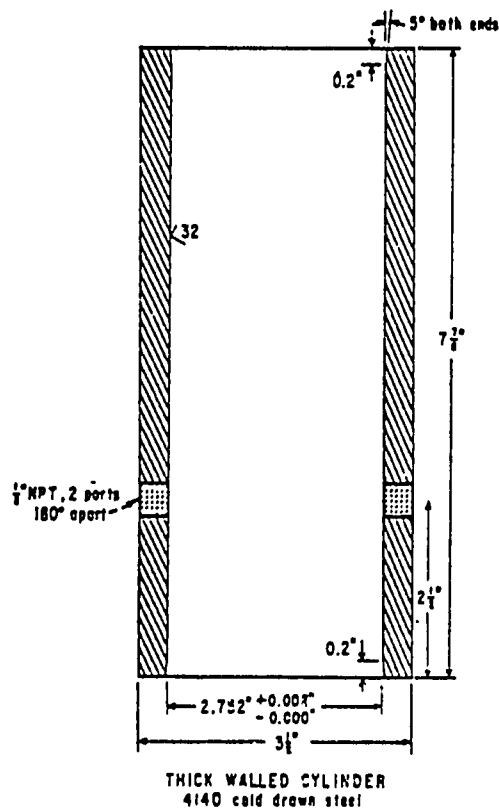
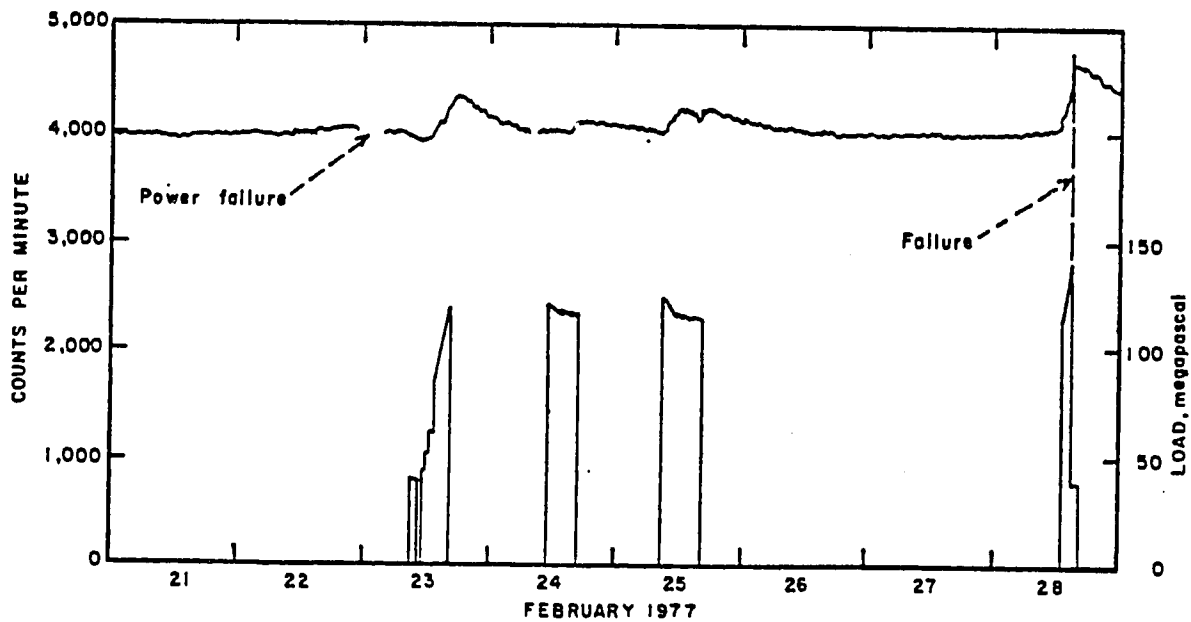
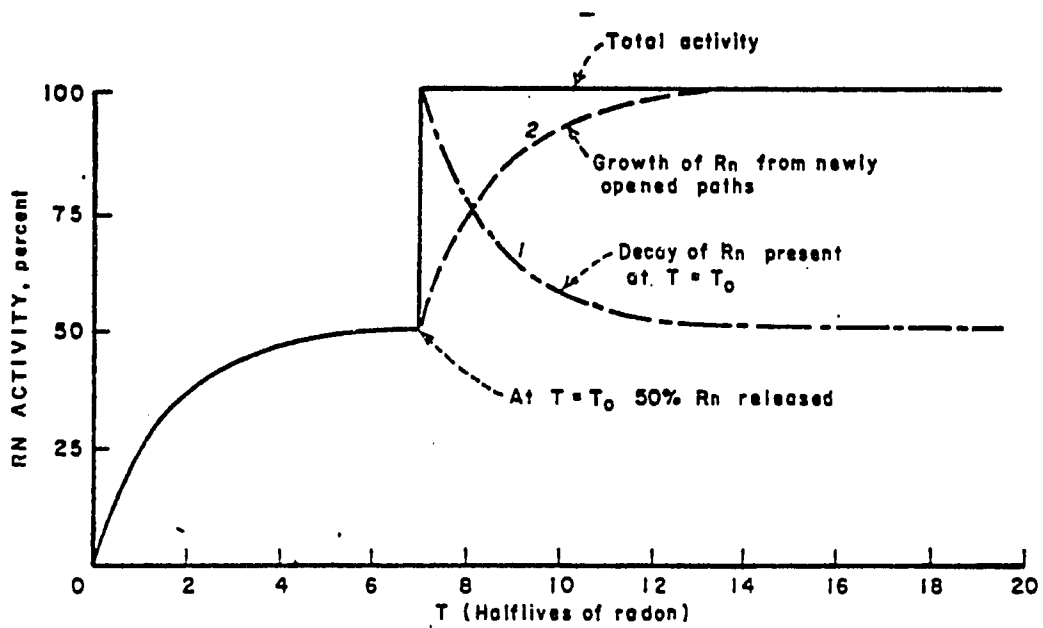


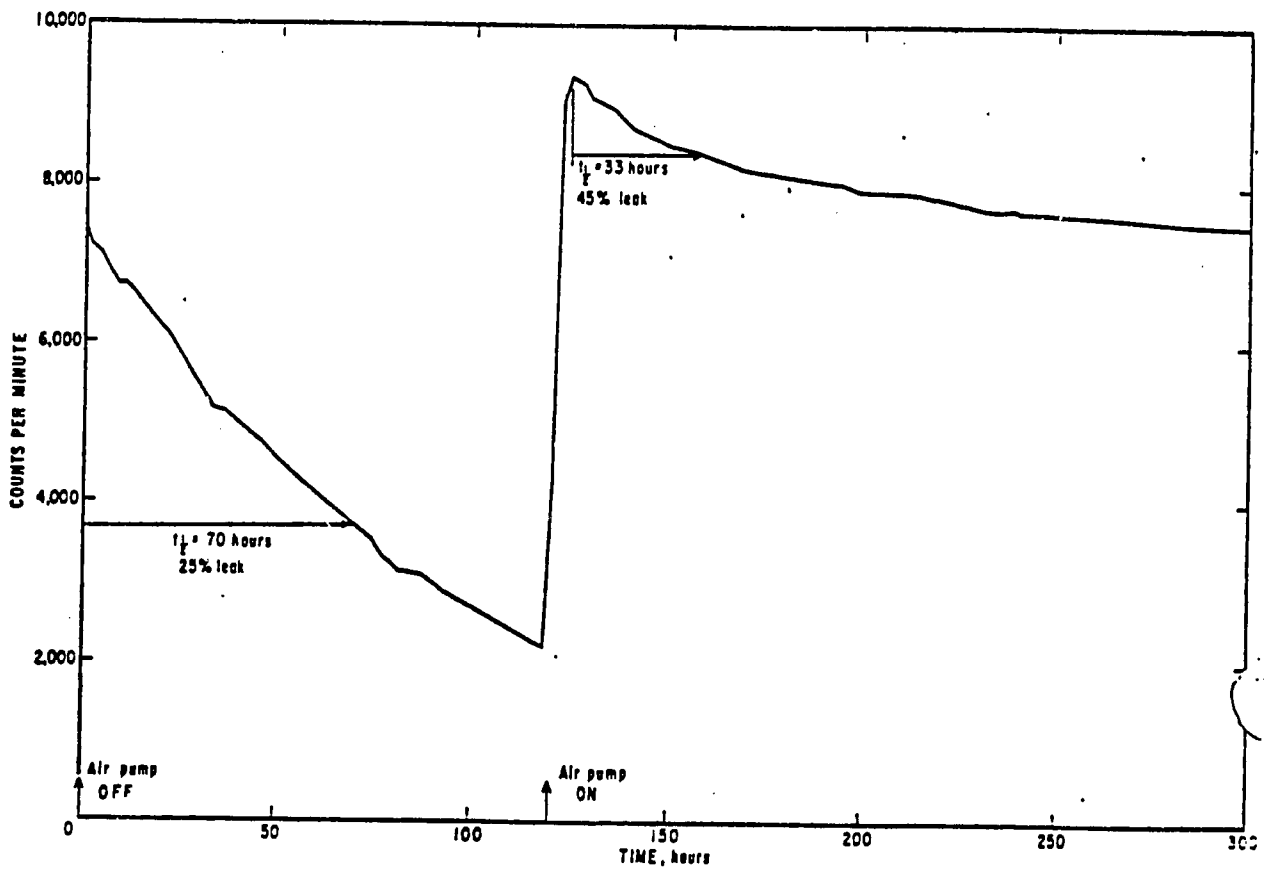
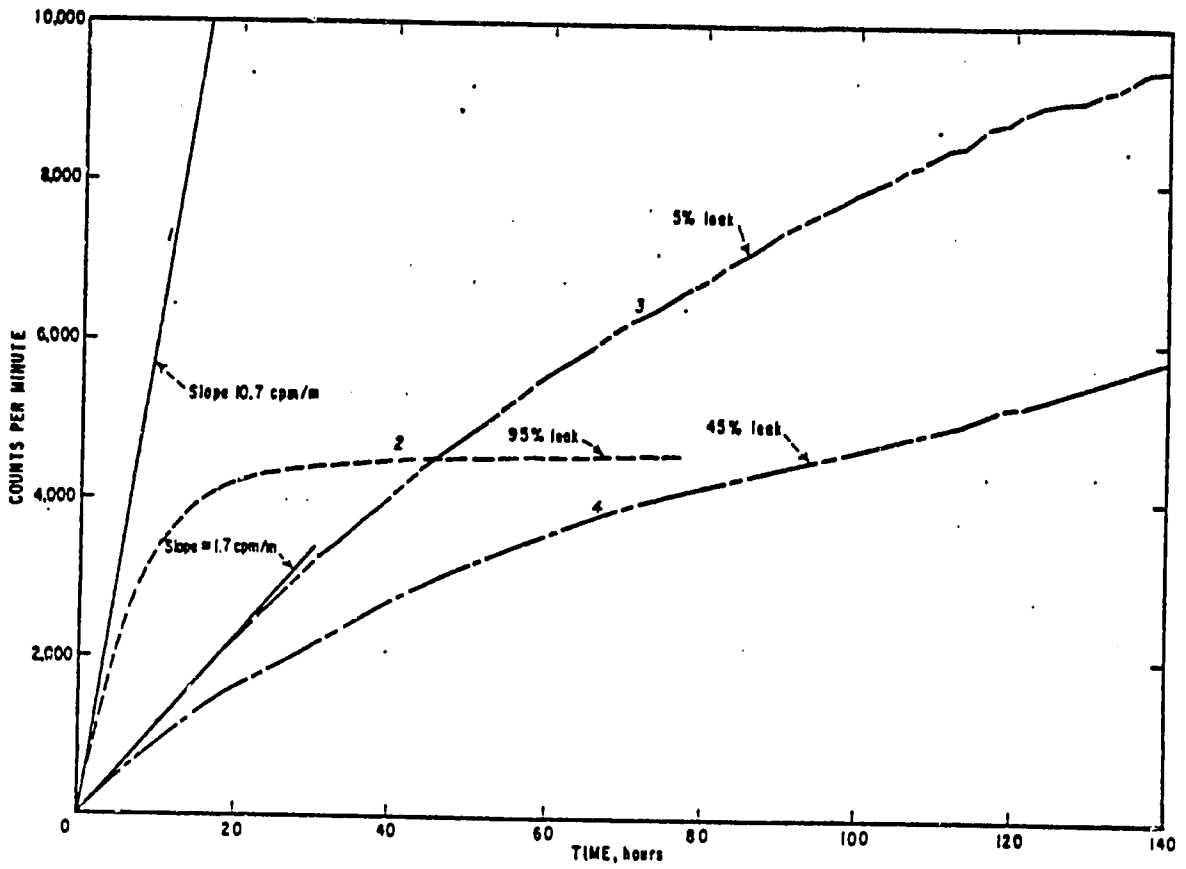
Fig. 1

Fig. 2

Fig. 3







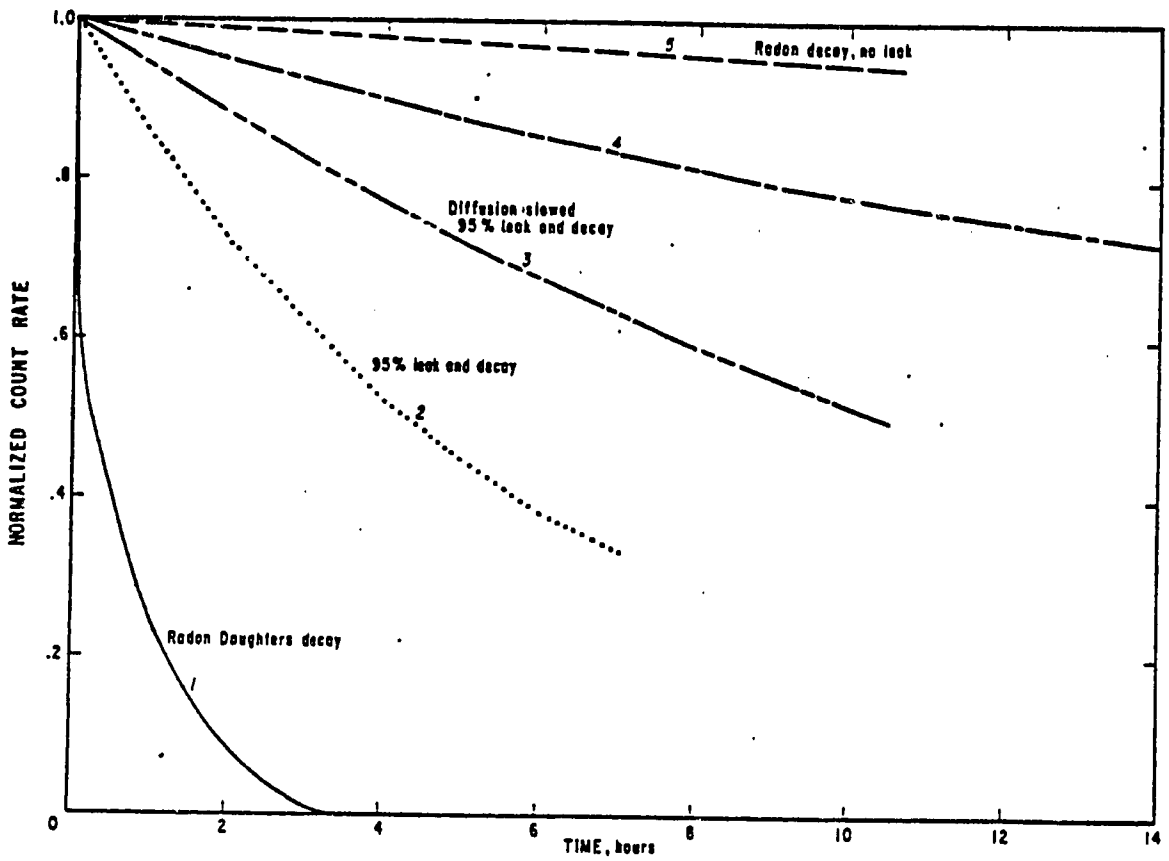
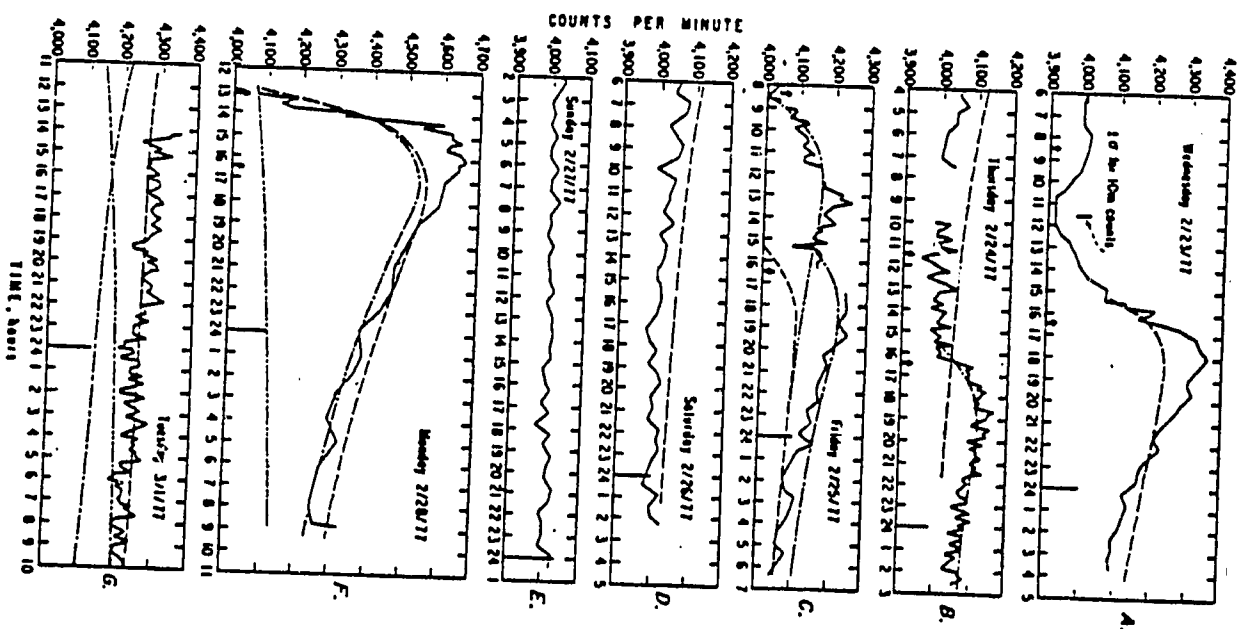


Fig. 2



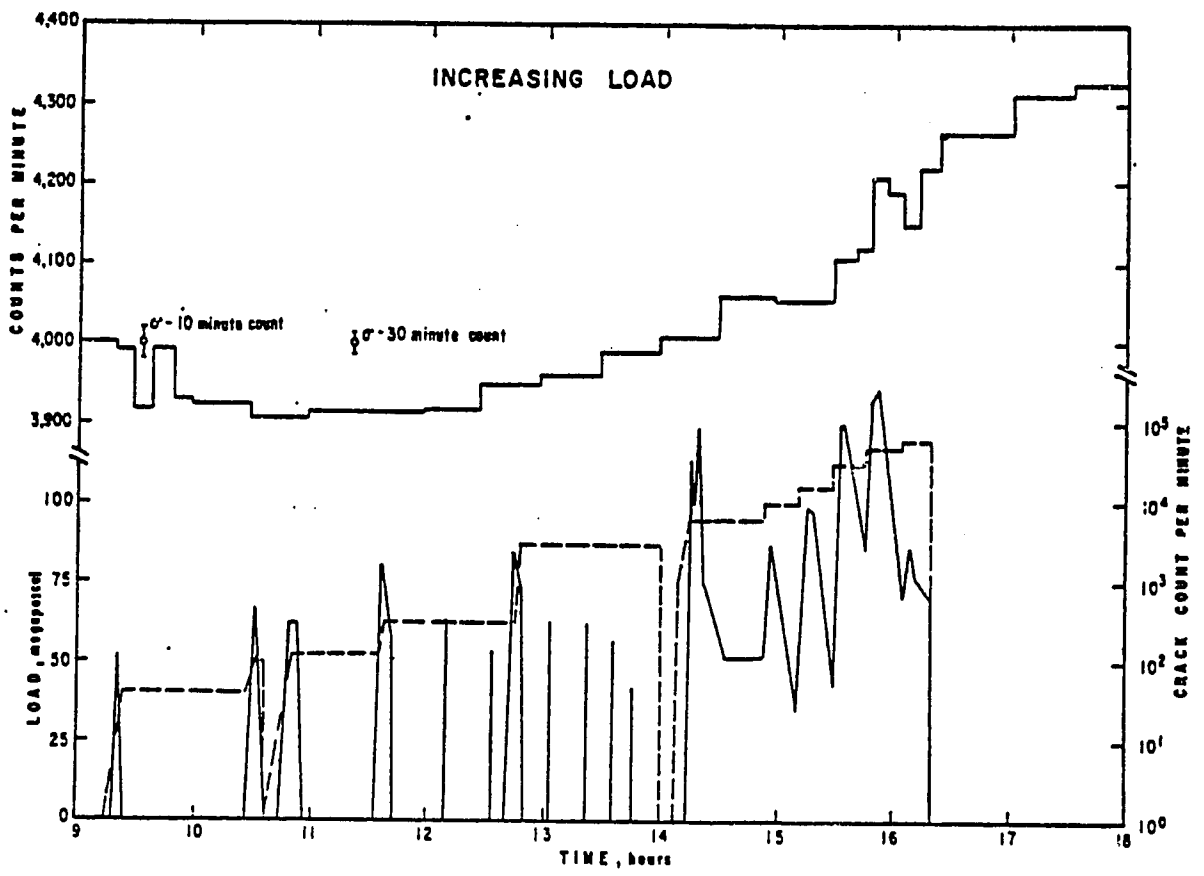
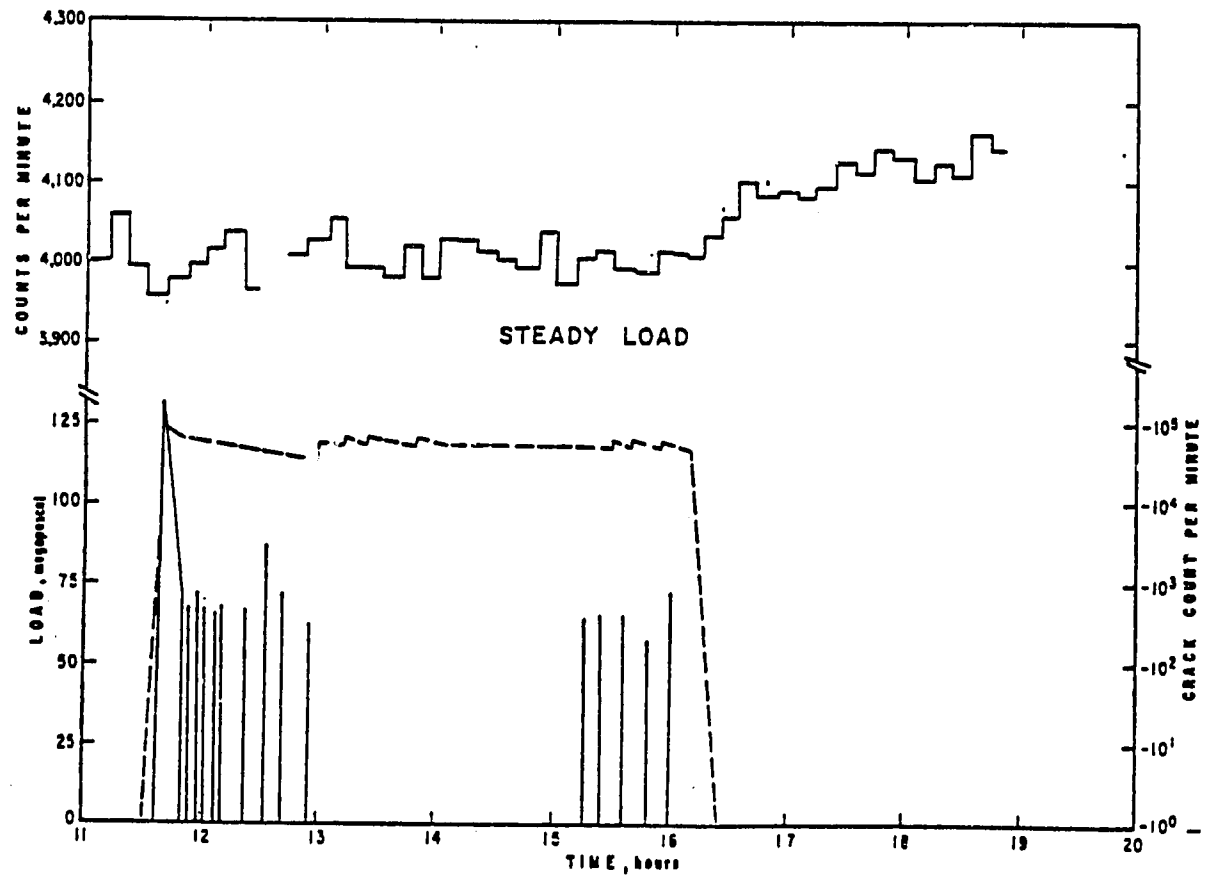


Fig. 10



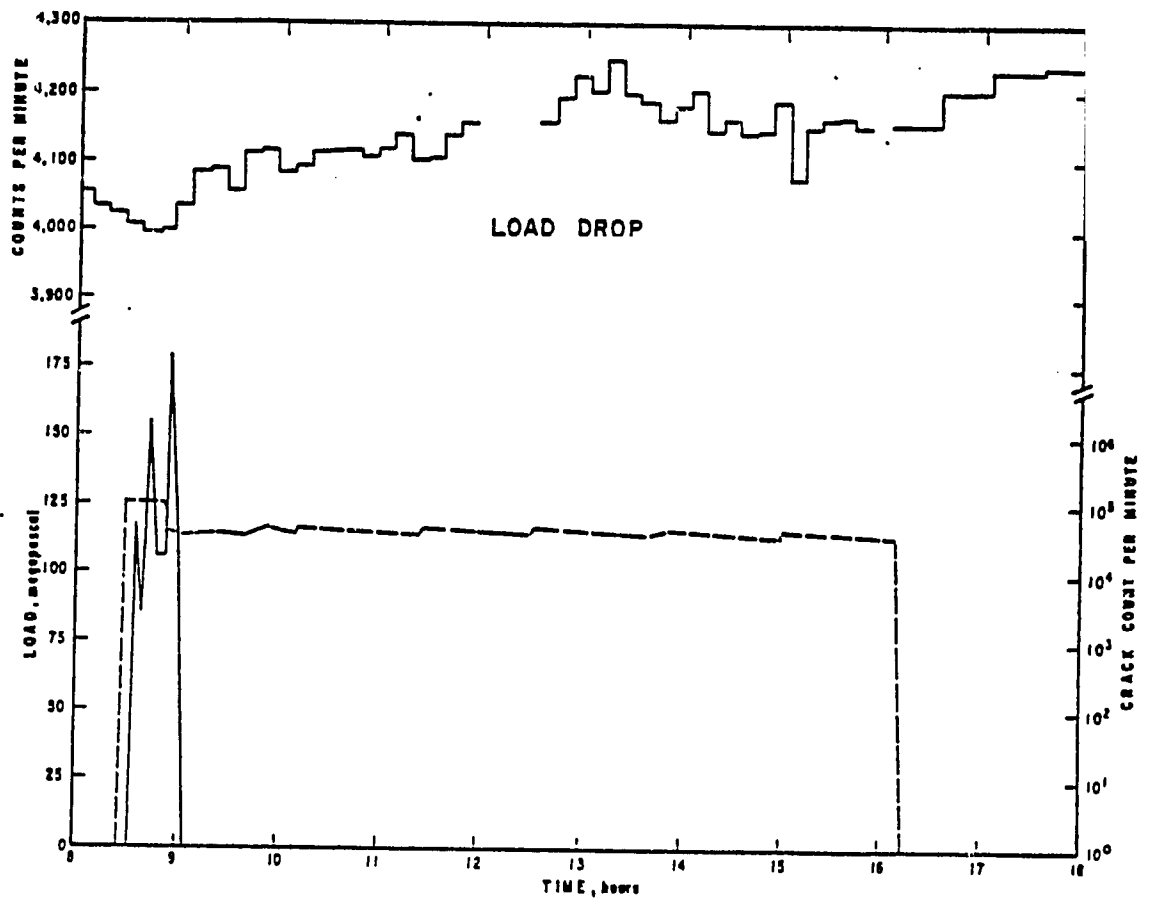
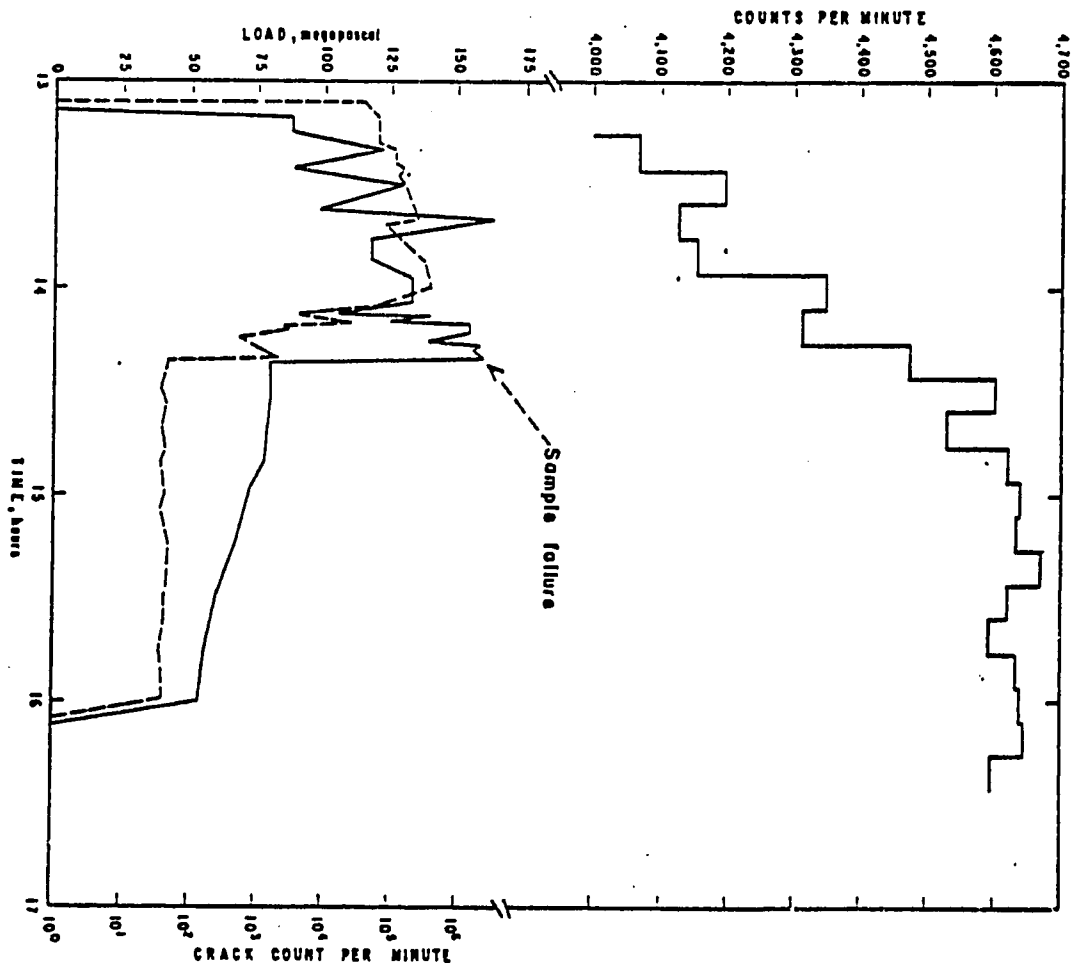


Fig. 12



Conference Report: Toward Earthquake Prediction on the Global Scale

Reprinted from
EOS
Vol. 59, No. 1, January 1978
Copyright 1978 by American Geophysical Union

Conference Report: Toward Earthquake Prediction on the Global Scale



Entrance to Lawrence C. Phipps Memorial Conference Center, University of Denver.

'From a practical standpoint, the prediction of . . . great earthquakes is at present the only way to avoid repetition of some of the terrible calamities of the past few hundred years.' (Sykes, 1976)

Only 10 years ago, most U.S. seismologists would have attributed to the dark arts any claim that earthquakes would be predictable. Yet at that very time the radical theory of global tectonics was being firmly established. Today, seismologists recognize numerous physical precursors to earthquakes. Earthquake prediction research is respectable in the scientific establishment.

A valid earthquake prediction specifies location, time of occurrence, size, and probability. Successful prediction of large earthquakes can lead to great reductions in economic and life losses; to increased safety and efficiency in critical facilities such as nuclear reactors, power grid control centers, and dams; and to the return of a populace to normal living patterns following a damaging earthquake.

During the preparation phases of great earthquakes, major changes in the associated regional stress fields

apparently occur. These stress changes result in a set of physical precursors to impending great earthquakes; some of these precursors are observable in the far field. Thus seismologists have the opportunity to use remote seismograph networks to monitor earthquake zones for possible earthquake precursors. In this way, regions can be identified for intensive local investigation, and this can lead to improved and rapidly accrued information on the preparation processes of great earthquakes. This information should prove valuable for our own national effort in earthquake prediction.

On September 22-24, 1976, the U.S. Geological Survey (USGS) Office of Earthquake Studies held a special conference to explore present and future research in global seismology, emphasizing global prediction of large earthquakes. The conference, 'Global Aspects of Earthquake-Hazard Reduction,' was held in the University of Denver's Lawrence C. Phipps Memorial Conference Center, where 32 participants from 11 institutions discussed and speculated on the questions at hand.

Highlights

From the large amount of information exchanged, certain themes predominated.

This meeting report was prepared by William Spence (meeting convener) and L. C. Pakiser, both at the U.S. Geological Survey Office of Earthquake Studies, Denver, Colorado 80225.

1. Temporal patterns of seismicity (and aseismicity) exist on a global scale, on a regional scale, and on a local scale. Certain of these seismicity patterns precede the occurrence of large earthquakes. The systematic location of worldwide earthquakes by the USGS National Earthquake Information Service provides a data base for monitoring zones of possible great earthquakes for precursory seismicity patterns.

2. The detection of P wave velocity variations precursory to a large earthquake is a complex and difficult task. Related practical problems, coupled with the poor understanding of the origin of these velocity variations, make this highly touted precursor far less useable than it was formerly thought to be.

3. Wave forms that originate from small to moderate earthquakes occurring in the region of a forthcoming great earthquake may change their character in relation to the evolving regional stress conditions. The new digital recording broadband seismograph systems now being installed by the USGS may permit monitoring of suspect seismic zones and detection of prognostic wave form changes as a large stress regime approaches failure.

Since this meeting, studies of seismicity patterns and the rupture dynamics of large earthquakes have been numerous. It is becoming increasingly clear that a definite reduction of low to intermediate magnitude earthquake activity occurs in what will be the aftershock zone of a large earthquake. At the same time there is often a small burst of activity near the hypocenter of the forthcoming large earthquake, which is then also followed by relative quiescence. These observations are consistent with the inclusion theory of earthquake occurrence [Brady, 1976]. Large earthquakes generally appear to be multiple-rupture phenomena, where the original failure nucleus dynamically ruptures into neighboring stress concentrations. This process continues until the regional stress field can no longer sustain crack growth. The multiple-rupture phenomenon may complicate the placement of an upper magnitude limit in an earthquake prediction.

Stress Drop and Earthquake Size

Appropriately, the conference began with discussions of the character of great earthquakes and quickly led into the nature of the related stress fields. Hiroo Kanamori (California Institute of Technology) began by emphasizing the difficulty of defining what a 'great' earthquake is. Conventional magnitude scales often lead to underestimation of inherent earthquake size, because the dimensions of large earthquakes often exceed the specific wavelengths used to determine magnitude. Thus body wave magnitudes (m_b), which are determined from P waves of about 1-s period, seldom exceed about 6.8, and 20-s surface wave magnitudes (M_S) never exceed about 8.6. Kanamori suggested that if a single parameter were to be used, then seismic moment would be a better measure of earthquake size. He compared the shallow Solomon Islands earthquake of February 1, 1974, with the disastrous shallow Chinese earthquake of July 27, 1976. The first event, with an M_S of 7.1, actually had a larger moment than the second event, which had an M_S of 8.0.

One of the most interesting topics discussed by Kanamori was that of 'silent earthquakes'—low stress drop events with little seismic wave excitation in conventional frequency bands, but nevertheless having large moments. As an example he mentioned the tsunami-producing Kurile Islands event of June 10, 1975, which had a body wave magnitude of 5.2 but was accompanied by large 200-s Airy phases. The 1896 Sanriku earthquake, which generated a great tsunami, had an M_S of only 7½. He said that the present tsunami warning system, which is based on M_S alone, is 'very dangerous.' Kanamori suggested that one practical tsunami warning system would use quick recovery of 100-s surface wave magnitudes from a special network. Data on seismic moment have also provided evidence that in the Kurile and Hokkaido Islands region about 70% of the motion required by plate tectonics occurs as aseismic slip.

Charles Archambeau (Cooperative Institute for Research in Environmen-

tal Sciences (CIRES), University of Colorado/NOAA) described studies of variations of the ratio of m_b to M_S in the Kurile-Kamchatka and Alaska-Aleutian regions. These data are interpreted with a model of the earthquake source that expands with a specified rupture velocity and is analogous to a generalized phase change. Synthetic seismograms can be computed from such a model with depth, stress drop, and source geometry as variables. Families of curves of m_b versus M_S based on these synthetic seismograms, lead to estimates of spatial variations of absolute stress within a region. For the Kurile-Kamchatka and Alaska-Aleutian data, inferred total stresses scatter between 10 and 1000 bars, the larger variability and higher stresses appearing more often for the smaller magnitude earthquakes.

Archambeau's m_b versus M_S data indicate high stresses in one of the seismic gaps of the Aleutians and a decrease of stress level after the occurrence of the large 1973 Hokkaido earthquake. Kanamori thought that differences in m_b/M_S were also caused by stress heterogeneities in the source regions. The smaller magnitude events characterized by high m_b/M_S ratios may reflect the higher stress concentrations within possibly 'locked' areas of faults, whereas low m_b/M_S values could be associated with large multiple-rupture earthquakes. Some participants advocated the concept of 'asperities' in fault zones as the points of nucleation of earthquakes and as points at which additional bursts of energy are released in large earthquakes. Don Anderson (California Institute of Technology) sees several mechanisms by which effective asperities can be created on fault surfaces. For example, change in pore fluid pressure along the fault surface or changes in the orientation of fault surfaces could result in local regions of relatively high strength that would hold up slippage on a fault until catastrophic failure occurs.

There was considerable discussion on possible reconciliation of these results on stress drop with laboratory studies and other seismic studies. Bryan Isacks (Cornell) noted that the high stress drop (~1 kbar) thought to be associated with the failure of

asperities would lead to anomalously high accelerations on the ground surface. For example, the widely used source model of James Brune predicts ground accelerations from a 1-kbar stress drop an order of magnitude higher than accelerations heretofore observed on strong motion records. The consensus was that the 1-kbar stress drop associated with the failure of an asperity would occur over a small part of a fault surface and that the average stress drop of a large earthquake could be much lower, resulting in lower ground accelerations. Thus an earthquake rupture may nucleate in regions of high stress and dynamically rupture into regions of lower stress.

For shallow earthquakes whose fault dimensions could be determined, Kanamori noted that most have an average stress drop of about 30 bars, as shown in Figure 1. Comparable stress drops are calculated for rock bursts in South African gold mines. Max Wyss (CIRES) noted that stress drops in intermediate- to deep-focus earthquakes are of the order of 10 bars. These observations, if substantiated by more detailed studies, have important implications for the physical changes involved during the earthquake preparation and rupture processes.

Donald Helmberger (California Institute of Technology) showed how wave form modeling can be used to infer properties at an earthquake source. The initial fast rise and then slower falloff source function determined in this way for the 1968 Borrego Mountain earthquake was supported by strong motion recordings taken at an epicentral distance of 60 km. This wave form suggests a possible initial rupture at high stress which then propagates into a region of lower stress. Thus it is again concluded that mapping variations in the source wave forms may reveal important features of spatial variations of stress. This technique also yields a good estimate of source depth, because the waves reflected from the surface are important in the teleseismic wave forms. Helmberger pointed out that higher frequencies are efficiently removed from teleseismic signals by anelastic attenuation so that very high stress drops may be difficult to detect with

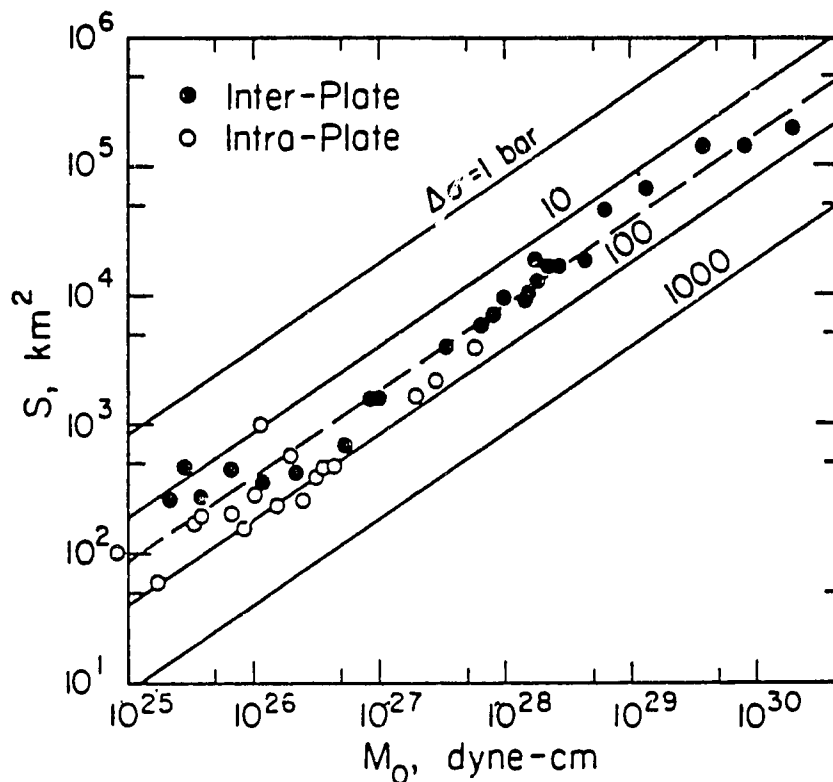


Fig. 1. Relation between S (fault surface area) and M_0 (seismic moment). The solid straight lines give the relations for circular cracks with constant stress drop $\Delta\sigma$. The dashed line is for $\Delta\sigma = 30$ bars. (Modified from Kanamori and Anderson [1975].)

teleseismic data. He proposed the deployment of digital strong motion seismographs in the aftershock zones of great earthquakes to gather data on stress drops associated with $M \approx 6-7$ aftershocks of these earthquakes.

Many conference participants called for additional research at both the very high and the very low frequency end of the seismic spectrum. Kanamori thought that very high peak frequency foreshocks to major earthquakes might be detectable with instruments sensitive to frequencies of 100 Hz and higher. At low frequencies (periods longer than 550 s), accelerated creep or some other preparatory process might be detectable prior to great earthquakes. Jon Peterson (USGS) gave a briefing on the new U.S. Geological Survey Seismic Research Observatory (SRO) data acquisition system. These seismograph systems are capable of recording from very short to tidal periods. They have a dynamic range of 120 dB, much superior to the analog records of the Worldwide Standardized Seismograph Network (WWSSN) but still insufficient to

record the full range of seismic motions between microseismic noise at a quiet site and the teleseismic ground motion of great earthquakes. Presently under discussion is a modification of a minimum of 20 WWSSN seismographs so that they record digitally also. Shelton Alexander (Pennsylvania State University) foresees major gains from the new SRO systems because they will greatly increase our ability to measure source parameters and transmission path effects. He foresees the application of pattern recognition methods to the comparison of the seismic signatures of different sources. Such methods may also be useful in studying temporal variations of stress in given source regions.

Space-Time Seismicity Patterns

A second part of this conference concerned earthquake space-time relations. Jack Healy (USGS) suggested that unusual seismic patterns could be foreshocks in a generalized sense and that searching for such pat-

terns could be a productive research area. He felt that foreshocks may have wave form or spectral properties that distinguish them from other earthquakes and that searching for such properties could result in useful predictive tools. John Kelleher (Nuclear Regulatory Commission) dealt with suggestive correlations between subduction of topographically varied sea floor and the mode of release of seismic energy along subduction zones. He found that if the inner wall of an island arc trench has a series of rugged and broken ridges, scarps, and terraces, then this zone is a likely source area for large tsunami-producing earthquakes that have maximum rupture lengths of about 150 km. Conversely, if the inner wall has long and relatively unbroken ridges, scarps, and terraces, then this zone is a likely source region for great earthquakes that have rupture lengths greater than 150 km.

Moreover, the rupture zones of major earthquakes ($M_S \geq 7.7$) at subduction zones appear not to overlap but systematically fill each arc segment. This process is related to the overall relative plate motions and leads to the formation of seismic gaps (Figure 2). These gaps have a high degree of earthquake expectancy (at least seven recognized and published gaps have been filled by large earthquakes), and the detailed low-magnitude seismicity occurring in and on the periphery of gaps may provide clues as to when the gap-filling earthquake will occur. George Plafker (USGS) discussed geologic studies showing that some sections of Alaska's Denali Fault have not had major slippage in the last 1500 yr, although long-term displacement across the fault zone is thought to average 1 cm/yr. These sections of the fault would seem to be likely sources of future great earthquakes.

William Spence (USGS) described a detailed study of the space-time character of the aftershocks of the 1965 Rat Islands earthquake. These aftershocks were relocated to compensate for location bias introduced by the high P wave velocities in the descending slab. Walter Elsasser's model of Newtonian (linear) stress propagation in an elastic plate overlying a viscous half-space was used to

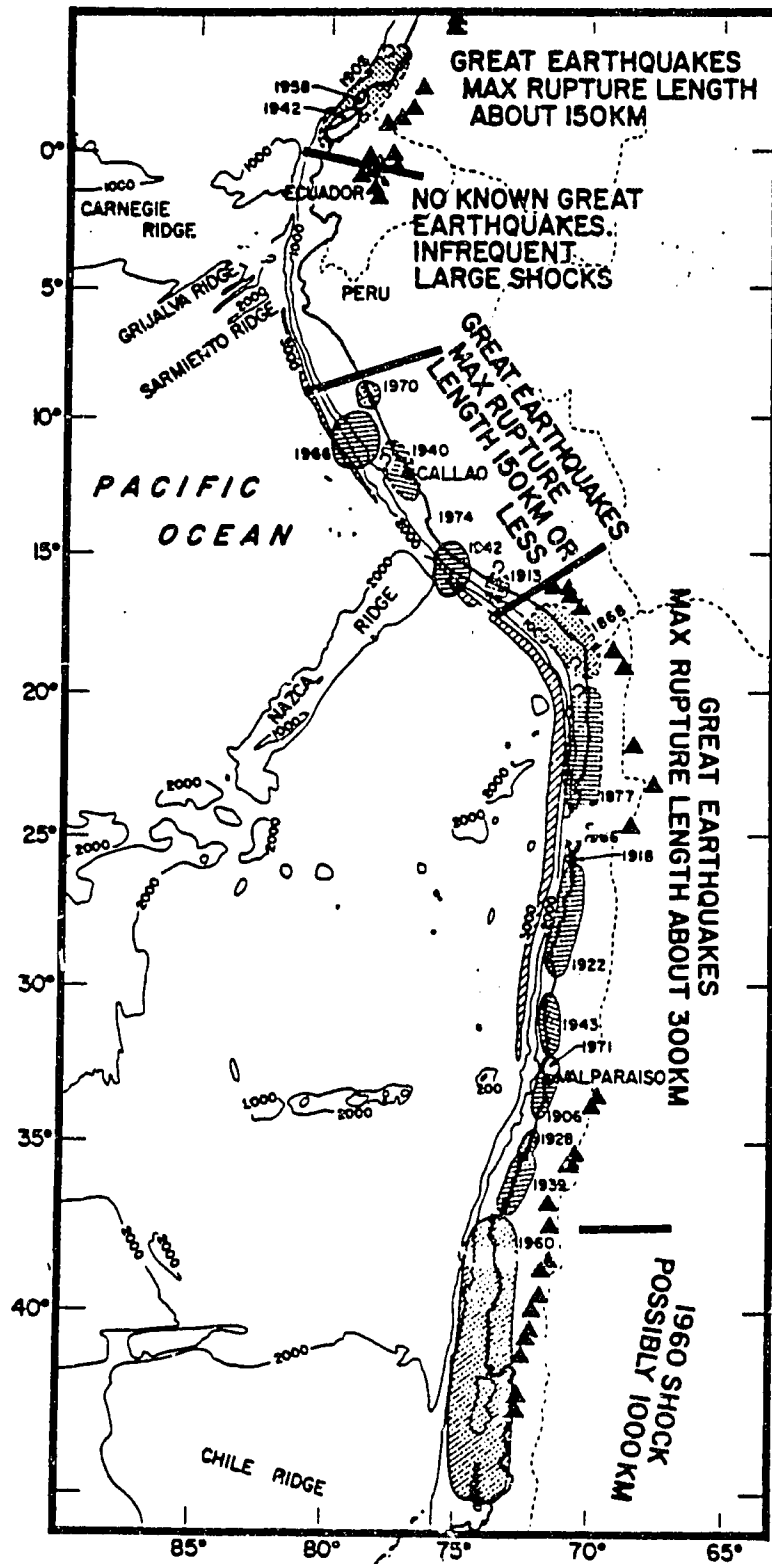


Fig. 2. Inferred rupture zones of major earthquakes near western South America, indicated by cross-hatching, do not overlap but appear to link so as to cover most of this plate boundary [Kelleher and McCann, 1976]. Note the absence of great shocks near the intersection of the massive Carnegie ridge complex with Peru-Ecuador. A seismic gap at about 13°S was filled by the magnitude 7.8 Peru earthquake of October 1974. The zone of southern Peru and northern Chile last had great earthquakes in 1868 and 1877 and may now be a candidate for another great earthquake. Solid triangles show active volcanoes and indicate the segmented nature of zones of active volcanism in western South America.

explain the observed relation of the stress release of the main event to the locations and focal mechanisms of many of the large 'aftershocks.' This interpretation of the observed definite space-time-focal mechanism sequence requires that following the main shock, in addition to the rebound of the island arc, a compressive strain pulse slowly diffused down the oceanic plate and an extensional pulse moved oceanward in the oceanic plate. The velocities of these strain pulses (actual plate motions) indicate an effective mantle viscosity of 6.0×10^{19} poise. Earthquake periodicities and migration patterns, particularly those described by K. Mogi, were discussed. Anderson noted that this simple model of linear mantle viscosity is consistent with many of the observed 'velocities' of earthquake migration. Yan Kagan (University of California at Los Angeles) described a method of statistically modeling earthquake sequences. He used the Duda world catalog and California catalogs and concluded that the largest aftershocks occur soonest and that large aftershocks migrate with velocities of the order of kilometers per day. His method may be useful in statistically testing claimed observations of earthquake migration or earthquake periodicity.

Animated discussion arose from talks by Michael Chinnery (Massachusetts Institute of Technology) and Brian Brady (U.S. Bureau of Mines) on correlations between earthquake occurrences and changes in the length of day (LOD). Chinnery's data consisted of earthquake time series constructed by making regional and global counts per unit time for earthquakes whose magnitudes were greater than a chosen threshold. He demonstrated striking correlations of activity between widely separated geographic regions and numerous correlations between shallow earthquake activity of one region with deep-focus activity in another region. The implication drawn was that there exists an unidentified global mechanism of earthquake (or stress) generation capable of rapid long-distance energy transfer. However, most of Chinnery's presentation dealt with correlations of global seismicity with changes in the

LOD. He showed apparent correlations of peaks in earthquake activity with peaks in LOD changes, after removal of seasonal effects. A search for periodicities in the earthquake catalogs using maximum entropy spectral techniques gave rise to a strong peak at a 235-day period based on worldwide data. No explanation is readily available for this phenomenon; it may be due to a beat frequency between other obviously periodic observations, such as the 40-yr peak. A major portion of Brady's presentation also dealt with long-term correlations of earthquake activity with changes in LOD. He feels that the great energy required by the inclusion model of earthquake occurrence implies that the preparation phases of large crustal earthquakes will cause stress changes at far greater distances from the eventual rupture surfaces than is generally accepted. Brady calculates that such stress changes can naturally involve the viscous upper mantle and that therefore upper mantle rheology can be a significant factor in the earthquake preparation process. He argued that these tectonic processes could provide the energy for changes in the LOD and for the excitation of the Chandler Wobble. Anderson also believes that great earthquakes may be correlated with excitation of the Chandler Wobble and LOD changes but noted that establishing cause or effect is the subject of heated debate.

Failure Theory and Some Seismic Precursors

Another primary theme addressed the physical basis of earthquake occurrence and the success of using seismic precursors in the prediction of earthquakes. Barry Raleigh (USGS) noted that although many tantalizing observations of earthquake premonitory phenomena have been made, we seem to be further from understanding them than we thought we were a few years ago. He proposed that precursory fault slip is necessary to generate the instability that culminates in an earthquake; perhaps dehydration or other thermally activated processes provide the mechanism for the instability. Brady presented a model for earthquake occurrence. He began with a discussion of

microscale characteristics of rock failure and a discussion of the energy required to break molecular bonds. He argued that initial cracks (due to tensile failure) are oriented parallel to the direction of maximum principal stress and that the initial dilatant volume consists of such cracks. His model then calls for crack coalescence and a localized crack concentration. This localized soft zone, the 'inclusion zone,' leads to higher stresses in the stiffer adjacent region and causes a 90° rotation of the local direction of maximum principal stress. A repetition of this process leads to conditions that power a jerky crack growth (multiple rupture). Brady suggested that this process is scale invariant and showed precursor time versus fault length data that plot linearly (Figure 3) from the scales of laboratory failure and mine rock bursts to the scale of major earthquakes. These data lead to the important implication that the physical basis for earthquake occurrence may be very similar to the mechanics of rock failure in mines or in the laboratory. He calculates a seismic efficiency factor of 0.5%, most energy being used to power crack growth or dissipated in frictional processes. Wyss recommended more extensive study of precursors to rock bursts in mines to bridge the gap between laboratory studies of hand specimens and teleseismic study of great earthquakes.

The Palmdale bulge was briefly considered. Raleigh reported that the region affected by the uplift has been found to be considerably larger than had at first been realized, extending nearly to the Imperial Valley. Moreover, triangulation data, obtained independently of the level lines, showed anomalous behavior at the time the uplift occurred. He noted that Wayne Thatcher has had considerable success at explaining the apparently complex spatial and temporal pattern of the uplift in terms of a simple model of a creep zone propagating upward along the San Fernando thrust fault prior to the 1971 San Fernando earthquake. Brady observed distinctive seismicity patterns here, occurring in the early 1960's, that are consistent with his inclusion model and thus independently tied the Palmdale bulge to the

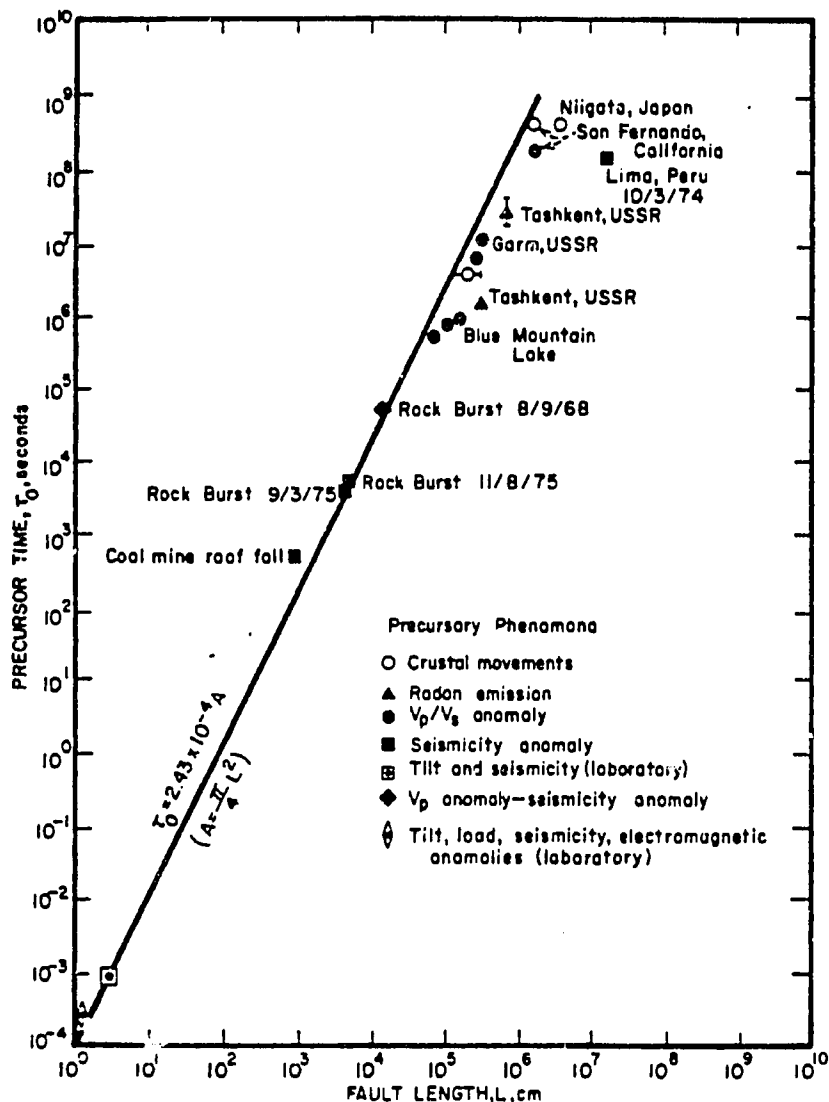


Fig. 3. Precursor (preparation) time τ_0 versus fault length L for selected earthquakes, mine failures, and laboratory failures [Brady, 1976]. The τ_0 refers to the time interval between the initiation of the process that leads to the occurrence of the failure and the actual occurrence of the failure; L refers to an average linear dimension of the aftershock region produced by the failure.

same stress anomaly that produced the San Fernando earthquake. Plafker noted that Alaskan geodetic studies have shown a long-term decrease in the rate of uplift of marine terraces in the Montague Island region prior to the 1964 Alaska earthquake.

William Ellsworth (USGS) brought to the group's attention that there are now 37 published studies on V_p residual and V_p/V_s variations reported to precede shallow earthquakes. Each study was characterized by Ellsworth with a given signal-to-noise ratio (S/N) based on the magnitude of the anomaly and the error bound within which the anomaly developed. The

results are listed below. (None refers to observations for which no data on the error bound were available.)

S/N	Number of Studies
<1	5
1	7
2	10
>2	2
none	13

According to Ellsworth, it is significant that the 'best' studies reported in the literature observe little or no variations in P wave delays or V_p/V_s ratios prior to earthquakes.

Wyss and Robert Engdahl (CIRES) discussed use of P wave delays to

detect possible dilatant zones and showed that anomalous ray paths, due to lateral variations in earth structure, create considerable problems. They suggested that some of this difficulty can be lessened by primarily using earthquakes that have focal depths of at least 500 km. It is apparent, on the basis of discussion during and following these presentations, that P wave delay data require considerable care to extract meaningful information. Wyss proposed that because the existing worldwide seismic network lacks density, a mobile array of compatible instrumentation, say, six in number, be made available to monitor local V_p time histories in zones that are thought to be due for major earthquakes.

Engdahl discussed Aleutian P wave delay data from deep Tonga earthquakes, obtained by using the wave correlation method, and showed convincingly that this method produces tight bounds on P wave delay variations for station separations less than 100 km. His primary conclusion was that the scatter in relative residuals between more widely separated Alaskan-Aleutian stations arises from lateral variations in earth structure along the ray paths.

Techniques for determining local structure and possible time-dependent velocity anomalies were presented by Ellsworth, HelMBERGER, and Bruce Julian (USGS). Ellsworth used P wave delays with the inverse technique of Keiiti Aki to determine the best upper mantle velocity structure in the regions of Hawaii and Lake Oroville. In each example, local earthquake data were used to predetermine local crustal structure. He found that relative P wave residuals prior to the $M_s = 7.2$, November 1975 Hawaiian earthquake, which were corrected for local structure effects, could not resolve perceptible V_p anomalies during the 5 yr preceding the event. HelMBERGER found unusual crust and upper mantle structure in the Puget Sound region, including a low-velocity zone at depths of about 40-60 km, as indicated by analysis of the teleseismic wave forms of the Puget Sound earthquakes as well as by analysis of body wave signals from distant earthquakes. Julian proposed use of surface waves to monitor

velocity changes beneath a seismometer array as an alternative to use of local or teleseismic travel time variations to detect possible precursory velocity anomalies in the crust. Such a technique would not depend on the occurrence of local seismicity and would be relatively insensitive to subcrustal velocity changes or to lateral velocity variations. Kanamori said that he had tried this method for southern California, but the effects of structural heterogeneity and multimode contamination must be considered before this method is applied.

An important consensus from this conference is that a prediction program based solely on detecting velocity anomalies may be premature and should be approached cautiously until earth structure effects can be more fully accounted for and until more reliable and accurate models of the earthquake preparation process are advanced or existing ones understood.

Conclusion

The conference was concluded by recapping the principal results, outlin-

ing some new areas for research, discussing the requirements for a new generation of seismic instrumentation, and noting how existing data handling procedures could be improved. Discussion was guided through a panel consisting of L. C. Pakiser (moderator), Anderson, Engdahl, Healy, and Kanamori. Many specific suggestions were given to assist the National Earthquake Information Service in improving its service to the seismological community.

The conference participants generally felt stimulated by the breadth and candor that pervaded these sessions. The authors of this report thank these participants for permission to summarize their comments.

Selected References

- Brady, B. T., Theory of earthquakes. IV, General implications for earthquake prediction, *Pure Appl. Geophys.*, 114, 1031-1082, 1976.
- Chinnery, M. A., and T. E. Landers, Evidence for earthquake triggering stress, *Nature*, 258, 490-493, 1975.
- Engdahl, E. R., J. A. Sindorf, and R. A. Eppley, Interpretation of relative teleseismic P wave residuals, *J. Geophys. Res.*, 82, in press, 1977.
- Kagan, Y., and L. Knopoff, Statistical search for non-random features of the seismicity of strong earthquakes, *Phys. Earth Planet. Interiors*, 12, 291-318, 1976.
- Kanamori, H., The energy release in great earthquakes, *J. Geophys. Res.*, 82, 2981-2987, 1977.
- Kanamori, H., and D. L. Anderson, Theoretical basis of some empirical relations in seismology, *Bull. Seismol. Soc. Amer.*, 65, 1078-1095, 1975.
- Kelleher, J., and W. McCann, Buoyant zones, great earthquakes, and unstable boundaries of subduction, *J. Geophys. Res.*, 81, 4885-4896, 1976.
- Kelleher, J., and J. Savino, Distribution of seismicity before large strike-slip and thrust-type earthquakes, *J. Geophys. Res.*, 80, 260-271, 1975.
- Langston, C. A., and D. V. Helmberger, A procedure for modelling shallow dislocation sources, *Geophys. J. Roy. Astron. Soc.*, 42, 117-130, 1975.
- Spence, W., The Aleutian arc: Tectonic blocks, episodic subduction, strain diffusion, and magma generation, *J. Geophys. Res.*, 82, 213-230, 1977.
- Sykes, L. R., Earthquake-prediction research outside the United States, Appendix B, in *Predicting Earthquakes, A Scientific and Technical Evaluation - With Implications for Society*, pp. 51-62, National Academy of Sciences, Washington, D. C., 1976.
- Wyss, M., Local changes of sea level before large earthquakes in South America, *Bull. Seismol. Soc. Amer.*, 66, 903-914, 1976.

Reprint from the Review
PURE AND APPLIED GEOPHYSICS (PAGEOPH)
Formerly 'Geofisica pura e applicata'

Vol. 117 No. 6 (1979)

Pages 1148-1171

Seismic Gaps and Source Zones of Recent
Large Earthquakes in Coastal Peru

by

J. W. Dewey and W. Spence

BIRKHÄUSER VERLAG BASEL

Seismic Gaps and Source Zones of Recent Large Earthquakes in Coastal Peru

By JAMES W. DEWEY and WILLIAM SPENCE¹⁾

Abstract – The earthquakes of central coastal Peru occur principally in two distinct zones of shallow earthquake activity that are inland of and parallel to the axis of the Peru Trench. The interface-thrust (IT) zone includes the great thrust-fault earthquakes of 17 October 1966 and 3 October 1974. The coastal-plate interior (CPI) zone includes the great earthquake of 31 May 1970, and is located about 50 km inland of and 30 km deeper than the interface thrust zone. The occurrence of a large earthquake in one zone may not relieve elastic strain in the adjoining zone, thus complicating the application of the seismic gap concept to central coastal Peru. However, recognition of two seismic zones may facilitate detection of seismicity precursory to a large earthquake in a given zone; removal of probable CPI-zone earthquakes from plots of seismicity prior to the 1974 main shock dramatically emphasizes the high seismic activity near the rupture zone of that earthquake in the five years preceding the main shock. Other conclusions on the seismicity of coastal Peru that affect the application of the seismic gap concept to this region are: (1) Aftershocks of the great earthquakes of 1966, 1970, and 1974 occurred in spatially separated clusters. Some clusters may represent distinct small source regions triggered by the main shock rather than delimiting the total extent of main-shock rupture. The uncertainty in the interpretation of aftershock clusters results in corresponding uncertainties in estimates of stress drop and estimates of the dimensions of the seismic gap that has been filled by a major earthquake. (2) Aftershocks of the great thrust-fault earthquakes of 1966 and 1974 generally did not extend seaward as far as the Peru Trench. (3) None of the three great earthquakes produced significant teleseismic activity in the following month in the source regions of the other two earthquakes. The earthquake hypocenters that form the basis of this study were relocated using station adjustments computed by the method of joint hypocenter determination.

Key words: Earthquake Prediction; Seismic Gaps; Tectonics of Peru.

Introduction

The purpose of this paper is to use accurately relocated hypocenters of earthquakes from the central Peruvian coastal region (Fig. 1) to test and refine hypotheses on seismic gaps and source zones of large earthquakes on active plate margins. For the time period of this study, 1964–74, the region experienced three great ($M_s \geq 7\frac{1}{2}$) earthquakes: 66.10.17 ($M_s = 7\frac{1}{2}$ –8), 70.05.31 ($M_s = 7.8$), and 74.10.03 ($M_s = 7.8$) (dates of earthquakes are given as year.month.day). The catalogs for this time period are

¹⁾ U.S. Geological Survey, Branch of Global Seismology, Box 25046, Mail Stop 967, Denver, Colorado 80225, USA.

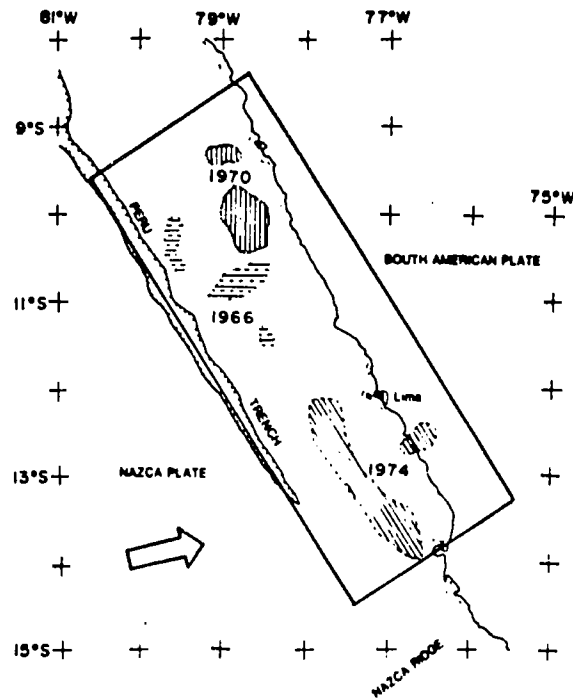


Figure 1

Reference map of central Peru coastal area. We redetermined hypocenters for earthquakes that were teleseismically located in the region bounded by crosses. The rectangle encloses the seismic zone shown in Figs. 2 through 11; shaded regions are our aftershock zones for the 1966, 1970, and 1974 earthquakes. 3000-fathom isobath indicates the location of the Peru Trench. Arrow shows direction of motion of Nazca plate relative to South American plate (MINSTER *et al.*, 1974).

complete for earthquakes of magnitude (m_b) 4.7 and greater (LANGER, 1977). We consider the type of seismic gap studied by MCCANN *et al.* (1978) – a segment of an active plate boundary that has been quiescent for a time long enough to permit accumulation of elastic strain sufficient to produce a large earthquake.

Initially we assume that the spatial distribution of well-located teleseismically-recorded aftershocks occurring within 31 days of each main shock provides an approximate map of the fault plane of the main shock, and we consider the following questions that bear on defining the extent of a gap that has been filled by a large earthquake or that bear on recognizing a plate boundary segment that is about to experience a great earthquake:

1. How completely do the hypocenters of teleseismically-recorded aftershocks represent the rupture areas of these earthquakes?
2. During the years prior to each great earthquake was the rupture area of the future earthquake largely free of moderate-sized earthquakes, except perhaps the region near the hypocenter of the future main shock?

3. Was there unusual seismic activity in the broad region surrounding and including each main shock rupture surface that could have been interpreted as precursory activity to the main shock?
4. Did the occurrence of a great earthquake trigger earthquake activity in a nearby seismic gap that was soon to experience its own major earthquake?

Analysis of seismic gaps in coastal Peru is complicated by the presence of at least two modes of faulting within the principal seismic source region of the Peruvian subduction zone from 60 km to 200 km landward of the Peru Trench. Thrust-fault mechanisms have been determined for the earthquakes of 66.10.17 (ABE, 1972; HUACO, 1978) and 74.10.03 (SPENCE *et al.*, 1975); these earthquakes probably occurred on the interface between the subducting Nazca plate and the overriding South American plate. The earthquake of 70.05.31 involved normal faulting (ABE, 1972; HUACO, 1978) and many of its aftershocks had reverse-fault mechanisms that are apparently inconsistent with thrust faulting on the interface between the Nazca and South American plates (STAUDER, 1975; ISACKS and BARAZANGI, 1977). ABE, STAUDER, and ISACKS and BARAZANGI have explained the 1970 earthquake in terms of stresses within the Nazca plate. Evidently there are at least two different stress environments, within the most active region of the Peruvian subduction zone, that are capable of producing destructive earthquakes.

Relocation of hypocenters

In order to better define the seismicity of coastal Peru, we have relocated the hypocenters of teleseismically recorded earthquakes; our conclusions are based on the hypocenters estimated to be most precisely located. Routinely determined hypocenters from the Peruvian region, plotted without selection criteria, reveal little about the fine structure of the subduction zone (Fig. 2); many of the hypocenters are biased by lateral variations in seismic-wave velocity or mislocated because the earthquakes were recorded through only a limited range of azimuths (BARAZANGI and ISACKS, 1979). In the relocated hypocenters (Figs. 3-11) the bias introduced by lateral velocity variations has been minimized by applying station adjustments to the travel time tables.

We used the method of Joint Hypocenter Determination (JHD) (the program is modified from DEWEY, 1971) on two groups of 15 well-recorded earthquakes, respectively north and south of 11°S, to estimate both the variances of different seismic phase arrivals (P, S, pP, PKP) to be used in phase weighting factors, and the station adjustments for each phase. The JHD-computed station adjustments and variances were then used in a single event location method to determine the hypocenters of all earthquakes in the corresponding latitude range. The precision of a redetermined hypocenter is estimated from 90% confidence ellipses (e.g., FLINN, 1965; EVERNDEN, 1969) on the pairs of hypocentral coordinates.

The JHD calibration event for the southern group of earthquakes was the shock of

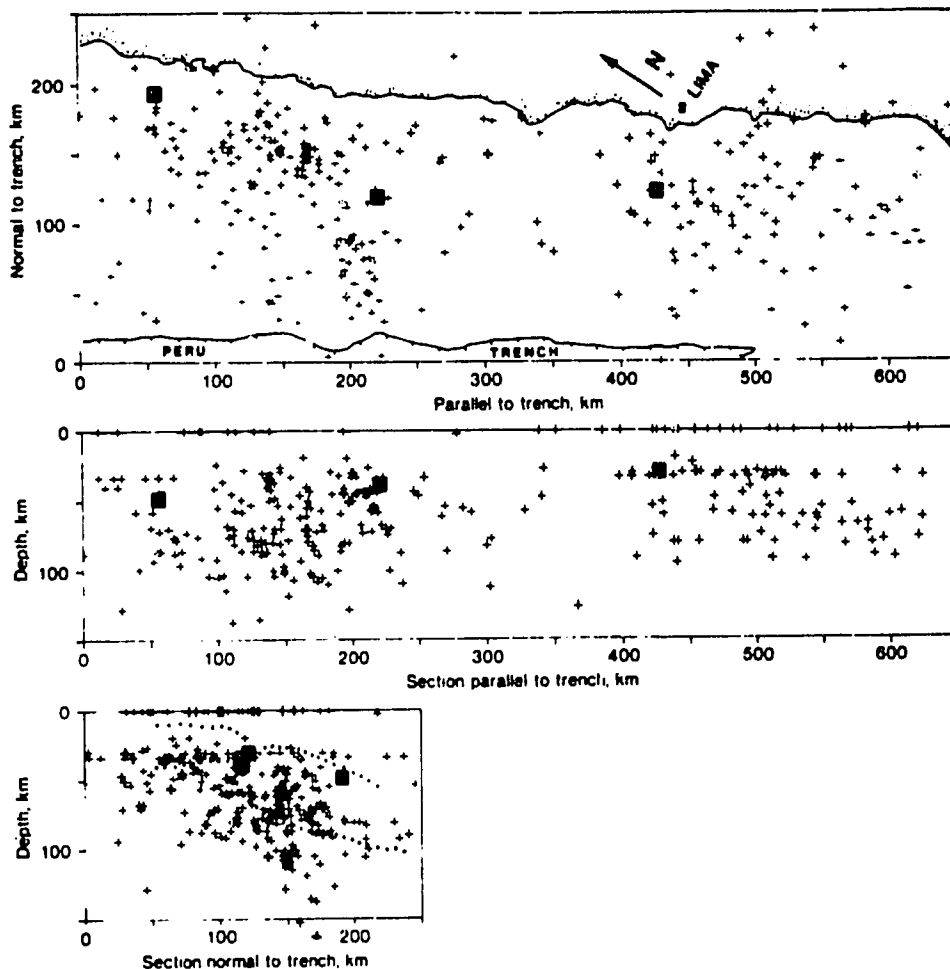


Figure 2

Hypocenters determined by the International Seismological Centre for the region of study (Fig. 1). Squares indicate hypocenters of the major shocks of 66.10.17, 70.05.31, and 74.10.03. Dotted lines on the section perpendicular to the trench indicate source regions defined by the b-quality relocated hypocenters of Fig. 3.

74.10.10 195300.7 UTC ($m_b = 5.3$, USGS), restrained to the location (12.52°S , 77.62°W , $h = 23.4$ km) determined by LANGER and SPENCE (1978) using data from a temporary regional network of seismographs. The JHD calibration event for the group of hypocenters lying north of lat. 11°S was the shock of 70.06.04, 040927.9 UTC, ($m_b = 5.8$, USGS), whose hypocenter (9.97°S , 78.68°W , $h = 54.6$ km) had been first located using the station weights and adjustments computed for the southern group of hypocenters.

Earthquakes relocated were those originally assigned by the International Seismological Centre (ISC) to the region indicated in Fig. 1. Arrival-time data consisted

for the most part of P, pP, S, and PKP readings listed in Bulletins of the ISC. We read seismograms of selected stations of the Worldwide Standardized Seismograph Network to obtain readings of pP to supplement readings of depth phases reported in the Bulletins. Arrival time data listed in the Bulletins of the ISC for aftershocks of the earthquake of 74.10.03 were supplemented by numerous P- and S-readings from the temporary network of LANGER and SPENCE (1978).

We relocated 478 teleseismically-recorded earthquakes. For 37% of these shocks, 90% confidence ellipses on the epicentral coordinates have semi-major axes less than

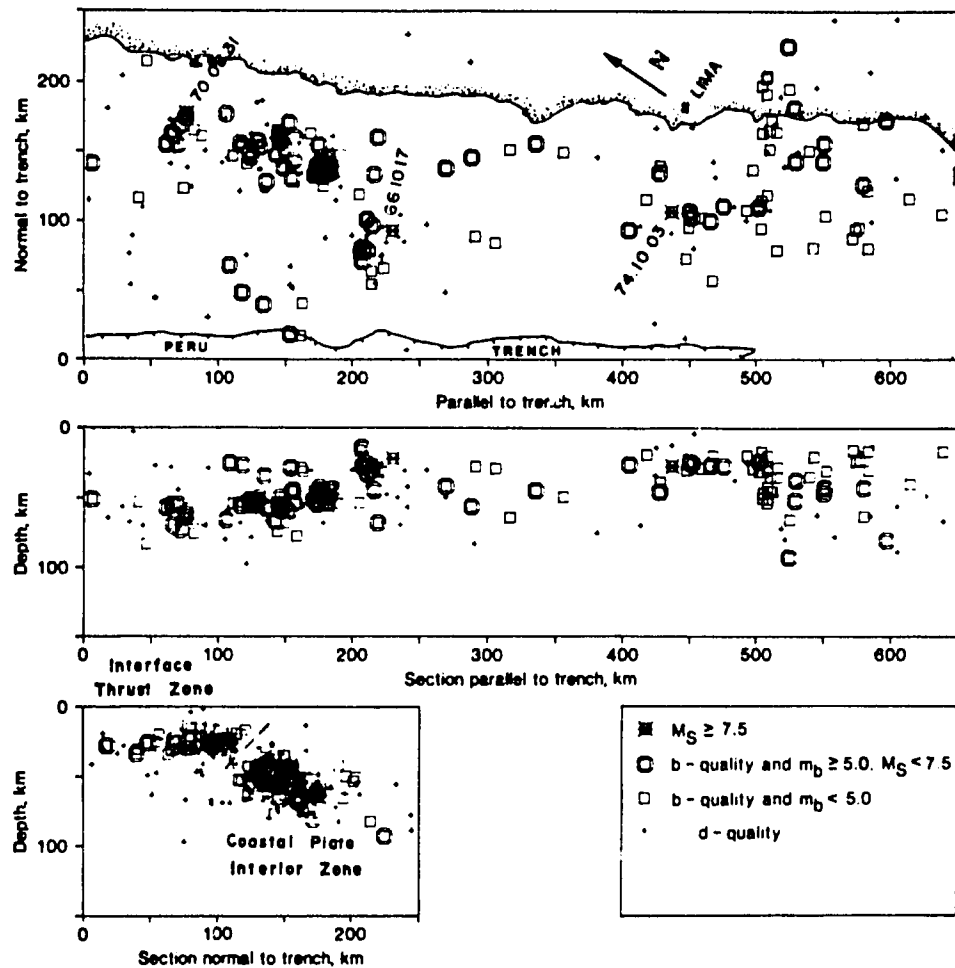


Figure 3

Hypocenters of b-quality (semi-major axes of 90% confidence ellipses on epicenter less than 20 km long) and d-quality (semi-major axes of 90% confidence ellipses on epicenter between 20 km and 50 km long) occurring in the study area (Fig. 1). 73% of the shocks plotted in Fig. 2 were relocated to b- or d-quality. Most of our inferences are based on the 37% of all shocks in Fig. 2 that were relocated to b-quality. The dashed line (in the section perpendicular to the trench) is the trenchward boundary of the coastal plate-interior (CPI) zone. Focal depths are likely to be least reliable near the trench.

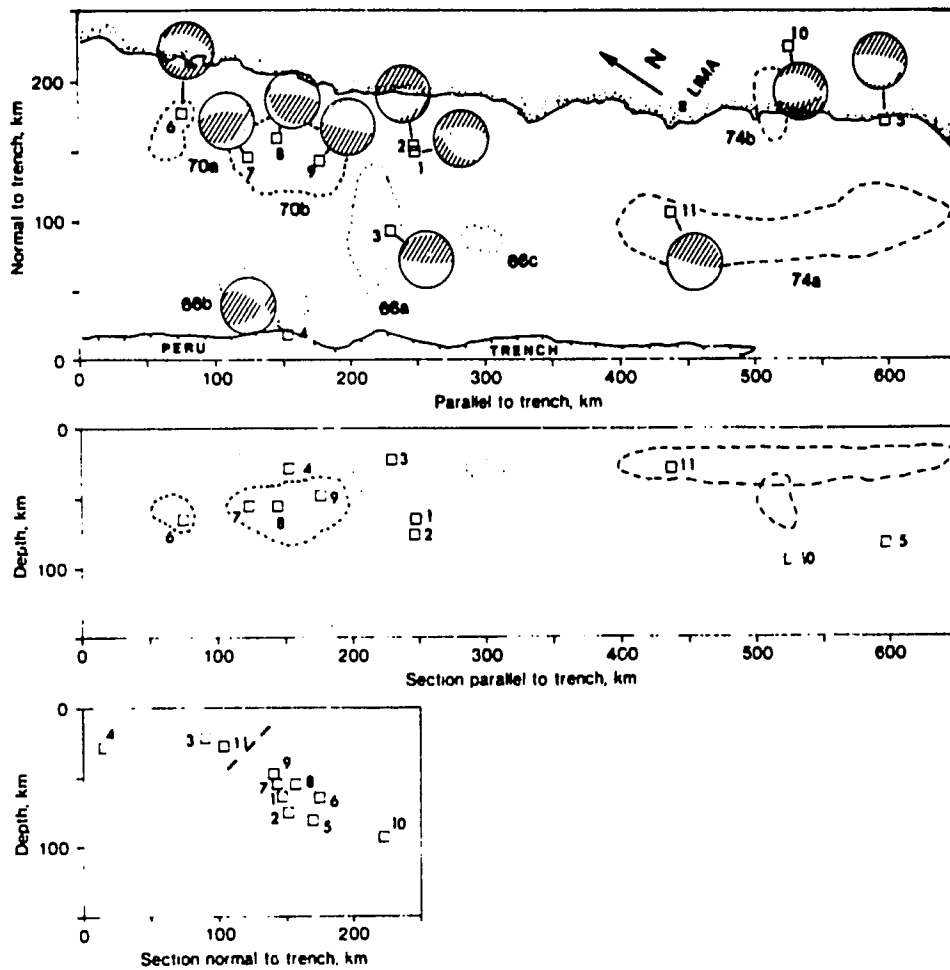


Figure 4

Focal mechanisms available for earthquakes in the region studied; earthquake hypocenters shown by squares. Parameters and sources of focal mechanisms given in Table 1. Dotted lines show after-shock zones from Figs. 5-7. All mechanisms are represented by the lower hemisphere of the focal sphere; quadrants of compressional P-wave motions are shaded. Dashed line in section perpendicular to trench is trenchward boundary of CPI zone from Fig. 3.

20 km in length (hereafter designated *b*-quality locations). For 36% of the earthquakes, 90% confidence ellipses on the epicentral coordinates have semi-major axes between 20 km and 50 km in length (hereafter designated *d*-quality locations). The remainder (27%) of the shocks could not be located to an estimated precision of 50 km or better; these shocks are not plotted in Figs. 3-11. The precision of focal depth determination is, for most shocks, roughly comparable to the precision of the determination of epicentral coordinates. Two-thirds of the hypocenters were located with the use of depth phases and many shocks were deep enough and near enough to the local seismograph stations NNA (Ñaña) and HUA (Huancayo) that P-wave times from

these stations enabled a reliable depth computation. The apparent deepening of the hypocenters toward the Peru Trench in the region of 0-100 km from the trench axis may be an effect of systematic errors in depth determination. Shocks near the trench axis would tend to be located too deep relative to shocks nearer the coast for two reasons: (1) a shallower M-discontinuity near the trench would cause earlier P_n -arrivals at the local stations and a consequent overestimation of focal depth, and (2), the interpretation of the pwP-phase as pP would cause deeper focal depths to be estimated for shocks occurring beneath the deeper water of the trench (MENDIGUREN, 1971).

P-wave readings at the nearest stations ($\Delta < 5^\circ$, variance typically 3 sec^2) and at teleseismic stations ($\Delta > 20^\circ$, variance typically $1\text{--}4 \text{ sec}^2$) were the most consistent.

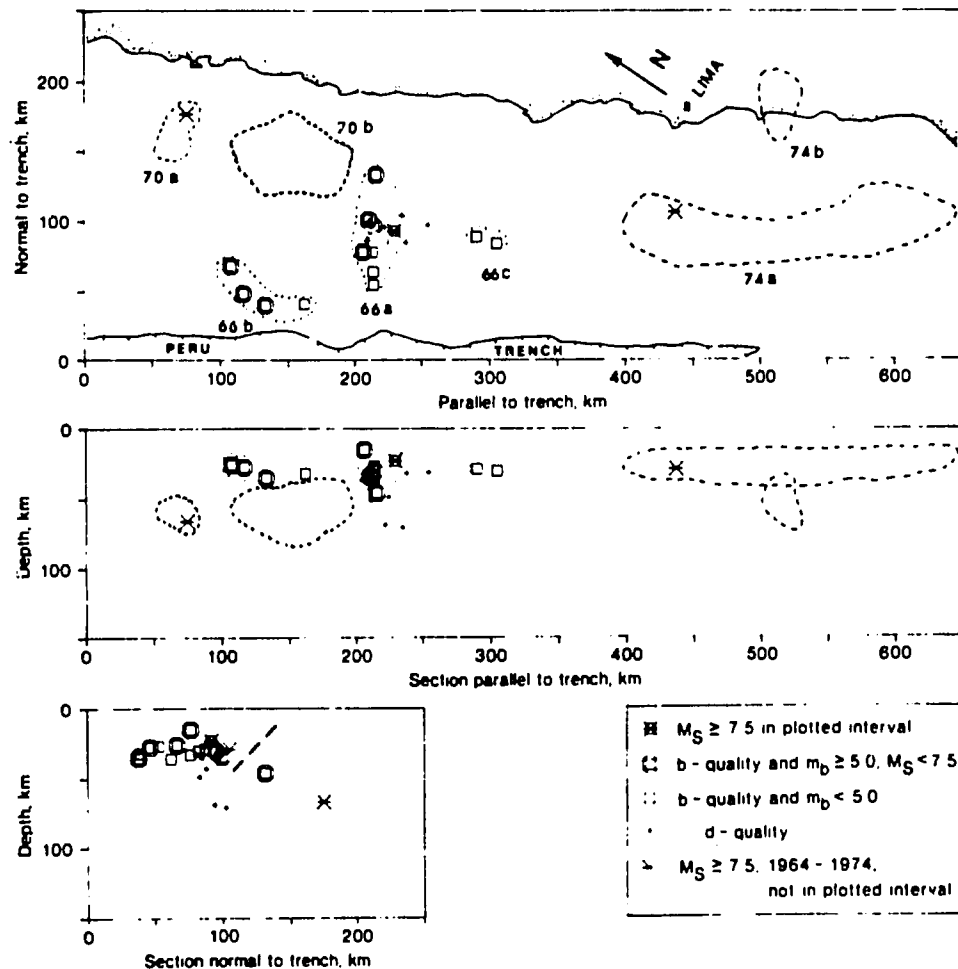


Figure 5

Aftershocks occurring within 31 days of the earthquake of 66.10.17. Principal aftershock zones (66a,b,c) are outlined on the basis of b-quality hypocenters. Also plotted are the hypocenters and aftershock regions of the yet-to-occur earthquakes of 70.05.31 (70a,b) and 74.10.03 (74a,b). Dashed line in section perpendicular to trench is the trenchward boundary of CPI zone from Fig. 3.

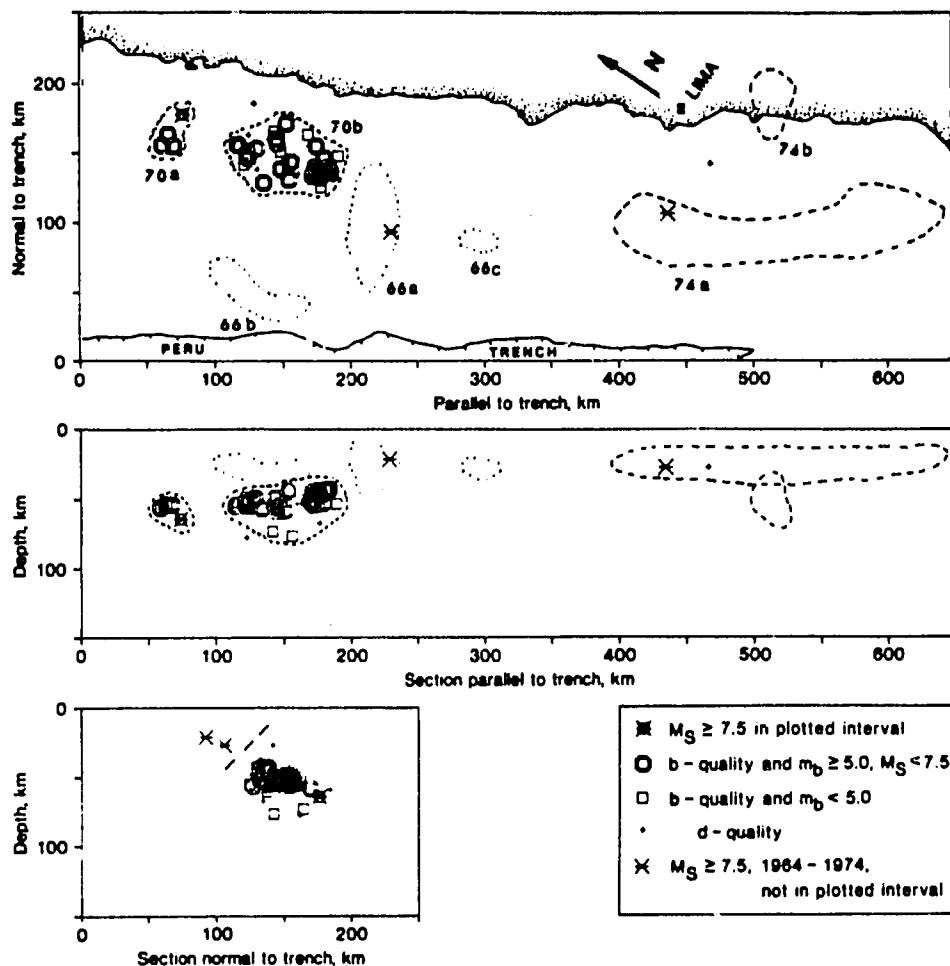


Figure 6

Aftershocks occurring within 31 days of the earthquake of 70.05.31. Principal aftershock zones (70a,b) are outlined on the basis of *b*-quality hypocenters. Also plotted are the hypocenters and aftershock zones of the previous shock of 66.10.17 (66a,b,c) and the yet to occur shock of 74.10.03 (74a,b). Because the focal depth of the main shock may be important in the interpretation of the aftershock sequence, we note that our focal depth (64 km) was estimated without depth phases and is estimated to be accurate to within 10 km at a 90% level of confidence. Dashed line in section perpendicular to trench is the trenchward boundary of CPI zone from Fig. 3.

P-wave arrival times at stations in the range of $\Delta = 8^\circ - 15^\circ$ were generally less consistent (variance typically 8 sec^2). The high variance regional stations include such normally reliable stations as ARE (Arequipa), PNS (Peñas) and LPB (La Paz). Inspection of seismograms at ARE and LBP shows that the initial P-waves from shocks in the region under study are very emergent and of low amplitude, probably the effect of a P-wave shadow zone (GUTENBERG and RICHTER, 1939), and later arriving P-waves likely are often reported as the initial P-wave. Computer location programs

will tend to interpret such late arrivals as indicating greater focal depth than is actually the case. The variance of the set of pP readings was about 6 sec^2 , corresponding to an uncertainty of somewhat more than 10 km in focal depth determination based on a single pP datum. The somewhat high variances of pP times relative to those of teleseismic P-wave times may arise in part from some pwP- or sP-phases being read as pP. The regional S-waves reported in the ISC bulletins had a high variance (typically 50 sec^2) and correspondingly were assigned low weights in the computation of hypocenters. The S-wave data provided by the aftershock network of LANGER and SPENCE (1978) did prove highly consistent (variance approximately 3 sec^2) and were most useful in determining hypocenters of aftershocks of 74.10.03.

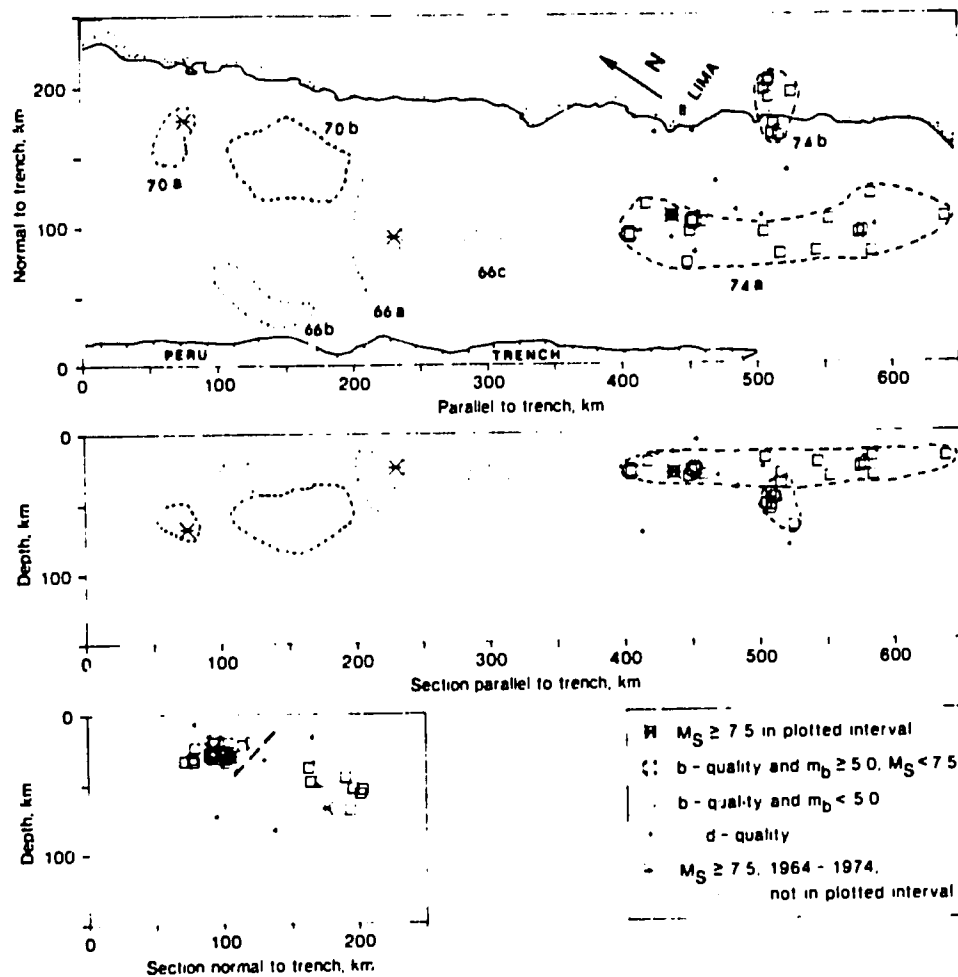


Figure 7

Aftershocks occurring within 31 days of the earthquake of 74.10.03. Principal aftershock zones (74a,b) are outlined on the basis of b-quality hypocenters. Also plotted are the hypocenters and aftershock zones of the previous shocks of 66.10.17 (66a,b,c) and 70.05.31 (70a,b). Dashed line in section perpendicular to trench is the trenchward boundary of CPI zone from Fig. 3.

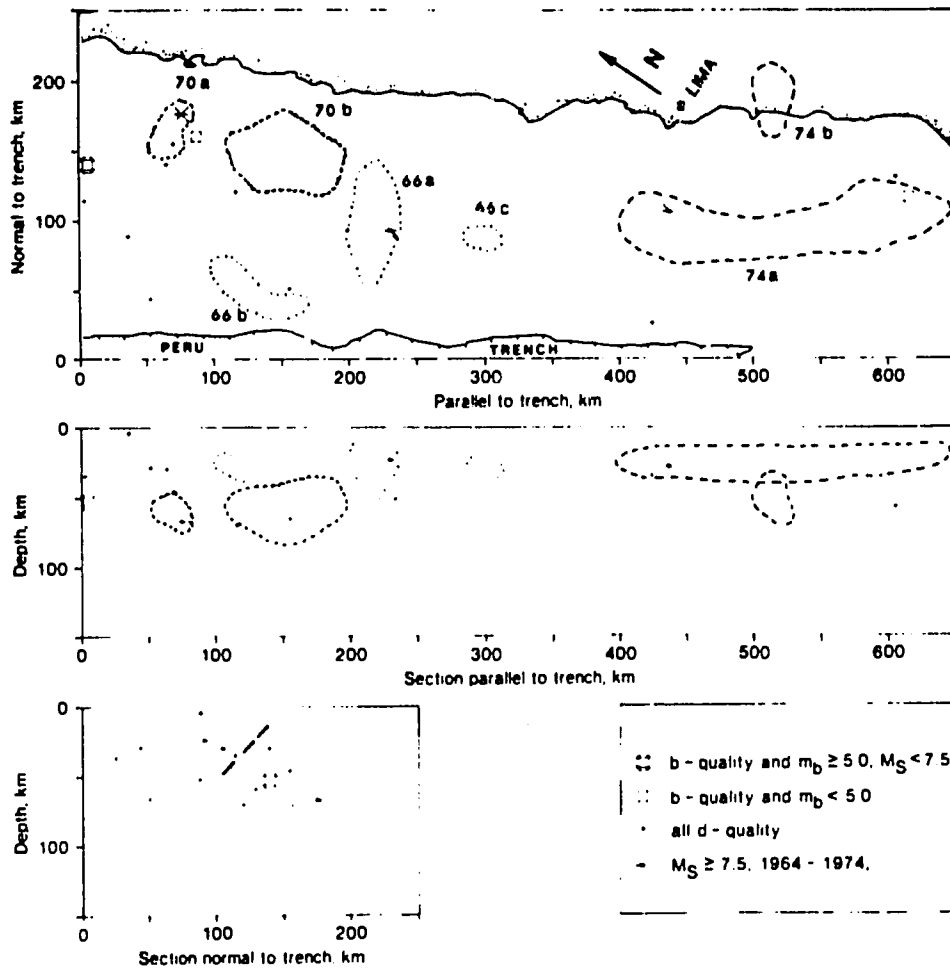


Figure 8

Seismic activity occurring from 64.01.01 through 66.10.16. Main shock hypocenters and aftershock zones of 66.10.17 (66a,b,c), 70.05.31 (70a,b), and 74.10.03 (74a,b) are shown. Dashed line in section perpendicular to trench is the trenchward boundary of CPI zone from Fig. 3.

Interface-thrust and coastal plate-interior seismic zones

Projection of a 650 km long segment of the seismic zone (Fig. 1) onto a depth section normal to the Peru trench (Fig. 3) shows two prominent zones of activity separated by a region of low activity. The seaward and shallower of the two zones is defined principally by aftershocks of the thrust-fault earthquakes of 66.10.17 and 74.10.03, and by a series of moderate shocks that preceded the earthquake of 74.10.03. We call this zone the interface thrust (IT) zone. The second zone includes hypocenters of eight earthquakes whose slip vectors are inconsistent with thrust motion on the interface between the subducting Nazca plate and the overriding South American plate

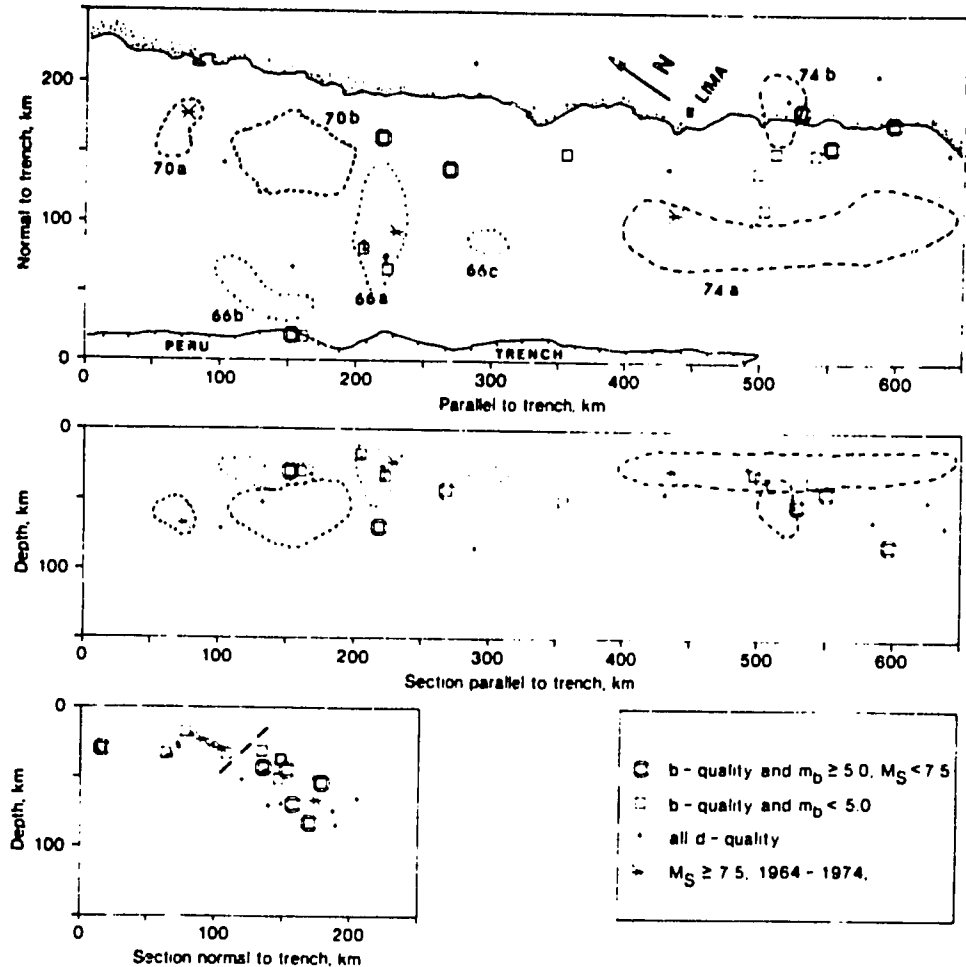


Figure 9

Seismic activity occurring from 66.11.17 through 70.05.30. Main shock hypocenters and aftershock zones of 66.10.17 (66a,b,c), 70.05.31 (70a,b), and 74.10.03 (74a,b) are shown. Dashed line in section perpendicular to trench is the trenchward boundary of CPI zone from Fig. 3.

(Table 1, Fig. 4). These earthquakes are interpreted as occurring within a plate interior (ABE, 1972; STAUDER, 1975; ISACKS and BARAZANGI, 1977), and we denote the second zone the coastal plate interior (CPI) zone.

The existence of two extensive shallow ($h < 70$ km) seismic zones, each capable of producing destructive earthquakes, may indicate that a given segment of the central Peruvian subduction zone inland from the Peru Trench has the potential to produce two great earthquakes, or, equivalently, that the occurrence of one great earthquake does not necessarily preclude the occurrence of another great earthquake in the same section of arc but at a different distance from the trench. Because CPI-zone earthquakes are postulated to result from large-scale deformation of the subducting Nazca

plate (ABE, 1972; STAUDER, 1975; ISACKS and BARAZANGI, 1977), the seismic gap concept as considered by MCCANN *et al.* (1978) may not be helpful in estimating the recurrence times of these earthquakes. Although the earthquake of 70.05.31 was the only major CPI earthquake in this region during 1964–74, the earthquake of 40.05.24, $M_s = 8.0$, may also have been a plate interior earthquake originating south of the focal region of 70.05.31 and inland from the southern portion of the focal region of the thrust fault earthquake of 66.10.17 (SILGADO, 1973).

The presence of two nearby seismic zones also complicates the detection of unusual seismic activity precursory to a great earthquake in one of the two zones. For example, because of the different stress regimes in the zones, the CPI zone could quite possibly

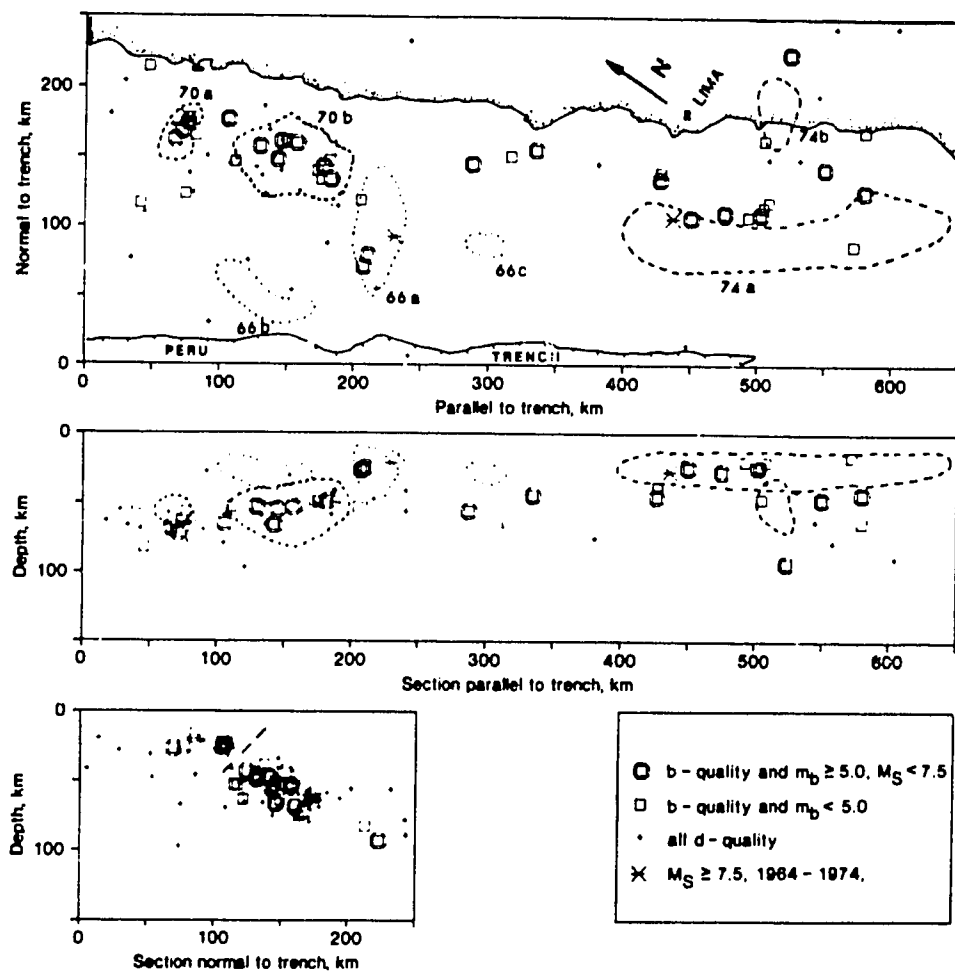


Figure 10

Seismic activity occurring from 70.07.01 through 74.10.02. Hypocenters and aftershock zones of 66.10.17 (66a,b,c), 70.05.31 (70a,b), and 74.10.03 (74a,b) are shown. Dashed line in section normal to trench is the trenchward boundary of CPI zone from Fig. 3.

be seismically active when the IT zone is inactive, and a resumption of distinctive activity in the IT zone prior to a major interface earthquake could go unnoticed amidst the general CPI zone activity.

Although the existence of two zones seems established from the locations of earthquakes and their focal mechanisms, the geometry of the boundary between the two zones is not well defined. For the purpose of summarizing the seismicity data of Fig. 3 and the focal mechanism data of Fig. 4, we have drawn in Figs. 3-11 (sections normal to the trench) a planar boundary that passes between the two prominent zones of hypocenters (Fig. 3), so as to separate the hypocenters of plate interior earthquakes

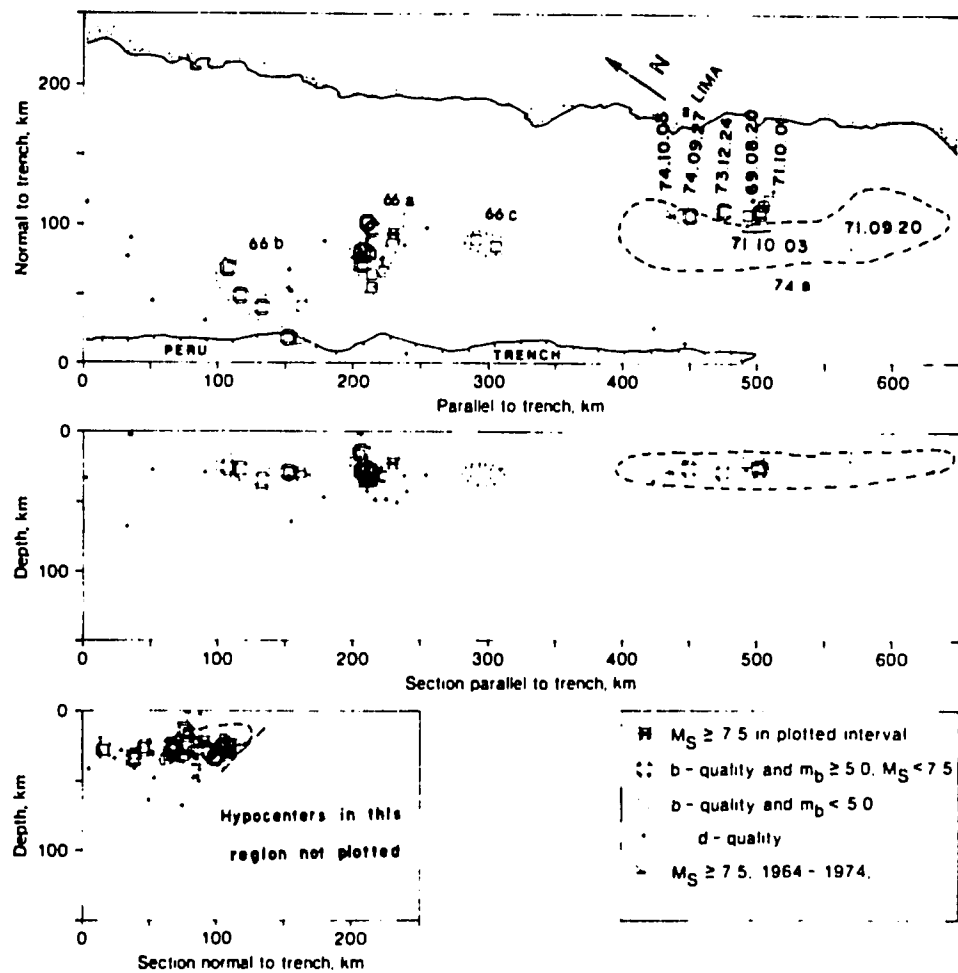


Figure 11

Shocks occurring from 64.01.01 through 74.10.02 west of the trenchward boundary of the CPI zone. Main shocks and aftershock regions not in the CPI zone are shown for 66.10.17 (66a,b,c) and 74.10.03 (74a). Dates of shocks near the 74a focal region are shown. The seismic gap identified by KELLEHER (1972) prior to 74.10.03 would correspond, in our coordinate system, to the region from 430 km to 640 km parallel to the trench.

Table 1

Source-parameter data for earthquakes whose focal mechanisms are shown in Fig. 4. Hypocenters are our joint hypocenter determination results. Magnitudes are M_s values unless otherwise indicated. The strike and dip are given in degrees for each nodal plane, with strike measured clockwise from north and dip measured clockwise from horizontal while looking in the direction of strike; the trend and plunge are given in degrees for the axes of greatest and least compressive stress

N	Date	H GMT	λ S	ϕ W	h km	Mag ^a	Nodal plane				Stress axes				Reference
							1st St	Dp	2nd St	Dp	P Tr	Pl	T Tr	Pl	
1	63.09.17	0554	10.78	78.26	64	6 $\frac{1}{2}$	328	53	187	44	180	69	76	5	WAGNER (1972)
2	63.09.24	1630	10.75	78.23	75	7	325	75	90	25	261	56	39	27	WAGNER (1972)
3	66.10.17	2141	10.92	78.79	21	7 $\frac{1}{4}$ -8	310	13	150	78	236	33	66	57	STAUDER (1975)
4	67.09.03	2107	10.69	79.74	28	6 $\frac{1}{2}$ -7	113	56	0	60	57	2	325	49	WAGNER (1972)
5	68.09.28	1353	13.21	76.33	80	6	336	78	121	15	257	57	59	32	WAGNER (1972)
6	70.05.31	2023	9.36	78.87	64	7.8	340	50	160	40	250	85	70	5	STAUDER (1975)
7	70.06.02	0137	9.87	78.89	54	5.7(m_b)	320	65	95	33	33	17	267	63	STAUDER (1975)
8	70.06.04	0409	9.96	78.68	55	5.8(m_b)	190	20	114	74	70	28	223	59	STAUDER (1975)
9	70.07.02	0045	10.28	78.66	47	5.8(m_b)	270	11	158	86	79	48	239	40	STAUDER (1975)
10	74.01.05	0833	12.42	76.31	93	6.6	356	40	133	58	352	67	240	10	**
11	74.10.03	1421	12.39	77.66	27	7.8	160	80	6	11	252	45	65	45	**

^a Magnitude determined by USGS and predecessors going back to the U.S. Coast and Geodetic Survey.

** W. Spence, C. J. Langer, and J. N. Jordan, unpublished data.

identified by focal mechanism solutions (Fig. 4) from hypocenters of interface thrust earthquakes identified by focal mechanism solutions. It seems clear, however, that the boundary could be greatly modified from the form of Figs. 3–11 and still satisfy the available seismicity and focal mechanism data. For example, the position of the boundary may change with distance parallel to the strike of the subduction zone. In addition, the stress-generating mechanism responsible for the CPI-zone earthquakes is not well-enough understood that we can confidently predict that the existence of CPI-zone earthquakes should preclude the occurrence of thrust-fault earthquakes on the immediately adjacent plate interface, down-dip from the known IT-zone earthquakes.

Clusters within the aftershock zones – implications for estimates of source parameters

Teleseismically-recorded aftershocks for 31 days following each of the three major earthquakes under study (66.10.17, 70.05.31, and 74.10.03) show a tendency to occur in clusters rather than to be distributed evenly along a planar structure that could be interpreted as a simple fault plane. These clusters are outlined in Figs. 5, 6, and 7. The clustering of teleseismically-recorded aftershocks makes it difficult to assess from teleseismic data how much of a seismic gap has been filled by a particular earthquake. Has the rupture extended to include all the regions of aftershock clusters, or do some of the aftershock clusters in fact represent activity triggered in highly strained regions, in and around which there is still the potential to produce a damaging earthquake in the near future?

Some of the clustering effect may be due to our considering only well-located teleseismically-recorded events. However, LANGER and SPENCE (1978), using data from a temporary local seismograph network, found that locally recorded aftershocks ($m_b \geq 3.0$), occurring during October 7–24, 1974, cluster in the same zones outlined by the teleseismically recorded aftershocks of 74.10.03 (Fig. 7). BILLINGTON and ENGBAHL (1978) found similar clustering among locally recorded aftershocks ($m_b \geq 3.0$) of the Aleutian Islands' earthquake of 77.11.04 ($m_b = 6.5$, depth = 18 km), with one cluster separated by a 35 km quiet zone from the main shock hypocenter.

66.10.17 earthquake. ABE (1972) estimated the seismic moment of the earthquake of 66.10.17 as 2.0×10^{28} dyne cm. Using a source area of 11 200 km² and a shear modulus of 7.0×10^{11} dyne cm², he inferred an average fault displacement of 2.6 m. The stress drop was estimated to be 42 bars using a formula derived for circular faults by KEILIS-BOROK (1959). In Fig. 5, these source parameters could correspond approximately to a convex area encompassing both 66a and 66b, or to a 50 km wide zone extending from the northwest end of 66b to the southeast end of 66c. One could also postulate that the main shock rupture was confined to 66a, and that 66b,c, and the regions between the clusters did not rupture in the earthquake. This model would require that 66b and 66c be triggered by the elastic readjustment of stress following the

main shock, since both 66b and 66c had become active within eight hours of the main shock. The source area would thus be about 5000 km². The average fault displacement (5.7 m) and stress drop (140 bars) under this hypothesis do not seem to be physically unreasonable. In other words, based on different interpretations of the aftershocks of 66.10.17, one could postulate that elastic stress had been relieved along the entire IT zone between and including 66b and 66c, or one could postulate that one or both of the 50 km long zones between the aftershock clusters continue to be stressed and capable of producing a large earthquake.

70.05.31 earthquake. We have defined two clusters, 70a and 70b, in the aftershock zone of the 70.05.31 earthquake (Fig. 6). The normal faulting main shock occurred in cluster 70a. The first teleseismically-recorded aftershock occurred at the south end of cluster 70b. However, the underlying mechanism by which many aftershocks were triggered by the main shock is not clear to us. Many of the aftershock hypocenters are at nearly the same depth, distributed over a zone several tens of kilometers wide (Fig. 6), and their locations are not consistent with their occurring on one of the planes of dip 40°–50° defined by the main shock focal mechanism solution (shock 6, Fig. 4). Moreover, the focal mechanisms of many of the aftershocks involve reverse faulting, apparently within the Nazca plate, in contrast to the normal faulting mechanism indicated by P-wave first motions of the 70.05.31 main shock (STAUDER, 1975; ISACKS and BARAZANGI, 1977). The three aftershocks with most completely defined mechanism solutions (STAUDER, 1975) have focal mechanisms very different from that of the main shock and all are in our 70b zone.

ISACKS and BARAZANGI (1977) studied P-wave first motions at selected stations for 28 of the aftershocks of Fig. 6 and 3 aftershocks occurring in the two months following the interval plotted in Fig. 6. They characterized the aftershock focal mechanisms as 'down-dip compression' or 'down dip tension,' depending on whether the first motions at the selected stations were consistent with the well-determined, respectively down-dip compression or down-dip tension, focal mechanisms of the larger earthquakes of the 1970 Peru sequence. Twenty-seven of their shocks lay in the region of our aftershock zone 70b, and 26 of these 27 were identified as down-dip compression shocks (B. ISACKS, written communication, 1979). Of the four aftershocks they studied that occurred in zone 70a, all are identified as down-dip tension shocks.

The rapid change in focal mechanisms between aftershock zones 70a and 70b is similar to changes of focal mechanism with distance parallel to the strike of the Benioff zone observed for intermediate depth earthquakes in the Aleutian Islands (ENGDahl and SCHOLZ, 1977). Such changes of focal mechanism parallel to the strike of the subduction zone evidently require models that consider the variations of stress and rheology in the subduction zone as functions of distance along strike. The characteristics of the aftershock sequence of 70.05.31 would, in addition, support models that predict that the readjustment of stress following a large earthquake in a region of down-dip tension should favor the occurrence of aftershocks in a nearby region of down-dip compression.

LOMNITZ (1971) observed that the 70.05.31 earthquake was a 'multiple event' and that prominent later events during the main shock appeared to have focal mechanisms different than that of the first event. It is possible that the main shock may have involved spatially separated events from source regions 70a and 70b, with focal mechanisms characteristic of both the down-dip compression aftershocks and the down-dip tension aftershocks identified by STAUDER (1975) and ISACKS and BARAZANGI (1977). In this case, individual events in the mainshock would have had stress drops substantially higher (e.g., MADARIAGA, 1979) than the overall stress drop of 23–35 bars inferred for this earthquake by ABE (1972).

74.10.03 earthquake. We assume that the principal source of energy for the earthquake of 74.10.03 was the aftershock zone 74a. We use source dimensions of 40 km × 240 km, the moment of 1.5×10^{28} dyne cm obtained for this earthquake by G. S. Stewart (reported by KANAMORI, 1977), and the value of rigidity and equation for stress-drop assumed by ABE (1972) in his study of the two earlier Peru earthquakes. The stress drop is then estimated to be 39 bars.

Discussion. Strong motion data reported by CLOUD and PEREZ (1971) are qualitatively consistent with the sources of 66.10.17 and 70.05.31 comprising high stress-drop events whose dimensions were significantly smaller than the overall aftershock zones of these earthquakes. Peak accelerations recorded at Lima for 66.10.17 and 70.05.31 were substantially larger than would have been expected on the basis of strong motion data from 18 other moderate-to-large earthquakes in the Western Hemisphere. The high accelerations recorded for 66.10.17 and 70.05.31 were associated with unusually high predominant frequencies (CLOUD and PEREZ, 1971). Peak accelerations measured at Lima from the 74.10.03 earthquake were more consistent with the primary data set of CLOUD and PEREZ, and the damage pattern in Lima from the earthquake of 74.10.03 suggested lower frequency strong ground motion than had been the case in 66.10.17 (ESPINOSA *et al.*, 1977). The transmission to Lima of anomalously high frequency accelerations from the 66.10.17 and 70.05.31 sources may also imply anomalously low attenuation for those source-receiver paths.

The shocks of 66.10.17 (Fig. 5) and 74.10.03 (Fig. 7) were both followed by aftershocks in the CPI zone. After the 74.10.03 shock, there was a cluster of aftershock activity (74b), well located by the temporary stations of LANGER and SPENCE (1978), inland from and deeper than the principal aftershock-region 74a. Langer and Spence (personal communication, 1978) have studied focal mechanisms and overall geometry of the 74.10.03 aftershock zone as defined by both teleseismically- and locally-recorded data and conclude that the 74b aftershocks probably represent internal deformation of the Nazca plate. The occurrence in the CPI zone of aftershocks of IT zone earthquakes is evidence of a linkage between the seismicity of the two zones.

For most of their lengths, the aftershock zones of 66.10.17 and 74.10.03 extended no closer to the axis of the Peru Trench than 50 km to 75 km (Figs. 5 and 7). The broad areas trenchward of aftershock zones 66a, 66c, 70a (Figs. 4 and 6) could conceivably represent source regions for future large earthquakes. Alternatively, the dip of the

fault surface associated with 66.10.17 and 74.10.03 may have steepened trenchward of the earthquake focus, and the surface may have intersected the sea bottom well inland from the trench axis. PLAFKER (1972) has postulated that the principal fault plane or planes of the 1960 Chilean earthquake and the 1964 Alaskan earthquake may have steepened trenchward of the respective hypocenters and broken through the overriding plate, and PRINCE and KULM (1975) have suggested that a similar phenomenon may occur off the coast of Peru. FUKAO (1979) finds in the Kurile arc and northern Japan that fault surfaces on which great earthquakes occur may both be steeper toward the trench and remain unbroken during the main shock at their trenchward extremities. These trenchward regions may later produce tsunami earthquakes. The focal mechanism of earthquake 67.09.03 (Fig. 4) is consistent with steeply dipping reverse faulting near the Peru Trench; this mechanism also requires a component of left-lateral, strike-slip motion. Although the computed focal depth (28 km) of 67.09.03 and those of neighboring shocks would place them below the interface between the Nazca and South American plates, the computed depths of these shocks may be systematically too great (see section on 'Relocation of hypocenters').

*Seismicity prior to the earthquakes of 17 October 1966, 31 May 1970,
and 3 October 1974*

A number of studies (e.g., MOGI, 1969; KELLEHER and SAVINO, 1975; BRADY, 1976; OHTAKE *et al.*, 1977) have postulated that for some years prior to the occurrence of a major earthquake, the source region of the shock is largely quiescent except for a distinctive pattern of moderate earthquake activity that might indicate the point of initial rupture or the origin time of the future main shock. The patterns recognized by various workers differ in detail, and we use, for convenience, the pattern recognized by KELLEHER and SAVINO (1975, p. 260) as the type with which we compare the Peruvian data:

1. Extensive portions of the interior of the rupture zones remain aseismic until the time of the main shocks. The aseismic character of most of the zone extended to at least several magnitudes below the magnitude of the pending main shock.
2. Prior seismicity that did occur was generally confined to the vicinity of the epicenters (points of initial rupture) of the pending main shocks and/or the edges of the rupture zones. There are some indications that the level of this prior activity, particularly in the vicinity of the epicenter, increased as the time of the main shock approached.

There are too few well-located (b-quality) epicenters occurring during the time interval 64.01.01-66.10.16 (Fig. 8) to define any characteristic patterns of seismicity prior to the Peruvian earthquake of 66.10.17. The pattern of seismicity prior to the earthquake of 70.05.31 (Figs. 8 and 9) is consistent with the pattern recognized by Kelleher and Savino although, as discussed earlier, the earthquake of 70.05.31

occurred within a plate rather than at the interface between plates. There is one b-quality shock, occurring on 65.11.06, located within 20 km of the hypocenter of earthquake 70.05.31 (Fig. 8). Otherwise, the focal region of 70.05.31 is devoid of well-located hypocenters. There were, however, other regions in the study area that seemed similar to the future source region of 70.05.31 (Figs. 8 and 9), in that a number of seismically quiet regions in the CPI zone could have been identified and associated with hypocenters that could be considered possible sites of future main-shock hypocenters. The nearness in space and time of the earthquakes of 66.10.17 and 70.05.31 may indicate either that the nonelastic readjustments of the regional strain field after 66.10.17 ultimately triggered 70.05.31, or that the two earthquakes were responding to the same tectonic phenomenon, the greatly different source mechanisms of the shocks notwithstanding.

The seismicity occurring prior to 74.10.03 is most like the pattern recognized by KELLEHER and SAVINO (1975). The principal rupture zone, 74a, was largely quiescent for the more than ten years prior to the main shock. Moreover, seismicity increased, during this time period, on the landward edge of 74a. We observed significant seismic activity in the region immediately down dip from the principal source region (Figs. 9 and 10).

Previous work on the source region of the earthquake of 74.10.03 had essentially considered the IT and CPI zones as a single seismic zone. KELLEHER (1972, p. 2097) had recognized the region of the 74.10.03 shock as a zone of 'relatively high earthquake risk.' His seismic gap lay between the aftershock zones of the earthquakes of 40.05.24 ($M = 8$, GUTENBERG and RICHTER, 1954) and 42.08.24 ($M = 8.1$, GUTENBERG and RICHTER, 1954). Kelleher's gap corresponds more closely to the source region of 74.10.03 than does the 'gap' defined in the distribution of teleseismically-recorded IT-zone earthquakes for 64.01.01-74.10.02 (Fig. 11). However, as noted earlier, the earthquake of 40.05.24 may have occurred within the CPI zone rather than in the IT zone. BRADY (1976), using routinely determined USGS hypocenters, pointed out that earthquakes had occurred in the region of the 1974 source prior to 74.10.03 and identified as precursory activity some shocks that we have included in the CPI zone, as well as moderate earthquakes included in our IT zone. The characteristics of Peruvian seismicity seen by Kelleher and Brady may be further evidence of a seismo-tectonic coupling of the two different local stress regions.

We wish to also consider the prior seismicity of the source region of 74.10.03 by examining only the seismicity of the region oceanward of our inferred boundary between the IT zone and the CPI zone (Fig. 11). When the CPI-zone earthquakes are removed from the seismicity catalogue, the IT zone earthquakes from the region of the 1974 source region assume considerable prominence. They are, in fact, the only well-located earthquakes (b-quality) in the 650 km long section of the IT zone that are not within or immediately adjacent to the aftershock zones 66a, 66b, and 66c (Fig. 11). KELLEHER *et al.* (1973) have observed a tendency for large thrust-fault earthquakes to initiate at depth and propagate upward and along the interface between the two

plates. The distribution of main-shock and aftershock epicenters of 74.10.03 is consistent with this observation; the main shock is near the landward edge of the principal aftershock zone 74a (Fig. 7). Again, the striking feature of Fig. 11 is that the IT zone seismicity near and prior to 74.10.03 was also concentrated at the landward edge of the aftershock-zone 74a. For a little more than five years, seismic rupture was concentrated at approximately the same depth and distance from the trench as the main-shock hypocenter of 74.10.03, along 60 km of the lower edge of the future rupture surface of 74.10.03. The shocks of 71.10.03, 73.12.24, and 74.09.27 were the largest three earthquakes, having magnitudes (m_b , USGS) of 5.2, 5.4, and 5.0, respectively. Earthquakes of this magnitude (m_b) would not be expected to rupture the entire 60 km long segment of the lower edge of the IT zone in which the earthquakes occurred unless the shocks had very low stress drops. It is therefore unlikely that the prior seismicity from the source region of 74.10.03 represents the continuous seismic rupture of the 60 km segment of the IT zone.

The occurrence of these shocks as activity premonitory to 74.10.03 would be consistent with two general mechanisms proposed to account for precursory seismic activity. On the one hand, such premonitory activity may be a result of the redistribution of stresses due to preliminary failure within the future rupture zone itself. For example, the formation of microcracks (e.g., MYACHKIN *et al.*, 1972; BRADY, 1976), or the occurrence of aseismic fault slippage (e.g., DIETERICH, 1978) within the rupture zone could increase stresses near the boundary of the focal region to the point where moderate earthquakes occur. On the other hand, moderate earthquake activity could also be the result of generally high stresses in the broad region within which 74.10.03 occurred. From this second viewpoint, it could be postulated that the critical stress level necessary for seismic slippage is reached first at a distance of about 100 km inland from the axis of the Peru Trench, at the landward edge of the IT zone, because hypocenters of the postulated precursory seismicity to 74.10.03 and of the main shocks of 66.10.17 and 74.10.03 are concentrated at this distance from the trench axis.

*No short-term positive correlation between activity in
three principal source regions*

Figures 5, 6, and 7 show that in the month following each of the major shocks of 66.10.17, 70.05.31, and 74.10.03, there was no increase in the number of teleseismically-recorded shocks from the other two source regions. Apparently the changes in elastic strain associated with each of the main shocks were insufficient to immediately trigger numerous earthquakes in the other two source regions. This is of interest because, for example, by the time of the 1966 earthquake, the source regions of the 1970 and 1974 earthquakes were also approaching the end in time of strain cycles that were to result in their respective earthquakes. We had thought that we might find a phenomenon similar to that reported by FEDOTOV (1969), in which many early aftershocks of one

great Kurile Island earthquake (6 November 1958) occurred at the hypocenter of a subsequent great earthquake (13 October 1963). The rupture zones of these two great earthquakes abutted or overlapped one another. However, the source region of the Peru thrust-fault earthquake of 74.10.03 was probably about 100 km distant from the source region of 66.10.17 (Fig. 5). The known focal mechanisms in the 70b cluster (Fig. 6) are dissimilar to the focal mechanism for the 66.10.17 main shock (Fig. 4); thus although the zone 70b is very near to zone 66a it perhaps is not surprising that the 66.10.17 main shock did not trigger activity in cluster 70b. In any case, no part of the 1970 or 1974 source regions produced a teleseismically recorded earthquake in the month following 66.10.17. One shock (occurring on 70.06.19) is located (d-quality) in the region between 74a and 74b in the month following 70.05.31 (Fig. 6).

Conclusions

We have used the joint hypocenter determination method to relocate teleseismically-recorded earthquakes of central coastal Peru for the period 1964–74. Based on these relocated data, two distinct coastal zones of shallow seismicity can be identified. The first zone corresponds to earthquakes occurring on the thrust interface while the second zone, which is deeper than and inland from the first, corresponds to earthquakes occurring within a plate removed from the subduction interface.

The seismicity of coastal Peru offers examples of difficulties that have been anticipated by many seismologists (e.g., MCCANN *et al.*, 1978) in the application of the gap concept to specific regions. *First*, the region of coastal Peru experiences destructive earthquakes that occur near the interface between the plates but are actually plate-interior earthquakes (in our CPI zone). The presence of two nearby seismic zones, each corresponding to different stress regimes, may greatly hinder the identification of seismic gaps or anomalous precursory activity in either zone if the hypocenters of earthquakes in the two zones cannot be distinguished by accurate location methods or, possibly, by focal-mechanism studies. *Second*, there may be a significant uncertainty in the dimensions of a main-shock rupture as estimated from teleseismically-recorded aftershocks. The aftershocks tend to occur in spatially separated clusters, and it is possible that some clusters occur in source regions that are distinct from that of the main shock and that remain highly strained and capable of producing a future strong earthquake. There are corresponding uncertainties in estimates of average fault displacement and stress drop for the main-shock rupture and in estimates of dimensions of possibly unfilled seismic gaps. *Third*, aftershock zones of the large thrust-fault earthquakes of 66.10.17 and 74.10.03 did not extend out to the Peru Trench but left, free of aftershocks, long regions of 50–75 km width immediately inland from the trench axis. Either this region is not completely decoupled and there remain zones that are still stressed and capable of producing large earthquakes, or in central Peru the width of the rupture zone of the largest probable interface thrust earthquakes cannot be

reliably estimated from the distance between the trench axis and the epicenters of the deepest interface-thrust earthquakes, as is sometimes done in other regions. It is notable that no normal-faulting earthquakes are known to have occurred near the Peru Trench, following the earthquakes of 66.10.17 and 74.10.03. Trench-associated, normal-faulting earthquakes have been postulated to occur when subduction zone decoupling occurs between oceanic and continental plates (KANAMORI, 1972; ABE, 1972; SPENCE, 1977; HANKS, 1979) as a consequence of accelerated movement of the oceanic plate past the trench region.

In searching for seismic activity precursory to a large earthquake, it may be advantageous to consider the seismicity of the IT-zone and the CPI-zone both jointly and separately. The nearness in space and time of the earthquakes of 66.10.17 and 70.05.31 suggest that they are related tectonically, despite the great differences in focal mechanism and, similarly, we have noted the possibility that foreshocks to the IT-zone earthquake of 74.10.03 occurred in the CPI-zone. However, by considering IT zone seismicity separately from CPI zone seismicity, we may be able to recognize possible systematic differences in the characteristics of precursory phenomena in the two zones. We have shown that removal of CPI zone earthquake data from regional seismicity plots prior to 74.10.03 dramatically emphasized a group of moderate earthquakes that occurred near the main-shock rupture of 74.10.03.

Hypocenters of aftershocks to 70.05.31 defined two clusters. The main shock, which began as a normal faulting earthquake, had its point of initial rupture in the northern cluster. Aftershocks in this cluster also have focal mechanisms consistent with their being produced by extensional stresses oriented down-dip, parallel to the general dip of the seismic zone. The southern cluster of aftershocks contained many more teleseismically-recorded aftershocks than the northern cluster, and the large majority of these aftershocks had focal mechanisms consistent with their being produced by compressional stresses oriented down-dip. Because these two clusters of aftershocks occur at the same distance from the Peru Trench and over the same depth interval, the different focal mechanism characteristic of each cluster may indicate rather rapid variation of stress or plate rheology parallel to the Benioff Zone within the Nazca plate. The main shock of 70.05.31 may have been a multiple event, with significant energy contributed from the regions of both the northern and southern clusters.

Acknowledgements

The P-wave arrival-time data used for this study were derived from ISC data and reformatted by A. C. Johnston. We gratefully acknowledge the helpful suggestions and criticism of D. Huaco, B. Isacks, J. Taggart, A. Tarr, and M. Wyss. J. W. Dewey would like to acknowledge, in particular, that the comments of Huaco and Isacks encouraged him to accept the view of his co-author, W. Spence, that more emphasis should be given to the possibility of a correlation between seismicity in the IT zone

and CPI zone. We thank B. ISACKS for sending us the data that formed the basis of the discussion of the 1970 earthquake sequence in ISACKS and BARAZANGI (1977).

REFERENCES

- ABE, K. (1972a), *Lithospheric normal faulting beneath the Aleutian Trench*, Phys. Earth Planet. Interiors 5, 190-198.
- ABE, K. (1972b), *Mechanisms and tectonic implications of the 1966 and 1970 Peru earthquakes*, Phys. Earth Planet. Interiors 5, 367-379.
- BARAZANGI, M. and ISACKS, B. L. (1979), *Subduction of the Nazca Plate beneath Peru: evidence from the spatial distribution of earthquakes*, Geophys. J. R. astr. Soc. 57, 537-555.
- BILLINGTON, S. and ENGDAHL, E. R. (1978), *A shallow earthquake sequence in the central Aleutian Islands* (abs.), EOS, Trans. Amer. Geophys. U. 59, 1127.
- BRADY, B. T. (1976), *Theory of earthquakes, IV, General implications for earthquake prediction*, Pure appl. Geophys. 114, 1031-1082.
- CLOUD, W. K. and PEREZ, V. (1971), *Unusual accelerograms recorded at Lima, Peru*, Bull. Seism. Soc. Am. 61, 633-640.
- DEWEY, J. W. (1971), *Seismicity studies with the method of joint hypocenter determination*, Ph.D. Dissertation, Univ. Calif. Berkeley.
- DIETERICH, J. H. (1978), *Preseismic fault slip and earthquake prediction*, J. Geophys. Res. 83, 3940-3948.
- ESPINOSA, A. F., HUSID, R., ALGERMISSEN, S. T. and DE LAS CASAS, J. (1977), *The Lima earthquake of October 3, 1974: intensity distribution*, Bull. Seism. Soc. Am. 67, 1429-1439.
- ENGDAHL, E. R. and SCHOLZ, C. (1977), *A double Benioff Zone beneath the Central Aleutians: An unbending of the lithosphere*, Geophys. Res. Lett. 4, 473-476.
- EVERNDEN, J. F. (1969), *Precision of epicenters obtained by small number of world-wide stations*, Bull. Seism. Soc. Am. 59, 1365-1398.
- FEDOTOV, S. A. (1969), *Chapter Four, Zemletryasaniya i glubinnoe stroenie yuga Kuril'skoi ostrovnnoi dugi*, Edited by S. A. Fedotov, Izdatel'stvo 'Nauka,' Moskva.
- FLINN, E. A. (1965), *Confidence regions and error determinations for seismic event location*, Rev. Geophys. Sp. Phys. 5, 157-185.
- FUKAO, Y. (1979), *Tsunami earthquakes and subduction processes near deep-sea trenches*, J. Geophys. Res. 84, 2303-2314.
- GUTENBERG, B. and RICHTER, C. F. (1959), *New evidence for a change in physical conditions at depths near 100 kilometers*, Bull. Seism. Soc. Am. 29, 531-538.
- GUTENBERG, B. and RICHTER, C. F. (1954), *Seismicity of the earth and associated phenomena*, reprinted by Hafner Press (1965), New York, 310 p.
- HANKS, T. C. (1979), *Deviatoric stresses and earthquake occurrence at the outer rise*, J. Geophys. Res. 84, 2343-2347.
- HUACO, D. (1978), *Source parameters and the static field of earthquakes at near distances*, Ph.D. Dissertation, St. Louis University, St. Louis, Mo.
- ISACKS, B. L. and BARAZANGI, M. (1977), *Geometry of Benioff zones: lateral segmentation and downward bending of the subducted lithosphere*, Maurice Ewing Series 1, 99-114.
- KANAMORI, H. (1972), *Mechanism of tsunami earthquakes*, Phys. Earth Planet. Interiors 6, 346-359.
- KANAMORI, H. (1977), *The energy release in great earthquakes*, J. Geophys. Res. 82, 2981-2987.
- KEILIS-BOROK, V. (1959), *An estimation of the displacement in an earthquake source and of source dimensions*, Ann. Geofis. (Rome) 12, 205-214.
- KELLEHER, J. (1972), *Rupture zones of large South American earthquakes and some predictions*, J. Geophys. Res. 77, 2087-2103.
- KELLEHER, J., SYKES, L. and OLIVER, J. (1973), *Possible criteria for predicting earthquake locations and their application to major plate boundaries of the Pacific and the Caribbean*, J. Geophys. Res. 78, 2547-2585.

- KELLEHER, J., SAVINO, J., ROWLETT, H. and McCANN, W. (1974), *Why and where great thrust earthquakes occur along island areas*, J. Geophys. Res. 79, 4889-4899.
- KELLEHER, J. and SAVINO, J. (1975), *Distribution of seismicity before large strike slip and thrust-type earthquakes*, J. Geophys. Res. 80, 260-271.
- LANGER, C. (1977), *The locations and characteristics of the aftershocks of the October 3, 1974, Peruvian earthquake*, M.S. thesis, Virginia Poly. Inst., Blacksburg, Va.
- LANGER, C. J. and SPENCE, W. (1978), *A study of aftershocks of the October 3, 1974, Peru earthquake* [abs.], Earthquake Notes 49, 54.
- LOMNITZ, C. (1971), *The Peru earthquake of May 31, 1970: some preliminary seismological results*, Bull. Seism. Soc. Am. 61, 535-542.
- MADARIAGA, R. (1979), *On the relation between seismic moment and stress drop in the presence of stress and strength heterogeneity*, J. Geophys. Res. 84, 2243-2250.
- MCCANN, W. R., NISHENKO, S. P., SYKES, L. R. and KRAUSE, J. (1978), *Seismic gaps and plate tectonics: seismic potential for major plate boundaries*, USGS Open-File Report 78-943, 441-584.
- MENDIGUREN, J. A. (1971), *Focal mechanism of a shock in the middle of the Nazca plate*, J. Geophys. Res. 76, 3861-3879.
- MINSTER, J. B., JORDAN, T. H., MOLNAR, P. and HAINES, E. (1974), *Numerical modelling of instantaneous plate tectonics*, Geophys. J. R. astr. Soc. 36, 541-576.
- MOGI, K. (1969), *Some features of recent seismic activity in and near Japan, 2, activity before and after great earthquakes*, Bull. Earthquake Res. Inst. Tokyo Univ. 47, 395-416.
- MOGI, K. (1973), *Relationship between shallow and deep seismicity in the western Pacific region*, Tectonophysics 17, 1-22.
- MYACHKIN, V. I., SOBOLEV, G. A., DOLBILKINA, N. A., MOROZOW, V. N. and PREOBRAZENSKY, V. B. (1972), *The study of variations in geophysical fields near focal zones of Kamchatka*, Tectonophysics 14, 287-293.
- OHTAKE, M., MATUMOTO, T. and LATHAM, G. V. (1977), *Seismicity gap near Oaxaca, southern Mexico as a probable precursor to a large earthquake*, Pure appl. Geophys. 115, 375-385.
- PLAFKER, G. (1972), *Alaskan earthquake of 1964 and Chilean earthquake of 1960: implications for arc tectonics*, J. Geophys. Res. 77, 901-925.
- PRINCE, R. A. and KULM, L. D. (1975), *Crustal rupture and the initiation of imbricate thrusting in the Peru-Chile Trench*, Geol. Soc. Am. Bull. 86, 1639-1653.
- SILGADO, E. (1973), *Historia de los sismos mas notables ocurridos en el Peru (1555-1970)*, Geofisica Panamerica 2, 179-243.
- SPENCE, W. (1977), *The Aleutian arc: tectonic blocks, episodic subduction, strain diffusion, and magma generation*, J. Geophys. Res. 82, 213-230.
- SPENCE, W., GIESECKE, A., LANGER, C. J., OCOLA, L., DILLINGER, W. H. and JORDAN, J. N. (1975), *The Lima, Peru earthquake series* [abs.], Earthquake Notes 46, 38.
- STAUDER, W. (1975), *Subduction of the Nazca Plate under Peru as evidenced by focal mechanisms and by seismicity*, J. Geophys. Res. 80, 1053-1064.
- SYKES, L. R. (1971), *Aftershock zones of great earthquakes, seismicity gaps, and earthquake prediction for Alaska and the Aleutians*, J. Geophys. Res. 76, 8021-8041.
- WAGNER, D. (1972), *Statistical decision theory applied to the focal mechanisms of Peruvian earthquakes*, Ph.D. Dissertation, St Louis Univ., St Louis, Mo., 176 pp.

(Received 8th August 1979)

PHYSICAL PRECURSORS OF ROCK FAILURE: A LABORATORY INVESTIGATION

by

B. T. Brady¹, Glen A. Rowell, and Larry P. Yoder

ABSTRACT

Anomalous behavior prior to failure of Barre granite has been observed in each of seven different parameters monitored under laboratory testing conditions. These anomalies are observed to develop at a lead time that is proportional to the size of the failure to be produced; in the laboratory the lead time is of the order of 100 μ sec. The seven parameters monitored were axial load, tilt in two orthogonal directions, confining pressure, seismicity, piezoelectric effect as monitored by changes in electric field potential between two points on the specimen surface, and acceleration in axial displacement of the sample. Our evidence suggests that fracture of laboratory size rock samples may result from a series of much smaller failures, each with apparent stress drops of 5-8 MPa (50-80 bars), and that each failure is accompanied by a localized minimization of dilatancy (dilatancy recovery). The observational data are discussed and compared with existing theories of the failure preparation process (dilatancy-diffusion, Soviet model, and inclusion model). Several implications of the data to the problem of failure prediction are considered.

¹ U.S. Department of the Interior, Bureau of Mines, Denver Mining Research Center, Denver, Colo.

INTRODUCTION

Two sources of instability in brittle rock have been identified and studied extensively in the laboratory. The first includes fracture of intact rock in either compression or tension. The second includes phenomena characterized by stick-slip instabilities that are apparently nucleated along pre-existing crack surfaces (see for example, Byerlee, 1970; Byerlee and Brace, 1968; Scholz, 1967, 1968). Both sources of instability have been postulated to be relevant to mine failures and/or earthquake processes (Byerlee and Brace, 1968; Scholz, 1968; Brady, 1974, 1976a, 1976b, 1978; Brady and Leighton, 1977).

In order to model intermediate and large scale failures, such as mine failures and earthquakes, laboratory tests are usually performed under moderate-to-large confining pressures (several tens of MPa) and, in some instances, moderate temperatures (several hundred degrees Celsius). However, it is found that even when these test conditions are met, there are still a number of significant discrepancies between laboratory and field measurements. These discrepancies include much higher stress drops in the laboratory, quantitative differences in seismicity, and anomalous precursory behavior in V_p/V_s , tilt, and electromagnetic emission that are unresolved in the laboratory (Byerlee and Brace, 1968; Aggarwal et al., 1975; Hadley, 1975; Nersisov et al., 1975; Scholz, et al., 1973; Brune, 1970; Wyss, 1970; Wyss and Molnar, 1972; Hanks, 1977). For example, it is now well established that laboratory stress drop magnitudes (equal to the difference between the maximum principal stress just prior to and immediately follow-

ing the instability) are comparable for either intact or faulted rock (Byerlee and Brace, 1968; Byerlee, 1970). Typical laboratory determined stress drops are observed to be on the order of 100-to-200 MPa (several kilobars) (Byerlee, 1970). On the other hand, stress drops measured from earthquakes are calculated to be on the order of 1 to 6 MPa (10-60 bars) (Brune, 1970; Wyss, 1970; Wyss and Molnar, 1972; Hanks, 1977). Regarding seismicity, laboratory studies suggest that rock fails when the seismicity attains some critical value, or equivalently, that dilatancy (crack formation) peaks at the inception of failure (Obert and Duvall, 1942; Vinogradov, 1957; Brace, et al., 1966; Scholz, 1968). Yet, observational data from mine failures and some earthquakes indicate that seismicity decreases dramatically prior to failure (Aggarwal, et al., 1975; Brady, 1976b, 1977b; Mogi, 1973, 1968). There are some laboratory results which suggest that seismicity does decrease prior to failure (Brady, 1976a, b; 1978); however, this behavior is reported to occur milliseconds before the initiation of catastrophic fault growth, a time interval too short for detection and analysis of the physical behavior of the material during this interval in most rock mechanics laboratories. Certainly, further studies of such precursory phenomena under laboratory test conditions are required. If discrepancies in stress drop and precursory phenomena between field and laboratory data cannot be reconciled. We must conclude that laboratory modeling of failure has little, if any, relevance to mine failures and earthquakes.] ?

Recent studies of failure precursors on the small (laboratory)

intermediate (mine), and large (earthquake) scale suggest that rock failure may satisfy a scale invariant process (Brady, 1974b, 1976b). "Scale invariance" in failure means that the physics of fracture is identical for all failures, regardless of size; scale invariance does not imply simple scaling laws.

Figure 1 illustrates preparation times (τ_0) as a function of "effective" length, L, for selected failures, including several mine failures and earthquakes (see Brady, 1974a, 1978, 1977b, 1976b; Brady and Leighton, 1977; Aggarwal, et al., 1975; Anderson and Whitcomb, 1975; Scholz et al., 1973; Mersesov et al., 1974). The "effective" length, L, denotes an average linear dimension of the aftershock region generated by the failure. For the laboratory failure, L was estimated to be the length of the test sample (~ 10 cm), (Brady, 1974). Several important observations can be drawn from the data shown in fig. 1. First, there is an apparent linear relationship between τ_0 and $A (=4L^2)$ extending from large scale failures down to laboratory-scale failures. Thus, an understanding of the physical processes which produce failure on the small scale may admit an understanding of the physical processes producing failure on the intermediate and large scales. Second, because the functional relationship between τ_0 and A is approximately linear, and because observational data suggest that earthquakes occur repeatedly in the same region, apparently on preexisting fault planes (Mogi, 1968, 1974), it appears that similar physical processes lead irrevocably to failure both in fresh, relatively unbroken laboratory material and along preexisting earthquake fault zones. These data suggest fault zones may heal following their failure. The experimental

results of Byerlee and Brace (1968) emphasize the similarities between fracture of intact and faulted rock samples in the laboratory. Third, the diversity of scale shown in fig. 1 (~ six orders of magnitude in L , ~ 13 orders of magnitude in τ_0) indicate that the physical processes leading to failure may be independent of rock type. Thus, failure may satisfy a "material invariance" or universality principle. Laboratory data also indicate that the anomaly time is independent of rock type for a wide variety of rock materials (Brady, 1976a). Fourth, and of particular importance to this article, the apparent scale invariant properties of rock failure suggest that while precursors identical to those reported as occurring on the intermediate and large scale will occur on the laboratory scale, they will be present only during a time interval which is too short (several hundred μ sec) to be detected in most rock mechanics laboratories. This, phenomena such as dilatancy and seismicity which appear to peak at laboratory failure (Brace et al., 1966; Scholz, 1968) may not be "true" precursors of impending failure. We therefore suggest that increased dilatancy (as evidenced by seismicity) is only a necessary, but not a sufficient condition of impending failure.

The above considerations prompted the experimental program by the Bureau of Mines on the physics of rock failure. We show in this article that laboratory studies provide valuable insight into the failure preparation process, but only when the process is studied during the very short time interval of 10^{-4} - 10^{-3} sec prior to failure. We also propose to show that stress drops occurring during the failure preparation time are comparable (several MPa) to those calculated from earthquakes. Although we report

results only for Barre Granite, similar failure precursors have been observed for a wide variety of rock types deformed to failure in our laboratory.

EXPERIMENTAL PROCEDURE

1X-size cores (5/8 in diameter) of Barre granite were drilled, cut, and ground to a final length of 135 mm. The variation in axial length of each core was held to less than .02 mm, insuring that the loading surfaces were nearly parallel. The perpendicular tolerance of the end planes to the axis of the specimen was less than 2°. All specimens were deformed to failure under a confining pressure of 6.9 MPa (70 bars) in a servo-controlled materials-testing system (MTS, Systems Corp.², 2.7×10^6 newton capacity) instrumented as shown in fig. 2. Reaction time of the MTS to changes in load or displacement rate is approximately 200 milliseconds. Lateral compression was developed and maintained in the pressure chamber by a servocontrolled mechanism with a reaction time on the order of 200 milliseconds. All tests were performed with a displacement rate of 12.7 μ m/sec.

The load cell (Interface model 1240 HF, 9×10^5 newton and 16×10^3 newton-meter capacity) used in the testing program allowed monitoring of both the x- and y-moments (M_x and M_y), in addition to the total load, F_z . Load changes greater than 90 newtons within the sample can be detected. The bending moments, similar to tilt measurements in earthquake-prone regions, are measured about two perpendicular axes intersecting at the center of the transducer and normal to the load axis. Maximum thrust and moment deflection

² Reference to specific trade names is made for identification only and does not imply endorsement by the Bureau of Mines.

in this cell are 1×10^{-4} m and 0.15° , respectively. M_x , M_y , and F_x are measured and recorded on separate channels as a function of time. The load cell exhibits characteristic resonant frequencies of approximately 800 Hz, 1100 Hz, and 3300 Hz that are excited when the rock specimen fails. The Q-value of the load cell is approximately 10.

The piezoelectric polymer transducer (PPT) and electromagnetic detection device (EDD) were placed directly onto the rock surface (fig. 2) and pressed into place by the flexible bladder when the pressure chamber is pressurized. The PPTs were supplied to the Bureau of Mines by the National Bureau of Standards (Cohen and Edelman, 1971). The PPT is primarily sensitive to changes in pressure; thus, it is a useful device for sensing the pressure waves of acoustic emissions. The PPT is also affected by changes in chamber pressure, temperature, and strain. Therefore, acoustic emission may not be the only source of output. However, our laboratory experience with this device strongly suggests that prior to failure, PPT output is primarily associated with acoustic emission. The primary advantages of the PPT are its short ring-down time (several μ sec) and its flexibility in conforming to the shape of the rock. The rapid ring-down time allows a possible discrimination of a "quiet" period predicted to occur several hundred μ sec prior to rupture.

The EDD consists simply of two copper electrodes, 0.02 mm thickness, and approximately 160 mm² area that are placed directly on the rock surface. The electrode near the upper edge of the rock is driven to the same potential as the electrode near the center of the rock specimen by a high impedance,

low capacitance electrometer follower (Monroe Electronics, Inc., model 145 Mosfet). The frequency range of the electrometer follower is from near dc to 2 MHz. The output from the EDD represents the difference in potential between the two areas of rock in contact with the electrodes. Barre granite is a slightly piezoelectric material. Therefore it is reasonable to expect nonhomogeneous volume changes to appear as potential differences. It is also possible that bond breaking is reflected in the EDD output.

The dynamic pressure transducer (PCB Piezoelectronics, Inc.) was inserted into the wall of the pressure chamber with the base of the pressure transducer nearly flush with the chamber surface, separated from the rock by the bladder and hydraulic fluid. The rise time, resolution, and time constant of the pressure transducer are 1 μ sec, 300 Pa, and 100 sec, respectively. The AET acoustic emission transducer (Dunegan/Endevco, model S 9201) located on the baseplate (fig. 2) primarily responds to frequencies in the range of 100 kHz to 1 MHz with a peak response at 200 kHz. The output of the AET can be related to acceleration, and will be referred to as acceleration.

Moments, load, pressure, acceleration, seismicity, and electric field intensity were recorded on three digital memory scopes (Nicolet Corp., model 1090) and on an FM tape recorder (Sangamo, model 3500). Each digital scope has a sampling rate that can be varied from .5 μ sec to 200 sec per point. Frequency response for the tape deck is dc - 10 kHz at 40 cm/sec. Both PPT and EDD outputs from the rock sample were measured initially with a Dunegan/Endevco 3000 series system that includes a totalizer, log converter, and reset clock. (Note: the reset clock signal is superimposed on the output from

this system. Each peak, of about one-half division, in the output represents the passage of 100 μ records of time. Further, the inherent filtering quality of the tape deck has a tendency to spread out the timing signal. Therefore the apparent noise seen in figures 3E and 3F is not noise from the PPT or EDD; it is timing signals.) In later experiments, the PPT and EDD output were fed directly into the digital scope because of the following circumstances. In earlier reported tests (Brady, 1976a), the PPT signal was sent through a 200 kHz - 2 MHz (40 dB) preamplifier followed by adjustable passband filters and a variable gain amplifier. The count rate was determined using a threshold event detector with a time window adjustable from 100 μ sec to 1.2 sec, with a 100-200 μ sec time window typically being used. As further tests of the instrumentation were made, it became apparent that band pass filters can confuse high amplitude lower frequency signals with higher frequencies in the passband. Further, it was found that high amplitude signals (including signals whose frequencies were below the passband) paralyzed the amplifier; that is, the null signal was transmitted from shortly after the amplifiers were overdriven until a short time after the input amplitude had fallen back below limits. Therefore we suspect that near failure, the PPT signal "overdrove" the amplifiers, thus rendering the null output questionable for physical interpretation of the failure process. It was reported elsewhere (Brady, 1976a) that prior to failure the sample appeared to "quiet" down. Recognition of the "overdrive" problem then made ambiguous the interpretation that a seismic shutdown within the test sample had actually occurred. By connecting the PPT and EDD/electrometer follower

directly to the scope, the problems associated with amplification were eliminated, but the time window of looking at the output was considerably shortened. We will show shortly that the output of the PPT does, in fact, decrease dramatically just prior to failure. Since the output of the PPT cannot be uniquely related solely to acoustic emission and the EDD output may not be related solely to the piezoelectric charge effect in the rock (i.e., electron emission) the output of both the PPT and EDD are recorded in millivolts.

In order to accurately compare the time of occurrence of the various events taking place, the relative times from seismic event to signal pickup must be considered. For example, the physical location of the load cell is approximately 200 mm above the top of the sample. This implies that after a change in rock configuration occurs, the P-wave ($V_p \approx 5$ km/sec) signal requires approximately 40 μ sec to travel from the top of the rock sample to the load cell. There are additional time delays of nearly 35 μ sec within the load cell due perhaps to the web-type design of the cell. Bridge amplifier electronics may contribute to time delays; however, they amount to less than several μ sec at most and will be neglected in this report. There is also a time delay of 0 - 30 μ sec for the signal to travel from the source location to the top of the rock sample. The net result is an absolute time delay in load and moments of 90 μ sec \pm 15 μ sec from event occurrence. The other measured quantities, pressure, PPT, EDD, and AET, also experience a time delay from event occurrence to detection because of the physical distance between source and detector. When the signals are simultaneously recorded on

the analog tape deck, there is an additional effect due to the slight misalignment of the record and playback heads. This time delay was determined using a Fast Fourier Transform analyzer. The relative time delay between tracks was as much as 80 μ sec. Table 1 lists a summary of these time delays. The time axis of all graphical data presented below has been adjusted to take these delays into account.

EXPERIMENTAL RESULTS - Barre Granite Core - 28

The following results required both high frequency and amplitude resolution of both the testing and recording systems. Full use was made of the capabilities of both the digital oscilloscopes and the FM tape deck. The following data is not available in conventional rock mechanics laboratories where system response is limited to tenths or hundredths of

Table 1. - Time Delay Chart

Sensor	Time delay from event to change in signal, μ sec	Time delay relative to PPT μ sec (used for data digitized during experiment)	Time delay relative to PPT including tape deck μ sec (used for data retrieved from analog tape deck)
1. PPT	10 \pm 10	0	0
2. EDD	10 \pm 10	0 \pm 10	0 \pm 10
3. Pressure	15 \pm 10	5 \pm 10	20 \pm 10
4. Load	90 \pm 15	75 \pm 15	50 \pm 15
5. M_x	90 \pm 15	75 \pm 15	85 \pm 15
6. M_y	90 \pm 15	75 \pm 15	70 \pm 15
7. AET	55 \pm 15	40 \pm 10	70 \pm 10

seconds. Consequently, the fractures discussed below would appear as single, instantaneous, catastrophic failures with no anomalous behavior prior to their occurrence.

Figure 3 illustrates the time variation of the acoustic emission transducer (AET), confining pressure, x and y moments, piezoelectric polymer transducer (PPT), electromagnetic detection device (EDD), and load for Barre granite core 28. The sample was tested using the threshold event detector with an 100 μ sec time window to count events recorded by the PPT and EDD. Prior to failure, we feel that figures 3E and 3F accurately portray event occurrences, even though the frequencies of the signal input to the threshold detector may have been altered by the preamplifier and the amplifier. After failure, the "quiet" periods may have been caused by either an overdriven preamp or by actual quiet periods. Figures 3B and 3G are from data recorded during the experiment using the digital scopes at a digitizing rate of 5 μ sec/point. The other figures were first recorded on the analog tape deck and later played back into the digital scopes. All the digital data were stored on a magnetic tape, played into a computer, adjusted in time according to table 1, and plotted on a graphic display terminal. Note the absence of analog tape noise on the load and pressure data.

Several observations of these data should be noted. First, there is a period of gradual increase in output from both the AET and pressure transducer approximately 1.2 msec prior to failure, figures 3A, B. This increase correlates with an increase in seismicity, fig. 3E, but no apparent change in EDD output (fig. 3F). The bending moment began to show "tilt" in a direction which was to be the rupture propagation direction, fig. 3C. For this failure, the rupture propagated in the negative (downward) x-axis direction (note the "permanent" change in moment). There was less permanent change in

y-moment during this fracture. Therefore the anomalous behavior in y-moment, though present, is less apparent. Second, moment ("tilt"), confining pressure, AET (apparent axial acceleration of the sample), and seismicity began to exhibit more rapid changes approximately $300 \pm 50 \mu\text{sec}$ prior to failure. Third, the "tilt" direction reversed as the load began to rapidly decrease. This can best be seen in fig. 4A, an expanded time view of fig. 3C. The decrease in axial load was followed shortly by a decrease in confining pressure of nearly 0.3 MPa (3 bars, fig. 4P, a time expanded view of fig. 3B). In addition, the output of the PPT decreased (fig. 3E) and the EDD increased (fig. 3F) during this time interval. These anomalies all developed within a time interval of approximately $300 \mu\text{sec}$ prior to failure.

Failure of Barre granite core 28 was taken to coincide with the extremely rapid load drop, confining pressure increase, and increased AET output. The anomalous period, τ_0 , before failure, begins when the output from the PPT, AET, and confining pressure all start showing anomalous behavior. It must be noted that anomalous behavior in only seismicity (PPT) would lead to ambiguity in the choice of τ_0 . However, this ambiguity is removed by considering all three indicators.

The AET (acceleration) output during τ_0 indicates that strain waves emanating from the sample were not only coherent in phase relationships to one another, but also suggests that their amplitudes were increasing during this time interval.

The variation in confining pressure (fig. 4B) merits further discussion. It is probable that the advancing steel platens (fig. 2) cause the dramatic

increase ($\sim 5 \text{ MPa}$) in confining pressure after failure of the rock specimen. The test was run at a nominal pressure of 6.9 MPa (1000 psi). The interesting feature of the pressure data is the small drop of ($\sim 0.3 \text{ MPa}$) at the moment of failure. It should be noted that this pressure drop occurs at a time when the load is decreasing; that is, a time when the loading platens are advancing on the specimen. This pressure drop must be caused by either the testing system or the rock specimen. If the pressure drop is due to a sudden decrease in confining pressure caused by, perhaps, a resonant response of the pressure chamber or loading system, then a similar pressure drop would be seen in all tests because it would be a function of the testing machine. In fact, when this pressure drop is observed, its character (magnitude and time of onset) is often different. An alternative explanation is that the pressure drop is caused by a coherent withdrawing motion of a portion of the rock produced by a localized minimization of dilatancy prior to failure (i.e., during the preparation phase). If this is true, then the observation of a pressure drop would be a function of the point of fault nucleation with respect to the location of the pressure transducer. The data from our experiments are consistent with this explanation.

Not shown in this data set is the observation that failure of core 28 was a multiple fracture event. The event shown in figures 3 and 4 is the first of 3 failures. During this first failure, the load drop was about 110 kN (an apparent stress drop of 48 MPa) out of a total load of about 620 kN. The apparent stress drop during the preparation time ($\lesssim 200 \mu\text{sec}$) is approximately 5 MPa (50 bars).

Note also that the seismicity and EDD are measured during each 100 μ sec time window. The drop-off in fig. 3E occurred during the 100 μ sec time interval prior to the failure. The precise time when PPT output decreased is uncertain. This difficulty with interpreting PPT and EDD output was eliminated in the test on Barre granite core 34 where both the PPT and EDD output were recorded directly onto the scope, thereby eliminating counting difficulties and possible amplifier blockage and contamination, but limiting the time window of looking at PPT and EDD to 4 msec.

EXPERIMENTAL RESULTS - BARRE GRANITE CORE - 28

For Barre granite core 34, the PPT and EDD outputs were recorded directly on 2 digital oscilloscopes using sampling rates of 2 MHz and 0.5 MHz. Pressure and load were recorded on the third digital scope at 2 MHz. The pressure increase at failure was used to simultaneously trigger the scopes. Except for the PPT and EDD outputs (due to the low input impedance of the tape deck), the monitored parameters were recorded on the FM tape deck during the entire experiment. The results shown in figures 5 and 6 have been adjusted in time according to table 1 so that graphs with the same time units are synchronous to within $\pm 15 \mu$ sec of event occurrence.

In these figures, the failure points are taken to be the peaks in the EDD output (fig. 5D) because of the piezoelectric effect of the quartz present in the granite specimen. For convenience, the failure points have been located on the other figures. Figure 6F was recorded at 0.5 μ sec/point. Note the relative quiet of the EDD output prior to the sequence of failures.

From fig. 5A the fracture seems to be composed of a series of at least three separate failures. Such a statement may be speculative as the response time of the load cell is not fast enough to detect rapid changes in load. It may be possible to explain the load inflections using load cell resonances as the basis for argument, however, load cell resonances are not transmitted to the rock. A recent experiment with strain gages fastened to the top steel platen (refer to fig. 2) showed that the ringing of the load cell, seen best in fig. 5i, was not present in the steel platen, and therefore, not present in the rock specimen. If one tries to explain the inflections in load by load cell resonances, then the associated variations in pressure, PPT, and EDD outputs have to be attributed to chance coincidence. It is our view that the load cell response merely filters higher frequency variations in load. For example, the remaining peaks in EDD output may also represent failures. A series of experiments is planned using a higher frequency response load cell to clarify uncertainties in load response.

Referring to fig. 5A, the load drop corresponding to failures 1 and 2 are about 11 kN and 18 kN, respectively, small parts of the total load on the specimen prior to fracture, about 620 kN. Failure 3 is marked with a question mark, because the load response is not known after the end of the graph. The load history recorded on the FM tape deck is too noisy to have any real meaning on the scale of events shown in fig. 5A, but it did show that the load continued to drop. The apparent stress drops associated with failures 1 and 2 are 5 MPa and 8 MPa, respectively. It must be emphasized that the apparent stress drop is merely the drop in load averaged across the

entire cross section of the specimen. It is quite possible that the load drop was caused by a localized failure that affected only a small portion of the cross section at the point of failure.

The pressure curve shows similar results to those seen in Barre granite core 28, namely a drop in pressure or at least a point of inflection, during the moments of failure. If this is caused by momentary volume decreases of small volumes of the rock, then varying degrees of pressure change are expected depending upon the location of the volume relative to the transducer.

The beginnings of the preparation phases, τ_0 , prior to failure, are taken as the inflection points on the rising PPT curve prior to the failures. An imaginary smooth curve is drawn through the PPT output in order to determine the inflection location. This point is chosen because past experience with mine failures and earthquakes has shown that a seismicity buildup is a necessary, though not sufficient, condition for failure. The point of inflection approximately represents the beginning of this buildup. Figure 6E shows a longer time window of the PPT output. The failure points are shown for reference. Relative "quiet" in PPT output prior to each failure is readily apparent.

In looking at the x- and y-moments in fig. 6A,B, the tilt shows the normal behavior of going toward the eventual rupture direction, reversing, and finally giving way toward the rupture. As seen through the analog tape deck, failures 1, 2, and 3 blend together as one larger failure on this time scale. The outputs of the pressure transducer and the AET, as recorded by the analog tape deck, fig. 6C, D are similar to those from Barre granite core 28.

In summarizing the results of Barre granite core 34, there is evidence that this failure, which would have appeared as a single load drop in most laboratories, may be the result of a series of much smaller failures or slips which occurred in rapid succession. Each of these small failures represents an apparent stress drop of approximately 5 - 8 MPa, a stress drop similar to those inferred from mine failures and earthquakes. There is evidence of a seismicity (PPT) increase and decrease prior to each of the failures seen in figure 5. This, too, is similar to observations of large scale fractures. In order to show, or disprove these conclusions more clearly, tests will be conducted with a more responsive load and moments cell. Also, further clarification must be made of the PPT, EDD, and AET outputs.

DISCUSSION AND CONCLUSIONS

As shown in fig. 1, laboratory data presented in this article and elsewhere lend support to the hypothesis that failure, at least for rock materials, may satisfy a scale invariant principle. Reliable prediction of impending failure on the intermediate and large scale may be a distinct possibility because of this principle.

The time durations (τ_0) of the anomalies observed prior to fault growth in Barre granite may be functionally related to the size of the anomalous region associated with the impending failure. The anomalous region, or equivalently, the activation volume of the failure denotes an upper bound to the volume which can be fractured by an event. This bound is determined when there is no energy dissipated by frictional sliding in a growing rupture.

Typical preparation times for Barre granite, as well as other rock types deformed to failure in our laboratory are on the order of 100 μ sec. Experimental results presented above suggest these failures produce activation volumes whose dimensions are comparable to that of the sample, since tilt reversals must pervade substantial portions of the sample to be detected.

Our studies indicate multiple fractures are the rule rather than the exception. This result suggests multiple deformation bands, within which each fracture is nucleated, may exist within the test specimen prior to catastrophic fault growth. It is also possible that these deformation bands may be induced to form within the time interval that the "primary" fracture is growing. Thus, nucleation of a failure (fault) within a specific deformation band could load an adjacent band and, possibly, prematurely trigger its failure. Our results indicate that typical times (not to be confused with precursor or preparation time) between growths of these multiple fractures may range anywhere from several tens of μ sec to tens of milliseconds.

These precursory data conform with precursory data reported to precede some mine failures and earthquakes, such as shown in fig. 1. Here, preparation time, τ_0 , and aftershock area, A , are functionally related by $\tau_0 = \gamma_0 A$, where $\gamma_0 = 2.43 \times 10^{-4}$ sec/cm² (Brady, 1977, 1978a). This gives a diffusion coefficient, b ($= \frac{i}{\gamma_0}$), for the failure preparatory process to be approximately $D = 4 \times 10^3$ cm²/sec. This result suggests that creep-related processes, such as ion diffusion along crack surfaces, can be neglected in the laboratory failures and by inference for the mine failure and earthquake data shown in fig. 1, as diffusion coefficients for ion diffusion processes are typically

on the order of 0.04 cm²/sec (Cottrell, 1961). It is important to note that the relation $\tau_0 = \gamma_0 A$ is only applicable when the far-field boundary conditions (FFBC) are not changing during τ_0 and when deformation due to creep induced effects, such as fluid diffusion, can be neglected. FFBC refer to stress, strain, and strain rate conditions prevailing at distances far removed from the aftershock zone. These facts may account for the good linear fit of the laboratory data and mine failure data in fig. 1. Here, the FFBC can be assumed constant during the failure preparation time. Some of the earthquake data in fig. 1, particularly the large magnitude events, exhibit marked deviations from the trend of this curve. Physical causes for a decrease in the preparation times for moderate-to-large earthquakes have been discussed elsewhere (Brady, 1976b, Brady 1979).

Table 2 lists a comparison of the laboratory results presented earlier and various model predictions. Shown are model predictions for the dilatancy-diffusion model (without water) (Nur, 1972; Scholz, et al., 1973), the Soviet model (Mjachkin, et al., 1975), and the inclusion model (Brady, 1976h) for laboratory-sized rock failures. The Soviet model is identical to the model independently presented by Stuart (1974). Because the Soviet model is postulated as dependent upon a generally accelerating increase in displacement parallel to the applied maximum principal stress, we assume that the electric field intensity and frequency will both increase. Note also that the inclusion model predicts an increase in the average pressure within the impending aftershock zone and, to a lesser extent, within the activation volume of the impending failure during the preparation time τ_0 . The principal stresses will decrease outside the activation volume. Thus, since the

dimensions of the inclusion zone and its focal region are small ($l \sim 1$ cm) and the sample dimensions are larger than a mean average length of the activation volume; this model predicts that the applied axial load will decrease during τ_0 . Very briefly, rock failure by the inclusion model goes through three phases: ① A zone of concentrated dilatancy develops, where local σ_3 is perpendicular to the ultimate direction of fault growth. Seismic events that radiate anomalous levels of long-period energy occur during this phase. ② The local stress field rotates through 90° and the cracks in the intensely dilated zone are forced shut by the local σ_3 . The former zone of concentrated dilatancy is now elastically stiffer than the surrounding material and is capable of storing higher stresses than the surrounding material. ③ The local σ_1 now follows the elongated inclusion zone in the same direction as originally. Failure occurs when σ_1 increases (by drawing stress from the surrounding medium) and σ_3 decreases to failure-inducing levels of tension.

As shown in table 2, the observational data rule out the dilatancy-diffusion model. The confining pressure decrease during τ_0 is inconsistent with the Soviet model prediction. In addition, the Soviet model predicts recovery once the sample enters the post-failure (load decrease) period of deformation. Our experiments indicate that there is not recovery during this period which usually begins in our tests several tens of seconds prior to rupture. Rather, recovery only occurs approximately several hundred μ sec prior to rupture. The inclusion model is the only theory consistent with these data.

Summarizing, we find that the observational data on failure of Barre granite and similar results on other rock types are consistent with the

scale invariant inclusion theory of failure. These data do not constitute "proof" of this theory. The theory is merely consistent with the data.

Table 2. - Comparison of Observational Data and Various Model Predictions for Laboratory Scale Failures

Anomaly	Failure Theory			
	Dilatancy-diffusion	Soviet model	Inclusion model	Observation
Axial load	decrease	decrease	decrease*	decrease
Tilt reversal	no	no	yes	yes
Confining pressure	increase	increase	decrease	decrease
Axial acceleration	increase	increase	increase	increase
Seismicity	decrease	decrease	decrease	decrease
Electric field	?	?(increase)	increase	increase
Electric field frequency	?	?(increase)	increase	increase

* There will be an increase in the average pressure [$\approx \frac{1}{3}(\sigma_1 + \sigma_2 + \sigma_3)$] within the focal volume of the impending failure.

In order to adequately test the applicability of the inclusion theory to failure prediction, we must determine where and when the primary inclusion zone (PIZ) forms and be able to correlate other precursory phenomena to PIZ formation. This requires location of seismic events within the test sample, a problem now under active investigation by the Bureau of Mines. In addition, preparation times are functionally related to other parameters, such as intrinsic porosity and ambient temperature (Brady 1977b). The apparent correlation of PIZ length (l_1) to grain size of Barre granite

(~ 0.02 cm) observed in this study suggests that grain size within a rock mass may influence crack dimensions and, by inference, the preparation time required for the failure. Future investigations by the Bureau of Mines will be concerned with these problems. The existing data, however, suggest the following four interpretations about the physical processes that produce failure. First, dilatancy, as measured by an increase in apparent volume of material, does not peak at failure. Rather, data presented here suggest that dilatancy attains a minimum value within a localized zone where a fracture (fault) will be nucleated. Second, the sample appears to experience a general decrease in volume during the preparation time, τ_0 , required to produce the fracture (fig. 7). This collective behavior is interpreted as an implosion or an "inward type of motion" as the activation volume obtains strain energy for the impending rupture. The activation volume is defined to be the volume of material affected by the withdrawing motion. This motion is evidenced by a simultaneous decrease (during τ_0) of axial load and confining pressure. This behavior also suggests that it is during the preparation time that the energy, which will be dissipated as elastic wave radiation and heat during the growth phase of the failure, is stored. Hence, we suggest that creep deformation (time-dependent motion under constant far-field conditions) precedes failure and failure does not precede creep, thus providing a basis for resolving the question: "does creep precede failure, or does failure precede creep?" (Savage and Mohanty, 1969; Steketee, 1958). Briefly, the inclusion theory requires that (for failure under triaxial compression), creep deformation in the direction of the maximum principal local stress

axis, say $\delta\epsilon_{11}^*$, must precede failure. At the time of the mainshock, constancy of volume ($\delta\epsilon_{11}^* = 0$) requires the component of creep strain, say $\delta\epsilon_{33}^*$, normal to the direction of fracture propagation to be equal to $-1/2 \delta\epsilon_{11}^*$, where $\delta\epsilon_{33}^* = \delta\epsilon_{22}^*$. Thus, strain $\delta\epsilon_{33}^*$ follows the shock. Third, stress drop, in the laboratory tests inferred from a decrease in axial load, is calculated to be on the order of several MPa, in good agreement with field observations of large scale failures such as earthquakes and rock bursts in deep mines. Fourth, the physical processes leading to failure are scale invariant.

Lastly, we emphasize the use of the term precursor of an impending instability. As used in this article, the existence of a precursor(s) implies that the process leading to instability (failure) has become self-sustaining. In other words, we use the term precursor only during the time interval when the conditions of thermodynamic stability are no longer valid.

The conditions of thermodynamic stability are

$$\begin{aligned} \beta &> 0 \text{ (mechanical stability)} \\ C_v &> 0 \text{ (thermal stability)} \\ \Delta\mu_1 &> 0 \text{ (diffusion stability)} . \end{aligned}$$

Stability with respect to diffusion requires that diffusion of a given species always occurs in the direction of increasing concentration (decreasing chemical potential of that species). β refers to the isothermal compressibility and C_v is the specific heat at constant volume. Negative values of β , C_v , and $\Delta\mu_1$ imply thermodynamic instability.

Experimental evidence presented earlier showing that both axial load and confining pressure decrease during the failure preparation time provides direct evidence that β has become negative (sample volume is decreasing as

the total applied pressure decreases) within a localized volume (failure nucleation zone) prior to rupture. Conditions for mechanical stability are violated during this time interval.

Our experimental evidence for a negative value of C_1 within the failure nucleation zone is indirect. For example, it is not difficult to show that a negative specific heat within the nucleation volume (primary inclusion zone-PIZ) would require that the temperature of the material within this volume increases during the implosion phase. The temperature increase causes this zone to (thermally) radiate and that this process (temperature increase and radiation) would be self-sustaining and increasing at an exponential rate during the preparation time. Thus as the surface area of the nucleation zone is decreasing, its temperature will increase. This process would be evidenced by an ever increasing strain rate outside the zone and if the material displays a piezoelectric effect, an increasing electric current would be measured on the specimen surface. When the temperature within the nucleation zone approached the value necessary to cause bond breakage (~ several thousand degrees Kelvin), bound electrons would be freed and the growth phase of the failure would occur. The existence of a "spike" in the surface EM field could easily be explained by this process. Thus the data on EM radiation and increases in the rate of sample "acceleration" during the failure preparation time are consistent with a violation of the thermal stability criterion. In addition, the implosion process also suggests that the system has become unstable with respect to diffusion during the preparatory phase. A violation of this criterion implies the movement of matter in a direction (toward the nucleation zone) of decreasing concentration (soft inclusion-like phase) and of increasing chemical potential.

The violation of mechanical, thermal, and diffusion stability are essential ingredients of the inclusion theory of instability (Brady 1979a). Their violation is shown to be necessary and sufficient conditions that the failure preparation process has been initiated.

REFERENCES

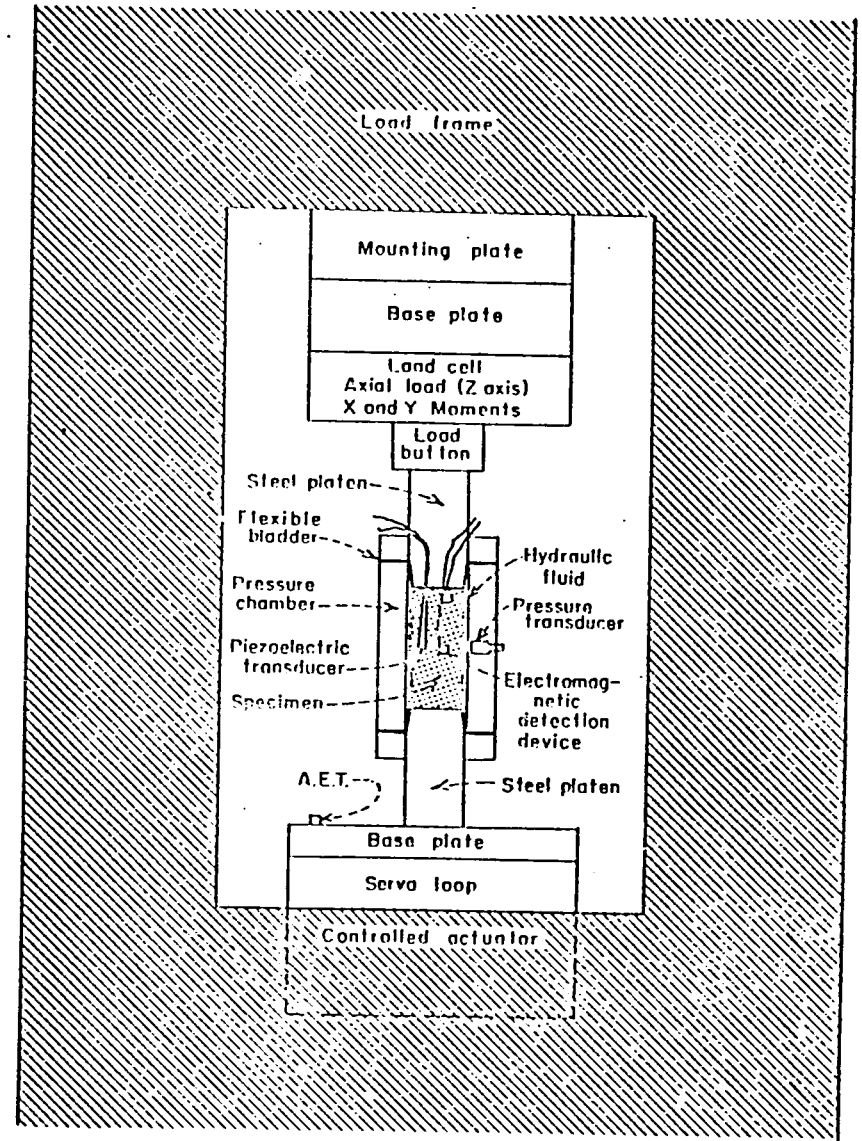
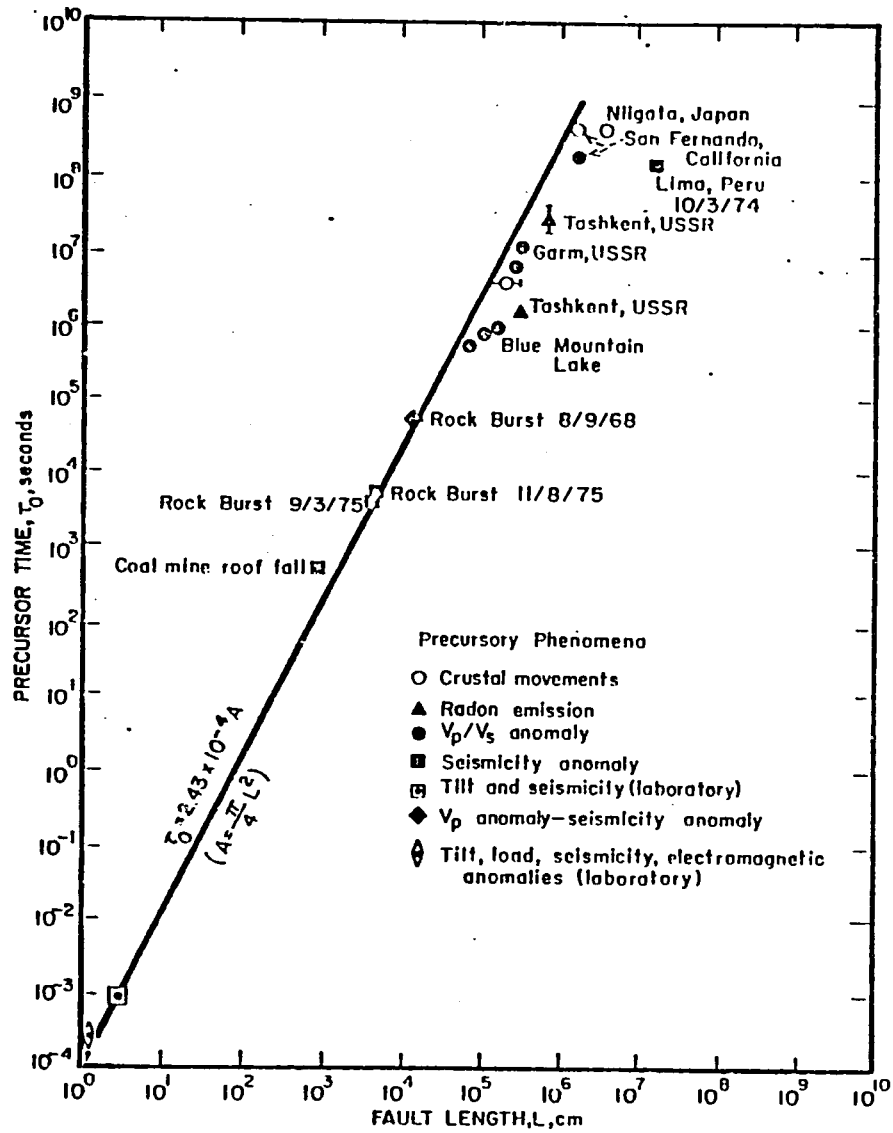
1. Aggarwal, Y.P., L.R. Sykes, D.W. Simpson, and P.C. Richards. Spatial Variations in τ_x/τ_y and in P-Wave Residuals at Blue Mountain Lake, New York: Application to Earthquake Prediction, J. Geophys. Res., vol. 80, No. 5, pp. 718-732, 1975.
2. Anderson, D.L., and J.H. Whitcomb. Time-Dependent Seismology, J. Geophys. Res., vol. 80, No. 11, pp. 1497-1503, 1975.
3. Brace, W.F., B.W. Paulding, and C. Scholz. Dilatancy in the Fracture of Crystalline Rocks, J. Geophys. Res., vol. 77, No. 16, pp. 3939-3955, 1966.
4. Brady, B.T. Seismic Precursors Prior to Rock Failures in Underground Mines, Nature, vol. 252, No. 5484, pp. 544-552, 1974.
5. Brady, B.T. Laboratory Investigation of Tilt and Seismicity Anomalies in Rock Before Failure, Nature, vol. 260, No. 5547, pp. 108-111, 1976a.
6. Brady, B.T. Theory of Earthquakes IV. General Implications for Earthquake Prediction, Pure and Applied Geophysics, vol. 114, pp. 1031-1082, 1976b.
7. Brady, B.T. An Investigation of the Scale Invariant Properties of Failure, Int. J. Rock Mech. Min. Sci., vol. 14, No. 3, pp. 121-126, 1977a.
8. Brady, B.T. Anomalous Seismicity Prior to Rockbursts: Implications for Earthquake Prediction, Pure and Applied Geophysics, vol. 115, Nos. 1-2, pp. 357-375, 1977b.
9. Brady, B.T. Thermodynamics of Failure (in preparation, 1979a).
10. Brady, B.T., and F.W. Leighton. Seismicity Anomaly Prior to a Moderate Rock Burst: A Case Study, Int. J. Rock Mech. Min. Sci., vol. 14, No. 3, pp. 127-132, 1977.
11. Brady, B.T. The October 3 - November 9, 1974, Peru Earthquake Sequence: Seismological Implications and a Prediction Update, (submitted to Science), 1979b.
12. Byerlee, J.D. The Mechanics of Stick-Slip, Tectonophysics, vol. 9, pp. 475-488, 1970.
13. Byerlee, J.D., and W.F. Brace. Stick-Slip, Stable Sliding and Earthquakes - Effect of Rock Type, Pressure, Strain Rate, and Stiffness, J. Geophys. Res., vol. 73, pp. 6031-6046, 1968.

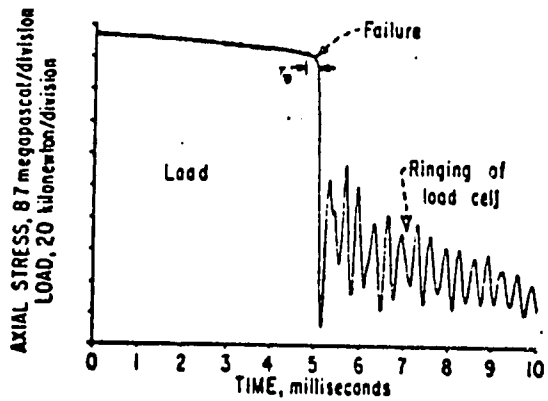
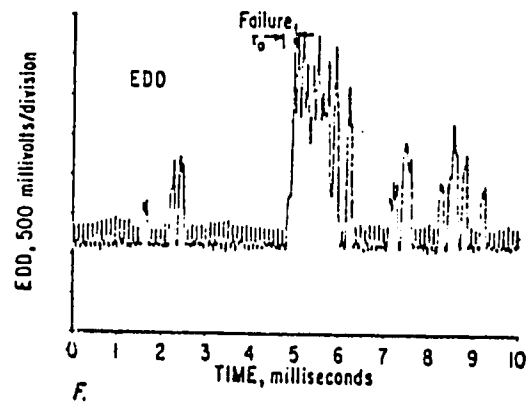
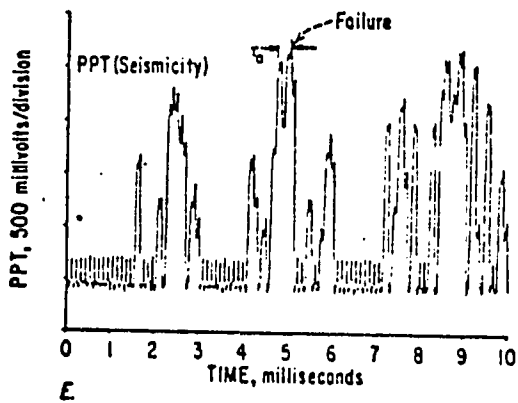
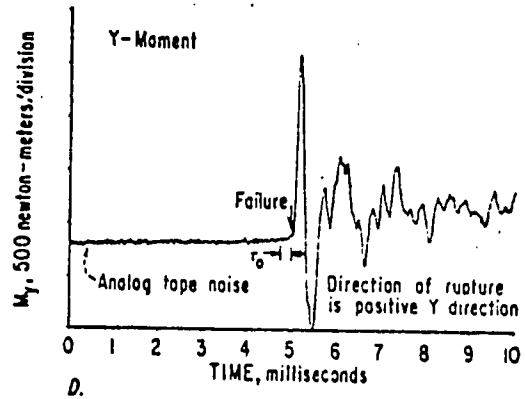
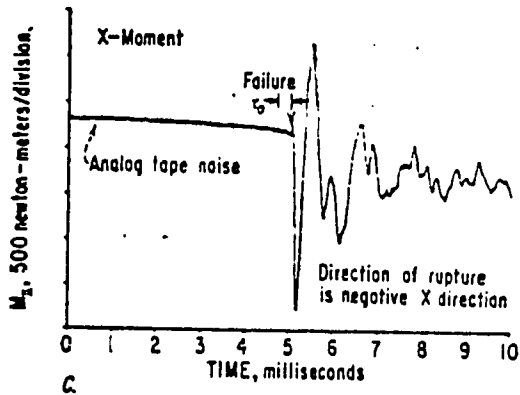
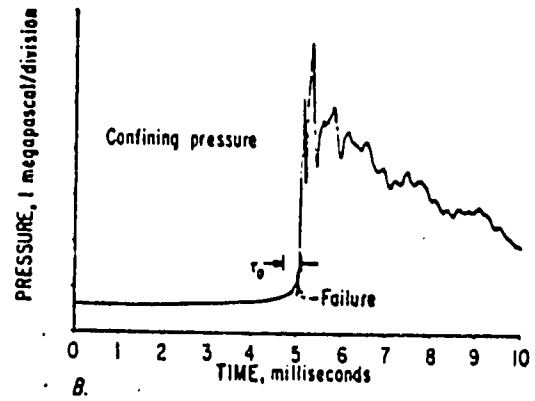
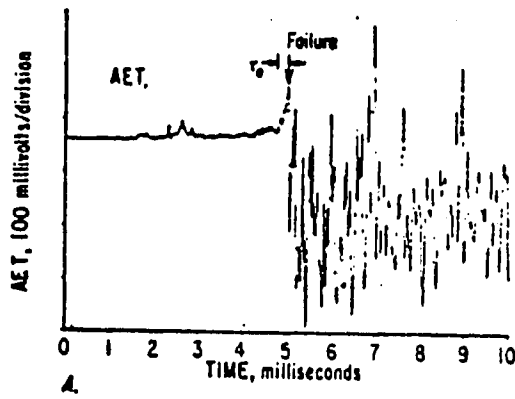
14. Brune, J.N. Tectonic Stress and the Spectra of Seismic Shear Waves, J. Geophys. Res., vol. 75, pp. 4997-5009, 1970.
15. Hanks, T.C. Earthquake Stress Drops, Ambient Tectonic Stresses, and Stresses that Drive Plate Motions, Pure and Applied Geophysics, vol. 115, Nos. 1-2, pp. 441-458, 1977.
16. Cohen, J., and S. Edelman. Piezoelectric Effect in Oriented Polyvinylchloride and Polyvinylfluoride, J. of App. Phys., vol. 42, No. 8, pp. 3072-3074, 1971.
17. Cottrell, A.H. Dislocations and Plastic Flow in Crystals, Oxford at the Clarendon Press, 223 pp., 1961.
18. Hadley, K. V_p/V_s Anomalies in Dilatant Rock Samples, Pure and Applied Geophysics, vol. 113, No. 112, pp. 1-25, 1975.
19. Hardy, H.R. Application of Acoustic Emission Techniques to Rock Mechanics Research, Am. Soc. Test. Mat., Spec. Tech. Publ., p. 505, 1972.
20. Hjachkin, V.I., W.F. Brace, G.A. Sobolev, and J.H. Dietrich. Two Models for Earthquake Forerunners., Pure and Applied Geophysics, vol. 113, No. 1/2, pp. 169-183, 1974.
21. Nersisov, I.L., A.A. Likk, V.S. Ponomarev, T.G. Ravitain, B.G. Rubev, A.V. Semenas, and I.G. Simbrieva. Possibilities of Earthquake Prediction, Exemplified by the Garm Area of the Tadzhik, S.S.R., in Earthquake Precursors, ed. M.A. Sadovskii, I.L. Nersisov, and L.G. Latynina (Academy of Science of the U.S.S.R., Moscow, pp. 79-99, 1975).
22. Richter, C.F. Elementary Seismology, W.H. Freeman, San Francisco, 768 pp, 1958.
23. Savage, J.C. Steketee's Paradox, Bull. Seismol. Soc. Am., vol. 59, pp. 381-384, 1969.
24. Savage, J.C., and B.B. Mohanty. Does Creep Cause Fracture in Brittle Rocks?, J. Geophys. Res., vol. 74, No. 17, pp. 4329-4332, 1969.
25. Scholz, C.H. Frequency - Magnitude Relationship of Micro-Fracture Events During the Triaxial Compression of Rock, Trans. Am Geophys. Union, vol. 48, No. 1, p. 205, 1967.
26. Scholz, C.H. Microfracturing and the Inelastic Deformation of Rock in Compression, J. Geophys. Res., vol. 73, No. 4, pp. 1417-1432, 1968.

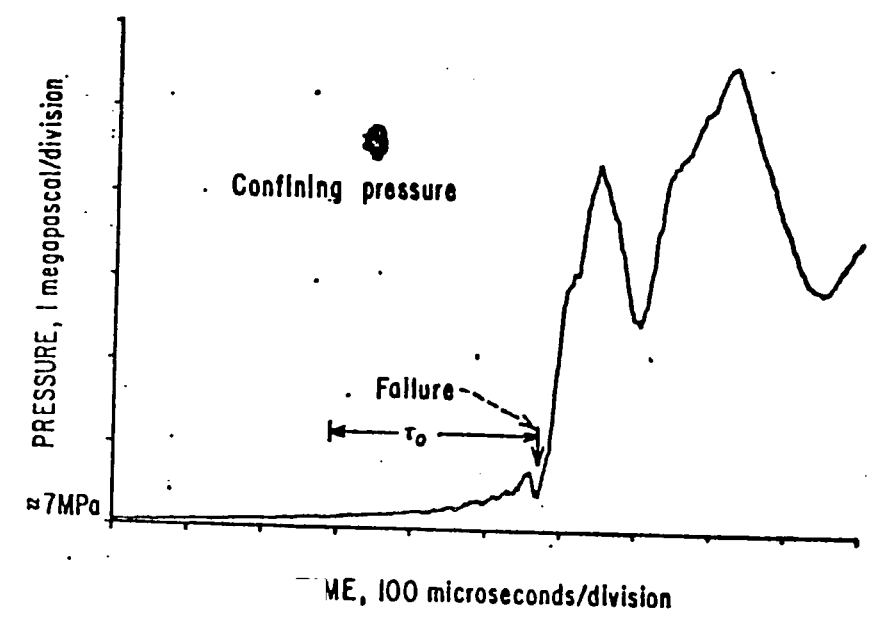
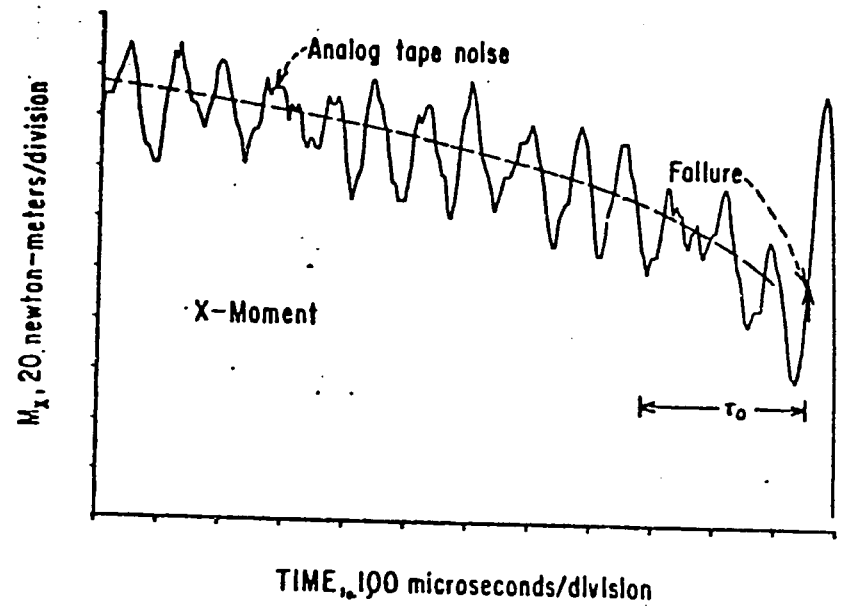
27. Scholz, C.H., L.R. Sykes, and Y.P. Aggarwal. The Physical Basis for Earthquake Prediction, Science, vol. 181, No. 4102, pp. 803-810, 1973.
28. Steketee, J.A. Some Geophysical Applications of the Elasticity Theory of Dislocations, Can. J. Phys., vol. 36, No. 17, pp. 1168-1198, 1958.
29. Stetsky, R.H., W.F. Brace, D.K. Riley, and P.Y.F. Robin. Friction in Faulted Rock at High Temperature and Pressure, Tectonophysics, vol. 23, vol. 1-2, pp. 177-203, 1974.
30. Stuart, W.D. Diffusionless Dilatancy Model for Earthquake Precursors, Geophys. Res. Lett., vol. 1, pp. 261-264, 1974.
31. Wyss, M. Stress Estimate for South American Shallow and Deep Earthquakes, J. Geophys. Res., vol. 75, pp. 1529-1544, 1970.
32. Wyss, M., and P. Molnar. Sources Parameters of Intermediate and Deep Focus Earthquakes in the Tonga Arc, Phys. Earth Planet. Interiors, vol. 6, pp. 279-292, 1972.

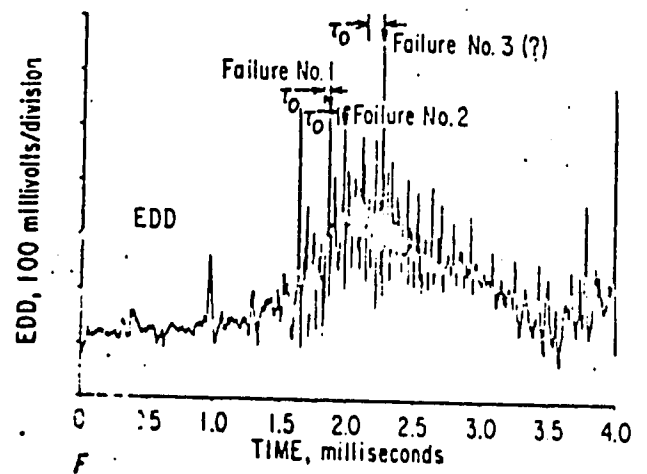
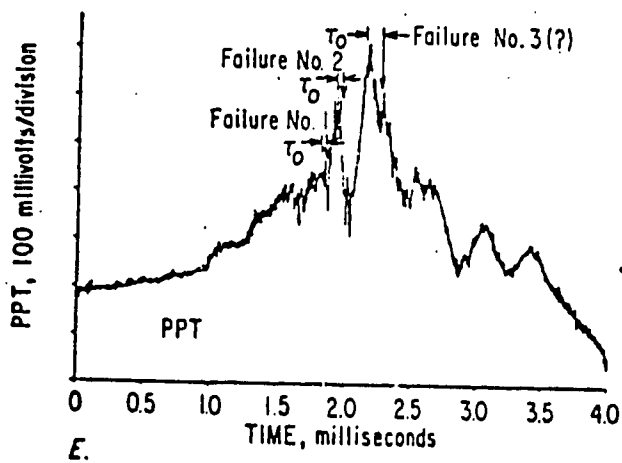
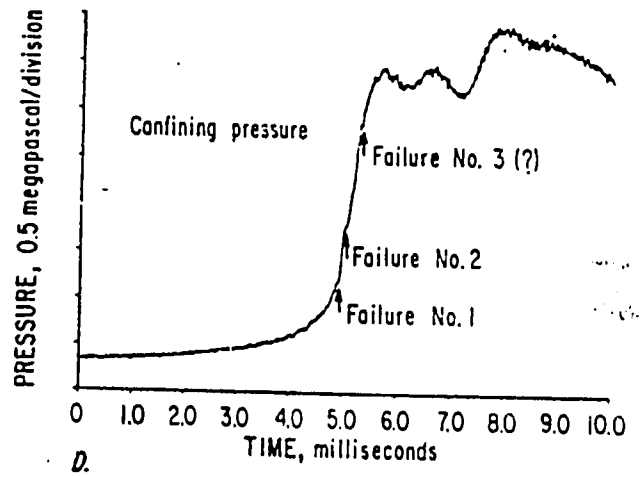
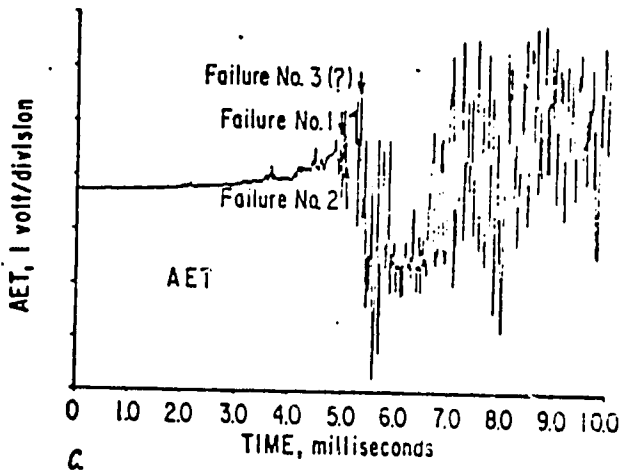
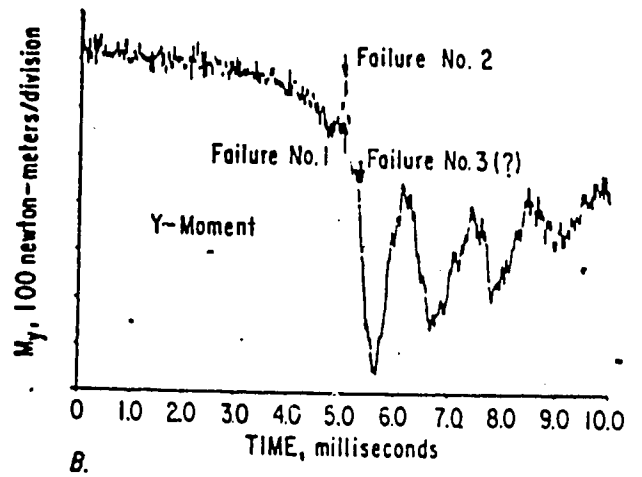
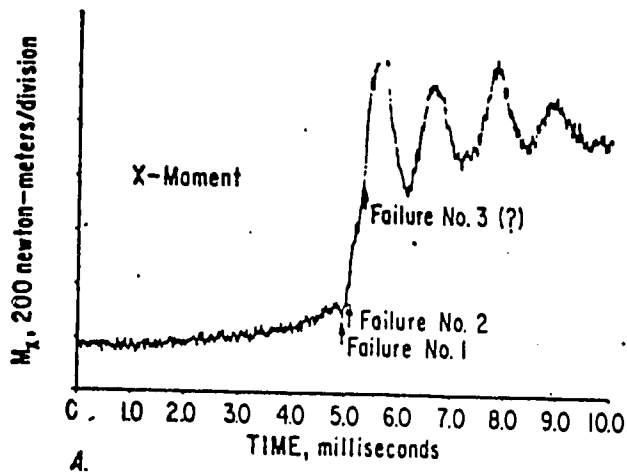
FIGURE CAPTIONS

1. Failure preparation (precursor) times for laboratory, mine, and selected earthquake failures. Fault lengths refer to an average linear dimension of the aftershock region. Precursor time is the time interval from the moment failure becomes inevitable to the actual failure.
2. Experimental arrangement used in laboratory experiments.
3. Test results from Barre granite core 28. Signal delay times have been removed, according to table 1, so that each graph is synchronous with respect to event occurrence to within $\pm 15 \mu$ sec. Each graph shows relative changes in the indicated quantities. In figures E and F, the number of counts during each 100 μ sec time window, N, may be determined from $N = 10^6 v$, where v is the voltage above the zero level. The apparent noise in E and F is due to the reset clock signal.
4. Expanded time view of figures 3C and 3B, nonsynchronous. Note especially the direction changes in H_x and the drop in confining pressure near failure.
5. Test results from Barre granite core 34 as recorded directly on the digital scope during the experiment, 0.5 μ sec/point. Only relative changes are shown.
6. Further test results from Barre granite core 34. Figures A, B, C, and D were obtained from the analog tape deck.
7. Illustration of activity within the anomalous region induced by the formation of the PIZ. Arrows depict motion of material as distortional strain energy is converted into volumetric energy within the activation volume during the failure preparation time.

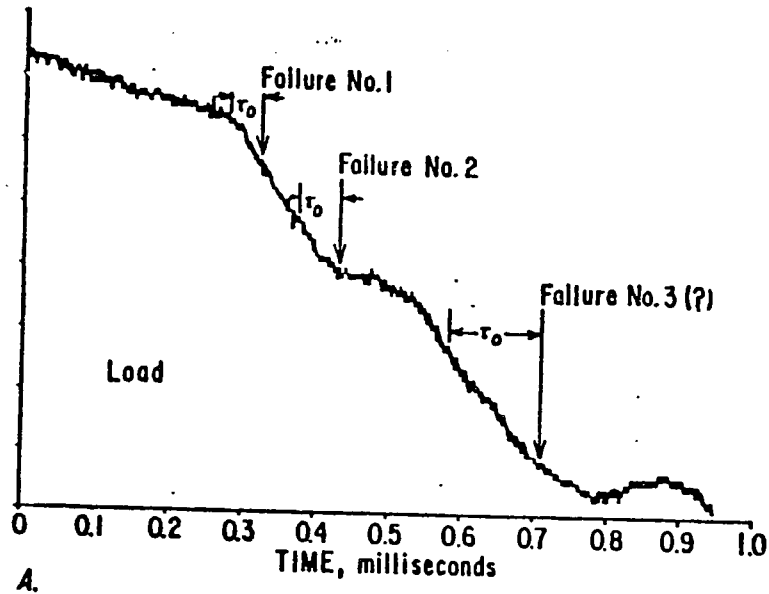




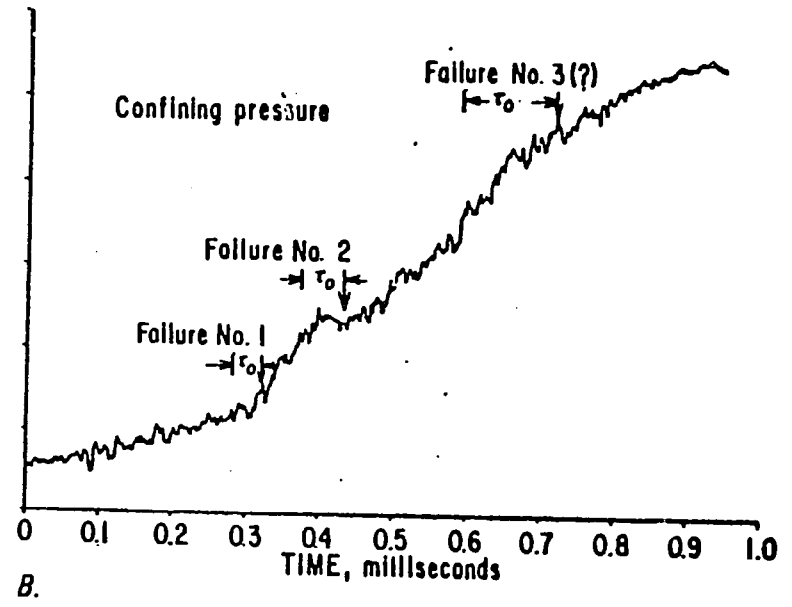




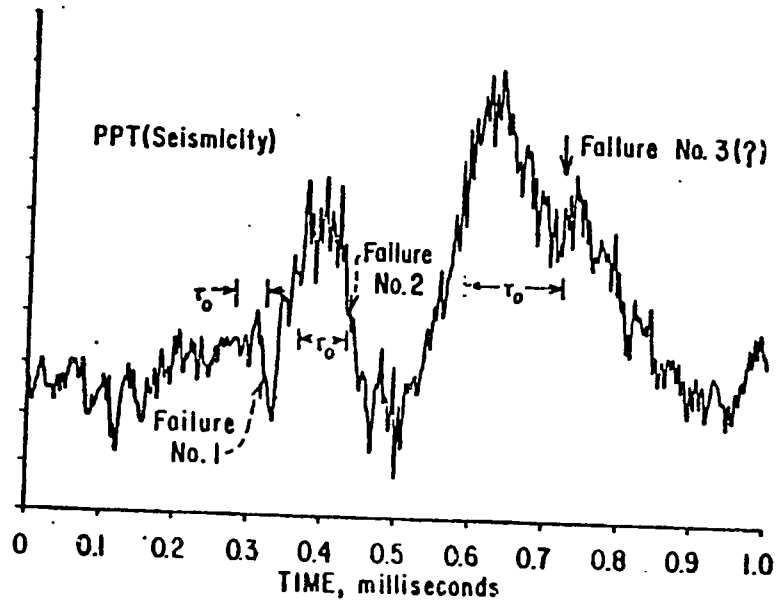
AXIAL STRESS, 2.2 megapascal/division
LOAD, 5 kilonewton/division



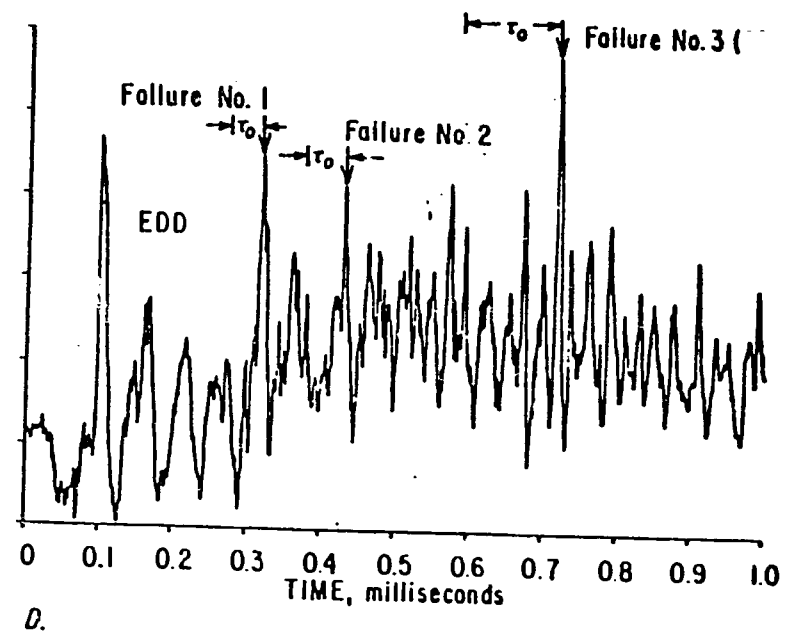
PRESSURE, 0.5 megapascal/division

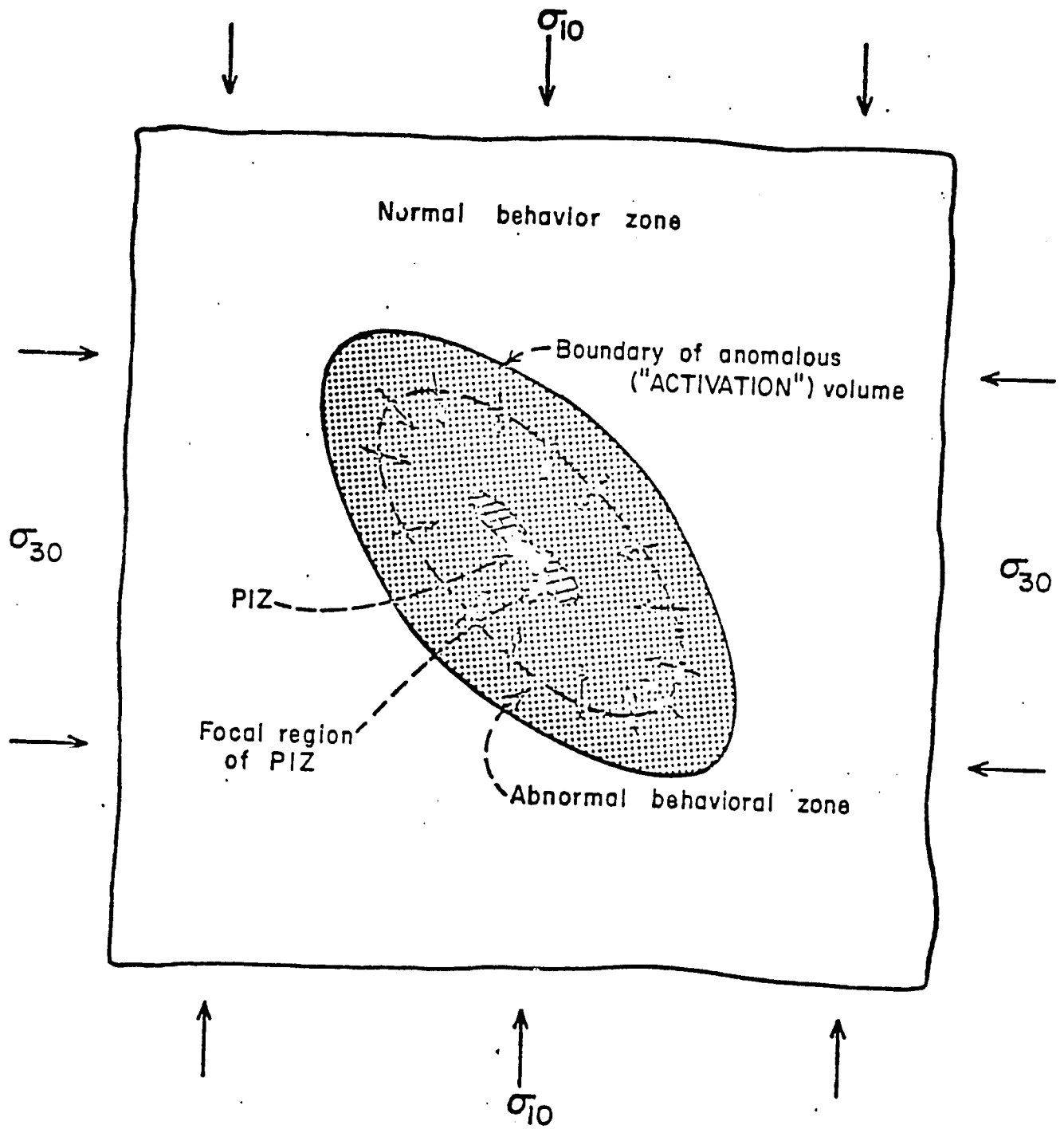


PPT, 50 millivolts/division



EDD, 100 millivolts/division





-  Aftershock region ("FOCAL REGION OF PIZ")
-  Implosion region ("STRAIN ENERGY STORAGE ZONE")
(Implosion region contains aftershock region)

INFORME

PREDICCIÓN SISMICA EN EL PERU:
PARAMETROS IMPORTANTES, PROGRAMA GENERAL,
Y EQUIPAMIENTO

POR :
LEONIDAS OCOLA

DIRECCION DE INVESTIGACION CIENTIFICA DE
GEOFISICA APLICADA

LIMA, ABRIL 1980

TABLA DE CONTENIDO

	Página
INTRODUCCION	1
<u>PARTE 1:</u> IDENTIFICACION Y CATEGORIZACION DE PARAMETROS IMPORTANTES	2
1. SISMICIDAD	3
2. DEFORMACION GEODESICA	4
3. DEFORMACIONES PUNTUALES	4
4. CAMPOS POTENCIALES	6
4.1 Campo gravimétrico	6
4.2 Campo geomagnético	6
4.3 Campo geoeléctrico	7
5. GEOQUIMICA	7
6. VARIACIONES DEL NIVEL FREATICO	8
7. GEOLOGIA	8
8. RESUMEN	8
<u>PARTE 2:</u> PROGRAMA GENERAL	9
1. GENERALIDADES	9
I. FASE 1: DETECCION Y ADQUISICION DE DATOS	10
2. SISMICIDAD	10
2.1 Redes Sísmicas	11
2.1.1 Red Telesísmica	11
2.1.2 Red Sísmica de Arequipa	12
2.1.3 Red Sísmica de Lima y Dptos. del sur del Perú.	12
2.1.4 Red Sísmica del Reservorio de Poechos y estaciones de INIE	12
2.2 Comentarios sobre las redes sísmicas existentes	13
2.3 Red sísmica para el programa de predicción	14
2.3.1 Características de la red sísmica principal.	14
2.3.2 Red sísmica principal	15
2.3.3 Red sísmica especial	16
3. DEFORMACION GEODESICA	16
3.1 Re-ocupación geodésica	16
3.2 Determinación del nivel medio del mar	17
3.3 Fechamiento de terrazas marinas	18
3.4 Resumen	19
4. DEFORMACIONES PUNTUALES	19
5. ESTUDIO DE NEOTECTONICA	20
6. FLUJO DE RADON	20
7. VARIACIONES DE LOS CAMPOS GEOELECTRICOS Y GEOMAGNETICOS	21

II. FASE 2: ANALISIS Y PROCESAMIENTO DE DATOS	21
1. SISMICIDAD	21
1.1 Procesamiento	22
1.2 Digitalización	23
2. DEFORMACIONES GEODESICAS	24
2.1 Análisis-Procesamiento	24
2.2 Digitalización	24
3. DEFORMACIONES PUNTUALES	24
3.1 Análisis-Procesamiento	24
3.2 Digitalización	25
III. FASE 3: USO Y DISPERSION DE DATOS	25
<u>PARTE 3:</u> RECOMENDACIONES SOBRE LA ADQUISICION DE EQUIPO	26
I. DETECCION Y ADQUISICION DE DATOS	26
1. SISMICIDAD	26
1.1 Red Sísmica Principal	26
1.1.1 Generalidades	26
1.1.2 Equipo de detección, transmisión, registro: Red Sísmica Principal.	27
1.2 Equipo de Detección y Registro in situ: Red Sísmica Principal	28
1.2.1 Generalidades	28
1.2.2 Equipo a adquirirse	28
1.3 Estaciones de amplio rango dinámico	28
1.3.1 Generalidades	28
1.3.2 Equipo	29
2. DEFORMACION GEODESICA	29
2.1 Control geodésico horizontal	29
2.2 Control geodésico vertical	30
2.3 Variaciones del campo gravimétrico	30
2.4 Determinación de edades de las terrazas	30
2.5 Variaciones del nivel medio del mar	30
3. DEFORMACIONES PUNTUALES	30
4. CAMPO GEOMAGNETICO	31
5. GEOQUIMICA	31
II. ANALISIS Y PROCESAMIENTO DE DATOS	31
1. ANALISIS	31
1.1 Generalidades	31
1.2 Equipo	32
2. PROCESAMIENTO	32
2.1 Generalidades	32
2.2 Equipo	33
AGRADECIMIENTOS,	35
A P E N D I C E:	37

I N T R O D U C C I O N

El 16 de Marzo de 1980, el suscrito recibió, de parte del Jefe del Instituto Geofísico del Perú (IGP), la tarea de reunir información sobre experiencias científicas, equipo y procedimientos actualmente en uso en el programa de predicción sísmica del Servicio Geológico de los Estados Unidos de Norteamérica. La tarea se cumplió del 23 de Marzo al 6 de Abril del presente.

En vista que los fondos puestos a disposición del IGP por el Gobierno del Perú son para un programa de predicción sísmica a nivel nacional, y teniendo en cuenta que existe una predicción a mediano plazo para la zona litoral del departamento de Lima, se juzgó conveniente sostener sesiones de trabajo con investigadores científicos de gran experiencia y de reconocido prestigio internacional en las diferentes disciplinas de investigación del programa de predicción sísmica del Servicio Geológico, con el fin de identificar los parámetros más significativos que permitieran implementar un programa de predicción sísmica nacional dentro de las posibilidades económicas y técnicas presentes. Se sostuvo además varias sesiones de trabajo con el Dr. B. Brady, autor de la predicción, para tratar en detalle lo que para su teoría eran las observaciones más significativas.

En el presente informe se resumen los resultados en tres partes. En la primera, concierne principalmente al grado de importancia de los 'parámetros' físicos y químicos actualmente utilizados en la predicción. En la segunda, se sugiere un programa de trabajo; y en la tercera parte, se presenta una recomendación sobre el equipo a adquirirse.

PARTE I :

IDENTIFICACION Y CATEGORIZACION DE PARAMETROS IMPORTANTES

Los programas nacionales de predicción sísmica de Estados Unidos de Norteamérica, Japón, China, Rusia, etc. han hecho, a través de varios años, observaciones de las variaciones en tiempo y espacio, de un gran número de propiedades físicas y físico-químicas con miras a identificar anomalías asociadas con la etapa de 'preparación' de sismos destructores. Varios de estos programas involucran observaciones masivas a costo de una inversión de varios millones de dólares en equipo de adquisición y procesamiento de datos, con la participación de varias centenas de científicos y técnicos altamente especializados. Como resultado de este gran esfuerzo, se han identificado algunos parámetros o indicadores que tienen relevancia en la predicción sísmica.

La mayoría de los estudios aún están en la etapa de investigación. Nadie puede asegurar exactamente "qué es lo que se va a encontrar", y aún "no se sabe qué es lo que se está buscando ..." en las observaciones de los fenómenos pre-terremoto. Aún cuando cualquiera de los programas avanzados de predicción de terremoto de las naciones mencionadas anteriormente, logren predecir con cierto grado de certeza, los fenómenos (anomalías) asociadas con la ocurrencia misma del evento serán, probablemente, diferentes en carácter.

Teniendo en cuenta los factores brevemente mencionados arriba, durante las sesiones de trabajo, se ha hecho esfuerzos para establecer su importancia y el nivel de variación en el tiempo y en el espacio de los parámetros físicos y químicos comunmente observados.

Los parámetros tratados con amplitud son: 1) sismicidad, 2) deformación geodésica, 3) 'deformaciones' puntuales

4) campos potenciales: gravimétricos, geomagnéticos, eléctricos, 5) geoquímica, 6) varios.

1. SISMICIDAD

Hay un consenso, salvo la opinión de un investigador científico en Menlo Park, sobre la primerísima importancia de seguimiento y caracterización de la evolución de la sismicidad en tiempo y espacio con fines de predicción. Según la experiencia del Dr. Eaton, al iniciarse el programa de predicción en California, se hizo un esfuerzo grande para la implementación, primero, de una red básica (master net), y luego en el establecimiento de procedimientos de análisis standard para la producción de datos altamente confiables y exactos - sin requerir gran interacción con la investigación científica en su producción. Esto requiere que los datos producidos por personal de nivel intermedio deben ser autocontrolados. Posteriormente, se desarrolló la red actual, cuya implementación en el área de manejo de datos, y procesamiento en línea (tiempo real) aún continúa.

El Dr. Brady considera la sismicidad, según su teoría, como 'el parámetro 'necesario y suficiente' para la predicción sísmica. Los otros parámetros, entre ellos las variaciones de 'esfuerzos', son 'curiosidades científicas'. Según él, es necesario ubicar los eventos sísmicos con magnitud igual o mayor que 4 m_b con una exactitud ± 10 km. Con el fin de mejorar la estimación de la magnitud del evento principal, la zona de inclusión primaria (PIZ) debe mapearse con gran exactitud. Esto implica detectar y localizar eventos con magnitudes mayores que 1 m_b .

El estudio de la sismicidad requiere del conocimiento de las propiedades físicas del medio, por lo menos, las velocidades de propagación de las ondas sísmicas en la región cu -

bierta por la red sísmica. Con este fin, en California, además del programa de estudio de eventos naturales tiene el de fuentes controladas (refracción y reflexión sísmicas).

2. DEFORMACION GEODESICA

Este es otro de los 'parámetros' sobre los cuales hay una opinión unánime, salvo la opinión de un investigador científico en Menlo Park, que debe estudiarse. Es de primera necesidad establecer el modo y la razón (rate) de deformación horizontal, las variaciones de altitud y la razón de levantamiento del borde continental. La determinación de estos valores y su variación en tiempo y espacio requieren de un estudio sistemático y cuidadoso de los datos provenientes de las re-ocupaciones de redes de triangulación o poligonación, de líneas de nivelación geodésica; del análisis de los mareogramas, y finalmente del fechamiento de las terrazas marinas recientes.

Según el Dr. J. Savage, los resultados encontrados en California son muy confiables y coherentes. Este tipo de mediciones de deformación minimiza los efectos de lluvia, movimientos locales del suelo, cambios por temperaturas, o cualquier movimiento en un punto individual. Las medidas deben tener una resolución de 10^{-7} y re-ocuparse cada año, por lo menos; lo ideal sería tener un monitoreo continuo.

3. DEFORMACIONES 'PUNTUALES'

Bajo la denominación de mediciones de 'deformaciones puntuales' se involucra las mediciones in situ de 'esfuerzos' y su monitoreo, la detección de variaciones de 'deformaciones', incluyendo inclinación, con tiempo y espacio.

benefició grandemente de los resultados del programa japonés. Según el Dr. S. Sacks, se ha encontrado que para obtener medidas de 'deformaciones' posiblemente relacionadas al proceso tectónico causante de la ocurrencia de los sismos, es necesario: i) detectar cambios de deformaciones del orden de 10^{-9} ; ii) medidas de 'deformaciones' a profundidades menores que 50 m son fuertemente influenciadas por los elementos meteorológicos, descarga-carga de reservorios de agua subterránea; iii) instrumental instalado en minas en trabajo por lo general son muy ruidosas; iv) las rocas en las minas, por lo general, están altamente fracturadas por lo tanto efectos locales, aún a profundidades de 100 m, pueden ser grandes; v) las medidas obtenidas de los extensómetros de cuarzo, alambre invar, inclinómetros, tales como las que hay en el Perú, no se sabe qué significan. El Dr. Sacks mencionó que actualmente en el Japón tienen 34 'deformómetros' (strainmeter) en pozos profundos, y que han detectado anomalías relacionadas al sismo de Izu (6.8 Ms). Actualmente, tienen programado aumentar significativamente el número de sensores profundos.

El Dr. Brady había sugerido medir 'esfuerzos' in situ en un gran número de puntos. Sobre este tema se cambió ideas ampliamente. Se llegó a la conclusión que el material en el volumen hipocentral de la PIZ antes del inicio de la etapa de ruptura, la variación con el tiempo de las deformaciones es del orden de 10^{-12} - 10^{-11} , y que durante la etapa de inestabilidad probablemente alcancen órdenes de 10^{-5} . Estas apreciaciones son concordantes, en términos generales, con las del Dr. Sacks. Las experiencias en S. de California sobre las observaciones de deformación e inclinación es que los niveles de 'ruido' son muy altos. A la fecha, no se ha obtenido un 'set' de datos que no tenga problemas y sea asociable sin cuestionamiento a un evento sísmico.

- 914 -

Hay un consenso general sobre: 1) las medidas de deformación ó esfuerzos a poca profundidad, no son significativos; 2)

son complejos; 3) que la detección de 'deformaciones' del orden de 10^{-9} es muy difícil con la tecnología presente; 4) la detección debe hacerse a una profundidad tal que elimine los efectos superficiales y lejos de la influencia de perturbaciones locales (fallas, fracturas, movimientos masivos de agua subterránea, etc.).

4. CAMPOS POTENCIALES

Bajo esta denominación se agrupan la detección y monitoreo de las variaciones del campo gravitatorio, geomagnético y geoelectrico. En general, la confianza que los científicos de Menlo Park tienen sobre estos parámetros es baja, y la experiencia no muy amplia.

4.1 Campo Gravitatorio

De los tres campos potenciales mencionados líneas arriba, éste es el menos problemático. Las observaciones relacionadas con la predicción requieren medidas del orden de 10 microgales, en áreas donde hay variaciones en altitudes significativas. Se espera que este parámetro sea un buen complemento al geodésico, considerando el costo y facilidad de observación.

4.2 Campo Geomagnético

Las anomalías se establecen utilizando observaciones simultáneas en pares de estaciones. Se esperan anomalías de 3-10 gammas. Las observaciones no muestran consistencia. En California, instrumentos con 1/4 gamma de sensibilidad, en las cercanías del epicentro de sismos de regular magnitud, no dieron anomalía alguna.

4.3 Campo Geoelectrico

Lo que actualmente se monitorea en S. de California son las variaciones del autopotencial y de la resistividad. A la fecha, aparentemente, no hay mayores resultados. Ninguno de los especialistas tiene su centro de operación en Menlo Park.

5. GEOQUIMICA

Las investigaciones en Menlo Park están dirigidas hacia el monitoreo de radón, helio y la relación entre los isótopos estables. La experiencia del Dr. Chi-Yu King, en el monitoreo de radón en pozos de 2 1/2 pies de profundidad utilizando el método de la 'taza invertida', y tomando promedios semanales de 'conteo' de los trazos dejados por las partículas en la película fotográfica, es la siguiente: 1) como regla no hay cambios en el flujo de Rn fuera de la zona de falla, 2) para detectar variaciones en el flujo de Rn, las observaciones deben hacerse sobre la falla, 3) para obtener algún resultado relacionado a efectos pre-sismos se tiene que monitorear muchas estaciones.

De las discusiones con el Dr. R. Holub, en el laboratorio del Bureau of Mines en Denver, es evidente que las variaciones del flujo del gas radón reflejan las variaciones del campo de esfuerzos; por lo tanto los problemas de detección y análisis, están influenciados significativamente por las condiciones locales. Se propuso, al Dr. Holub, la alternativa de hacer un monitoreo en la fase acuosa en pozos perforados en rocas cuyo contenido radioactivo es alto. En su opinión, el experimento podría dar mejores resultados que las observaciones hechas actualmente en sedimentos y otras clases de rocas o medios.

6. VARIACIONES DEL NIVEL FREÁTICO

Las investigaciones de este parámetro son, al parecer, muy limitadas ya que su relación a procesos tectónicos es muy difícil de establecer.

7. GEOLOGIA

Los procesos geológicos y los sísmicos están íntimamente relacionados. La predicción de los segundos requiere del entendimiento de los primeros. Para este fin, se requiere del mapeo geológico a una escala razonable tanto de la geología como de la estructura geológica asociada. En especial, es de gran relevancia al programa de predicción sísmica los estudios de la neotectónica andina, i.e., tectónica de fines del Terciario y Cuaternario, y la identificación del patrón sismotectónico andino. La identificación de fallas activas o potencialmente activables es vital para la toma de medidas de prevención en la 'zona' activa continental.

Por lo tanto, un programa de predicción sísmica es incompleto si es que no se complementa con un programa de estudio de fenómenos geológicos neotectónicos y un mapeo de fallamiento activo reciente.

8. RESUMEN

De la descripción anterior, es evidente el siguiente orden de importancia de los diferentes parámetros observables para la predicción sísmica a nivel nacional: i) sismicidad, ii) deformación geodésica, iii) fenómenos neotectónicos, iv) deformaciones puntuales, v) variaciones del flujo de radón, vi) variaciones del campo magnético, vii) variación del nivel de la napa freática, viii) variaciones del campo eléctrico. - 917 -

PARTE 2 :

PROGRAMA GENERAL

1. GENERALIDADES

En la presente parte se esboza un programa general para la predicción de sismos en el Perú. El programa da lineamientos generales para cada uno de los parámetros descritos en la Parte 1. Varios de los puntos expuestos en esta sección incluyen sugerencias de algunos científicos con los cuales se intercambi6 ideas.

Para asegurar un programa continuado, es necesario prever redundancia, en especial en las dos primeras fases del programa. El equipamiento utilizado, así como el procedimiento implementado para el procesamiento de datos deben tener la resolución suficiente para asegurar la obtención de la información básica relevante al proceso sísmico mismo. El énfasis del programa en general debe ser hacia la ejecución de 'observaciones fundamentales del proceso sísmico' en vez del 'seguimiento de fenómenos precursoros' sin un fundamento científico sólido, y el análisis e interpretación de dichos datos resultantes de dichas observaciones.

Se debe tener presente que aún 'no se sabe qué es lo que se busca exactamente' o 'qué es lo que se debe ver'. Por lo tanto, se debe tener una actitud amplia, cuidadosa y crítica ante la presencia de anomalías y fenómenos que frecuentemente se les relaciona al proceso pre-evento sísmico.

Es igualmente importante definir el nivel mínimo del evento sísmico que se desea pronosticar o finalmente predecir, ya que éste incide directamente en la densidad del muestreo, amplitud y tamaño de los fenómenos transitorios o anomalías de los parámetros a estudiarse.

es reducir los daños y pérdida de vidas. El éxito del programa de predicción se mediará en el grado de confianza que el público tenga en los resultados, y de su participación en el programa de predicción mismo como usuario de la información producida o como observador, y sobre todo en el grado en que la información y resultados alcanzados sean integrados en el Programa de Prevención Sísmica. Por lo tanto, es indispensable dotar al programa de predicción de una infraestructura que le permita integrar el interés regional, tanto para la etapa de investigación científica y estudio como para la implementación del uso de los resultados. Bajo este punto de vista se considera importante la implementación de Centros Regionales integrados a un Centro Nacional de Predicción Sísmica.

Para facilidad de exposición, el programa considera tres fases principales: 1) detección y adquisición de datos, 2) análisis y procesamiento de datos, y 3) uso y dispersión de datos.

I. FASE 1.- DETECCION Y ADQUISICION DE DATOS

La detección y adquisición de datos es una de las fases fundamentales en cualquier programa de investigación. Esta requiere la conjugación de financiamiento, experiencia, y una infraestructura apropiada.

A continuación se hace una evaluación somera del estado de estudio de los principales parámetros utilizables para la predicción sísmica en el Perú y se esboza, en términos generales, el plan de trabajo inmediato.

2. SISMICIDAD

Como se mencionó en la Parte 1, éste es el parámetro más importante utilizado en la predicción sísmica. La ocurrencia de sismos refleja inestabilidad mecánica que afectan masas de material cuyas dimensiones (volumen) están íntimamente relacionadas con la magnitud del sismo y su proceso de gestación. 919

2.1 Redes Sísmicas

A Diciembre de 1979, el Perú contó con las siguientes redes sísmicas: i) Red Telesísmica, ii) Red Sísmica de Arequipa, iii) Red Sísmica de Lima y Departamentos del Sur del Perú, iv) Red Sísmica de Poechos y estaciones de Energía (INIE). A continuación se hace una breve descripción de las características de las Redes y se está en el estado de análisis y procesamiento de datos.

2.1.1 Red Telesísmica

Esta red está constituida, principalmente, por las estaciones standard NOAA: Arequipa y Naña; y la estación de Huancayo. Estas estaciones están instrumentadas con equipos de período corto y largo. El análisis de los sismogramas se mantiene al día y se reporta al National Earthquake Information Service en Golden, U.S.A.

Además de estas estaciones telesísmicas existen las estaciones del Cuzco y Trujillo. Ambas instaladas y operadas bajo la responsabilidad del Department of Terrestrial Magnetism (DTM) de la Carnegie Institution of Washington en colaboración con el IGP. Actualmente, se obtiene un registro en papel de la estación del Cuzco. Ningún registro visible se obtiene de la de Trujillo ya que su registro es en cinta magnética. Los datos del Cuzco se registrarán con los de la Red de Lima y Dptos. del Sur del Perú.

Se tiene aproximadamente 20 años de datos para las estaciones de Arequipa y Naña. Para la Huancayo, se han obtenido datos por aproximadamente 45 años. Sin embargo, los sismogramas para un buen número de años, los primeros de operación, se encuentran en Caltech, U.S.A.

2.1.2 Red Sísmica de Arequipa

La Red Sísmica de Arequipa es operada, descontinuada, por el Instituto Geofísico de Arequipa (IGA) de la Universidad Nacional de San Agustín de Arequipa, el DTM; y últimamente con la cooperación del IGP. La primera temporada de operación se inició alrededor de 1964.

La red sísmica IGA-DTM comprendía estaciones en Arequipa (5), Puno (1), y Cuzco (1). El análisis y procesamiento no se ha completado.

2.1.3 Red Sísmica de Lima y Dptos. del Sur del Perú

Esta red opera bajo la responsabilidad completa del IGP: Dirección de Investigación Científica de Geofísica Aplicada (DICGA), y comprende instalaciones semiportátiles y radio telemétricas. La red cuenta con instalaciones en los siguientes departamentos: Lima (3), Ica (3), Ayacucho (1), Apurímac (1), Arequipa (2), Cuzco (1), Junín (1) -tele sísmica. La red funcionó continuamente desde mediados de 1976 a fines de 1977. En 1978 y 1979 funcionó parcialmente.

El análisis se encuentra completo desde Octubre 1976 a Junio 1977. No se ha iniciado el procesamiento por falta de computadora y de personal técnico.

2.1.4 Red Sísmica del Reservorio de Poehos y Estaciones INIE

La operación de la red sísmica de Poehos así como de las estaciones de INIE son responsabilidad del IGP: Dirección de Investigación Científica de Sismología (DICS).

La red sísmica de Poechos fue diseñada e implementada para monitorear la actividad sísmica en la vecindad del reservorio de Poechos sobre el río Chira, departamento de Piura. En la actualidad cuenta con 5-estaciones remotas con transmisión radial a la estación central de registro en las instalaciones del IGP en Negritos.

Las estaciones de INIE se encuentran instaladas en Ayacucho (1), Puerto Ocopa (1), Huánuco (1), Pucallpa (1), y en Tarapoto (1).

2.2 Comentarios sobre las Redes Sísmicas Existentes

Las redes sísmicas existentes fueron diseñadas e implementadas para resolver problemas locales de interés de un grupo de investigadores científicos locales y/o extranjeros, en el caso de las redes locales de Arequipa y Lima, o para la obtención de datos con uso potencial en proyectos de ingeniería: caso de la red de INIE o como medidas preventivas en el caso de la Red del Reservorio de Poechos. Como resultado se tiene información sísmica en diversos grados de resolución y calidad, cubriendo períodos diferentes.

Además, el instrumental es altamente heterogéneo, las prácticas de análisis y procesamiento disimilares.

Quando todas las estaciones se juzgan en conjunto, su distribución geográfica así como su equipamiento está muy lejos del mínimo que requiere una red sísmica para fines de predicción. Sin embargo, a pesar de estas deficiencias, la información que se puede extraer después de un análisis cuidadoso y crítico es invaluable; y serviría para guiar los estudios inmediatos y sobre todo para caracterizar el proceso sísmico en la plataforma continental al frente del departamento de Lima.

2.3 Red Sísmica para el Programa de Predicción

Las zonas sismogénicas en el oeste de Sudamérica, en las latitudes que comprende el Perú, influyen prácticamente la República en su totalidad, en especial el área comprendida entre la zona del mar territorial y las estribaciones subandinas. Por lo tanto, la red sísmica que se implemente, deberá cubrir este vasto territorio teniendo en cuenta que los niveles más altos de recurrencia están a lo largo de la plataforma continental y los sismos más destructores en la región subandina, futura área de desarrollo del país.

En el caso que se logre identificar un área en la cual se pronostique la ocurrencia de un evento sísmico importante, la Red Nacional deberá complementarse con una red sísmica especial cuya apertura dependerá del tipo de sismo y su impacto en la economía nacional, y sobre todo, de los posibles efectos en la población.

Se debe tener en cuenta que los resultados de los estudios serán útiles y el programa de predicción alcanzará su cometido, en la medida que tanto los representantes del Gobierno y el pueblo en general hagan uso de dicha información para mejorar el conocimiento general del grado de peligro sísmico local y regional, y del grado en que dichos resultados sean utilizados en el PROGRAMA DE PREVENCIÓN SISMICA para reducir los daños y pérdida de vidas humanas.

Teniendo en cuenta el principio de duplicidad, es recomendable implementar varios centros de acopio, procesamiento y distribución de información proveniente del programa de predicción.

2.3.1 Características de la Red Principal

La red sísmica con fines de predicción sísmica deberá tener las siguientes características:

- i. Equipo uniforme de detección, transmisión de información, análisis, procesamiento y presentación de datos.
- ii. Uniformidad en el nivel de detección para todo el territorio nacional.
- iii. Centros regionales de acopio, procesamiento preliminar en tiempo real, y distribución de información sísmica.
- iv. Dualidad en los sistemas de adquisición de información sísmica.
- v. Equipamiento de estaciones con 110 dB de rango dinámico para el estudio de características dinámicas de sismos fuertes y débiles.

ARE.
LIM.
CHIC.

2.3.2 Red Sísmica Principal

Se propone una red sísmica principal constituida por lo siguiente: 1) 35-estaciones radio telemétricas remotas, sin contar con las estaciones radio telemétricas existentes; 2) 15-estaciones con registro in situ, estas estaciones proveen la duplicidad del sistema de detección; 3) 3-estaciones con 110 dB de rango dinámico; 4) 3-centros regionales de registro, análisis, y procesamiento de datos en tiempo real; 5) 1-Centro Nacional de estudio e investigación sísmica para fines de predicción.

Se propone como centros regionales a Chiclayo, Lima y Arequipa. Siendo Lima, además, el centro de estudio de investigación nacional. El ámbito de influencia de cada uno de los centros regionales dependerá de las facilidades logísticas existen

facilidades de análisis, y procesamiento de datos (digitalizadoras, y minicomputadoras); además debe dotárseles del personal técnico apropiado, sin el cual todo esfuerzo será inútil.

2.3.3 Red Sísmica Especial

La red sísmica especial es aquella que permite mejorar el nivel de detección y la resolución espacial en la ubicación de los eventos sísmicos asociados con una predicción, o el monitoreo de actividad sísmica post-evento.

Las características principales de la instrumentación deben ser: alta movilidad, fácil instalación y mantenimiento del registro apto para procesamiento automático por computadoras, la respuesta dinámica del equipo similares al de la red principal

Se propone contar con unos 10-sistemas de detección y registro.

3. DEFORMACION GEODESICA

El objetivo principal de este programa de investigación debe ser determinar la variación espacial y temporal de acumulación de deformaciones a través de los Andes, y a lo largo de la costa. El programa corresponde a tres áreas principales: i) re-ocupación geodésica, ii) determinación de variación del nivel medio del mar y 3) fechamiento de terrazas marinas. A continuación se esboza brevemente los trabajos y requerimientos de cada una de estas áreas de estudio.

3.1 Re-ocupación geodésica

La determinación de "deformaciones geodésicas" requieren: 1) una evaluación cuidadosa y exhaustiva de re-ocu

ciones de redes de triangulación y poligonación, así como un estudio completo de las líneas de nivelación geodésicas; 2) identificación de zonas con alto grado de deformación; 3) re-ocupación de los monumentos cuidadosamente seleccionados para mediciones con equipos altamente estables y con resolución de por lo menos 10^{-7} ; 4) implementación de control rutinario y periódico.

El equipo utilizado para las medidas de deformación horizontal es altamente sofisticado y costoso.

El análisis de datos históricos y aún de re-ocupaciones recientes requiere gran cuidado y experiencia. Sin embargo, investigadores del USGS Menlo Park tienen implementados procedimientos en computadoras digitales que permiten garantizar un procesamiento correcto.

La re-ocupación gravimétrica con equipo altamente estable y con sensibilidad del orden del microgal corrobora, usualmente, los resultados de la nivelación. Estas medidas son más económicas y rápidas que las nivelaciones, pero, su "significado algunas veces es difícil de establecer".

Los estudios de re-ocupación geodésica, en particular el control horizontal y vertical por lo menos en su etapa inicial, requerirán el apoyo y guía de especialistas que estén trabajando en el área de predicción. El equipamiento, por ser muy costoso, se deberá pensar en programas cooperativos

El Instituto Geográfico Militar (IGM) es la institución indicada a realizar los trabajos geodésicos. Sin embargo, se debe establecer una estrecha coordinación del estudio con el IGP en todas las etapas.

3.2 Determinación del Nivel Medio del Mar

- 926 -

Existe en el país datos sobre el monitoreo del nivel medio del mar para algo más de 20 años en aproximada-

damente 10 puntos a lo largo de la costa peruana. Estos registros constituyen una fuente de datos muy valiosa para la determinación del nivel medio del mar en función del tiempo. Los resultados permitirán delinear, posibles, grandes zonas de deformación y correlacionarlos con la ocurrencia de sismos destructores. Claro está que la mayor tarea es poner los datos analógicos en forma digital para su procesamiento y análisis. La instalación de nuevas estaciones mareográficas, debe resultar de las recomendaciones de esta etapa previa.

El trabajo de digitalización y procesamiento de los datos provenientes de los mareogramas deberían ser ejecutados por la Marina del Perú a través de la dependencia apropiada, y en estrecha coordinación con el IGP.

3.3 Fechamiento de Terrazas Marinas

Uno de los elementos de primera magnitud, que indicaría el grado de deformación vertical a través de los últimos milenios de años, es el fechamiento y establecimiento de la altitud de las terrazas marinas a lo largo de la costa peruana. Esta es una línea de investigación muy promisoras y usándose con buenos resultados no sólo en las costas de Alaska y California, sino también en terrazas fluviales en el continente.

El Dr. K. La Joie ha hecho un estudio en el S. de California utilizando ^{14}C , aminoácidos, y series de uranio en corales, como medios de fechamiento. Los resultados son sorprendentes.

El ambiente sísmico en Alaska es similar al de Sudamérica: zonas de subducción. El Dr. G. Plafker está estudiando en Alaska las terrazas para determinar la historia de la deformación mediante la correlación de terrazas. Uno de los resultados, además de establecer la historia del levantamiento continental, es la estimación del tiempo de recurrencia de eventos sísmicos, posible -

El estudio de terrazas requiere indefectiblemente, la transferencia de experiencia a geólogos peruanos. El Dr. R. Bucknam, quien está haciendo estudios similares pero en terrazas de ríos, estaría dispuesto a colaborar en la etapa de entrenamiento. El Dr. La Joie también ofreció su colaboración.

3.4 Resumen

De la exposición anterior es evidente que los trabajos relacionados con la "deformación geodésica" requiere de la experiencia de especialistas actualmente ejecutando trabajos en esta disciplina para la predicción sísmica. Asimismo, el monitoreo de deformaciones horizontales requerirá la gestión previa de un préstamo de equipo, por ser éste muy costoso.

4. DEFORMACIONES PUNTUALES

En el Perú se cuenta con abundantes datos sobre observaciones de "deformaciones puntuales" provenientes de la estación tensométrica de Naña, y las estaciones del Proyecto Cooperativo de Deformaciones Corticales IGP-Universidad de Kyoto, Japón.

La mayoría de investigadores científicos trabajando en la predicción sísmica, están convencidos que los datos que producen instrumentos como los que equipan las estaciones mencionadas, tienen poca o ninguna relevancia en el programa de predicción sísmica. Sin embargo, se debe hacer un análisis exhaustivo e investigar si hubo o no anomalías significativas asociadas con la ocurrencia de los sismos de 1966, 1969, 1970, 1974.

En la denominación de deformaciones puntuales, se incluyen observaciones a través de fallas activas, de acuerdo a uno de los investigadores científicos de Menlo Park, es lo único que tiene sentido. Al respecto, muchos de los observatorios de deformación del programa chino se encuentran sobre las fallas: un pilar en cada lado de la traza de la falla. En el Perú son pocos los sitios donde se pueden implementar tales medi-

~~das de inmediato. Hace falta un mapa geológico exhaustivo.~~

Existe gran interés de parte del Dr. Brady en las medidas de deformación por la técnica de 'overcoring' y la determinación del módulo elástico para evaluar el nivel de 'esfuerzos' pre-sismo; es deseable que una vez que él decida ejecutar dichas medidas a través del Bureau of Mines, U.S.A., se le preste el apoyo logístico apropiado para la ejecución de tales medidas. La decisión depende de la ocurrencia del evento sísmico premonitor pronosticado para Setiembre de 1980.

5. ESTUDIO DE NEOTECTONICA

Los estudios de neotectónica deberán concentrarse en el mapeo de fallas activas recientes y determinación del patrón de movimiento tectónico. Estos estudios, a nivel nacional, deberán ser ejecutados por el INGEMMET en coordinación con el IGP. La determinación de los ejes de deformación mediante observaciones de la microtectónica en períodos recientes, geológicamente hablando, es de gran importancia.

6. FLUJO DE RADON

Los trabajos bajo este rubro deben ser muy limitados. Se debe usar la fase acuosa en la adquisición de muestras. Los pozos de muestreo deberían estar en rocas ígneas ácidas; en las cuales se perforarían huecos con diamantina y se mantendrían llenos de agua. El pozo se protegería contra la contaminación ambiental y la muestra se obtendría del fondo del pozo por bombeo. Se debe medir la temperatura del agua in situ. El flujo de radón es sensible a la temperatura. Según resultados del Dr. Holub.

En el caso de Lima, se tiene un pozo en La Molina que penetra en el basamento: roca ígnea. Este debe ser el primer punto de estudio.

7. VARIACIONES DE LOS CAMPOS GEOELECTRICOS Y GEOMAGNETICOS

Según el Dr. E. Eufar, del Ames Research Center, no existe comercialmente el equipo magnético que reúna las condiciones de sensibilidad y estabilidad que permita detectar anomalías magnéticas atribuibles a procesos sísmicas. Por lo tanto, estos estudios deben diferirse a una segunda etapa de estudio.

En cuanto a las variaciones del campo geoelectrico: autopotencial y resistividad, no hay mayor experiencia. Esta es un área de investigación actualmente.

II. FASE 2.- ANALISIS Y PROCESAMIENTO DE DATOS

1. SISMICIDAD

Actualmente la interpretación y análisis de sismogramas, en el Perú, se hacen manualmente con el auxilio de reglas milimetradas y/o lupas con varios factores de aumento. Este es un procedimiento lento y propenso a un sinnúmero de errores y de una variabilidad grande en la resolución tanto en las lecturas del tiempo como las medidas de las amplitudes de las ondas sísmicas.

En USGS, Menlo Park, este problema se ha resuelto parcialmente utilizando medios electrónicos de la lectura. Aún se requiere la participación del interpretador. La tendencia actual, sin embargo, es substituir, o por lo menos disminuir la labor del interpretador utilizando el flujo de datos en forma digital y la implementación de algoritmos inteligentes para la detección de las fases y amplitudes de las diferentes ondas sísmicas. En esta última área el impacto de los minicomputadores y microprocesadores es muy grande y su costo relativamente modesto. Sin embargo, la implementación del 'software' apropiado es lento y costoso, si es que se le tiene que

desarrollar íntegramente. Es muy económico si se intercambia con otras instituciones que trabajan en la misma problemática.

Volviendo al caso del Perú, la DICGA ha implementado un procedimiento que utiliza el medio electrónico: digitalizadora de INIE, y el interpretador. El programa de cómputo respectivo está en la etapa de prueba final dentro de poco ha de entrar en producción.

Se requerirá varias mesas de digitalización y múltiples turnos para sólo poner al día el análisis de sismogramas de los años anteriores. La situación del análisis de sismogramas producidos por DICS e IGA no es diferente.

El análisis de sismogramas debe mantenerse al día o con un desfase razonable en tiempo. Para alcanzar este objetivo, es indispensable que se dote a los Centros Regionales de varios sistemas digitalizadores del tipo tablero con la electrónica correspondiente.

1.1 Procesamiento

El procesamiento de datos sísmicos deberá consistir, por lo menos, en chequear por consistencia de los datos calcular las coordenadas hipocentrales y magnitudes de cada uno de los eventos sísmicos y producción del boletín sísmico mensual. Actualmente, sea por el número reducido de estaciones sísmicas o por no contar frecuentemente con el acceso a una computadora, los cálculos se hacen manualmente. Este cálculo es imposible hacerlo cuando el número de estaciones crece significativamente y/o cuando la actividad sísmica es muy alta; y el requerimiento de publicar la información sísmica es a corto plazo..

Por lo tanto, es indispensable contar con el acceso permanente a una computadora que permita procesar la

información sísmica y producir el boletín sísmico en cada Centro Regional.

El Centro Nacional de procesamiento de datos estaría ubicado en las oficinas del IGP en Lima. Considerando la presente situación del IGP, parece lógico, aumentar la capacidad de memoria de la computadora Harris 6-6D, y proveerla con los periféricos necesarios e investigar la posibilidad de adquirir una minicomputadora que actúe como 'manager' en la transmisión de datos vía micro-ondas al centro de cómputo del IGP en Jicamarca. El Centro de Cómputo del IGP, en Jicamarca, estaría constituido por las dos computadoras Datacraft y la Harris interconectadas. De esta manera se satisface el principio de duplicidad.

1.2 Digitalización

La geofísica moderna demanda el tratamiento de señales en forma digital tanto para el estudio del contenido dinámico como para el uso de la información cinemática. Por esta razón, es imprescindible contar con sistemas de digitalización de señales analógicas no solamente sísmicas sino de otras índoles tales como mareogramas, registros de deformaciones, etc.

Como se ha mencionado anteriormente, la tendencia actual es aprovechar el manejo de señales digitales no solo para mejorar el entendimiento del fenómeno físico, sino para liberar al investigador científico o al analista de tareas que requieren interacción de carácter rutinario.

La implementación de los sistemas de digitalización de señales se hará, en principio, en el Centro Nacional: Lima.

2. DEFORMACIONES GEODESICAS

2.1 Análisis-Procesamiento

El análisis y cómputo de las deformaciones geodésicas involucran, esencialmente, procesamiento de los datos con programas de cómputo especialmente escritos para este fin. Probablemente, sólo se tenga que adaptar programas escritos para otras computadoras. El procesamiento de los datos gravimétricos y los de mareogramas sólo requieren el acceso a una máquina de propósito general.

2.2 Digitalización

La información de las variaciones del nivel medio del mar tiene que ser extraída de los mareogramas. Los mareogramas, salvo cuando son afectados por tempestades y/o maremotos, contienen señales que varían lentamente con el tiempo. Esta característica los hacen apropiados para ser digitalizados a una 'razón' fija, siguiendo la curva diaria de variación del nivel del mar. Al implementarse el sistema de digitalización en el Centro Nacional debe tenerse en cuenta este problema.

3. DEFORMACIONES PUNTUALES

3.1 Análisis-Procesamiento

El análisis y procesamiento de la información proveniente de las observaciones puntuales requieren de la disponibilidad de una computadora de propósito general implementada con los periféricos standard. Actualmente, el suscrito desconoce el volumen de datos a procesar, sin embargo, a juzgar por el número de estaciones y los años de funcionamiento de las mismas, se espera que éste sea comparable con el volumen de datos de sismicidad. 933

3.2 Digitalización

Al igual que los mareógrafos se obtiene registros analógicos en papel; sin embargo, algunas estaciones, ya registran actualmente en forma digital. Pero el mayor volumen de la información analógica sobre deformaciones puntuales se encuentran en papel. Se desconoce cuál es el estado actual de la digitalización. De todas maneras se estima que para el análisis de los datos de la red de deformaciones de Ica y la de Arequipa, y en parte la de Naña se requiere la disponibilidad de una digitalizadora de tablero en el Centro Nacional.

III. FASE 3.- USO Y DISPERSION DE DATOS

El éxito último del programa de predicción, no sólo de penderá de la exactitud con la cual se pronostique el sismo en cuanto a su magnitud, ubicación y tiempo de ocurrencia, sino también de cómo se utilicen los resultados para la implementación de los programas de prevención. Es muy importante que la información técnica que se adquiera y procese en el programa de predicción llegue tanto a las autoridades gubernamentales como al poblador en general. Este propósito ha de lograr se con la publicación periódica y frecuente de boletines informativos sobre la evolución del ambiente sísmico, y la publicación de boletines especializados para usos de las autoridades y profesionales encargados de la planificación y construcción en el territorio nacional.

Los boletines informativos diarios y mensuales serían producidos por los Centros Regionales, y los especializados por el Centro Nacional.

PARTE 3 :

RECOMENDACIONES SOBRE LA ADQUISICION DE EQUIPO

I. DETECCION Y ADQUISICION DE DATOS

1. SISMICIDAD

1.1 Red Sísmica Principal

1.1.1 Generalidades

La filosofía sobre equipamiento de estaciones sísmicas remotas y la transmisión de datos a la estación central de registro, varía entre el grupo de Golden y la de Menlo Park. Los de Menlo Park, prefieren los equipos diseñados y construidos por ellos mismos. En cambio los de Golden, prefieren aquellos equipos comerciales que son confiables. En este aspecto, dada la limitada disponibilidad de mano de obra especializada disponible en el IGP y a brevedad de tiempo, es más conveniente adoptar la filosofía de Golden.

El grupo de Golden tiene alta confianza en las unidades de Teledyne Geotech. Ellos mismos han hecho mejoras a ciertas unidades, especialmente, de registro. En cuanto a las unidades de radio transmisión tienen muy alto concepto y confianza al equipo REPCO. Este equipo es modular, estable y durable. Investigadores de Golden tienen varias redes sísmicas equipadas con este instrumental.

No hay consenso como registrar los datos. Unos

~~registran en papel térmico, otros en película foto-~~

- 1-unidad de reproducción de cinta (Sangamo),
- 70-antenas Yagi más el número correspondiente de las repetidoras,
- Repuestos para todas las unidades,
- Equipo de prueba.

1.2 Equipo de Detección y Registro in situ: Red Sísmica Principal

1.2.1 Generalidades

Este equipo lo constituyen esencialmente los utilizados en las redes actuales. Se debe mejorar el control de tiempo y algunos registradores y se les reubicaría para complementar la Red Telemétrica. Sin embargo, debido a la edad, algunas unidades deben reemplazarse. Su reemplazo se recomienda sea con equipo MEQ-800, ya que el equivalente Microcorder de Teledyne Geotech tiene, según los usuarios de Golden, problemas técnicos, y no son equipos para labor 'pesada'.

El grupo de California Menlo Park, no requiere de esta red de registro in situ porque la redundancia de estaciones telemétricas es altísima y la accesibilidad a cualquier estación es fácil.

1.2.2 Equipo a adquirirse

El número de sistemas a adquirirse dependerá de la evaluación física que se haga de las unidades actuales en operación.

1.3 Estaciones de amplio rango dinámico

- 936 -

1.3.1 Generalidades

Estaciones sísmicas de 110 dB de rango dinámico no

ma de detección y registro de la Universidad de Wisconsin, cuyas especificaciones se dan en el Apéndice I.

Estas unidades han sido probadas en el terremoto de México y en los estudios de réplicas del sismo de Colombia del 12.12.79

1.3.2 Equipo

- 3-sistemas de registro, 3 componentes cada uno,
- 1-sistema de reproducción con terminal SR-232.

2. DEFORMACION GEODESICA

2.1 Control Geodésico Horizontal

Hay, por lo menos, dos sistemas de medidas de distancia que se utilizan actualmente: en primera clase están el Geodolite M-8, y el Range Master y con alcances hasta de 50 km, rangos de detectividad hasta 10^{-6} . Las observaciones requieren determinar la densidad, presión, temperatura, y humedad durante la ejecución de las medidas. El costo de cada uno es alrededor de 20 mil dólares, siendo el segundo mejor que el primero. A la segunda clase pertenece el "two-color terrameter" con sensibilidad 10^{-7} y es independiente de los elementos meteorológicos, maximum range: 20 km, realísticamente 10 km. El precio por unidad es 200 mil dólares.

Estos equipos actualmente los usan las agencias encargadas de mapeo cartográfico de U.S.A. Es posible implementar un plan de cooperación, por el cual se solicitaría en préstamo el equipo pertinente y darían el entrenamiento al personal peruano que ejecutaría la labor.

Otra alternativa es adquirir el Range Master y soli

citar la cooperación de la aviación peruana para -
las medidas de los elementos meteorológicos.

2.2 Control Geodésico Vertical

El control geodésico vertical requiere la disponibilidad de niveles y miras de alta precisión, que probablemente el IGM cuenta.

2.3 Variaciones del Campo Gravimétrico

Un gravímetro Modelo D con sensitivity de 1 microgal y 200 mgl de rango. El equipo cuesta 29 mil dólares.

2.4 Determinación de Edades de las Terrazas

El equipo para ejecutar este estudio es muy poco. Unos 3 ó 4 pares de lentes estereoscópicas, bolsas para la colección de muestras, etc.

Se debe reservar fondos para la determinación de - edades y transporte de muestras al extranjero, compra de fotografías aéreas, etc.

2.5 Variaciones del Nivel Medio del Mar

La mejora del equipo existente y la implementación de nuevas estaciones debe estar supeditada al resultado de los análisis de los datos existentes.

3. DEFORMACIONES PUNTUALES

El equipamiento de una o dos estaciones en el norte del país debe estar supeditado a los resultados de los análisis de los datos existentes.

4. CAMPO GEOMAGNETICO

El equipamiento con fines de predicción deberá posponerse; sin embargo, es recomendable iniciar las gestiones pertinentes a través de NASA para lograr el préstamo de las estaciones del tipo que el Dr. E. Eufar ha diseñado y construido para S. de California, U.S.A.

5. GEOQUIMICA

Se recomienda la compra de equipo para el estudio del flujo de radón, utilizando muestras de agua. Los precios FOB, Canadá son:

1 RDU-200 US\$ 2,000

1 RD200 4,000

Con fecha de entrega de dos semanas.

(cotización telefónica)

II. ANALISIS Y PROCESAMIENTO DE DATOS

1. ANALISIS

1.1 Generalidades

Se debe adquirir equipo que permita la implementación automática de lecturas sísmicas. Como primera etapa se debe adoptar el sistema de una digitalizadora de 0.001" de resolución con salida en tarjetas. Posteriormente se le puede acoplar un microprocesador que permita la salida en 'disket' o directamente a un sector del disco de una de las computadoras del centro de cómputo del IGP. 939

de investigadores utilizan en Menlo Park es mesa, y unidades electrónicas de la marca Bendix. Este sistema es similar al de INIE: marca Del Foster. Desafortunadamente, no se pudo hacer contacto con dichas firmas. Este mismo equipo se usaría para digitalizar los mareogramas, registros de deformación, sismogramas, etc. Además de utilizarlos para hacer lecturas sísmicas.

1.2 Equipo

- 3-sistemas Bendix o Del Foster de digitalización. Cada uno de los sistemas Bendix cuesta alrededor de 20 mil dólares.

2. PROCESAMIENTO

2.1 Generalidades

En el Perú, un área en que los estudios de física de la tierra necesitan apoyo aún sin el incremento de nuevas unidades de detección y adquisición de datos, es la de procesamiento digital. Muchos de los programas de estudio e investigación se encuentran paralizados por la falta de facilidades de cómputo y graficación. A pesar del esfuerzo que hizo el IGP en la adquisición de una computadora adicional, debido a la situación económica y las restricciones gubernamentales y al hecho de que la computadora tuvo ya cierto número de años de trabajo, no ha sido posible ponerla operativa a la fecha. Sin embargo, se tiene esperanzas que una vez que se tenga las partes electrónicas de repuestos, y se contrate personal electrónico para atender la adquisición de datos, el personal técnico especializado se dedicará 100% a poner operativa dicha unidad.

Además el IGP cuenta con una computadora nueva recientemente adquirida y específicamente

al manejo del radar de Jicamarca. Esta computadora se le puede convertir en una unidad de propósito general - añadiéndole unidades periféricas de 'input-output' y aumentando su capacidad de memoria y almacenamiento de datos. Para asegurar duplicidad se propone el traslado de la computadora Datacraft 6024/3-UW a Jicamarca y su interconexión a la nueva Harris 6-6D. En el futuro, para aumentar la accesibilidad al Centro de Cómputo se debe instalar un canal de comunicación por micro-ondas entre Lima y Jicamarca que permita la transmisión de un alto número de bits por segundo entre ambos sitios. Esto implica la adquisición de un microprocesador, que serviría de 'manager' en Lima y, por lo menos, dos terminales (pantallas) de interacción.

En resumen se propone que en una primera etapa :

- 1) se implemente el Centro de Cómputo del IGP en Jicamarca trasladando la computadora Datacraft 6024/3-UW interconectándola a la Harris 6-6D , 2) se aumente la memoria, y la capacidad de almacenamiento de datos de la Harris 6-6D , 3) se provea de los periféricos básicos: impresora, ploteador, pantalla de graficación y copiador, y pantallas de interacción. En una segunda etapa: 1) establecimiento de canal de comunicación de micro-ondas: Jicamarca-Lima, 2) adquisición de un microprocesador y unidades de 'input' interactivo, y de 'output' simples. Por último en una tercera etapa: se le implemente a la unidad de Lima con un sistema de detección en 'línea' (tiempo real) de sismos.

2.2 Equipo

El equipo para la primera etapa, se recomienda lo siguiente:

	Precio aprcx.
1. una tarjeta de memoria de 389K bytes	\$ 10,000
2. un disco de cabeza removible, 40 megabytes	30,000
3. un multiplexor (8310)	3,000
4. un 8360-1 'interface' para CRT modelo 8610	750
5. dos 8340-1 'interfaces' para el impresor y ploteador, provee conector standard RS-232	1,500
6. un 8335 'interface' para 'gráficos' en pan- talla (CRT Tetronix 4010 con opción # 6)	6,000
7. un copiador acoplado al CRT Tetronix 4010	6,000
8. un impresor (i.e., LA-180, 180 caracteres/sec, conector RS-2B2)	2,000
9. un ploteador (i.e., Calcomp)	(no hay precio)
10. dos pantallas CRT modelo 9610 (Harris)	7,000
(se puede adquirir otros modelos más económicos).	

AGRADECIMIENTOS

El suscrito expresa su agradecimiento a las siguientes - personas del U.S. Geological Survey que dedicaron parte de su tiempo para expresar puntos de vista personales sobre la problemática de la predicción sísmica, compartir experiencias, y ofrecer consejos sobre futuros programas de investigación en la línea de predicción y pronóstico sísmico:

1. En Golden, Colorado:
 - Dr. T. Algermissen
 - Dr. R. Bucknam
 - Dr. B. Engdahl
 - Dr. S. Harding
 - Dr. J. Jordan
 - Dr. W. Spence

2. En Denver, Colorado:
 - Dr. F. Lee

3. En Menlo Park, California:
 - Dr. J. Eaton
 - Dr. J. F. Evernden
 - Dr. M. Johnston
 - Dr. C-Y King
 - Dr. K. La Joie
 - Dr. W. Lee
 - Dr. M. McGarr
 - Dr. G. Plafker
 - Dr. C. B. Raleigh
 - Dr. J. Savage

En la parte instrumental y procesamiento de datos, el programa propuesto se benefició de las experiencias y consejos de las siguientes personas:

1. En Denver, Colorado:
 - Mr. T. Bice
 - Mr. D. Dobbs
 - Mr. D. Ketchum
 - Mr. C. Langer
 - Mr. R. Henrissi

2. En Menlo Park, California:
 - Dr. R. Allen
 - Dr. W. Lee
 - Mr. W. Van Schaack
 - Dr. P. Ward

La coordinación y programación de actividades en Golden, Colorado, fue hecha por el Dr. J. Jordan y en Menlo Park por el Dr. W. Kenoshita. La colaboración del Dr. W. Mooney fue muy importante en Menlo Park. A ellos quedo muy agradecido. Asimismo, agradezco al Dr. J. Filson por hacer las coordinaciones previas.

Además de las conversaciones con el personal científico y técnico del U.S. Geological Survey, se contó con la colaboración de los Drs. B. Brady y R. Holub del Bureau of Mines, U.S.A., y del Dr. S. Sacks del Department of Terrestrial Magnetism, Carnegie Institution of Washington, U.S.A.. Sus opiniones contribuyeron significativamente en el delineamiento del programa propuesto.

Lima, 10 de Abril de 1980

LO:ma

Leonidas Ocola

A P E N D I C E - I

UNIVERSITY OF WISCONSIN DIGITAL RECORDING SYSTEM
General Specifications (3-Component System)

RECORDER: 5" real-to-real 1/4" tape

TAPE: 1800 feet (audio grade)

FORMAT: 4 tracks digital 1 channel/track.
 System status, time, and Omega phase
 are distributed with the data.
 One track = error correction.
 5 hours recording (360 3-component 60-second
 events at 100 samples/second/channel).

DELAY: 5.12 seconds/channel

DYNAMIC RANGE: 105 dB
 Input noise - 0.25 μ v P-P
 Clipped = 0.05 v P-P input

MODES: Programmed and/or triggered with
 trigger arm and disarm programmable

PROGRAMMING: Keyboard "day-time-function" entry
 with a 99 day range

INTERNAL TIMING: TCXO clock to 99 days

EXTERNAL TIMING: n x 10 seconds from pattern of Omega
 radio navigation broadcasts

POSITIONING: Differential Omega between recording
 stations, using recorded phase

POWER: 12.5 v DC \pm 20%
 25 ma quiescent current
 400 ma recording

DIMENSIONS: 56 x 33 x 40 cm

WEIGHT: 22 kg

TEMPERATURE: 0° - 50° C normal operating range
 -20° - 70° C at reduced specifications
 -40° - 60° C storage

Reflections on a forecast which may lead to the prediction of a strong earthquake near Lima, Peru.

Dr. John Roberts
Dec. 1980

For the period 20/24 October the writer attended a seminar arranged under the auspices of the following organisations:-

DECEMBER 1980

Institute Nacional de Prevencion Sismica de la Argentina - INPRES

Control Regional de Sismologia para America del Sur - CERESIS

United Nations Educational Scientific and Cultural Organisation - UNESCO.

United Nations Disaster Relief Office - UNDRO

United Nations Environment Programme - UNEP

The subject of the seminar was Seismic Prediction and the Evaluation of Seismic Risk. It was held at the premises of INPRES in the city of San Juan in Northwestern Argentina, a region of considerable seismic activity. It is interesting to note the involvement of the United Nations agencies all of which were sponsoring participants at an International Symposium on Earthquake Prediction held in Paris in April 1979.

The San Juan meeting attracted about eighty participants from twenty-one countries. The largest group came from South American states but there were, in addition, participants from the United States, U.S.S.R., the People's Republic of China, Switzerland, Italy, Germany, Indonesia and New Zealand.

A large number of papers was presented to the Conference (a copy of the programme is annexed) but it is not the purpose of this report to offer any general comment upon them except to say that as a non-specialist (as far as I am aware I was the only social scientist attending) the writer found it intensely valuable to be present at sessions on scientific and technological matters. There is no doubt that although the subtleties of the arguments may be missed, the effort involved in understanding the methods employed to study seismic phenomenon vastly increases the non-specialist's ability to assess the significance, the difficulties and the many ambiguities of earthquake prediction. The writer concludes from the experience in San Juan that if progress is to be made towards understanding the wider social implications of prediction,

politicians, administrators and social scientists must be exposed to discussions of the developing scientific and technological concepts similar to those presented at San Juan. This proposition is particularly relevant to the points developed later in this report and requires elaboration.

The Implications of Earthquake Prediction

There is as yet no conclusive scientific basis for earthquake prediction in the sense that a reliable probability can be attached to a statement that an event of a certain magnitude will occur within a specified and socially useful time range in a precisely located region. Of course, reliable forecasts may be made of seismic vulnerability both on the basis of historic data and in terms of the rapidly developing understanding of the physical mechanisms operating in the earth's crust but it is only recently that the relevant sciences seismology, geophysics and geology - have given promise that careful measurement and analysis of certain phenomena may indicate an imminent earthquake with useful precision. It is of compelling interest that a combination of empirical techniques were employed in the People's Republic of China to predict the severe earthquake at Haicheng on 4 February 1975, with the result that an evacuation was ordered within five and a half hours of the event. It is equally relevant that a devastating earthquake on the 1976 was not predicted and appalling loss of life occurred. These two events indicate a possible process in the evolution of earthquake prediction which those who must react would be prudent to assume. First, as the meeting in Paris last year and San Juan this year indicated, earthquake prediction is now firmly established as a legitimate objective of scientific enquiry. Second, a proportion of the predictions that will arise from this activity will prove to be unreliable and a number of strong earthquakes will not be predicted at all. These conclusions raise very difficult questions for scientists, politicians and administrators. Answers can only be found if every one involved shares a common philosophy springing from an understanding of the problems facing the scientists.

An unavoidable dilemma arises in prediction. Normally a scientific hypothesis that the occurrence of certain phenomena will lead to a given result tends to be verified or refuted when the result occurs or fails to occur. This does not prove the causal relationship but it may provide a powerful impulse to the development of a valid theory of causation. A scientist may propose an hypothesis and a series of observations. He may also evolve a tentative theoretical explanation based upon the hypothesis. Normally it would not be expected that society should act upon hypotheses or theory until events have occurred which allow some index of probability to be stated.

The case of earthquake prediction raises extraordinary objections to this procedure. Prediction, as we have seen, involves specification of time, place and magnitude. If an earthquake of high magnitude is predicted, disastrous consequences will follow for the inhabitants of the area affected. The scientist may take one of three possible actions as follows:-

- (a) He may decide not to publish his prediction on the grounds that it is not scientifically significant until the verifying event occurs;
- (b) He may publish his prediction only in scientific papers on the grounds that the scientific community should be in a position to weigh his hypothesis and develop programmes in advance of the event to test its validity;
- (c) He may communicate his prediction to governmental authorities in order that they may, if they wish, take steps to mitigate the hazards of the event if it occurs.

If the scientist decides to follow the first course no precautions can be taken and the opportunity to reduce human suffering will be lost. If he decides to take the second option, it may be that the same result will follow.

Alternatively, the prediction may come to the notice of the society at large causing social and economic disruption. This may eventually lead to the intervention of government to preserve social order. If he adopts the third course, the scientist conveys important information to government for which, he can, at the moment, give no reliable estimate of probability in the knowledge

that the prediction itself may have harmful consequences for the society.

The status of hypotheses will differ, of course. Some may be of such a tentative nature that no responsible scientist would consider giving them publicity. Nonetheless, there seemed to be a consensus at San Juan that an increasing number of scientists will be engaged in studying a wide range of phenomena now thought to be precursors of imminent earthquakes and that, as a result, predictions will be made in increasing numbers as confidence in the scientific arguments develops.

It is my conclusion, based on attendance at four extensive conference on this subject, that the only rational course should the observations of precursory events satisfy the scientist that a destructive earthquake will occur within a reasonably specific time range at a specific location, is to communicate this opinion to the appropriate authorities. This conclusion has been reached despite the difficulties that such information will raise. These difficulties will be examined in the light of an actual case later in this report. For the moment I shall discuss only the problem of communication and official reaction to the scientific information.

It is possible to propose a logic of events which is almost certain to be followed given that predictions are likely to be made in areas where there are political systems which have already active programmes for the study of seismic phenomena.

Hypothesis

This is necessarily a scientific activity. (Earthquake prediction may emerge from non-rational sources such as astrology or sooth-saying but it is dubious that any response would be invoked from government.) Those members of the scientific community working on prediction will of course be members of a community who exercise a powerful influence on the standards observed in professional activity, although there is no guarantee that such standards will always be deserved.

Predictions

When the data analysed by the scientist appears to be congruent with the sequence assumed by the hypothesis to the point where the scientist is satisfied that a specific event called for by the hypothesis will occur at a certain place and time, he may decide to make a prediction.

Communication of the Prediction

Supposing the scientists' satisfaction with the quality and congruence of the data leads him to believe that he should communicate the prediction, it is inevitable that he will inform the government executive who are responsible for civil order, relief of those affected by disaster, social and economic support of the community, land use control and physical planning.

Evaluation

The government executive will have to assess the credibility of the prediction. Since any credible prediction will involve complex scientific analysis it is certain that a responsible government will seek an independent qualified opinion on the validity of the hypothesis, the quality of the data and the vigour of the analysis. It is here that the need for a merging of scientific and political considerations is urgently required.

When evaluation is completed the political executive may act upon the prediction as it decides. The possible courses open will be discussed later. For the moment, I shall turn to the requirements for effective evaluation.

Experience in Four political systems

Thus far the People's Republic of China, Japan, the Federal Government of the United States of America and the State of California have set up procedures for the receipt and evaluation of earthquake predictions.

People's Republic of China

Although the specific rules governing earthquake prediction in the People's Republic of China have not been published in English as far as the author can determine, various papers indicate that the following process, is employed. The

State Seismological Bureau in Peking and Provincial Seismological Bureaux are monitoring data to identify seismic anomalies. They are assisted in this work by a network of amateur seismic observation activity. Previously, the Provincial Seismological Bureau could act on its own initiative in evaluating predictive phenomena and passing on details for consideration of the provincial executive authorities. This does not appear to have happened when the Seismological Bureau of Liaoning Province predicted the Haicheng earthquake. In that case the State Seismological Bureau, acting on information collected by observers of seismic phenomena in the Province, advised the Provincial Party-Committee that a large earthquake could be expected shortly. Continuous monitoring then led to an order for evacuation.

At San Juan in October 1980, Dr Ma Xing Yuan of the State Seismological Bureau in response to a question, advised that the Chinese authorities now require that all predictions should be transmitted for consideration by the State Seismological Bureau although in conditions of urgency the Provincial Bureaux retain the power to act independently.

Japan

There were no Japanese scientists associated with the structure established to deal with earthquake predictions in that country at San Juan. This must be regretted as the Japanese seem to have produced a more formal and more active process than anyone else so far. The Large Scale Earthquake Countermeasures Act of 1978 not only revises the procedures for political action in the event of an earthquake but also anticipates the possibility of short-term predictions providing a structure for communication between scientists and the government. There is a Committee for Earthquake Prediction in the Science and Technology Agency in Tokyo which apparently meets regularly to consider long-term prediction information. This group has a sub-committee for more concentrated attention upon predictions for the area adjacent to the great conurbation centred on Tokyo. These scientists are in constant communication with those processing information and may, if the information warrants, set the prediction process in motion.

Under the 1978 Act, the formal responsibility for communicating information lies with the head of the Japan Meteorological Agency who advises the Prime Minister. The Prime Minister may take different steps on long-term and short-term predictions.

Long term

If information received from scientific sources indicates that there is an "especially great danger of a large scale earthquake occurring, the Prime Minister shall designate the area where it is necessary to take intensified measures against earthquake disaster." (Article 3) The Prime Minister is required to consult with the provincial governors who in turn are required to consult with mayors of municipalities in the "intensified area". Following this process the Prime Minister makes a suitable public announcement and the Central Disaster Provincial Council in terms of Article 5 "formulates a basic plan of earthquake disaster prevention for the intensified area and promote(s) its implementation".

Short term Prediction

When advised by the Director General of the Meteorological Agency of a short term prediction under Article 9 the Prime Minister may, if he believes action should be taken, after consultation with the Cabinet issue an earthquake warning statement. This entails as well passing specific information to residents in the area, advising general agencies and setting in motion various disaster prevention processes including the establishment of a "National Headquarters for Earthquake Disaster Prevention" whose Director General is the Prime Minister himself.

One interesting point is that the Prime Minister is given power under the legislation to "make the Director General of the Meteorological Agency explain technical matters regarding the earthquake prediction information." (Article 9(2)) In the context of the section it is clear that this explanation has to form part of the warning information to the citizen.

United States of America

The U.S.A. has recently updated its legislative provisions in the National Earthquake Predictions Act of 1977. Under this Act a National Earthquake Prediction Program has been established which provides that responsibility for evaluating and communicating earthquake predictions shall lie with the Director of the U.S. Geological Survey. To assist him in evaluating information a National Earthquake Prediction Evaluation Council (NEPEC) has been set up with a membership which includes both government and non government scientists. Under the programme, state and local governments bear the "responsibilities for preparedness response, warning, regulating construction and regulating the use of land" (The National Earthquake Hazards Prediction Program, Executive Office of the President, Washington D.C.). It appears that the function of NEPEC will be to assist each level of government to assess predictions. The fundamental responsibility lies with each Governor of a state affected by a prediction since it is with this office that the power to declare an "emergency" lies: But the Governor may request the President to declare an "emergency" or a "major disaster" thus inviting Federal government action to mitigate hazards. It is not clear from the literature whether these provisions could be used to cover a prediction but it is rational to suggest that they should if NEPEC - a Federal entity - advises a Governor or Governors that a given prediction has sufficient credibility to warrant hazard reduction action.

State of California

In 1975-76 the State of California established two bodies to advise the State's Office of Emergency Services. The California Earthquake Prediction Evaluation Council (CEPEC) receives predictions and establishes the validity of the scientific argument. A public evaluation of the prediction is then issued. The Advisory Panel on State Government Response to Earthquake Prediction on the other hand recommends the policy and administrative steps "to mitigate the effects of both the prediction and of the impending earthquake (Earthquake

Hazards Prediction Issues for an Implementation Plan: Working Group on Earthquake Hazards Prediction, Office of Science and Technology Policy, Executive Office of the President, Washington 1978, p.31) This report also summarises action taken by the U.S. Geological Survey and CEPEC in two interesting cases.

Since 1975, several geophysical and geological anomalies have come to light that have caused official concern. The Earthquake Prediction Council of the USGS has reviewed the data on several geophysical anomalies that have been recognized by its scientists. One, termed the southern California uplift or bulge, was considered to be of sufficient concern that the Director of the USGS officially notified the Governor of the State of California of the uplift at a meeting in March 1976 in Sacramento. The Director of the USGS and staff representatives met with representatives of the Governor's office and staffs of various State agencies, including the Seismic Safety Commission, the Office of Emergency Services, and the Division of Mines and Geology. Even though the recognition and announcement of the southern California uplift was not represented as being an earthquake prediction, it did raise official concern above normal levels, and the California Office of Emergency Services did issue a statement to local communities about the uplift and included the suggestion that they review emergency preparedness plans. In addition, a closely spaced instrumental network was set up to monitor the area. Also in 1976 the Earthquake Prediction Evaluation Council of the State of California formally reviewed a report construed by the press to be a prediction of a potentially damaging earthquake in southern California. The Council concluded that the chances of the earthquake occurring were not significantly higher than those of a randomly occurring event in the same region.

Some researchers have concluded that an earthquake prediction will be significant only if large numbers of people take it seriously, and that will happen only if the pronouncement is in effect "certified" by an expert body or scientific consensus.

Responsibility for Predictions and Warnings

The structures analysed above show certain common elements which spread the political responsibility for predictions and warnings. Broadly one can suggest that the following elements will always be present when predictions come to the notice of the political community.

- (a) Scientific theory and empirical records indicating that strong earthquakes may occur in a given area. This will be accepted by all qualified people and consequently by politicians.
- (b) Scientific observation of anomalies leading to the hypothesis that a strong earthquake is imminent.

(c) Development of a programme of observations to test the precursory pattern hypothesized by the scientists.

Note that this and the previous step may originate from any of the following sources:-

1. Teams of qualified scientists employed in a public agency to identify and confirm precursory phenomena. (This seems to be the position in the People's Republic of China.)
2. Qualified scientists in a government agency working on independent research generated by information secured in performing professional duties. (This seems to be the situation of the Brody/Spence prediction discussed later in this paper.)
3. Qualified scientists working within a university research project intended to identify precursory phenomena and develop a theory of prediction. (This seems to be the case in a major inter-university programme in Japan).
4. Qualified scientists working in research programmes within university departments either collectively or individually on research programmes of their own choice.
5. Qualified scientist or scientists working in private employment (e.g. oil company) providing information of a precursory nature.
6. Qualified scientists not pursuing observations in the course of employment but making private observations in their own time.
7. Unqualified or partially qualified observers of phenomena linked to an overall programme of collating and analysing precursory data. (This seems to be an element in the People's Republic of China programme.)
8. Unqualified or partially qualified observations by private individuals acting independently of any recognized scientific agency.

(d) Communication of Prediction

A procedure for communication of a prediction raises immediate questions about the time, place and magnitude of the predicted event, the confidentiality of the prediction, and the formality or informality of the contract with government. There are two points upon which we may assume those who communicate a prediction will want reassurance. First they will prefer that the communication should not expose them to public odium or to legal liability for damage. Second, they will want to be sure that the scientific basis for the prediction is fully understood by the recipient. Without that assurance the scientist could not be content with a refusal to act on his arguments. Very complex issues of scientific ethics arise here. These will be discussed later.

(e) Evaluation

An attempt to judge the quality of the scientific basis for any prediction will have to be made. It is interesting to note that in three of the four jurisdictions with established evaluation procedures the same general concept has prevailed. That is, the prediction together with its scientific reasoning and supporting data is passed to a committee composed of technically qualified individuals some of whom hold public office; this committee submits its evaluation to a technical or scientific government agency which in turn advises the highest executive authority in the jurisdiction.

We may draw the following conclusions:

1. the political executive cannot assess the scientific credibility of a prediction and will seek help from those who are appropriately qualified;
2. it has become the practice in these circumstances to reinforce the reputation for impartiality and objective assessment by establishing a procedure demonstrably independent to some degree of commitments to the political executive and to the person or group which has

developed the prediction. Thus both the scientist and the public can be expected to have confidence in the evaluation. The evaluation also protects those who make predictions from public odium and may be a legitimate reason to absolve them from possible legal liability. Public order can be more easily sustained by a sober authoritative assessment and, of course, subsequent political action can be justified in the light of the evaluation. At the same time, the constitutional link between the responsible administrator and his political chief is maintained to permit confidential deliberations on executive action. Only time will tell whether this will be a politically successful procedure but it does appear to be sound in concept.

(f) Warning

This is clearly a political responsibility and will lie with that level of executive authority which can mobilize resources and move the political community to appropriate action. In the cases we have examined the responsible levels appear to be as follows:-

1. China The provincial administration and the Communist Party executive advised by the Head of the State Seismological Bureau.
2. Japan The Prime Minister in consultation with the Cabinet advised by the Director General of the Japan Meteorological Agency.
3. U.S.A. Federal Government: the Governors of the States affected by the prediction advised by the Director of the U.S. Geological Survey.
4. California The Governor of the State advised by the Director of the Office of Emergency services.

A warning implies of course that the prediction has been evaluated and is regarded as sufficiently credible to put the citizens in possession of information that may allow them to reduce the hazards of the predicted event by individual action. It seems improbable however that any responsible politician would or could decide to limit action to this step. We may

assume that a warning would be accompanied or followed up by a statement of intended action by the political executive. Obviously the lead time would have a major influence on the steps to be taken but they might include:-

1. Instructions to all appropriate services (e.g. civil defence, hospitals, communications, water supply and sanitation, energy delivery, police, army, transport) to prepare contingency plans for the emergency. This may also include involvement of international disaster relief organisations.
2. Arrangements for evacuation if practicable or, if not, instructions to reduce activity in areas of high vulnerability (e.g. central business district, public transport systems) over the emergency period.
3. Stockpiling of supplies in a secure area for immediate availability during the emergency.
4. Programme to sustain investment, economic activity and employment between the date of warning and the event.
5. Review of provisions for insurance of property with the objective of maintaining public confidence in recovery.
6. Emergency programme to remove or rehabilitate hazardous structures.
7. Preliminary planning and marshalling of resources for reconstruction, including potential contributions from international financial and aid sources.

We may conclude that a warning ~~is~~ definitive notice to the society that the political leaders have accepted the credibility of a prediction, assumed the burden of responsibility to act and absolved the scientists of further liability beyond intensive monitoring of the phenomena that will tend to confirm the prediction or invalidate it.

Confidentiality

It takes little imagination to appreciate the damage that may be done by an earthquake prediction which is interpreted as a credible warning by the community. A dramatic failure in social and economic confidence in the future of the affected region is, at least, probable even when the political executive announces a hazard mitigation programme along with the warning. No sensible scientist, politician or administrator will want to disturb social order unnecessarily. There is a good argument that the process should be kept confidential until the point where the political authorities are satisfied that the balance of community advantage lies with the promulgation of an official warning. Unfortunately, this may be difficult. A number of factors work against confidentiality.

(a) Scientific communication

Scientific progress is thought to be dependent upon an open exchange of argument and data. By exposure to the review and criticism of his scientific peers, the scientists can remedy error and develop theory. As we shall see in the ensuing case study, the development of a bold theoretical analysis of earthquake mechanisms led to the prediction of an earthquake in Lima which has caused some embarrassment to governmental officers. Should the author of this theory have refrained from following his argument to a conclusion which allows his critics to investigate the practical consequences of his theory?

(b) Human Rights

Social order is a legitimate objective of government but there is an undeniable claim by the citizen to exercise individual judgement on issues affecting personal safety and prosperity. Rules imposing confidentiality upon the development and announcement of prediction hypothesis may be thought to offend against the citizens' rights.

The rights of the scientist as citizen are also brought into question. Is it justifiable to require him or her to withhold information believed to

be of the greatest importance to fellow citizens. Suppose a scientific hypothesis has been processed by an evaluation committee and rejected as a reliable earthquake prediction. If the scientist (or scientists) responsible for the hypothesis does not accept the evaluation, should he/she remain silent or persist with publication of the prediction?

(c) Open Government

There are powerful arguments for the proposition that government conduct its affairs, as far as possible under the scrutiny of public opinion. This is held to be especially important for bodies undertaking enquiries into the public interest such as a prediction evaluation committee. It is interesting to note that CEPEC has held its meetings in public and the Chairman of NEPEC, Dr Clarence Allen reported to the San Juan Seminar that this body had also decided that its proceedings would be completely open.

(d) The Probability of Disclosure

In those political systems where the media is not subject to official control, it is highly unlikely that evaluation of a prediction would remain confidential for long. Earthquakes are front page news. The media are bound to consider that the public's interest in them cannot be denied. The case study describes a prediction which has now become world news. Official recognition by the evaluation process confers newsworthiness, even where the prediction is rejected and it is difficult to conceive that the information would not leak.

Public Responsibility

These considerations suggest that the California and Federal evaluation authorities have sound arguments for conducting their affairs in open session. In the writer's opinion any attempt to impose legal constraints on the publication of earthquake predictions or upon subsequent evaluation proceedings would be misconstrued. That said, it does seem desirable that it would be wise to develop and publish a set of guidelines for those who may be involved with prediction

or evaluation in order that they may proceed soberly to the most advantageous result for the society at large. This may be achieved in the following conditions:-

1. Widespread understanding of the principles of prediction

Following the major UNESCO Conference in Paris last year and the establishment of official procedures in the People's Republic of China, Japan, U.S. Federal Government and the State of California it is reasonable to suggest that earthquake prediction is no longer a marginal issue of speculative science. An increasing number of scientists are giving attention to the development of a theory of prediction and to the study of precursory phenomena. Earthquake vulnerable societies must accept the possibility that predictions will be made. It will be to their advantage if the citizen is aware of the scientific arguments involved and understand the uncertainties surrounding prediction. At the official level, agencies concerned with hazard reduction should commission studies of earthquake prediction and in consultation with informed scientists adjust existing public policies to deal with the situations arising from a prediction and the promulgation of a warning. The political executive should designate responsibility for responding to predictions and promulgating warnings. In my opinion it is essential for politicians to allocate time for a thorough briefing on the scientific principles involved.

2. Establishment of formal evaluation process

The arguments for an established process of evaluation in which scientists and politicians can have confidence seems to be irresistible. All those societies where seismic risk is high should at least define their policy for evaluation and the qualifications and responsibilities of an evaluation committee to the point where a credible body of qualified people can be assembled without delay should a prediction come to the notice of the government. The precedents of the Japanese and American process seem to be sound. Any committee should comprise qualified government and independent scientists and should convey their evaluations to

appropriate administrator with access to the highest executive authority. Obviously, if any member of the committee is associated scientifically with the development of a prediction referred to the committee he should disqualify himself from the evaluation deliberations. On the arguments advanced above it seems to me that the committee should meet in open session.

One interesting problem arises from the choices made so far of an appropriate agent to advise the government. Japan and U.S. Federal Government give this task to the Head of a scientific agency - the Japan Meteorological Agency and the U.S. Geological Service. In California, however, it rests with the Head of the Office of Emergency Services. On balance it seems to me that the scientific adviser is more appropriate although, of course, it is understood that the emergency services or civil defence agency should be informed immediately of any intention to issue a warning and should be commissioned to bring the organisation up to the level of preparedness appropriate to the potential emergency.

3. Location of Political Responsibility

The responsibility for earthquake warnings must fall on the highest level of the political executive in the affected jurisdiction. This will vary according to the constitutional arrangements. Broadly we may say that in Federal systems such as the United States the official corresponding to the State Governor should accept responsibility and in unitary systems such as New Zealand the level of Prime Minister will be appropriate. Wherever seismic risk is high, government should consider the formal designation of responsibility by legislation or executive order as may appear constitutionally appropriate. The Japanese Large Scale Earthquakes Countermeasures Act 1978 appears to be a most useful basis for discussion of appropriate legislation.

In addition to formal designation, it would be useful to consider the nature of the responsibility which the politicians will assume. However careful and skilfull the evaluation, any earthquake prediction will be

attended by considerable uncertainty. Evaluation will not relieve the politician of difficult choices in the light of the index of probability or perhaps credibility attached to it by the evaluation committee. The specification of time, place and magnitude may be so broad as to raise questions about the usefulness of any warning. It is possible that the evaluation committee and the administrator who advises the politician may take different views of the significance of the prediction. It will be prudent for the politician to commission a review of the situations that may possibly arise. Clearly, once an evaluation has been made public the politician will be expected to act promptly. A grasp of the potential problems will be helpful to him in acting wisely as well.

As proposed above a warning necessarily implies a programme of hazard reduction and maintenance of public confidence. The possible areas for consideration are set out on page 13. Again there are obvious advantages in revising existing policies in the light of a potential warning and devising the necessary additional policies. This seems to be a field in which the techniques of modelling and scenario writing might be particularly helpful and, in my opinion, would have immediate value in subjecting existing policies to critical review. The Government should also initiate consultation with socio-economic groups such as unions, employers, property investors, insurance companies, engineers, education authorities. Of course, it would be essential as well to coordinate policy with local government agencies.

4. Legal liability and Earthquake Prediction

It is possible that an earthquake prediction may damage economic or other interests and give rise to a claim for compensation against the scientists making or evaluating the prediction. This should be investigated by legal experts. If it is thought that liability may lie it seems appropriate that statutory protection should be extended at least to those who follow the procedure for referral to an evaluation committee and those who carry out the evaluation on behalf of the government. What further

protection against liability might be necessary is a complex problem requiring specialist investigation.

5. Code of Practice for Scientists

If the proposals listed above are carried out, there seems to be no reason why a scientist who may wish to communicate an earthquake prediction should lack confidence in the opportunity for careful evaluation of the scientific argument and the determination of the political community to protect the interests of the society. Scientists may in those circumstances agree to observe a code of practice issued perhaps by an appropriate professional body to guide the process of communication. Compliance with these should be voluntary and there should of course be no suggestion of political intervention in independent scientific investigation. With these provisos, it seems probable that responsible scientists would welcome a code developed along the following lines:-

- (a) A scientist engaged in studying earthquake prediction or in work which he believes may have a bearing on prediction should advise the secretary of the evaluation committee giving details of the nature of the project and the data that he may be collecting.
(A register of current research would be valuable in the evaluation process.)
- (b) The evaluation committee should provide a general indication of the conditions they believe should be fulfilled before a prediction can be usefully evaluated. This might cover such matters as levels of probability, specification of time, place and magnitude, identification and confirmation of precursory data etc. While exceptional circumstances may well arise in such a fluid field, scientists would be expected to observe the requirements of the committee in deciding whether or not to communicate a prediction.

- (c) Scientists who have developed a prediction which in their opinion meets the conditions specified by the committee (or requires evaluation on other grounds) should communicate their findings to the committee before submitting them for publication elsewhere and withhold publication until it is possible to attach to the findings any note that the evaluation committee sees fit to issue.
- (d) Editors of scientific journals receiving papers in which predictions are made for regions covered by evaluation committees should decline to publish until they are satisfied that the committee has had a reasonable opportunity to evaluate the prediction and to provide a note of their findings as suggested in (c) above.
- (e) Scientists should refrain from discussing any specific prediction in circumstances where their remarks are likely to generate wide publicity until the evaluation committee has had a reasonable opportunity to consider the prediction.
- (f) In so far as may be practicable scientists who communicate predictions to the evaluation committee would help to carry out observations of precursory phenomena to test the prediction hypotheses and assist in periodic reviews of the prediction.

Case Study : The Brady/Spence Prediction

Dr B.T. Brady, a physicist employed at the Research Centre of the Bureau of Mines, an agency of the U.S. Department of the Interior published a series of articles on the Theory of Earthquakes in the Journal of Pure and Applied Physics. In the last of these which is sub-titled General Implications for Earthquake Prediction (1970, p.1031). Dr Brady analysed the phenomena considered to be precursors of earthquakes and proposed relationships between these manifestations of tectonic strain and the physical explanations provided in his theory of laboratory experiments in rock failure, the process of rock bursts in mines and the ruptures which produce earthquakes.

As part of his argument he subjected certain past events to analysis including an earthquake sequence which occurred off the coast of central Peru between 3rd October and 9th November 1974. He came to the conclusion that in terms of his theory these events indicated the possibility that an area of strain was building up in the subduction zone of the Nazca and Americas Plates which could lead to an earthquake of large magnitude in a period ranging from 7.1 years to 14 years from mid November 1974.

Dr Brady attended the San Juan seminar and provided details of further study of this hypothesis carried out in association with Dr W. Spence of the U.S. Geological Survey. He confirmed then and in subsequent discussions with the writer that in his view the data that had come to light since his 1977 paper conformed in terms of his theory to the proposition that an earthquake was imminent. In his view, the most probable timing was in August 1981. I gained the impression that Dr Brady felt that the magnitude 8.2 proposed in his 1977 paper was too low and that the evidence supported the proposition that an earthquake of extraordinary violence might occur.

Dr A. Giesecke, the Director of Central Regional de Sismologia para America del Sur (CERESIS), which is located in Lima, Peru, invited Dr Brady, Dr Spence, Dr E. Algermissen and the writer to visit Lima following the seminar on Earthquake Prediction in San Juan, Argentina, to discuss the Brady/Spence prediction. Formal machinery for evaluation has not yet been established in Peru although there is, as would be expected in an area exceptionally vulnerable to strong earthquakes, an active programme of seismological observation.

At the San Juan seminar Dr Giesecke presented an analysis of the reaction by the media to the Brady/Spence prediction. This appears to have ranged from sober investigation of the progress towards predictive theory to emphatic condemnation of the two American scientists for their action in publishing their scientific arguments. As far as the writer is aware, there had been no reaction to the prediction from the government executive, although it had been agreed

that additional effort should be devoted to identifying precursory phenomena relevant to the Brady/Spence hypothesis.

One factor had important implications for the procedure followed on 29th October in Lima. Dr Brady and Dr Spence both live in Colorado. Both are employed by federal agencies of the United States Government. The possibility that a prediction may be made by a reputable scientist living outside the boundaries of the country for which the event is predicted is by no means remote. Dr M.S. Ordone presented a paper to the UNESCO Seminar on Earthquake Prediction held in Paris in 1979 in which he describes the consequences of a telegram originating from the United States predicting an earthquake at a specific location on a specific date. The prediction proved to be false but it came to the notice of the people living in the area of prediction and started a series of irrational rumours. Dr Ordone concludes from this experience that the release of information in this way (which is, of course, similar to the present situation in Peru) should be, in his words "stopped at source."

Dr G.A. Eiby recounts a similar event when "an English academic (not a seismologist) considered that he had found a method of predicting earthquakes, and decided to tell the press. He added that he was expecting a large one in New Zealand. The British press passed the news on by cable. Fortunately their New Zealand colleagues decided to get expert comment before printing the story, and only very timid souls were upset. New Zealand's official displeasure was conveyed to the prophet, who is understood to have muttered darkly about interference with academic freedom." (Earthquakes, G.A. Eiby, Heinemann Educational Books, Auckland, 1980, p. 95.)

These may seem to be of little significance but they are interesting in the light of the Brady/Spence prediction. Certainly, it would be foolish to ignore the problems that may arise when the prediction is made by a scientist outside the political jurisdiction of the area affected by the prediction.

In the Brady/Spence case Dr Giesecke prudently proposed to the U.S. Embassy in Lima that the implications should be discussed. Two officials of the U.S.

Aid Agency had come to Lima from the conference in San Juan and had intimated that their Agency would be willing to consider a proposal to help fund intensified monitoring of phenomena that might tend to confirm or deny the validity of the Brady/Spence prediction. It was obviously desirable that U.S. officials should be aware of this possibility since relations between Peru and the United States might be affected by a decision to act upon Brady/Spence prediction. Dr Brady and Dr Spence are both employees of Federal agencies in the United States. If both the government of Peru and the United States stood on common ground in relation to the prediction, the opportunities for embarrassment of both governments would be reduced.

In the event, the meeting at the U.S. Embassy was attended by Doctors Brady, Spence, Algermissen, Mr Cole and Mr Krumpke of the U.S. Aid agency, Dr Giesecke and colleagues from the Geophysical Institute of Peru, the writer, the Chargé d'Affaires of the U.S. Embassy and a number of other Embassy officials.

The meeting was informal in the sense that there was no fixed agenda but as discussion progressed three main themes emerged.

1. Was it possible to carry out a series of observations to test the Brady/Spence hypothesis and establish a set of criteria by which the prediction would be confirmed or abandoned? This inevitably involved some argument about the scientific basis of the prediction and the specialised techniques required to test the hypothesis. It seem to me that the exchanges between the scientists present did not go very far to enlighten the nonspecialist. It is worth remarking that in any earthquake prediction process, it may become necessary to explain the basis of the prediction to intelligent laymen if for no other reason than to persuade them to give the scientists money. Some thought should be given to the development of a simple but accurate resumé of the physical processes involved drawing attention to the phenomena that indicate imminence of rupture.
2. Could the United States Government expect to receive requests from

Peru for aid? Most of the discussion was centred on scientific programmes but the group gave cursory attention to the possibility of hazard reduction aid.

The Chargé, doubtless speaking from experience suggested that any response from Washington would take many months to implement. From the remarks of the AID officials present however it seemed that, as they had prior notice of the Brady/Spence prediction it was likely that on request from the Peruvian government they would be able to provide useful assistance for scientific work without undue delay. The practical outcome of this discussion was an agreement to convene a meeting of the U.S. and Peruvian scientists and the U.S. AID officials to prepare a schedule of the assistance needed to test the Brady/Spence hypothesis.

3. What was to be conveyed to the President of Peru at a meeting to be held later in the day? It was agreed that common ground should be established but beyond the communication of the basis for the Brady/Spence hypothesis, it was not immediately clear what the agreed points were. There seemed to be a consensus on the need to convey some information on the requirements of the scientific programme and, perhaps, some indication of the procedures established in other states for evaluation of predictions. It also seemed to be desirable to provide a brief summation of the issues involved in hazard mitigation.

Meeting with President of Peru

Most of the participants at the U.S. Embassy attended this meeting in the Presidential palace at 5 p.m. on 29th October. Dr Giesecke outlines the events leading up to the meeting and invited Dr Brady to summarise the process by which he had arrived at his prediction. In the course of this exposition Dr Brady invited Dr Spence to add details on the seismicity of the region and its relationship to the prediction hypothesis.

President Belaunde asked about the source of the data employed by the two scientists. He asked particularly for information on the likelihood of earthquake damage in a particular region of Peru where the government had a development programme. In one aside, the President appeared to hold the opinion that little could be done to prepare for a very large earthquake. There was no opportunity to discuss this point. The Chargé referred to the possibility of U.S. aid for the collection and integration of data. Dr Giesecke outlines the content of a proposed press statement giving brief details of the purpose of the meeting. It was agreed that this should be referred to the President's staff.

Assessment

Before attempting to spell out some of the lessons that might be learnt from the experience in Lima two points can be made. First, as far as the writer is aware this is the first time that anyone has predicted a high magnitude earthquake at a specific place and time to a head of state. Whatever may follow it will be of great value to analyse the process and the outcome. In my opinion, it is highly likely that a number of predictions will be made in the near future. It is certain that the reaction of the communities affected by the prediction will be complex and may be counter productive in terms of reducing casualties and mitigating hazards. All earthquake-vulnerable societies will therefore have an interest in the procedures to be adopted by the Peruvian authorities. Second, it quickly became apparent in Lima that once a prediction is conveyed officially to the highest government authority its status will alter.

Although the Brady/Spence prediction had become common property in Peru it had no claim to recognition beyond the personal conviction of the two scientists involved. That situation is now definitively changed. By agreeing to receive the prediction, the President has assumed political obligation to respond to it. Naturally he will seek the advice of the qualified scientists working in Peru's Institute of Geophysics. It appears that they have an obligation therefore to interpret data in the light of the Brady/Spence hypothesis

and, probably to refer the data also to Dr Brady and Dr Spence for analysis. It may be appropriate also for the Peruvian government to propose to the American National Earthquake Prediction Evaluation Council that, as Dr Brady and Dr Spence are both employees of U.S. Federal agencies the Council may wish to evaluate their conclusions and advise the Peruvian government. Dr Clarence Allen, the Chairman of the NEPEC indicated to the writer that the Council might feel itself obliged to respond to such a request.

Thus before the Government is in a position to accept or reject the prediction a substantial scientific investigation should be carried out. If this becomes widely known it will confer status on the Brady/Spence prediction and there will be intense interest in the results of the investigation. Dr Brady has indicated that unless certain phenomena manifest themselves before the end of 1980 he will feel obliged to withdraw his prediction. No doubt this would be the most welcome outcome for the Peruvian Government and people.

What will be the situation if the observations conform to Dr Brady's theoretical propositions? The matter will remain ambiguous. There may be scientific dispute about the evidence itself. In discussions at San Juan and Lima it was clear that no scientific consensus exists on the causal relationships predicated by the theory. Much will depend upon the steps now to be taken. The options and their consequences appear to be the following:-

- (a) The President, reflecting upon the information provided by Dr Spence and Dr Brady may conclude that there is insufficient agreement upon the validity of their theory to warrant a request to the Peruvian scientific establishment to carry out a special programme of observations. If this decision were to be taken the President and his governmental colleagues would have to decide whether or not they should communicate their conclusion to the citizens. An announcement to this effect should have the effect of preventing any social or economic description arising from public anxiety. On the other hand, if the event predicted by Brady occurred, the government would find itself exposed to criticism.

(b) The President may require the scientists to undertake a programme of observations, or allow them to exercise independent judgement in the matter. Whichever course is adopted the President will expect to be advised of the results. Suppose a first case in which Dr Brady and Dr Spence consider that the results conform to their theory but the Peruvian scientific authorities (and possibly scientists from other countries) remain unconvinced. There is an uncomfortable factor in this outcome. Dr Brady and Dr Spence have invested a great deal of effort in the development of their theory. If it is validated by events, there is no doubt that very considerable scientific acclaim will follow. While there is not the slightest doubt that both scientists are accomplished and honourable men they are also enthusiasts who may be unconsciously impelled to read more into the data than scientific objectivity would warrant. On the other hand, the Peruvian scientists will be influenced by an opposite impulse. The Brady/Spence hypothesis does not yet enjoy general support. It predicts an utterly calamitous event for all Peruvians. Scepticism reinforced by a natural reluctance to admit the possibility of a terrible catastrophe may - again unconsciously - influence the interpretation of data. It would require heroic detachment to avoid some resentment against a foreign expert who will be in no way affected by the prediction except in his professional reputation.

The Peruvian government may therefore be confronted by a conflict of opinion on the significance of the data. They will be exposed on the one hand to criticism that they have set aside the opinion of the Peruvian scientists in favour of that of foreign experts. If they decide to take no further action on the prediction they run the risk of allegations that they are failing in their duty to protect the citizens.

(c) The Peruvian scientists, having carried out a programme of observations, may come to the conclusion that the data appear to conform sufficiently.

with the Brady/Spence hypothesis to attach some index of probability to the prediction. No doubt this would be immediately referred to the President. Subsequent action would depend upon several factors:-

1. the degree of probability attached to the prediction;
2. the publicity surrounding the scientific advice;
3. the public policy priorities of the government;
4. residual political scepticism about earthquake prediction;
5. the strength of the opinion that very little can be done to mitigate the hazards of an earthquake.

Governmental Response to Prediction

In my view, a popularly elected government can avoid response to a confirmed prediction - even one confirmed at a low order of probability - only in circumstances where the scientific advice is never made public. Given the present situation in Peru, it seems doubtful that it will be possible to enforce secrecy. However, if that is the wish of the Government, the scientists and administrators involved should develop a plan to protect their scientific programme from public scrutiny and to bind all participants (including those in other countries if possible) to a contract of confidentiality. I have to confess that the chances of success seem to me to be nil.

I have argued above that the possibility of establishing earthquake prediction evaluation committees should be considered in all highly seismic countries. Obviously this must apply to Peru but in my opinion it is too late to establish an evaluation procedure drawn solely from qualified Peruvian scientists. Having become involved in the process of discussing the Brady/Spence hypothesis and in developing, even tentatively, a programme of monitoring relevant phenomena too many of the qualified scientists who would be essential to the success of such a committee have become sufficiently involved to make it difficult for them to recover their proper stance of neutrality towards the prediction. Therefore, for this particular case only, I believe that the

Government of Peru should authorize the Director of the Geophysical Institute to approach a number of qualified scientists from countries other than Peru to join with an equal number of Peruvian scientists to review Dr Brady's thesis on the mechanism of earthquakes, analyse the significance of the data employed to support the theory, and, if necessary, apply the theory to the data available for the location proposed by Dr Brady and Dr Spence for the earthquake in 1981.

I believe that the committee should be convened in Lima early in 1981 and asked to announce publicly its advice as to whether the Brady/Spence hypothesis is sufficiently compelling to suggest that the government of Peru should consider acting upon it. The mixed composition of the committee would help increase public confidence in the advice and develop support for any subsequent government action.

I do not favour reference to NEPEC. While I am sure that the members would be skilful and objective the position of NEPEC would be anomalous. Since the Government of the United States may be deeply involved in subsequent negotiations with the Government of Peru in financial and other matters bearing on the predicted earthquake. This, of course, says nothing about the possibility of inviting U.S. scientists to join in the evaluation process in their individual capacity. In such a case their obligation would lie not to their own government but to the Peruvian Agency which had sought their advice.

1/20/81

A PROBABILISTIC SYNTHESIS OF PRECURSORY PHENOMENA

Keiiti Aki

Department of Earth and Planetary Sciences

Massachusetts Institute of Technology

Abstract

The concept of probability gain associated with a precursor may be useful for unifying various areas of earthquake prediction research. Judging from the success of predicting the Haicheng earthquake of 1975, the probability gain at each stage of long-term, intermediate-term, short-term and imminent prediction in this case is estimated as a factor of about 30. For many independent precursors, the Bayesian theorem shows that the total probability gain is approximately the product of individual gains.

The probability gain for an individual precursor may be calculated as its success rate divided by the precursor time (Utsu, 1979). The success rate can only be determined from the accumulation of experiences with actual earthquakes. The precursor time, on the other hand, may be studied experimentally and theoretically. A review of these studies leads to a suggestion that the loading rate may be faster for smaller earthquakes. The existence of so called "sensitive spots" where precursory strain, radon or other geochemical anomalies to show up even for distant earthquakes suggest that some sites may have stress amplification (concentration) effect which may also account for higher loading rate for a small earthquake.

The concept of fractals (a family of irregular or fragmented shapes) developed by Mandelbrot (1977) is applied to the fault plane to gain some insight into its geometry. If we use the idea of barrier model in which smaller earthquakes are generated by the segmentation of a large earthquake, the fractal dimension of the fault plane becomes equal to $3b/c$ where b is the b value of magnitude-frequency relation, and c is the log-moment vs magnitude slope ($c \sim 1.5$). For $1 < b < 1.5$, which is usually observed, the fractal dimension varies from 2 (filling up plane) to 3 (filling up volume). For $0.5 < b < 1.0$, which is sometimes observed for foreshocks, the model corresponds to fault lines trying to fill up a plane. The Goishi model of Otsuka (1972) and branching model of Vere-Jones (1976) have such geometry. Assuming that the total length of branches is proportional to earthquake energy, the b value for these models becomes 0.75, corresponding to the fractal dimension of 1.5.

The probability gain for the tectonic stress increase by $\Delta\sigma$ can be expressed as $\exp(\beta\Delta\sigma)$. The coefficient β has been obtained in laboratories and in field using various methods. The value of β varies wildly, but tends to show higher value when the stress is applied in a large scale. This may also be explained by a stress amplification due to the fractal nature of fault plane. Deterministic studies of inhomogeneities, irregularity and fragmentation of fault zone will be important for understanding precursor phenomena.

Introduction

The most impressive accomplishment in seismology during the last decade was the success of our Chinese colleagues in predicting several major earthquakes. Let us take the Haicheng earthquake of 1975 and consider the probability of its occurrence before the earthquake. When the warning of earthquake occurrence was issued and people were kept outdoors in cold winter temperatures, the hazard rate, that is, the probability of earthquake occurrence per unit time, must have been on the order of 1 per several hours. The area is normally aseismic and historic records indicate the hazard rate to be on the order of 1 per thousand years. In other words, the information gathered by Chinese colleagues was able to raise the probability by a factor of about 10^6 . This remarkable accomplishment was made in four stages, namely, long-term, intermediate-term, short-term and imminent prediction. Figure 1 illustrates schematically how the unconditional hazard rate estimated from historic data was raised by each stage of prediction. Assuming an equal gain for all the stages, we find that each stage contributed to the probability gain of a factor of about 30. In order to achieve this amount of probability gain, many, many specialists and non-specialists were engaged in collecting information on various precursory phenomena. Some of the key precursors at each stage are indicated in Figure 1.

The purpose of the present paper is to unify various areas of earthquake prediction research by the concept of probability gain. The probability gain for a particular precursor may be studied empirically using past experiences with actual earthquakes. It may be studied in a laboratory

scale model under controlled conditions. More fundamentally, the probability gain may be determined by the increase of tectonic stress, which can be estimated from geodetic data. If these studies can develop a means to determine probability gain as a function of given precursors, the results can be translated into objective quantitative measure for the grade of concern about an earthquake occurrence, which will be helpful to the public offices in charge of public safety.

Let us start with a few definitions.

Definitions

First we specify the area in which an earthquake is predicted to occur. Then, we can define the average frequency of occurrence of earthquakes with a certain magnitude range in that area. For example, if the number $N(M)$ of earthquakes with magnitude greater than M is recorded during the total time period T , the average rate of occurrence p_0 per unit time is given by

$$p_0 = \frac{N(M)}{T} \quad (1)$$

For a short time interval τ , then, the unconditional probability $P(M)$ of occurrence of an earthquake with magnitude greater than M in that area is given by

$$P(M) = p_0 \tau \quad (2)$$

We shall divide the time axis into consecutive segments with the constant interval τ as shown in Figure 2. The crosses indicate the occurrence

of an earthquake with magnitude greater than M . The interval τ is taken short enough so that each segment contains at most one earthquake. We shall write the total number of segments as

$$N_0 = \frac{T}{\tau} \quad (3)$$

Let us now introduce precursors, and designate them as A, B, C, For example, A may be a swarm of small earthquakes which may be characterized by the duration, the maximum magnitude and the b value. B may be a ground upheaval characterized by the duration, extent and amount of uplift. C may be a Radon anomaly observed in the area characterized by the duration and amplitude. Suppose that, in the total period of observation, the precursor A showed up for time intervals shown in Figure 3.

Consider those segments during which the precursor A existed. Of those segments, let the number of segments containing an earthquake be n_A , and the number of segments containing no earthquake be \tilde{n}_A . Then, we can define the conditional probability $P(M|A)$ of occurrence of an earthquake within a time interval τ under the condition that the precursor A is existing as

$$P(M|A) = \frac{n_A}{n_A + \tilde{n}_A} \quad (4)$$

Since, for small τ , $P(M|A)$ is proportional to τ , we can write

$$P(M|A) = p_A \tau \quad (5)$$

P_A is the probability of an earthquake per unit time under the condition that the precursor A is existing.

We define similarly n_B , \tilde{n}_B and p_B for the precursor B, and so on. Here, we simplified our problem by neglecting the details of each precursor phenomenon, which may be included by the explicit use of multiple parameters as done by Rhoades and Evison (1979).

Conditional Probability for Multiple Independent Precursors

Let us find the probability $P(M|A,B,C,\dots)$ of occurrence of an earthquake (with magnitude greater than M in a specified area) under the condition that n independent precursors A,B,C,\dots appeared simultaneously. According to the Bayes' theorem,

$$\begin{aligned} P(M|A,B,C) &= \frac{P(A,B,C|M) P(M)}{P(A,B,C)} \\ &= \frac{P(A,B,C|M) P(M)}{P(A,B,C|M) P(M) + P(A,B,C|\tilde{M}) P(\tilde{M})} \end{aligned} \quad (6)$$

where \tilde{M} means the non-occurrence of an earthquake.

Since we assume the statistical independence among the precursors,

$$P(A,B,C|M) = P(A|M) P(B|M) P(C|M) \quad (7)$$

and

$$P(A,B,C|\tilde{M}) = P(A|\tilde{M}) P(B|\tilde{M}) P(C|\tilde{M}) \quad (8)$$

On the other hand, from the definitions given in the preceding section,

$$P(A|M) = \frac{n_A}{N} \quad (9)$$

$$P(M) = \frac{N}{N_0} \quad (10)$$

$$P(A|\tilde{M}) = \frac{\tilde{n}_A}{N_0 - N} \quad (11)$$

and

$$P(\tilde{M}) = \frac{N_0 - N}{N_0} \quad (12)$$

Putting the equations (7) through (12) into (6), we obtain

$$P(M|A, B, C) = \frac{1}{1 + \left(\frac{\tilde{n}_A}{n_A} \frac{\tilde{n}_B}{n_B} \frac{\tilde{n}_C}{n_C} \dots \right) \left(\frac{N}{N_0 - N} \right)^{n-1}} \quad (13)$$

Using equation (4), the above relation can be rewritten as

$$P(M|A, B, C) = \frac{1}{1 + \left(\frac{1}{P(M|A)} - 1 \right) \left(\frac{1}{P(M|B)} - 1 \right) \left(\frac{1}{P(M|C)} - 1 \right) \dots / \left(\frac{1}{P(M)} - 1 \right)^{n-1}} \quad (14)$$

The above equation was obtained by Utsu (1979) without the use of the Bayes' theorem. For a small τ the above probability is proportional to τ . We can, then write

$$P(M|A, B, C) \sim P\tau,$$

where

$$P = P_0 \cdot \frac{P_A}{P_0} \frac{P_B}{P_0} \frac{P_C}{P_0} \quad (15)$$

The above extremely simple relation shows that, for multiple independent precursors, the conditional rate of earthquake occurrence can be obtained by multiplying the unconditional rate p_0 by the ratios,

$$\frac{\text{conditional probability}}{\text{unconditional probability}}$$

for all the precursors. We shall call the above ratio as the probability gain of a precursor.

A quantitative measure of the grade of concern on an earthquake occurrence is illustrated in Figure 4, which shows the probability of occurrence per day of an earthquake with magnitude greater than a specified value. The unconditional probability is determined from the precursor data by equation (1). The precursors A, B, and C increase this probability approximately by a factor of $\frac{P_A}{P_0} \frac{P_B}{P_0} \frac{P_C}{P_0}$ as shown in equation (15). The example shown in Figure 4 corresponds to the earthquake with $M > 6 \frac{1}{2}$ in the Izu-Oshima area in Japan just before the earthquake of Jan. 14, 1978. Precursors A, B, and C are uplift (including gravity change), foreshocks, and Radon anomalies (including water-level change) respectively. The probability gain for each precursor was assigned by Utsu (1979) in a manner described later. The conditional probability for the three precursors almost reached the highest grade of concern VI. Although the evaluation of conditional probability was not made in real time, the Japan Meteorological Agency nevertheless issued an earthquake information at 10h50m, on Jan. 14 stating

that there was a possibility of occurrence of an earthquake causing a minor damage. An earthquake with $M = 7$ took place at 12h24m on the same day.

How to Assign the Probability Gain for a Particular Precursor

The evaluation of an earthquake prediction is very simple using the procedure described in the preceding section, if we know the probability gain p_A/p_0 , p_B/p_0 , ... for given precursors.

For the Izu-Oshima earthquake of 1978, Utsu (1979) estimated the probability gain in the following manner. The precursor A is the uplift in Izu Peninsula which was confirmed also by gravity change. The diameter of uplifted area is about 25 km, which may correspond to the source size of an earthquake with $M = 6 \frac{1}{2}$. According to a summary by Sato and Iuchi quoted in Utsu (1979), only 17% of anomalous uplifts were connected directly to earthquake occurrence. However, since the uplift in this case is so conspicuous, Utsu assigned the probability of $1/3$ instead of 17%. He also assigned the life-time uplift (or precursor time) to be five years. This gives the conditional probability rate $p_A = \frac{1}{3 \times 5 \times 365}$ per day.

The precursor B is the earthquake swarm taking place in the area. According to statistics, one out of twenty swarms may be followed by a major earthquake. However, the Izu area is known for relatively frequent foreshocks. Utsu, thus, assigns the probability of $1/10$ instead of $1/20$ for the chance of a swarm to be followed by a major earthquake in this area. Utsu made a study of foreshocks for 26 major earthquakes, and found that the mainshock occurred with three days from the biggest foreshock for 19 cases out

of 26, and that the difference between the magnitude of main shock and that of the biggest foreshock was greater than 1.6 for 10 cases out of 26. Since the biggest foreshock in the present case was M 4.9, the difference between the magnitude of presumed main shock (M 6.5) and that of the biggest foreshock is 1.6. Thus, he assigned the conditional probability rate p_B to be

$$\frac{1}{10} \frac{19}{26} \frac{10}{26} \frac{1}{3} \approx 10^{-2} \text{ per day.}$$

Finally, the precursor C for the Izu-Oshima earthquake is the composite of Radon anomaly, anomalous water table change, and volumetric strain anomaly. He considers that these three precursors may be closely related, and treats them as one precursor. He just assigns the precursor time of 1 month, and the probability that the precursor is followed by a major earthquake to be 1/10. This gives $p_C = \frac{1}{300}$ per day,

With the above estimates of conditional probability rates p_A , p_B , p_C and the unconditional probability/^{rate} p_0 based on the past seismicity in the area, he calculates the probability gains as shown in Figure 4. The precursor A (uplift) gives only the probability gain of about 2, while the precursors B (radon) and C (foreshock) gives the gain of about 100. The former, however, was important for assigning the magnitude of predicted earthquake. The main reason for the high gain of latter precursors is their short lifetime.

The probability gain is a function of magnitude of earthquake to be predicted. For a given earthquake swarm the probability that the swarm be accompanied by a major earthquake will decrease sharply with the magnitude of the latter. The longer lifetime of precursor for greater earthquakes as

proposed by various people also tend to diminish the probability gain for precursors of greater earthquakes.

On the other hand, a tremendous gain is possible, if a particular short-term precursor is expected with a high degree of certainty. For example, Sieh's (1978) suggestion that one out of several Parkfield earthquakes may become a foreshock of the next 1857 great California earthquake will give a very high conditional probability rate, say, 10^{-1} per day. This means the probability gain of more than 10^4 . With several additional precursors of moderate or small gains, it may be possible to issue a high-grade concern before the next 1857 earthquake.

Precursor Time for Various Models of Rock Failure

As described in the preceding section, Utsu (1979) estimates the probability gain for a given precursor to be equal its success rate divided by the precursor time. The success rate can only be determined from the accumulation of experiences with actual earthquakes. The precursor time, on the other hand, may be studied using rock samples in the laboratory under various conditions, or by analyzing models of rock failure theoretically. Here we shall make a review of proposed models with regard to the question "what determines the precursor time?".

Theoretical studies of the above problem were made by Rice (1979) and Rice and Rudnicki (1979) for a fluid-filled porous medium, and they concluded that not only the fault length of the impending earthquake but also the loading rate and the constitutive relation may play important parts. Their result showed that the precursor time is closer to proportional to L (fault

length) rather than to L^2 as suggested in various empirical formulas (Tsubokawa [1969], Scholtz, et al. [1973], Rikidake [1976]). Dieterich (1979) also suggests that the precursor time may be proportional to L on the basis of the precursory creep observed in his laboratory experiment and reproduced theoretically by a frictional model of slip-weakening instability. His precursor time is the travel time of precursory creep over the fault length, thus proportional to the latter.

Brady (1974) claims that the L^2 dependence of precursory time on fault length can be derived for a dry-dilatancy model without fluid diffusion. A close look at the derivation of his equation (19) reveals an unacceptable assumption made on the average strain $\bar{\epsilon}$ within a volume element dV_{fr} due to closure of an average sized microcrack. The average strain can be written as

$$\bar{\epsilon} = \frac{\int \epsilon(x) dV}{dV_{fr}}$$

Since $\epsilon(x)$ is a decreasing function with distance from the microcrack, beyond a certain size of dV_{fr} , the numerator will reach a constant asymptotically. Since, by definition, dV_{fr} should be large enough to include many cracks, $\bar{\epsilon}$ will be inversely proportional to dV_{fr} instead of a constant as assumed by Brady. If we correct for this, the precursor time becomes independent of L .

This conclusion is expected from a simple consideration that the successive stages of dilatancy model (Miachkin et al., 1975, Sobolev, et al., 1978) are primarily determined by the stress relative to the failure stress (independent of L), and the precursory time is mainly determined by the

loading rate. There is no obvious reason why the precursory time should depend on fault length, for a dry dilatancy model.

If the loading rate determines the precursor time, the empirical relation between precursor time and fault length means that the loading rate is higher for smaller earthquakes.

This magnitude dependence of loading rate is somewhat difficult to conceive for a homogenous continuum model of the earth and a common source model of stress for all earthquakes, that is, the plate motion.

One disturbing thing about the empirical relation between the precursor time and earthquake magnitude is the fact pointed out by Tsubokawa (1969) and Anderson and Whitcom (1975) that the slope of log precursor time vs. magnitude is identical to that of log recurrence time vs. magnitude. This means that the observed precursor time is roughly a fixed fraction of the recurrence time. Since no one tries to pick up a precursor for an earthquake before the time of occurrence of the preceding one, it may be suspected that those precursors may be just noises. On the other hand, these precursors may be real signals as demonstrated by the successful prediction of the Haicheng and other earthquakes.

If we accept the reality of precursors and the magnitude dependence of precursor time, we may have to accept also that the loading rate may be higher for smaller earthquakes.

A higher loading rate for a localized region relative to the surrounding is possible if the stress in the region is somehow amplified. Inhomogeneities such as joints and inclusions can cause such an amplification through stress concentration. The existence of so called "sensitive spots"

where precursory strain, radon or other geochemical anomalies tend to show up even for distant earthquakes, as well as the fact that even in the near-field of an earthquake, some precursory phenomena (such as the anomalous water table change) occur only at a small number of sites (wells) also suggest that some sites may be more sensitive because of the greater stress amplification.

Barrier Model and Fractal Dimensions of Fault Planes

The inhomogeneity of the fault zone, sometimes called "patches", "barriers" and "asperities", also introduce stress concentration. These inhomogeneities appear to exist in all scales. Microscopic pictures of the sections of rock sample after failure show that the zone of failure is not a continuous plane but fragmented. Similar fragmentation of fault has been observed at the site of rock burst in a deep mine (e.g., Spottiswoode and McGarr, 1975) and in the epicentral areas of major earthquakes (e.g., Tchalenko and Berberian, 1975). Das and Aki (1977) made a numerical experiment on rupture propagation over a fault plane with distributed barriers, and showed that some of the barriers may remain unbroken after the rupture propagation, offering a mechanism to account for fragmented fault.

The stress concentration around unbroken barriers may become the source of aftershocks (Otsuka, 1976). Aki (1978) summarized the relation between the barrier interval and the maximum slip obtained by various methods, and found that the barrier interval increases with the slip even for the same fault zone. This is consistent with the observed high Griffith fracture energy for greater earthquakes (Aki, 1979), because greater earthquakes break stronger fracture energy barriers with resultant longer barrier intervals.

Andrews (1978) pointed out, from a consideration of energetics, that the stationary occurrence of a large number of small earthquakes cannot be explained by the load of smoothly varying tectonic stress alone, but requires a generation of short wavelength self stress by a large earthquake, unless fault creep, varying in amplitude of all length scales prepares the fault for small earthquakes. The barrier model offers a physical mechanism for such a roughening of self stress in the fault zone after a major earthquake.

The above line of reasoning suggests a generic process of the whole ensemble of earthquakes, in which an earthquake prepares the stress field for the smaller earthquakes. This is similar to the phenomena of turbulence, in which a large eddy splits into smaller ones, generating a hierarchy of eddies linked by a cascade.

The concept of "fractals" developed in a book by Mandelbrot (1977) may be useful for describing the geometry of the assemblage of fault planes. A fractal is a family of irregular or fragmented shapes. An example is the length of the coast of Britain, which increases indefinitely as the scales of map is made finer. Topologically, a coast is a line with dimension 1. To describe the departure of the coast line from a simple line with finite length, he introduces the fractal dimension. For example, the trace of Brownian motion of a particle has the fractal dimension of 2 because it fills up the plane, and the fractal dimension of west coast of Britain is determined to be about 1.25. One way to obtain the fractal dimension D is, given a segment, to find the number N of subsegments which has a linear dimension r times the segment. Then, D is given by $\log N / \log(1/r)$. For example, if a straight line is divided into N segments, $r = 1/N$ and therefore $D = 1$. If a square is divided into N squares, $r = 1/\sqrt{N}$ and therefore $D = 2$.

Assuming a process in which smaller earthquakes are generated by a large earthquake in the manner in which aftershocks are generated by the barrier model, we can interpret the magnitude-frequency relation and find the fractal dimension of fault plane (we allow an overlap of fault planes, in accordance with the barrier model). Let the number of earthquakes (in a given time-space range) with fault length greater than L be $N(L)$. The slope of $\log N(L)$ against $\log L$ is $3b/c$, where b is the slope of \log frequency-magnitude relation and c is the slope of \log moment-magnitude relation, and we assume that the seismic moment is proportional to L^3 (self-similarity). To be compatible with the process for generating segments, we shall restrict the possible fault length to be $L_n = r^n L_0$, where n is the integer.

From the n to $(n + 1)$ step, the length is reduced by a factor r . In this process, the number of earthquakes is multiplied by $(1/r)^{3b/c}$, because $\Delta L = (L_{n+1} - L_n)$ is proportional to L and $\Delta L \, dN/dL$ is proportional to $L^{3b/c}$. Thus, the fractal dimension of fault plane is $D = 3b/c$. We shall consider the usual case of $c = 1.5$ (Hanks and Kanarmori, 1979). Then, if $b = 1$, the fractal dimension of fault plane is 2, same as its topological dimension. If $b = 1.5$, on the other hand, the fractal dimension becomes 3, which corresponds to filling up volume with fault planes. In most cases, the observed b value falls between the above two extremes. The value slightly greater than 1 observed for the world, imply that the assemblage of fault planes, "the plate boundary" in the context of plate tectonics, is a little more than a plane.

For $0.5 < b < 1.0$, the fractal dimension becomes between 1 and 2. For them, one can no longer consider the fault as a plane, because the fractal dimension must be greater than the topological dimension. It is possible, however, to imagine fault lines trying to fill up a plane. As a matter of

fact, the goishi model of Otsuka (1972) (see also Saito et al., 1973 and Maruyama, 1978) and the branching model of Vere-Jones (1976) have such geometry. In fact, the corresponding log frequency-magnitude relation becomes linear (in the critical case) with the b value equal to 0.75, assuming that the total length of branches is proportional to earthquake energy. This suggests that the fractal dimension of the branching model is 1.5.

Otsuka's model has been shown to be essentially the same as the model used in the study of percolation process. Otsuka proposed this model to describe the growth of an earthquake fault. His model is not based on the elasto-dynamics of rupture propagation along a fault plane, but is based on a probabilistic growth of a tree-like shape. Seismological observations clearly show that an earthquake involves a propagation of rupture with the speed comparable to elastic wave velocities and is not a percolation process. On the other hand, his model may be useful for studying the stage of preparation of a large earthquake. The barrier model used for generating a hierarchy of earthquakes is adequate for aftershocks and probably for the normal earthquake, but not for foreshocks which will precede a larger earthquake. If there is a basic generic difference between foreshocks and normal earthquakes, there remains a hope to discriminate them. Smaller b values observed for some foreshocks than for aftershocks certainly agree with the idea that the percolation model applies to the former and the barrier model to the latter. Needless to say, the precursor time will be longer for larger earthquakes if the percolation model is applicable to the preparation stage. The cross section of branches at the earth's surface will be points, and may be very difficult to be detected without numerous observations. This may explain the reason for the Chinese successful predictions.

Probability Gain by an Increase in Tectonic Stress

So far, we have mainly considered the geometry of the assemblage of fault planes, somewhat phenomenologically without paying much attention to the detailed state of stress and dynamic process going on over the fault plane. More explicit discussions of these subjects have been given by Hanks (1979) and Andrews (1980). Here we shall stay out of the stress distribution in the fault zone and consider only its response to applied external stress, namely, the problem of estimating the probability gain of an earthquake occurrence by an increase in tectonic stress.

How the probability of earthquake occurrence depends on the tectonic stress is an extremely complex problem. According to Mogi (1962), the probability of occurrence of fracture in a rock sample increases exponentially with the applied stress. When a constant stress σ is applied at $t = 0$, he found that the probability of occurrence of fracture between t and $t + dt$ is independent of t and given by

$$\mu(t)dt = \mu_0 \exp(\beta\sigma) \quad (16)$$

where $\mu(t)$ is what we called "hazard rate" earlier, and β is determined as 0.37 bar^{-1} for the tensile fracture of granite samples in the atmosphere. The experiment by Scholtz (1972) on static fatigue of quartz under uniaxial compression shows the same functional dependence on stress, but with β about one hundred times smaller than Mogi's value. The probability gain due to stress increase by $\Delta\sigma$ is simply $\exp(\beta\Delta\sigma)$, which will be wildly different whether we use Mogi's value or Scholtz's value for β .

The coefficient β can be estimated from the recurrence time of major earthquakes in a fault zone and the associated stress drop. For the Hokkaido-Kuril region, Utsu (1972) constructed a statistical model based on equation (16) and determined the model parameter by fitting the data on recurrence time. Combining Utsu's result with the average stress accumulation rate (0.3 bar per year) inferred from the stress drops in major earthquakes in this zone (Fukao and Furumoto, 1979), we find that β is 1.1 bar^{-1} . Earlier, Hagiwara (1974) obtained β of about 0.3 bar^{-1} by applying equation (16) to the statistical distribution of ultimate strain obtained by geodetic measurements.

From time to time, we find reports on an apparent sensitivity of earthquake occurrence to small stress changes such as due to earth tide and atmospheric pressure. For example, Conrad (1932) showed an impressive evidence for the increase of local earthquake frequency by 30% due to the atmospheric pressure gradient across the Alps by 5^{mm} Hg (6.7×10^{-3} bars) or greater. This gives β to be about 40 bar^{-1} .

In this conference, Barry Raleigh reported about the increase of seismicity in southern California by a factor of 2 which was associated with a strain change of 10^{-6} . This corresponds to the value of β about 2 bar^{-1} , which is much greater than laboratory values but comparable to the Hokkaido-Kuril result.

The value of β estimated by various methods, thus, ranges from 0.004 to 40 bar^{-1} over 4 decades. There is some suggestion of increasing β with increasing scale length. In other words, the probability of earthquake occurrence is more sensitive to stress change, when stress is applied in a larger scale.

Earlier, we have discussed about the scale dependence of loading rate, and suggested that stress concentration or amplification may be occurring in a cascade from a larger scale to successively smaller scales. The scale dependence of β may also be attributed to such stress amplification.

Discussion

I feel that fractal models of fault planes would be useful for understanding the precursory phenomena, especially with regard to their sensitivity to tectonic stress. The currently most reliable data for estimating tectonic stress are geodetic data supplied from levelling and geodimeter survey. One promising approach toward understanding precursory phenomena is to determine the stress change at depth from geodetic data, and then correlate the estimated stress change with the stress-sensitive phenomena such as changes in seismicity and magnetic field. A preliminary result from the Palmdale area obtained by Ikeda (1980) is encouraging. He inverted the geodetic data into 3-D stress distribution and found that the state of incremental stress during the downwarp period was in agreement with the fault plane solutions for the swarm of earthquakes during the same period given by McNally et al. (1978). From the magnitude of incremental stress (estimated at about 10 bars) and increase in the frequency of small earthquakes, the β -value was estimated to be about 0.3 bar. This magnitude of stress increase was consistent with that estimated by Johnston, et al. (1979) from the observed magnetic anomaly.

In the present paper, we discussed the fractal aspect of fault planes only from the statistical point. For the purpose of earthquake prediction, however, it may be necessary to study them deterministically. For example, we need to know where the sensitive spots are in order to observe precursors. Recent work by Bakun et al. (1980) on the relation between detailed seismicity and geometry of fault fragmentation along a part of the the San Andreas fault demonstrated that such a deterministic approach may be feasible and promising.

Acknowledgement

I thank Joe Andrews for directing me to the most interesting book by Mandelbrot. This work was supported by the U.S. Geological Survey under contract 14-08-0001-19150.

Reference

- Aki, K., A quantitative model of stress in a seismic region as a basis for earthquake prediction Proc. Conf. III, Fault Mechanics and its relation to earthquake prediction, U.S. Geological Survey Open-file Report 78-380, 7-30, 1978.
- Aki, K., Characterization of Barriers on an Earthquake Fault, J. Geophys. Res., 84, 6140-6148, 1979.
- Anderson, D. L. and J. H. Whitcom, Time-dependent seismology, J. Geophys. Res., 80, 718-732, 1975.
- Andrews, D. J., Coupling of energy between tectonic processes and earthquakes, J. Geophys. Res., 83, 2259-2264, 1978.
- Andrews, D. J., Stochastic Fault model - I Static Case, J. Geophys. Res., in press, 1980.
- Bakun, W. H., R. M. Stewart, C. G. Bufe, and S. M. Marks, Implication of seismicity for failure of a section of the San Andreas fault, Bull. Seis. Soc. Am., 70, 185-201; 1;980.
- Brady, B. T., Theory of earthquakes, I. A scale independent theory of rock failure, Pageoph 112, 701-725, 1974.
- Conrad, V., Die Zietlich Folge der Erdbeben und Bebenaulosande Ursachem, Handbuch der Geophysik, Bd. IV, 1997-1185, 1932.
- Das, S. and K. Aki, Fault plane with barriers: A versatile earthquake model, J. Geophys. Res., 82, 5658-5670, 1977.

- Dieterich, J. H., Modeling of Rock Friction. 1. Experimental results and constitutive equations. 2. Simulation of preseismic slip, J. Geophys. Res., 84, 2161-2175.
- Fukao, Y., and M. Furumoto, Stress drop, wave spectrum and recurrence interval of great earthquakes - implication from the Etorofu earthquake of Nov. 6, 1958, Geophys. J. Roy. Astr. Soc., 57 23-40, 1979.
- Hagiwara, Y., Probability of earthquake occurrence estimated from results of rock fracture experiments, Tectonophysics, 23, 99-103, 1974.
- Hanks, T. C., b-values and $\omega^{-\gamma}$ seismic source models: Implications for tectonic stress variations along active crustal fault zones and the estimation of high-frequency strong-ground motion, J. Geophys. Res., 84 2235-2242, 1979.
- Hanks, T. C. and H. Kanamori, A moment magnitude scale, J. Geophys. Res., 84, 2348-2350, 1979.
- Ikeda, K., 3-dimensional geodetic inversion method for stress modelling in the lithosphere, MS thesis, M.I.T., Jan. 1980.
- Johnston, M. J. S., F. J. Williams, J. McWhister and B. E. Williams, Tectonomagnetic anomaly during the southern California downwarp, J. Geophys. Reviews, 84, 6026-6030, 1979.
- Mandelbrot, B. B., Fractals, W. H. Freeman and Co., San Francisco, pp. 365, 1977.
- Maruyama, T., Frequency distribution of the sizes of fractures generated in the Branching Process -- Elementary Analysis, Bull. Earth. Res. Inst. 53, 407-421, 1978.
- Miachkin, V. I., W. F. Brace, G. A. Sobolev, J. H. Dieterich, Two models for earthquake forerunners, Pure Appl., Geophys. 113.

- McNally, K. C., H. Kanamori, J., Pechmann and G. Enis, Seismicity increase along the San Andreas fault, southern California, *Science*, 201, 814, 1978,
- Mogi, K., Study of elastic shocks caused by the fracture of heterogeneous material and its relation to earthquake phenomena, *Bull. Earth. Res. Inst., Univ. Tokyo*, 40, 125-173, 1962.
- Otsuka, M. A simulation of earthquake occurrence, 5, an interpretation of aftershock phenomena, *Zisin, Ser. II*, 29, 137-146, 1976.
- Otsuka, M., A chain-reaction type source model as a tool to interpret the magnitude-frequency relation of earthquakes, *J. Phys. Earth.*, 20, 35-45, 1972.
- Rhoades, D. A., and F. F. Evison, Long-range earthquake forecasting based on a single predictor, *Geoph. J. R., Astro. Soc.* 59, 43-56, 1979
- Rice, J.R., and J. W. Rudnicki, Earthquake precursor effects due to pore fluid stabilization of weakening fault, *J. Geophys. Res.*, 84, 2177-2194, 1979,
- Rice, J. R., Theory of precursory processes in the inception of earthquake rupture, *Gerl. Beitr. Geoph. Leipzig* 88, 91-127, 1979.
- Rikitake, T., *Earthquake prediction*. Elsevier, Amsterdam, 1976
- Saito, M., M. Kikuchi and K. Kudo, An analytic solution for Otsuka's goishi model, *Zisin, II*, 26, 19-25, 1973.
- Scholtz, C. H., L. R. Sykes and Y. P. Aggarwal, Earthquake prediction: A physical basis, *Science*, 181, 803-810, 1973.
- Scholtz, C. H., Static fatigue of quartz, *J. Geophys. Res.*, 77, 2104-2114, 1972.

- Sieh, K. E., 1978, Central California foreshocks of the great 1857 earthquakes, Bull. Seis. Soc. Am., 68, 1731-1750, 1978.
- Sobolvev, G., H. Spetzler and B. Salov, Precursors to failure in rocks while undergoing anelastic deformations, J. Geophys. Res., 83, 1775.
- Spottiswoode, S. M. and A. McGarr, Source parameters of tremors in a deep-level gold mine, Bull Seis. Soc. Am., 65, 93-112, 1975.
- Tchalenko, J. S. and M. Berberian, Dasht-e Bayas Fault, Iran: Earthquake and earlier related structures in bedrock, Geol. Soc. Am. Bull., 86, 703-709, 1975.
- Tsubokawa, I., 1969, On relation between duration of crustal movement and magnitude of earthquake expected, J. Geod. Soc. Japan, 15, 75-88, 1969.
- Utsu, T., Large earthquakes near Hokkaido and the expectancy of the occurrence of a large earthquake off Nemuro, Rep. Coord. Comm. for Earthq. Prediction, Geographic Survey Inst. Ministry of Construction, Japan, 7, 7-13, 1972.
- Utsu, T., Calculation of the probability of success of an earthquake prediction (in the case of Izu-Oshima-Kinkai earthquake of 1978), Rep. Coord. Comm. for Earthquake Prediction, 164-166, 1979.
- Vere-Jones, D., A branching model for crack propagation, Pageoph, 114, 711-725, 1976.

Figure Captions

- Fig. 1. The successful prediction of the Haicheng earthquake implies that the hazard rate (probability of occurrence of earthquake per unit time) had been increased from about 1 per 1000 years to 1 per several hours through acquisition of precursory information. The probability gain at each of four stages of prediction is about a factor of 30.
- Fig. 2. The cross indicates an earthquake. The time interval τ is taken short enough so that each interval contains, at most, one earthquake.
- Fig. 3. The precursor A occurs in time intervals marked A.
- Fig. 4. The probability gains calculated by Utsu (1979) for precursors A (uplift), B (foreshock) and C (radon and water table) for the Izu-Oshima earthquake of 1978.

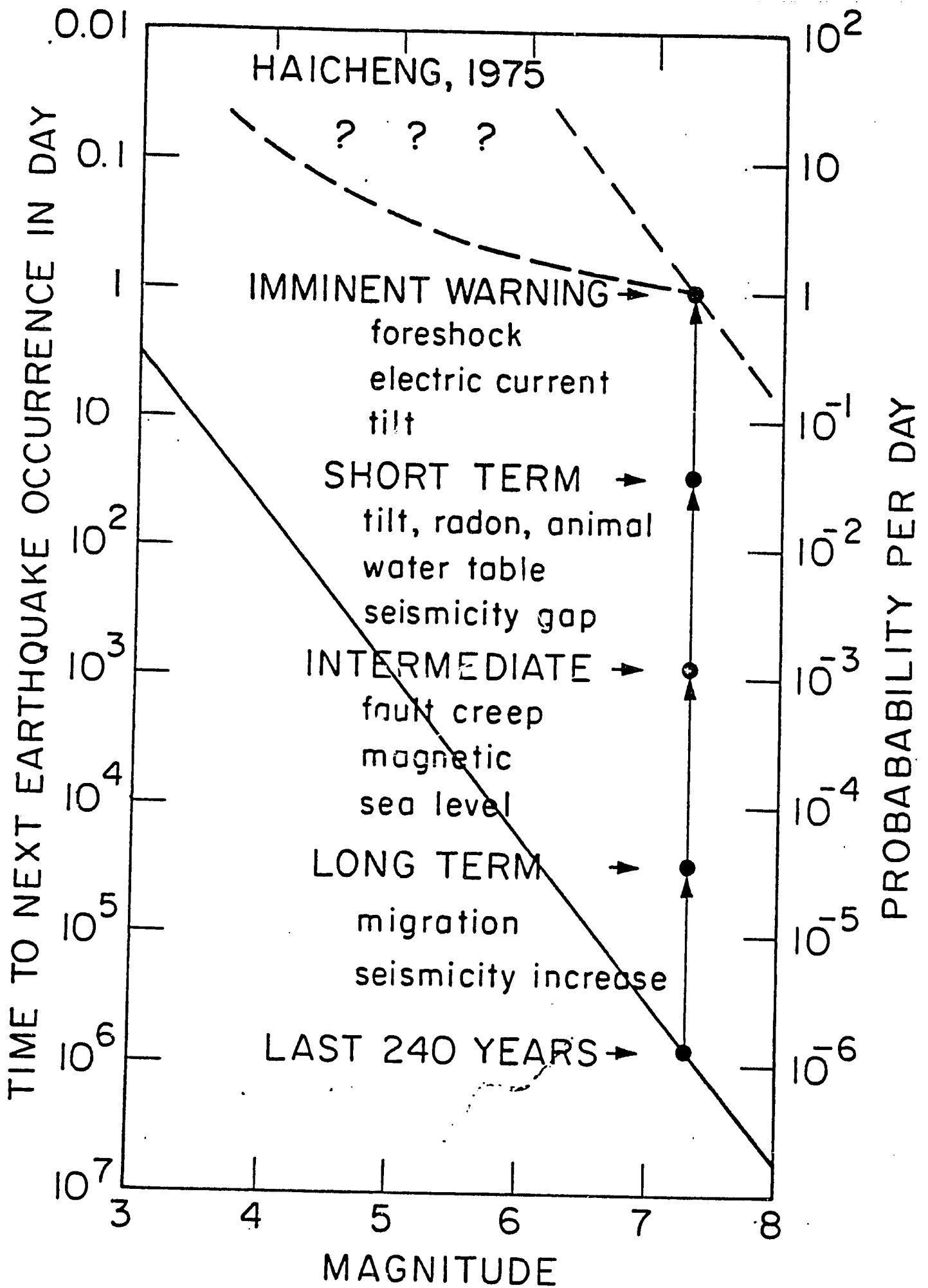


FIG 2

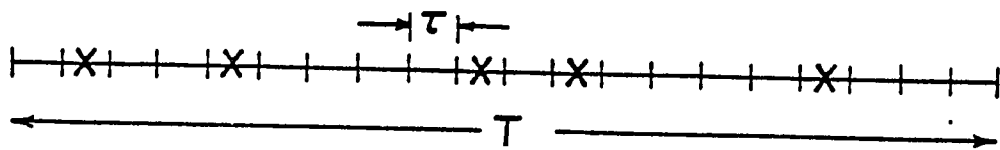
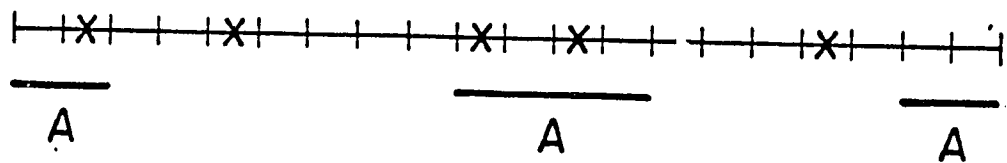
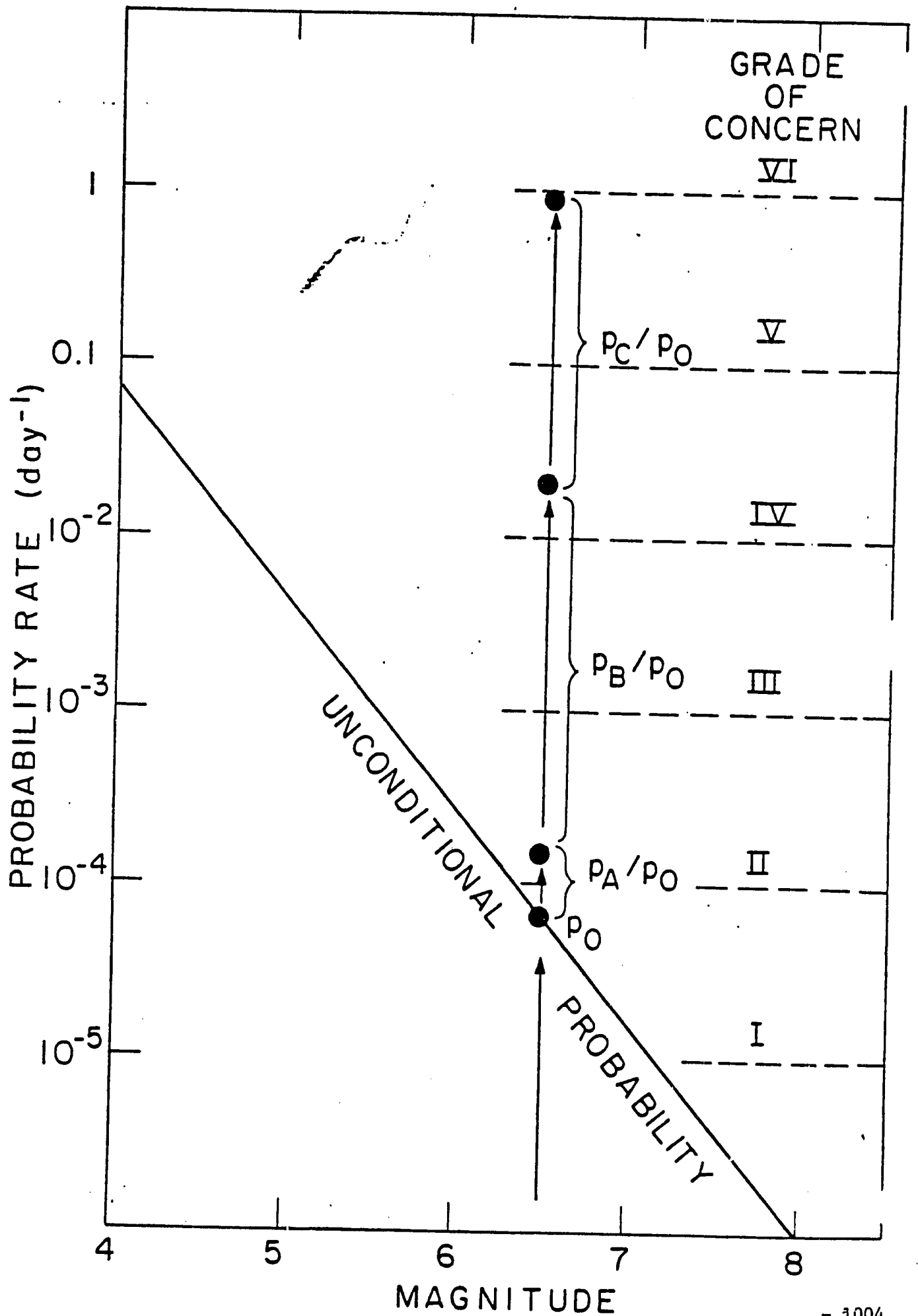


FIG 3





Unesco Seminar on Earthquake Prediction Case Histories

Notes on procedure for conveying earthquake forecasts by foreign scientists suggested by experience of forecasts issued for central coastal area of Peru in October 1980. by J.L. Roberts, Dept. of Public Administration Victoria University of Wellington, New Zealand

This paper deals with certain forecasts made by Dr B.T. Brady of the U.S. Bureau of Mines and Dr W. Spence of the U.S. Geological Survey concerning possible events in the sub-duction zone of the Nazca and Americas plates off the coast of Central Peru. The writer is not a physical scientist and offers no judgement on the validity of the theories developed or observations made by Drs Brady and Spence. As a student of politics and administration he is concerned only to study the consequences for those public authorities who came to learn of the arguments put forward by the two scientists and from an examination of the response to consider the case for some consistent procedure when scientists who are not resident within a particular country decide that they are in a position to forecast an earthquake at some place in that country within a period sufficiently specified to suggest that some counter-measures should be taken by the community. It is relevant to mention that the author has been actively engaged in the study of political and administrative consequences of earthquake prediction for some ten years. (Cf. Roberts 1973, 1977, 1979, 1979, 1981, 1981.) The author was also present at the audience with the President of Peru when Drs Brady and Spence officially conveyed their forecast that a series of strong earthquakes would occur near Lima in the second half of 1981. He has had the advantage of several discussions with the American and Peruvian scientists and administrators involved.

The Need for Definitions

The most cursory acquaintance with earthquake prediction will reveal that there are a number of stages in the process involving an increasing number of actors. The first stage involves the continuing work of the earth science community in gathering information on the phenomena of earthquake causation and frequency. We could call this the risk probability stage. From this data, it is customary to find a response in the technical and politico administrative community which attempts to assess the exposure of structures and land use to earthquake risk and to specify standards of construction, land use and civil defence procedures to mitigate risk according to the degree of hazard established. We could call this the hazard mitigation stage. With the development of enquiry into the scientific possibility of forecasting of time, place and magnitude of events the scientist may be faced with a situation in which his observations convince him that an earthquake may take place at a near date in a given location; this could be called the forecast stage. Naturally, the validity of this forecast will be assessed (if it comes to notice) and the possibility that a prediction should be formally issued will be considered. Several countries (China, Japan, the United States) have evolved machinery for what might be called the prediction evaluation stage. At this point, national authority may have to consider their reaction to the evaluation and decide whether they wish to advance to the prediction stage at which point the possibility of an event is formally put before the community at large. Once a prediction is made the precursory phenomena will come under close scrutiny

in what may be termed the risk monitoring stage. Finally, if the sequence of events forecast as precursors to the predicted earthquake occur with sufficient congruity the authorities will be compelled to decide whether or not to advance to the warning stage at which point disaster mitigation programmes would be put in train.

Forecasts from Foreign Sources

Much geological information is international in the sense of availability to earth scientists. The desire to gather information and develop theory takes as little account of national boundaries as do plate tectonics. Naturally, many of those devoted to the cause of scientific enquiry will support a philosophy of open access to data and untrammelled analysis. But the sequence of events involved in earthquake prediction is not only a scientific problem. Once given currency a forecast becomes a matter of intense interest and concern to individuals whose life and property are seen to be at risk and to those private and public institutions which may want to react or are under duty to react. One may expect that in those countries where the geological conditions and historical record indicate a possibility of strong earthquakes, there will be active public institutions for the study of seismic phenomena capable of advising public authorities on such forecasts. It is likely that they will be in touch with the main lines of scientific investigation in this field and will be available for consultation by any scientist who may consider that he has information that the public authorities should consider.

However, the scientist working outside the country may not be in touch with these institutions. Even where the scientist develops scholarly exchanges with colleagues and establishes working relationships with the relevant public agencies, the extent of these contacts will vary with each individual case.

In this exploratory phase of earthquake forecasting, it seems that the greatest care should be employed to avoid undesirable consequences for the community. This depends upon the establishment and maintenance of clear channels of communication between scientist and community but there are difficulties as the forecast made by Drs Brady and Spence demonstrates.

The Brady/Spence Forecast

It is not useful to investigate here the scientific background to the forecast of a great earthquake off the coast of Central Peru in August 1981. No doubt other and competent analysis will be available. It is sufficient to point out that in 1976 Dr Brady concluded a series of four articles on the theory of earthquakes with the deduction that strain building in the subduction zone of the Nazca and Americas plates might result in an earthquake of large magnitude within a period of seven to fourteen years from mid November 1974 (Brady: 1976).

This information reached a journalist in Peru who contacted Dr Brady and confirmed the general circumstances of the forecast. Wide publication and media comment followed. This was the subject of an analysis by Dr Alberto Giesecke, Director of the Centro Regional de Sismologia para America del Sur (CERESIS) located in Lima, at a Seminar organised by a number of national and international institutes at San Juan, Argentina, in October 1980. This revealed a reaction ranging from sober commentary

on the progress towards a theory of forecasting to somewhat sensationalist condemnation of Drs Brady and Spence. The latter also presented a paper at San Juan outlining the theory, commenting upon the investigation of empirical data and confirming their forecast.

Subsequent to this seminar Drs Brady and Spence, Dr S.T. Algermissen of U.S. Geological Survey and the writer met in Lima at the invitation of Dr Giesecke. This group joined with officials of the U.S. Government at the U.S. Embassy in Peru to discuss the implications of the forecast on 29 October 1980, and subsequently on the same day, most of this group attended an audience with the President of Peru where Drs Brady and Spence communicated the substance of their investigations and their forecast of a series of large magnitude earthquakes in the second half of 1981.

It was agreed at the meeting in the U.S. Embassy that data on seismicity in the region should be communicated to Drs Brady and Spence and there was some discussion on a possible contribution by U.S. sources to the scientific programme. I am not aware that this was forthcoming although it is clear that Peruvian scientists did supply seismic data to Dr Brady through 1981.

It is of interest to note that Dr Clarence Allen of the California Institute of Technology and Chairman of the U.S. National Earthquake Prediction Evaluation Council (NEPEC) attended the Seminar at San Juan and in conversation with the writer indicated that, in his opinion, the Council would react to the Brady/Spence forecast if requested by the Peruvian Government. Obviously, such a request was made very shortly after the communication of the forecast on 29 October. NEPEC convened at Golden, Colorado and issued the statement on 27 January 1981 appended to this paper. The operational part of their evaluation reads:

The members of the Council are unconvinced of the scientific validity of the Brady/Spence prediction. The Council has been shown nothing in the observed seismicity data, or in the theory insofar as presented, that lends substance to the predicted times, locations and magnitudes of the earthquakes.

The Council regrets that an earthquake prediction based on such speculative and vague evidence has received widespread credence outside the scientific community. We recommend that the prediction not be given serious consideration by the Government of Peru.

We cannot say with complete confidence that major earthquakes will not occur at the predicted times but we judge the probability of this happening to be very low indeed. On the basis of the data and interpretation currently available, none of the members of the Council would have serious reservations about being present personally in Lima at the times of the predicted earthquakes.

Notwithstanding this uncompromising rejection, Dr Brady maintained that his forecast was correct and my information is that as late as early May 1981 Dr Brady confirmed a forecast that there would be at least three earthquakes on or about July 6, August 18 and September 24 1981 respectively. His colleague, Dr Spence, who had looked at "... the prediction that Brady made... to determine if it was plausible given the region's tectonics" - 1007 (EOS: 1981) is reported in EOS as follows:

"I think that there's a very small chance of the predictions being correct.... Even if there's a small chance however the risk is extremely great." In light of the prediction "keeping an eye on the zone" to test the prediction would be "very prudent".

"I think scientists should be very careful about issuing predictions because of the social consequences... predictions should be supported with well documented details".

(EOS: 1981)

In July 1981 Richard A. Kerr, writing in Science reported that Brian Brady of the U.S. Bureau of Mines in Golden, Colorado, has formally withdrawn his predictions of two mammoth earthquakes off the coast of Peru. Because the prerequisite seismic activity had not occurred "The probability of the last two [large] events occurring is extremely small" he said (Kerr: 1981). Kerr also reports that despite the evaluation by NEPEC many Peruvians had continued to take the Brady forecast "very seriously" according to Dr John Filson of U.S. Geological Survey and Vice Chairman of NEPEC. Not until the first event forecast by Dr Brady had failed to occur were they relieved of their anxiety (Kerr: 1981).

Assessment

This narrative raises several important questions about the nature of scientific and public obligation. To take the scientific aspect first, it could be said that a scientist has a right to be wrong and a duty to make every effort to be right. That is, no condemnation should fall upon a scientist who publishes an hypothesis which he has earnestly and, in a professional manner endeavoured to verify but which subsequently proves to be false. It is not for a layman to judge whether Dr Brady had attained that standard of verification when he published his paper in the Journal of Pure and Applied Geophysics but it is not unreasonable to assume that the editor or editorial board of that Journal made the usual efforts to ensure that qualified authority considered the paper worthy of publication. It is my understanding that Dr Brady continued to publicise his conclusions before the San Juan meeting but so far as I am aware no systematic refutation appeared in public prior to the prediction evaluation of NEPEC in January 1981. Since Dr Brady had made in 1976 and subsequently a specific forecast of a series of large and probably devastating earthquakes, public anxiety was to be expected. Independent scientific comment could have guided lay assessment of the forecast. The problem is one of time; to coin a phrase scientia longa vita brevis. No doubt in time, the scientific community in its ordinary process of examining hypotheses would have got round to Dr Brady's theory and forecast. But one may doubt that this would have occurred soon enough to be of much use to the Peruvian community.

This raises the second problem of obligation. When a scientific hypothesis is likely to cause anxiety, economic loss and, perhaps, public disorder, has the scientist a duty to modify his method of proceeding by accommodating his scientific activity in some way to the requirements of community interest?

It would be misleading to dodge the underlying individual moral dilemma in this. If one has information whose release it is sincerely believed may increase the chances of life for others there must be an ethical duty to make the information available other things being equal. Suppose the possessor of the information believes that to resign this duty to some independent body may lead to the neglect, misinterpretation or even the suppression of the information. The establishment of NEPEC is one answer to this dilemma since the Council is composed of qualified scientists, meets in public and issues a public evaluation. Yet in the case under consideration, Dr Brady did not accept the NEPEC evaluation. To the contrary he persisted with his forecast for nearly six months after the NEPEC pronouncement. May we say that this is his proper privilege taking into account both the cause of promoting scientific advances and his duty to fellow human beings in Peru?

I know of no unqualified answer to these questions but I believe that a special set of considerations should apply to a scientist who makes forecasts for a community in which he does not live and to which he feels no more responsibility than may be evoked by common humanity.

It is obvious that a scientist living in the community must feel a greater weight of local opinion than a foreigner. Dr Clarence Allen, then President of the Geological Society of America, speaking to his fellow American scientists suggested "The next ten years are going to be tough ones.... We're going to have to work hard to maintain public support" (Spall: 1978). Dr Allen speaks of the great interest of the media in prediction and the determination of reporters to pursue any and all rumours. A prudent scientist, realising this will be fully alive to the need for caution in publishing a forecast affecting the area where he lives. One can expect that he will take every precaution to consult with colleagues and, where scientific support is forthcoming, advise the civil authorities if only to avoid personal harassment or even liability. These pressures may not be felt by a non-resident. An excess of enthusiasm may tempt him to publish without considering the implications for the society affected by his forecast. While it is not suggested that Drs Brady and Spence succumbed to such temptation it is relevant to point out that foreign predictions have been issued for areas other than Peru. A telegram from the United States was received in Mexico predicting an earthquake at Pinotepa Nacional on 23 April 1978. The municipal authorities made the contents of the telegram known and there was widespread anxiety in the region. The forecast, whose source is still not known as far as the writer is aware, turned out to be false. Clearly it was also irresponsible (Ordonez: 1979). G.A. Eiby records that an English academic following a theory of causation forecast a large event in New Zealand. This reached New Zealand from press sources but fortunately the local journalists sought expert comment before publishing the story and any disturbance of public calm was avoided. According to Dr Eiby "New Zealand's displeasure was conveyed to the prophet, who is understood to have muttered darkly about interference with academic freedom" (Eiby: 1980).

In the final analysis this is the issue. Academic freedom is a central principle of scientific advance. It is also breached constantly for commercial reasons, for reasons of state and to maintain civil order. A scientist must always weigh his scientific obligation against his obligation as a member of a local, national or international community. Brady/Spence suggest that some scientists will find it difficult to maintain equilibrium and that they need a reliable, independent and qualified consultative mechanism to help them in reaching a decision to public a forecast.

Prediction Evaluation

At some point a forecast may become a prediction. This will follow upon an assessment process which this paper calls the prediction evaluation stage. This terminology seems to be useful in signifying a possible change of status for the forecast. The evaluation of a forecast is not only concerned with its scientific validity but also with the question of a potential response of the public authorities and the community. Thus NEPEC in evaluating the Brady/Spence forecast not only stated that the members were 'unconvinced of the scientific validity of the Brady/Spence prediction' but also recommended that it should 'not be given serious consideration by the Government of Peru'. That evaluation having passed to the government of Peru it was up to the Government to decide whether to issue a "prediction" - that is a formal notification to the community that responsible public authorities accept the possibility that an earthquake will or will not occur in accordance with the terms of the evaluation. It would be naive to imagine that this will relieve a forecaster entirely of any further burdens but, at least, he may reasonably claim that a defensible procedure has been followed.

In the writer's opinion, the discussion of 'earthquake prediction' has now reached the point where responsible national and international bodies should consider encouraging the establishment of prediction evaluation procedures and advising those scientists who may develop forecasts to submit their findings to the relevant national evaluation procedure. This should not be read as an endorsement of the NEPEC form of evaluation. While NEPEC may suit the particular conditions of the United States, it may be inappropriate for other societies. As the experience of the People's Republic of China and of Japan demonstrates, there are other valuable precedents to assist in the development of a procedure adapted to the scientific and political conditions of each country. To venture briefly into an area beyond the writer's proper competence, it seems that in this palaeotechnic period of earthquake forecasting we have been misled by the drama of a possible prediction certain in time, place and magnitude - a sort of one shot scenario of disaster, to which the NEPEC procedure with its open theatre of conflict lends some support. The writer is much impressed by the reasoning of two colleagues at Victoria University of Wellington who in a paper on the subject of what they term 'synoptic forecasting' argue that

earthquake forecasting is essentially an estimation of probabilities - a statement of risk - and thus represents things as they really are.

Up to the present, most thinking about earthquake prediction has been based on the concept of the isolated prediction of a single earthquake - what might be called (to borrow a word from oil prospecting) a wildcat prediction.

(Evison and Rhoades: 1981)

While probabilistic forecasts may pose problems for the public authorities responsible for hazard mitigation programmes, it does seem that both in testing hypotheses and in establishing operating estimates of risk, they offer opportunities for sensible policy development. Clearly the NEPEC procedure would not be appropriate to probabilistic evaluation and its associated monitoring.

The writer is well aware that there is nothing new in these suggestions for evaluation procedures. An Ad hoc Working Group convened under Unesco auspices in 1981 to consider the selection of international experimental sites for research on earthquake prediction pointed out that 'guidelines for the formulation, evaluation and communication of such predictions should have previously been drawn up, to which host countries and participating institutions would already have signified their agreement'. (Unesco: 1981). Earlier in 1979 a Panel of Experts convened to review aspects of earthquake prediction recognized 'that scientific observations pertaining to earthquake predictions may have an immediate impact on society' and recommended that 'Unesco encourage the development of guidelines to assist individual scientists, scientific institutions and governments in the presentation of such information' (Unesco: 1979). Last year the General Assembly of the 'International Association of Seismology and Physics of the Earth's Interior' resolved as follows:

Noting the valuable past contributions of Unesco, UNEP and UNDRRO towards the development of multidisciplinary studies of earthquake prediction and its social implications,

Recognizing the need for the world seismological community to develop a code of practice on the formulation, assessment and communication of earthquake predictions, especially when the crossing of international boundaries is involved,

Recommends that ICSU be invited to encourage these United Nations Agencies to address this need in implementing their work programmes related to seismology and the mitigation of earthquake risk.

Suppose that the professional association and government organisations to which Drs Brady and Spence belong had promoted discussion of the need for caution in publishing specific forecasts and wide dissemination of information on the procedures available for referring any forecasts to, inter alia, Peruvian authorities for testing and, if necessary, evaluation, would it have been reasonable for Dr Brady to have refrained from incorporating in his 1976 publication the specific forecast referred to above and to have submitted this information in confidence to the specified procedure in Peru? The answer to this question depends upon the confidence the individual scientist has in the response to his submission. This is a matter of some moment. The whole purpose of an evaluation procedure is to prevent unofficial prediction. If scientists believe that their findings have not received thoroughly professional and sympathetic examination they may decide to publicise them whatever conclusion may be reached in the evaluation process. It seems to me that standards of evaluation including the process of consultation with the forecasting scientist deserve the closest attention by national and international associations. If anyone doubts that forecasts may remain current against sustained criticism it would be wise to consider the experience of U.S. authorities in the Brady/Spence case.

A lesson learned from the experience some scientists say, is that the federal government's handling of earthquake predictions can still be improved. In particular, scientists have censured the Agency for International Development's Office of Foreign Disaster Assistance (OFDA). Filson notes that for 2 years the USGS had emphasized to OFDA that Brady's predictions totally lacked support in the scientific community, outside of Spence's feasibility arguments. These "early informal reviews by the Survey were not taken as seriously as we would have liked". Clarence Allen... says "Many of us

were upset with OFDA's handling of this". In spite of the lack of scientific support, OFDA continued to place credence in Brady's prediction and even promoted the idea, he says. (Kerr: 1981)

It is of interest to note that officials of AID/OFDA were present in Lima at the meetings of 29 October 1980.

The lesson seems to be that "early informal reviews" in a foreign country are not enough. Reason suggests that Lima should have been the appropriate place and the Peruvian scientific establishment the proper authority to consider the Brady/Spence forecast. From observation, it seems to the writer that having no precedent to refer to and no canons of judgement, the Peruvian's were not equipped for this task. They tended to feel that as Drs Brady and Spence were U.S. nationals and employees of the U.S. Federal Government it was largely up to the United States to dispose of the matter. While the writer accepts that this was inevitable in the given circumstances steps should be taken to see that a similar situation does not recur.

Conclusion

Discussions on earthquake prediction so far convinces the writer that a prediction which is given wide currency and is generally believed will be a disaster for the affected community whether or not the predicted events occur. In the Brady/Spence case it was fortunate that NEPEC existed and was able to refute the prediction sufficiently early to avoid the worst consequences. That may not always be the case and the circumstances reveal an urgent need for an authoritative evaluation process in countries vulnerable to strong earthquakes. Although it is possible to argue that scientific freedom may be inhibited by such procedures, it is clear that such freedoms are frequently subject to constraints of a national or commercial interest, and in any event compulsion is not contemplated as an element in the procedures. National and international bodies concerned to promote responsible scientific activity should consider their duty to propose and assist in the establishment of evaluation procedures and to encourage the scientific community to submit their findings to the appropriate institutions. In the specific case of forecasts developed by scientists not resident in the country to which the forecast refers, the need for caution and for early and confidential consultation should be strongly emphasized.

J.L. Roberts
Professor of Public Administration,
Victoria University of Wellington,
New Zealand.

1. "Problems of Earthquake Policy", in proceedings of Seminar on High Earthquake Risk Buildings. Wellington, 1973.
2. "Central Government and Earthquake Prediction", in proceedings of Seminar on Social and Economic Effects of Earthquake Prediction. Wellington, 1977.
3. "Political and Administrative Consequences of Prediction" in proceedings of Unesco International Symposium on Earthquake Prediction. Paris, 1979.
4. "Reflections on Environmental Hazard" in Nature and Resources, October/December 1979, Paris, pp.24-30.
5. "Political and Administrative considerations in the Establishment of an Earthquake Prediction and Warning Procedure" in proceedings of International Seminar on Earthquake Prediction and Evaluation of Dangers and Seismic Risks. San Juan, 1980.
6. "The Prediction of Earthquake Hazards" in Large Earthquakes in New Zealand, Royal Society of New Zealand, Wellington, 1981, pp.3-9.
7. "Refleccions on a forecast which may lead to the prediction of a strong earthquake near Lima, Peru" in Revista Geofisica, No.10-11.
8. "General Implications for Earthquake Prediction". Journal of Pure and Applied Geophysics, 1976, p.1031.
9. "Prediction of Peru Quakes Rejected". Report in EOS, 13 March 1981.
10. Ibid.
11. "Earthquake Prediction Retracted". Science, 31 July 1981, p.527.
12. Ibid.
13. "Clarence Allen Talks About the Responsibilities of Earthquake Prediction". Earthquake Information Bulletin, Vol. 10, 1978, p.117.
14. "Causes and Effects of a False Prediction of an Earthquake at Pinotepa Nacional", M.S. Ordoneo, paper delivered to International Symposium on Earthquake Prediction, Unesco, Paris, 1979.
15. Earthquakes, G.A. Eiby, Heineman Educational Books. Auckland: 1980 pp.9-5.
16. "Synoptic Earthquake Forecasting as a Basis for Disaster Prevention". F.F. Evison and D.A. Rhoades in Large Earthquakes in New Zealand, op. cit., 1981, p.26.
17. Report of Ad hoc Working Group on International Experimental Sites for Research on Earthquake Prediction: Unesco report, SC/CONF.81/629.8 Recommendation 3.
18. Report of Panel of Experts on the Scientific, Social and Economic Aspects of Earthquake Prediction: Unesco report, SC-79/CONF.801/2.
19. Resolution of General Assembly of IASPEI, July 1981.
20. "Earthquake Prediction Retracted" in Science, op. cit., 1981, p.527.

UNDRO-UNESCO SEMINAR ON EARTHQUAKE PREDICTION

CASE HISTORIES

GENEVA, 12-15 OCTOBER 1982

CASE HISTORY OF THE PERU PREDICTION FOR 1980-81

Alberto A. Giesecke M.
Director
Regional Center for Seismology
for South America (CERESIS)

ABSTRACT

The case history of a scientific specific prediction of a large earthquake to occur off the coast of central Peru on June 28, 1981, but which did not take place, begins five years earlier with the publication of a forecast by Dr. Brian T. Brady, in Pure and Applied Geophysics (1976). Dr. Brady is a Supervisory Physicist employed by the United States Bureau of Mines, since 1967.

The formal prediction was based on the observed seismicity patterns in central Peru and Dr. Brady's interpretation of those patterns with his theoretical model of the failure preparation process in rocks, and on the plausability of major decoupling events along the Peruvian and Chilean coasts.

The scientific community in the United States (or else where) was not prompted by Brady's work to take active interest in the prediction. The U.S. Geological Survey, at the request of the Instituto Geofisico del Peru, arranged for two meetings, in 1977 and 1979, for Dr. Brady to present his work to USGS and IGP scientists; the meeting took place under the label of "cooperation to analyze the seismic hazard in Peru". Also at IGP's initiative and a request from the peruvian government, the U. S. National Earthquake Prediction Evaluation Council (NEPFC) met in January, 1981, to hear Dr. Brady. The Council concluded that its members were unconvinced of the scientific validity of the prediction, and advised the government of Peru to disregard it. At none of the major international Simposia concerned with earthquake prediction, held during the period from 1978 through 1980, was there any mention of this particular prediction. It may be that scientists felt that the state of the art was such that any precise prediction, such as Dr. Brady's was not to be taken seriously; given the professional credentials of Dr. Brady and his responsible position with a United States government bureau, this would seem to be the wrong attitude. I concur with Dr. William Spence, who states that the very occurrence of great earthquakes makes attempts to predict these catastrophic events, which kill people and disrupt society, an endeavor that the seismological community is forced to live with. The problem of earthquake prediction must be approached in such a way that the social benefits greatly outweigh the social detriments.

The rather detailed report on management of the prediction by peruvian government agencies was possible because of the author's position as head of the Instituto Geofisico del Peru and his access to the highest levels of government. It is more difficult to learn about the United States government because the Peru prediction still is a sensitive issue.

In the first three years (1976-79) the prediction did not come to the attention of the general public. During the last twelve months of the period when the prediction was widely publicized (1979-81), recently elected (1980) President Belaunde decided to give little or no public importance to it; this seems to have been the correct decision.

The impact of the prediction is evaluated in terms of schools, insurance, tourism, real estate and newsmedia. The latter did not fully realize its responsibility in attenuating or exacerbating the public's reaction to the prediction. Brady did not seek publicity for the prediction; he talked to the press only after it became front-page news in Peru. Some of the interviews with him were invented; others distorted his remarks.

The change of government, after twelve years of military rule, in mid-1980, the rising inflation and economic hardship were issues that attenuated the news value of the prediction as the date for the earthquake to occur neared.

The concluding remarks suggest that a mechanism should be adopted so that the scientific community be urged to evaluate published scientific forecasts, which can be construed as predictions that will affect people. The problem of managing a prediction will become more difficult as the state of the art progresses, the data base improves and the probability of a prediction being correct becomes greater. Brady's prediction was not entirely negative in its effects on Peru; the sustained campaign of the newsmedia, during almost two years, was most effective in increasing peruvians' awareness of their seismic hazard and, as a result, some have responded with rational actions to mitigate their risk.

1. THE PREDICTION AND ITS PROCESS

The prediction that a massive ($M_w = 9.0$) thrust-fault earthquake would occur in 1981, in the coastal region of central Peru, began in 1976 as a forecast formulated at about the same time and which attracted much less attention than others that were investigated (Cape Yakutaga, Oaxaca, Nicaragua), probably because they were based on the generally accepted empirical paradigm of the seismic gap (Spence 1979). The author of the forecast for Peru is Dr. Brian T. Brady, (M. Sc. Geophysics, M.I.T., 1964; Ph. D. Applied Mathematics, Colorado School of Mines, 1969) employed from 1967 to the present, by the United States Bureau of Mines, as Supervisory Physicist. He is the author of more than forty scientific publications in respected and well known journals. His research experience includes studies of rock fracture, physical processes involved in earthquake development and in producing plate motions.

In September 1976, a conference on "Global Aspects of Earthquake Hazard Reduction" held in Denver, Colorado, USA, was attended by 32 well known scientists from 11 institutions, including Dr. Brady. The meeting report was prepared by Drs. William Spence (meeting convener) and L.C. Pakiser, both with the U. S. Geological Survey Office of Earthquake Studies. Brady's presentation described microscale characteristics of rock failure and suggested that the process is scale invariant. He showed precursor time versus fault length data that plot linearly from the scales of laboratory failure and mine rock bursts to the scale of major earthquakes. These data lead to the important conclusion that the physical basis for earthquake occurrence may be very similar to the mechanics of rock failure in mines or in the laboratory. The meeting report includes a reference to Brady's paper "Theory of Earthquakes, IV, General Implications for Earthquake Prediction", Pure and Applied Geophysics, 114, 1031-1082, 1976. This paper discusses the earthquake sequence that occurred approximately 60 km off the coast of central Peru, between 3 October and 9 November, 1974, within a well documented seismic gap and suggests that it could have important seismological and sociological consequences. His arguments led to the possibility that the region in question, between $11.5^{\circ}\text{S} - 14^{\circ}\text{S}$ and $76^{\circ}\text{W} - 79^{\circ}\text{W}$, might have again approached a critical

state and be in the process of preparation for an earthquake of magnitude at least M8.2. Brady goes on to state that if there were no further de-stressing seismic events then the precursor times for a range of predicted magnitudes of 8.2, 8.3 and 8.5 would be 7.1 yr, 8.9 yr and 14 yr, respectively, measured from November, 1974. It is important to note that Brady also stated that the hypothesis could be tested by detailed monitoring of sea-level changes, anomalous Vp, Vs and/or Vp/Vs, radon emanations, possible secular variations in the geomagnetic field and seismicity.

We received at the Instituto Geofisico del Peru (IGP) and CERESIS the reprint of Brady's paper from Dr. William Spence of the United States Geological Survey (USGS), in late 1976. It was highly unlikely that anybody else in Peru would have known at the time of Brady's article in Pure and Applied Geophysics; we believe that only six persons in Peru, (Casaverde, Deza, Giesecke, Huaco, Ocola and Silgado) were aware of the forecast.

We began corresponding with Dr. Brady immediately. We questioned the completeness and accuracy of his data base, the applicability of the Utsu relationship between aftershock area and magnitude and his selection of certain precursory events on which he based his calculations to arrive at the specific date for the main event.

As a result of the Denver conference, held in September, 1976, Dr. L. C. Pakiser, at the time acting chief of the Branch of Seismicity and Earth Structure of the U. S. Geological Survey, and Dr. William Spence, requested Brady to update his studies of the Peru seismicity. Brady's report to Dr. Pakiser, dated 25 August, 1977, reiterated his belief that a serious situation had developed near Lima, since November 9, 1974, and that supportive data, including theoretical studies, led him to estimate the epicenter (12.5°S, 77,7°W), magnitude (M8.4 ± 0.2) and minimum preparation time measured from 14 November, 1974 (5.9 years), i.e. circa, October, 1980. we do not know how this report was circulated officially but many people in the USGS had a copy. In fact, copies of this report and of other internal USGS documents apparently were readily available to outsiders; some were reproduced and published in the Lima newspapers in 1980 and 1981. At the Geophysical Institute and at CERESIS we decided that we should treat the prediction with the utmost reserve and do our best to monitor at

least some of the Class 1 precursors that have been observed prior to major earthquakes.

In view of Brady's report to Dr. Pakiser, I informed the U. S. Ambassador in Lima of the predicted earthquake to occur in or about 1980/81, and requested his support to propose a meeting with experts of the USGS. Dr. Robert Hamilton, Chief of the Office of Earthquake Studies of the USGS, in Reston, Virginia, who knew of Brady's forecast, which he considered "far-out", kindly arranged with Dr. Pakiser to convene a meeting in Golden, Colorado on 18 November, 1977, a date on which I was able to attend. There was relatively little discussion of the theory but nevertheless my impression was that most of those present agreed that it had scientific merit. The accuracy of the location of the seismic events selected by Brady as precursors for his forecast was questioned and it was agreed that the epicenters should be recalculated. We were informed by Dr. Pakiser that Brady's report had been submitted to the Earthquake Prediction Panel of the USGS for evaluation, as well as recent results from Drs. Spence and Brady, supporting the prediction. The Panel had not responded, very likely because the prediction was for a foreign country. Dr. Robert Wallace, of the USGS at Menlo Park, who was present at the meeting, commented that if the Brady prediction were for the United States, the USGS and others would be working quite seriously to determine its validity. At my request, Dr. Brady agreed at the time not to publish any paper that would further support his prediction, without prior approval by the Peruvian government.

The Minister of Education, on whom IGP depends, was kept verbally informed of developments from the beginning. He asked for a written report in August 1978, for him to present to the President. In that report I stressed the importance of additional funding for IGP to enable it to carry out a program to detect and identify precursors, regardless of the degree of credibility given to the Brady prediction. However, no additional funds were allocated at the time.

Early in 1979 Dr. Brady told me that his latest results confirmed his belief that his prediction was more correct than not. I requested Dr. H. W. Menard, Director of the U.S. Geological Survey in Reston, Virginia, to agree on a joint meeting of USGS and IGP seismologists. The Oaxaca, December 1978, event which took place in an identified seismic gap had

reinforced our concern about the credibility to be given to predictions. Dr. John Filson, on behalf of Dr. Menard, agreed to a meeting on 24 May 1979, in Golden, Colorado "to review and discuss matters related to earthquake prediction and hazards in Peru". It was understood that the USGS would not, as a result of the meeting, formally endorse, condemn or otherwise indicate any official evaluation but would assist IGP in the assessment of the current status of earthquake prediction research and its relevance to Peru. Dr. Brady was invited to present the latest results of his earthquake research.

The month before we met in Golden, the International Symposium on Earthquake Prediction was held in Paris, April 2-6, 1979. It is interesting that there was no mention of the Brady prediction for Peru in any of the papers nor by the Experts invited by UNESCO to evaluate the Symposium and to discuss social and economic aspects of earthquake prediction, during the following week.

The meeting in Golden on 24 May, 1979, was attended by 15 scientists: 9 from the USGS, 4 from IGP, 1 each from the Bureau of Mines and the Carnegie Institution of Washington; also present were representatives of the Office for Foreign Disaster Assistance of the U. S. State Department, the Bureau of Mines and the Peruvian Embassy in Washington.

In the course of his presentation Brady made the formal prediction that in September 1980 a foreshock series would begin and would last about nine months, with a sequence of 13 events; the mainshock would take place in July, 1981, magnitude M_w 9.8 (7×10^{26} ergs), with a rupture from $12.5^\circ S$ latitude to $24.5^\circ S$, off the coast of Peru and Chile. This shock would be followed by another large shock in April, 1982, M_w 8.7, rupturing from $12.5^\circ S$ to $8.5^\circ S$. This formal prediction was based on two lines of argument. In Brady's own words the first relied solely on the observed seismicity patterns in central Peru and his interpretation of those patterns with his theoretical model of the failure preparation process in rock materials. The model was, and continues to be, in the developmental phase. The second argument was based on the plausibility of major decoupling events along the Peruvian and Chilean coasts (approximately $7^\circ S$ - $28^\circ S$). The plausibility arguments (geological, geophysical, space-time seismicity patterns during the 1974 sequence) were developed jointly

by Spence and Brady. That phase of the investigation was undertaken in response to Brady's theoretical arguments that the offshore zone had approached a critical state. The plausibility arguments remain plausible as they are obviously independent of any theoretical model. Spence argued that there is strong coupling between the Nazca and South American plates and offered evidence against aseismic slip; others, like H. W. Dewey, who have analyzed the potential for a massive thrust-fault earthquake in the region of Brady's prediction from the seismic gap point of view, come to the conclusion that such an earthquake is most unlikely to occur in the next decade, based on evidence that supports the assumption that much of the motion of the South American plate relative to the Nazca plate is accommodated by aseismic deformation. Dewey did not consider Brady's prediction in terms of its theoretical model or precursory phenomena.

Brady was challenged because he was reminded that the scientific community requires publication in such detail that other researchers can replicate results and derive the same conclusions, based on equivalent data sets, - replication of results being essential to validation, acceptance and use of a prediction model.

Both Brady and Spence informed the meeting that a complete analysis of the data leading to the prediction was in preparation and that a report would be ready by September 1980, to be published should the predicted foreshock series begin; Brady stated that he had not published his work bearing in mind IGP's request, at the prior meeting in November 1977 meeting, that he not do so. The meeting report which IGP presented to the government of Peru stated that the majority of those present remained unconvinced that Brady's prediction was valid, but nevertheless it stressed the importance of improving IGP's capability to monitor and interpret precursory phenomena.

Because the first of the primary foreshocks gave only a ten-month lead time before the mainshock, it became important that a comprehensive program to gather a wide range of precursory data, in terms of the inclusion theory of earthquakes, be ready to implement by September 1980. In a private communication dated 26 October 1979, Brady and Spence refer to two developments that increased the probability of occurrence of the

predicted earthquake: (1) the "El Centro" (California) earthquake, forecast by Brady during an OES Seminar in Golden on May 11, 1978 and again during the May 24, 1979 meeting with IGP, which did occur in the target area (Salton Sea), with a magnitude and on a date compatible with the forecast, and (2) the independent finding by Dr. V. Kulm of Oregon State University of major subsidence on the Peruvian continental shelf between about 11.8°S and 13.5°S of some 500 meters in the central portion increasing to about 1,000 meters, there being no evidence of either subsidence or uplift north or south of this zone. Kulm thought this subsidence to have occurred near the end of the last five million years, a time consistent with Brady's theoretical preparation time for the predicted 1981 earthquakes. In the same communication Brady and Spence outlined what they considered to be the most relevant measurements that should be carried out to permit a continuing evaluation of the prediction status and stressing again that a critical part of the prediction was the foreshock series to begin about September, 1980.

During the next several months the Instituto Geofisico del Peru provided Brady on a somewhat timely basis with seismic data detected by the Peruvian national network, and additional information on horizontal geodetic control along the coast, sea-level changes, secular changes in the geomagnetic field, strain and inclination.

CERESIS, with financial aid from UNESCO, UNDRO and UNEP, organized a Regional Seminar on Earthquake Prediction and Seismic Risk. It was held in San Juan, Argentina, in October, 1980, hosted by INPRES. Brady's prediction might have influenced the UN agencies in their decision to fund the seminar, which was well attended by scientists from all over the world. Drs. Brady and Spence presented a paper on the Peru prediction which the newsmedia publicized. On the other hand, the scientists were not excited and their formal discussion of the Peru prediction was rather perfunctory. One of the participants at San Juan was Dr. Clarence Allen, President of the U. S. National Earthquake Prediction Evaluation Council (NEPEC), which was established to evaluate predictions affecting the United States. I asked Dr. Allen if NEPEC would evaluate the Brady prediction should the peruvian government request it; Dr. Allen replied that in view of the circumstances NEPEC would probably make an exception and accede.

We arranged for Brady, Spence and other participants to visit Lima, Peru, after the San Juan Seminar. Private meetings were arranged with the President of Peru, Arq. Fernando Belaunde Terry, and the U. S. Embassy. President Belaunde, after listening to Brady, Spence and others, was not convinced that an emergency situation had developed and concluded that Brady's prediction did not increase the probability for the occurrence of a very large earthquake as compared to Peru's "normal" probability for such catastrophes. He agreed that it was logical and necessary that IGP do its best to monitor precursory evidence and asked me to act on behalf of the government with regard to possible assistance from the United States government including a request to NEPEC for an evaluation of Brady's prediction; I did so on 25 November 1980. NEPEC met on January 26-27, 1981. NEPEC claims that its work was hampered by the fact that no recent paper setting forth Dr. Brady's theory, model or current status of his prediction was available to the council members for review; furthermore, in one and a half days it was impossible for comprehensive follow-up of lines of questioning by Council members particularly on the theoretical basis of Brady's prediction or the complex mathematical formulations on which his model is based.

The members of the Council were unconvinced of the scientific validity of the prediction. The Council stated that they had been shown nothing in the observed seismicity data or in the theory, in so far as presented, that lended substance to the predicted times, locations and magnitudes of the earthquakes. The Council recommended that the Government of Peru not give serious consideration to the prediction, although it could not, of course, state with complete confidence that major earthquake could not occur at the predicted times, but that such probability was very low indeed. The U.S. Geological Survey endorsed the conclusions reached by the Council.

NEPEC's official report to the peruvian government was made public to the press in general. Coverage in the Lima papers was not impressive, although government spokesmen, including President Belaunde, expressed their satisfaction with NEPEC. Science, Vol. 112, 20 February 1981, had an article entitled "Prediction of Euge Peruvian Quakes Quashed" and several foreign newspapers carried the news.

The Council's pronouncement did not, of course, reduce the earthquake hazard to the region. Dr. Brady held steadfastly to his prediction and continued to do so not out of hubris, or obstinacy, but out of a moral conviction that there was a large enough chance that he was right and that people should be forewarned.

On August 14, 1980 an M_L 4.0 event was detected in the expected foreshock area. Sixteen additional events were recorded with magnitudes ranging from M_L 3.0 to M_L 4.5 up to 10 April 1981; one of them on 20 September, 1980. As this sequence developed, Brady believed that the overall characteristics of the final foreshock phase were occurring as indicated by the prediction.

Between October 1980 and May 1981, a large number of earthquakes occurred in Ayacucho (central Peru, inland), which caused loss of life and considerable damage in rural areas. These were superficial events with magnitudes in the order of M_S 5.0. Brady associated this activity with the coincident period of the predicted foreshock series in the nucleation zone but IGP public_{ly} reported that there was no evidence which related Ayacucho to the Brady prediction. However the prolonged seismic activity in Ayacucho gave rise to speculation in the newsmedia.

Brady's status report dated May 7, 1981, to Dr. Moravelli, Director, Division of Minerals, Health and Safety Technology of the Bureau of Mines, specifies preliminary dates, subject to change as additional data from the Peruvian seismic network became available, for three large predicted events: the first to occur on or about July 6, 1981, with a magnitude M_W 8.1-8.3, the second, on or about August 18, M_W 9.2 and the third on or about September 24, M_W 9.9 +. A Memorandum dated June 19, 1981, directed to Dr. John Filson, Head of the Office of Earthquake Studies, confirmed Brady's prediction that the mainshock was to occur between June 26 and June 30, 1981.

However, in a letter dated 28 April, 1981, Brady informed me that the first large event would occur on June 28, 1981, and not on or about July 6; should it not occur he would withdraw the prediction. While convinced that the area affected by the predicted shocks is capable of sustaining earthquakes of the predicted magnitudes and that the Nazca and

South American Plates are locked between the latitude limits of 7°S to 28°S, Brady also stated he would be remiss in not conveying his reservations concerning the validity of the prediction. He was convinced that the space-time off-shore seismicity patterns were real and conformed to his theory but that this did not prove that the theory was correct and that large earthquakes would occur. Whether those patterns were unique or just random fluctuations remained a question of conjecture at the time. Although Brady personally believed his prediction was correct, his letter was useful to indicate the uncertainty of the prediction.

In late May, 1981, Dr. Spence officially announced that he believed Brady's specific prediction to be incorrect and that none of the earthquakes, as predicted, would actually occur. The main reasons for his disavowal were: (1) only one of the foreshock series between October, 1980 and May, 1981 was actually located exactly in the target zone; (2) the second foreshock series to begin in mid-May, 1981 (teleseismically detected) did not occur; and (3) numerous low-magnitude seismic events, recorded by IGP in or near the target zone, are quite likely representative of continuing long-term, low-magnitude seismicity characteristic of the region near the boundary between the Nazca and the South American Plates and thus the uniqueness of the activity detected could not be demonstrated. If no earthquakes occurred that could reasonably be interpreted as foreshocks then the prediction of the mainshock(s) could effectively be considered withdrawn. Furthermore, independent evidence of geophysical anomalies that could be construed as precursors were not reported by IGP; given the size of the predicted earthquakes such anomalies should have been quite evident. Spence recognized that there remains considerable evidence for a high, present-day seismic risk throughout the zone of the predicted earthquakes and, in particular, he considers southern Peru and northern Chile as a region of very high, present-day seismic potential. He concluded by stating that he did not doubt Dr. Brady's sincerity and that he appreciated the stimulating effect of a creative scientific mind, such as Brady has. However, he reluctantly realized Brady believed too much in the correctness of his prediction to function self-critically in assessing the relevant seismic data.

Although the press was not informed by IGP or other peruvian government agencies of Brady's May 7, 1981, status report to Dr. Moravelli,

or his April 28, 1981, letter to me, June 28, 1981, was soon known by the public as the date for the predicted mainshock.

Fortunately, the earthquake did not occur and I can end this aspect of the prediction by referring to a letter from Dr. Brady to me, dated July 20, 1981, wherein he recognizes that his prediction of the large seismic events off the coast of central Peru, as presented at the NEPEC meeting in January 1981, was incorrect. Without the occurrence of the first large event, on or about 28 June, 1981, which would initiate the decoupling process between the Nazca and South American Plates, the probability of the occurrence of the two remaining large events became exceedingly low. Dr. Brady concluded by saying that he was greatly relieved that his interpretation of the space-time seismicity patterns in central Peru was not correct.

2. GOVERNMENT RESPONSE TO THE PREDICTION

2.1 Government of Peru

As has been mentioned, we in Peru knew of Brady's forecast and subsequent prediction in 1976; a process which lasted approximately five years. The responsibility for action on such knowledge, during the first three years, fell on the Instituto Geofisico del Peru (IGP) and CERESIS. The Minister of Education was given copies of pertinent correspondence and scientific reports, starting in 1977, because of the potential social and economic implications of such a catastrophic prediction, regardless of its scientific validity. The Minister was of the same opinion as IGP, - that the matter be handled confidentially. At his request, during the second semester of 1978, we informed the highest authorities in the Ministry of Foreign Affairs, the Institute of Planning and the Executive Secretariat of the National Committee for Civil Defence. It was not until November 9, 1979, that I was asked to make a formal presentation of the situation, at Civil Defence headquarters, to the Vice-Ministers and the Directors of all government agencies, including the Red Cross. The meeting had two objectives. One, to decide on a reasonable effort, in terms of government funding, to improve IGP's capability to detect and interpreta relevant precursory phenomena, bearing in mind that such an investment was reasonable and logical, in the

light of Peru's seismic hazard, Brady or no Brady, and second, to learn the state of preparedness in the several areas of government and to decide on priorities for what needed to be done.

The group endorsed a strong recommendation to the President and his Cabinet to allocate about one million dollars to IGP. As to the state of preparedness for disasters in general, much had been accomplished with very modest resources. Civil Defence was created in 1972 to cope with vulnerability and risk analysis, planning and implementation of protective measures prior to a disaster and relief operations after the disaster, including, besides earthquakes and tsunamis, landslides, avalanches, inundations, electrical storms, explosions, pollution, fire, drought and others. Civil Defence has a Scientific Advisory Committee and a small technical staff, but it is able to call for and coordinate action of military and relevant civil agencies.

Soon after the November 9, 1979, meeting at Civil Defence there was a marked increase in newspaper space dedicated to the possibility that a major earthquake would hit Lima by 1980. The large number of people present at the meeting made it impossible to continue treating the Brady prediction as a confidential matter.

Early in 1980, American consultants at the Instituto Peruano de Energía Nuclear (IPEN) provided their peruvian counterparts with several USGS documents on the Brady prediction. Some of this material subsequently reached the newsmedia.

Fortunately, press coverage of the Brady prediction decreased to occasional articles or to tabloid "specials" due to the intense political campaign to elect a new government, after 12 years of military rule.

As a result of my presentation at Civil Defence, the Peruvian Red Cross decided to make an international appeal requesting aid "as a precaution against disasters". The pertinent document covers a very broad range of items and was obviously designed to meet the disaster that would result from the earthquake(s) predicted by Brady. It included food, medicaments, plastic bags for cadavers, hospitals, housing, communications

equipment, vehicles and technical assistance, all to be delivered during the period between May 1980 and May 1981. Because of the huge amounts requested the petition could not possibly be met; even so, the Peruvian Red Cross benefited from the exercise as it had to evaluate its own capability to cope with a major disaster and to identify needs and assign priorities, useful information for international disaster relief agencies.

UNDRO sent a Mission to Peru in October, 1980, and came to the conclusion that few specific preparedness measures had actually been taken. Most people in Peru have little alternative but to continue living in their present houses and working in their present workplaces. However, because of the Brady prediction, in a few cases, people who could afford it had their houses inspected and spent money to improve their resistance to earthquakes.

In February, 1980, I was called by the President of Peru to present to him and his Cabinet a situation report on the Brady prediction. I took the opportunity to request additional funds for IGP to improve its operational capability and to recommend that an official agency be appointed to assume responsibility for all government action with regard to the prediction. A few days later, I was informed that approximately one million dollars were to be allocated to IGP. About one third of this amount was authorized in March, 1980. I was asked to approach foreign governments to explore possible donations of equipment or availability of soft credits for the purchase of equipment before requesting from the Treasury the remaining two thirds. The government also provided funds for Civil Defence. The president appointed the Executive Secretariat for National Defence, under Executive Secretary General Ramón Miranda Ampuero, as the agency responsible for handling the Brady prediction. National Defence has to do with military and non-military problems; Civil Defence is a subsystem of National Defence. This arrangement subsisted until the end of the military government in June, 1980.

The new government revoked legislation imposed by the former regime, changed institutional structures and appointed different people to responsible levels of the public administration, - a common and understandable pattern of behaviour under the circumstances. This attitude

may also explain why some of the new Ministers and Congressmen labelled the military as "believers" of the earthquake prediction and denounced Brady as an international terrorist. However, the new government did support IGP's joint proposal with Carnegie Institution of Washington, to the U.S. Agency for International Development, for a project to study seismicity in Peru, by obligating counterpart funds in the 1981 and 1982 budgets; the project includes purchase of seismometers, telemetry and a central data processing facility with an approximate value of \$800,000 dollars. Although the proposal did not mention Brady or the prediction, its origin, timing and acceptance were influenced by the Brady prediction.

In May, 1981 the National Council for Science and Technology of Peru (CONCYTEC) asked CERESIS for an opinion on the Brady prediction. Father Cabré, President of the CERESIS Directive Council, in consultation with other Council members and myself, prepared a report summarizing the situation, stressing the fact that Lima, as well as other parts of Peru, should permanently improve the earthquake-resistant characteristics of its buildings, regardless of any given prediction (it must be remembered that, on the average, Lima has suffered four destructive earthquakes each century). Father Cabré as a member of the UNESCO reconnaissance mission to Lima, after the 1966 earthquake, was well aware that many buildings, specially the older structures, do not meet earthquake-resistant standards. The report recommended that Peru improve its capability to detect and analyze seismic events on a national and regional scale, and mentioned the importance of providing the newsmedia with credible and timely official information. CONCYTEC reported to President Belaunde, on May 22, 1981.

The National Census for 1981 was originally scheduled for June 28, 1981. Because of the prediction, it was postponed until July 12 1981. It was believed that population data would be distorted because of the significant number of people expected to leave their homes on June 28, because of the prediction.

2.2 U. S. Government

Reference has been made to the participation and role of U. S. government agencies involved in the Brady prediction. These were

the U.S. Geological Survey, the Bureau of Mines and the Office of Foreign Disaster Assistance of the Agency for International Development (Department of State). The U.S. Geological Survey did not at any time endorse or support Brady's prediction. Nevertheless, they were extremely cooperative in arranging for the two formal meetings held in Golden, Colorado, at the request of the Instituto Geofisico del Peru "to assist Peruvians in their assessment of earthquake hazards in Peru", and for NEPEC's evaluation of Brady's prediction. The USGS also authorized Dr. Jerry Eaton to work with IGP in Peru in connection with a program for the detection and analysis of earthquake precursors. At the individual level, IGP scientists and executives benefited from the friendship and understanding of their U.S. colleagues.

Dr. Brady had the support of his employers, the Bureau of Mines, throughout the whole process. He continues to hold a responsible position and is respected by his superiors and fellow workers. As an outsider, I can only venture to state that there probably could have been a better working relationship between Dr. Brady and his scientific colleagues in the USGS had there been a decision at a sufficiently high level, in the USGS and the Bureau of Mines, to examine the situation jointly, bearing in mind that the problem was not solely seismology or physics but that it had to do with important social and economic questions and international relations.

We received courteous and helpful attention from the Office of Foreign Disaster Assistance (OFDA). They realized the serious implications of the Brady prediction and stressed the importance of being prepared for a disaster, which undoubtedly Peru will suffer sooner or later. However, the Peru prediction was and still is a sensitive issue and I have been told that open discussion concerning its management by agencies and individuals within the U.S. Government remains difficult. This is complicated by the fact that Dr. Brady continues to examine the theory and its application with respect to possible future events. He is not the only one concerned by the possibility that the coastal segment off central Peru may not have been distressed by the number and severity of seismic events which have recurred since 1746. This region is currently exhibiting an unusual quiescence, which may be an indication that a strong earthquake could occur in the not too distant future.

Seismic data from the IGP local network was relayed to Dr. Brady by the U.S. Embassy at regular intervals. IGP kept in touch with officers of the Embassy who handled information relevant to the prediction; on several occasions we met with the Ambassador to discuss the situation. The U.S. Embassy apparently felt obligated to cooperate with Peruvian authorities because Dr. Brady was a U.S. government employee in good standing. The Embassy maintained a low profile except when it publicized the findings of the NEPEC and when, a few days before the first large earthquake was to occur, June 28, 1981, Ambassador Corr announced that he was bringing his mother and father from the United States to have them with him in Lima on the day of the earthquake. The story, with pictures of their arrival, was on the front pages and on T.V. The U.S. Embassy arranged for Dr. John Filson, head of the Office of Earthquake Studies of the USGS, to come to Lima for a press conference and to remain until after the predicted date, and for experts in disaster preparedness to come to work with Civil Defence.

The U.S. Embassy recommended favourable action on proposals by IGP and CERESIS to U.S. funding agencies. Two projects were approved. First, OFDA transferred \$ 500,000 dollars to the U.S. Geological Survey for CERESIS to carry out the initial phase of a four-year earthquake disaster mitigation program in the Andean region (Project SISRA). The objectives are to produce national and regional catalogues of earthquake hypocenters and intensities, seismotectonic and neotectonic maps and uniform seismic hazard maps for various probability levels and parameters. Second, the IGP - Carnegie Institution proposal to OFDA to upgrade and modernize Peru's earthquake monitoring network, a most appropriate and cost-effective project, given the magnitude of possible disaster which permanently threatens Peru.

3. SOCIAL AND ECONOMIC IMPACT

3.1 Schools

The school system in Peru has both public and private schools. In 1981, 3,238,000 students ages 6-12 attended primary grades, 1,257,000 ages 13-18 attended secondary grades and 250,000 adults were enrolled in primary or secondary schools. Thus, the school population in 1981 was

4,745,000 approximately one quarter of the total population of Peru. There are 90,000 teachers in primary and 50,000 in secondary, in some 25,000 school units.

The effect of the Brady prediction in schools is therefore significant as a reference for the behaviour of the population. My impressions are derived from interviews with teachers and students in several Lima schools of different categories. This sample appears to be representative of a general pattern.

Before Brady, there was no significant effort in schools to increase the awareness of the seismic environment, with two exceptions: (1) at Reina de los Angeles, which had suffered partial collapse of its modern building due to the 1974 Lima earthquake possibly because of faulty construction and higher-than-expected soil response, and (2) at San Silvestre, also a good private school for girls (1,200 students) which for years has had orderly drills at least once each semester and maintains a well organized system for evacuation, disconnecting power and gas mains, quick access to fire extinguishers, first-aid stations and signs; students and teachers are permanently trained and assigned specific tasks. At both of these schools the Brady prediction motivated further improvement in design and construction of their buildings, removal of dangerous objects that could fall on people, widening of stairs and doorways, rounding off all sharp edges, more frequent unannounced emergency drills, involvement of parent-teachers associations through teaching aids - films, text-books and talks with students, parents and teachers, thus gaining a better understanding of earthquake hazard and risk.

Because of the prediction, Civil Defence and the Ministry of Education inspected school buildings, designed and posted evacuation routes with cardboard or painted signs and lectured on the subject. The people we interviewed report that (1) there was general indifference to the prediction; speakers and teachers designated to discuss the problem only partially complied and attendance to such talks was minimal; typically, a seminar was attended by 20 teachers out of a possible 300; (2) the competence of the speakers was, in general, poor; at ESAN, a post-graduate institution for executives in business administration, the lecturer (a lawyer commissioned by Civil Defence) began his talk disqualifying Brady because, "as far as he knew, Brady had never personally inspected the subduction zone in a submarine"; (3) the recommendations to reduce the

- 1032 -

vulnerability of the structures were impossible to carry out because of high cost and bureaucratic impediments; (4) printed instructions for preventive measures were distributed via the Ministry of Education; a first version, which unfortunately was widely circulated and given publicity by the official T.V. Channel 7, recommended that the refrigerator be kept well stocked; that a two to three week supply of canned food be purchased; that fresh water be kept in large containers and changed twice a week adding chlorine pills; that at least two large flashlights be handy with replacements cells; that a well-equipped first-aid kit, sleeping bags and a transistor radio, be readily accessible and in a safe place. For probably more than 85% of Lima's population, such recommendations, probably valid for the U.S., Germany, the Soviet Union or Japan, were meaningless. People still buy water daily, in cans, and thousands go to the market to purchase a subsistence amount of food each day; perhaps the irrelevance of recommended action for preparedness in the light of their economies led the majority of the population to come to the conclusion that the Brady prediction was a problem for the rich.

An ambitious exercise was carried out by Civil Defence on November 29, 1980. At schools throughout Peru, bells and alarms sounded during 30 seconds to simulate the occurrence of a severe earthquake. Several days of practice preceded this exercise, including rapid and orderly evacuation, tending to the wounded and fighting fires. To be effective, this type of action must be a sustained program at each school, students change class-rooms every year, as they grow their own perspective changes.

A few positive effects have been detected, - occasional evacuation drills are carried out and in a disciplined manner; some new schools are to be one-story buildings with direct exit to open areas; in some places, students are instructed on what to do during and immediately after an earthquake. However, in general, class-rooms and assembly halls are again being filled well beyond capacity; signs to show evacuation routes have either been painted over or removed; no major program has been implemented to reduce the vulnerability of school buildings; there is no sustained effort on the part of Civil Defence, directly or through the Ministry of Education, to improve the situation, according to the teachers interviewed. It would seem that without Brady, Peru's earthquake problem has disappeared.

We wanted to correlate absenteeism of students with rumors of impending earthquakes, earthquake headlines and the dates of the predicted large earthquakes. One conclusion is that there is a correlation between absenteeism and the economic level of the families of the students. In the public schools and the poorer private schools there was no apparent effect of the prediction on school attendance; in the rich private schools there was a noticeable effect; for example, about 1 1/2 % of the families took their children to some other country; others left Lima for cities in the interior. Rumors had an effect at all schools; it is almost impossible to know how rumors start but, typically, some teacher would receive a call stating that the Geophysical Institute or the Ministry of Education had announced that the earthquake would take place two or three hours later; the usual reaction was to have the students go home. This happened rather frequently but the rumors did not affect more than a few schools at a time.

Perhaps as a result of the Brady prediction UNESCO's Program for Environmental Education asked CERESIS, in 1980, to carry out a pilot project in the area of seismology. This was implemented with the cooperation of the Ministry of Education. Visual aids, cartoons, slides and texts have been prepared and will be included in the regular school program after a period of evaluation.

3.2 Insurance

Rates for earthquake insurance did not change in response to the Brady prediction. Some 85% of large and medium large Lima industry is normally covered by such insurance, whereas the number of policies for residences has been rather low. In 1981 there was an increase of about 35% in the number of policies for residences. Many homeowners and small businesses who did not have the infrastructure to analyze their risk management problem in the light of the prediction's real implications decided anyway not to assume such an "imminent" risk. This seems a reasonable decision specially because of the relatively low cost, since the frequency component of the insurance rate was apparently favoring them. However, in 1982 there is evidence that some of those residence policies will not be renewed.

Some of the large and medium large industries did modify their normal practice by adding coverage of "loss of profit" due to earthquake damage, so as to be covered during the period that their plants were non-operative. There is also some evidence that this type of added coverage is not being generally renewed in 1982. Most large industries apparently analyzed their risk management practice with respect to earthquakes and Brady's prediction of a terrible catastrophe and have decided that there are not enough elements as to make them change their traditional practice.

In 1980, the total amount of earthquake insurance in Peru was of the order of 4,900 million dollars as compared to 6,400 million in 1981. The increase of 1,500 million dollars may not be too significant, considering normal growth and inflation, but certainly the increase in number of policies, specially for individual homes, does seem to be a direct effect of the prediction.

3.3 Tourism

Statistics on the number of foreigners that enter Peru may not lead us to a valid conclusion as to the effect of the prediction on tourism. 293,447 entered in 1978, 338,468 in 1979, 372,790 in 1980 and 334,819 in 1981. The numbers typically increase by 10% to 15% from one year to the next, as noted from the figures for 1978 to 1980 and in preceding years. One would expect that in 1981, some 420,000 people, mostly tourists, should have come to Peru; the actual number was 25% below that estimate. There may be other reasons for this decrease besides the Brady prediction, but this needs to be investigated. Monthly figures for 1981 do point to the decrease in the high-season months of June and July, and tourist agencies state that the number of tourists was 35% less than expected. The loss of revenue to Peru, on the basis of such information, can be estimated to have been about one hundred million dollars. Two lawyers initiated formal legal action to sue Dr. Brady, but the case was rejected by the District Attorney and by the Court of Appeals on the grounds that there was insufficient evidence. These same lawyers also asked the Congress on Problems of Latin American Nations, sponsored by the Universities of Yale, Harvard and Georgetown, to take notice of the situation and condemn Brady.

The total number of nationals leaving Peru in 1981 would seem to indicate that fewer people did so than what could have been expected from the normal year to year increase, except for the fact that in July, 1981, more peruvians left Peru than during any one month in the previous four years. Tourist agencies and airlines stated that all flights leaving Peru in May, June and July, 1981, were booked solid. There is some evidence that more foreign employees of embassies, international agencies and transnational companies requested vacations during this three-month period than usual.

3.4 Real Estate

The effect of the prediction on value of property was noticeable in La Punta, a small upper-middle class suburb, on a peninsula adjacent to the port of Callao, only one meter above sea-level on the average.

The Naval Academy and the Hydrographic Office are located in La Punta. The Hydrographic Office is responsible for the tide-gauges along the peruvian coast and participates in the Tsunami Warning System for the Pacific Ocean. Early in 1981 they put under the door of all the homes and establishments in La Punta a brochure with technical information on tsunamis, as a normal service to the community. Although the brochure did not refer to the prediction, people associated the timing of its distribution with concurrent prediction publicity in the newsmedia, and this heightened awareness of potential danger was the reason for dozens of homeowners to try to sell their La Punta homes. Those that were able to find buyers did so at a significant loss. In other areas of greater Lima there is no evidence of a similar large-scale effect, but more research on the subject is required.

3.5 Newsmedia

Press coverage of the Brady prediction does not start until the last quarter of 1979, three years from the date Brady published his paper in Pure and Applied Geophysics.

A Harvard professor attending the VIth Panamerican Congress of Soil Mechanics and Foundation Engineers, which took place in Lima, December 2-7, 1979, was quoted as being of the opinion that the Brady

prediction for 1980 had a 20% probability of being correct ; another participant, a peruvian engineer with strong political views, thought that the "Beard" (meaning Brady) prediction was a plot of the military government to remain in power; a Dr. Sowers was quoted as being the real author of the prediction and as stating that the tsunami generated by the earthquake would endanger 2,000 million people living on the coasts of the Pacific ocean; a geologist, supposed to be an authority, said that the cause of earthquakes was the energy released by the river sediments dropping 5,868 m. into the deep trench off the coast, and that the whole coastal highway would drop into the sea. The two most widely read weekly magazines, Gente and Caretas, published rather accurate information and avoided statements that would cause undue alarm.

During the following 18 months the Brady prediction was well publicized in the twelve Lima daily papers, the three principal weekly magazines and radio, but not much on T.V. The total space dedicated by newspapers and magazines is equivalent to approximately a 6-cm wide colum, more than 600 meters long, or nearly 400,000 square centimeters. Not more than about 25% was useful, relevant, reliable, and timely information. The rest, mostly in tabloids, even went so far as to invent interviews with Brady, quote "authorities" such as the winner of a Miss Bikini contest, head-lined that Brady confirmed Saint Rose' sixteenth century prediction that the sea would cover the Plaza de Armas of Lima (in fact there is no historical evidence that St. Rose of Lima ever made such a prediction, but it is popular belief). This type of press, and even the more conservation newspapers, discovered a great number of peruvian experts on earthquake prediction, who were quoted at length on why Brady's theory was correct or incorrect, although it is certain that none of them had ever read any of Brady's papers. Between March and October, 1980, the prediction was almost forgotten; this was because of the election campaign and change of government after 12 years of military rule.

One particular tabloid (P.M.) printed on its front page during 35 consecutive days sensational news about the earthquake; its central page was a blank with only a small caption which stated: "Mr. President: this space is reserved for your message to our people concerning the earthquake". Some papers, and the weekly magazines, published

results of polls, according to which 75% of the people were simply not interested or worried about the forthcoming earthquake.

Rumors and their effects received considerable press attention. There were four occasions when rumors caused panic. These occurred on 14 January 1980, 18 March 1980, 16 March 1981 and 25 June 1981, and in all cases they related to tsunamis that would destroy the city of Callao, Lima's port. People evacuated homes and headed for Lima causing incredible traffic jams. It was necessary for Civil Defence, police and government officials to intervene before a return to normality. It is curious that this source of fear can not be eradicated in as much as a tsunami is the kind of catastrophe which can be foretold. The Pacific Warning System can estimate arrival times for tsunamis generated off distant shores; tsunamis generated near the coast can only be dangerous after a strong earthquake occurs. This is an area where public education, through the newsmedia, can be very effective.

The seminar on earthquake prediction, in San Juan, Argentina, in October 1980, motivated considerable press coverage in San Juan, some of which was reproduced in the Buenos Aires papers - specially Brady's prediction for Peru. The international news services circulated the story all over the world and the same story was recycled back and forth between Peru and foreign newsmedia. There were two peak periods in the newsmedia, one from November, 1980 through February, 1981, and the other from April to July, 1981, during which almost every newspaper had some reference to the prediction itself or of the general earthquake hazard two or three times a week. It is undeniable that a prediction is newsworthy and such news increase sales. El "Diario de Marka" (a serious paper) had a one-week series of well-written articles on the earthquake prediction and it sold about 50% more copies than on the average. Daily sales of Lima newspapers were of the order of 600,000 to 650,000 in the period 1975-80, when the press was under government control. Since 1980 with a free press, sales have increased to about 900,000 daily. The change from a controlled to a free press, in mid-1980, distorts the prediction effect on circulation figures and, in addition, statistics on day to day circulation of many newspapers are not readily available.

Our estimate of radio time dedicated to the prediction during

the same 18 month period is about one thousand hours. One particular station mentioned the prediction in at least 50% of its daily morning broadcasts during the first semester of 1981.

One of the important television companies produced a documental film on the prediction, including interviews with Brady and Spence. It illustrated the geophysical and geological characteristics of Peru and, its seismic environment; it was quite good. However, for some reason, the decision was to cancel its public release scheduled for a date before that of the predicted earthquake, and has gone into the files.

4. CONCLUDING REMARKS

4.1 A mechanism should be adopted by the scientific community to bring about automatic peer review of any bonafide scientific paper that forecasts or predicts a specific earthquake that will have destructive effects anywhere, in particular in countries that are not able to evaluate such a prediction by themselves. In the case of Dr. Brady, his paper was accepted for publication in an accredited international scientific journal, on the basis of its scientific merits. The reference to a possible catastrophic earthquake in central Peru was somewhat buried in the text, and perhaps this explains why neither the U.S. scientific community, as such, nor that of other advanced countries took the time or had the interest to analyze this prediction. The general reaction might have been that Brady's forecast was not to be taken at face value. It was only because of the persistence and interest of peruvians that the USGS and NEPEC got involved.

A mechanism whereby immediate evaluation and pertinent recommendations are formulated and, as the prediction evolves, active cooperation, could be the responsibility of IASPEI or ICSU, as a first step, and subsequently of inter - governmental agencies such as UNESCO and UNDRO.

Dr. Spence's experience with the Brady prediction should not be ignored. We are thankful for his participation and are glad to know his scientific stature did not suffer from his association with Brady but to the contrary. Spence believes that as scientists better understand

the physics of the earthquake process and are tempted to predict earthquake occurrences, they should move slowly and rationally, with plenty of discussion, hypothesis testing, hard thinking prior to publication, and to couch predictions in terms of well-defined conditional probabilities which can be up-dated. A predicting scientist should maintain a perspective that can change pro por con with the acquisition of new data and, if so, should expect help and not reprisals from the seismological community. Spence believes that the precise prediction of an earthquake is an extremely difficult scientific problem; however, the very occurrence of great earthquakes makes attempts to predict these potentially catastrophic events an endeavor that the seismological community is forced to live with; the problem must be approached with the view that the social benefits greatly outweigh the social detriments. Responsible agencies should encourage earthquake prediction research and should document prediction scenarios and case histories to really understand the complex social, political, and economic ramifications of what must remain a purely scientific endeavor.

It must be realized that as science progresses the Brady effect will become worse before it becomes better. In other words, one must assume that future Bradys may be more knowledgeable, with a better data base, new insight as to the genesis of earthquake and so on, - hence the prediction should be relatively more reliable than Brady's and the probability of a successful prediction will be greater but certainly the chances for failure will still be more than those for success, for some time to come. Therefore the problem of handling a prediction becomes more and more difficult as the science progresses and predictions can not be ignored, making it more difficult for governments to take decisions and guide public reaction.

4.2 There have been some benefits to Peru from the Brady prediction:

- a) IGP is now better equipped to cope with the problem of detection, location and real-time analysis of earthquake events.
- b) The Ministry of Education is giving support to the project of Environmental Education in Seismology, begun

- under auspices of UNESCO and CERESIS, to educate the population to better cope with the earthquake hazard.
- c) The Brady experience has called our attention to a problem that is not unique to Peru: Government institutions do not readily cooperate or help each other. They have an aversion to free exchange of data and know-how, because of a competitive attitude which some times places institutional prestige above national objectives; institutions compete for limited financial resources; each wants to be hegemonic in its field even when its competence may be minimal. At a personal level, institution heads and staff members do maintain a working relationship, but institutional behaviour needs to be greatly improved.
 - d) The Brady experience has made the government receptive to the proposition that an international site for research oriented to the prediction of earthquakes be established in southern Peru. The area of southern Peru and northern Chile was proposed for such a site by the Group of Experts, invited by UNESCO, which met in London, Ontario, Canada, during the IASPEI General Assembly last year.

4.3 This paper does not attempt to be more than a partial and brief report of the Peru prediction from a personal point of view. Invited by CERESIS, a group of experts from the United States, New Zealand and Peru is considering the suggestion that a formal Working Group be established to produce a well-documented, comprehensive, and unbiased analysis.

References

Brady, B.T. Theory of Earthquakes, IV, General Implications for Earthquake Prediction, Pure and Applied Geophysics, 114, 1031 - 1082, 1976.

Spence, W. Conference Report: Toward Earthquake Prediction on the Global Scale. EOS, Vol. 59, No. 1, January 1978.

BRADY File at Instituto Geofísico del Peru (IGP) and at Regional Center for Seismology for South America (CERESIS).

NEWSMEDIA file at CERESIS